UNIVERSIDAD COMPLUTENSE DE MADRID

FACULTAD DE VETERINARIA

Departamento de Fisiología

LAS CÉLULAS INTERSTICIALES DE CAJAL COMO MEDIADORAS DE LA NEUROTRANSMISIÓN URETRAL

MEMORIA PARA OPTAR AL GRADO DE DOCTOR
PRESENTADA POR

María Sancho González

Bajo la dirección de los doctores

Ángeles García Pascual
Domingo Triguero Robles

MADRID, 2013

UNIVERSIDAD COMPLUTENSE DE MADRID
FACULTAD DE VETERINARIA
DEPARTAMENTO DE FISIOLOGÍA

Las células intersticiales de Cajal como mediadoras de la neurotransmisión uretral

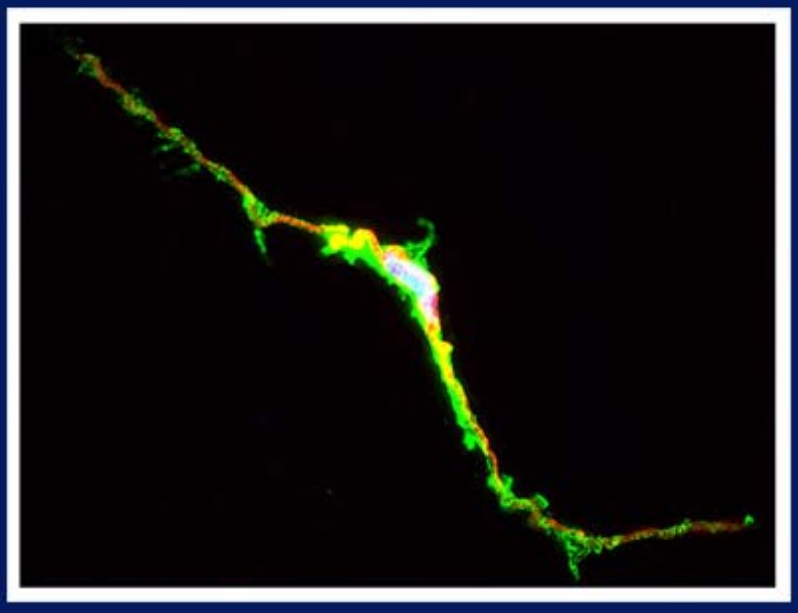

Tesis Doctoral
María Sancho González
Madrid, 2013

UNIVERSIDAD COMPLUTENSE DE MADRID

FACULTAD DE VETERINARIA

DEPARTAMENTO DE FISIOLOGÍA

Las células intersticiales de Cajal como mediadoras de la neurotransmisión uretral

Tesis doctoral

María Sancho González

Madrid, 2013

UNIVERSIDAD COMPLUTENSE DE MADRID
FACULTAD DE VETERINARIA
DEPARTAMENTO DE FISIOLOGÍA

Las células intersticiales de Cajal como mediadoras de la neurotransmisión uretral

Memoria presentada por María Sancho González para optar al grado de Doctor Europeo

Directores de la tesis: Dra. Ángeles García Pascual y Dr. Domingo Triguero Robles

Madrid, 2013

Vº Bº Directores

Ángeles García Pascual **Domingo Triguero Robles**

Trabajo financiado por: Ministerio de Educación y Ciencia (BFU2006-15135-C02-01). Universidad Complutense de Madrid (UCM GR85/06); UCM- Comunidad de Madrid (CCG07-UCM/SAL-2150), UCM-Banco Santander Central Hispano (920307-GR58/08, GR35/10-A-920307) y Fundación Mutua Madrileña (FMN 2011). El desarrollo de la tesis ha sido posible gracias a la percepción de una beca FPU del MEC (AP2008-00281).

Bueno, pensé que este momento no llegaría nunca, pero sí, aquí estoy frente al ordenador escribiendo las últimas páginas de mi tesis, y no por ello menos importantes. Si me paro a pensar en todas las cosas he hecho y aprendido durante todo este tiempo, y a quien tengo que agradecer que esta tesis haya salido adelante, son muchos los recuerdos y caras que me vienen a la mente, pero a la vez me da la sensación de que esta etapa se haya pasado volando, y quizás haya sido una de las que más he disfrutado. Esto es en parte gracias a mis directores de tesis, Ángeles y Domingo. Muchas gracias por confiar en mí desde el primer momento en que os conocí, por enseñarme a cómo crear ciencia, por apoyarme en los malos momentos y ayudarme a conseguir aquella beca que parecía inalcanzable, por vuestras horas de dedicación y esfuerzo, y sobre todo por estar siempre ahí para darme el último "empujoncito" que siempre he necesitado.

Una de las personas imprescindibles para mí en el departamento ha sido Gonzalo. Muchas gracias por tu incondicional ayuda para todo, por todas las horas que hemos pasado en los baños de órganos codo con codo, por todas las veces que me has hecho reír, por nuestras discusiones futbolísticas. Como ves, al final he intentado resumir la tesis en un único tomo, ya te avisaré cuando salgan los fascículos coleccionables a la venta.

Si a alguien tengo que darle las gracias una y otra vez es a mi compañera de *curro* y de piso, pero principalmente gran amiga, Arantxa. Muchas gracias por estar siempre ahí dándome ánimos, por todo el tiempo que hemos pasado juntas dentro y fuera del laboratorio, para nosotras se quedan todas nuestras perfusiones juntas, horas de baños de órganos al borde del delirio, prácticas de manejo y no manejo, *tuppers* compartidos (unos mejores que otros…), viajes al animalario en moto…..Pero no todo ha sido trabajo, muchas gracias por todos los buenos momentos en el piso, por las risas hasta terminar llorando, per les teues classes de valencià, nuestros viajes juntas, y las salidas de cañitas madrileñas. Llegados a este punto es necesario hacer una mención especial a *Pepe el Guarro* y sus alitas, y es que no sé cuántas horas habremos pasado dentro de aquel *garito*.

Jose, muchas gracias a ti también por todos los momentos que pasamos juntos en el laboratorio, por esos maratones de *Westerns* (*Blots*, no de películas de vaqueros…) mano a mano. Seguro que a ninguno de los dos se nos olvida la experiencia con "Andresito" y sus ratas. Espero que te vaya todo muy bien con tu tesis, seguro que sí.

Muchas gracias a todos los profesores del departamento de Fisiología por hacerme sentir como en casa y estar ahí para cualquier cosa que he necesitado, en especial a Alicia, Rosana, Pedro, Luis, y Rosa. También me gustaría dar las gracias a Marta, por todo el tiempo que empleaste enseñándome tus protocolos de biología molecular, y a Bene, por toda la ayuda que he recibido por tu parte y por traerme las muestras fresquitas del matadero.

Quería también dar las gracias a Magdalena, por toda tu "ayuda molecular", tu amabilidad, y todo lo que he aprendido contigo, y a Pepe, gracias a vosotros esta tesis ha podido finalizar como se merecía. También quería dar las gracias a todos los pre- y

postdoctorales del Departamento de Bioquímica que están y han pasado a lo largo de todo este tiempo, por su ayuda para cualquier cosa y todos los materiales prestados.

Gracias a todo el personal de la Facultad de Veterinaria, secretaría, conserjería, biblioteca, reprografía, informática, cafetería y limpieza, por hacerme siempre las cosas más fáciles y responder siempre con una sonrisa.

Soriana, tú me has enseñado a leer entre líneas, muchas gracias a ti también.

Últimamente he pasado más horas en el centro de microscopia confocal que en mi propia casa. Muchas gracias a Alfonso, Luis y Teresa por su ayuda técnica, y por su capacidad a la hora de resolver todos los problemas que me han ido surgiendo.

Gracias a la Dr. Pilar Bringas y a todo el personal del animalario de la Facultad de Medicina, por su buena disposición para todo, así como por sus animales prestados.

My predoctoral stay in Dundalk was a really nice experience. I would like to thank to Dr. Gerard Sergeant, it was a great pleasure working with you and your colleagues. My thanks to Dr. Mark Hollywood, Dr. Keith Thornbury and Prof. Noel McHale, for their great hospitality during my stay in the Smooth Muscle Research Centre. Billie, Adebola, Tim, Eamonn, Subrangsu, Claire, Roddy and Bernard, thanks for warmly welcoming me and making me feel at home during the time spent at Dundalk. I owe special thanks to Rishiparna, who has become a good friend, thanks to you and Subrangsu for your delicious Indian cuisine. I wish you all the best! Con referencia a mi estancia en Irlanda, Dani muchas gracias por toda tu ayuda, por acogerme en ese *pisito* tan caluroso (no sé las mantas que me podía llegar a poner), pero sobre todo por nuestras salidas de pintas por Dublín.

Y por último, muchas gracias a toda aquella gente que me ha hecho ver que hay vida detrás de la tesis. Muchas gracias a todas mis amigas/os de Tudela, por lo bien que nos lo seguimos pasando aunque vayamos camino de los 30… (seguro que a estas alturas más de una ya los ha cumplido….), y todo lo que nos queda por disfrutar juntos. Sarica, muchas gracias por todas tus visitas a Madrid, aunque cada vez que vengas acabemos las dos con gastroenteritis. Muchas gracias a mis colegas de profesión, Isa, Miche y Perón, porque sólo nosotras sabemos lo *jod*….que estamos, pero lo que disfrutamos con la Biología. María, muchas gracias por todo, por tu surtido de *pendrives*, y porque sin nuestras rutas y conciertos mi estancia en Madrid no hubiera sido lo mismo. También tengo que dar las gracias a los demás compañeros de piso que he tenido durante todo este tiempo: Cace, Parrote y Alber, por hacer la convivencia mucho más fácil, y porque sólo nosotros sabemos *lo cómodo que es ese sofá...*Y ya que estamos, muchas gracias a Juan Antonio, mi casero, por poner facilidades siempre para todo (aunque deberías de saber *lo cómodo que es ese sofá...*).

Y lo más importante, muchas gracias a mis padres (pocas cosas hay más anti-estrés que la vida del jubilado en Cascante, se te olvida que estás escribiendo la tesis), y

a mis hermanos. Al nuevo fichaje de la familia, “Sofiota”, por dejarme ser su *babysitter*. A Melo y Tata.

Abreviaturas:

AC	Adenilato ciclasa
ACh	Acetilcolina
ANO1	Anoctamina 1
ATP	Adenosina trifosfato
AVP	Arginina vasopresina
BH_4	Tetrahidrobiopterina
CaCC	Canales de cloro activados por Ca^{2+}
CaM	Calmodulina
cAMP	Adenosina monofosfato cíclico
CCE	Sistema de calcio capacitativo
CCK	Colecistoquinina
cGMP	Guanosina monofosfato cíclico
CGRP	Péptido relacionado con el gen de la calcitonina.
CNG	Canales iónicos operados por nucleótidos cíclicos
cNOS	NO sintasa constitutiva
CO	Monóxido de carbono
COX	Ciclooxigenasa
Cx	Conexina
CYP	Ciclofosfamida
DEA-NO	Dietilamina de NO
DIDS	Sal disódica del ácido 4,4´-diisotiocianatostilbeno-2,2-disulfónico
E_{Cl}	Potencial de equilibrio para el Cl^-
EFS	Estimulación eléctrica transmural
E_m	Potencial de membrana
eNOS	NO sintasa endotelial
ET	Endotelina
EUE	Esfínter uretral externo
EUI	Esfínter uretral interno
FAD	Flavín-adenosin-dinucleótido
FMN	Flavín mononucleótido

αGA	Ácido 18α- glicirretínico
GIST	Tumores gastrointestinales de estroma
GJ	Unión gap
GTP	Guanosina trifosfato
G3PDH	Gliceraldehido-3-fosfato-deshidrogenasa
HC	Cistitis hemorrágica
HSP90	Chaperona "*Heat Shock Protein 90"*
ICC	Células intersticiales de Cajal
ICC-DMP	ICC situadas en la capa muscular profunda de intestino delgado
ICC-IM	ICC intramusculares
ICC-LP	ICC situadas en la lámina propia
ICC-M	ICC intramusculares
ICC-MY	ICC situadas en el plexo mientérico
ICC-SEP	ICC septales
ICC-SM	ICC situadas en la submucosa
ICC-SMP	ICC situadas en el plexo submuscular del colon
ICC-SR	ICC situadas en la serosa
IFNγ	Interferon γ
IL-1β	Interleucina 1β
iNOS	NO sintasa inducible
IP_3	Inositol trifosfato
ir	Inmunoreactividad
L-MNNA	N^G-monometil-L-arginina
L-NAME	N"-nitro-L-arginina metil éster
L-NNA	N^G-nitro-L-arginina
LPS	Lipopolisacárido bacteriano
LUTS	Síntomas del tracto urinario inferior
Mesna	2-mercaptoetano sulfonato
NE	Noradrenalina
NADPH	Nicotinamida adenina dinucleotidofosfato
NANC	No adrenérgico-no colinérgico
NK1	Neurokinina 1
nNOS	NO sintasa neuronal

NO	Óxido nítrico
NOS	NO sintasa
NPY	Neuropéptido Y
ODQ	1H-‹1,2,4› oxadiazolo ‹4,3› alquinoxalin-1-one
PDE	Fosfodiesterasa
PDGFR-α	Receptor del factor de crecimiento derivado de plaquetas
pGC	Guanilato ciclasa particulada
PK	Proteína kinasa
PKC	Proteína kinasa C
PKG	Proteína kinasa cGMP dependiente
RyR	Receptor de Rianodina
scf	Factor estimulante de colonias
sGC	Guanilato ciclasa soluble
SMC	Células musculares lisas
SNC	Nitrocisteína
SNP	Nitroprusiato sódico
SP	Sustancia P
STIS	Ácido 4-acetamido-4´-isotiocianato-2,2´-stilbenodisulfónico hidrato de sal disódica
TNF-α	Factor de necrosis tumoral α
t-PA	Activador tisular de plasminógeno
TTX	Tetrodotoxina
VIP	Péptido intestinal vasoactivo
YC-1	3-‹5´-hidroximetil-2´-furil›-1-benzilindazol
5-HT	Serotonina
9-AC	Antraceno 9-carboxilato

SUMMARY

1. Introduction

The study of interstitial cells of Cajal (ICC) in the gastrointestinal tract has revolutionized the way the researches understand gut motility and neurotransmission. ICC, described in the intestine by Ramón y Cajal a century ago (Cajal, 1911), are now considered to be a specialized class of noncontractile but excitable cells. Gastrointestinal ICC have been suggested to act as **pacemakers** of the slow waves, to play a **key role in the neurotransmission** from cholinergic and nitrergic nerves to smooth muscle or even to act as mechanoreceptors (Komuro, 2006). Outside de gastrointestinal system, ICC have been widely studied in many regions of the urinary tract, from the ureter to the bladder and the urethra, of different species including humans (Metzger et al., 2004; McCloskey and Gurney, 2002; Sergeant et al., 2000; Brading and McCloskey, 2005). The discovery of these cells in urinary tissues provides new opportunities to advance our knowledge on their cellular interactions within these tissues and it could lead to the development of new therapies to treat urinary tract disorders.

The study of urethral ICC is arguably more advanced in terms of cellular physiology. The first evidence that the urethra contained ICC-like cells was reported by Sergeant et al. (2000), who observed a mixed population of enzymatically dispersed cells from the rabbit muscular urethra. It was composed of a majority of spindle-shaped smooth muscle cells (SMC) and a smaller population of branched stellate- or elongated shaped cells, which were morphologically reminiscent of gut ICC. Sergeant et al. (2000) used vimentin immunochemistry to distinguish the branched cells from the spindle-shaped SMC, which contained myosin filaments but no vimentin positive ones. In addition, they demonstrated that these branched cells showed similar ultrastructural characteristics than gastrointestinal ICC.

These first studies described urethral ICC as not positive to **c-kit** (Sergeant et al. 2000), a receptor tyrosine kinase extensively used as an ICC marker in gastrointestinal tract (Torihashi et al., 1997; Vanderwinden et al., 1996) and other tissues (Lammie et al., 1994). Nevertheless, recent studies have effectively demonstrated c-kit staining in ICC throughout the urinary tract (McHale et al., 2006; Lyons et al., 2007; McCloskey, 2011). It has to be pointed out that c-kit-ir does not always mark "ICC-like cells" (Pezzone et al., 2003; Torihashi et al., 1999; Wang et al., 2003) as it can also be present in other cells including mast cells, melanocytes, nerve cells and glial cells (Zhang and Fedoroff, 1997). As described above, another marker used for the recognition of ICC is **vimentin** because it reacts with intermediate filaments, which are not expressed in the neighboring SMC (Rumessen and Thuneberg, 1996). Alternative ICC markers used has been **CD34**, a glycoprotein present in endothelial and mesenchymal cells (Pusztaszeri et al., 2006), although some researchers believe that it is present in fibroblasts but not in ICC (Vanderwinden et al., 2000; Pieri et al., 2008). Finally, the platelet-derived growth factor receptor α (**PDGFRα**) has recently been proposed as a new marker of a sub-population of c-kit negative ICC in gastrointestinal tract (Iino et al., 2009; Iino and

Nojyo, 2009; Kurahashi et al., 2012) and urinary bladder (Koh et al., 2012). The current debate focus on whether vimentin, CD34 or PDGFRα positive, but c-kit negative, cells would be true ICC and if so, the possible existence of different types of ICC with different functions (Vanderwinden et al., 2000).

The morphological description of those c-kit-positive cells in the urethra made by Lyons et al. (2007) were consistent with those previously found in the cell dispersals of Sergeant et al. (2000). Unipolar, bipolar, stellate, and elongated cells with several lateral branches, which can be classified into several subtypes, similarly to that described in the gastrointestinal tract and the bladder (Sergeant et al., 2000; Lyons et al., 2007). Subpopulations of urethral ICC are: ICC of the lamina propria (ICC-LP), ICC inside the muscle bundles (intramuscular ICC, ICC-IM) or in between them (interbundle ICC; ICC-IB) and ICC associated with the serosa (ICC-SR). One of the objectives of this study was to analyze the presence and distribution of ICC in the urethra by using different ICC markers (c-kit, vimentin, CD34, and PDGFRα), and to show its structural relationship to SMC and intramural nerves.

Investigation of urethral ICC with patch-clamp electrophysiology and fluorescent Ca^{2+}-imaging has established that these cells possess properties of pacemaker cells. In a tonically contracted organ like the urethra, a pacemaker has been suggested to support the asynchronous recruitment of muscle units to maintain tone, very much alike skeletal muscle (Sergeant et al., 2000). The ionic mechanisms underlying this activity were described in the rabbit urethra (Johnston et al., 2005) and it is initiated by inositol 1,4,5-triphosphate (IP_3)-mediated Ca^{2+} release from intracellular stores and the subsequent opening of Ca^{2+}-activated Cl^- channels (CaCC). However, other studies in the guinea pig (Hashitani and Edwards., 1999), sheep (Sergeant et al., 2001) and even the rabbit urethra (Hashitani and Suzuki, 2007) have reported that not only ICC, but also SMC, were able to develop spontaneous depolarization mediated by CaCC and to generate Ca^{2+} transients. Recently, it has been suggested that both ICC and SMC may simultaneously be involved in urethral pacemaking in the intact rabbit urethra (Hashitani et al., 2006).

The pacemaker activity of isolated rabbit urethral ICC is defined by the ionic balance of chloride, which have lead even to the proposal that specific CaCC inhibitors, such as 9-AC and niflumic acid, may be used to generate “pharmacological knock-out” of ICC (Sergeant et al., 2002). Chloride-dependent currents have also been implicated in the control of smooth muscle contraction in the bladder and the urethra of several species (Chipperfield and Harper, 2000). In this sense, the recently cloned and characterized anoctamin 1 (**ANO1**; also known as TMEM16A) was identified as the main CaCC. While ANO1 is absent from SMC in the gastrointestinal tract, it has been localized to a conspicuous network of ICC (Huang et al., 2009) though to mediate autorhythmicity and neurotransmission (Caputo et al., 2008; Sanders, 1996). Thus, ANO1 has been proposed as a specific marker of ICC in the gut, as it is c-kit (Gomez-Pinilla et al., 2009). However, in the mouse urethra ANO1 was absent in SMC and ICC, suggesting differences between gastrointestinal ICC and those cells in urinary tissues

(Huang et al., 2009). In this work, we investigated the distribution of ANO1 in the urethra of sheep, rat and mouse by both immunofluorescence and PCR, and their involvement in excitatory (mainly noradrenergic) and inhibitory (nitrergic) neurotransmission.

The urethral smooth muscle sphincter has a high spontaneous tone during continence, which is maintained by neurally released norepinephrine (NE) and abruptly lost during micturition by neurally released nitric oxide (NO; Arensbak et al., 2001). It has been shown that NE increased the frequency of the spontaneous depolarizations in ICC isolated from the rabbit urethra through the activation of CaCC channels (Li et al., 2007). By contrast, this electrical activity was inhibited by the NO donor DEA-NO, as well as by activators of the cGMP pathway, probably by inhibiting the IP_3-mediated Ca^{2+} release from intracellular stores (McCloskey et al., 2009). Indeed, SIN-1 (another NO donor) reduced the amplitude of ICC Ca^{2+} transients in the intact rabbit urethra, while phenylephrine increased their frequency and induced a sustained rise in Ca^{2+} (Haefliger et al., 2002). Furthermore, several investigations have shown a close association between ICC and nerves within the muscular layer giving morphological support for the association of these two kinds of cells in the urethra (Lyons et al., 2007, Smet et al., 1996). These results suggest that, like in the gut, neurotransmitters in the urethra may act through ICC, although this hypothesis has to be tested in experiments where the release of the endogenous neurotransmitters from intramural nerves is elicited.

Micturition is iniciated by an abrupt loss of urethral smooth muscle sphincter tone that is mediated by the release of NO from the local nitrergic fiber network (Andersson and Wein, 2004). It is generally accepted that this process involves the NO-dependent activation of soluble guanylate cyclase (sGC), which provokes a transient increase in intracellular **cGMP levels** and the subsequent activation of PKG in urethral smooth muscle cells (Andersson and Wein, 2004; Persson et al., 2000). Smet et al (1996) and Waldeck et al (1998) presented the first studies suggesting that ICC may act as a new cellular element in the NO/cGMP pathway. Their immunohistochemical studies demonstrated the presence of branched ICC in human, guinea-pig and rabbit urethras, which were immunopositive for cGMP following exposure to NO donors. Hence, ICC appear to express the second messengers necessary to transduce NO signals, including sGC. However, the involvement of ICC in the relaxation induced by selective stimulation of nitrergic nerves in the urethra has yet to be demonstrated (urethral tissue responds quite differently to exogenous NO or NO donors and to the endogenous release of the nitrergic transmitter; Gillespie et al., 2004). In the present study we have addressed this issue in the rat and sheep urethra, where cGMP production and relaxation were compared in preparations subjected to electrical field stimulation (EFS) of nitrergic nerves or to an exogenous NO donor (SNC; S-nitroso-L-cysteine).

The **cyclic nucleotide-gated** (**CNG**) **channels** are ion channels directly gated by the binding of intracellular cAMP and/or cGMP. These channels, first known in sensory cells, have now been described in a variety of tissues participating in a plethora of

physiological processes (Craven and Zagotta, 2006), although their functional role seems to be complex and poorly understood (Craven and Zagotta, 2006; Hofmann et al., 2005). CNG channels can conduct currents carried by mono- and divalent cations and there is growing interest in this family as they provide an alternative pathway for Ca^{2+} entry that is virtually independent of membrane voltage and that couples the activity of Ca^{2+}-regulated proteins to cAMP/cGMP signaling without involving protein kinases. One of the most widely used specific inhibitors of cGMP-gated CNG channels is L-cis-Diltiazem (Hofmann et al., 2005), which has been shown previously to inhibit relaxation elicited by stimulation of intrinsic nitrergic nerves (Triguero et al., 2003), suggesting that CNG channels are involved in the urethral NO/cGMP signaling pathway. In the present work, we further examine the possibility that CNGA1, a functional subtype of CNG channels selectively gated by cGMP, is present in the rat urethra and its involvement in the urethral neurotransmission process (both excitatory and inhibitory), specially focusing on the role of ICC in these processes. Furthermore, we have addressed the expression of CNG1 channels in SMC and ICC isolated from the rabbit urethra, and the effects of L-cis-Diltiazem on Ca^{2+} oscillations developed in these cells either spontaneously or after activation of the NO/cGMP pathway.

The underlying mechanism of communication between ICC, nerves and the final effectors, SMC, is still unknown. In the gastrointestinal tract, it is generally believed that ICC are connected to each other through **gap junctions** (**GJ**), facilitating their behavior as pacemakers (Belzer et al., 2002). However, there is scant evidence for the existence of GJ between ICC and SMC, and some studies failed to demonstrate this connexion (Daniel et al., 1998; Powley et al., 2008). Nevertheless, it has been often assumed that ICC can influence the behavior of SMC through rapid electrical synapses (Sanders and Ward, 2006). Alternatively, low-molecular-weight second messengers (cGMP, calcium, etc.) could freely diffuse through GJ from ICC to SMC (Kumar and Gilula, 1996). The subunit that forms GJ is called connexin (Cx), and at least 20 different types of Cx have been described, named according to their expected molecular weight (Willecke et al., 2002). Thus, a wide variety of GJ can exist, with different attributes in terms of permeability to low-molecular-weight substances (Kanaporis et al., 2008), justifying the need to identify the Cxs present in any given tissue. Several studies have described the presence of Cx43, Cx40 and Cx37 in the bladder of different species (Ikeda et al., 2007; Neuhaus et al 2002a; 2002b; 2009). Some of these Cx have been localized in subepithelial and intramuscular ICC (Sui et al., 2002), suggesting their implication in the homocellular or heterocellular GJ communication involving ICC. In the present work, we investigated the distribution of different Cx (Cx43, Cx40, and Cx37) in the sheep and rat urethra, as well as their possible role in neurotransmission.

The study of ICC is one of the most promising areas in the knowledge of urinary tract function and dysfunction. Therefore, it will be interesting to investigate if ICC are also associated with disorders of the urinary tract and to show whether defects in either the number or function of urethral ICC may be implicated in the pathogenicity of several types of LUTS (lower urinary tract symptoms). Within this term is included a

cluster of urinary symptoms associated to several pathological conditions of the urinary tract. In this context, **hemorrhagic cystitis (HC)** induced by **cyclophosphamide (CYP)** is considered to be one of the most severe forms of chemotherapy-induced bladder injuries leading to irritative LUTS up to severe hemorrhage (Stillwell and Benson, 1988). CYP or ifosfamide (Seber et al., 1999) are alkylating agents with therapeutic efficacies in multiple solid tumors, and also used as part of a conditioning regimen for hematopoietic cell transplantation (Korkmaz et al., 2007). Well-known animal models consisting in the systemic injections of CYP or ifosfamide (Cox, 1979; Bon et al., 1998) have been developed in rats and mice, which are characterized by the induction of bladder inflammation and interstitial cystitis accompanied by overactive bladder symptoms (Bon et al., 1998; Yoshimura and de Groat, 1999). However, the effect of CYP on the urethra remains unexplored, despite the possible contribution of urethral inflammation to the overactive symptomatology.

Among the increasing number of mediators suggested to be implicated in the pathogenicity of CYP-induced cystitis, NO overproduction plays a key role (Souza-Filho et al., 1997; Alfieri and Cubeddu, 2000; Korkmaz et al., 2007; Andersson et al., 2008; Linares-Fernandez and Alfieri, 2007). This increased production of NO is often assumed to result for the expression of the inducible isoform of NO synthase (iNOS; Souza-Filho et al., 1997; Linares-Fernandez and Alfieri, 2007; Xu et al., 2001) while the production of NO by the other two constitutively expressed NOS isoforms, endothelial (eNOS) and neural (nNOS), has not yet been studied. In addition, c-kit and vimentin-positive ICC are one of the many cellular targets of NO in the bladder and urethra (Gillespie et al., 2004); although no information exists regarding changes in ICC and their role in the altered NO production during CYP-induced inflammation. In the present work, we analyzed the changes in expression and distribution of ICC, iNOS, eNOS and nNOS. Furthermore, alterations in nerve-mediated contractility in the bladder and urethra of CYP-treated rats were investigated.

2. Results

2.1 Involvement of ICC in the urethral inhibitory neurotransmission: role as effectors of NO

In the present study, we have used cGMP immunofluorescence to identify the specific cell types in the sheep and rat urethra that respond to nitrergic stimulation by elevating their intracellular cGMP levels. Tissues were subjected to EFS of nitrergic nerves or exposed to SNC, the NO donor that produces the fastest relaxation and highest levels of cGMP in the sheep urethra (García-Pascual et al., 1999). Both relaxations and cGMP immunoreactivity (-ir) were compared directly in the same preparation. Furthermore, PGP 9.5-ir or nNOS-ir in nerve structures was combined with cGMP labeling to identify nerves and their relationship with the effector cells. Finally, vimentin/cGMP and c-kit/cGMP double labeling was used to confirm the mesenchymal nature of the cGMP-containing cells.

Upon EFS, cGMP-ir was observed in both SMC and spindle-shaped cells that contained c-kit (in the sheep) and vimentin (in both species) and had the characteristic features of ICC. Similarly, cGMP-ir was preferentially, but inconsistently, found in ICC of the outer muscle layer on exposure to SNC. We found separate functional groups of ICC within the urethra. Among these, only ICC present in the muscle layers (ICC-M) but not those in the serosa (ICC-SR) and lamina propria (ICC-LP) seem to be specifically influenced by activation of nNOS. Thus, the increase in cGMP-ir induced by EFS in ICC-M was prevented by either NOS (N^{ω}-nitro-L-arginine, L-NNA) or sGC inhibitors (ODQ). Urethral ICC did not express nNOS, although they were closely associated with nitrergic nerves. cGMP-ir was also present in the urothelium (in the rat) and the vascular endothelium, but not in neural structures (either nerve trunks or nerve terminals). Together, these results suggest a model of parallel innervation in which both SMC and ICC-M are effectors of nerve-released NO in the urethra.

2.2 Involvement of CNG channels in the nerve-mediated nitrergic relaxation of the urethra: role of ICC

Here, we analyzed the possibility that CNGA1, the functional subtype of CNG channels specifically gated by cGMP, are present in the rat urethra. We studied the cellular distribution of CNGA1 channels by immunofluorescence as well as the mRNA expression of the different subunits of the channel. In addition we characterized the functional effects of L-cis-Diltiazem, a widely used specific inhibitor of cGMP-gated CNG channels, on both relaxant and contractile nerve mediated responses induced by EFS.

Functional studies showed that L-cis-Diltiazem leads to the rapid inhibition of urethral relaxation induced either by NO released from nerves or by direct activation of

sGC with YC-1. By contrast, nerve-mediated noradrenergic contractions were only slowly and middly reduced by L-cis-Diltiazem. This effect was mimicked by lower concentrations of the D-diltiazem isomer probably due to the nonspecific inhibition of voltage-dependent calcium channels. Accordingly, D-Diltiazem did not affect relaxation responses.

The expression of heteromeric retinal-like CNGA1 channels was demonstrated by conventional PCR. Furthermore, by immunofluorescence we showed that CNGA1-ir was mainly present in a subpopulation of urethral ICC, but they were only weakly expressed in SMC. CNG channels could not be visualized in any nervous structure within the urethral wall. These results are in agreement with the emerging view that a subset of ICC serves as targets for NO. We hypothesize that CNG channels could be a suitable link between the activation of the NO/cGMP pathway and the modulation of the nitrergic control of SMC activity by ICC.

2.3 Involvement of CNG channels in the spontaneous Ca^{2+} oscillations of isolated ICC and SMC and in those changes induced by activation of the NO/cGMP pathway

Here, we used confocal imaging on freshly dispersed ICC and SMC from the rabbit urethra to examine the effects of L-cis-Diltiazem on spontaneous Ca^{2+} waves as well as on those changes in Ca^{2+} waves induced by increases in intracellular cGMP levels elicited by the following treatments: 1) a cGMP permeant-analogue (8-Br-cGMP); 2) a sGC activator (YC-1); 3) a mixture of phosphodiesterase (PDE) inhibitors (IBMX, zaprinast); or 4) a NO donor (DEA-NO). Furthermore, we analyze the inmunoreactivity of CNG1 by immunofluorescence in isolated ICC and SMC.

Confocal imaging on freshly dispersed SMC and ICC showed that L-cis-Diltiazem significantly reduced both the frequency and amplitude of Ca^{2+} waves as well as the basal calcium in both type of cells. In contrast, the isomer D-Diltiazem was only efective in SMC by acting on L-type voltage-gated Ca^{2+} channels. Reductions of intracellular Ca^{2+} events were observed when both type of cells were exposed to different procedures increasing cGMP levels. The following order of potency was found: DEA-NO > YC-1 > PDE inhibitors > 8-Br-cGMP. L-cis-Diltiazem did not inhibit these changes but even showed an additive effect to the previous reduction in Ca^{2+} oscillations. This action is probably due to their unspecific effect on L-type Ca^{2+} channels.

Weak and diffuse CNG1-ir was present in SMC (also showing α-actin-ir), while it was very intense in vimentine-ir ICC. It is worthwhile the fact that CNG1-ir was mostly located in very thin spines emerging from the ICC body and prolongations, from where they can contact with other cells. Together, these results suggest that CNG channels could provide a new and exclusive pathway for Ca^{2+} entry in ICC that

participates in the generation and maintenance of spontaneous Ca^{2+} waves, but not in the reduction in Ca^{2+} events induced by cGMP in both cells.

2.4 Involvement of the direct coupling through gap junctions in urethral neurotransmission

In the present work, we used RT-PCR and immunofluorescence to investigate the expression and location of Cx43, Cx40, and Cx37 in the sheep and rat urethra. Furthermore, the possible functional involvement of GJ in both the excitatory (noradrenergic) or inhibitory (nitrergic) neurotransmission in the urethra was evaluated by using GJ blockers in tissues subjected to EFS. We used 18α-glycyrrhetinic acid (α-GA) as a nonselective GJ blocker (Davidson and Baumgarten, 1988), as well as a mixture of different Cx mimetic peptides (GAP peptides) that are considered to be the more selective tools to block GJ formed by specific Cx (Evans and Boitano, 2001; Wang et al., 2007).

Conventional PCR confirmed that Cx43, Cx40, and Cx37 are expressed in the urethra. Moreover, by immunofluorescence we showed that both Cx43- and Cx37-ir were present in SMC, ICC, and the urothelium, being Cx37-ir significantly weaker and Cx40-ir was limited to the vascular endothelium. While these results suggest that intercellular communication through GJ could occur between SMC and ICC, neither the contractile (noradrenergic) nor the relaxant (nitrergic) responses to EFS were significantly modified by the different GJ inhibitors used. By contrast, contractions induced by high K^+ were effectively reduced showing that they effectively inhibit intercellular communication. These results suggest that GJ are not implicated in urethral neurotransmission. Whether ICC modulates neurotransmission through some other mechanism remains to be determined.

2.5 Involvement of CaCC in the urethral excitatory neurotransmission: role of ICC

We analyzed the distribution of ANO1 in the urethra of sheep, rat and mouse, by both conventional PCR and immunofluorescence. In addition, we studied its role in urethral contractility by examining the effects of chloride-free medium and of several CaCC inhibitors (niflumic acid, 9-AC, and STIS) in urethral preparations subjected to EFS or to the addition of exogenous agonists.

In all species analyzed, chloride-free medium as well as niflumic acid and 9-AC inhibited noradrenergic urethral contractions, while their effects on relaxant nitrergic responses were negligible. Since contractile responses were only slightly inhibited in the sheep, but not in the rat and the mouse urethra, by the IP_3 receptor antagonist 2-

APB, it could be suggested that activation of CaCC is probably due to calcium influx with a minor contribution of IP_3-mediated calcium release.

Strong ANO1 immunolabeling was consistently observed in SMC, and the urothelium, but not in ICC, strongly suggesting that ANO1 is not a specific marker of ICC in the urethra, in contrast to that described in the gastrointestinal tract (Gomez-Pinilla et al., 2009). RT-PCR confirmed the strong expression of ANO1 mRNA in the rat urethra. The lack of ANO1 in ICC challenges the proposed role of these cells as regulators of urethral contractility, at least in a manner similar to that observed in the gut.

2.6 Changes in the production of NO in the bladder and urethra in an experimental model of CYP-induced cystitis in the rat

Increased production of NO seems to play a key role in CYP-induced cystitis but the underlying mechanism and the involvement of ICC remain to be established. Furthermore, the role of the urethra in this process is unknown. The present study addresses the changes of expression and distribution of ICC, iNOS, eNOS, and nNOS as well as the possible alterations in nerve-mediated contractility in the bladder and the urethra of CYP treated rats. Wistar rats received either acute (4 h) or intermediate (48 h) CYP treatment (150 mg/kg), or chronic treatment (70 mg/kg every third day for 10 days) before sacrifice in comparison with time-matched controls. Changes in protein expression were assessed and quantified by immunofluorescence and Western Blot, and altered mRNA expression was assessed by conventional/quantitative PCR.

Our results showed prominent inflammatory reactions in the urethra and bladder, although contractility was only modified in the bladder. A surprising lack of iNOS expression was observed in both organs following CYP treatments, while nNOS and eNOS expression were decreased and increased, respectively. These findings suggest that spatiotemporal alterations in NO production by constitutive NOS may be involved in the pathogenicity of CYP.

2.7 Involvement of ICC in CYP-induced cystitis

Changes in the density and distribution of ICC immunoreactives to four different markers: c-kit, vimentin, CD34 and PDGFRα, were analyzed by immunofluorescence in the bladder and urethra of CYP-treated rats. In addition, we investigated the possible protective effect of Glivec (imatinib mesylate), a drug currently used for the treatment of lymphomas and solid tumors of the gastrointestinal tract characterized as c-kit positive (Kubota et al., 2004; Joensuu et al., 2001). Glivec is a receptor tyrosine kinase inhibitor and is known to be capable of inhibiting c-kit and PDGFR receptors (Druker et al., 1996), whose activation appears to be critical to maintain ICC phenotypic

characteristics and regulate ICC proliferation (Maeda et al., 1992; Torihashi et al., 1995). In this case, only two CYP-treatments were performed: intermediate (48 h; 150 mg Kg^{-1}), and chronic (10 days, 50 mg Kg^{-1} every 3 days), with their respective controls. Finally, eNOS expression in ICC of the bladder and urethra of CYP treated rats was analyzed.

Our results showed that CYP treatment induced pronounced increases in the density of ICC positive to c-kit, vimentin, CD34 and PDGFRα. These increases were similar in both the lamina propria and the muscle layer of the bladder and the urethra and progressively increased with the duration of the CYP treatment. It was remarkable a special accumulation of cells beneath the urothelium. The degree of colocalization in the same cell was higher than 60% for all the pairs of antibodies assayed (c-kit-vimentin, c-kit-CD34, vimentin-CD34, vimentin-PDGFRα y CD34-PDGFRα) in both tissue layers. The treatment with CYP did not modify in any case the colocalization percentages, suggesting that all the antibodies are equally useful in marking those cells that proliferate upon CYP treatment. In addition, we showed in the CYP treated bladder and urethra, but not in controls, the expression of eNOS in cells positive to vimentin or CD34 and with morphological characteristics of ICC. Finally, pretreatment with Glivec significantly inhibited both ICC proliferation and the overactive bladder symptoms that accompanied the treatment with CYP. These results strongly suggest that ICC proliferation is behind the pathogenicity of CYP induced cystitis and eNOS expression may be involved. Glivec may have a possible therapeutic application in preventing bladder disorders that are secondary to chemotherapy treatment with CYP.

3. Conclusions

3.1 Stimulation of urethral nitrergic nerves causes cGMP accumulation in both SMC and ICC, suggesting a parallel innervation model, in which both type of cells are direct effectors of the NO released by nerves. The close relationship between ICC and nitrergic nerves supports this suggestion. Different functional types of cGMP-ir ICC form interconnecting networks at different locations in the urethral wall, but only ICC-IM seem to be involved in nitrergic transmission.

3.2 We have described the expression of CNG channels (subtype CNGA1) in the urethra located in SMC but more intensely in ICC. CNG expression in isolated ICC is intense in very thin spines emerging from the cell body and prolongations. The functionality of these channels seems to be essential to the urethral relaxation elicited by activation of the NO/cGMP pathway, although the precise mechanisms involved remain to be elucidated.

3.3 CNG channels could be involved in the pacemaker function of ICC, but not of SMC, by providing an alternative route of Ca^{2+} entry. However, they are not involved in the reduction of spontaneous Ca^{2+} waves caused by cGMP, suggesting that this is not the mechanism by which CNG channels mediate the NO/cGMP-induced relaxation in the urethra.

3.4 We demonstrate the expression of connexins (Cx37, Cx40, and Cx43) in the urethra, located both in SMC and ICC. However, the failure of GJ inhibitors to modify either contractile or relaxant responses induced by nerve stimulation does not support the involvement of an electrical communication mechanism between ICC and SMC in the urethral neurotransmission.

3.5 We detected strong ANO1 expression in SMC of the urethra that seems to be involved in the noradrenergic urethral contraction, but not in the nitrergic relaxation. In sharp contrast to the gastrointestinal tract, we failed to demonstrate ANO1 expression in any of the different subtypes of urethral ICC.

3.6 CYP treatment in the rat induces prominent inflammatory reactions in the urethra and the bladder, although contractility was only modified in the bladder. The main observation was the lack of iNOS expression in both organs following CYP treatment, which was accompanied by changes in the expression of the constitutive NOS isoforms providing a new source of NO that could participate in the pathogenicity of the inflammatory process.

3.7 CYP treatment in the rat induced a prominent increase in c-kit-, vimentin-, CD34-, and PDGFRα-positive ICC in the bladder and the urethra that were accompanied by the expression of eNOS "*de novo*" in these cells, providing a new source of NO that may contribute to the pathogenicity of the inflammatory process. Glivec inhibited both ICC proliferation and overactive bladder symptoms, further supporting the role of ICC and

allowing us to suggest its possible therapeutic application in preventing bladder disorders that are secondary to chemotherapy treatment with CYP.

4. References

Alfieri AB, Cubeddu LX. Nitric oxide and NK_1-tachykinin receptors in cyclophosphamide-induced cystitis in rats. *J Pharmacol Exp Ther* 295: 824-829, 2000.

Andersson KE, Wein AJ. Pharmacology of the Lower Urinary Tract: Basis for Current and Future Treatments of Urinary Incontinence. *Pharmacol Rev* 56(4): 581-631, 2004.

Andersson MC, Tobin G, Giglio D. Cholinergic nitric oxide release from the urinary bladder mucosa in cyclophosphamide-induced cystitis of the anaesthetized rat. *Br J Pharmacol* 153: 1438-1444, 2008.

Arensbak B, Mikkelsen HB, Gustafsson F, Christensen T and Holstein- Rathlou N-H. Expression of connexin 37, 40 and 43 mRNA and protein in renal preglomerular arterioles. *Histochem Cell Biol* 115: 479-487, 2001.

Belzer V, Kobilo T, Rich A, Hanani M. Intercellular coupling among interstitial cells of Cajal in the guinea pig small intestine. *Cell Tissue Res* 307:15-21, 2002.

Bon K, Lanteri-Minet M, Michiels JF, Menetrey D. Cyclophosphamide cystitis as a model of visceral pain in rats: a c-fos and Krox-24 study at telencephalic levels, with a note on pituitary adenylate cyclase activating polypeptide (PACAP). *Exp Brain Res* 122: 165-174, 1998.

Brading AF, McCloskey KD. Mechanisms of disease: specialized interstitial cells of the urinary tract-an assessment of current knowledge. *Nat Clin Pract Urol* 2: 546–554, 2005.

Cajal SR. Histologie du système nerveux de l´homme et des vertébrés. Paris: Maloine, 891-942, 1911.

Caputo A, Caci E, Ferrera L, Pedemonte N, Barsanti C, Sondo E, Pfeffer U, Ravazzolo R, Zegarra-Moran O, Galietta JV. TMEM16A, a membrane protein associated with calcium-dependent chloride channel activity. *Science* 322: 590–594, 2008.

Chipperfield AR, Harper AA. Chloride in smooth muscle. *Prog Biophys Mol Biol* 74: 175–221, 2000.

Gillespie JI, Markerink-van Ittersum M and DeVente J. cGMP generating cells in the bladder wall: identification of distinct networks of interstitial cells. *BJU Int*. **94**:1114-1124., 2004.

Cox PJ. Cyclophosphamide cystitis—identification of acrolein as the causative agent. *Biochem Pharmacol* 28(13): 2045-2049, 1979.

Craven KB, Zagotta WN. CNG and HCN channels: Two peas, one pod. *Annu. Rev. Physiol* 68:375-401, 2006.

Daniel EE, Wang YF, Cayabyab F. Role of Gap junctions in structural arrangements of interstitial cells of Cajal and canine ileal smooth muscle. *Am J Physiol Gastrointestinal Liver Physiol* 274:G1125-G1141, 1998.

Davidson JS, Baumgarten IM. Glycyrrhetinic acid derivatives: a novel class of inhibitors of gap-junctional intercellular communication. Structure-activity relationships. *J Pharmacol Exp Ther* 246: 1104-1107, 1988.

Druker BJ, Tamura S, Buchdunger E, Ohno S, Segal GM, Fanning S, Zimmermann J, Lydon NB. Effects of a selective inhibitor of the Abl tyrosine kinase on the growth of Bcr-Abl positive cells. *Nat Med* 2: 561-566, 1996.

Evans WH, Boitano S. Connexin mimetic peptides: specific inhibitors of gap junctional intercellular communication. *Biochem Soc Trans* 29: 606-612, 2001.

García-Pascual A, Costa G, Labadía A, Jimenez E, Triguero D. Differential mechanisms of urethral smooth muscle relaxation by several NO donors and nitric oxide. *Naunyn Schmiedebergs Arch Pharmacol* 360: 80-91, 1999.

Gillespie JI, Markerink- van Ittersum M, de Vente J. cGMP generating cells in the bladder wall: identification of distinct networks of interstitial cells. *BJU International* 94:1114-1124, 2004.

Gomez-Pinilla PJ, Gibbons SJ, Bardsley MR, Lorincz A, Pozo MJ, Pasricha PJ, Van de Rijn M, West RB, Sarr MG, Kendrick ML, Cima RR, Dozois EJ, Larson DW, Ordog T, Farrugia G. Ano1 is a selective marker of interstitial cells of Cajal in the human and mouse gastrointestinal tract. *Am J Physiol Gastrointest Liver Physiol* 296: 1370–1381, 2009.

Haefliger J-A, Tissières P, Tawadros T, Formenton A, Bény J-L, Nicod P, Frey P, Meda P. Connexins 43 and 26 are differentially increased after bladder outlet obstruction. *Exp Cell Res* 274: 216-225, 2002.

Hashitani H, Edwards FR. Spontaneous and neurally activated depolarization in smooth muscle cells of the guinea-pig urethra. *J Physiol* 514: 459–470, 1999.

Hashitani H, Suzuki H. Properties of spontaneous Ca^{2+} transients recorded from interstitial cells of Cajal-like cells of the rabbit urethra in situ. *J Physiol* 583: 505-519, 2007.

Hashitani H, Yanai Y, Kohri K, Suzuki H. Heterogeneous CPA sensitivity of spontaneous excitation in smooth muscle of the rabbit urethra. *Br J Pharmacol* 148: 340–349, 2006.

Hofmann F, Biel M, Kaupp UB. International Union of Pharmacology. LI. Nomenclature and structure-function relationships of cyclic nucleotide-regulated channels. *Pharmacol Rev*. 57 (4): 455-462, 2005.

Huang F, Rock JR, Harfe BD, Cheng T, Huang X, Jan YN, Jan LY. Studies on expression of the TMEM16A calcium-activated chloride channel. *Proc Natl Acad Sci USA* 106: 21413–21418, 2009.

Iino S, Horiguchi K, Horiguchi S, Nojyo Y. c-Kit-negative fibroblast-like cells express platelet-derived growth factor receptor *a* in the murine gastrointestinal musculature. *Histochem Cell Biol* 131: 691-702, 2009.

Iino S, Nojyo Y. Immunohistochemical demonstration of c-kit-negative fibroblast-like cells in murine gastrointestinal musculature. *Arch Histol Cytol* 72(2): 107-115, 2009.

Ikeda Y, Fry C, Hayashi F, Stolz D, Griffiths D, Kanai A. Role of gap junctions in spontaneous activity of the rat bladder. *Am J Physiol Renal Physiol* 293: 1018-1025, 2007.

Joensuu H, Roberts PJ, Sarlomo-Rikala M, Andersson LC, Tervahartiala P, Tuveson D, Silberman S, Capdeville R, Dimitrijevic S, Druker B, Demetri GD. Effect of the tyrosine kinase inhibitor STI571 in a patient with a metastaticgastrointestinal stromal tumor. *N. Engl.J. Med.*344, 1052–1056, 2001.

Johnston L, Sergeant GP, Hollywod MA, Thornbury KD, McHale NG. Calcium oscillation in the interstitial cells of the rabbit urethra. *J Physiol* 565:449-461, 2005.

Kanaporis G, Mese G, Valiuniene L, White TW, Brink PR, Valiunas V. Gap junction channels exhibit connexin-specific permeability to cyclic nucleotides. *J Gen Physiol* 131: 293-305, 2008

Koh BH, Roy R, Hollywood MA, Thornbury KD, McHale NG, Sergeant GP, Hatton WJ, Ward SM, Sanders KM, Koh SD. Platelet-derived growth factor receptor-a cells in mouse urinary bladder: a new class of interstitial cells. *J Cell Mol Med* 16(4): 691-700, 2012.

Komuro T. Structure and organization of interstitial cells of Cajal in the gastrointestinal tract. *J Physiol* 576:653-658, 2006.

Korkmaz A, Topal T, Oter S. Pathophysiological aspects of cyclophosphamide and ifosfamide induced hemorrhagic cystitis; implication of reactive oxygen and nitrogen species as well as PARP activation. *Cell Biol Toxicol* 23: 303-312, 2007.

Kubota Y, Kajioka S, Biers M, Yokota E, kohri K, Brading AF. Investigation of the effect of the c-kit inhibitor Givec on isolated guinea-pig detrusor preparations. *Auton Neurosci* 115: 64-73, 2004.

Kumar NM, Gilula NB. The gap junction communication channels. *Cell* 84: 381-388, 1996.

Kurahashi M, Nakano Y, Hennig GH, Ward SM, Sanders KM. Platelet-derived growth factor receptor α-positive cells in the tunica muscularis of human colon. *J Cell Mol Med* 16: 1397-1404, 2012.

Lammie A, Drobnjak M, Gerald W, Saad A, Cote R, Cordon-Cardo C. Expression of c-kit and kit ligand proteins in normal human tissues. *J. Histochem Cytochem*. 42: 1417, 1994.

Li L, Jiang C, Hao P, Li W, Song C, Song B. Changes of gap junctional cell-cell communication in overactive detrusor in rats. *Am J Physiol Cell Physiol* 293: C1627-C1635, 2007.

Linares-Fernandez BE, Alfieri AB. Cyclophosphamide-induced cystitis: Role of nitric oxide synthase, cyclooxygenase-1 and 2, and NK_1 receptors. *J Urol* 177: 1531-1536, 2007.

Lyons AD, Gardiner TA, McCloskey KD. Kit-positive interstitial cells in the rabbit urethra: structural relationships with nerves and smooth muscle. *BJU Int* 99: 687-694, 2007.

Maeda H, Yamagata A, Nishikawa S, Yoshinga K, Kobayashi S, Nishi K, Nishikawa S-I. Requirement of c-kit for development of intestinal pacemaker system. *Development* 116:369-375, 1992.

McCloskey KD, Anderson UA, Davidson RA, Bayguinov YR, Sanders KM, Ward SM. Comparison of mechanical and electrical activity and interstitial cells of Cajal in urinary bladders from wild-type and *W/Wv* mice. *Br J Pharmacol* 156:273-283, 2009.

McCloskey KD, Gurney AM. Kit-positive cells in the guinea pig bladder. *J Urol* 168: 832-836, 2002.

McCloskey KD. Interstitial cells of Cajal in the urinary tract. *Handb Exp Pharmacol* 202: 233-254, 2011.

McHale NG, Hollywood MA, Sergeant GP, Shafei M, Thornbury KT, Ward SM. Organization and function of ICC in the urinary tract. *J Physiol* 576(3): 689-694, 2006.

Metzger R, Schuster T, Till H, Stehr M, Franke FE, Dietz HG. Cajal-like cells in the human upper urinary tract. *J Urol* 172:769-772, 2004.

Neuhaus J, Heinrich M, Schwalenberg T, Stolzenburg J-U. TGF-β1 inhibits Cx43 expression and formation of functional syncitia in cultured smooth muscle cells from human detrusor. *Eur Urol* 55: 491-498, 2009.

Neuhaus J, Weimann A, Stolzenburg J-U, Wolburg H, Horn L-C, Dorschner W. Smooth muscle cells from human urinary bladder express connexin 43 in vivo and in vitro. *World J Urol* 20: 250-254, 2002a.

Neuhaus J, Wolburg H, Hermsdorf T, Stolzenburg J-U, Dorschner W. Detrusor smooth muscle cells of the guinea-pig are functionally coupled via gap junctions in situ and in cell culture. *Cell Tissue Res* 309: 301-311, 2002b.

Persson K, Pandita RK, Aszodi A, Ahmad M, Pfeifer A, Fässler R, Andersson KE. Functional characteristic of urinary tract smooth muscles in mice laking cGMP protein kinase type I. *Am J Physiol* 279: 1112-1120, 2000.

Pezzone MA, Watkins SC, Alber SM, King WE, de Groat WC, Chancellor MB, Fraser MO. Identification of c-kit-positive cells in the mouse ureter: the interstitial cells of Cajal of the urinary tract. *Am J Physiol Renal Physiol* 284:925-929, 2003.

Pieri L, Vannucchi MG, Faussone-Pellegrini MS. Histochemical and ultrastructural characteristics of an interstitial cell type different from ICC and resident in the muscle coat of human gut. *J Cell Mol Med* 12:1944-1955, 2008.

Powley TL, Wang, X-Y, Fox EA, Phillips, RJ, Liu LWC, Huizinga, JD. Ultrastructural evidence for communication between intramuscular vagal mechanoreceptors and interstitial cells of Cajal in the rat fundus. *Neurogastroenterol Motil* 20: 69-79, 2008.

Pusztaszeri MP, Seelentag W, Bosman FT. Immunohistochemical expression of endothelial markers CD31, CD34, von Willebrand factor, and Fli-1 in normal tissues. *J Histochem Cytochem*. 54(4):385-95, 2006.

Rumessen JJ, Thuneberg L. Pacemaker cells in the gastrointestinal tract: interstitial cells of Cajal. *Scand J Gastroenterol Suppl* 216:82-94, 1996.

Sanders KM. A case for interstitial cells of Cajal as pacemakers and mediators of neurotransmission in the gastrointestinal tract. *Gastroenterology* 111:492-515, 1996.

Sanders KM, Ward SM. Interstitial cells of Cajal: a new perspective on smooth muscle function. *J Physiol* 576.3: 721-726, 2006.

Seber A, Shu XO, Defor T, Sencer S, Ramsay N. Risk factors for severe hemorrhagic cystitis following BMT. *Bone Marrow Transplant* 23 (1): 35-40, 1999.

Sergeant GP, Hollywood MA, McCloskey KD, Thornbury KD, McHale NG. Specialised pacemaking cells in the rabbit urethra. *J Physiol* 526:359-366, 2000.

Sergeant GP, Hollywood MA, McHale NG, Thornbury KD. Spontaneous Ca^{2+} activated Cl^- currents in isolated urethral smooth muscle cells. *J Urol* 166: 1161–1166, 2001.

Sergeant GP, Thornbury KD, McHale NG, Hollywood MA. Characterization of norepinephrine-evoked inward currents in interstitial cells isolated from the rabbit urethra. *Am J Physiol Cell Physiol* 283: 885-894, 2002.

Smet PJ, Jonavicius J, Marshall VR, de Vente J. Distribution of nitric oxide synthase-immunoreactive nerves and identification of the cellular targets of nitric oxide in guinea-pig and human urinary bladder by cGMP immunohistochemistry. *Neuroscience* 71:337-348, 1996.

Souza-Filho MVP, Lima MVA, Pompeu MML, Ballejo G, Cunha FQ, Ribeiro RA. Involvement of nitric oxide in the pathogenesis of cyclophosphamide-induced hemorrhagic cystitis. *Am J Pathol* 150: 247-256, 1997.

Stillwell TJ, Benson RC Jr. Cyclophosphamide-induced hemorrhagic cystitis: a review of 100 patients. *Cancer* 61: 451-457, 1988.

Sui GP, Rothery S, Dupont E, Fry CH, Severs NJ. Gap junctions and connexin expression in human suburothelial interstitial cells. *BJU Int* 90: 118-129, 2002.

Torihashi S, Horisawa M, Watanabe Y. c-Kit inmunoreactive interstitial cells in the human gastrointestinal tract. *J Auton Nerv Syst* 75:38-50, 1999.

Torihashi S, Ward SM, Nishikawa S, Nishi K, Kobayashi S, Sanders KM. c-kit-dependent development of interstitial cells and electrical activity in the murine gastrointestinal tract. *Cell Tissue Res*. 280:97-111, 1995.

Torihashi S, Ward SM, Sanders KM. Development of c-kit-positive cells and the onset of electrical rhythmicity in murine small intestine. *Gastroenterology* 112:144-155, 1997.

Triguero D, González M, García-Pascual A, Costa G. Atypical relaxation by scorpion venom in the lamb urethral smooth muscle involves both NO-dependent and –independent responses. *Naunyn-Schmiedeberg´s Arch Pharmacol* 361: 151-159, 2003.

Vanderwinden JM, Rumessen JJ, De Laet MH, Vanderhaeghen JJ, Schiffmann SN. CD34 immunoreactivity and interstitial cells of Cajal in the human and mouse gastrointestinal tract. *Cell Tissue Res* 302: 145-153, 2000.

Vanderwinden JM, Rumessen JJ, Liu H, Descamps D, De Laet MH, Vanderhaeghen JJ. Interstitial cells of Cajal in human colon and in Hirchsprung´s disease. *Gastroenterology* 111:901-910, 1996.

Waldeck K, Ny L, Persson K, Andersson KE. Mediators and mechanisms of relaxation in rabbit urethral smooth muscle. *Br J Pharmacol* 123: 617-624, 1998.

Wang J, Ma M, Locovei S, Keane RW, Dahl G. Modulation of membrane channel currents by gap junction protein mimetic peptides: size matters. *Am J Physiol Cell Physiol* 293: C1112-C1119, 2007.

Wang XY, Paterson C, Huizinga JD. Cholinergic and nitrergic innervation of ICC-DMP and ICC-IM in the human small intestine. *Neurogastroenterol Motil* 15:531-543, 2003.

Willecke K, Eiberger J, Degen J, Eckardt D, Romualdi A, Guldenagel M, Deutsch U, Söhl G. Structural and functional diversity of conexin genes in the mouse and human genome. *Biol Chem* 383:725-737, 2002.

Xu X, Cubeddu LX, Malave A. Expression of inducible nitric oxide synthase in primary culture of rat bladder smooth muscle cells by plasma from cyclophosphamide-treated rats. *Eur J Pharmacol* 416: 1-9, 2001.

Yoshimura N, de Groat WC. Increased excitability of afferent neurons innervating rat urinary bladder after chronic bladder inflammation. *J Neurosci* 19: 4644-4653, 1999.

Zhang SC, Fedoroff S. Cellular localization of stem cell factor and c-kit receptor in the mouse nervous system. *J Neurosci Res* 47: 1-15, 1997.

INTRODUCCIÓN

El almacenamiento y la eliminación periódica de orina se encuentran regulados por un complejo sistema de control neural, tanto central como periférico, que coordina la actividad autónoma y somática de varios órganos efectores, incluyendo el cuerpo y la base de la vejiga, la unión ureterovesical, la uretra y los músculos del suelo de la pelvis (Lincoln y Burnstock, 1993). Todo este proceso está regulado por centros nerviosos supraespinales, responsables tanto de reflejos inhibidores como excitadores (Zhou y Ling, 1999).

El proceso de micción implica el vaciado total de orina de la vejiga urinaria; ello supone el mantenimiento de la contracción del músculo detrusor de la vejiga, la apertura de la uretra y el cierre de la unión ureterovesical durante el tiempo necesario para evacuar toda la orina almacenada. Por el contrario, durante la fase de continencia la uretra genera una presión intraluminal superior a la presión vesical. Mientras, la vejiga mantiene un estado de relajación adaptativa permitiendo aumentar el volumen de orina almacenado sin modificar la presión intravesical (Brading, 1999).

1. Anatomofisiología de la vejiga y uretra

1.1 Anatomía de la vejiga y uretra

La vejiga urinaria es un órgano muscular hueco con forma de saco situado en el suelo de la fosa pélvica y que se compone de: 1) cuerpo vesical, que ocupa la mayor parte del órgano y tiene la función de almacenar la orina; 2) el trígono, localizado en la pared posteroinferior de la vejiga por cuyos ángulos superiores penetran, oblicuamente, los uréteres; y 3) el cuello vesical, que conecta con la uretra y está compuesto por músculo liso involuntario.

La uretra es un tubo muscular a través del cual la vejiga descarga su contenido de orina al exterior (Patel y Chapple, 2008). La continencia urinaria resulta de la participación de los dos esfínteres presentes en la uretra, uno de ellos externo compuesto por músculo estriado, voluntario, llamado esfínter uretral externo (EUE) o rabdoesfínter y otro interno, compuesto por músculo liso, involuntario, llamado esfínter uretral interno (EUI; Strasser et al., 2000) (**Fig. I**).

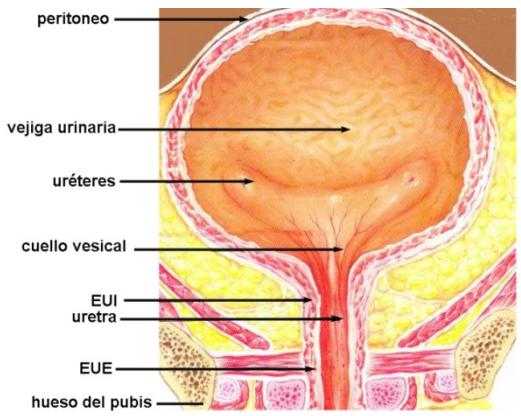

Figura I. Anatomía de la vejiga urinaria y la uretra femenina. EUI, esfínter uretral interno; EUE, esfínter uretral externo.

El presente estudio se ha centrado exclusivamente en uretras de hembras de rata, oveja, conejo y ratón, por lo que las descripciones que se presentan a continuación se centran en las características de la uretra femenina. En este sentido, la uretra de la hembra es más corta y sencilla que la masculina y más uniforme en estructura (Brading, 1999). Se dispone caudalmente sobre el suelo pélvico por debajo del tracto reproductor, y se relaciona dorsalmente con la vagina y ventralmente con la sínfisis púbica.

Desde el punto de vista histológico la uretra femenina está formada por cuatro capas, que desde la luz del tubo al exterior son:

a) Mucosa o urotelio: presenta pliegues longitudinales poco profundos, que determinan que la luz de la uretra sea semilunar. El epitelio de revestimiento en la proximidad de la vejiga es de transición, aunque va cambiando gradualmente hasta convertirse en escamoso estratificado según se aproxima al orificio externo. A lo largo de toda la longitud de esta capa se encuentran numerosas glándulas de Littre, claras secretoras de moco (Gartner y Hiatt, 2002).

b) Submucosa o lámina propia: es una capa de tejido conjuntivo, más compacta en la zona más cercana al epitelio y más laxa en su parte más profunda, con gran cantidad de fibras colágenas y elásticas, presentando ocasionalmente tejido linfático difuso y nódulos linfáticos. En esta capa abundan los vasos sanguíneos y las fibras elásticas, asociadas a las musculares, que aportan resistencia a esta estructura y forman un "cojín vascular" que contribuye al cierre pasivo de la uretra (Augsburger et al., 1993). También posee una densa red de terminaciones nerviosas aferentes responsables de transmitir información sensorial al sistema nervioso central.

c) Túnica muscular: formada a su vez por dos componentes musculares:

* El EUI de músculo liso que se localiza más internamente extendiéndose a lo largo de toda la uretra. Está a su vez formado por una gruesa capa interna de músculo liso circular, que alcanza su máximo espesor en la parte media de la uretra, donde se registra la máxima presión intrauretral durante el periodo de continencia. Exterior a ésta, existe una capa de músculo liso longitudinal que se continúa cranealmente con el músculo detrusor de la vejiga y que se ha sugerido que pudiera estar involucrada en el acortamiento de la uretra durante la micción (Augsburger et al., 1993; Dass et al., 2001).

* El EUE de músculo estriado forma una capa externa con fibras musculares estriadas dispuestas de forma circular, transversal y oblicua que comienza a partir de la uretra media aumentando su grosor caudalmente (Sautet et al., 1987).

De esta forma, si dividimos la uretra en tres regiones: proximal, media y distal, la distribución relativa de músculo liso y estriado cambia progresivamente. La uretra proximal estaría formada casi exclusivamente por músculo liso, la uretra media presentaría un componente preferente de músculo liso rodeado por una capa delgada de músculo estriado, mientras que la uretra distal presentaría tan solo una delgada capa interna de músculo liso y una gruesa capa externa de estriado.

d) Túnica adventicia o serosa: es una capa de tejido conjuntivo laxo que rodea la capa muscular.

Aunque se mantiene esta estructura general, existen diferencias interespecíficas en la morfología de la uretra femenina que afectan principalmente a la disposición de las fibras musculares lisas y estriadas. En este sentido, en la parte proximal de la uretra de oveja se distingue una capa de músculo liso circular interna y una longitudinal externa, y a nivel distal una capa de músculo estriado circular, lo que se asemeja a la disposición descrita en la uretra de la mujer. En la uretra de rata, conejo y ratón existe una mayor densidad de haces de músculo liso dispersos que adoptan una disposición longitudinal u oblicua en la submucosa. Además, la túnica muscular está constituida a nivel craneal por fibras de músculo liso con disposición circular, entre las que se imbrican fibras musculares estriadas, en una cuantía progresivamente mayor a medida que se avanza a nivel distal, por lo que resulta más difícil diferenciar ambos tipos de músculo (Andersson et al., 1990; Radziszewski et al., 1996) (**Fig.II**).

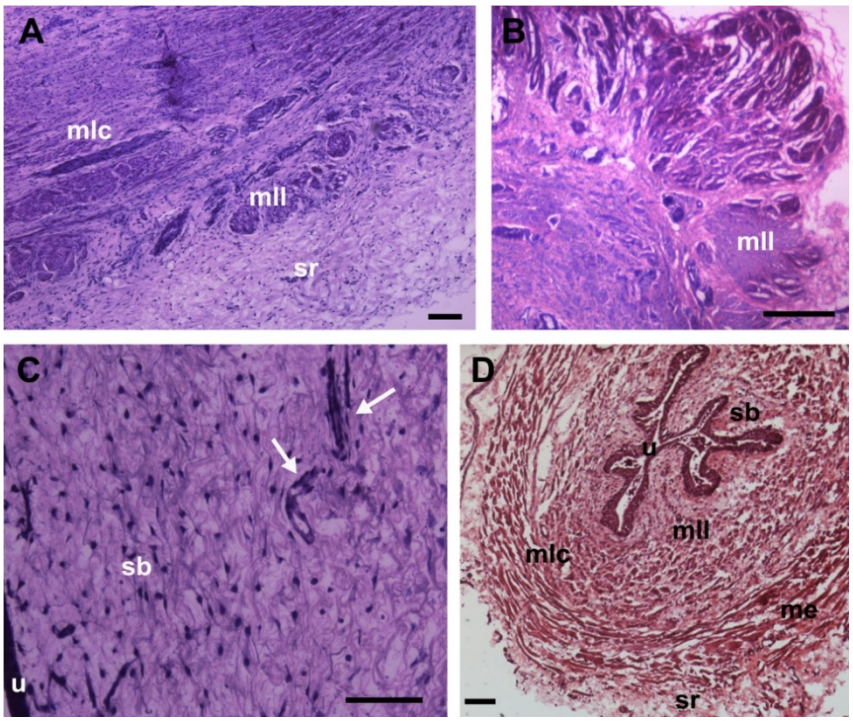

Figura II Capas histológicas de la uretra de oveja (*A, B*, y *C*) y de rata (*D*). *A*. Capas más externas de la uretra de oveja: serosa (sr), muscular lisa longitudinal (mll) y muscular lisa circular (mlc). *B*. Detalle a mayores aumentos de los fascículos de músculo liso longitudinal situados en la parte más externa de la zona ventral de la uretra de oveja. *C*. Capas de la uretra de oveja más cercanas a la luz tubular: urotelio (u) y submucosa (sb), donde abundan los vasos sanguíneos (señalados con flechas). *D*. Capas constituyentes de la uretra de rata: urotelio (u), submucosa (sb), muscular lisa longitudinal (mll), muscular lisa circular (mlc), muscular estriada (me) y serosa (sr). Barra = 40 µm.

1.2 Inervación de la uretra

La uretra femenina recibe inervación del sistema nervioso autónomo, constituida por fibras eferentes simpáticas y parasimpáticas, así como de fibras aferentes asociadas, procedentes del plexo vesical. El EUE además recibe inervación somática aferente y eferente procedente del nervio pudendo (Fowler et al., 2008).

El componente simpático es el responsable del mantenimiento del tono de la musculatura lisa de la porción craneal de la uretra, y está activo durante el almacenamiento de la orina, mientras que el componente parasimpático es el encargado de la relajación de la capa circular y posiblemente de la contracción en sentido longitudinal del músculo liso uretral, lo cual facilita la evacuación de la orina (Le Feber y Van Asselt, 1999).

La inervación simpática se origina en las astas laterales de los dos últimos segmentos medulares torácicos y los dos primeros lumbares (Fowler et al. 2008; Vera y Nadelhaft 1992). El nivel postganglionar se inicia con los nervios esplácnicos, éstos emiten ramas que se anastomosan para formar el plexo hipogástrico (Villanueva, 2001). Sus ramas vesicales se anastomosan con las de los nervios pélvicos y penetran en la vejiga y en la uretra (Andersson y Wein, 2004).

La inervación parasimpática tiene su origen en las astas laterales del segundo y cuarto segmento medular sacro, aunque en los roedores estas fibras parten de la zona caudal lumbar (Andersson y Arner 2004; Petras y Cummings, 1978). Los nervios sacros portan las fibras parasimpáticas que confluyen para formar los nervios pélvicos que terminan en pequeños ganglios (nivel preganglionar) cerca o en la propia pared de la vejiga y la uretra, y de ellos salen fibras postganglionares que terminan en receptores sensitivos y fibras musculares. En este sentido, cabe destacar que la rata es la única especie que no presenta ganglios parasimpáticos intramurales (McMurray et al., 2006).

La inervación somática se distribuye en el EUE regulando su contractilidad a través del nervio pudendo interno que se origina en las astas anteriores del segundo, tercer y cuarto segmento de la médula espinal sacra (Lincoln y Burnstock, 1993).

1.2.1 Inervación adrenérgica

Diversos estudios han revelado que las fibras adrenérgicas están distribuidas de forma dispersa en el músculo detrusor de la vejiga pero su densidad aumenta en la capa muscular del cuello vesical y en la uretra proximal (Hamberger y Norberg, 1965; El-Badawi y Schenk, 1966). Además, la presencia de receptores α y β-adrenérgicos ha sido demostrada en las células musculares lisas de la uretra en varias especies de mamíferos (Edvardsen, 1968, Persson y Andersson, 1976; Levin y Wein, 1979; Latifpour et al., 1990, Walden et al., 1997), con un predominio de los receptores α-adrenérgicos, especialmente los del subtipo α-1 (Andersson y Wein, 2004; Brading et al., 1999; García-Pascual et al., 1991a). Aunque también existen receptores β-adrenérgicos con un

predominio del subtipo β-2, y su estimulación provoca un efecto relajante (Takeda et al., 2003), que queda enmascarado por el predominio de la actividad α-adrenérgica.

Gran número de estudios funcionales han demostrado que tanto la estimulación eléctrica de los nervios hipogástricos, como la administración de agonistas adrenérgicos, provocan un incremento de la presión intrauretral atribuido a la presencia de receptores α-adrenérgicos (Frenier et al., 1992). Actualmente se admite que la descarga simpática es la principal responsable de la contracción de la capa circular uretral, manteniendo el cierre uretral y, por tanto, asegurando la continencia (Bagot y Chess-Williams, 2006). La importancia funcional de la inervación simpática uretral se pone también de manifiesto *in vitro* por el hecho de que tanto la estimulación eléctrica transmural (EFS, *electrical field stimulation)* como la despolarización con altas concentraciones de K^+ provocan la liberación de noradrenalina (NE) desde las terminaciones adrenérgicas y la consiguiente activación de receptores postsinápticos α_1-adrenérgicos (García-Pascual et al., 1991b).

1.2.2 Inervación colinérgica

Aunque en la uretra se ha demostrado la existencia de nervios colinérgicos que discurren y se ramifican por los fascículos de músculo liso, con actividad acetilcolinesterasa positivas ($AChE^+$), constituyendo un plexo neuromuscular muy rico en algunas especies (Alm, 1978), la significación funcional de los nervios colinérgicos en la uretra es todavía un asunto controvertido.

Aunque en un principio se postuló que la acetilcolina (ACh) actuaba como relajante uretral, posteriormente estudios *in vitro* realizados en varias especies animales mostraron que los agonistas colinérgicos producen la contracción de preparaciones orientadas longitudinalmente, interpretándose que la contracción en sentido longitudinal de la uretra durante la micción actuaría acortando su longitud y favoreciendo el paso de la orina (Hassouna et al., 1983).

Por otro lado, la presencia de receptores muscarínicos presinápticos en las terminaciones adrenérgicas podría inhibir la liberación de NE, lo que a su vez provocaría disminución del tono uretral y la presión intrauretral (Andersson y Wein, 2004), constituyendo un mecanismo funcional por el que la descarga parasimpática colinérgica contribuiría a la relajación uretral durante la fase de micción.

1.2.3 Inervación no adrenérgica-no colinérgica

Esta denominación, no-adrenérgica no-colinérgica (NANC), procede de los primeros descubrimientos de la existencia de otros tipos de inervación autónoma no relacionada con la liberación de NE o de ACh. En la uretra son muchos los estudios en diferentes especies animales que han mostrado en respuesta a EFS, la aparición de

respuestas contráctiles o relajantes que no podían ser afectadas por bloqueantes α- o β-adrenérgicos, ni por bloqueantes de receptores muscarínicos como la atropina, pero que sí podían ser inhibidas por tetrodotoxina (TTX) (García-Pascual et al., 1991c). La TTX bloquea los canales de sodio, y por tanto, inhibe la despolarización neuronal y la liberación de los neurotransmisores, indicando el origen neuronal de los mediadores implicados.

En este sentido se ha sugerido la participación de diferentes moléculas en la neurotransmisión uretral tales como óxido nítrico (NO), adenosina trifosfato (ATP), monóxido de carbono (CO), diversos neuropéptidos tales como péptido intestinal vasoactivo (VIP), neuropéptido Y (NPY), péptido relacionado con el gen de la calcitonina (CGRP) o endotelinas (ET); además de taquininas como sustancia P (SP) o neuroquinina A, y prostanoides o serotonina (5-HT) (Para una revisión ver: Andersson y Wein, 2004).

Especialmente importante es la existencia de una **inervación NANC mediada por NO** y denominada **inervación nitrérgica**, debida a la presencia de la isoforma neuronal de NO sintasa (nNOS) en nervios intramurales. Una rica inervación nitrérgica ha sido demostrada en el EUI de diferentes especies incluidas la rata (McNeil et al, 1992; Persson et al, 1997), la oveja (Triguero et al., 1993), el conejo (Dokita et al, 1991; Zygmunt et al, 1993), el cerdo (Persson et al, 1993), y la especie humana (Smet et al., 1994; Leone et al., 1994). También en el EUE, se ha demostrado una inervación nitrérgica en el sarcolema de las fibras rápidas, concentrada en la unión neuromuscular (García-Pascual et al., 2005).

El NO liberado de los nervios actúa a través de incrementos en los niveles de guanosina monofosfato cíclico (cGMP) del músculo liso uretral (García-Pascual y Triguero, 1994). Así, se ha descrito que la estimulación eléctrica de preparaciones uretrales precontraídas provocaba la aparición de pronunciadas relajaciones NANC que eran inhibidas por TTX y por inhibidores de la síntesis de NO y de guanilato ciclasa soluble (sGC; Andersson et al., 1991; Andersson et al., 1992; Dokita et al., 1991; García-Pascual et al., 1991c; Persson et al 1992, Persson y Andersson, 1992). Del mismo modo, la administración exógena de donantes de NO da lugar a una relajación concentración-dependiente que también es sensible a inhibidores de la sGC (Persson et al., 1992).

Además, estudios funcionales han demostrado que el NO está implicado en el descenso de la presión intrauretral que se produce al comienzo de la micción (Andersson 1993; Persson et al, 2000). De hecho, se ha observado como la infusión de donantes de NO en la uretra de rata *in vivo* reduce la presión intrauretral (Persson et al, 1992), mientras que la administración de inhibidores de NOS, causan anormalidades en la micción e hiperactividad vesical en ratas (Bennett et al., 1995; Persson et al., 1992) y en fetos de oveja (Mevorach et al., 1994). Asimismo, ratones con deleciones de nNOS demuestran el papel fundamental del NO en la función del tracto urinario inferior (Burnett et al., 1997; Sutherland et al., 1997). Todas estas evidencias han permitido

sugerir que el NO sea considerado como el principal neurotransmisor NANC inhibitorio en la uretra (Persson y Andersson, 1994).

2. El óxido nítrico

Desde el descubrimiento del NO como mediador biológico en 1987, esta sencilla molécula ha creado una gran conmoción en el mundo científico y tras vencer el escepticismo inicial de numerosos investigadores, hoy se reconoce su participación en casi cualquier aspecto de la biología y la medicina, desde su papel como vasodilatador y regulador de la coagulación sanguínea, hasta su función como neurotransmisor tanto central como periférico y su papel central en los procesos de inflamación y defensa inmunológica. Su trascendencia científica fue reconocida a finales del siglo pasado, recibiendo en 1992 el nombramiento de molécula del año y tan solo 6 años después, tres de los pioneros en su descubrimiento, *L. Ignarro, R. Furchgott y F. Murad,* recibieron el premio Nobel de fisiología y medicina.

El NO es un radical libre no cargado compuesto por un átomo de nitrógeno y otro de oxígeno, y que presenta un electrón desapareado condenado a una frenética búsqueda de otra molécula que pueda aceptarlo (Nathan, 1992). Estas características lo convierten en una molécula ideal para atravesar sin límite las membranas biológicas, ya que al no tener carga difunde libremente a través de la capa lipídica y al tener un electrón libre desapareado es una molécula altamente reactiva. Las moléculas diana incluyen oxígeno, otros radicales, grupos tiol y metales.

El NO posee una vida media corta (de 0.1 a 5 segundos, después de la cual se degrada a compuestos como nitritos y nitratos), aunque suficiente, dada su rápida migración hacia las moléculas diana, lo cual le permite actuar como primer mensajero en células adyacentes. Producido en grandes cantidades, en presencia de O_2, es capaz de formar peroxinitrito ($ONOO^-$), radical libre altamente reactivo, responsable de los efectos tóxicos mediados por el NO. Esta molécula puede dar lugar a reacciones de nitración de residuos de tirosina de muchas proteínas afectando a su función. A su vez el peroxinitrito puede descomponerse en radicales libres tóxicos y dióxido de nitrógeno (Álvarez et al., 1995).

2.1 Síntesis de NO

La síntesis de NO es llevada a cabo por una familia de enzimas denominadas óxido nítrico sintasas (NOS), que catalizan la oxidación de uno de los dos grupos amidino equivalentes del aminoácido L-arginina produciendo la liberación de una molécula de L-citrulina, pasando por un intermediario conocido como N^G-hidroxi-L-arginina (Stuehr et al., 1991a) y actuando como cofactor una molécula de nicotinamida adenina dinucleotidofosfato (NADPH) (**Fig. III**).

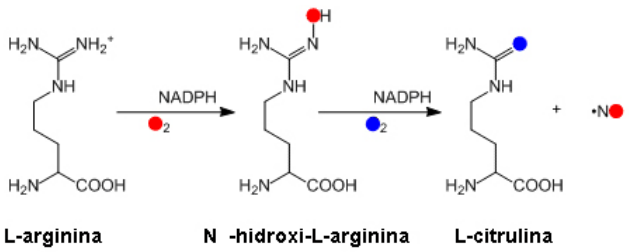

Figura III. Esquema de la reacción de síntesis de NO.

Existen tres isoformas de esta enzima en mamíferos, que difieren en cuanto a su localización, regulación y expresión: neural (nNOS o NOS 1), endotelial (eNOS o NOS 3) e inducible (iNOS o NOS 2). Estas tres isoformas tienen en común que todas utilizan flavín mononucleótido (FMN), flavin-adenin-dinucleótido (FAD), tetrahidrobiopterina (BH_4) y el grupo hemo como cofactores enzimáticos.

La NOS está constituida por un homodímero, presentando las tres isoformas un alto grado de homología (50-60%). Las subunidades idénticas que conforman el dímero presentan un peso molecular de 125-155 kDa (Knowles y Moncada, 1994) y están constituidas por dos dominios. El dominio N-terminal es de tipo oxigenasa y presenta las secuencias de unión al cofactor BH_4, al sustrato L-arginina y al grupo hemo. El dominio C-terminal es un dominio reductasa que permite la unión de los cofactores de óxido-reducción (NADPH, FAD y FMN) y de la proteína calmodulina (CaM) de carácter regulador (Ghosh y Stuehr, 1995; McMillan y Masters, 1995; Richards y Marletta, 1994). La unión a CaM parece ser el "interruptor molecular" que permite el flujo de electrones desde el dominio reductasa hacia el grupo hemo, permitiendo así la transformación de O_2 y L-arginina en NO y L-citrulina (Kelly et al., 1996).

Dos de estas isoformas; la endotelial (eNOS) y la neuronal (nNOS), se encuentran siempre presentes en la célula y se denominan **constitutivas** (cNOS), mientras que la tercera isoforma es **inducible** (iNOS), es decir, se expresa en las células tan sólo después de su estimulación por citoquinas, microbios o productos microbianos. Ambas cNOS se activan sólo cuando el Ca^{2+} liberado en la célula forma complejos con CaM y se une a la enzima. La unión a la CaM permite el paso de electrones de los grupos flavina al grupo activo hemo (Abu-Soud y Stuehr, 1993; Kelly et al., 1996). Por lo tanto las cNOS son activadas por estímulos que aumentan los niveles de Ca^{2+} intracelular (Moncada et al., 1991) y generan niveles moderados de NO (picomoles) de forma pasajera, lo que permite al NO producido actuar como señalizador celular y mensajero intercelular. En cambio, la iNOS posee una unión fija a CaM, circunstancia que permite a la enzima ser activada por los niveles basales de Ca^{2+} en las células y mantenerla así en estado activo (Cho et al., 1992) generando altas cantidades de NO (micromoles) por largos periodos de tiempo, pudiendo llegar a tener efectos citotóxicos sobre las propias células productoras o células vecinas. Aunque en condiciones fisiológicas no se expresan niveles suficientes de iNOS para originar estos efectos indeseables, en respuesta a estímulos inflamatorios o infecciosos se produce la

inducción de su expresión (Salkowski et al, 1997; Landry y Oliver, 2001). Sin embargo, no solamente iNOS es susceptible de modificar su expresión, también las isoformas constitutivas sufren *"up and down regulation"* (sobre- y subexpresión) en respuesta a diversos estímulos presentando una mayor adaptabilidad funcional de lo que en un principio se pensaba (Nathan y Xie, 1994; Fleming y Busse, 1999).

La **NOS neural** se expresa constitutivamente en el sistema nervioso central y periférico (Bredt, 1999), localizándose en la fracción soluble citosólica con un peso molecular de 150-160 kDa. Esta isoforma fue por primera vez purificada en el cerebelo de rata y cerdo (Mayer et al., 1990; Bredt y Snyder, 1990; Bredt 1999), pero además de expresarse en el sistema nervioso central también está presente en médula espinal (Dun et al., 1992), ganglios simpáticos y glándulas adrenales (Dun et al., 1993; Sheng et al., 1993), células epiteliales de pulmón, útero y estómago (Schimidt et al., 1992a), células de la mácula densa de riñón (Schimidt et al., 1992a), células pancreáticas (Schimdt et al., 1992b), células intersticiales de colón (Vannucchi et al., 2002) y en músculo esquelético (Nakane et al., 1993; Kobzic et al., 1994). Hay que destacar la participación del NO como neurotransmisor periférico del sistema nervioso autónomo formando parte de los mediadores NANC, atribuyéndole numerosas funciones en los sistemas gastrointestinal, urogenital, respiratorio y vascular (Rand y Li, 1995).

Con relación al tracto urinario inferior, diversos estudios han mostrado en diversas especies animales y en el hombre inmunorreactividad (-ir) a nNOS y actividad enzimática NOS predominante en la uretra y trígono, mientras que en el músculo detrusor de la vejiga es escasa o incluso inexistente (Triguero et al., 1993; Persson et al., 1995; García-Pascual et al., 1996; Ho et al., 1999), lo cual explica su función como relajante muscular provocando la rápida apertura del cuello vesical y la uretra durante la micción.

También se ha observado la presencia de nNOS-ir en el músculo estriado del EUE, localizada en el sarcolema de las fibras rápidas y en terminaciones nerviosas finas (Ho et al, 1999; García-Pascual et al., 2005). Aunque su papel fisiológico en esta estructura está todavía por determinar, la mayor densidad de nNOS-ir y cGMP-ir en la placa motora, sugiere su participación como neuromodulador de la transmisión neuromuscular colinérgica (García-Pascual et al., 2005).

Hay que señalar también la existencia de varias isoformas de nNOS resultantes de un proceso de "*splicing"* alternativo de su mRNA (Laine y Montellano, 1998). Una de ellas conocida como nNOS-μ, se ha comprobado que se expresa específicamente en músculo esquelético, músculo cardíaco, tejido peneano y uretra (Lin et al., 1998; Magee et al., 1996). Esta isoforma aparece ligada a la membrana por su unión al complejo distrofina-glicoproteína mediante el dominio PDZ de la sintrofina-α-1, miembro de la familia de las distrofinas asociada a membrana y fuertemente expresada en el sarcolema de la fibra muscular (Grozdanovic et al., 1997). Por el contrario, la isoforma predominante en cerebro es nNOS-α (Mungrue y Bredt, 2004), que difiere en la

inserción de 34 residuos aminoacídicos entre los dominios de la CaM y de la flavina (Laine y Montellano, 1998).

La **NOS endotelial** además de su localización en el endotelio vascular (Pollock et al., 1993) donde fue originalmente aislada, se ha descubierto su presencia en otras muchas localizaciones como por ejemplo en epitelio renal (Tracey et al., 1994), células intersticiales de colon (Xue et al., 1994) e hipocampo y otras regiones del cerebro (Dinerman et al., 1994). En el músculo estriado se la ha encontrado asociada a la membrana mitocondrial (Kobzic et al., 1995). En el tracto urinario inferior, se ha revelado la presencia de eNOS en el urotelio de uretra de diferentes especies (Persson et al., 1999, Pinna et al, 1999) y se ha sugerido su participación en la modulación de la relajación nitrérgica del músculo liso (Pinna et al., 1996).

La isoforma eNOS comparte los mismos mecanismos de activación con la nNOS e igualmente presenta una expresión constitutiva en sus respectivos tejidos, pero difiere de la isoforma neural en el peso molecular (134 kDa) y en su carácter de proteína particulada asociada a la membrana con capacidad para trasladarse al citosol mediante un proceso de fosforilación de sus residuos de serina (Förstermann et al., 1991; Michel et al., 1993). La actividad eNOS está regulada a nivel de su expresión por medio de polimorfismos y a nivel transcripcional por interacciones con su promotor. Además, es susceptible de regulación por fosforilación y nitrosilación (Searles, 2006). También es capaz de sufrir modificaciones postraduccionales como son la miristoilación irreversible, esencial para su unión a la proteína caveolina-1 presente en las caveolas de la membrana de la célula endotelial (Shaul et al., 1996; Ju et al., 1997), necesaria para su actividad enzimática, o la palmitoilación reversible inducida por agonistas que aumentan la concentración de Ca^{2+} intracelular (Prabhakar et al., 1998) y provocan su traslado al citosol y su inactivación. Además, se ha demostrado que esta enzima es susceptible de modificar su expresión en respuesta a la estimulación de receptores de superficie de la célula endotelial (como por ejemplo por ACh) o por fenómenos físicos como el efecto de cizalladura sobre la pared vascular ejercido por el flujo sanguíneo (*shear stress,* Fleming y Busse, 1999).

La **NOS inducible** presenta un peso molecular entre 125-135 kDa, y al igual que la nNOS-α se localiza en la fracción soluble (Hevel et al., 1991, Stuehr et al., 1991b). Esta isoenzima se expresa en macrófagos (Hevel et al., 1991), condrocitos (Charles et al., 1993), neutrófilos y eosinófilos (Sethi y Dikshit, 2000), hepatocitos (Billiard et al., 1990), células musculares lisas (Stuehr, 1999), islotes pancreáticos de ratas diabéticas (Kleemann et al., 1993) y otros muchos tejidos. Su expresión es el resultado de la exposición de las células a microorganismos o productos microbianos liberados durante episodios inflamatorios o infecciosos, y a citoquinas (Morris y Billiar, 1994) tales como el factor de necrosis tumoral α (TNF-α), la interleuquina-1β (IL-1β) o el interferón γ (IFN γ). La iNOS produce mayores cantidades de NO que las isoenzimas constitutivas (Gordge, 1998) y una de sus principales funciones durante la reacción de inflamación es debida al efecto bactericida del NO al inactivar enzimas imprescindibles en el metabolismo de determinados patógenos (Hibbs et al., 1988). Sin embargo este efecto

del NO tiene una doble cara, ya que aunque es capaz de disminuir la activación linfocítica consiguiendo un efecto antiinflamatorio, también produce disminución de la adhesión leucocitaria y aumento de la migración de leucocitos con un efecto potenciador de la inflamación (Kubes et al., 1991).

En el tracto urinario inferior, se ha identificado su presencia en el urotelio de la uretra (Persson et al., 1999) y aunque ha sido descrita en músculo liso de uretra de conejo (Dokita et al., 1994), parece ser que no se expresa en condiciones fisiológicas (García-Pascual et al., 1996), sino que podría estar relacionada con la presencia de células inflamatorias infiltradas (Smith et al., 1994).

2.2 Mecanismos de acción del NO

El principal receptor biológico para el NO es la sGC, presente en el citoplasma celular. La activación de la sGC por el NO (cuando la concentración de éste es baja, normalmente producido por las isoformas constitutivas de NOS) causa un aumento de la concentración intracelular de cGMP a partir de GTP (Schmidt et al., 1993; Bryan et al, 2009). Este aumento de cGMP intracelular origina a su vez una serie de respuestas en cascada actuando como segundo mensajero (**Fig. IV**):

1) Activación de **proteínas kinasas dependientes de cGMP (PKG)**, dando lugar a la fosforilación de diversas proteínas y por tanto, modificando su actividad. El efecto resultante depende de la especialización de la célula en que se produzca. La activación de la PKG se ha postulado como el principal mecanismo implicado en la relajación nitrérgica del músculo liso (Lincoln et al, 1995). Los mecanismos por los cuales la PKG provoca la relajación muscular parecen ser una reducción del Ca^{2+} intracelular (modulando los canales de Ca^{2+} de membrana celular y retículo sarcoplásmico) y una disminución en la sensibilidad del sistema contráctil al Ca^{2+} (Moncada, 1987; Warner et al, 1994). De las dos isoformas de la enzima (PKG I y PKG II) solamente PKG I se expresa en músculo liso, habiéndose comprobado mediante la utilización de ratones *"knockout"* que es el principal efector de la relajación nitrérgica de la uretra (Persson et al, 2000). En ciertas condiciones, el cGMP también puede activar PK dependientes de cAMP (Ruiz-Velasco et al, 1998), de la misma manera que el cAMP puede contribuir a la relajación del músculo liso por activación de PKG (Francis et al, 1988). Sin embargo, la relajación nitrérgica en la uretra parece estar únicamente asociada a incrementos en los niveles de cGMP, pero no de cAMP (García-Pascual y Triguero, 1994; Persson y Andersson, 1994).

2) Activación de **fosfodiesterasas (PDE),** que hidrolizan e inactivan el cGMP, y que también pueden modificar los niveles de otros segundos mensajeros como por ejemplo cAMP y Ca^{2+} intracelular (Bender y Beavo, 2006; Omori y Kotera, 2007). De los 11 diferentes isotipos de PDE, la PDE 5, que es altamente específica para cGMP (Soderling y Beavo, 2000) parece estar ampliamente distribuida en el músculo liso de la uretra (Werkstrom et al, 2006).

3) Apertura de **canales iónicos operados por nucleótidos cíclicos (CNG).** Los CNG son una familia de canales catiónicos no selectivos, cuya apertura está mediada por la unión directa de cAMP y/o cGMP intracelular y sólo se activan débilmente por cambios en el potencial de membrana. Estos canales conducen una corriente interna de Na^+ y Ca^{2+} que provoca la despolarización de la membrana o cambios locales en la concentración de Ca^{2+} citosólico. Aunque inicialmente fueron descritos en fotorreceptores (bastones) de la especie bovina (Koch y Kaupp, 1985) y posteriormente se demostró su participación en el control de la respuesta a la luz en los protozoos ciliados (Walerczyk et al, 2006), recientemente han sido identificados en otros tipos celulares tales como receptores sensoriales, epitelio, vasos sanguíneos, e incluso espermatozoides (Jain et al, 1998; Craven y Zagotta, 2006). Sin embargo, el papel funcional de estos canales iónicos es complejo y todavía no está bien definido (Craven y Zagotta, 2006; Hofmann et al, 2005) aunque existe un creciente interés en ellos, ya que pueden proporcionar una vía alternativa para la entrada de Ca^{2+} que es prácticamente independiente de los cambios de potencial de la membrana y que relaciona la actividad de las proteínas reguladas por Ca^{2+} con la vía de señalización de cGMP/cAMP sin la participación de PK. Hasta el momento, su presencia y posible función en el tracto urinario inferior no había sido descrita.

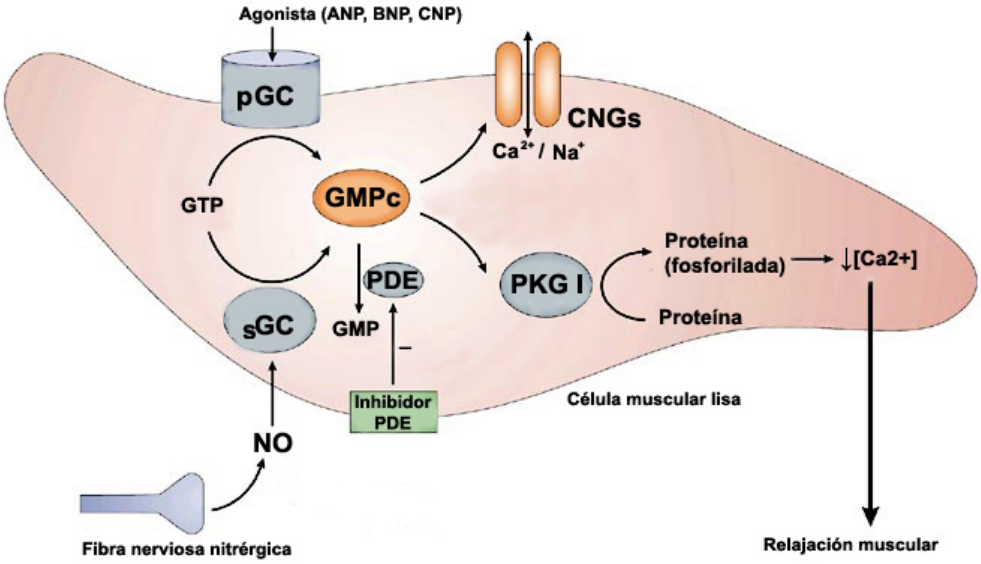

Figura IV. Esquema de la ruta de señalización por NO/cGMP en la célula muscular. (Adaptado de Hossein et al, 2006). NO, óxido nítrico; GTP, guanosina trifosfato; cGMP, guanosina monofosfato cíclico; sGC, guanilato ciclasa soluble; pGC, guanilato ciclasa particulada; PDE, fosfodiesterasa, PKG I, proteína kinasa dependiente de cGMP tipo I; CNG, canales iónicos operados por nucleótidos cíclicos.

Por otra parte, el NO también puede producir **efectos fisiológicos independientes de cGMP**, siendo las reacciones de nitrosilación las más importantes y extendidas. Debido a su capacidad de reaccionar con grupos tioles de muchas proteínas puede dar lugar a alteraciones en su actividad y por lo tanto, en su efecto biológico. Entre las proteínas susceptibles de nitrosilación se incluyen: proteínas plasmáticas,

como la albúmina, o la oxihemoglobina, que tras ser nitrosilada, modifican su afinidad por el O_2 (Stamler et al., 1992a); enzimas, como el activador tisular de plasminógeno (t-PA) (Stamler et al., 1992b), la gliceraldehído-3-fosfato-deshidrogenasa (G3PDH) (Mohr et al., 1996), o la propia NOS (Ravi et al., 2004) que al reaccionar con NO modifican su actividad; canales iónicos que modifican su conductancia, como los canales de K^+ presentes en músculo liso vascular, o el canal del receptor NMDA (Lei et al., 1992); proteínas G, como por ejemplo la $p21^{ras}$ (Lander et al., 1995) e incluso factores de transcripción, lo que explicaría la capacidad del NO de modular la expresión génica directamente, sin intervención del cGMP (Gross y Wolin, 1995).

Con herramientas farmacológicas específicas es posible actuar a diversos niveles del mecanismo de acción celular del NO y por lo tanto analizar su participación en un determinado proceso funcional. En este sentido, el empleo de los diferentes inhibidores de la NOS ha sido esencial, así como la utilización de L-arginina, precursor del NO y por tanto, potenciador de su efecto. La mayoría de los inhibidores de la NOS son análogos de la L-arginina o contienen un grupo guanidínico (Rees et al., 1990; Corbett et al., 1992). De ellos, la mayoría son inhibidores generales, no selectivos, que actúan sobre todas las isoformas de NOS. Como ejemplo N^G-monometil-L-arginina (L-NMMA), N^G-nitro-L-arginina (L-NNA) y su metil éster (L-NAME) entre otros, aunque su potencia no es la misma frente a todas las isoenzimas. También existen inhibidores relativamente selectivos de cada una de las isoformas como por ejemplo S-metil-L-tiocitrulina para nNOS (Melikian et al., 2009) o aminoguanidina para iNOS (Garvey et al., 1997), pero aún hoy no se dispone de inhibidores completamente selectivos. Por otro lado, la acción del NO sobre su diana fundamental, la sGC, puede modificarse mediante sustancias inhibidoras o activadoras de la cascada de cGMP. Así, por ejemplo ODQ (1H-‹1,2,4› oxadiazolo ‹4,3› alquinoxalin-1-one), (Wu y Dun, 1996) actúa inhibiendo la sGC mientras que YC-1 (3-‹5´-hidroximetil-2´-furil›-1-benzilindazol) (Friebe y Koesling, 1998) aumenta la sensibilidad de la sGC al NO. Otras posibles herramientas son los inhibidores de las PDE que al inhibir la degradación de cGMP potencian su efecto, como por ejemplo IBMX, inhibidor general de PDE o Zaprinast y Sildenafilo, inhibidores específicos de PDE5 (Kass et al., 2007); inhibidores de la PKG como Rp-8-Br-cGMPS, o de los canales CNG como L-cis-diltiazem (Xu et al., 1999), e incluso sustancias permeables análogas a cGMP como 8-Br-cGMP (Pineda et al., 1996), que imitarían las acciones de este nucleótido. Por último, el estudio del efecto de NO presenta el hándicap de su administración exógena a muestras biológicas dada su alta reactividad y corta vida media, recurriéndose al empleo de sustancias donantes de NO. Los donantes de NO son sustancias capaces de descomponerse en soluciones fisiológicas liberando NO del resto de la molécula. Existen diversos tipos de donantes de NO, desde la nitroglicerina (la más antigua) o el nitroprusiato sódico (SNP), que requieren su metabolización a NO por el tejido, los S-nitrosotioles como la S-nitrocisteína (SNC) que son capaces de liberar NO extracelularmente en presencia de metales, o los más modernos como la dietilamina de NO (DEA-NO) que libera NO extracelularmente en un medio neutro (Li y Lancaster, 2009).

3. Las células intersticiales de Cajal (ICC)

3.1 Breve historia de ICC

La aparición de D. Santiago Ramón y Cajal en el mundo de la neurociencia provocó un cambio radical en el curso de su historia. A diferencia de otros grandes investigadores, Cajal no hizo un solo descubrimiento, sino que realizó numerosas e importantes contribuciones al conocimiento de la estructura y función del sistema nervioso.

Dentro de su fructífera labor investigadora, una pequeña parte de su obra, posiblemente la menos conocida, la dedica al estudio del sistema nervioso vegetativo. En relación con los plexos nerviosos del intestino de rana (1892) y de mamíferos (1911), descubre la presencia de "ciertos corpúsculos nerviosos" que describe como: *"células fusiformes o triangulares de pequeña talla, pobres en protoplasma, del cual parten varias expansiones varicosas, larguísimas y de ordinario ramificadas en ángulo recto"*.

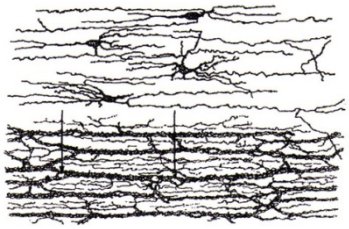

Figura V. Dibujo realizado por Cajal en 1911 de las células intersticiales situadas en el plexo muscular profundo del intestino. En la parte superior se muestran éstas, mientras que en la parte inferior están acompañadas de las fibras nerviosas. Las flechas indican los huecos reconocidos por Cajal como los cuerpos celulares de las ICC. (Cajal, 1911).

Por su morfología (expansiones largas, varicosas y ramificadas), características tintoriales (se teñían muy bien con azul de metileno y cromato de plata mostrando neurofibrillas) y relación con las fibras nerviosas, Cajal las consideró *"positivamente neuronas pero de carácter primitivo… a la manera de los elementos nerviosos más rudimentarios de la hidra y otros invertebrados"*. Estas células fueron confirmadas por otros autores de la época siendo precisamente Dogiel quien al reconocer su paternidad, les atribuye el nombre con el que hoy en día son reconocidas universalmente: Células Intersticiales de Cajal. También Kölliker ve en sus preparaciones estas células y en contra de la opinión de Cajal (neuronas primitivas) se inclina a estimarlas como células conectivas, iniciándose así una polémica que ha llegado hasta nuestros días. Desechando su carácter neural, hoy en día se considera que las ICC son de naturaleza mesenquimatosa (Young et al., 1996; Lecoin et al., 1996), al igual que las células musculares lisas produciéndose la transformación fenotípica de unas en otras en función del ambiente químico (Sanders, 2006). Sin embargo, hace algunos años, diversos autores establecen que, al menos una parte de las ICC, se originaría a partir de células

totipotentes procedentes de la parte ventral del tubo neural (células VENT = *ventrally emigrating neural tube*) (Sohal et al., 2002), lo cual estaría de acuerdo con los planteamientos de Cajal acerca del origen neural de las ICC. Aún hoy en día, el verdadero origen de las ICC no está del todo aclarado, incluso pudiera ser posible la existencia de diferentes tipos de ICC con distinto origen embriológico y papel funcional (Sanders, 2006).

La ausencia de un marcador específico que las distinguiera de otras células (neuronas, fibroblastos y células musculares lisas) con las que comparten características, ha hecho que su naturaleza, origen embrionario y función, hayan sido tema de debate entre los distintos grupos de investigadores. Es más, hasta hace pocos años podíamos encontrar importantes revisiones sobre la funcionalidad del tubo digestivo en las que no se mencionaban las ICC, no eran necesarias para explicar la motilidad intestinal, simplemente porque estas células no existían para muchos investigadores, aunque Cajal las había descrito perfectamente 100 años atrás.

Las descripciones ultraestructurales apuntaron ya su importante papel funcional: las *ondas lentas*, generadas en las ICC, que marcan el ritmo (*pacemakers*) de la actividad de la musculatura lisa del aparato digestivo. Las ICC intramusculares y las del plexo muscular profundo actuarían como mediadoras entre la señal motora llegada del Sistema Nervioso Entérico y la musculatura lisa. Aunque parezca sorprendente, dados los conocimientos de la época, Cajal ya propuso este modelo funcional.

Cajal describe también estas células en el páncreas. Deduce, razonablemente, que éstas células estarán, "casi con seguridad", presentes como neuronas intersticiales en todas las glándulas y en aquellas localizaciones terminales del simpático en las que coexistan músculo liso e inervación autónoma. Efectivamente, en estos últimos años se ha demostrado la presencia de células similares a las descritas por Cajal en diferentes estructuras musculares lisas que reciben inervación autónoma como la próstata (Exintaris et al., 2002; Popescu et al., 2005; Shafik et al., 2005a), vasos sanguíneos (Harhun et al., 2005; Povstyan et al., 2003), pene (Hashitani y Suzuki, 2004; Shafik, 2007), vagina (Shafik et al., 2005b), útero (Shafik et al., 2004a), vejiga (Shafik et al., 2004b), uréter (Metzger et al., 2004), útero (Duquette et al., 2005) y uretra (Sergeant et al., 2000) entre otras.

3.2 ICC en el tracto digestivo

Debido a que las ICC fueron inicialmente descubiertas en el tracto digestivo y la mayor parte de los conocimientos de que se disponen actualmente proceden de este órgano, realizaremos unas consideraciones generales sobre las características de las ICC gastrointestinales antes de centrarnos en las ICC del tracto urinario y en particular de la uretra.

3.2.1 Generalidades, morfología, funciones, tipos y distribución

Las ICC podrían considerarse como una población especializada de células musculares lisas (SMC: *smooth muscle cells*) puesto que ambas provienen de células mesenquimatosas comunes (Lecoin et al, 1996; Young, 1999). Sin embargo, mientras las SMC poseen elementos contráctiles, las ICC disponen de muy pocos. Estas últimas presentan un cuerpo celular fusiforme con escaso citoplasma, un núcleo ovoide y una gran cantidad de prolongaciones dendríticas celulares (Sanders, 1996). Desde dos a cinco prolongaciones dendríticas primarias pueden ramificarse en diversos procesos secundarios y hasta terciarios (Faussone-Pellegrini y Thuneberg, 1999). Estudios de microscopía electrónica muestran las características principales de las ICC incluyendo la presencia de filamentos intermedios, gran cantidad de mitocondrias, abundante retículo endoplásmico, ribosomas libres, canales iónicos de membrana, caveolina, lámina basal, íntimos contactos con varicosidades nerviosas y la formación de uniones intercelulares comunicantes (GJ: del inglés *gap junctions*) entre ellas y con las SMC (Faussone-Pellegrini y Thuneberg, 1999; Faussone-Pellegrini et al, 1989; Rumessen et al., 1992). Sin embargo, no todas las ICC presentan las mismas características estructurales.

Una gran parte de las ICC expresan el receptor **c-kit**, un receptor tirosin kinasa específico de membrana. El desarrollo de anticuerpos específicos anti c-kit (Sanders, 1996) ha permitido su reconocimiento en diferentes tejidos animales y humanos (Torihashi et al., 1997; Lammie et al., 1994; Vanderwinden et al., 1996). El ligando natural de c-kit es un factor de crecimiento llamado scf (*stem cell factor o steel factor:* factor estimulante de colonias), producido por SMC y células nerviosas y conocido por su papel esencial en el desarrollo y diferenciación de ciertas células incluidos melanocitos, células hematopoyéticas, mastocitos e ICC (Huizinga et al., 1995), pero ninguna otra a nivel del tubo digestivo. Por esto, el receptor c-kit permite diferenciar a las ICC como una categoría celular independiente a la de los fibroblastos. El reconocimiento de la expresión de c-kit se ha usado como marcador histológico de ICC (Maeda et al., 1992). En este sentido, se ha demostrado que existen al menos tres tipos diferentes de ICC positivas para c-kit, 1) algunas de ellas son más parecidas a SMC, presentando lámina basal y abundante caveolina, 2) otras difieren de las SMC puesto que no contienen ni lámina basal ni caveolina, y por último 3) aquellas intermedias que presentan caveolina y una lámina basal muy escasa, casi inexistente (Komuro, 2006). Estas diferencias probablemente representan diferentes tipos funcionales de ICC.

Sin embargo, no todas las ICC expresan c-kit. Se ha comprobado que las ICC presentes en la capa muscular profunda (ICC-DMP) del intestino delgado humano no poseen receptor específico c-kit (Torihashi et al., 1999; Wang et al., 2003a). Además otras células tales como mastocitos, melanocitos, neuronas y células de la glía también expresan c-kit, por lo que hay que tener en cuenta que no es un marcador específico de ICC y por lo tanto su uso exclusivo podría llevar a equivocaciones a la hora de identificar ICC en determinadas circunstancias (Zhang y Fedoroff, 1997). Otro de los marcadores utilizados para el reconocimiento de estas células es **vimentina**, marcador

de filamentos intermedios, la cual no se expresa en las SMC vecinas (Rumessen y Thuneberg, 1996). **CD34**, glicoproteína presente en células endoteliales y mesenquimatosas (Pusztaszeri et al., 2006), también ha sido empleado como marcador alternativo de ICC, aunque algunos investigadores consideran que éste es un marcador de fibroblastos pero no de ICC (Vanderwinden et al., 1999, 2000; Pieri et al., 2008). No obstante, estudios de PCR inversa y microscopía confocal han demostrado la co-expresión de c-kit y CD34 en ICC (Robinson et al., 2000; Hirota et al., 1998). Por último, el receptor del factor de crecimiento derivado de plaquetas (**PDGFRα**) también ha sido recientemente propuesto como un nuevo marcador de células similares a ICC pero c-kit negativas en el tracto gastrointestinal, sugiriéndose que al igual que CD34 es un marcador de fibroblastos (Iino et al., 2009; Iino y Nojyo, 2009; Kurahashi et al., 2012). El debate actual se centra en si las células positivas a estos marcadores alternativos, pero negativas a c-kit, serían o no verdaderas ICC con diferente función (Vanderwinden et al., 2000).

Se ha sugerido que las ICC pueden cumplir tres funciones principales en el tracto gastrointestinal: 1) Servir como células marcapasos mediante la generación de oscilaciones rítmicas eléctricas espontáneas, también llamadas ondas lentas, que dan lugar a contracciones en el músculo liso (Torihashi et al., 1995; Dickens et al., 1999; Sanders et al., 2000), y facilitar la propagación activa de los eventos eléctricos (Faussone-Pellegrini et al., 1977; Thuneberg, 1982), debido a la existencia de GJ entre ICC y SMC; 2) Actuar como conexión entre nervios entéricos y células musculares lisas, participando en la neurotransmisión y en la regulación de la motilidad gastrointestinal (Sanders, 1996; Ward, 2000); y 3) Participar en la transmisión aferente o sensorial. Sin embargo**,** esta última función hasta el momento no ha recibido suficiente contrastación experimental aunque se han descrito asociaciones íntimas entre las ICC y terminales aferentes intramusculares y algunos autores han sugerido que las ICC pueden comportarse como mecanorreceptores (Faussone-Pellegrini, 1992, Won et al., 2005).

Las ICC están distribuidas en localizaciones específicas del tracto digestivo (Ward, 2000), desde el esófago inferior hasta el ano (Torihashi et al., 1999) y dependiendo de su localización se pueden clasificar en distintos subtipos que presentan morfología y funciones diferentes:

En la mayor parte del tubo digestivo existe una extensa red de ICC en el plexo mientérico, entre la capa muscular longitudinal y circular: **ICC-MY** (también llamadas **ICC-AP o ICC-MP**). Se localizan principalmente en estómago e intestino delgado y actúan como células marcapasos generando ondas lentas en la túnica muscular (Ward et al., 2000a). Son células multipolares que están intercaladas entre las neuronas intramurales y las células musculares lisas formando un retículo, y suelen estar asociadas a terminaciones nerviosas y capilares sanguíneos (Huizinga, 2001; Ward y Sanders, 2001). Presentan grandes prolongaciones y conectan con otras ICC adyacentes mediante GJ. Poseen una abundancia de mitocondrias y retículo endoplásmico o aparato de Golgi, ribosomas libres, un abundante y electrodenso citoplasma, así como gránulos

electrodensos que contienen caveolina en la membrana plasmática (Takayama et al., 2002).

Existe una segunda población de ICC denominadas intramusculares: **ICC-IM (**o **ICC-M)**, que se localizan dispersas tanto en la capa muscular longitudinal como circular, generalmente en la proximidad de nervios entéricos motores (Ward et al., 2000b). En el intestino delgado, las ICC-IM principales están concentradas en la cara interna de la capa circular y son las encargadas de propagar la onda de activación. Parece ser que estas células también pueden generar ondas lentas en el corpus del estómago que carece de ICC-MY (Hashitani et al., 2005). Las ICC-IM poseen menos mitocondrias y retículo endoplásmico, pero tienen gran cantidad de filamentos intermedios en su citoplasma y abundantes GJ con las SMC, permitiendo un contacto directo entre ellas. Aunque también se ha demostrado la formación de uniones similares a sinapsis entre ICC y la célula muscular lisa adyacente, sugiriendo la posible existencia de una comunicación química (Harhun et al., 2004). Se caracterizan por ser alargadas y bipolares y se considera que son las mediadoras de la neurotransmisión entérica neuromuscular (Ward, 2000). Forman íntimos contactos con varicosidades de neuronas motoras entéricas y median entradas neurales excitatorias e inhibitorias al músculo liso (Ward, 2000; Ward et al., 2000b; Manneschi et al., 2004). Estudios funcionales han confirmado que estas células actúan como diana de numerosos transmisores como NO, SP, ACh, entre otros (Ward et al., 2000b; Forrest et al., 2006). Además, debido a la presencia de receptores para autacoides y hormonas circulantes como la colecistoquinina (CCK), podrían participar en la regulación hormonal muscular (Takayama et al., 2002). En algunos casos las ICC-IM también están asociadas a terminales nerviosas aferentes que transmiten información mecanorreceptiva procedente de la pared muscular (Iino y Horiguchi, 2006; Fox et al., 2000).

Horiguchi et al., (2001) describen una tercera población de ICC denominada **ICC-SEP**, que se sitúa entre los fascículos de músculo liso circular, y que probablemente juegue un papel importante en la transmisión de la información eléctrica desde el plexo mientérico hasta la capa muscular circular. Aunque este subtipo celular puede generar ondas lentas no es el principal foco marcapasos del tracto gastrointestinal sino que, en analogía con las fibras de Purkinje del corazón, su función sería la de conducir dicha actividad eléctrica hacia tejidos distantes (Hirst, 2001).

Otra población ya descrita por Cajal en 1893 son las **ICC-DMP** (*deep muscular plexus*), que están localizadas en la capa muscular profunda del intestino delgado, normalmente en íntimo contacto con varicosidades y troncos nerviosos. Suelen estar interconectadas entre ellas y con el músculo liso mediante GJ, formando una unidad dentro de la pared muscular que está sincronizada eléctricamente. También poseen un citoplasma electrodenso, numerosas mitocondrias y caveolina en la membrana plasmática. Posiblemente este subtipo de células también podrían tener un papel como mediadoras de la neurotransmisión y la regulación humoral muscular (Takayama et al., 2002). Una de sus características más destacada es su falta de reactividad a c-kit (Torihashi et al., 1999; Wang et al., 2003a).

Además en la capa submucosa del estómago y en el plexo submuscular del colon residen dos grupos de ICC denominadas **ICC-SM** e **ICC-SMP** respectivamente. Sus ejes celulares discurren paralelos a algunas células musculares lisas de la capa circular, aunque en otras ocasiones se trata de células multipolares que forman redes no muy densas entre ellas (Kunisawa y Komuro, 2004). En la actualidad se cree que las ICC-SMP son las principales células marcapasos en el colon (Pluja et al., 2001; Takaki, 2003).

Por último, se ha descrito una población de ICC con morfología estrellada en la capa serosa de intestino delgado y colon de ratón, denominada **ICC-SR** (Thuneberg, 1982; Vanderwinden et al., 2000), cuya función está todavía por determinar.

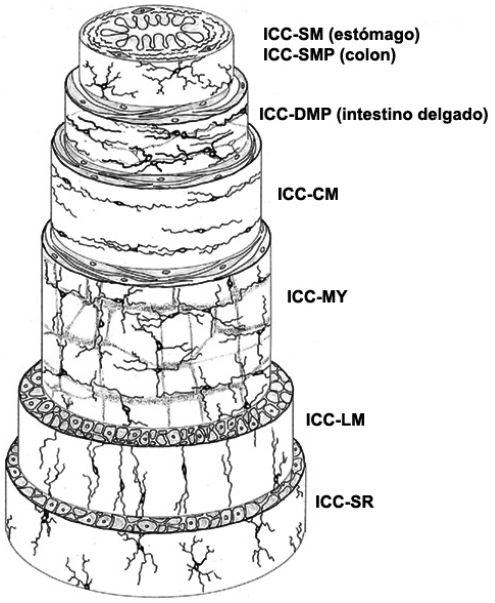

Figura VI. Representación esquemática de la distribución de las ICC en las diferentes capas histológicas a lo largo del tracto gastrointestinal. Adaptado de Hanani et al., 2005.

3.2.2 Papel marcapasos de ICC gastrointestinales

Muchos segmentos del tubo digestivo, al ser estudiados en tiras de tejidos aisladas, exhiben actividad contráctil rítmica aunque no reciban estímulos eléctricos u hormonales. Cuando se registran simultáneamente los potenciales de acción y la contracción mecánica, cada contracción es generada por una onda de despolarización. Por su baja frecuencia y larga duración, estas ondas se han denominado *"ondas lentas"*. Estas consisten en una rápida despolarización, una repolarización parcial y una fase de meseta sostenida seguida de una progresiva y completa repolarización hasta alcanzar el potencial de membrana en reposo (**Fig. VIIA**). Estas oscilaciones espontáneas del potencial de membrana no se inhiben con bloqueantes de canales de Ca^{2+} de tipo L (Cayabyab et al., 1996), aunque sí que son eliminadas con bloqueantes del receptor IP_3, responsable de la liberación de Ca^{2+} intracelular (Henning et al., 2004).

Hoy se admite que las principales generadoras de las ondas lentas gastrointestinales son las ICC, ICC-MY en estómago e intestino, ICC-IM en el corpus del estómago e ICC-SMP en el colón, fundamentalmente. Numerosas evidencias experimentales apoyan este papel marcapasos de las ICC. La disección de ICC-SMP en el colon bloquea la generación de ondas lentas en diversas especies (Smith et al., 1987; Du y Conklin, 1989; Pluja et al., 2001) y músculos gástricos carentes de ICC-MY (o con pérdida parcial de éstas), no son capaces de generar ondas lentas (Ördög et al., 1999). El empleo de drogas que lesionan a las ICC, como son el azul de metileno y la Rodamina 123, bloquea las ondas lentas e inhibe la actividad espontánea (Ward y Sanders, 1990). Además, estudios electrofisiológicos realizados en cultivos celulares de ICC o ICC aisladas han mostrado que estas células generan actividad eléctrica espontánea (Ward y Sanders, 2001), mientras que las SMC colindantes no poseen mecanismos de generación y regeneración de las ondas lentas (Horowitz et al., 1999). Además, se han utilizado modelos animales mutantes como el ratón W/W^V y la rata Ws/Ws que al presentar mutaciones en el protooncogen c-kit, localizado en el locus *W* (*white spotting*) en el ratón y en *Ws* en la rata, que codifica el receptor tirosinquinasa, dan lugar a una proteína kit anormal que impide el desarrollo normal de ciertas clases de ICC, permitiendo así estudiar el papel de estas células en diversas funciones (Huizinga et al., 1995). Otros modelos empleados son el ratón mutante Sl/Sl^d que tiene una mutación en el *"steel"* locus que afecta al gen que codifica el scf y el reciente ratón mutante W^{jic}/W^{jic} (Iino et al., 2011), los cuales también han mostrado alteraciones en algunas ICC y en la generación de ondas lentas. Así, en ratones W/W^V, las ICC-MY del intestino delgado están altamente disminuidas en número (Daniel et al., 2004) y las ondas lentas son abolidas (Huizinga et al., 1995), (**Fig. VII**). El estómago de los ratones W/W^V también carece de ICC-IM, pero sí poseen ICC-MY (Huizinga, 2001). En ratones Sl/Sl^d no existen ICC-MY en intestino delgado y no se generan ondas lentas (Beckett et al., 2002).

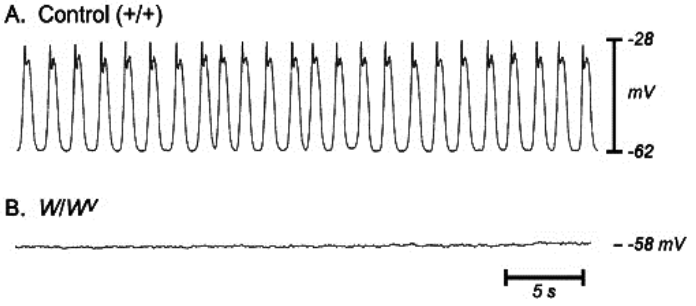

Figura VII. Actividad eléctrica registrada en intestino delgado de ratón control (*A*) y de ratón mutante W/W^V (*B*). Se observa la ausencia de ondas lentas en ratones W/W^V (Sanders y Ward, 2007).

La actividad marcapasos de las ICC depende del movimiento de Ca^{2+} entre compartimentos intracelulares (mitocondrias y retículo endoplásmico), mediado por bombas, canales específicos y receptores IP_3 (Liu et al., 1995; Sanders et al., 2000; Ward et al., 2000a) originando oscilaciones rítmicas del Ca^{2+} citosólico. Parece ser que la liberación de Ca^{2+} desde el retículo endoplásmico mediada por receptores de IP_3 es el evento celular fundamental que dispara la actividad marcapasos. Además, diversas

investigaciones han sugerido que la actividad eléctrica rítmica es la consecuencia de la apertura periódica de canales catiónicos no selectivos, no sensibles a voltaje (Takeda et al., 2008), o canales de Cl^- (Huizinga et al., 2002; Zhu et al., 2009), siendo su apertura causada a su vez por oscilaciones del Ca^{2+} intracelular (Ward et al., 2000a). De esta forma, la corriente de Cl^- sería activada por el Ca^{2+} liberado a consecuencia de la activación de los receptores de IP_3 en ICC (Hirst et al., 2002). Este hecho ha sido demostrado en experimentos farmacológicos usando cultivos de ICC o tiras musculares lisas intactas (Ward et al., 2000b), y experimentos con ratones mutantes carentes del receptor IP_3 (Suzuki et al., 2000). Estudios recientes han mostrado la expresión de canales de Cl^- activados por Ca^{2+} (CaCC) en ICC del tracto digestivo (Gómez-Pinilla et al., 2009) y su importancia en la generación de las ondas lentas (Hwang et al., 2009).

La activación de las ondas lentas y su propagación activa posterior, constaría de 4 fases. En la primera de ellas, los receptores de IP_3 liberan una pequeña ráfaga de Ca^{2+} en el espacio presente entre el retículo endoplásmico y la mitocondria. En la segunda fase, este Ca^{2+} da lugar a la apertura de un transportador de Ca^{2+} de la membrana mitocondrial, causando la entrada del catión a la mitocondria con el consecuente descenso de la concentración del Ca^{2+} en el espacio citoplasmático existente entre la mitocondria y la membrana plasmática. Este descenso local del Ca^{2+} citoplasmático produce la apertura de un canal catiónico no selectivo de la membrana plasmática y la corriente entrante de Ca^{2+} da lugar a la despolarización de la célula marcapasos primaria o unidad marcapasos. En la cuarta y última fase, las células vecinas a la unidad marcapasos (células marcapasos secundarias) son despolarizadas, dando lugar a la propagación de la onda lenta (Ward et al., 2000a; Kim et al., 2002; Suzuki et al., 2000).

Las conexiones entre unas ICC y otras, así como entre éstas y las SMC es un aspecto crítico en la función marcapasos. En el tracto gastrointestinal se cree que estas ICC están conectadas entre sí mediante GJ, permitiendo que los mensajes eléctricos se transmitan rápidamente entre la red interconectada de ICC, lo que facilita su comportamiento como marcapasos (Belzer et al., 2002; 2004). Las GJ son canales intercelulares formados por el acoplamiento de dos conexones o hemicanales en células vecinas. Cada conexón está formado por la asociación de 6 subunidades proteicas o conexinas (Cx), de las cuales se han descrito al menos 20 tipos diferentes, nombradas de acuerdo a su peso molecular (Willecke et al., 2002), formando así conexones homo- o heteroméricos, formados por Cx iguales o diferentes, respectivamente que dan lugar a su vez a GJ homo- o heterotípicas dependiendo de si se han formado por el acoplamiento de dos conexones iguales o distintos. Mediante la combinación de técnicas electrofisiológicas y experimentos de disección se ha visto que las ondas lentas se propagan en tres direcciones en la capa de músculo circular mediante un proceso activo y regenerativo (Bauer et al., 1985). Esta propagación sigue la siguiente secuencia: ICC-MY→ICC-IM→SMC, dando lugar a la contracción del músculo liso (Henning et al., 2004). Así, las ICC-MY actuarían generando las ondas lentas, mientras que las ICC-IM regenerarían la respuesta eléctrica y permitirían su propagación hacía el músculo liso.

3.2.3 Papel de ICC como mediadoras de la neurotransmisión

El Sistema Nervioso Entérico regula la excitabilidad del músculo liso que a su vez es generada por las células marcapasos. En éste intervienen neuronas aferentes, interneuronas y neuronas motoras. La mayoría de las neuronas motoras que inervan la capa de músculo circular liberan neurotransmisores inhibitorios tales como NO (posiblemente junto a CO) (Szurszewski y Farrugia, 2004), ATP y VIP (Okishio et al., 2000). Sin embargo, la capa longitudinal está inervada por neuronas motoras excitatorias, las cuales liberan ACh y taquininas.

El concepto clásico de transmisión neuromuscular postula que ésta ocurre a través de la liberación y difusión del neurotransmisor desde las terminaciones nerviosas motoras y su posterior unión y activación de los receptores postsinápticos presentes en las SMC vecinas (**Fig. VIIIA**). Sin embargo, estudios morfofisiológicos recientes consideran que este concepto está incompleto y exponen un modelo alternativo o *"teoría de la intercalación"* (**Fig. VIIIB**), ya propuesta en 1911 por Santiago Ramón y Cajal, en el cual el neurotransmisor liberado por la neurona motora se uniría en primer lugar a sus receptores específicos expresados en las ICC.

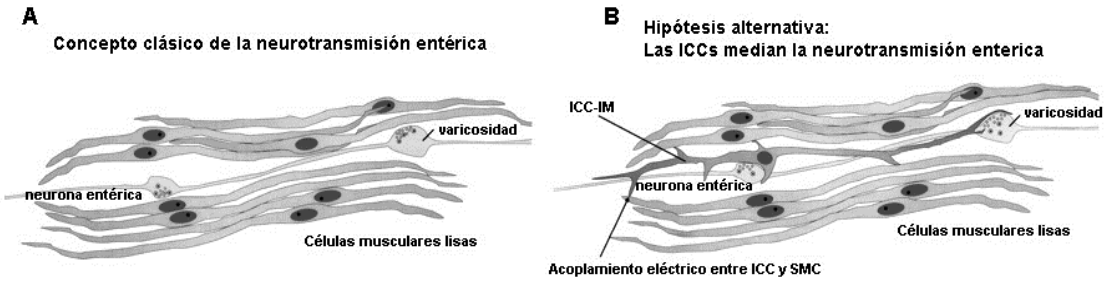

Figura VIII. Concepto clásico de la neurotransmisión entérica (A) y modelo alternativo ya propuesto anteriormente por Santiago Ramón y Cajal, en el cual las ICC actuarían como mediadoras de la neurotransmisión localizándose entre las terminaciones nerviosas motoras y las SMC (B). Adaptado de Ward, 2000.

Se ha demostrado la existencia de uniones sinápticas entre varicosidades nerviosas entéricas e ICC en varias regiones del tracto gastrointestinal lo que permitiría una efectiva neurotransmisión. Así, estudios ultraestructurales describen las varicosidades nerviosas en íntimo contacto con el cuerpo celular y prolongaciones de las ICC, mediante uniones de aproximadamente 20 nm, las cuales presentan tanto vesículas sinápticas pequeñas agranuladas como grandes y granuladas (Faussone-Pellegrini et al., 1989; Faussone-Pellegrini 1992). Estudios inmunohistoquímicos y fisiológicos en diferentes áreas han mostrado la existencia de una íntima relación entre ICC y las terminaciones nerviosas tanto excitadoras, conteniendo ACh o SP como inhibitorias, conteniendo NO (Ward et al., 2000b; Manneschi et al., 2004), sugiriendo su función como diana de los diferentes neurotransmisores.

Las principales evidencias que apoyan el papel intermediario de las ICC en la neurotransmisión provienen de diversos estudios que muestran la presencia de receptores específicos para los diversos transmisores localizados en ICC (Wang et al., 2000). Estos receptores son entre otros, muscarínicos para ACh, neurokininas para SP y VIP, y sGC en el caso de NO. El uso de técnicas moleculares ha permitido también demostrar la expresión de mRNA de los receptores proteicos presentes en estas células (Epperson et al., 2000; Hirst y Ward, 2003). Un resumen de los receptores descubiertos en ICC se presenta en la **Tabla I**. Hay autores que sugieren que aunque los mecanismos de transducción de señales de los neurotransmisores sean expresados tanto en SMC como por ICC, la íntima proximidad de éstas últimas con las terminaciones nerviosas puede hacer que reciban mayor concentración de sustancias neurotransmisoras (Sanders, 2000).

Tabla I. Receptores presentes en ICC

Receptores	Subtipo de ICC	Referencias
5-HT3, 5-HT4	ICC-MY, -DMP	Liu et al., 2005; Poole et al., 2006
Bombesina-3	Todas ICC	Porcher et al., 2005
CCK	Todas ICC	Patterson et al., 2001
PKA, PKC	Todas ICC	Southwell, 2003; Poole et al., 2004
M2, M3 (ACh)	ICC-IM, -MY, -DMP	Epperson et al, 2000; Iino y Nojyo, 2006
NK1, NK3	ICC-IM, -MY, -DMP	Epperson et al, 2000; Iino et al., 2004
P2Y1,P2Y4,	ICC-IM,-MY,-DMP	Burnstock y Lavin, 2002; Chen et al, 2007
P2X2, P2X5	ICC-IM,-MY,-DMP	Van Nassauw et al, 2006
Somatostatina 2A	ICC-DMP	Sternini et al, 1997
VIP	ICC-IM, -MY	Epperson et al, 2000
sGC	Todas ICC	Salmhofer et al., 2001; Iino et al, 2005

5-HT, serotonina; PKA, proteína kinasa A; PKC, proteína kinasa C; M2 y M3, receptores muscarínicos; NK, neuroquinina; P2Y1, P2Y4, P2X2, P2X5, receptores purinérgicos; VIP, péptido intestinal vasoactivo, sGC, guanilato ciclasa.

Estudios con ratones mutantes han demostrado que las respuestas a estimulación nerviosa en el músculo del estómago o del esfínter esofágico inferior, carentes de ICC-IM están enormemente reducidas (Ward et al., 2000b; Beckett et al., 2002). Asimismo, en estudios *in vitro* con ratones W/W^V (Ward et al., 2000b; Burns et al., 1996) y Sl/Sl^d (Beckett et al., 2002) se ha observado que las ICC-IM son esenciales para la neurotransmisión colinérgica y especialmente nitrérgica tanto en el estómago como en el esfínter esofágico inferior. En el intestino delgado, sin embargo, las ICC que parecen

estar más implicadas en la neurotransmisión son las ICC-DMP concentradas en la capa muscular profunda (Wang et al., 2003a; Iino et al., 2004; Ward et al., 2006).

Si bien parece claro el papel mediador de las ICC en la neurotransmisión entérica, en la actualidad no se conoce como se transmite el mensaje desde las ICC a las SMC. La hipótesis clásica asume una transmisión eléctrica directa gracias a la existencia de GJ entre ICC y SMC, aunque algunos trabajos apuntan que estas GJ no son esenciales para esta transmisión nerviosa (Daniel, 2004; Daniel et al., 2007).

3.2.4 ICC como mecanorreceptores

La hipótesis de que las ICC podrían actuar como sensores de estiramiento ha sido propuesta en repetidas ocasiones (Faussone-Pellegrini y Thuneberg, 1999; Thuneberg, 1989) en base a la existencia de unas estructuras denominadas uniones *"peg and socket"* a través de las cuales una SMC puede formar una extensión citoplasmática dentro de otra SMC o de una ICC. Con un tamaño de unos 5 μm constituyen la zona más vulnerable a la tensión en las SMC y su morfología y orientación sugieren que podrían actuar como mecanosensores de estiramiento, regulando el acoplamiento entre SMC e ICC y la sensibilidad de la capa muscular frente al mismo (Thuneberg y Peters, 2001).

Pero quizás, la evidencia fisiológica más solida que apoya la función de las ICC como mecanorreceptores se obtuvo mediante la aplicación de rampas de estiramiento y el registro simultáneo de la actividad intracelular eléctrica y la fuerza isométrica en preparaciones musculares del estómago de ratones (Won et al., 2005). El aumento de la longitud muscular daba lugar a la despolarización de la membrana y un aumento en la frecuencia de generación de ondas lentas. Se demostró que esta respuesta estaba mediada por ICC-IM puesto que estaba ausente en ratones W/W^V, y que en ella se hallaba implicada la enzima ciclooxigenasa II (COX-II) ya que era inhibida por indometacina y no estaba presente en ratones carentes de esta enzima (Won et al., 2005). COX-II se sabe que se expresa de forma constitutiva en ICC-IM (Porcher et al., 2002) y está implicada en la cascada de las prostaglandinas. Por lo tanto, se ha sugerido que productos derivados del metabolismo del ácido araquidónico, tales como la prostaglandina E2 (PGE_2) puedan ser los mediadores de las respuestas inducidas por estiramiento.

3.2.5 Implicación de ICC en patologías gastrointestinales

La implicación de las ICC en la actividad rítmica del tubo digestivo explica que su disminución o desaparición genere trastornos motores del estómago o del intestino, como ha sido observado en humanos (Sanders, 2006).

La serie de patologías digestivas que se piensa son producidas por la pérdida, reducción o daño de las ICC son: perforación gástrica idiopática, estenosis pilórica hipertrófica, pseudoobstrucción intestinal en neonatos, enfermedad de Hirschprung, aganglionosis colónica, displasia neuronal intestinal, hipoganglionosis, gastroparesis, pseudoobstrucción intestinal idiopática crónica, gastroenteropatía diabética, enfermedad de Chagas, o enfermedades inflamatorias intestinales como la colitis ulcerativa y la enfermedad de Crohn (ver revisión de Streutker et al., 2007).

Las ICC también están involucradas en la formación de los tumores gastrointestinales del estroma (GIST), previamente clasificados como tumores del músculo liso, y que constituyen la mayoría de los tumores mesenquimatosos del tubo digestivo, siendo más comunes en estómago (50-60%) e intestino delgado (20-30%). La mayor parte de estos surgen por una mutación en el gen c-kit que se independiza de la activación por scf, lo que origina división celular incontrolada e inestabilidad genómica (Taniguchi et al., 1999). Diseñar terapias para estos tumores será posible en la medida en que se conozcan las bases moleculares y genéticas de esta transformación (Sanders et al., 2002). En modelos preclínicos, la administración oral de un fármaco denominado mesilato de imatinib o Glivec®, antagonista de los receptores c-kit, mostró una eficaz inhibición de los GIST (Joensuu et al., 2001). Desde entonces, varios ensayos clínicos se han llevado a cabo con excelentes resultados (Verweij et al., 2004; Scaife el at., 2003). Más recientemente, dos nuevos inhibidores de c-kit, sunitinib (Demetri et al., 2006; Goodman et al., 2007) y PKC412 (Debiec-Rychter et al., 2005; Growney et al., 2005) han mostrado resultados prometedores contra tumores GIST resistentes a imatinib.

3.3 ICC en el tracto urinario

El tracto urinario muestra cierta similitud con el tracto gastrointestinal inferior, ya que podría ser considerado como el sistema de eliminación de desechos líquidos, por analogía con el sistema de eliminación de residuos sólidos que es el tracto digestivo inferior. Ambos sistemas excretores podrían presentar mecanismos de control similares puesto que sólo la divergencia evolutiva los ha separado en mamíferos y otros vertebrados superiores, y por lo tanto su origen común podría ser la explicación de que mantengan esquemas estructurales equiparables.

Subyacente a sus funciones aparentemente muy diferentes, lo que estos órganos tienen en común es que todos ellos poseen una actividad rítmica eléctrica espontánea. En el caso del uréter la existencia de un marcapasos es bastante evidente puesto que inicia la propulsión de fluido desde el cáliz renal a la vejiga por medio de ondas peristálticas bien coordinadas cuyo origen es la pelvis renal. Éste es menos evidente en la vejiga y en la uretra, puesto que la mayor parte del tiempo la primera actúa como un órgano de almacenamiento, y la segunda permanece contraída tónicamente. No obstante, mediante la utilización de electrodos extra- (Prosser et al., 1955) e

intracelulares (Hashitani et al., 1996; Bradley et al 2004), se ha demostrado la existencia de esta actividad eléctrica espontánea en los tres órganos.

La presencia de ICC ha sido ampliamente estudiada en diferentes tejidos del tracto urinario por numerosos grupos de investigación. Las ICC del tracto urinario presentan las mismas características ultraestructurales que las gastrointestinales: un citoplasma con abundantes mitocondrias, caveolina, retículo endoplásmico, aparato de Golgi, filamentos finos (5 nm) e intermedios (10 nm) y una lámina basal incompleta (Sergeant et al., 2000). Su descubrimiento en la pelvis renal, uréter, vejiga y uretra no sólo ofrece nuevas oportunidades para avanzar en el estudio de las interacciones celulares en estos tejidos sino que también permite el desarrollo de nuevas terapias para el tratamiento de diferentes trastornos del tracto urinario (McCloskey, 2011).

Actualmente existe un amplio debate acerca de la nomenclatura que se debe adoptar para referirse a las ICC presentes en otros sistemas diferentes al gastrointestinal. En este sentido podemos encontrar diversos nombres en la literatura: células intersticiales (IC), células intersticiales de Cajal (ICC), células similares a ICC (*ICC-like cells*) o miofibroblastos. Esta cuestión fue objeto de discusión en el "5º Simposio Internacional de ICC", celebrado en Irlanda en Julio de 2007, donde se llegó al acuerdo de que estas células deben de ser denominadas como ICC con objeto de unificar la nomenclatura y permitir su comparación directa con las ICC gastrointestinales. Esta terminología actualmente define a una familia heterogénea de células presentes en muchos tejidos diferentes, incluyendo vejiga, uretra, uréteres, pelvis renal y en otros tejidos urogenitales y vasos sanguíneos, que posean propiedades morfológicas, ultraestructurales y fisiológicas características de las ICC.

3.3.1 Tracto urinario superior

Gracias a estudios inmunohistoquímicos utilizando el marcador específico c-kit, las ICC han sido descritas en el tracto urinario superior de varias especies animales (Metzger et al., 2005; 2008, Pezzone et al., 2003), así como en la especie humana (Metzger et al., 2004; Lee et al., 2011). Su distribución, morfología y características inmunohistoquímicas son similares a las ICC gastrointestinales (Pezzone et al., 2003). Se distinguen dos tipos, uno de ellos reside en el urotelio, mientras que el otro se encuentra entre las capas musculares y la lámina propia. Sin embargo, se considera que el marcapasos responsable de la peristalsis ureteral no reside en ICC sino en SMC modificadas localizadas en la región proximal de la pelvis renal, mientras que las ICC actuarían conduciendo y amplificando la señal marcapasos para iniciar el potencial de acción en el músculo liso (McHale et al., 2006). Lang et al., (2006) consideran la existencia de dos posibles tipos de células marcapasos, SMC atípicas e ICC, cuya participación relativa varía en los distintos segmentos ureterales. Incluso en situaciones de desconexión con el marcapasos primario de la pelvis renal (obstrucción pieloureteral o pieloplastia), las ICC serían capaces de mantener una peristalsis rudimentaria que

permitiera un adecuado movimiento de la orina desde el riñón hacia la vejiga (Lang et al., 2006).

3.3.2 Vejiga

Numerosos trabajos han confirmado la existencia de ICC situadas en la lámina propia y a lo largo del músculo detrusor de la vejiga de diferentes especies mediante la utilización de anticuerpos para c-kit, el marcador de ICC en el tracto gastrointestinal (McCloskey and Gurney, 2002; Hashitani et al., 2004; Biers et al., 2006; Shafik et al., 2004a; Piaseczna Piotrowska et al., 2004; Roosen et al., 2009). No obstante, en otros muchos casos la reacción a c-kit se describe como débil o inexistente (Smet et al., 1996; Sergeant et al., 2000; Pezzone et al., 2003; Brading y McCloskey, 2005), mientras que sí son positivas para vimentina (Sanders y Ward, 2006). Recientemente, en vejiga humana se ha identificado una población de ICC negativas para c-kit pero inmunoreactivas a CD34, y que presentan una morfología estrellada con largas prolongaciones que envuelven y se entremezclan entre los fascículos de músculo liso (Rasmussen et al., 2007). Existe controversia respecto a si estas células deben considerarse como verdaderas ICC. En este sentido, un trabajo reciente de Koh et al (2012) muestra un tipo de células positivas a PDGFRα, que también lo son para la vimentina y que se encuentran rodeando los fascículos musculares lisos y en estrecha relación con las terminaciones nerviosas, aunque no se puede probar la colocalización con c-kit ya que no se obtuvo señal alguna para este anticuerpo. El hecho de que en el tracto gastrointestinal, también aparezcan células negativas para c-kit (por ejemplo las ICC-DMP) ha sugerido la posibilidad de la existencia de diferentes subtipos de ICC con diferentes características morfológicas y/o funcionales (Vanderwinden et al., 2000).

En la vejiga podemos diferenciar la existencia de diferentes tipos de ICC en función de su localización. Una población está situada en la región de la lámina propia (**ICC-LP**), entre el urotelio y la capa muscular del detrusor (Sui et al., 2002; Davidson y McCloskey 2005). Estas ICC-LP presentan una morfología estrellada con numerosas prolongaciones muy cortas que emanan del cuerpo celular central (Davidson y McCloskey, 2005), y establecen conexiones entre sí mediante GJ compuestas principalmente por Cx43 (Sui et al., 2002; Wiseman et al., 2003), dando lugar a una red interconectada de células, íntimamente asociada a terminales nerviosas aferentes presentes en la submucosa (Davidson y McCloskey, 2005; Wiseman et al., 2003).

Un estudio reciente en vejiga humana ha descrito una nueva población de ICC asociada a los vasos sanguíneos presentes en la lámina propia (Johnston et al., 2010). Éstas forman una red que rodea los vasos, de manera que cada una de sus prolongaciones establece contacto con hasta seis SMC vasculares. Esta disposición que recuerda extraordinariamente la que presentan los astrocitos del sistema nervioso central les permitiría ejercer un control local de la perfusión del tejido en respuesta a sus necesidades metabólicas. Aunque hasta el momento esto constituye tan sólo una

hipótesis, el hecho de que modelos animales *in vivo* de isquemia desarrollen hiperactividad vesical (Azadzoi et al., 1999) demuestra la importancia funcional de la perfusión vascular en la contractilidad vesical.

Otra población de ICC (**ICC-IM** o **ICC-M)** se localiza en el interior de los fascículos de músculo liso del detrusor, paralelamente a las fibras musculares (McCloskey y Gurney, 2002; Hashitani et al., 2004; Davidson and McCloskey, 2005; McCloskey et al., 2009; Johnston et al., 2010). Las ICC-IM presentan una morfología alargada con extensas prolongaciones, y son similares ultraestructuralmente a las ICC ICC-IM del tracto gastrointestinal (Cunningham et al., 2011) y al igual que ellas se encuentran asociadas a terminaciones nerviosas presentes en el músculo detrusor (Davidson y McCloskey, 2005; Johnston et al., 2008). Además, las ICC-IM muestran incrementos de Ca^{2+} intracelular por la adición de ACh, efecto mediado a través de receptores M_3 (McCloskey, 2010), sugiriendo su participación como mediadoras de la neurotransmisión colinérgica. Incluso recientemente se ha descrito que estas células contienen en su interior vesículas, quizás indicativo de una posible función secretora (Cunningham et al., 2011; Rasmussen et al., 2009).

En los espacios existentes entre los haces musculares del detrusor se ha descrito otra población diferente de ICC positivas tanto para c-kit como para vimentina denominada **ICC-SEP** o **ICC-IB** (*interbundle ICC*) que presentan una morfología estrellada muy similar a las ICC-LP y que contactan unas con otras mediante uniones "*peg and socket"* y GJ, apoyando la existencia de una red interconectada de ICC entre los haces musculares (Brading y McCloskey, 2005).

Las diferentes poblaciones de ICC presentes en vejiga podrían formar un circuito interconectado mediante el cual puede viajar la información desde el urotelio hasta el músculo detrusor. Así, las ICC-LP, que forman una extensa red bajo el urotelio, podrían participar como intermediarias en las respuestas sensoriales (Brading y McCloskey, 2005; Grol et al., 2008; Ikeda et al., 2007; Sui et al., 2004) amplificando esta respuesta y mediando la señalización entre el urotelio y los nervios aferentes o la capa muscular (Fry et al., 2007), modulación que podría producirse también en sentido inverso (Birder, 2006). Alternativamente, las ICC-LP también podrían actuar como mecanorreceptores, siendo responsables de las sensaciones de llenado vesical y transmitiendo esta información a las aferentes sensoriales de la mucosa (Sui et al., 2004). A su vez las ICC-SEP y las ICC-IM formarían una red que regularía la función muscular, transmitiendo la información entre y dentro de los haces musculares, respectivamente.

Al igual que en el tracto gastrointestinal, el músculo liso de la vejiga tiene actividad espontánea asociada con la formación de ondas lentas. La localización de las ICC vesicales en la capa muscular lisa vesical, zona donde se originan las ondas espontáneas de Ca^{2+} (McCloskey y Gurney, 2002) y su analogía morfológica con las ICC gastrointestinales (Shafik et al., 2004a) sugiere que estas células podrían actuar como el marcapasos principal de esta actividad eléctrica. Sin embargo, estudios electrofisiológicos han demostrado que las SMC aisladas del músculo detrusor son

capaces de generar por sí solas potenciales de acción espontáneos idénticos a los registrados en preparaciones completas de este músculo (Hashitani et al., 2001). Por lo tanto, actualmente se piensa que las ICC vesicales, aunque son capaces generar actividad eléctrica, no tienen un papel marcapasos y la actividad espontánea sería generada por las SMC directamente, participando las ICC en modular la señal mediada por neurotransmisores (Hashitani et al., 2004; McHale et al., 2006).

3.3.3 Uretra

El estudio de las ICC uretrales es sin duda el más avanzado dentro del sistema urinario, especialmente en términos de fisiología celular. La primera evidencia fisiológica de que las ICC estuvieran presentes en la uretra y pudieran actuar como células marcapasos especializadas fue expuesta por Sergeant et al., en el año 2000. Mediante dispersión enzimática de músculo liso uretral de conejo estos investigadores observaron que además de SMC, había otra población de células no contráctiles más oscuras y delgadas y que poseían varias ramificaciones laterales. Estas células constituían el 5-10% del total de células presentes en este tejido y fueron reconocidas como ICC. Estudios inmunohistoquímicos mostraron que estas ICC se marcaban con vimentina pero no con miosina, mientras que en el caso de las SMC sucedía lo contrario. Mediante examen ultraestructural, se comprobó que sus características morfológicas eran similares a las ICC del tracto gastrointestinal. Sin embargo, las ICC uretrales no presentaron inmunoreactividad para el marcador c-kit, aunque estudios posteriores en preparaciones completas de uretra de conejo si han podido demostrar su inmunoreactividad a este anticuerpo (McHale et al., 2006; Lyons et al., 2007). La apariencia de las ICC positivas a c-kit fue similar a la descrita por Sergeant et al., (2000), distinguiéndose diferentes subtipos morfológicos: unipolares, bipolares, estrelladas, y alargadas con varias ramificaciones laterales (**Fig. IX**). Al igual que en la vejiga, pueden distinguirse diferentes subpoblaciones de ICC según su localización a lo largo de la pared uretral; ICC de la lámina propia (ICC-LP) e ICC intramusculares en o entre las capas musculares, tanto circulares como longitudinales (ICC-IM) e ICC interfasciculares (ICC-IB).

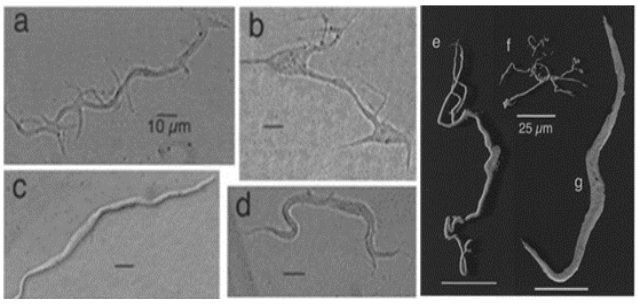

Figura IX. Morfología de ICC y SMC. Izquierda: imágenes obtenidas con microscopio de contraste de fases que muestran los diferentes subtipos morfológicos de las ICC uretrales (*a*, *b* y *d*) y la típica morfología de una SMC (*c*). Derecha: imágenes de microscopia confocal de dos ICC inmunoreactivas a vimentina (*e* y *f*) y una SMC marcada con miosina (*g*). Barra= 10 μm (*a- d*) y 25 μm (*e- g*). Adaptado de Sergeant et al., 2000.

El músculo liso de la uretra es capaz de jugar un papel importante en la continencia urinaria generando un tono suficiente para prevenir la salida de la orina desde la vejiga. Este tono es en parte de naturaleza miogénica y está también relacionado con la generación de ondas lentas. De hecho, en la mayoría de las especies estudiadas se observa actividad mecánica espontánea en la uretra, que también puede ser inducida por estimulación (Hashitani et al., 1996; Hashitani y Edwards, 1999). Mediante experimentos electrofisiológicos se ha observado que la actividad eléctrica registrada en ICC aisladas es semejante a la registrada en el tejido en su totalidad. Además, mientras sólo una pequeña minoría de SMC son activas espontáneamente, más del 80% de ICC generan actividad eléctrica (Sergeant et al., 2000). Por lo tanto, las despolarizaciones espontáneas registradas en el músculo liso uretral pueden atribuirse a corrientes internas generadas en las ICC (Hashitani et al., 1996). La suma de estas despolarizaciones espontáneas daría lugar a grandes despolarizaciones que alcanzarían el umbral necesario para abrir los canales de Ca^{2+}- tipo L del músculo (Hashitani y Edwards, 1999). Por lo tanto en la uretra, al menos en algunas especies, las ICC si parecen actuar como células marcapasos especializadas (Hollywood et al., 2003). La hipótesis actual sostiene que el disparo asincrónico de diferentes marcapasos simultáneamente permitiría el mantenimiento de un tono muscular continuo durante la fase de continencia (McHale et al., 2006), sobre el cual actuarían los neurotransmisores, aumentando o disminuyendo este tono basal.

Las bases iónicas que sustentan esta actividad eléctrica espontánea parecen no ser las mismas que en el tracto gastrointestinal. Dicha actividad en las ICC uretrales es inhibida en un medio libre de Ca^{2+} y por bloqueantes de canales CaCC (Sergeant et al., 2000), los cuales, al menos en la uretra de conejo, están distribuidos de forma específica en ICC pero no en SMC, sustentando su papel específico en la generación de la actividad eléctrica espontánea de las ICC uretrales (Sergeant et al., 2001a). Dentro de la extensa familia de los CaCC, el principal y más extendido es la Anoctamina-1 (ANO1; también conocido como TMEM16A) (Caputo et al., 2008; Schroeder et al., 2008; Yang et al., 2008). Mientras ANO1 está ausente en las SMC del tracto gastrointestinal, sí aparece expresado en una extensa red de ICC, lo que ha llevado a postular que ANO1 participe en la autorritmicidad y neurotransmisión del músculo liso gastrointestinal (Caputo et al., 2008; Sanders 1996; Zhu et al., 2009), y ha sido propuesto como un marcador específico de ICC en el tracto digestivo (Gómez-Pinilla et al., 2009). Sin embargo, hasta el momento no se había demostrado la presencia de ANO1 en SMC e ICC en la uretra de ratón, lo que pone de manifiesto que los sistemas gastrointestinal y urinario no comparten exactamente los mismos mecanismos (Huang et al., 2009).

La liberación de Ca^{2+} intracelular también sería, al igual que en las ICC del tracto digestivo, un elemento clave en la ritmicidad eléctrica de las ICC uretrales (Sergeant et al., 2001b). Sin embargo, en este caso el elemento desencadenante parece ser la activación de los receptores de rianodina (RyR) del retículo sarcoplásmico mientras que la activación de receptores de IP_3 contribuiría exclusivamente a la propagación posterior de la onda de Ca^{2+} hasta alcanzar el umbral para la apertura de

CaCC y la despolarización de la membrana (Johnston et al., 2005). Estos autores también establecieron la importancia de la entrada de Ca^{2+} extracelular en este proceso, aunque no se determinó la vía utilizada. Si se sabe que no parecen participar canales de calcio-voltaje dependientes (Sergeant et al., 2001b), y se ha sugerido la participación de la entrada de Ca^{2+} a través del intercambiador Na^{+}-Ca^{2+}, funcionando en sentido inverso (Bradley et al., 2006). Posteriormente se ha demostrado que la mitocondria también juega un papel esencial en la modulación de la actividad eléctrica espontánea en la uretra (Sergeant et al., 2008; Hashitani et al., 2010).

En resumen, un ciclo de actividad marcapasos en la uretra comprendería la siguiente secuencia de eventos (**Fig. X**): **1**) entrada de Ca^{2+} a través del intercambiador Na^{+}-Ca^{2+}, u otro sistema de entrada de Ca^{2+} extracelular aún no conocido; **2**) activación de los RyR, produciendo la liberación de Ca^{2+} desde los almacenes intracelulares, **3**) propagación de la onda de Ca^{2+} por activación de los receptores de IP_3, **4**) estimulación de los CaCC que da lugar a la despolarización y **5**) apertura de los canales de Ca^{2+} tipo L y la despolarización del músculo liso (Sergeant el a., 2006a).

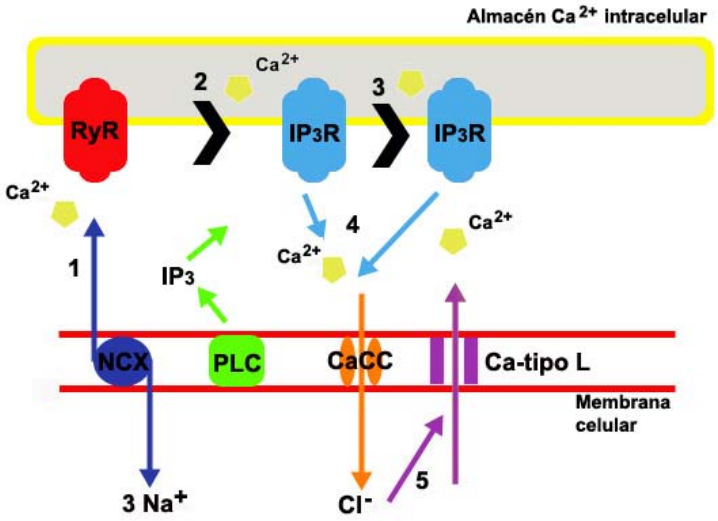

Figura X. Secuencia de eventos que comprende un ciclo de actividad marcapasos en las ICC uretrales (Adaptado de Sergeant el at., 2006a).

Si comparamos estos estudios con los descritos en el tracto gastrointestinal, podemos concluir la existencia de una considerable variación entre tejidos y especies en cuanto a los mecanismos desencadenantes de la generación y propagación de potenciales marcapasos. Diferentes tipos y subtipos funcionales de ICC podrían llevar a cabo funciones específicas en distintas localizaciones, posibilitando su modulación farmacológica selectiva.

De igual forma a las gastrointestinales, las ICC uretrales también podrían participar en mediar la neurotransmisión tanto excitatoria como inhibitoria en la uretra. Así, diversos estudios de inmunohistoquímica muestran una estrecha relación anatómica

entre ICC y estructuras nerviosas (Lyons et al., 2007, Smet et al., 1996). Además, agonistas α-adrenérgicos y purinérgicos en ICC aisladas de uretra de conejo incrementan su actividad espontánea por activación de CaCC (Hashitani y Suzuki, 2007; Sergeant et al, 2002; Sergeant et al., 2009; Bradley et al., 2010), mientras que donantes de NO y otros activadores de la vía cGMP/PKG origina una reducción de dicha actividad espontánea, probablemente debido a la inhibición de la liberación de Ca^{2+} intracelular inducida por IP_3 (Sergeant et al., 2006b). En este sentido, se ha descrito la acumulación de cGMP en ICC uretrales en respuesta a donantes de NO (Smet et al., 1996), al igual que en músculo detrusor (Smet et al., 1996; Gillespie et al., 2004), sugiriendo el papel de las ICC como efectoras de la acción del NO. Sin embargo, aún existen muchas dudas sobre la existencia de esta acción mediadora de la neurotransmisión en la uretra y los mecanismos implicados.

El hallazgo de que las ICC están presentes entre el músculo liso uretral ha abierto una nueva y emocionante vía para la investigación de los mecanismos responsables de la generación y modulación del tono uretral y la continencia urinaria. Actualmente nos encontramos en una etapa preliminar en la comprensión del verdadero papel fisiológico de las ICC en la uretra y todavía quedan por investigar múltiples mecanismos celulares implicados en su papel marcapasos y mediador de la neurotransmisión. A pesar de su importancia, el estudio de las escurridizas ICC presenta muchos retos metodológicos que explican el desconocimiento aún existente en su función. Con seguridad, futuros estudios, como el desarrollo de un buen cultivo de ICC (el cultivo de estas células se complica por el rápido cambio fenotípico hacia SMC; Epperson et al., 2000), estrategias moleculares que lesionen proteínas específicas, o modelos animales más específicos (recientemente se ha desarrollado un ratón transgénico con una proteína fluorescente-kit que facilita la identificación de las ICC; Ro et al., 2010), permitirán la investigación de las ICC en situaciones más fisiológicas.

4. ICC y patología del tracto urinario inferior

Teniendo en cuenta la estrecha similitud entre las características funcionales de las ICC gastrointestinales y las del tracto urinario sería lógico pensar que, al igual que las primeras (ver apartado 3.2.5), las ICC del tracto urinario participen en el desarrollo de patologías urinarias. En este sentido, la comparación en la densidad y actividad de las ICC en vejigas y uretras sanas y aquejadas de diferentes trastornos ayudarían a comprender la implicación de las ICC en un entorno más clínico, aunque hasta el momento se dispone de datos muy escasos al respecto. En preparaciones vesicales de animales con hiperactividad y obstrucción vesical, se ha descrito un incremento en el número de ICC y un mayor efecto inhibitorio de Glivec sobre las contracciones del músculo detrusor, en comparación con los tejidos normales (Biers et al., 2006; Kubota et al., 2008). La sección de la médula espinal en ratas adultas origina un aumento de la expresión de Cx43 en la lámina propia de la vejiga, asociado con una mayor

coordinación de la actividad espontánea (Ikeda et al., 2007). Además, en este caso, Glivec presentó un efecto inhibitorio sobre la actividad espontánea más marcado que en el caso de las vejigas control (Sui et al., 2008). Otros estudios en vejiga humana hiperactiva muestran un aumento en la inmunoreactividad a Cx43 aunque sin cambios en la expresión de c-kit, sugiriendo la sobreexpresión de Cx43 sin la modificación del número de ICC (Roosen et al., 2009). Por último, en pacientes que sufren el Síndrome de megavejiga-microcolon-hipoperistalsis intestinal, los cuales presentan una vejiga no obstruida y distendida, se ha observado una marcada reducción de la población de ICC (Piaseczna Piotrowska et al., 2004), hecho particularmente interesante puesto que está en concordancia con el aumento de ICC en vejigas obstruidas. Todos estos resultados parecen indicar que la disfunción vesical y el aumento/reducción de las ICC son dos fenómenos que están ligados, aunque se desconoce su secuencia. En la uretra, aunque la significación clínica de las ICC está todavía por determinar, sería interesante investigar si, al igual que en vejiga, se producen alteraciones en la población de ICC en relación a los diferentes desórdenes urinarios.

De nuevo, esclarecer el posible papel de las ICC en las patologías urinarias plantearía nuevas dianas terapéuticas, posibilitando el desarrollo de tratamientos eficaces de los que hoy carecemos pese a la relevancia de las patologías urinarias y su grave impacto en la calidad de vida de los pacientes afectados.

Diferentes desórdenes del tracto urinario inferior se caracterizan por presentar una sintomatología común, constituyendo un síndrome denominado LUTS (*lower urinary tract symptoms*). Estos síntomas pueden clasificarse en 1) síntomas asociados al llenado o irritativos, como la urgencia, frecuencia, disuria (micción difícil, dolorosa e incompleta) y nocturia (necesidad de orinar durante la noche); 2) síntomas asociados al vaciamiento vesical u obstructivos, como la hesitancia (demora para comenzar la micción) e incontinencia o flujo de micción pobre; así como 3) síntomas postmiccionales, como el vaciado incompleto o el goteo postmiccional; 4) incluyendo además otros síntomas asociados, como hematuria o dolor pélvico (Homma, 2008). Los LUTS no son específicos de género, suelen estar asociados a la edad, y son progresivos, siendo necesario el tratamiento de todos los síntomas en conjunto (Vishwajit y Andersson, 2009).

El síndrome LUTS está asociado a una serie de patologías muy diversas que normalmente presentan varios de estos síntomas simultáneamente. Este es el caso del síndrome de la vejiga hiperactiva (Stewart et al., 2003), la hiperactividad del detrusor (Abrams, 2003; Digesu et al., 2003), los síndromes de vejiga dolorosa e hipersensible, la cistitis intersticial o la cistitis hemorrágica (Hanno et al., 2009), así como la hiperplasia benigna prostática con obstrucción o diferentes infecciones del tracto urinario. En muchos de estos casos no se trata de procesos patológicos definidos o locales, sino de anormalidades funcionales con sintomatología múltiple y sin diagnóstico preciso dado el desconocimiento de su etiología (Homma, 2008).

4.1 Modelos animales de patologías urinarias: Cistitis hemorrágica

El desarrollo de modelos animales experimentales de una determinada patología constituye una herramienta muy útil en el estudio preclínico de los mecanismos implicados en el trastorno, así como de sus posibles tratamientos. En este trabajo destacamos el modelo de **cistitis hemorrágica** (**HC**) inducido en la rata mediante tratamiento con **ciclofosfamida** (**CYP**).

Una HC puede ser causada por varios agentes, tales como adenovirus, virus BK, citomegalovirus, enfermedad injerto-versus-huésped, o radiación, pero la causa más común es la quimioterapia, principalmente con oxazafosforinas como la CYP o la ifofosfamida (Seber et al., 1999). Se considera que la HC es la lesión vesical más grave inducida por la quimioterapia, y se define como un proceso inflamatorio vesical no infeccioso que presenta desde síntomas característicos de los LUTS hasta episodios severos de hemorragia (Stillwell y Benson, 1988). En pacientes con HC moderada, la hematuria puede causar anemia por deficiencia de hierro, pero en casos severos, puede dar lugar a una inestabilidad hemodinámica y a shock hipovolémico que puede llegar a ser mortal (4% de los casos; Philips et al., 1961). También existe la posibilidad de que la vejiga sufra fibrosis, necrosis y contractura, así como reflujo vesicouretral (Coggins et al., 1960). Además de los síntomas somáticos, la HC se acompaña de sufrimiento, depresión, limitaciones, y un claro deterioro de la calidad de vida.

La CYP es una oxazafosforina del grupo de las mostazas nitrogenadas que actúa como agente alquilante, usada desde 1958 en el tratamiento de tumores sólidos y enfermedades malignas de las células B como linfomas, mielomas, leucemia linfocítica crónica o macroglobulemia de Waldenstrom. Posteriormente, la CYP y la ifofosfamida, su análogo sintético, han sido empleadas para el tratamiento de un mayor número de enfermedades neoplásicas y como tratamiento preparatorio de un trasplante de células hematopoyéticas (Levine y Richie, 1989; Gupta et al., 2011, Korkmaz et al., 2005). La urotoxicidad de CYP se considera que es debida a la acumulación de metabolitos 4-hidrolixados, principalmente la acroleína, metabolizada por hidroxilación enzimática en el hígado (Brock et al., 1981). La acroleína es un aldehído altamente reactivo capaz de atacar al epitelio e iniciar un proceso inflamatorio que se extiende a lo largo de toda la pared vesical (Korkmaz et al., 2007). En este sentido, la vejiga es el órgano más afectado dado la función de almacenamiento de la orina y por lo tanto la larga exposición de su mucosa a la acroleína. Así, otros órganos urinarios, como la uretra, en principio no deberían verse afectados por la acroleína puesto que no están en contacto con la orina durante largos periodos de tiempo. Sin embargo, el efecto de la CYP en la uretra y su posible contribución a la sintomatología de la inflamación vesical que se produce en la HC todavía no han sido estudiados.

La incidencia de HC es variable y depende fundamentalmente del tratamiento pautado. Antes de utilizarse tratamientos profilácticos, la tasa de incidencia era del 10-40% en pacientes expuestos a quimioterapia con CYP para el tratamiento de diversos

tumores (Watson y Notley, 1973) y de hasta el 70% en pacientes que habían sufrido un trasplante de médula ósea (Shepherd et al., 1991). Sin embargo, la tasa de incidencia disminuyó hasta un 6-50% tras la utilización de diferentes tratamientos profilácticos (Shepherd et al., 1991; Vose et al., 1993; Meisenberg et al., 1994), como la hiperhidratación, la irrigación de la vejiga o la administración de mesna (2-mercaptoetano sulfonato), cuyo grupo sulfidrilo se une a la acroleína generando un tioéster que no daña el urotelio vesical (West, 1997; Morais et al., 1999). No obstante, estos tratamientos son sólo preventivos y no sirven una vez iniciados los síntomas clínicos, por lo que la HC todavía se presenta como un problema clínico que necesita el desarrollo de una mejor solución preventiva o de estrategias terapéuticas para su tratamiento.

Con el fin de estudiar los procesos implicados en la patogénesis de esta enfermedad se han creado modelos de experimentación animal, existiendo actualmente dos modelos de HC inducida por oxazafosforinas en rata o ratón: la administración sistémica de CYP o ifofosfamida mediante inyección intraperitoneal (Cox, 1979; Bon et al., 1998), o la inyección intravesical de acroleína (Batista et al., 2006).

La inyección intraperitoneal de CYP en la rata produce un cuadro de HC con aumento de la frecuencia y disminución del volumen de micción (Boucher et al., 2000; Lantéri-Minet et al., 1995) acompañado de signos claros de dolor como la disminución en la frecuencia respiratoria, cierre de los ojos y lagrimeo, piloerección, y la postura característica de dolor abdominal con el lomo arqueado (Lantéri-Minet et al., 1995; Boucher et al., 2000, **Fig. XI**). Además, se produce una hiperreflexia miccional asociada a la inducción de la inflamación vesical (Cox, 1979; Maggi et al., 1992; Lantéri-Minet et al., 1995) y cambios en la excitabilidad de las vías aferentes (Yoshimura y de Groat, 1999), que están relacionados con la alteración neuroquímica (Vizzard 2000; 2001; Qiao y Vizzard, 2002; 2004), electrofisiológica (Yoshimura y de Groat, 1999) y de organización (Vizzard, 1999) de las neuronas aferentes de la vejiga, originando grandes cambios en la función de la misma (Maggi et al., 1992).

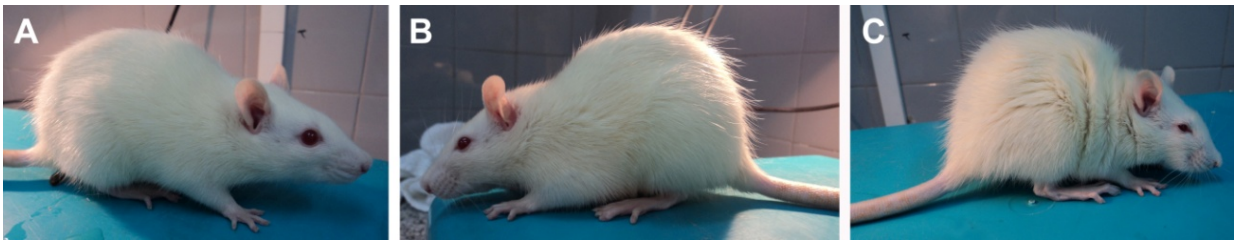

Figura XI. Aspecto externo de animales con cistitis hemorrágica inducida por inyección intraperitoneal de CYP. *A*. Rata control. *B*. Modelo agudo de cistitis hemorrágica inducida pasadas 48h de la inyección de una sola dosis de CYP (150 mg Kg^{-1}). *C*. Modelo crónico de cistitis hemorrágica inducida por tres dosis de CYP (70 mg Kg^{-1}) durante un total de 10 días. Se puede observar como en *B* y especialmente en *C*, el animal presenta cierre de los ojos, piloerección y postura característica de dolor abdominal con el lomo arqueado.

La inducción de HC por CYP en la rata se considera un modelo experimental establecido para el estudio del efecto de CYP en la vejiga, cuyo objetivo es encontrar un tratamiento adecuado para limitar su desarrollo como efecto secundario de la quimioterapia (Bon et al., 1998; Yoshimura y de Groat., 1999). Pero además, de forma más general, el estudio de los mecanismos patogénicos subyacentes puede aportar información sobre el resto de las patologías del tracto urinario inferior asociados al desarrollo de LUTS. Así, el modelo de HC en rata y ratón es un modelo establecido de inflamación vesical que ha sido ampliamente utilizado para el estudio de la cistitis intersticial humana y otros procesos que cursan con hiperactividad vesical (Ribeiro et al., 2012).

Entre la gran cantidad de mediadores que se ha sugerido que participan en la patogenicidad de la HC inducida por CYP, la **superproducción de NO** parece jugar un papel clave (Souza-Filho et al., 1997; Alfieri y Cubeddu, 2000; Korkmaz et al., 2007; Andersson et al., 2008; Linares-Fernández y Alfieri, 2007). Además del NO, existe una gran cantidad de mediadores inflamatorios implicados en esta patología (ver revisión de Ribeiro et al 2012), entre los que se encuentran el TNF-α, la IL-1β (Gomes et al., 1995, Ribeiro et al., 2002), las interleuquinas 4, 6, y 8 y otras citoquinas (Macedo et al., 2012; Malley y Vizzard, 2002; Smaldone et al., 2009), la bradiquinina (Maggi et al., 1993), la COX-II (Klinger et al., 2007; Macedo et al., 2011), el peroxinitrito (Korkmaz et al., 2005; 2007), el factor activador de plaquetas (Souza-Filho et al., 1997), o la SP (Alfieri et al., 2001). Sin embargo, aun no se conoce cuál es la cascada inflamatoria precisa. Tampoco se ha analizado la posible implicación de cambios en la funcionalidad de las ICC en este proceso. Dada la estrecha relación existente entre ICC del tracto urinario y las células productoras de NO, se podría sugerir que ante cambios en la expresión de las enzimas productoras de NO (las diferentes isoformas de NOS) asociadas a la HC se produzcan cambios en la distribución y función de las ICC que contribuyan a su vez al proceso patogénico.

OBJETIVOS

El **objetivo principal** de este estudio es investigar la posible implicación de las ICC en la neurotransmisión excitatoria (noradrenérgica principalmente) e inhibitoria (nitrérgica) de la uretra, tanto en condiciones fisiológicas como en situaciones patológicas del tracto urinario inferior, utilizando la oveja, rata, conejo y ratón como modelos experimentales. Los **objetivos concretos** se pueden resumir en los siguientes puntos:

1- Analizar el posible papel mediador de las ICC uretrales en la neurotransmisión inhibitoria nitrérgica uretral mediante un estudio comparativo de la acumulación de **cGMP** (como principal mediador de la acción del NO) y de la respuesta relajante (**manuscrito I**).

2- Investigar la participación de **CNG** en los procesos de neurotransmisión excitadora e inhibitoria uretral y la posible implicación de las ICC en dichos procesos (**manuscrito II**).

3- Analizar la participación de los canales **CNG** en las oscilaciones de Ca^{2+} que se producen en SMC e ICC aisladas de la uretra de conejo tanto de forma espontánea, como tras la activación de la vía NO/cGMP (**manuscrito III**).

4- Estudiar la presencia de **GJ** entre SMC e ICC en la uretra y su participación en la neurotransmisión excitatoria e inhibitoria (**manuscrito IV**).

5- Analizar la participación de **CaCC** en la neurotransmisión excitatoria e inhibitoria uretral y la posible implicación de ICC (**manuscrito V**).

6- Analizar los cambios en la expresión de las distintas **isoformas de NOS** y en la neurotransmisión excitatoria e inhibitoria en la vejiga y la uretra en un modelo de **HC inducida por CYP** en la rata (**manuscrito VI**).

7- Analizar los cambios en densidad y distribución de **ICC** en la vejiga y en la uretra en un modelo de **HC inducida por CYP** en la rata, así como el efecto preventivo del inhibidor de tirosina quinasas Glivec (mesilato de imatinib) (**manuscrito VII**).

RESULTADOS (RESUMEN)

En este capítulo se muestra un resumen de los hallazgos más significativos, manteniendo el orden correspondiente a los manuscritos independientes que la forman (manuscritos I a VII):

I. Participación de las ICC en la neurotransmisión inhibitoria uretral: papel como efectores de la acción del NO

Se ha analizado el papel relativo de las ICC y las SMC como efectoras del NO en uretra de rata y oveja. Para ello se ha realizado un estudio comparativo de la acumulación de inmunoreactividad a cGMP, con la relajación inducida tanto por la estimulación nitrérgica específica mediante EFS (2Hz, 4 min), como por la adición de SNC, un donante de NO elegido por ser el que produce la relajación más rápida y los niveles más altos de cGMP en la uretra de oveja (García-Pascual et al., 1999). Además, la naturaleza de las células positivas a cGMP se confirmó mediante marcajes dobles vimentina/cGMP y c-kit/cGMP y su relación con las terminaciones nerviosas se determinó utilizando marcajes dobles cGMP/PGP 9.5 (marcador panneuronal) o cGMP/nNOS (marcador de nervios nitrérgicos). Este ha sido el primer estudio que demuestra la acumulación de cGMP en ICC uretrales inducida por la estimulación selectiva de los nervios nitrérgicos.

I.1 Respuestas funcionales

Los estudios de relajación han sido realizados en preparaciones uretrales precontraídas con NE y en presencia de inhibidores de la PDE (IBMX y Zaprinast), con objeto de provocar la acumulación en el tejido de cGMP y por lo tanto permitir su posterior detección por inmunohistoquímica. Además la presencia de guanetidina, atropina y d-tubocurarina inhibió el efecto de la posible liberación de NE y/o ACh, permitiendo obtener con EFS una estimulación nitrérgica selectiva.

La adición de los inhibidores de PDE tuvo el inconveniente de producir por sí misma una respuesta relajante que dificultaba la evaluación de la relajación inducida por NO, especialmente en la rata donde se alcanzó una relajación casi máxima a pesar de haber reducido su exposición a tan solo 30 s antes y durante la estimulación nitrérgica específica (EFS o SNC). Este efecto enmascarador se redujo midiendo junto con la magnitud de la relajación la velocidad de la misma. Como puede observarse en las **figuras 1** y **2**, sólo en el caso de la oveja se obtuvieron con EFS y SNC relajaciones superiores al control (tratado únicamente con inhibidores de PDE), pero en ambos casos estas respuestas fueron significativamente más rápidas. La incubación tanto con el inhibidor de la NOS, L-NNA (0,1 mM), como con el inhibidor de la GC, ODQ (0,1 mM) originó una inhibición significativa de la respuesta relajante provocada por EFS, y del mismo modo, ODQ redujo la relajación inducida por SNC (**Figs. 1 y 2**). Estos resultados demuestran que las relajaciones estudiadas se pueden considerar

fundamentalmente de origen nitrérgico. En el caso de EFS serían debidas a la liberación de NO de los nervios nitrérgicos y la posterior activación de la GC soluble, mientras que en el caso de SNC se produciría la activación directa de ésta última.

I.2 Inmunoreactividad a cGMP

En las preparaciones control, tratadas sólo con los inhibidores de PDE, se observó una ligera cGMP-ir en algunas células con la morfología característica de las ICC, cuerpos celulares piriformes o fusiformes que contienen un gran núcleo ovoide rodeado con escaso citoplasma y largos procesos dendríticos (**Figs. 5 L y 6 D-E)**. Estas células se localizaron preferentemente en la capa serosa (ICC-SR), especialmente en la rata (**Fig. 3A**) y en la lámina propia (ICC-LP), particularmente en la oveja (Figura 4, manuscrito I), mientras que se observaron pocas ICC inmunoreactivas a cGMP en las capas musculares (ICC-M) (**Fig. 3A**). En las preparaciones control, la preincubación con ODQ y L-NNA no produjo una reducción significativa en la cGMP-ir (**Fig. 3B**).

La estimulación selectiva de los nervios nitrérgicos mediante EFS (2 Hz, 4 min) indujo un claro aumento de la cGMP-ir en la pared muscular de la uretra (**Fig. 3D**). Se observó una intensa cGMP-ir tanto en células con una morfología característica de ICC como en SMC. Este hecho hizo más difícil la diferenciación de ICC-M, distribuidas entre las fibras musculares, rodeando los fascículos de músculo liso, o localizadas en los septos que separan unos haces musculares de otros.

La adición de SNC (0,1 mM, 4 min) produjo un aumento claro de la cGMP-ir en grupos compactos de ICC localizadas a lo largo de la capa serosa de la rata y la capa muscular externa de ambas especies (**Fig. 3E**). Paradójicamente, cGMP-ir en SMC resultó ser más débil que en las preparaciones estimuladas con EFS, observándose las ICC inmunoreactivas más contrastadas frente a un fondo muscular menos marcado. Su distribución fue heterogénea, de forma que aparecen grupos densos de células en zonas concretas de la pared uretral, mientras que otras áreas carecen de células marcadas (**Fig. 3E**).

La inhibición de la NOS con L-NNA redujo la cGMP-ir en ICC-M inducida por EFS (**Fig. 3G**), mostrando así que la acumulación de cGMP en estas células está directamente relacionada con la activación de la nNOS en los nervios nitrérgicos. Además, la inhibición selectiva de la GC con ODQ (0,1 mM) también produjo una disminución significativa de cGMP-ir en ICC-M de preparaciones estimuladas con EFS (**Fig. 3F**) o con SNC (**Fig. 3H**). Sorprendentemente la cGMP-ir presente en ICC-LP en la uretra de oveja (Figuras 4 y 5 manuscrito I), y en ICC-SR en la uretra de rata no se vio afectada tras la exposición a L-NNA u ODQ sugiriendo la participación de una reacción inespecífica no relacionada con el NO.

I.3 Doble marcaje cGMP/vimentina y c-kit/vimentina

El doble marcaje cGMP/vimentina y c-kit/vimentina confirmó la naturaleza de las células inmunoreactivas a cGMP como ICC. Hay que destacar que mientras todas las ICC fueron positivas tanto para vimentina como para c-kit, solo una fracción de estas células presentaron cGMP-ir en preparaciones estimuladas por SNC o EFS (**Fig. 5**).

I.4 Dobles marcaje cGMP/nNOS y cGMP/PGP9.5: relación estructural entre ICC y estructuras nerviosas

Ambas combinaciones mostraron que en ningún caso el cGMP colocaliza con nNOS o PGP 9.5, aunque sí se observó una estrecha relación entre las ICC positivas a cGMP y las estructuras nerviosas (**Fig. 6)**. Se observaron múltiples varicosidades nerviosas inmunopositivas a PGP 9.5 o nNOS en íntimo contacto con las ICC positivas a cGMP a lo largo de toda la pared uretral, en la capa muscular, lámina propia, y serosa (**Fig. 6**).

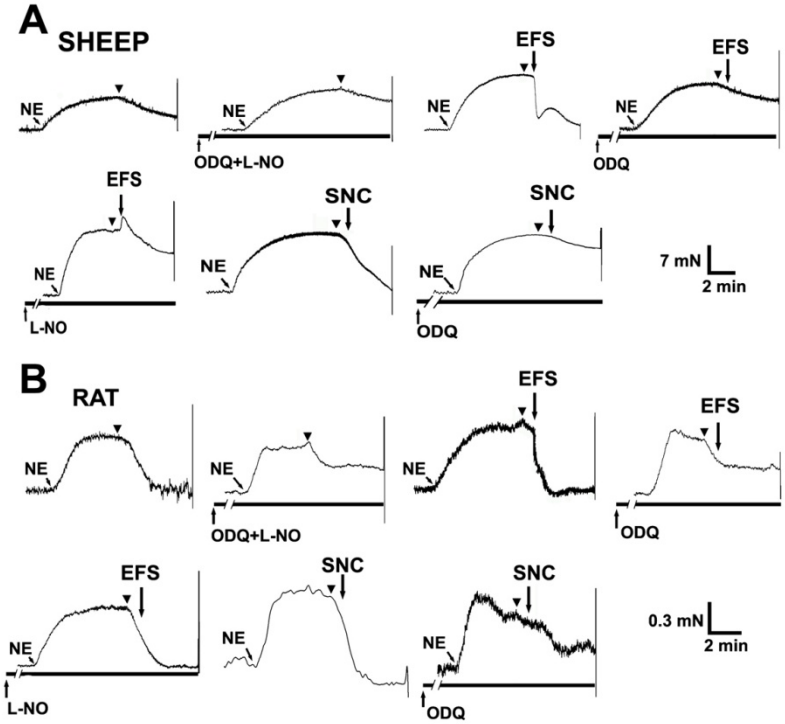

Figura 1. Registros característicos de las respuestas relajantes inducidas en preparaciones uretrales de oveja (*A*) y rata (*B*) bajo diferentes condiciones de estimulación nitrérgica. Se muestran preparaciones sometidas a estimulación eléctrica de campo (EFS; 2 Hz, 4 min) o S-nitroso-L-cisteína (SNC; 0.1 mM, 4 min) en presencia o ausencia de N^{ω}-nitro-L-arginina (L-NNA) y/u ODQ (0.1 mM, 30 min) en comparación con preparaciones control no estimuladas. Todas las preparaciones fueron precontraídas con noradrenalina (NE), las puntas de flecha indican el punto en el que fueron añadidos los inhibidores de la PDE (IBMX 1 mM and zaprinast 0.1 mM), presentes a partir de este momento durante todo el experimento. Las líneas verticales al final de cada registro indican la recogida rápida de la muestra para ser procesada por inmunofluorescencia.

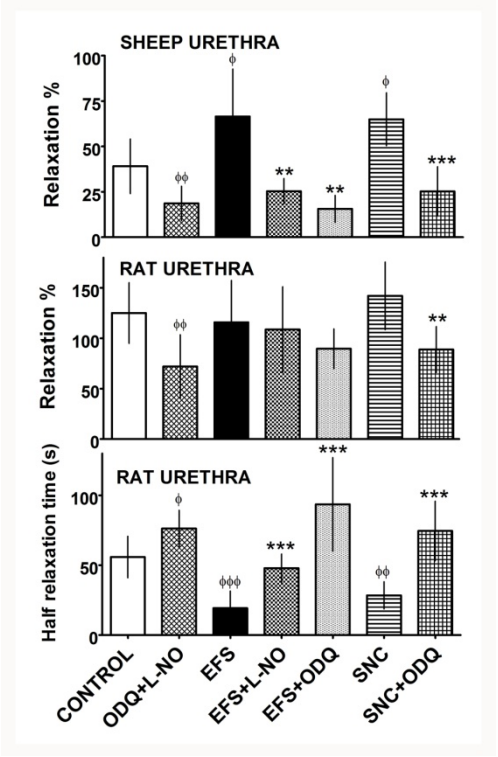

Figura 2. Valores medios de las respuestas relajantes inducidas por EFS y SNC en presencia o ausencia de L-NNA y/o ODQ, en comparación con las preparaciones control no estimuladas de uretra de oveja y de rata (n = 4-13). Los resultados que se expresan como media (SD), son el porcentaje de la tensión contráctil inducida por NE (% de Relajación) o el tiempo que tarda en alcanzar el 50% de la relajación total (tiempo de relajación medio). $\Phi P < 0.05$, $\Phi\Phi P < 0.01$, $\Phi\Phi\Phi P < 0.001$, diferencias con preparaciones control. $^{**}P < 0.01$ y $^{***}P < 0.001$, diferencias con preparaciones estimuladas con EFS o SNC pero no tratadas con L-NNA u ODQ (ANOVA de una vía seguido de *t*-test de Student no pareado).

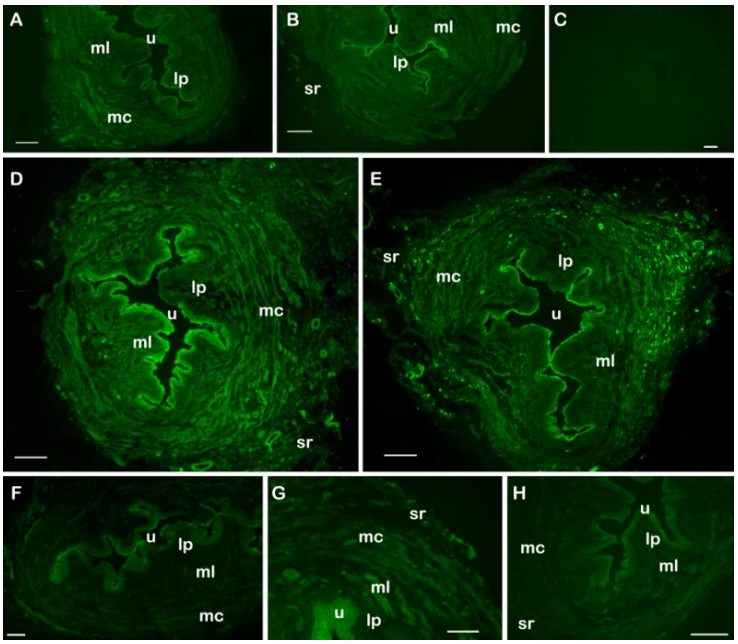

Figura 3. Comparación de la inmunoreactividad a cGMP (cGMP-ir) en secciones anulares de uretra de rata. *A*: bajo condiciones control, se observa una débil cGMP-ir en el epitelio y en algunas células en la capa muscular externa. *B*: leve reducción de la cGMP-ir basal en preparaciones no estimuladas previamente tratadas con L-NNA y ODQ. *C*: ausencia de cGMP-ir en el control negativo (sin anticuerpo primario), *D*: incremento pronunciado de cGMP-ir en preparaciones sometidas a EFS, mostrándose una intensa reacción en las células musculares lisas (SMC), células intersticiales de Cajal (ICC), vasos intramurales y urotelio. *E*: acumulaciones densas de ICC altamente reactivas a cGMP en la capa muscular externa de preparaciones estimuladas con SNC. *F-H*: inhibición pronunciada de la cGMP-ir en preparaciones estimuladas mediante EFS en presencia de ODQ (*F*) o L-NNA (*G*) y en preparaciones estimuladas con SNC en presencia de ODQ (*H*). u, urotelio; lp, lámina propia; ml, músculo longitudinal; mc, músculo circular; sr, serosa. Barra = 100 μm.

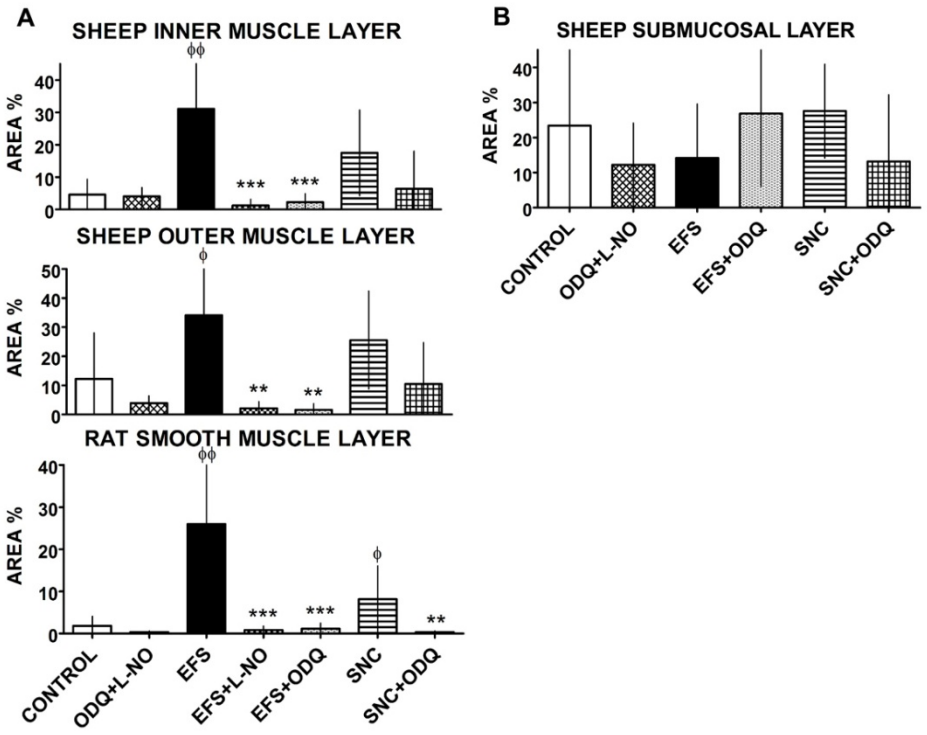

Figura 4. Cuantificación de la cGMP-ir en la uretra de oveja y rata bajo diferentes condiciones de estimulación nitrérgica. Las preparaciones fueron estimuladas por EFS (2 Hz, 4 min) o SNC (0.1 mM, 4 min) en presencia o ausencia de L-NNA (0.1 mM) y/u ODQ (0.1 mM) y comparadas con los controles no estimulados. Todas las preparaciones fueron precontraídas con NE (50 μM) y pretratadas con los inhibidores de la PDE e inmediatamente fijadas y procesadas para la inmunofluorescencia de cGMP. En campos seleccionados de las distintas secciones uretrales se calculó el porcentaje de área marcada con una intensidad por encima del umbral (% Area). En la uretra de oveja, se analizó de forma independiente la capa mucular circular interna, la capa muscular externa (ámbos en *A*) y la lámina propia (*B*), mientras que en las secciones de rata se analizaron todas las capas musculares conjuntamente (*A*). Los valores se expresan como media ± SD (n= 5-13 diferentes campos de al menos 3 animales distintos). ΦP < 0.05, ΦΦP < 0.01, diferencias con respecto al control. **P < 0.01, **P < 0.001, diferencias con respecto a las preparaciones estimuladas con EFS o SNC pero no tratadas con L-NNA ni ODQ (ANOVA de una vía seguido de t-test de Student no pareado).

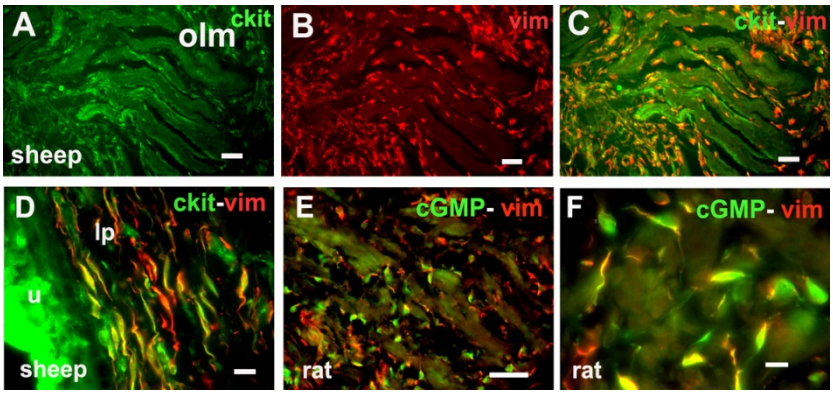

Figura 5. Colocalización de vimentina-ir (rojo) con c-kit-ir (verde) y cGMP-ir (verde) en ICC de uretra de oveja y de rata. Se muestran ejemplos de c-kit-ir (*A*) y vimentina-ir (*B*) junto con sus respectivas imágenes combinadas (*C* y *D*) en la capa muscular longitudinal externa (*A*-*C*) y la lámina propia (*D*) de la uretra de oveja, y de cGMP-ir y vimentina-ir (*E, F*) en la capa muscular de la uretra de rata estimulada con EFS (*E*) o con SNC (*F*). u, urotelio; lp, lámina propia; olm, músculo longitudinal externo. Barras = 100 μm (*A*- *E*) y = 20 μm (*F*).

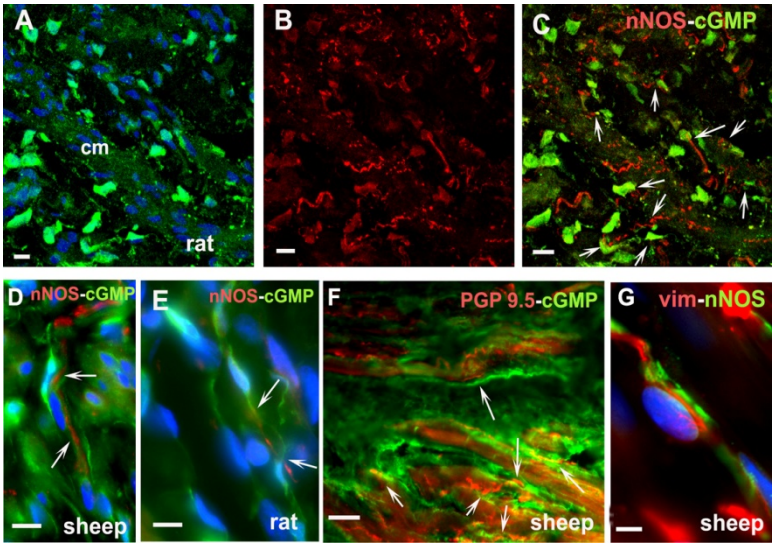

Figura 6. Se muestra la ausencia de colocalización y la existencia de una estrecha relación estructural entre ICC inmunoreactivas a cGMP y las estructuras nerviosas marcadas con nNOS o PGP 9.5. *A-C*: imágenes de microscopía confocal mostrando la superposición imágenes a lo largo del eje z de una sección de 12 µm procedente de la capa muscular circular de la uretra de oveja estimulada con SNC. *A*) Se muestra cGMP-ir (verde) en ICC, con sus núcleos teñidos con DAPI (azul) y *B*) nNOS-ir (rojo) en nervios intramurales, junto con su imagen combinada (*C*). *D-E*: imágenes a mayores aumentos de un doble marcaje cGMP/nNOS y contratinción de núcleos con DAPI que muestran una íntima relación estructural entre ICC y terminaciones nerviosas nitrérgicas localizadas en la capa muscular de la uretra de oveja tras la estimulación con EFS (*D*) y de rata expuesta a SNC (*E*). Dobles marcajes de PGP 9.5-ir /cGMP-ir (F) y vimentina-ir/ nNOS-ir (G) en la capa muscular de la uretra de oveja estimulada con SNC que revelan igualmente la ausencia de colocalización entre ambos marcajes. Las flechas indican los puntos de contacto entre las ICC y las estructuras nerviosas. cm, músculo circular. Barra = 20 µm excepto en *F* (100 µm).

II. Participación de los canales CNG en la neurotransmisión nitrérgica uretral: papel de las ICC

El presente trabajo, es el primero en el que se describe la presencia en la uretra de rata de un subtipo funcional de canales CNG, los CNGA1 conocidos por su presencia en la retina y porque son activados selectivamente por cGMP. Se estudió mediante inmunofluorescencia la distribución celular de los canales CNGA1, y se determinó por PCR la expresión del mRNA de las diferentes subunidades que componen el canal funcional CNG. Por último, se investigó la posible participación de los CNG en los procesos de neurotransmisión excitadora noradrenérgica e inhibitoria nitrérgica en la uretra y la posible implicación de las ICC en dichos procesos. Para ello se empleo el L-cis-Diltiazem como inhibidor selectivo de los canales CNG.

II.1 Efecto de L-cis-Diltiazem y D-Diltiazem en las respuestas relajantes

La preincubación con L-cis-Diltiazem (50µM, 30 min) redujo significativamente la relajación nitrérgica inducida por EFS en preparaciones previamente precontraídas

con arginina-vasopresina (AVP) a todas las frecuencias empleadas y tanto en estimulaciones de corta como de larga duración (**Fig. 7**). Este efecto inhibitorio se caracterizó por presentar un desarrollo muy rápido (**Fig. 8A**).

Por el contrario el isómero, D-Diltiazem, utilizado a una concentración capaz de bloquear los canales de Ca^{2+} dependientes de voltaje (1 μM), no modificó las relajaciones nitrérgicas a ninguna de las frecuencias ni duraciones de EFS empleadas (**Fig. 9**).

La relajación inducida por YC-1, un activador directo de la sGC independiente de NO, y que por lo tanto provoca un aumento en los niveles de cGMP intracelular, fue también abolida completamente por la preincubación con L-cis-Diltiazem (**Fig. 10)**.

II.2 Efecto de L-cis-Diltiazem y D-Diltiazem en las respuestas contráctiles

L-cis-Diltiazem provocó también una inhibición dosis-dependiente de las contracciones adrenérgicas inducidas por EFS, que alcanzó la inhibición completa a una concentración de 50 μM. Sin embargo, a diferencia de su efecto sobre la relajación nitrérgica, presentó una mayor latencia, necesitando un promedio de 15 EFS para inhibir las contracciones de forma significativa (**Fig. 8B**).

Con objeto de analizar la posible participación en el efecto de L-cis-Diltiazem sobre canales de calcio dependientes de voltaje se analizó el efecto de ambos isómeros sobre la contracción provocada por despolarización con altas concentraciones de K^+ extracelular. Como se puede observar, una vez eliminadas las influencias excitadoras de origen nervioso con atropina y guanetidina se puede considerar que la contracción restante es debida a la despolarización directa del músculo liso. La preincubación tanto con L-cis-Diltiazem como con D-Diltiazem (50 μM y 1 μM, respectivamente) inhibió significativamente esta contracción residual inducida por K^+, efecto que fue parcialmente revertido tras el lavado de ambos isómeros (**Fig. 11**). Por lo tanto se demuestra que L-cis-Diltiazem presenta también como efecto inespecífico una acción inhibidora sobre los canales de Ca^{2+} dependientes de voltaje de tipo L, aunque con un rango de potencia 50 veces inferior a su D-isómero.

II.3 Expresión del mRNA de CNGA1 y CNGB1 en la uretra de rata

Los canales CNG no habían sido previamente identificados en la uretra, y el presente estudio muestra la presencia en uretra de rata de un canal CNG heteromérico también presente en la retina, tejido utilizado como control positivo. Se llevó a cabo una PCR inversa utilizando cebadores basados en las secuencias específicas de los mRNA que codifican para las dos subunidades del canal: CNGA1 y CNGB1, y se amplificó una banda del tamaño previsto, que tras ser secuenciada mostró un 99% de identidad con la de CNGA1. Después de realizar una segunda ronda de amplificación o PCR anidada

con el mismo par de cebadores se obtuvo también una banda visible correspondiente a la secuencia de CNGB1 (**Fig. 12**).

II.4 Detección por inmunofluorescencia de los canales CNG1 en la pared uretral

Se observó una evidente inmunoreactividad específica para los canales CNG1 en dos tipos celulares de la uretra de rata: SMC e ICC (**Fig. 13**). Las células musculares lisas presentaron una débil y difusa inmunoreactividad a CNG1, que colocalizó con α-actina (**Fig. 13, A-C**). Por el contrario se observó una intensa CNG-ir en células con morfología fusiforme localizadas entre los haces musculares o en los septos de tejido conectivo (**Fig. 13, A-C**), y que recordaban a las ICC positivas a cGMP antes descritas. Esta subpoblación de células inmunoreactivas a CNG1 también lo fueron para vimentina (**Fig. 13, D-F**).

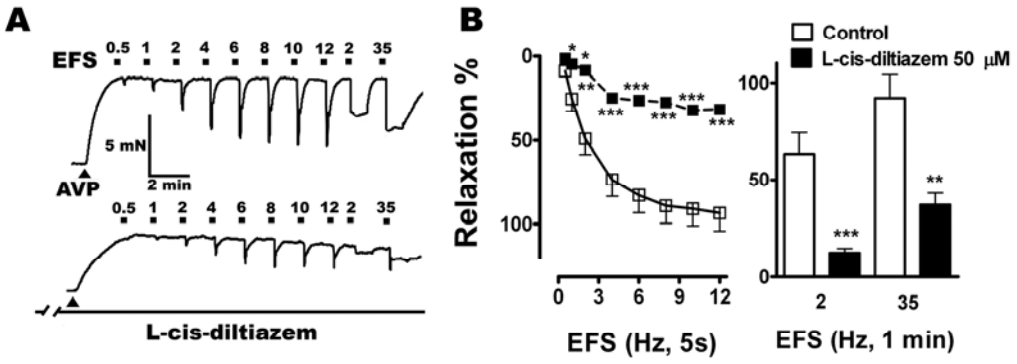

Figura 7. Efecto de L-cis-Diltiazem sobre la relajación nitrérgica. *A*: registros representativos de la relajación inducida por EFS (5 s, 0.5- 12 Hz y 1 min de duración, 2 y 35 Hz) en preparaciones de uretra de rata precontraídas con AVP (0.1 μM), en condiciones control (parte superior) y expuestas a L-cis-Diltiazem (30 min, 50 μM, parte inferior). *B*: Valores medios de las curvas frecuencia-respuesta de corta (5s, izquierda) y larga duración (1 min, derecha) en ausencia (símbolos y barras blancas) y presencia de L-cis-Diltiazem (50 μM, símbolos y barras negras). Los resultados se expresan como media ± SEM (n = 6, de diferentes animales). *$P < 0.05$, **$P < 0.01$, *** $P < 0.001$, diferencias significativas respecto al control. (ANOVA de una vía seguido de *t*-test de Student no pareado).

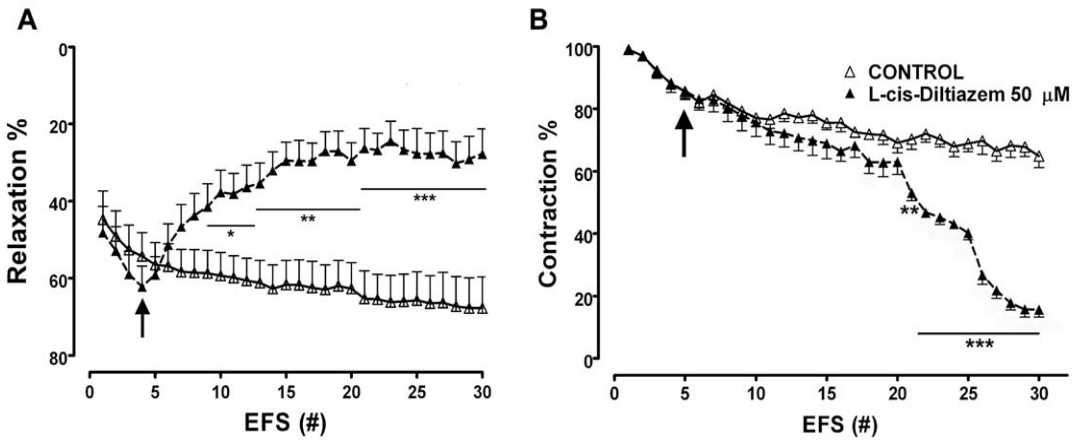

Figura 8. Evolución temporal del efecto inhibitorio de L-cis-Diltiazem sobre las respuestas relajantes y contráctiles inducidas por EFS. Valores medios de la evolución temporal de las relajaciones (*A*) y contracciones (*B*) inducidas por estimulaciones repetitivas (# indica el número del estímulo) en condiciones control (símbolos blancos) y tras la adición de L-cis-Diltiazem (50 μM, flecha, símbolos negros). Los resultados se expresan como media ± SEM ($n = 6$, de diferentes animales). *$P < 0.05$, **$P < 0.01$, *** $P < 0.001$, diferencias significativas respecto al control. (ANOVA de una vía seguido de *t*-test de Student no pareado).

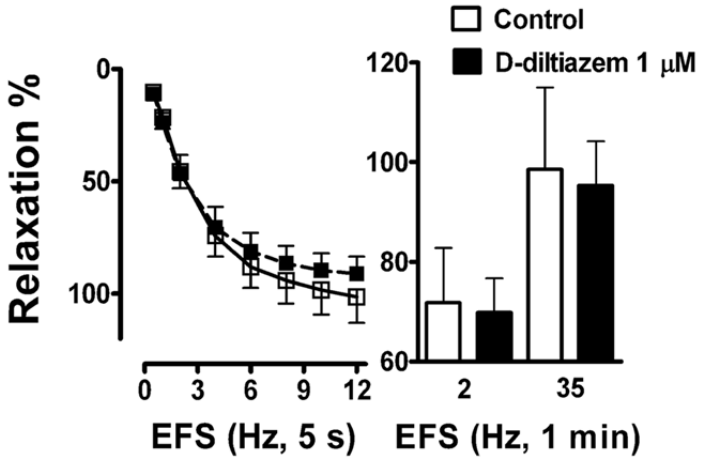

Figura 9. Curvas frecuencia-respuesta en preparaciones de rata precontraídas con AVP (0.1 μM) y sometidas a EFS de corta (5s, izquierda) y larga duración (1 min, derecha) en ausencia (símbolos y barras blancas) y presencia de D-Diltiazem (1 μM, símbolos y barras negras). Los resultados se expresan como media ± SEM ($n = 6$, de diferentes animales). No se observaron diferencias significativas entre ambos grupos (ANOVA de una vía).

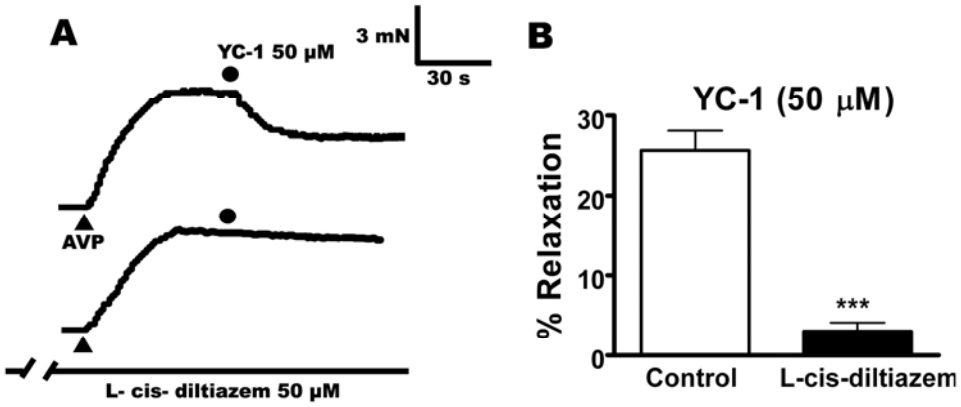

Figura 10. *A*: Registros característicos que muestran el efecto relajante de YC-1 (50 µM) en una preparación de uretra de rata precontraída con AVP (parte superior) y su inhibición con L-cis-Diltiazem (50 µM, parte inferior). *B*: Valores medios que muestra el potente efecto inhibitorio de L-cis-Diltiazem (50 µM, barra negra) sobre la relajación inducida por YC-1 (barra blanca). Los resultados se expresan como media ± SEM (n = 6, de diferentes animales). *** P <0.001, diferencias significativas respecto al control. (t-test de Student no pareado).

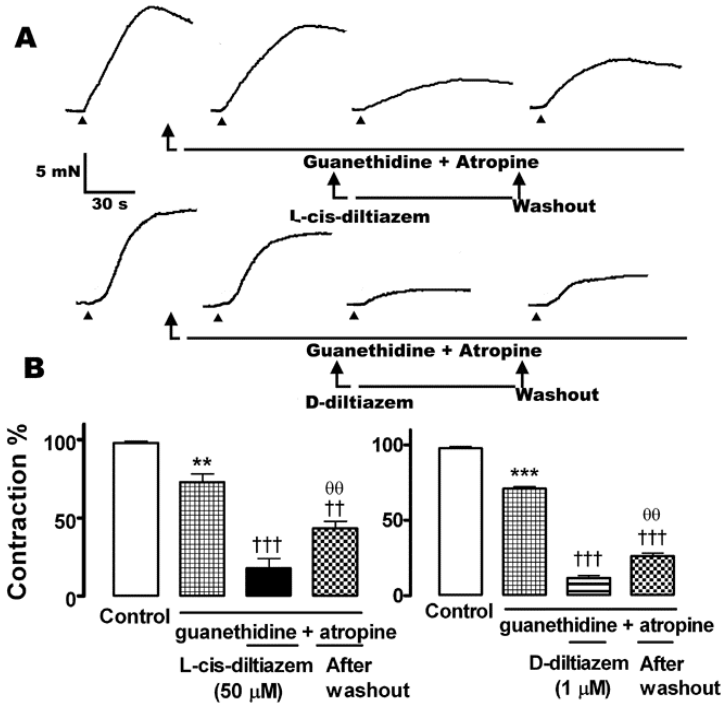

Figura 11. Efecto de L-cis-Diltiazem y D-Diltiazem sobre las contracciones inducidas por K^+ 120 mM. *A*: Registros característicos en condiciones control, en presencia de guanetidina (50 µM) y atropina (1 µM), y tras el tratamiento con L-cis-Diltiazem (50 µM, parte superior) o D-Diltiazem (1 µM, parte inferior), y después del lavado de ambos isómeros. *B*: valores medios de la contracción inducida por K^+ 120 mM en preparaciones de uretra de rata bajo las diferentes condiciones experimentales detalladas en A. Los resultados se expresan como media ± SEM (n = 6, de diferentes animales). **P < 0.01, *** P <0.001, diferencias significativas respecto al control. †† P < 0.01, ††† P <0.001, respecto a guanetidina + atropina. ΘΘ P < 0.01, respecto a los isómeros de Diltiazem (ANOVA de una vía seguido de t-test de Student no pareado).

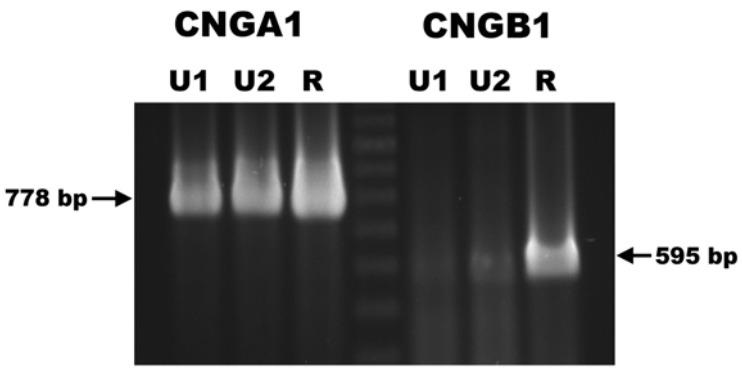

Figura 12. Amplificación de las dos subunidades que conforman el canal CNG: CNGA1 y CNGB1, visualizados en un gel de agarosa al 2% teñido con SYBR gold. Los transcritos de mRNA de tamaño apropiado correspondientes a ambas subunidades se expresaron en la uretra de dos ratas (U1 y U2) en comparación con los transcritos en la retina de rata (R), utilizada como control positivo. 778 bp para CNGA1 y 595 bp para CNGB1; carril central, escalera de 100 bp.

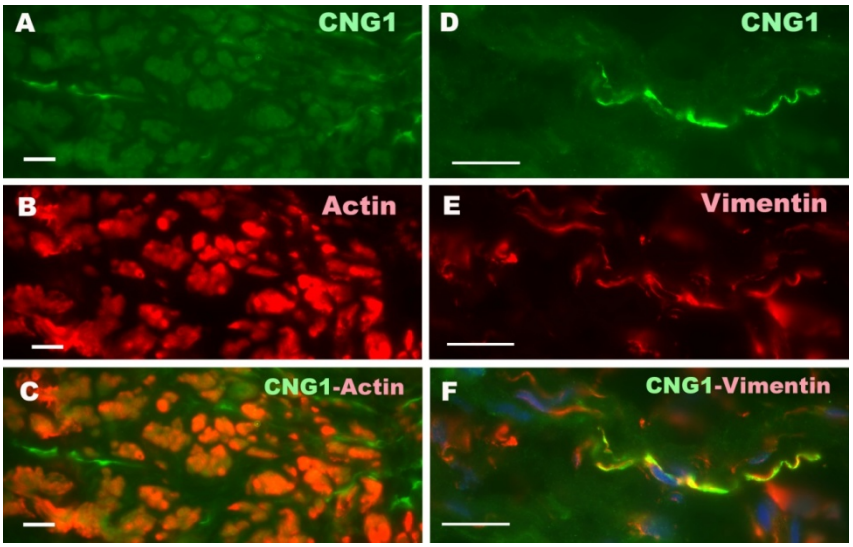

Figura 13. Microfotografías representativas que muestran la inmunolocalización de CNGA1 (verde, *A*, *C, D* y *F*), α-actina (rojo, *B* y *C*) y vimentina (rojo, *E* y *F*) en la capa muscular lisa de la uretra de rata. Se puede observar una débil inmunoreactividad (ir) a CNG1 en las células musculares lisas positivas para α-actina-ir, mientras que la CNG1-ir es muy intensa en células de morfología fusiforme que aparecen dispersas entre los haces musculares (*A*-*C*). A mayores aumentos se muestra la colocalización de CNG1-ir con vimentina, en ICC con característicos largos y finos procesos citoplasmáticos. Los núcleos celulares presentan contratinción con DAPI (azul) en F. Barra = 50 µm.

III. Participación de canales CNG sobre la actividad espontánea y en los cambios inducidos por la activación de la vía NO/cGMP de ICC y SMC aisladas

En este apartado, se utilizó un sistema de imagen de calcio por microscopía confocal para examinar el efecto de L-cis-Diltiazem, como inhibidor selectivo de

canales CNG, sobre las oscilaciones espontáneas de Ca^{2+} registradas en ICC y SMC aisladas por dispersión enzimática de la uretra de conejo. Asimismo se analizaron los cambios inducidos en las oscilaciones de Ca^{2+} intracelular por diversos procedimientos que originan un aumento de los niveles intracelulares de cGMP. Por último, mediante inmunocitoquímica se analizó la presencia de CNG-ir en SMC e ICC aisladas.

III.1 Efecto de los isómeros de Diltiazem sobre las ondas espontáneas de Ca^{2+}

Aproximadamente el 5% de las células dispersas de la uretra proximal (bajo microscopía de campo claro) mostró la típica apariencia de ICC, con la presencia de múltiples y finas prolongaciones (Sergeant et al., 2000). Cuando estas células fueron incubadas con el indicador de Ca^{2+} Fluo-4, más del 50% produjeron incrementos regulares espontáneos en la intensidad de fluorescencia. Por el contrario, las SMC identificadas por su característica forma fusiforme, raramente mostraron ondas espontáneas de Ca^{2+}. Su frecuencia media fue de 16.12 ± 2.60 min^{-1} en SMC, y 10.73 ± 1.25 min^{-1} en ICC. La **figura 14** muestra como la adición de L-cis-Diltiazem (50 μM) indujo una reducción significativa en la frecuencia y amplitud de las ondas de Ca^{2+}, así como en el Ca^{2+} basal en ambos tipos de células. Este efecto no pudo ser revertido tras el lavado con solución Hanks. Por el contrario, si bien la adición de D-Diltiazem (50 μM) produjo una reducción significativa en los valores de frecuencia media y amplitud de las ondas de Ca^{2+} en SMC, no afectó a los de ICC (**Fig. 15**). D-Diltiazem también redujo el nivel de Ca^{2+} basal de ambas células aunque el efecto fue mayor en SMC. El efecto del D-Dilitazem no pudo ser revertido tras el lavado con solución Hanks.

III.2 Efecto de L-cis-Diltiazem sobre los cambios inducidos en las oscilaciones intracelulares de Ca^{2+} por un aumento en los niveles de cGMP

Con objeto de provocar la activación de la vía NO/cGMP y la consecuente acumulación intracelular de cGMP se utilizaron los siguientes tratamientos: 1) adición de un análogo de cGMP permeable (8-Br-cGMP) que penetra lentamente en la célula; 2) inhibición de la degradación de cGMP por PDE mediante un cóctel compuesto por un inhibidor no específico (IBMX), y un inhibidor selectivo de la PDE V (Zaprinast); 3) activación directa de la GC con YC-1; y 4) adición directa de NO por medio de un compuesto donante (DEA-NO) que libera NO de forma espontánea.

La **figura 16** muestra un ejemplo de cómo las ondas espontáneas de Ca^{2+} no se modificaron de forma significativa por la adición de 8-Br-cGMP (1 mM) tanto en SMC como en ICC, aunque si se produjo una disminución significativa en el Ca^{2+} basal. Sin embargo, tras la adición de L-cis-Diltiazem (50 μM) disminuyeron de forma significativa tanto la frecuencia como la amplitud de las ondas de Ca^{2+}, y se produjo una mayor reducción del Ca^{2+} basal en ambas células. El efecto de L-cis-Diltiazem fue parcialmente revertido tras el lavado con solución Hanks.

La administración del cóctel inhibidor de PDE redujo significativamente la frecuencia y amplitud media de las ondas de Ca^{2+} así como el calcio basal en ambos tipos celulares. La adición posterior de L-cis-Diltiazem (50 μM) redujo aún más todos los parámetros estudiados. El efecto fue revertido tras el lavado (Figura 4 manuscrito III).

A diferencia de los tratamientos anteriores, la activación de la GC con YC-1 (60 μM) disminuyó rápidamente y de forma notable la frecuencia y amplitud media de las ondas de Ca^{2+} así como el Ca^{2+} basal en ambos tipos de células. En este caso, la posterior administración de L-cis-Diltiazem (50 μM) no produjo ningún cambio adicional en ninguno de los parámetros estudiados (Figura 5 manuscrito III). De forma similar, la adición directa de NO en forma de un compuesto donante (DEA-NO, 60 μM) disminuyó significativamente todos los parámetros. Tampoco L-cis-Diltiazem (50 μM) indujo nigún cambio adicional. El efecto del DEA-NO fue revertido tras el lavado con solución Hanks (**Fig. 17**).

III.3 Inmunoreactividad a CNG1 en SMC e ICC aisladas

Se detectó una gran diferencia en la presencia de CNG1-ir específica entre ambos tipos celulares. Así, mientras fue débil y difusa en SMC, donde colocalizó con α-actina (**Fig. 18 A-C**), en ICC, positivas a vimentina se observó una intensa CNG1-ir (**Fig. 18 D-I)**. Puede observarse como mientras las SMC mostraron una morfología típica fusiforme, la morfología de las ICC fue muy variable de acuerdo con lo descrito anteriormente (Sergeant et al., 2000). Así, algunas presentaron un aspecto estrellado con multiples prolongaciones que irradian desde la región central que contiene el núcleo (**Fig. 18 G-I**), mientras que otras eran de apariencia bipolar con el núcleo en posición central y prolongaciones citoplasmáticas largas y delgadas (**Fig. 18 D-F**). Hay que destacar la presencia de una intensa CNG-ir presente en las múltiples y finas espinas o espículas que irradian tanto del cuerpo celular como de las prolongaciones de las ICC (**Fig. 18 F, I**, señaladas con flechas).

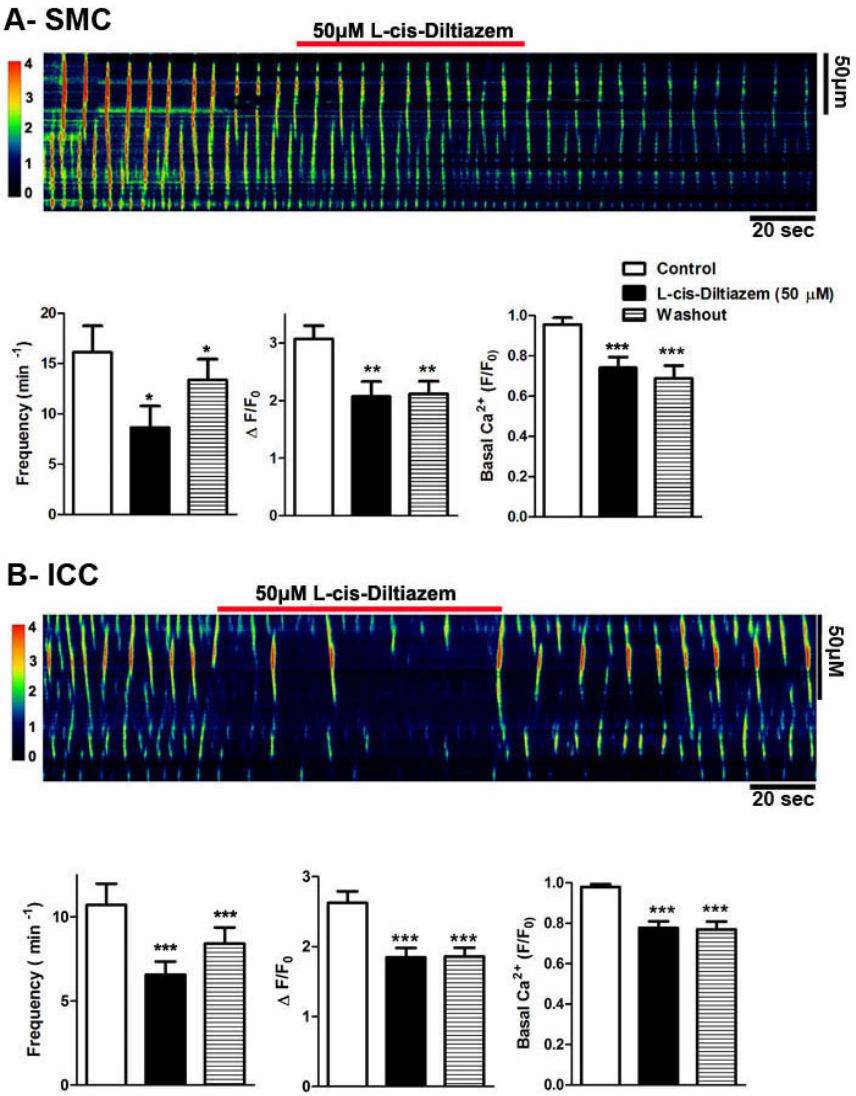

Figura 14. Efecto de L-cis-Diltiazem sobre las oscilaciones espontáneas de Ca^{2+} en SMC (*A*) e ICC (*B*) aisladas de la uretra de conejo e incubadas con Fluo-4AM. Los paneles superiores muestran un registro representativo, y los paneles inferiores muestran los valores medios de frecuencia (min $^{-1}$, izquierda), amplitud ($\Delta F/F_0$, centro) y Ca^{2+} basal (F/F_0; derecha). L-cis-Diltiazem se administró a una concentración de 50µM y estuvo presente durante 60-90 s antes del lavado con solución Hanks. Los resultados se expresan como media ± SEM (n = 13 SMC, n = 23 ICC). *P < 0.05, **P < 0.01, *** P <0.001, diferencias significativas respecto al control (t-test de Student pareado).

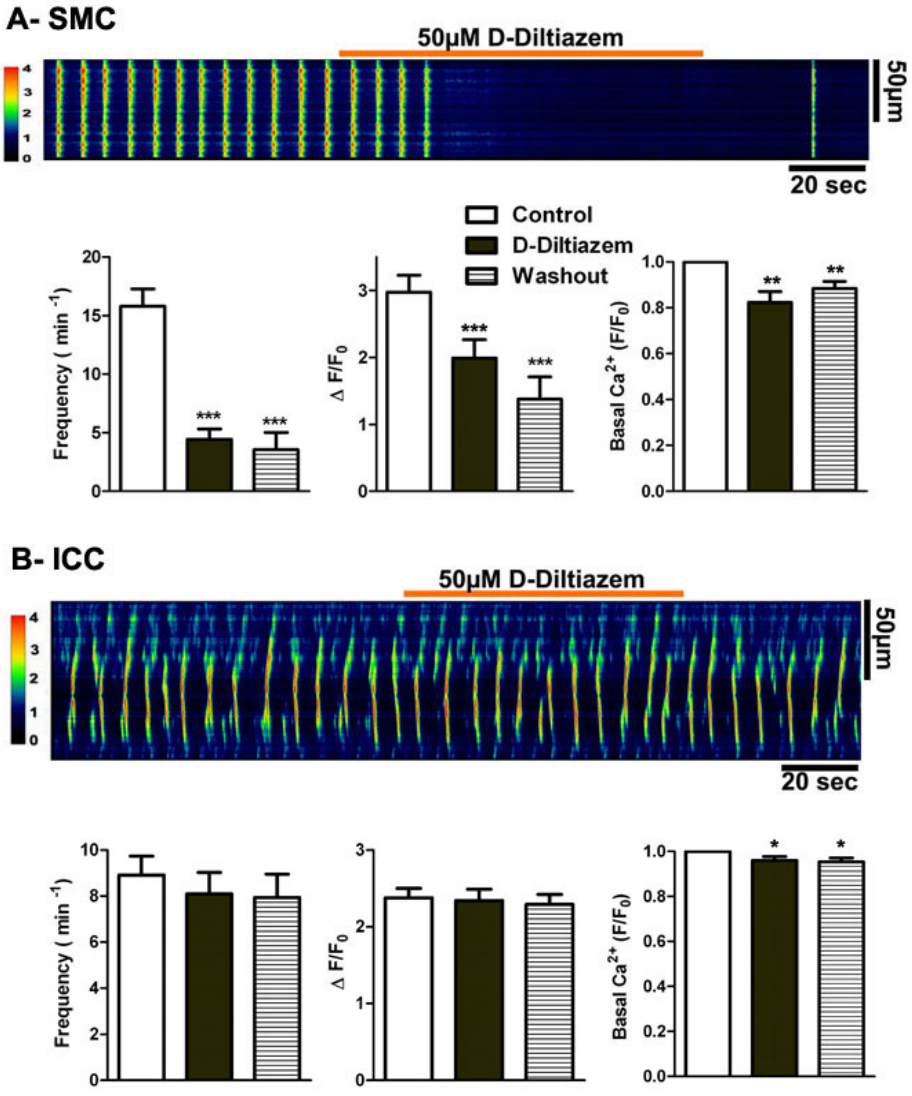

Figure 15. Efecto de D-Diltiazem sobre las oscilaciones espontáneas de Ca^{2+} en SMC (*A*) e ICC (*B*) aisladas de la uretra de conejo e incubadas con Fluo-4AM. Los paneles superiores muestran un registro representativo, y los paneles inferiores los valores medios de frecuencia (min $^{-1}$, izquierda), amplitud ($\Delta F/F_0$, centro) y Ca^{2+} basal (F/F_0; derecha). D-Diltiazem fue aplicado a una concentración de 50µM y estuvo presente durante 60-90 s antes del lavado con solución Hanks. Los resultados se expresan como media ± SEM (n = 14 SMC, n = 21 ICC). *$P < 0.05$, **$P < 0.01$, *** $P < 0.001$, diferencias significativas respecto al control (*t*-test de Student pareado).

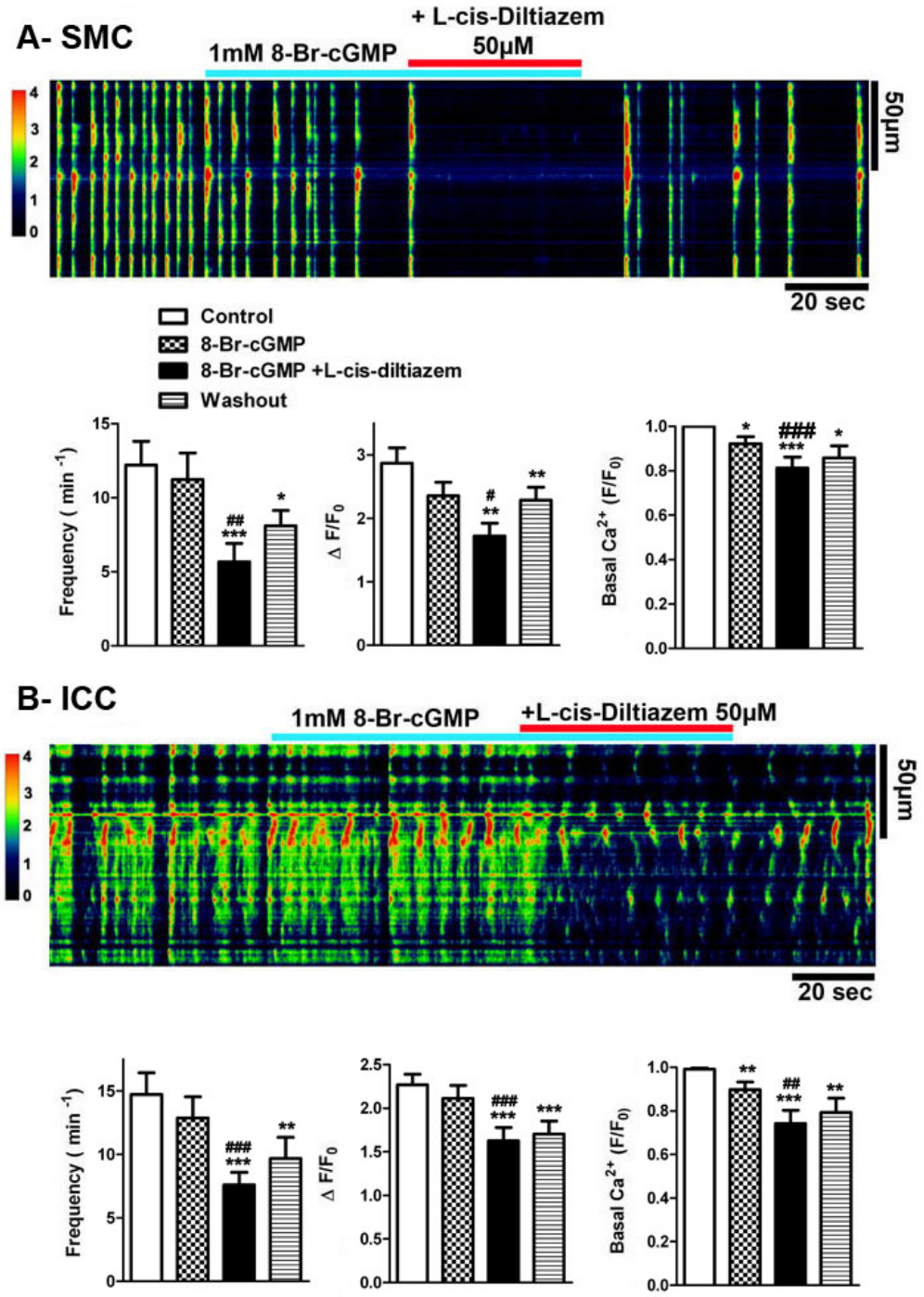

Figure 16. Efecto de L-cis-Diltiazem sobre los cambios en las oscilaciones de Ca^{2+} inducidos por 8-Br-cGMP en SMC (*A*) e ICC (*B*) aisladas de la uretra de conejo e incubadas con Fluo-4AM. Los paneles superiores muestran una imagen representativa, y los paneles inferiores muestran los valores medios de frecuencia (min $^{-1}$, izquierda), amplitud ($\Delta F/F_0$, centro) y Ca^{2+} basal (F/F_0; derecha). 8-Br-cGMP fue aplicado a una concentración de 1 mM durante 40-60 s, seguido de la posterior adición de L-cis-Diltiazem (50 µM). Ambos fármacos estuvieron presentes durante otros 40-60 s antes del lavado con solución Hanks. Los resultados se expresan como media ± SEM (n = 21 SMC, n = 22 ICC). *P < 0.05, **P < 0.01, *** P <0.001, diferencias significativas respecto al control; #P < 0.05, ## P < 0.01, ###P < 0.001 diferencias significativas respecto al tratamiento sólo con 8-Br-cGMP (*t*-test de Student pareado).

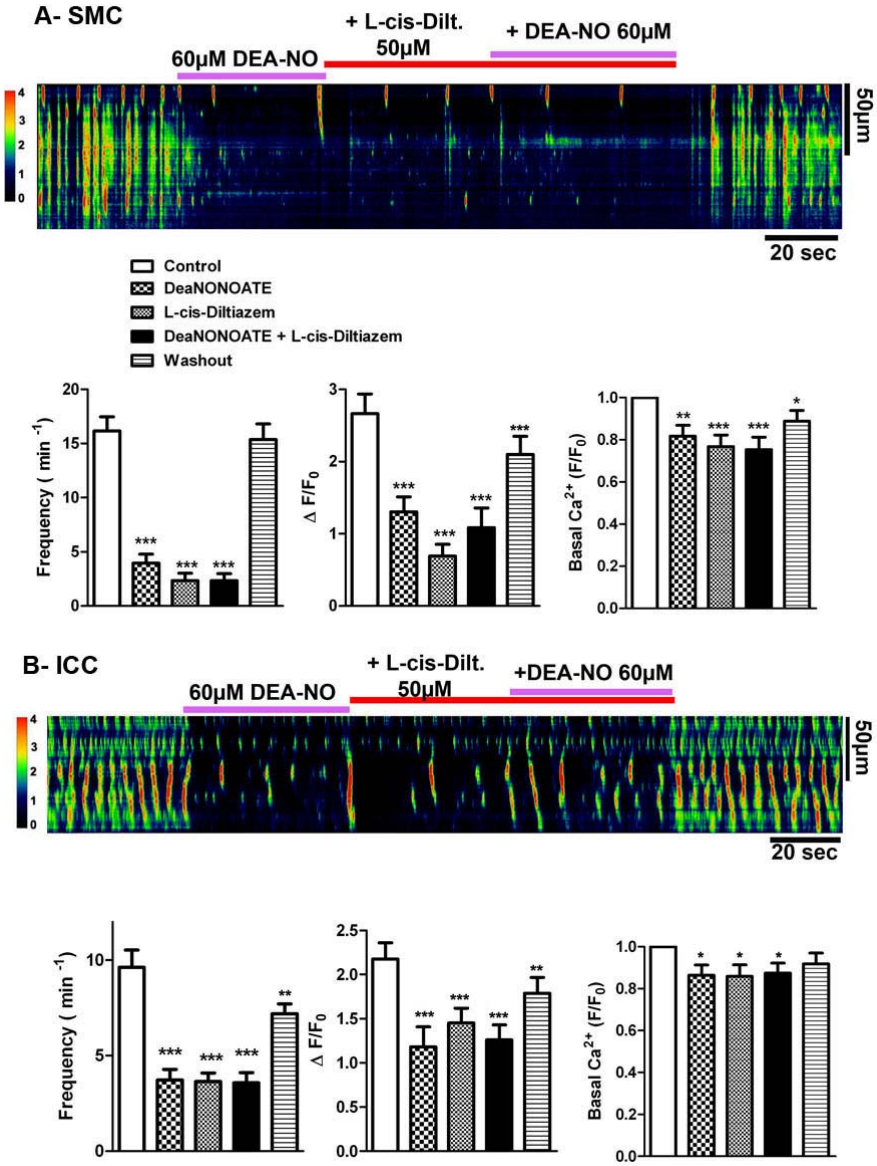

Figure 17. Efecto de L-cis-Diltiazem sobre los cambios en las oscilaciones de Ca^{2+} inducidas por DEA-NO en SMC (*A*) e ICC (*B*) aisladas de la uretra de conejo e incubadas con Fluo-4AM. Los paneles superiores muestran un registro representativo, y los paneles inferiores muestran los valores medios de frecuencia (min $^{-1}$, izquierda), amplitud ($\Delta F/F_0$, centro) y Ca^{2+} basal (F/F_0; derecha). DEA-NO fue aplicado a una concentración de 60 µM durante 40-50 s, seguido de la posterior adición de L-cis-Diltiazem (50 µM) durante otros 40-50 s. Por último, se realizó una nueva adición de DEA-NO, y ambos fármacos estuvieron presentes durante otros 40-50 s antes del lavado con solución Hanks. Los resultados se expresan como media ± SEM (n = 17 SMC, n = 14 ICC). *P < 0.05, **P < 0.01, *** P <0.001, diferencias significativas respecto al control (t-test de Student pareado).

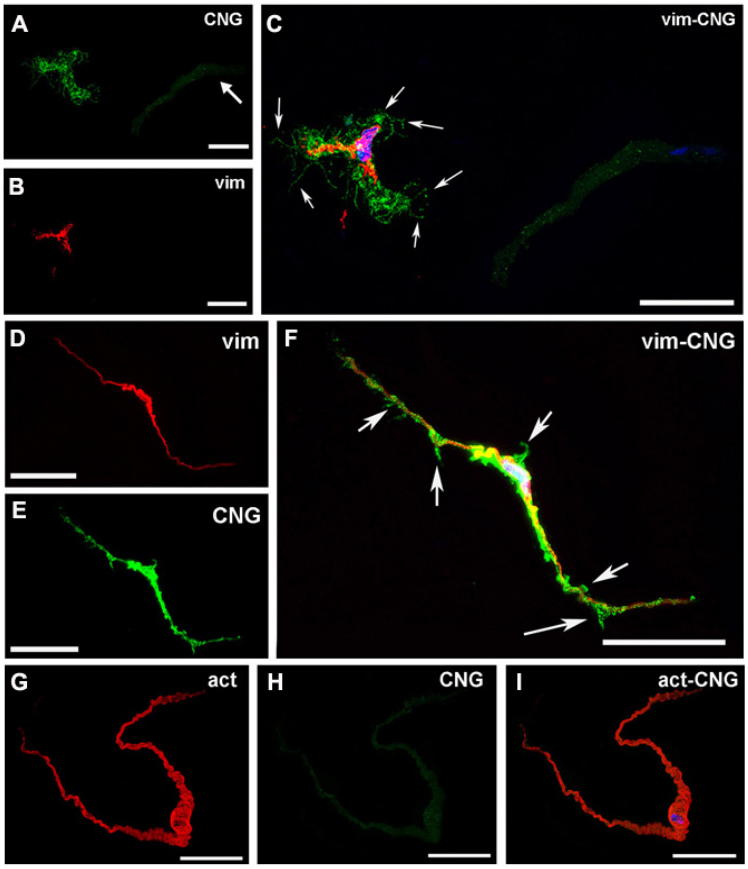

Figura 18. Comparación de la CNGA1-ir en SMC e ICC aisladas de la uretra de conejo. Microfotografías representativas que muestran la diferencia en la CNGA1-ir (verde) entre una SMC (señalada con flecha en *A*) y una ICC presentes en el mismo campo (*A-C*). Se puede observar una débil CNGA1-ir en SMC, mientras que existe una intensa CNGA1-ir en ICC con forma estrellada. Las ICC fueron también positivas para vimentina (rojo; *B, D*), que colocalizó con CNGA1-ir (*C, F*) mientras que las SMC lo fueron para α-actina (*G*) que colocalizó con la débil y difusa CNGA1-ir (*H*). *I* es la imagen combinada en la que la α-actina-ir roja enmascara a la CNGA1-ir verde. Nótese la presencia de CNGA1-ir en múltiples espículas muy finas que emergen del cuerpo celular y de las prolongaciones de las ICC (flechas). Los núcleos fueron marcados con DAPI (azul). Barra = 25 µm.

IV. Papel del acoplamiento eléctrico a través de uniones intercelulares comunicantes en la neurotransmisión uretral

En este apartado se analizó la posible implicación funcional de las uniones intercelulares comunicantes o GJ en la neurotransmisión tanto excitatoria (noradrenérgica) como inhibitoria (nitrérgica) uretral. Para ello se analizó el efecto funcional de diferentes bloqueantes de GJ en preparaciones uretrales de oveja y rata sometidas a EFS tanto excitatoria como inhibitoria. Se utilizó el ácido 18α-glicirretínico (α-GA), como bloqueante no selectivo de GJ (Davidson y Baumgarten, 1988), así como una mezcla de diferentes péptidos miméticos de Cx (péptidos GAP), considerados actualmente como la herramienta más selectiva para inhibir tipos específicos de GJ compuestas por determinadas Cx (Evans y Boitano, 2001; Wang et al., 2007). Por

último, se realizaron ensayos de RT-PCR e inmunofluorescencia con el fin de demostrar la presencia y distribución de Cx43, Cx40 y Cx37 en la uretra.

IV.1 Efecto de inhibidores de GJ en las respuestas neurogénicas contráctiles y relajantes

Se analizó el efecto de estos inhibidores tanto sobre las respuestas excitatorias adrenérgicas como sobre las inhibitorias nitrérgicas inducidas por EFS en preparaciones de uretra de oveja y de rata. La administración tanto de α-GA (50 μM, 30 min), como un cóctel de péptidos GAP (^{Cx43}Gap 26, $^{Cx37,\ 43Gap}$ 27, y ^{Cx40}Gap 27; 0.3mM cada uno, 2 h), no afectó en modo alguno tanto a las contracciones noradrenérgicas (**Fig. 19A**) como a las relajaciones nitrérgicas (**Fig. 19B**) en ninguna de las dos especies. Por lo tanto, la comunicación intercelular a través de GJ no parece jugar un papel esencial en la neurotransmisión uretral. La eficacia de los inhibidores empleados (α-GA y péptidos GAP) ha sido demostrada por el hecho de que fueron capaces de inhibir en ambas especies la respuesta contráctil inducida por la despolarización con una alta concentración de K^+ extracelular (**Fig. 20**).

IV.2 Expresión de mRNA de Cx43, Cx40, y Cx37 en la uretra de rata

Se llevó a cabo una PCR inversa utilizando cebadores específicos basados en las secuencias de mRNA que codifican Cx43, Cx40 y Cx37, y se amplificó una banda del tamaño previsto para cada una de ellas (627 bp, 503 bp y 509 bp, respectivamente), tanto en la uretra como en el corazón de la rata (**Fig. 21**), este último utilizado como control positivo.

IV.3 Expresión y distribución de Cx43, Cx40, y Cx37 en la uretra mediante inmunofluorescencia

De las tres Cx estudiadas, la que presentó una mayor expresión fue Cx43 detectada tanto en SMC como ICC de la uretra de oveja y de rata (**Fig. 22**). El marcaje en SMC se mostró en forma de un punteado fino o como una tinción irregular (**Fig. 22A**), mostrando en cualquier caso colocalización con el marcador de músculo liso α-actina (Figura 3 manuscrito IV). En ICC positivas a vimentina (**Fig. 22E-G**)**,** Cx43-ir apareció de forma típica en células fusiformes con múltiples y largas prolongaciones distribuidas entre los haces musculares o interconectadas entre ellas formando redes en la capa submucosa (Figuras 2 y 3 manuscrito IV). En ICC el patrón de marcaje de Cx43 fue más intenso y uniforme que en SMC, observándose intensa fluorescencia en toda la membrana, e incluso en el citoplasma (**Fig. 22E**).

Por otro lado, Cx37-ir se presentó en SMC (**Fig. 22C**) y en ICC distribuidas en las capas muscular y submucosa (**Fig. 22D**), aunque de forma mucho más débil que el marcaje de Cx43. Por último, se detectó una escasa Cx40-ir presente en el endotelio vascular y muy débilmente en las SMC, pero en ningún caso marcó ICC positivas a vimentina (Figura 2 manuscrito IV).

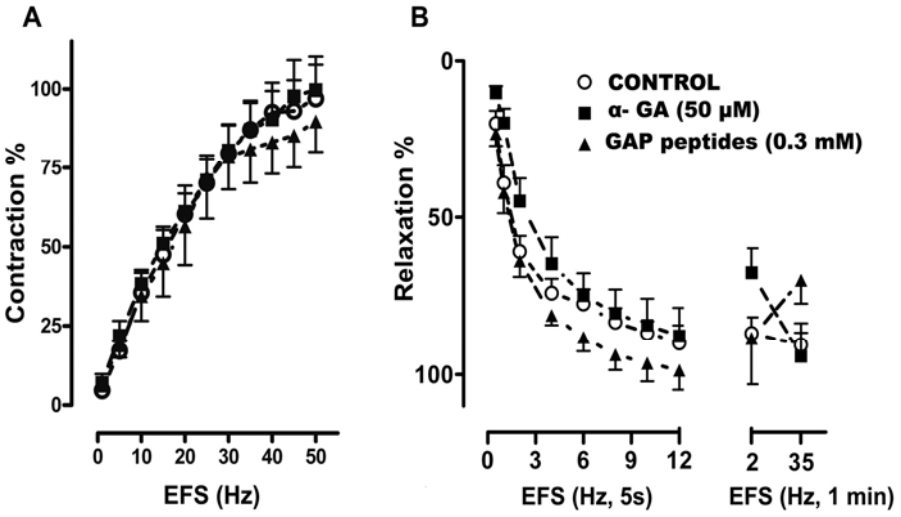

Figura 19. Curvas frecuencia-respuesta de contracción (*A*) y de relajación (*B*) en uretra de rata en presencia o ausencia (símbolos blancos) de los inhibidores de GJ: α-GA (50 μM, 30 min, ■) y péptidos GAP (0.3 mM, 2 h, ▲). Las preparaciones fueron sometidas a EFS de corta duración (5s, B izquierda) y larga duración (1 min, B derecha). Los resultados se expresan como media ± SEM (n = 7, de diferentes animales). No se observaron diferencias significativas entre ambos grupos (ANOVA de una vía). Resultados similares se obtuvieron en uretra de oveja.

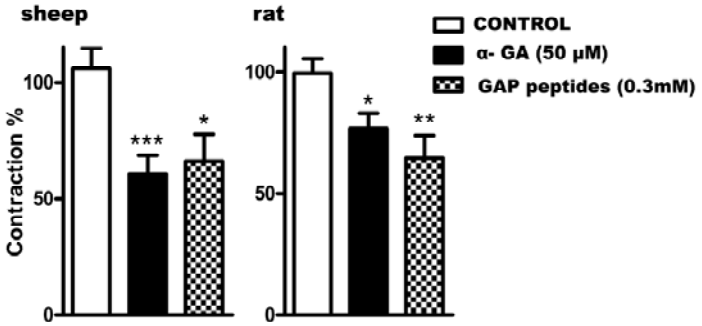

Figure 20. Efecto de los inhibidores de GJ en la contracción inducida por una alta concentración de K^+ extracelular (120 mM). Valores medios de la contracción inducida por la adición de K^+ 120 mM en la uretra de oveja (izquierda) y de rata (derecha) en condiciones control y tras el tratamiento con α-GA (50 μM, 30 min) o con los péptidos GAP (0.3 mM, 2 h). Los resultados se expresan como media ± SEM (n = 10, de diferentes animales de ambas especies). *P < 0.05, **P < 0.01, *** P <0.001, diferencias significativas respecto al control (ANOVA de una vía seguido de t-test de Student no pareado).

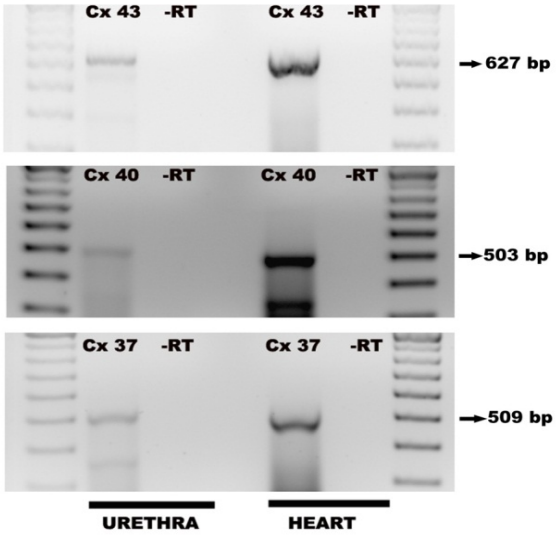

Figura 21. Productos amplificados por PCR correspondientes a las Cx43, Cx40 y Cx37, en uretra y corazón (control positivo) de rata. Los transcritos de mRNA para las tres Cx se corresponden con sus tamaños esperados: 627 bp para Cx43, 503 bp para Cx40, y 509 bp para Cx37 (carriles de la izquierda y derecha: escalera de 100 bp). Los controles negativos se llevaron a cabo sin realizar la transcripción inversa (–RT).

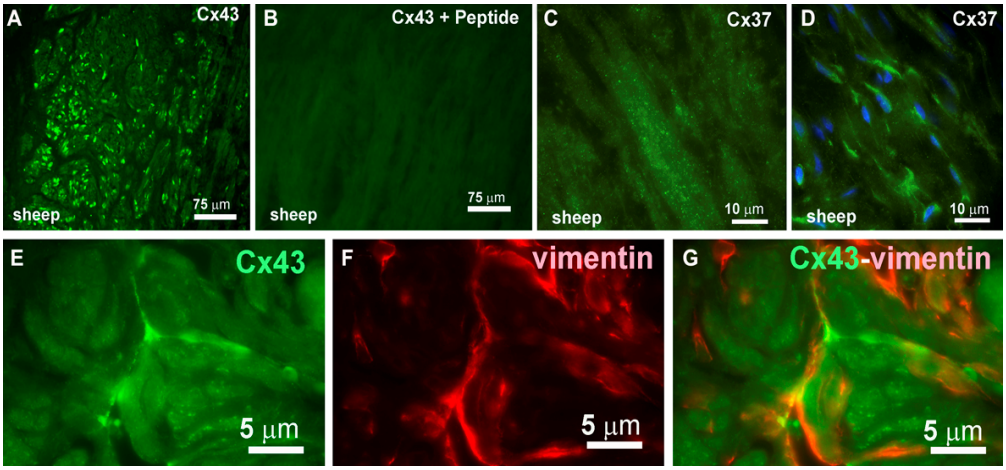

Figura 22. Inmunoreactividad a Cx43, Cx40, y Cx37 en la uretra de oveja y de rata. Nótese la expresión de Cx43 en forma de punteado irregular en las células musculares lisas (SMC) de la uretra de oveja (*A*) que desapareció cuando el tejido fue incubado con su correspondiente péptido bloqueante (*B*). También se observó débil Cx37-ir tanto en la capa muscular (*C*) como en la ICC presentes en la submucosa (*D*). Además se muestra la colocalización Cx43/vimentina en ICC de la uretra de rata. La inmunoreactividad a Cx43 (*E*) y vimentina (*F*) se muestra junto con su imagen combinada (*G*). Barra = 75 µm en A y B, 10 µm en C y D, 5 µm en E-G.

V. Participación de CaCC en la neurotransmisión excitatoria uretral: papel de las ICC

En el presente apartado se ha analizado la posible implicación de las ICC uretrales en la neurotransmisión excitatoria adrenérgica de la uretra por intermedio de CaCC. Mediante ensayos de inmunohistofluorescencia y PCR se analizó la distribución celular del canal de cloro ANO1 en la uretra de tres especies diferentes: oveja, rata y ratón. Además, se estudio el papel de los CaCC en la contractilidad neurogénica uretral mediante la exposición del tejido a un medio libre de cloruro, así como al efecto de varios inhibidores de dichos canales de cloro.

V.1 Efecto de la inhibición de los CaCC y de los receptores de IP_3 sobre la neurotransmisión uretral

Estudios preliminares en la uretra de rata y ratón permiten concluir que las respuestas contráctiles inducidas por EFS pueden considerarse debidas fundamentalmente a la liberación de NE desde terminaciones adrenérgicas, en concordancia con nuestros resultados anteriores en oveja (García-Pascual et al., 1991d). Así, estas respuestas fueron casi completamente inhibidas por fentolamina (10 μM), mientras que la posterior adición de TTX (1 μM) o de atropina (1 μM) no produjeron un mayor efecto inhibitorio. Sin embargo, cuando la atropina (1 μM) fue añadida antes que la fentolamina (Figura 3 manuscrito V), si se observó reducción significativa de las respuestas, tanto en la rata como en el ratón, sugiriendo la existencia de una liberación de ACh que posiblemente actúe presinápticamente sobre nervios adrenérgicos. Ambos neurotransmisores excitadores (NE y ACh) producen un efecto contráctil dosis-dependiente cuando se administran de forma exógena.

Aunque el inhibidor del transporte de aniones STIS (0.1 mM) no tuvo ningún efecto, inhibidores más específicos de los CaCC como ácido niflúmico (0.1 mM) o 9-AC (1 mM), originaron una inhibición significativa tanto de las contracciones inducidas por EFS como las provocadas por la adición acumulativa de NE o de ACh, especialmente en la uretra de rata y ratón (**Fig. 23 A-C**). De forma similar, la eliminación de Cl^- del medio extracelular provocó una reducción significativa de las respuestas contráctiles inducidas por EFS con mayor sensibilidad en la uretra de rata (**Fig. 24**).

Con objeto de evaluar si la estimulación de los CaCC se produce como consecuencia del aumento en los niveles intracelulares de Ca^{2+} que resulta de la activación de los receptores IP_3 presentes en los depósitos intracelulares de Ca^{2+}, se analizó el efecto de la inhibición del receptor IP_3 mediante 2-APB (60 μM; 30 min), aunque solamente se observó una reducción significativa de las respuestas contráctiles inducidas por EFS en el caso de la oveja. (**Fig. 25**).

A diferencia de las respuestas contráctiles, el pretratamiento con ácido niflúmico (50 μM), ni con 2-APB (60 μM) no fue capaz de modificar las respuestas relajantes

nitrérgicas inducidas por EFS en preparaciones de rata previamente precontraídas con AVP (0.1 μM) a ninguna de las frecuencias o duraciones de EFS probadas (Figuras 5 y 6 manuscrito V).

V.2 Expresión y distribución de los canales de cloro ANO1 en la uretra

Mediante RT-PCR se detectó la expresión de ANO1 en la uretra de rata. Se utilizaron para ello dos conjuntos de cebadores específicos diseñados a partir de secuencias conocidas de ANO1, dirigidas contra diferentes regiones del mRNA, que dieran lugar a productos de diferente tamaño y composición, para así garantizar una evaluación precisa de la expresión génica de ANO1 en la uretra. En ambos casos, cada conjunto de cebadores amplificó una banda específica del tamaño previsto a partir del mRNA obtenido tanto de la uretra como de la próstata, este último utilizado como control positivo. De hecho, el producto amplificado a partir del tejido uretral produjo una banda incluso de mayor intensidad que en la próstata. (**Fig. 26**).

Por inmunohistofluorescencia se detectó ANO1-ir exclusivamente en el músculo liso, donde colocaliza con α-actina, y en las células uroteliales de las tres especies estudiadas (**Fig. 27**). En ningún caso se observó la presencia de ANO1-ir en ICC positivas a vimentina, tanto las distribuidas en la lámina propia como entre los haces musculares lisos (**Fig. 27 D-F**). Tampoco se observó ANO1-ir en ninguna estructura nerviosa, incluidas fibras y troncos nerviosos.

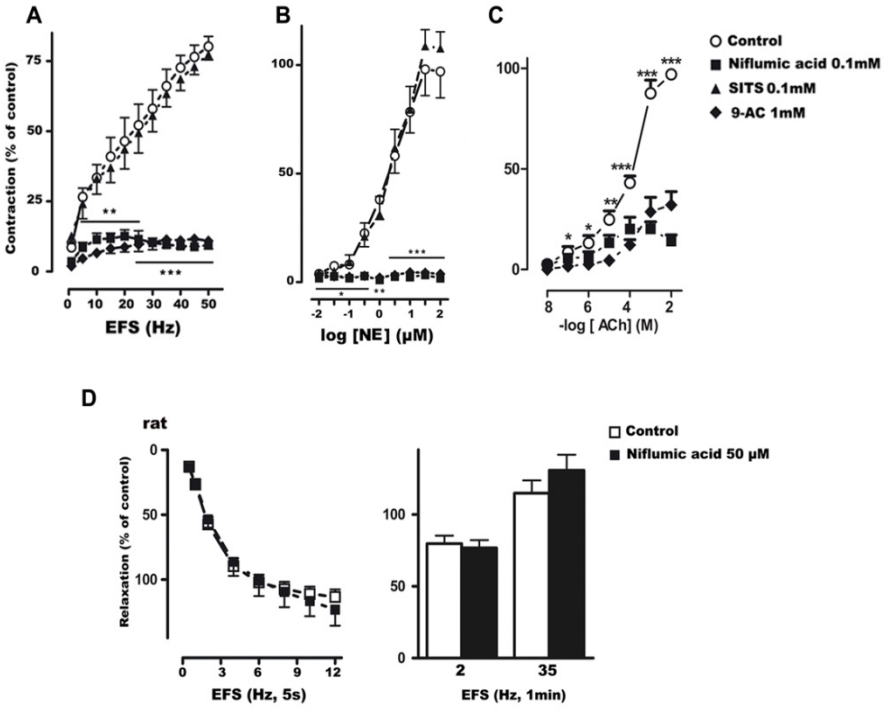

Figura 23. Efecto de los inhibidores de los canales de cloro (CaCC) sobre las respuestas contráctiles inducidas por EFS (*A*) o por la adición exógena de NE (*B*) y ACh (*C*) en comparación con su efecto sobre las respuestas relajantes inducidas por EFS (*D*) en uretra de rata. Las relajaciones fueron evaluadas en preparaciones previamente contraídas con AVP (0.1 μM). Los distintos inhibidores de CaCC: ácido 4-acetamido-4´-isotiocianato-2,2´-stilbenodisulfónico hidrato de sal disódica (STIS; 0.1 mM), ácido niflúmico (0.1 mM), y antraceno 9-carboxilato (9-AC; 1 mM) fueron incubados durante 30 min. Los resultados se expresan como porcentaje de sus respectivas curvas control en ausencia (símbolos blancos) o en presencia de STIS (0.1 mM; ▲), ácido niflúmico (0.1 mM; ■) o 9-AC (1mM; ♦) como media ± SEM (n = 5-8). *$P < 0.05$, **$P < 0.01$, *** $P < 0.001$, diferencias significativas respecto al control (ANOVA de una vía seguido de *t*-test de Student no pareado). Resultados similares se obtuvieron en la uretra de ratón y de oveja.

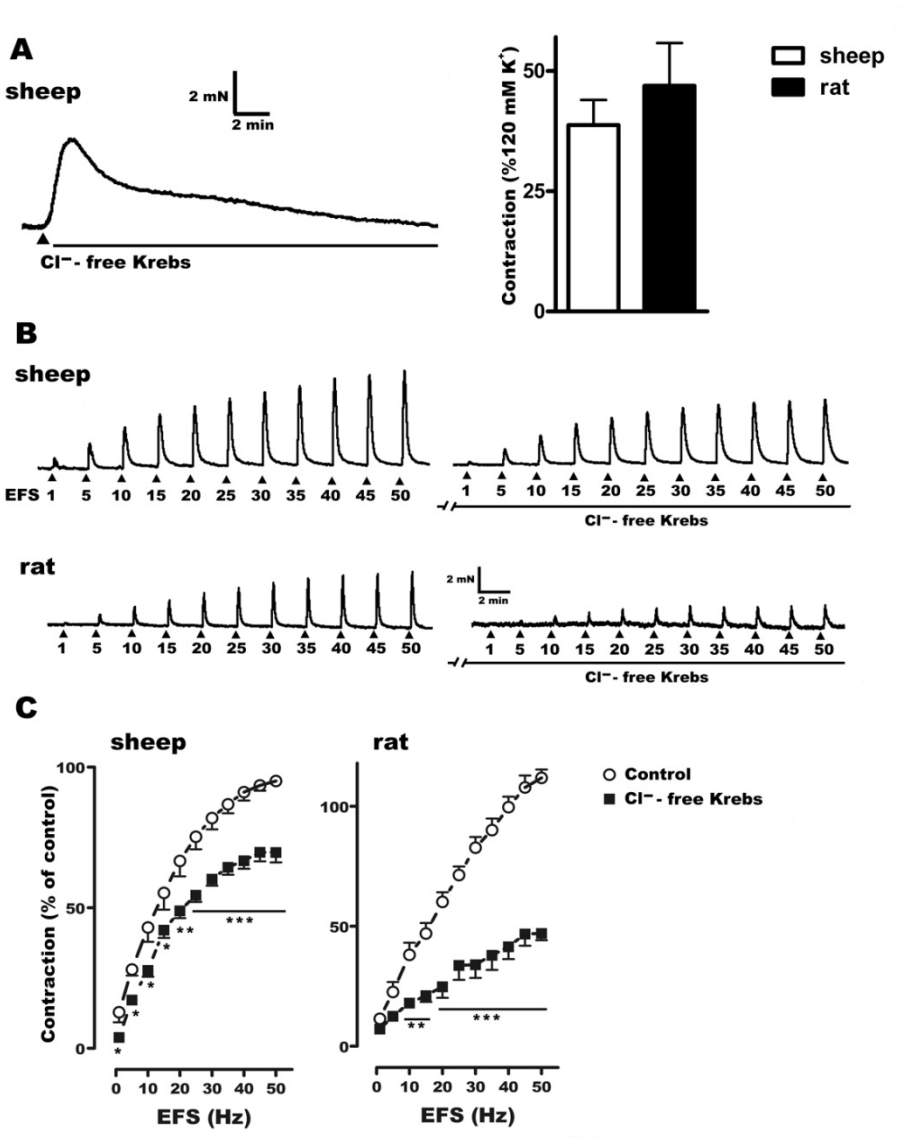

Figura 24. Efecto de la solución Krebs libre de Cl^- en las respuestas contráctiles nerviosas. *A*: curvas representativas (izquierda) que muestran la contracción uretral transitoria provocada por la exposición del tejido a la solución Krebs libre de Cl^- (punta de flecha). Derecha: diagrama de barras que muestra la reducción de la contracción inducida por K^+ 120mM en comparación la inducida previamente a la eliminación de Cl^- en la misma preparación. *B*: curvas representativas de la contracción inducida por EFS (5s, 1-50 Hz) en la uretra de oveja (parte superior) y de rata (parte inferior) en condiciones control (izquierda) y tras la incubación con la solución Krebs libre de Cl^- durante 30 min (derecha). *C*: Valores medios de las curvas frecuencia-respuesta en la uretra de oveja (izquierda) y de rata (derecha) en presencia de solución Krebs libre de Cl^- (símbolos negros) o en solución Krebs normal (símbolos blancos). Los resultados se expresan en porcentaje de la primera respuesta control en cada preparación y como media ± SEM (n = 8 en oveja, n = 7 en rata). *$P < 0.05$, **$P < 0.01$, *** $P <0.001$, diferencias significativas respecto al control (ANOVA de una vía seguido de *t*-test de Student no pareado).

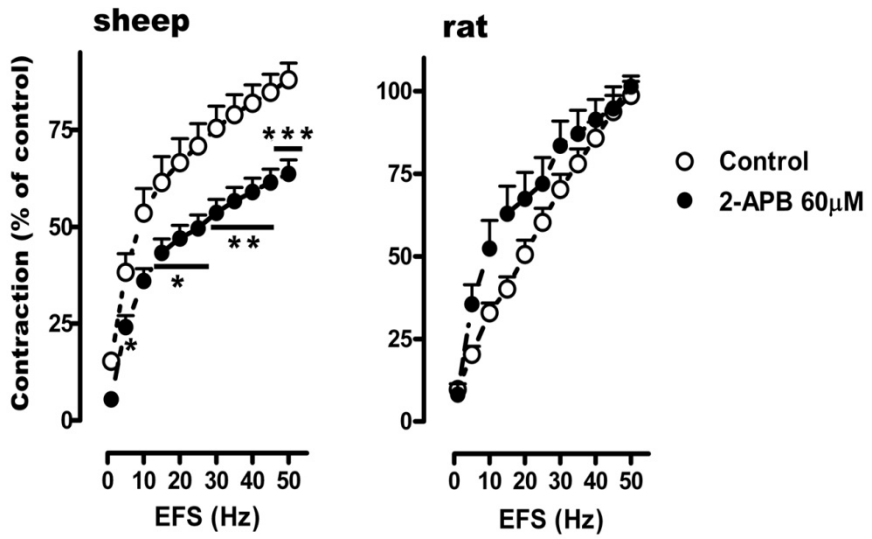

Figura 25. Efecto del inhibidor del receptor IP_3, 2-APB sobre las respuestas contráctiles inducidas por EFS en la uretra de oveja (izquierda) y rata (derecha). Los resultados se expresan como media ± SEM (n = 7 en oveja, n = 6-8 en rata). *$P < 0.05$, **$P < 0.01$, *** $P < 0.001$, diferencias significativas respecto al control (ANOVA de una vía seguido de t-test de Student no pareado).

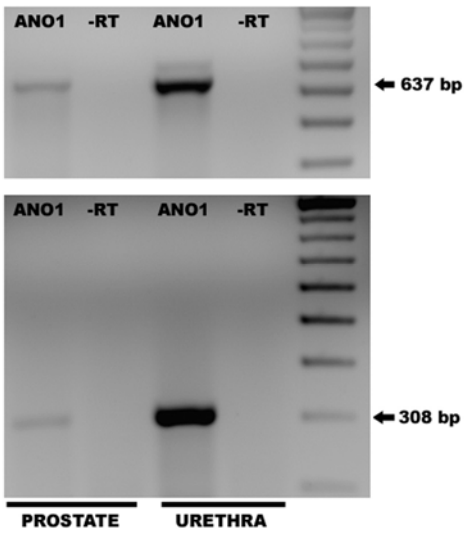

Figura 26. Expresión del mRNA de ANO1 en la uretra de rata. Los transcritos de mRNA fueron amplificados a partir de tejido uretral [637 bp para el primer conjunto de cebadores de ANO1 (parte superior), y 308 bp para el segundo conjunto de cebadores de ANO1 (parte inferior)], y se correspondieron con los trascritos amplificados a partir de tejido prostático de rata (control positivo). Los controles negativos se llevaron a cabo sin realizar la transcripción inversa (–RT). Carril derecho: escalera de 100 bp.

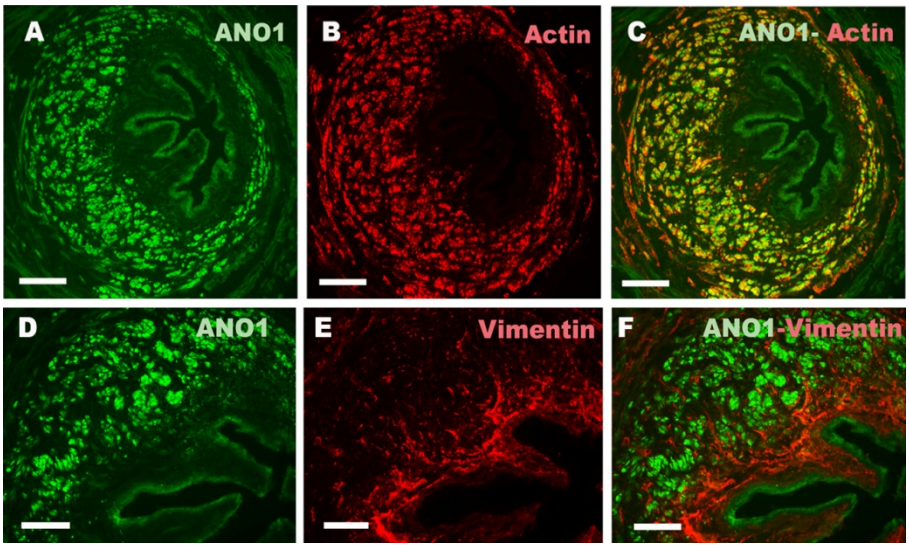

Figura 27. La inmunoreactividad a ANO1 (ANO1-ir; verde; *A*) colocaliza con α-actina (rojo; *B, C*) en fibras musculares pero no con ICC positivas a vimentina. Se muestran microfotografías representativas de la intensa ANO1-ir (verde; *A, D*) en la capa de músculo liso y algo más débil en el urotelio. En ningún caso se detectó ANO1-ir en la capa submucosa y no colocalizó (*F*) con vimentina (rojo; *E*) presente en ICC de la capa submucosa y entre los fascículos musculares. Barra = 50 μm.

VI. Cambios en la producción de NO en la vejiga y uretra en un modelo experimental de cistitis hemorrágica inducida por CYP en la rata

El siguiente objetivo de este estudio fue analizar desde un punto de vista fisiopatológico los cambios inducidos por un proceso inflamatorio en la producción de NO (cambios en la expresión y distribución de las diferentes isoformas de NOS: eNOS, nNOS e iNOS) con objeto de relacionarlo posteriormente con la posible implicación de ICC. Se empleó un modelo previamente estandarizado de cistitis hemorrágica inducida por CYP en la rata, extendiendo el estudio a su efecto sobre la uretra. Se realizaron tres tipos de tratamientos: agudo (4 h; 150 mg Kg^{-1}), intermedio (48 h; 150 mg Kg^{-1}), y crónico (10 días; 70 mg Kg^{-1} cada tres días) en comparación con sus respectivos controles. Se realizaron ensayos de inmunohistofluorescencia, Western Blot y PCR (convencional y cuantitativa) y se estudiaron las posibles alteraciones en la neurotransmisión excitatoria e inhibitoria de la vejiga y uretra.

Después del tratamiento con CYP, las ratas mostraron claros síntomas de dolor y algunos animales sometidos a tratamiento crónico presentaron sangrado de ojos y hocico, y aproximadamente el 10% murieron antes de la finalización del tratamiento, mostrando signos de hemorragia en diferentes órganos (hígado, riñón y pulmón) y sangre en la orina. Estos animales fueron excluidos del análisis.

A consecuencia del tratamiento con CYP se incrementó la frecuencia miccional, particularmente del número de micciones de pequeño volumen como indicativo de la aparición de síntomas de hiperactividad vesical (Figura 1 manuscrito VI). El peso del

tracto urinario inferior aumento significativamente y tanto la vejiga como la uretra de los animales tratados (especialmente en los tratamientos intermedio y crónico) mostraron signos claros de inflamación (Figura 2 manuscrito VI). Se observó la aparición de edema, lesión vascular, hemorragia, infiltración celular y erosión o proliferación del urotelio, en diversos grados, con alteraciones similares tanto en la vejiga como la uretra (Figura 2 y Tabla 2 manuscrito VI). Además, se demostró un incremento en el número de macrófagos (inmunoreactivos a CD163) infiltrados en la capa muscular y especialmente en la lámina propia de ambos órganos (Figura 3 manuscrito VI).

VI.1 Cambios en la expresión de las distintas isoformas de NOS inducidos por el tratamiento con CYP

A pesar de que diversos trabajos previos han sugerido que la inducción de iNOS es uno de los mecanismos patogénicos iniciales que desencadenan la cistitis por CYP, nuestros resultados no mostraron evidencias de que se produjera expresión de la isoforma inducible de NOS en ningún caso, ni en los animales control, ni siquiera en los animales tratados con CYP, tanto en la vejiga como en la uretra. No se detectó inmunoreactividad a iNOS (iNOS-ir) en ensayos de inmunohistoquímica ni se demostró la expresión de la proteína de iNOS mediante ensayos de inmunotransferencia por Western Blot (**Fig. 28**). Sin embargo, la especificidad del anticuerpo primario fue demostrada mediante el uso de dos proteínas recombinantes como controles positivos (**Fig. 28**). Por último, los transcritos de mRNA para iNOS no fueron amplificados ni para la vejiga ni para la uretra en los tratamientos control e intermedio (CYP 48h) utilizando tres pares de cebadores diferentes, mientras que a partir del control positivo si fue amplificada una banda del tamaño esperado (cDNA de iNOS de macrófago de ratón; **Fig. 28**).

Si se observaron sin embargo cambios significativos en la expresión de las isoformas constitutivas de NOS, tanto nNOS como eNOS, aunque en sentido inverso. Mientras que la expresión de nNOS disminuyó en los tratamientos agudo e intermedio recuperándose parcialmente en el tratamiento crónico, la expresión de la isoforma endotelial mostró un aumento progresivo a consecuencia del tratamiento con CYP. Así, la inmunoreactividad a nNOS (nNOS-ir) presente en gran densidad en nervios nitrérgicos, fundamentalmente de la región del trígono y de la uretra, disminuyó en respuesta al tratamiento con CYP agudo e intermedio, pero se recuperó parcialmente después del tratamiento crónico (**Fig. 29**). Esta misma evolución de la expresión de la proteína nNOS fue corroborada mediante ensayos de Western Blot (**Fig. 30**). Por el contrario, la débil inmunoreactividad a eNOS detectada en el endotelio vascular y urotelio de los tejidos control aumentó de forma dramática en los animales tratados con CYP, extendiéndose su presencia a las células musculares lisas vecinas y a otras células del intersticio (**Fig. 31**). Los ensayos de Western Blot mostraron la aparición de dos bandas específicas de eNOS en ambos órganos. De éstas, la más pequeña (60 KDa) es la

que presentó los aumentos más manifiestos tras los tratamientos con CYP intermedio y crónico, especialmente en la vejiga (**Fig. 32**). En experimentos de PCR cuantitativa sin embargo, no se detectó un aumento significativo en la expresión del mRNA de eNOS en cualquiera de los tejidos en respuesta al tratamiento con CYP intermedio (Figura 8 manuscrito VI).

VI.2 Cambios en la contractilidad vesical y uretral inducidos por el tratamiento con CYP

Con objeto de evaluar el efecto del tratamiento con CYP sobre las respuestas motoras o eferentes tanto en la vejiga como en la uretra, se analizaron las contracciones inducidas por una alta concentración de K^+ extracelular (120 mM), por EFS, o por la adición de agonistas exógenos. En el caso de la vejiga se observó una disminución significativa de todas las respuestas contráctiles (alta concentración de K^+, EFS o adición de ACh) tras el tratamiento intermedio con CYP, efecto que fue revertido en los animales sometidos a tratamiento crónico (**Fig. 33**). Sin embargo, el tratamiento con CYP en la uretra no presentó ningún efecto tanto sobre las respuestas contráctiles, inducidas por una alta concentración de K^+ o por NE exógena, como relajantes, inducidas por EFS o por la adición exógena de SNC (Figura 10 en manuscrito VI). Las relajaciones inducidas por EFS en la uretra fueron abolidas por L-NNA (0.1 mM), mostrando así su origen nitrérgico (no mostrado). El pretratamiento con L-NNA (0.1 mM) no modificó las respuestas contráctiles de la vejiga (**Fig. 33**) y de la uretra, sugiriendo que los cambios provocados en la vejiga por el tratamiento con CYP no parecen estar relacionados con cambios en la producción de NO.

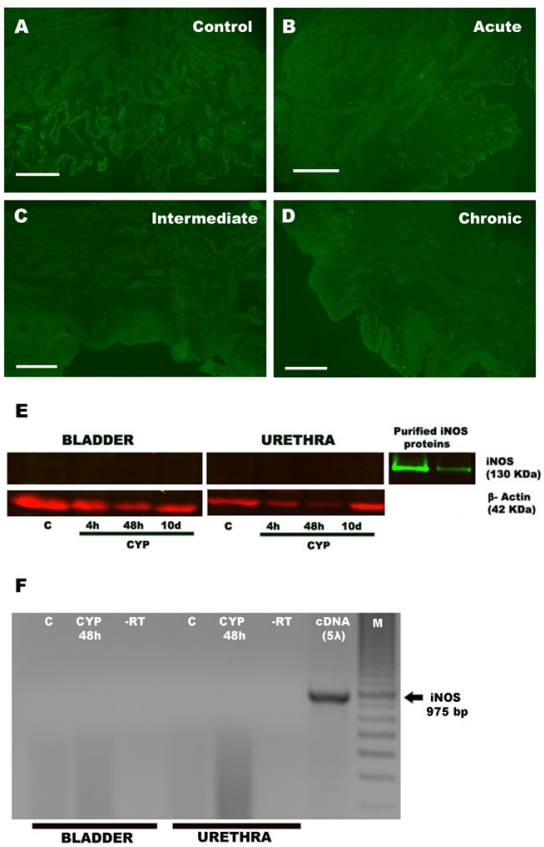

Figura 28. Ausencia en la expresión de iNOS en la uretra y vejiga tanto en condiciones control como después de cualquiera de los tratamientos inducidos por CYP.*A-D*: imágenes representativas de iNOS-ir en secciones de vejiga. Barra = 100 µm. *E*: Ausencia de inmunotransferencia de iNOS en la vejiga y uretra. Dos proteínas purificadas de iNOS (130 KDa) fueron incluidas como controles positivos (derecha). El anticuerpo anti- β-actina fue utilizado como control de carga. *F*: imagen de RT-PCR que muestra la ausencia de expresión del mRNA de iNOS en vejiga (izquierda) y uretra (derecha), tanto en preparaciones control como después del tratamiento intermedio con CYP (48h). Se utilizó como control positivo el cDNA de la iNOS presente en macrófagos de ratón. RT, control sin transcripción inversa; M, marcador molecular.

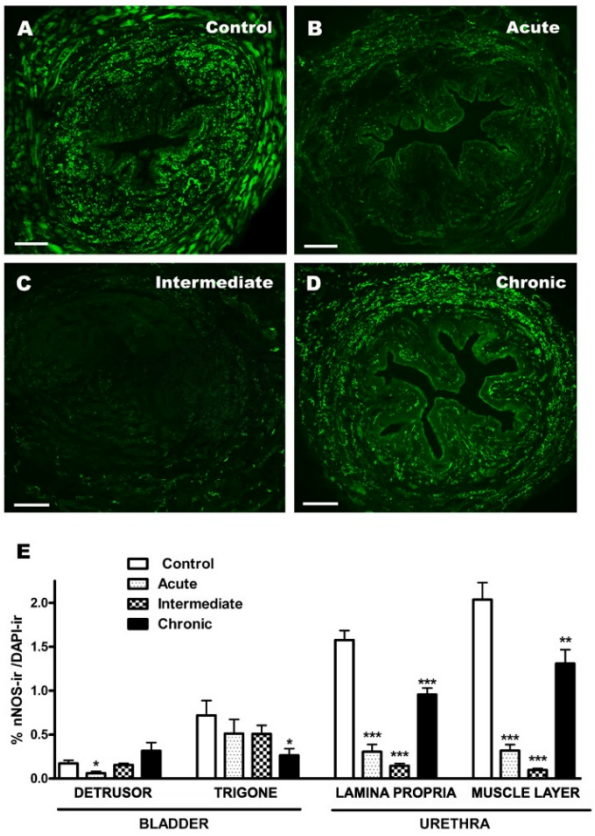

Figura 29. Reducción de la inmunoreactividad a nNOS a consecuencia del tratamiento con CYP en la vejiga y la uretra. *A-D*: imágenes representativas de nNOS-ir en la uretra. *E*: cuantificación de nNOS-ir en la vejiga y uretra. Barra = 50 μm. Las mediciones se realizaron de forma independiente en el músculo detrusor y trígono de la vejiga, y en la lámina propia y capa muscular lisa de la uretra. Se midió el área por encima del umbral de intensidad y se normalizó con el número de células presentes en dicha región (núcleos marcados con DAPI). Los resultados se expresan como media ± SEM (n = 6-7 campos diferentes de al menos 4 animales). *P <0.05 **P < 0.01, *** P <0.001, diferencias significativas respecto al control (ANOVA de una vía seguido de t-test de Student no pareado).

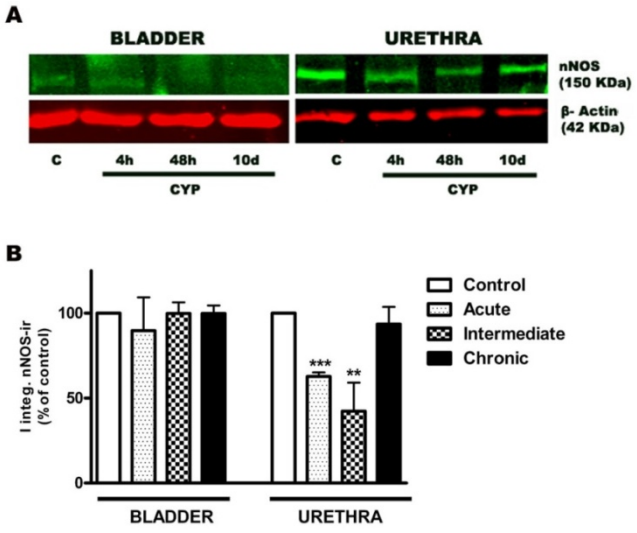

Figura 30. Efecto del tratamiento con CYP en la expresión de la proteína nNOS en la vejiga y la uretra. *A*: Imágenes representativas de Western Blots. *B*: cuantificación de la proteína nNOS en condiciones control y tras el tratamiento con CYP. Los resultados se normalizaron a los de β-actina (control de carga) y se expresaron como porcentaje de las muestras control. Los resultados se expresan como media ± SEM (n = 4). **P < 0.01, *** P <0.001, diferencias significativas respecto al control (ANOVA de una vía seguido de t-test de Student no pareado).

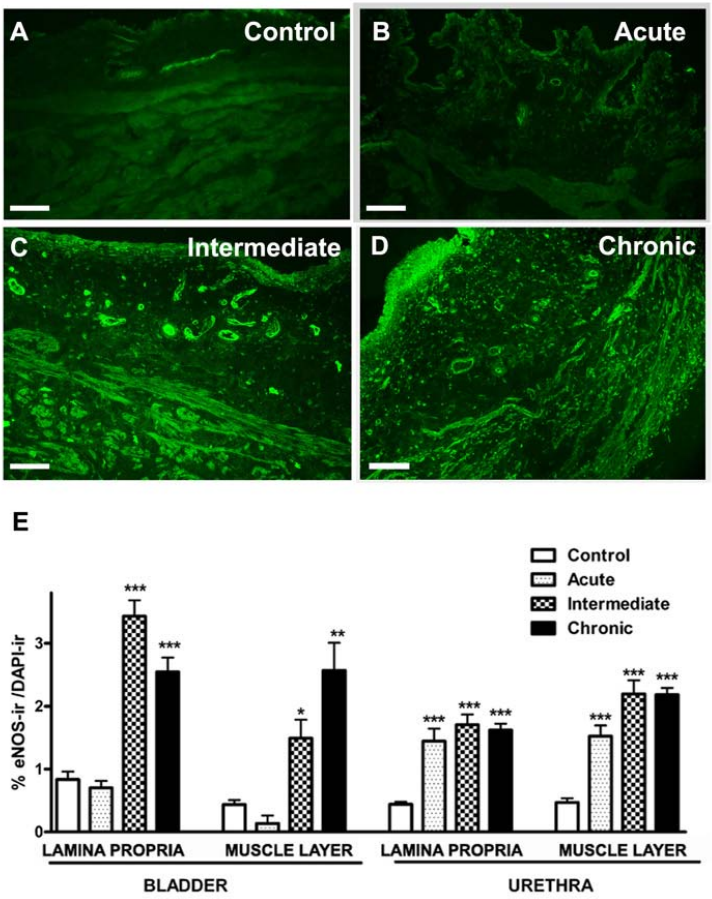

Figura 31. Prominente aumento en la inmunoreactividad a eNOS a consecuencia del tratamiento con CYP en la vejiga y la uretra. *A-D*: Imágenes representativas en la vejiga, Barra = 50 μm. *E*: cuantificación de la eNOS-ir en la vejiga y uretra. Las mediciones se realizaron de forma independiente en la lámina propia y capa muscular de ambos órganos. Se midió el área por encima del umbral de intensidad y se normalizó con el número de células presentes en dicha región (núcleos marcados con DAPI). Los resultados se expresan como media ± SEM (n = 6-7 campos diferentes de al menos 4 animales). *P <0.05 **P < 0.01, *** P <0.001, diferencias significativas respecto al control (ANOVA de una vía seguido de t-test de Student no pareado).

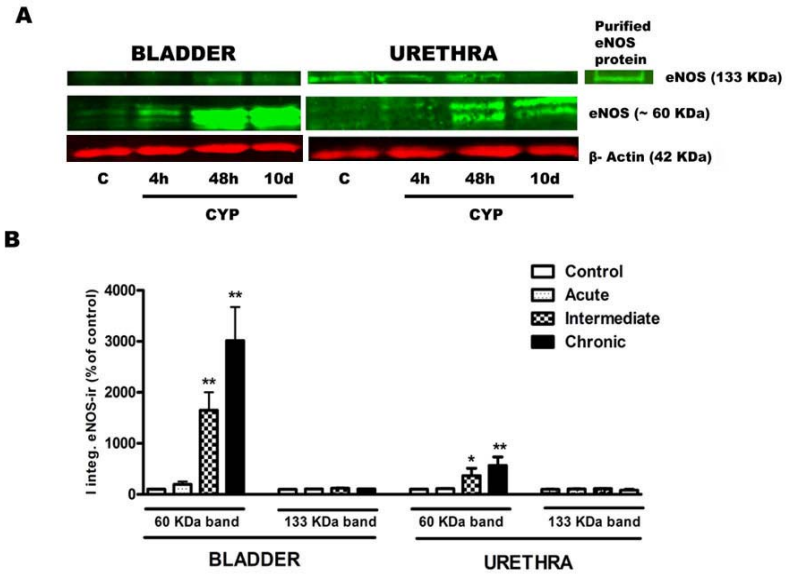

Figura 32. Efecto del tratamiento con CYP en la expresión de la proteína eNOS en la vejiga y la uretra. *A*: imágenes representativas de Western Blots, y *B*: cuantificación de la proteína eNOS. Se incluyó una proteína purificada bovina de eNOS como control positivo (~130 KDa, derecha). Los resultados cuantitativos muestran por separado las dos bandas (60 KDa y 133 KDa), y se expresan como porcentaje de las muestras control usando β-actina como control de carga. Los resultados se expresan como media ± SEM (n = 4). *P <0.05, **P < 0.01, diferencias significativas respecto al control (ANOVA de una vía seguido de t-test de Student no pareado).

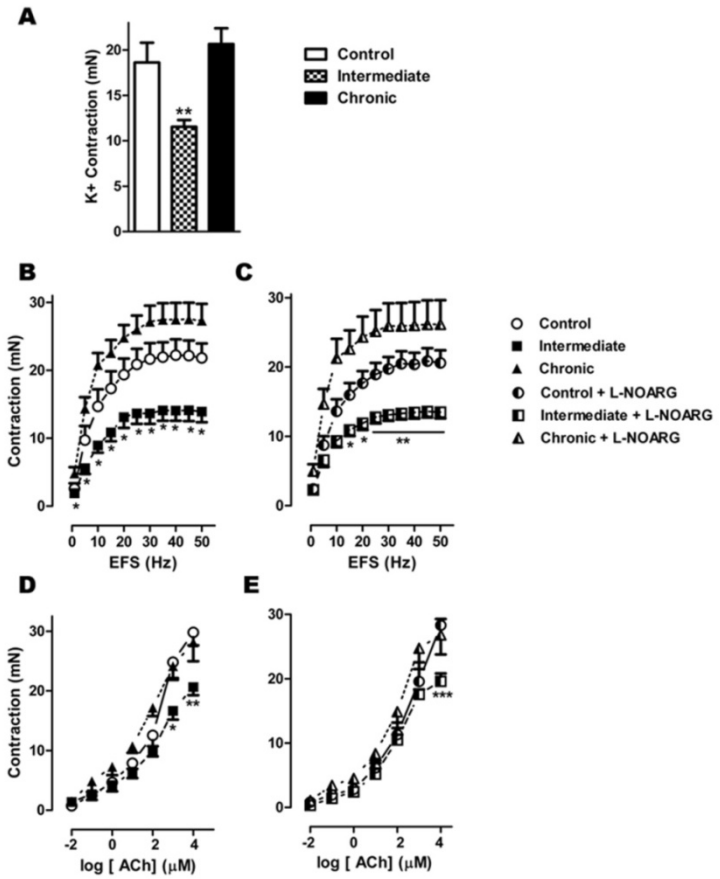

Figura 33. Efecto del tratamiento con CYP sobre la contractilidad vesical. *A*: respuestas contráctiles inducidas por K^+ 120mM. *B- C*: curvas frecuencia-respuesta, y *D- E*: curvas dosis-respuesta inducidas por la adición acumulativa de ACh en condiciones control (símbolos blancos) y tras el tratamiento con CYP intermedio (48 h; ■) y crónico (10 días; ▲), en presencia (C, y E) o ausencia (A, B, y D) de L-NNA (0.1 mM; símbolos rellenos a la mitad). Los resultados se expresan como valores absolutos (mN) y representan la media ± SEM (n = 6 por grupo). **P* <0.05, ***P* < 0.01, diferencias significativas respecto al control (ANOVA de una vía seguido de *t*-test de Student no pareado).

VII. Participación de ICC en la cistitis inducida por CYP

El último objetivo del presente estudio fue investigar los posibles cambios en el número y distribución de las diferentes subpoblaciones de ICC presentes en la vejiga y en la uretra de los animales tratados con CYP mediante el uso de 4 marcadores diferentes: vimentina, c-kit, CD34 y PDGFRα. Además, se investigó el posible efecto protector de un tratamiento previo con Glivec (mesilato de imatinib), un inhibidor de receptores tirosina quinasa y se sabe que es capaz de inhibir el receptor c-kit y el receptor PDGFR (Druker et al., 1996). En este caso se realizaron únicamente dos tratamientos con CYP: intermedio (48 h; 150 mg Kg^{-1}), y crónico (10 días; 50 mg Kg^{-1} cada 3 días) junto con sus respectivos controles. La dosis empleada en el tratamiento crónico fue inferior a la utilizada previamente con objeto de reducir sus efectos sistémicos. Paralelamente, otros grupos experimentales recibieron un tratamiento previo con Glivec (10 mg Kg^{-1} por vía oral, cinco días antes y durante todo el tratamiento con CYP). Por último, se analizó la aparición de expresión a eNOS en las diferentes subpoblaciones de ICC de los animales tratados con CYP.

VII.1 Cambios en la densidad y distribución de ICC inmunoreactivas a c-kit, vimentina, CD34 y PDGFRα

El tratamiento con CYP originó un notorio aumento en la densidad de ICC positivas a los cuatros marcadores utilizados (**Figs. 34, 35**; Figuras 2, 4 manuscrito VII), evidente tanto en la lámina propia como en la capa muscular de ambos órganos y que aumentó progresivamente con la duración del tratamiento (**Figs. 34, 35**). Destaca el intenso aumento en el número de ICC a nivel subepitelial formando una capa con tal densidad celular que en algunos casos impide distinguir las células individuales (**Figs. 36J, N, Q**; Figuras. 2B, 4I manuscrito VII**)** mientras que en la capa muscular, las ICC fueron especialmente densas en la periferia de los haces musculares, expandiéndose hacia la serosa, donde forman una densa corona celular, fundamentalmente en el caso de la uretra (**Figs. 35 H-I**; Figura 2 H-I manuscrito VII).

Los marcajes dobles, utilizando parejas de anticuerpos generados en diferentes especies, mostraron en todos los casos la existencia de un elevado grado de colocalización (**Fig. 36**) que pese a no ser completa en ningún caso, mostró porcentajes generalmente superiores al 60% (Tabla 1 manuscrito VII). Dicho porcentaje fue superior al 90 % entre CD34 y PDGFRα en ambos órganos, mientras que el menor grado de colocalización correspondió a las parejas vimentina-CD34. Los porcentajes de colocalización fueron similares en la lámina y propia y capa muscular (Tabla 1 manuscrito VII).

En ninguno de los casos el tratamiento con CYP modificó el grado de colocalización de ninguna de las parejas de anticuerpos analizados (Tabla 1, manuscrito VII), indicando que la población de ICC que prolifera como resultado del tratamiento con CYP es positiva a los cuatro marcadores empleados.

VII.2 Efecto preventivo del tratamiento con Glivec

El tratamiento previo con Glivec redujo significativamente el número de micciones totales y de pequeño tamaño (**Fig. 37**), y también atenuó significativamente el aumento en el peso del tracto urinario inferior que se observa tras el tratamiento intermedio con CYP (Figura 7 manuscrito VII).

En los estudios de inmunofluorescencia se observó una drástica reducción en el número de ICC en los animales sometidos a tratamiento previo con Glivec, que se manifestó con todos los marcadores empleados, tanto en la lámina propia como en la capa muscular lisa de ambos órganos y tanto en el tratamiento intermedio como en el crónico con CYP (**Figs. 34, 35**; Figuras 2, 4 manuscrito VII).

VII.3 Inducción de la expresión de eNOS en ICC: nueva fuente de NO durante la inflamación

Como se ha descrito previamente (manuscrito VI), en animales tratados con CYP se observó, por inmunofluorescencia simple, la extensión de la expresión de eNOS a células morfológicamente compatibles con ICC. En el presente estudio se han realizado marcajes dobles de eNOS con distintos marcadores de ICC, con el fin de determinar la naturaleza de estas células. Sólo pudieron realizarse comparaciones directas entre eNOS y vimentina o CD34 debido a la imposibilidad de encontrar anticuerpos eficaces frente a c-kit y PDGFRα que no hubieran sido generados en conejo, especie en la que se obtuvo el anticuerpo frente a eNOS.

Nuestros resultados muestran la colocalización de eNOS con vimentina y CD34 en células de morfología alargada, con escaso citoplasma y largas prolongaciones celulares, similares a las anteriormente descritas, y por lo tanto identificables como ICC (**Fig. 38 A-F**). Esta expresión se dio en ICC vesicales y uretrales con diferente localización: la lámina propia (ICC-LP; **Fig. 38 A-C**), el interior de los fascículos musculares (ICC-IM; **Fig. 38 D-F**), o rodeando los fascículos musculares (ICC-SEP, **Fig. 38 G-I**). Las ICC inmunoreactivas a vimentina y/o CD34 no mostraron sin embargo eNOS-ir en los animales control (no mostrado).

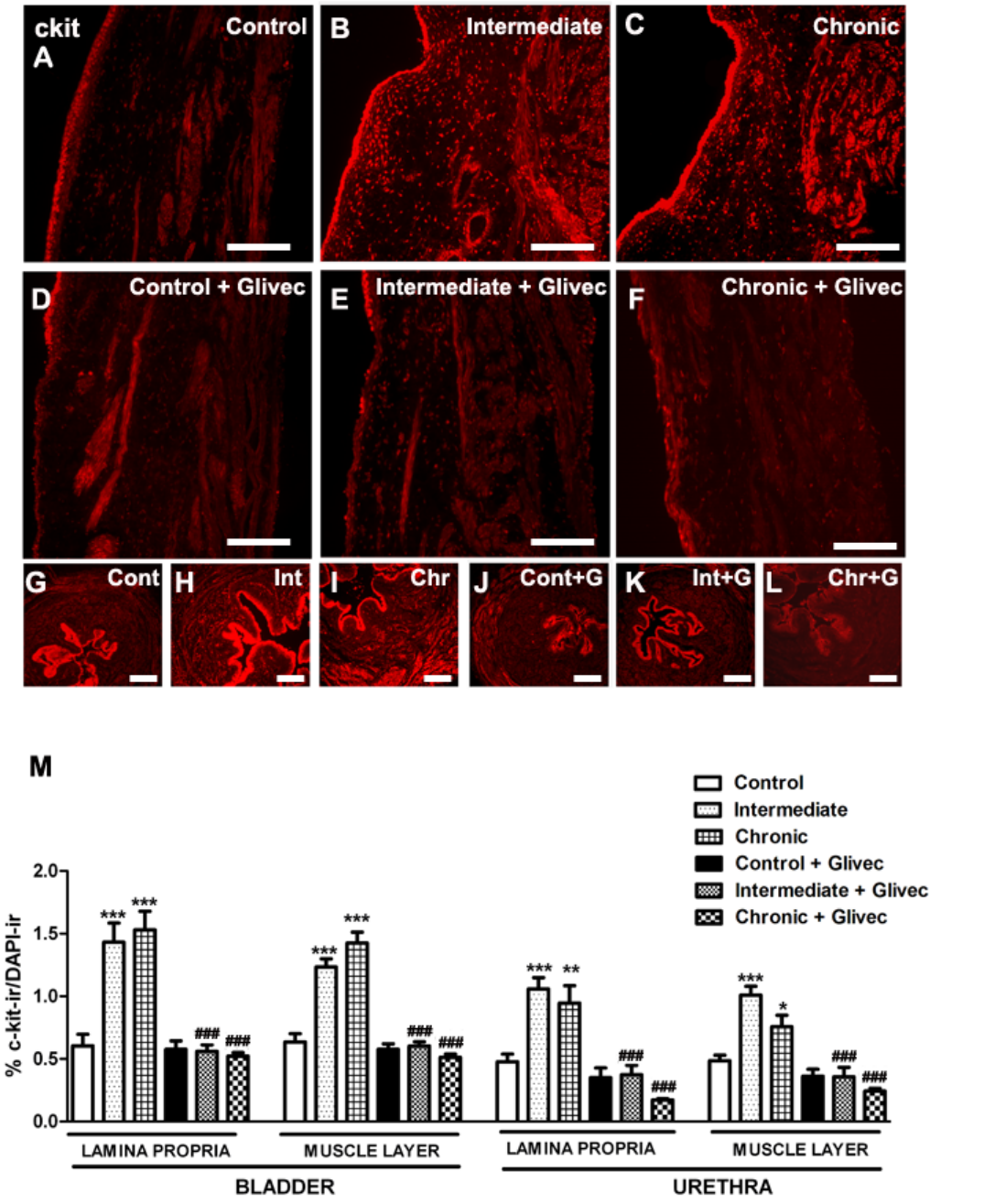

Figura 34. Prominente aumento en la inmunoreactividad a c-kit a consecuencia del tratamiento con CYP en la vejiga y en la uretra y el efecto preventivo de Glivec. Las ratas fueron tratadas con CYP durante 48 h (150mg Kg^{-1}, intermedio) o 10 días (50 mg Kg^{-1} cada 3 días, crónico) y comparadas con animales controles y con animales pretratados con Glivec (10 mg Kg^{-1} 5 días antes y durante el tratamiento con CYP) *A-F*: Imágenes representativas en la vejiga. Barras = 100 µm. *G-L*: Imágenes representativas en la uretra. Barras = 50 µm. *M:* Cuantificación de c-kit-ir en la vejiga y en la uretra. Las mediciones se realizaron de forma independiente en la lámina propia y capa muscular de ambos órganos. Se midió el área por encima del umbral de intensidad y se normalizó con el número de células presentes en dicha región (núcleos marcados con DAPI). Los resultados se expresan como media ± SEM (n = 6-7 campos diferentes de al menos 4 animales). *P <0.05, **P < 0.01, *** P <0.001, diferencias significativas respecto al control; ### P <0.001, diferencias respecto al tratamiento correspondiente sin Glivec (ANOVA de una vía seguido de test no paramétricos, Bonferroni y Newman-Keuls).

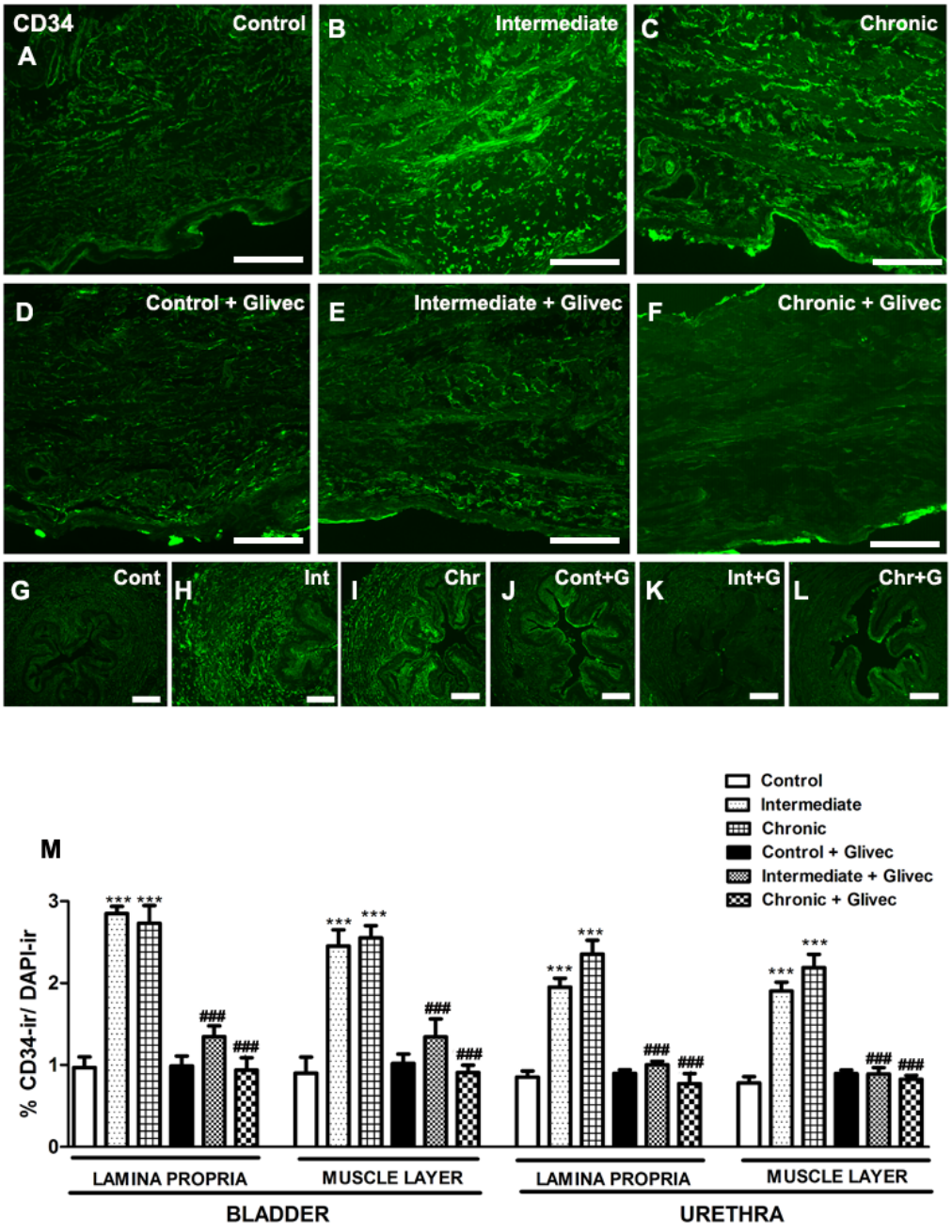

Figura 35. Prominente aumento en la inmunoreactividad a CD34 a consecuencia del tratamiento con CYP en la vejiga y en la uretra y el efecto preventivo de Glivec. Las ratas fueron tratadas con CYP durante 48 h (150mg Kg^{-1}, intermedio) o 10 días (50 mg Kg^{-1} cada 3 días, crónico) y comparadas con animales controles y con animales pretratados con Glivec (10 mg Kg^{-1} 5 días antes y durante el tratamiento con CYP).*A-F*: Imágenes representativas en la vejiga. Barras = 100 µm. *G-L*: Imágenes representativas en la uretra. Barras = 50 µm. *M:* Cuantificación de CD34-ir en la vejiga y en la uretra. Las mediciones se realizaron de forma independiente en la lámina propia y capa muscular de ambos órganos. Se midió el área por encima del umbral de intensidad y se normalizó con el número de células presentes en dicha región (núcleos marcados con DAPI). Los resultados se expresan como media ± SEM (n = 6-7 campos diferentes de al menos 4 animales). *** P <0.001, diferencias significativas respecto al control; $^{\#\#}P$ < 0.01, $^{\#\#\#}$ P <0.001, diferencias respecto al tratamiento correspondiente sin Glivec (ANOVA de una vía seguido de test no paramétricos, Bonferroni y Newman-Keuls).

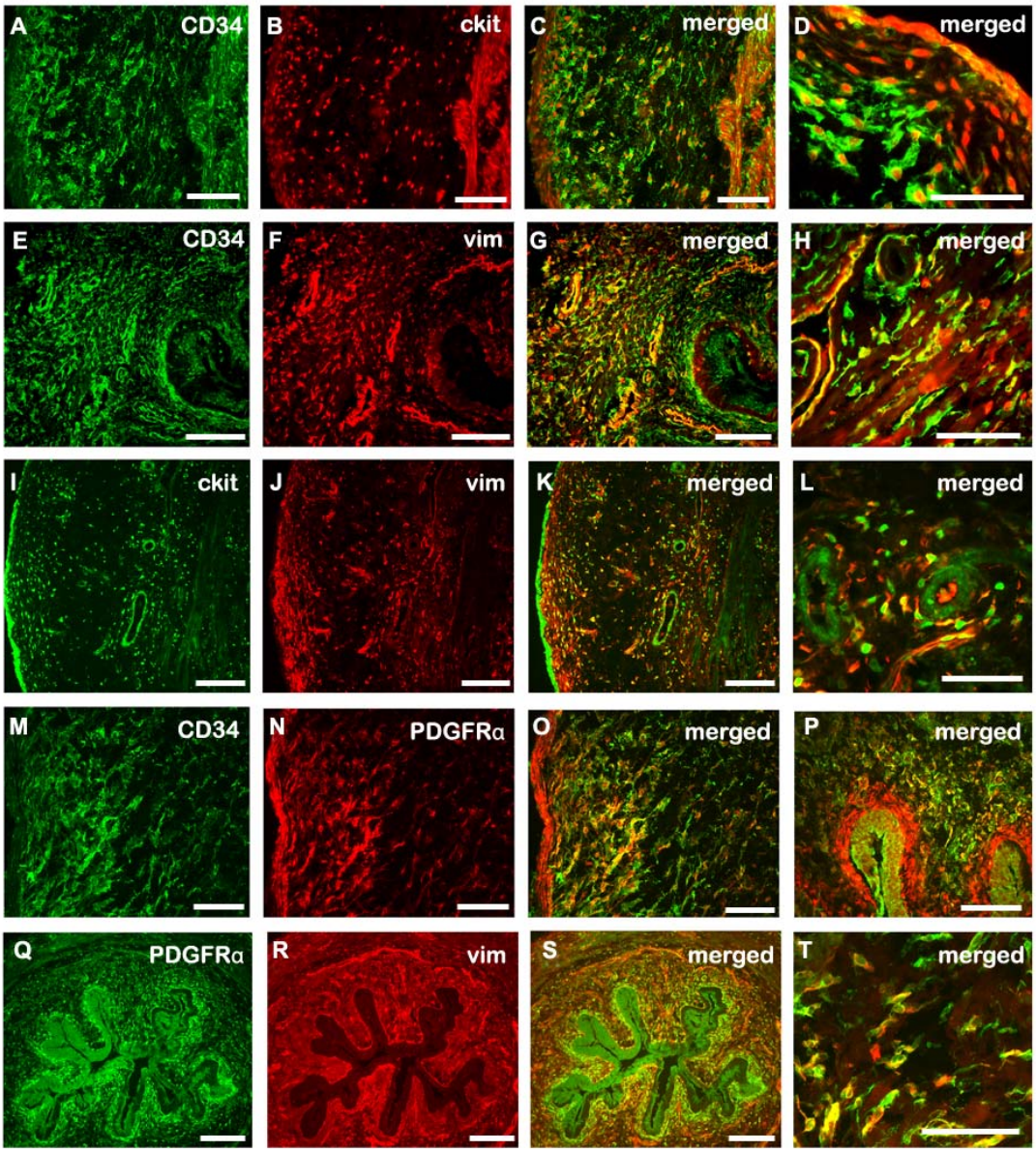

Figura 36. Imágenes representativas de la colocalización entre los diferentes marcadores de ICC. Todos los ejemplos proceden de ratas tratadas con CYP durante 48 h (150 mg Kg^{-1}, tratamiento intermedio). *A-D*: CD34 (verde)-c-kit (rojo) en vejiga. (*D*) La capa subepitelial de la misma preparación a mayores aumentos. *E-H*: CD34 (verde)-vimentina (rojo) en uretra. . (*H*) .Muestra la capa submucosa de la misma preparación a mayores aumentos. *I-L*: c-kit (verde)-vimentina (rojo) en vejiga. (*L*) A mayores aumentos la capa submucosa de la misma preparación. *M-P*: CD34 (verde)-PDGFRα (rojo) en vejiga (*M-O*) y uretra (*P*). *Q-T*: PDGFRα (verde)-vimentina (rojo) en uretra. (*T*) A mayores aumentos la capa muscular externa de la misma preparación. Barras = 100 μm, excepto *Q-S* (50 μm) y *D, H, L, T* (25 μm).

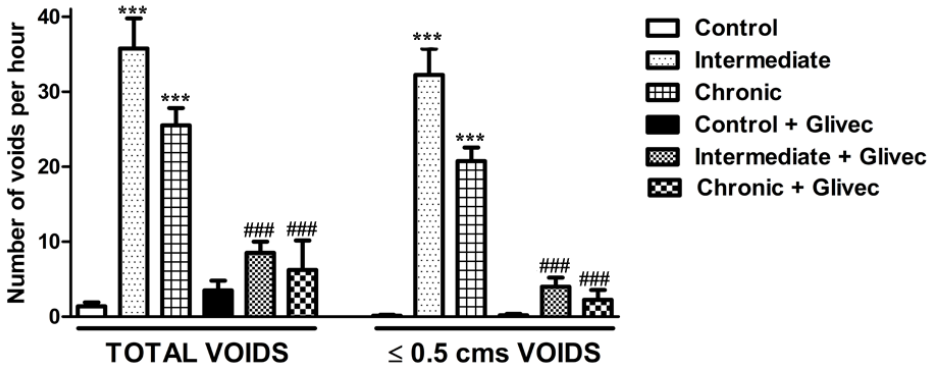

Figura 37. Cambios en la frecuencia de micción a consecuencia del tratamiento con CYP y el efecto preventivo de Glivec. El número de micciones por hora (totales y de pequeño tamaño) se determinaron en animales tratados sólo con CYP durante 48h (intermedio) o 10 días (crónico), y en aquellos que previamente recibieron un tratamiento con Glivec. Los resultados se expresan como media ± SEM (n = 6 por grupo). *** P <0.001, diferencias significativas respecto al control; $^{\#\#}P$ < 0.01, $^{\#\#\#}$ P <0.001, diferencias respecto al tratamiento correspondiente sin Glivec (ANOVA de una vía seguido de test no paramétricos, Bonferroni y Newman-Keuls).

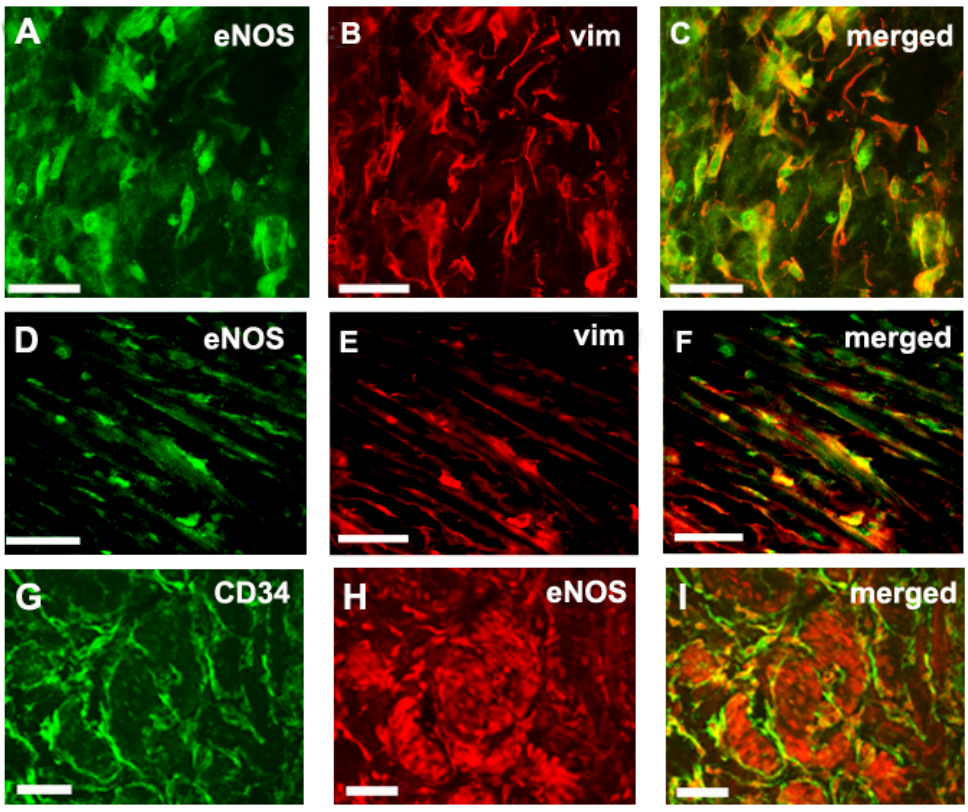

Figura 38. Imágenes representativas del doble marcaje con eNOS (verde, *A, C, D, F*; o rojo, *H* e *I*) y vimentina (rojo, *B, C, E,* y *F*), o CD34 (verde, *G* e *I*) en ICC de la lámina propia (ICC-LP, *A-C*), paralelas a los fascículos de músculo liso (ICC-IM, *D-F*) o entre los fascículos musculares (ICC-SEP, *G-I*) de vejigas tratadas con CYP durante 48h. Barras = 50 µm.

DISCUSIÓN

1. Participación de las ICC en la neurotransmisión inhibitoria uretral: papel como efectores de la acción del NO

Se puede considerar que en el músculo liso uretral el NO es el principal neurotransmisor responsable de la relajación uretral durante la micción, presentando la uretra una inervación nitrérgica más densa (McNeil et al, 1992; Zygmunt et al., 1993; Triguero et al, 1993; Persson et al, 1993; Leone et al., 1994), y respondiendo al NO con una relajación más prominente que otras regiones del tracto urinario como la vejiga o los uréteres (Triguero et al., 1993). El mecanismo por el cual el NO origina la relajación uretral está mediado por la activación de la sGC y la elevación en los niveles intracelulares de cGMP (García Pascual y Triguero, 1994; Persson y Andersson, 1994).

Se ha observado que la relajación uretral inducida por la adición exógena de diferentes donantes de NO origina acumulaciones de cGMP mucho mayores (hasta 200-300 veces superiores) para un mismo nivel de relajación que la inducida por EFS (García-Pascual y Triguero, 1994; García-Pascual et al., 1999), lo cual pone de manifiesto la existencia de mecanismos diferentes de relajación inducidos por NO endógeno (liberado por estimulación de los nervios nitrérgicos intramurales) y exógeno (añadido en forma de compuestos donantes de NO). Este aspecto es especialmente importante puesto que a menudo se extrapolan erróneamente los resultados obtenidos mediante el uso de un donante exógeno de NO a la neurotransmisión nitrérgica funcional.

En este sentido, el primer estudio que describe la acumulación de cGMP mediante inmunohistoquímica en la uretra de conejo y el hombre fue realizado por Smet et al., (1996). En éste, el tejido uretral fue activado por altas concentraciones de SNP, durante largos periodos de tiempo y en presencia de inhibidores de PDE y se describe la aparición de cGMP-ir en músculo liso, nervios y células ganglionares intramurales, así como en un elemento celular, morfológicamente similar a las ICC intestinales. Estudios posteriores han demostrado también la presencia de ICC inmunoreactivas para cGMP en la vejiga del cobaya (Gillespie et al., 2004; Gillespie y Drake, 2004) y del ratón (Fujiwara et al., 2000; Lagou et al., 2006), y en la uretra del cerdo (Werkström et al., 2006) y del conejo (Waldeck et al., 1998) e igualmente, en todos los casos las preparaciones fueron activadas mediante incubación con donantes de NO, no existiendo ningún estudio previo que haya analizado la distribución de cGMP-ir en respuesta a la estimulación de los nervios nitrérgicos uretrales.

En el presente estudio se describe por primera vez en la uretra la acumulación de cGMP en diferentes elementos celulares en respuesta a EFS de los nervios nitrérgicos, en comparación a la inducida por la adición exógena de NO en forma de SNC. Además, y también por vez primera se realiza una comparación directa en cada preparación entre la cGMP-ir y la respuesta relajante inducida por ambos tipos de estimulación. Los experimentos se llevaron a cabo en presencia de dos inhibidores de PDE (IBMX y Zaprinast), con objeto de permitir una acumulación suficiente de cGMP en el tejido para

su posterior detección inmunohistoquímica. El primer problema a resolver fue que la incubación con IBMX y Zaprinast, a las mismas concentraciones utilizadas por otros estudios en la vejiga urinaria (Fujiwara et al., 2000; Gillespie et al., 2004) y en la uretra (Smet et al., 1996), producía una depresión tan grande de la tensión contráctil que la relajación no podía ser monitorizada. Por ello se decidió añadir estos compuestos sobre la contracción inducida por NE tan solo 30 s antes de la estimulación, tiempo suficiente para reducir la tensión contráctil inicial no más del 40%, con objeto de aumentar la relación señal/ruido y evitar lo que parecía ser una acumulación basal de cGMP excesivamente grande.

En contra de lo esperado, esta relajación tan manifiesta inducida por los inhibidores de PDE no parecía ser debida exclusivamente a la acumulación de cGMP, ya que el tratamiento con ODQ y L-NNA (inhibidores de sGC y NOS, respectivamente), tan sólo redujeron parcialmente la relajación. El hecho de que la cGMP-ir basal (en preparaciones control) fuera poco intensa y además se redujera en preparaciones tratadas con ODQ y L-NNA apoya la hipótesis de que no se está produciendo una acumulación sustancial de cGMP en ausencia de estimulación nitrérgica y que el efecto relajante inducido por la adición de IBMX y Zaprinast, no está relacionado con la acumulación de este nucleótido. Otros autores, empleando incluso periodos de incubación muy largos (30 min) con estas sustancias, tampoco han observado una inmunoreactividad apreciable para cGMP en condiciones basales (Shuttleworth et al. 1993; Gillespie et al., 2004) lo que es coincidente con nuestros resultados. Dado que IBMX es un inhibidor inespecífico de PDE, tanto de cGMP como de cAMP, sería posible que originara también una acumulación de este segundo nucleótido, cuyo efecto en la uretra también es relajante. La incubación con SQ22536 (inhibidor de la adenilato ciclasa, AC) produjo una reducción significativa de la relajación provocada por los inhibidores de PDE, aunque sólo en la uretra de oveja. La activación de AC podría ser secundaria al aumento de cGMP puesto que al combinar ambos inhibidores (SQ22536 y ODQ) no se produjo una mayor inhibición de la relajación muscular que cuando se empleo ODQ sólo, sugiriendo una modulación cGMP-dependiente de las PDE de cAMP. No se puede descartar, sin embargo, la participación de otros mecanismos, como podría ser la activación de GC particulada (De Vente et al., 2007) o de canales de K^+ por los inhibidores de PDE utilizados (Medina et al., 2000).

Utilizando un paradigma de EFS característico de una estimulación nitrérgica se originó una relajación rápida en las preparaciones uretrales de ambas especies que se superpuso al efecto relajante lento de los inhibidores de PDE y que fue inhibida de forma efectiva por L-NNA y ODQ, demostrando así su carácter nitrérgico. La administración de una dosis maximal de SNC originó una respuesta relajante más lenta y sostenida que también fue inhibida por ODQ, indicando que es debida a la activación de sGC.

El análisis comparativo de la cGMP-ir en secciones histológicas de preparaciones sometidas a las distintas situaciones experimentales (preparaciones

control y estimuladas con EFS o SNC, en presencia y ausencia de L-NNA o ODQ) mostró la presencia de cGMP-ir en células alargadas o estrelladas, cuyas características morfológicas (núcleo ovoide con escaso citoplasma y una o varias prolongaciones alargadas) recuerdan a la descripción hecha por Cajal de las ICC del tracto digestivo. Sus características morfológicas junto con la existencia de colocalización con vimentina, su positividad a c-kit (al menos en la oveja) y la colocalización c-kit-vimentina, nos has permitido considerar estas células como ICC. En condiciones basales éstas ICC se distribuyen principalmente en la capa serosa (ICC-SR) de la uretra de rata, y en la lámina propia (ICC-LP) de la uretra de oveja, y su cGMP-ir parece ser independiente de NO y/o sGC ya que no se modificó en presencia de ODQ y L-NNA. Sin embargo, en preparaciones estimuladas por EFS o SNC, se observó un claro aumento en la densidad de cGMP-ir especialmente en ICC-IM e ICC-SEP (situadas dentro y rodeando los haces musculares de la capa muscular, respectivamente) que sí fue reducida por el tratamiento con L-NNA y ODQ, coincidiendo con una reducción significativa de la respuesta relajante inducida por ambos estímulos. Estos resultados demuestran claramente la acumulación de cGMP en ICC uretrales tanto por la adición exógena de NO como por su producción y liberación endógena.

La localización del aumento de cGMP-ir inducido por NO se produjo tanto en SMC, como en ICC-IM, especialmente en la estimulación con EFS, sugiriendo que ambos tipos celulares podrían estar actuando en la uretra como efectores de su acción. Esta situación no ha sido descrita previamente en el tracto urinario y contrasta con la observada en la vejiga urinaria en diferentes especies (Gillespie et al., 2004; Fujiwara et al., 2000; Lagou et al., 2006), donde sólo aparece cGMP-ir en ICC, pero nunca en SMC, hecho que podría estar directamente relacionado con la ausencia de relajaciones nitrérgicas inducidas por EFS en la vejiga (Triguero et al., 1993) y con la gran resistencia del músculo detrusor a ser relajado por NO y donantes de NO (Fujiwara et al., 2000), sugiriendo que este mediador no provoca la relajación vesical. El estudio pionero de Smet et al. (1996) en la uretra de cobaya y humana describe la aparición de una fuerte inmunoreactividad en la capa muscular lisa a consecuencia de la estimulación con nitroprusiato sódico. Por el contrario, los estudios de Waldeck et al (1998) en la uretra de conejo, estimulada también con nitroprusiato sódico, muestran cGMP-ir sólo en ICC, distribuidas fundamentalmente en la capa longitudinal externa. De hecho, estos autores no encuentran explicación a estos hallazgos, considerando que si, a diferencia de la vejiga, el NO si relaja efectivamente la uretra, debería producirse un aumento de cGMP en el último efector que es el músculo liso. Este hecho unido a la presencia de ICC especialmente en la capa muscular longitudinal, pero no en la capa circular, les hace dudar de su papel en la relajación uretral, puesto que ésta última capa es la más importante para la relajación de este órgano. Por último, Werkström et al. (2006) en la uretra del cerdo estimulada con el donante de NO, DEA-NO describen la aparición de cGMP-ir en el músculo liso, pero ésta es mayor en ICC distribuidas entre los haces de fibras musculares, fundamentalmente de la capa muscular longitudinal externa.

Estos resultados, obtenidos en la uretra de diferentes especies por la adición de un donante de NO, serían más similares a los descritos en el presente estudio en las preparaciones estimuladas con SNC. Redes interconectadas de ICC intensamente fluorescentes a cGMP que rodean los fascículos de músculo liso menos inmunoreactivos. Esto podría ser debido a una mayor capacidad de las ICC, en comparación con las SMC, para acumular cGMP en respuesta a las altas concentraciones de NO liberado por el donante en presencia de inhibidores de PDE. Al igual que en los trabajos anteriormente descritos, la distribución de estas redes celulares inmunoreactivas a cGMP predomina en la capa muscular externa longitudinal, en el caso de la oveja, mientras que en la rata se distribuyen en toda la pared uretral. Hay que señalar, no obstante, que la presencia de ICC con intensa cGMP-ir no se produjo en todas las preparaciones analizadas, a pesar de que todas ellas relajaron con potencia similar a SNC y además, las ICC inmunoreactivas no se distribuían de forma uniforme en toda la pared uretral sino que aparecían concentradas en algunas zonas, pero ausentes en otras. La razón de esta variabilidad se desconoce y podría explicar la ausencia de diferencias significativas al comparar el % de área marcada por encima del umbral de las preparaciones tratadas con SNC frente a las preparaciones control o a las preparaciones expuestas a SNC pero preincubadas con ODQ.

En la actualidad se considera que el principal indicio de que un tejido contiene ICC es su positividad a c-kit, aunque ello no es ni suficiente ni necesario para identificar una célula como ICC, ya que otros tipos celulares como mastocitos, melanocitos, fibroblastos o macrófagos también expresan el receptor c-kit (Zhang y Fedoroff, 1997), mientras que algunas ICC se muestran negativas a c-kit, como por ejemplo las ICC-DMP del intestino (Wang et al., 2003a), claras mediadoras de la neurotransmisión entérica. Parece ser que en muchos casos la negatividad a c-kit por métodos inmunohistoquímicos se debe a problemas técnicos. Así los estudios pioneros en la uretra del conejo (Sergeant et al., 2000) y del ratón (Pezzone et al., 2003) indican la negatividad a c-kit en células cuya morfología y propiedades electrofisiológicas son similares a las ICC intestinales, aunque estudios recientes en tejido no fijado han podido demostrar la positividad a c-kit en ICC en la uretra y uréter de diversas especies (Van der AA et al., 2004; Lyons et al., 2007; Metzger et al., 2005). Nuestro estudio se realizó en tejido fijado con paraformaldehído, necesario para el uso de los anticuerpos contra cGMP, y en esas condiciones no se pudo observar reactividad manifiesta para c-kit con dos anticuerpos distintos (policlonal de conejo, anti c-kit humano, clones Ab-1 y H-300) en la uretra de rata, mientras que en la oveja si se detectó inmunoreactividad débil pero evidente para el anticuerpo c-kit H-300 en ICC donde colocaliza con vimentina. Las ICC de ambas especies fueron intensamente marcadas con vimentina, diferenciándolas claramente de las SMC que no muestran inmunoreactividad a este marcador de filamentos intermedios. Por lo tanto, la identificación de ICC en el presente estudio se ha basado fundamentalmente en la utilización de vimentina como marcador de ICC, junto con sus peculiares características morfológicas, como ya ha sido previamente descrito en otras especies (Sergeant et al., 2000). No se puede descartar que algunas células consideradas como ICC sean en realidad otros parientes cercanos, como

mastocitos o fibroblastos, cuya diferenciación requeriría el uso de marcadores específicos (Metzger et al., 2004). En cualquier caso, los mastocitos poseen importantes diferencias morfológicas con las ICC (núcleo redondeado y ausencia de prolongaciones) por lo que sólo hemos identificado claramente como ICC aquellas células positivas a cGMP, vimentina y a veces a c-kit con grandes núcleos ovoides, escaso citoplasma y una o varias prolongaciones. Hay que señalar que la vimentina marcó más intensamente la periferia de las células, especialmente las prolongaciones, mientras que el anticuerpo para cGMP marcó preferentemente el citoplasma. Además, no todas las células positivas para vimentina lo fueron para cGMP, resultados coincidentes con otros estudios realizados en vejiga humana y de cobaya (Smet et al., 1996), que sugiere que no todas las ICC actuarían como efectores directos de NO y que, al igual que en el tracto digestivo, podrían existir diferentes subtipos de ICC con distintas funciones dentro del mismo órgano. Así, las ICC-MY del intestino delgado (Ward et al., 1994) o las ICC-SM del colon (Smith et al., 1987) actúan fundamentalmente como marcapasos generando las ondas lentas intestinales, mientras que las ICC-IM (Burns et al., 1996) y las ICC-DMP (Torihashi et al. 1995) actúan como mediadoras de la neurotransmisión. De forma similar, en la uretra sería posible la coexistencia de distintos tipos de ICC, con diferentes características morfológicas y funcionales, distribuidas en zonas concretas de la pared uretral.

Los diferentes subtipos de ICC encontrados en nuestro estudio han sido nombrados empleando la misma nomenclatura utilizada en el tracto digestivo en función de su localización y distribución a lo largo de la pared uretral. Las ICC de la lámina propia (**ICC-LP**) observadas especialmente en la uretra de oveja, son células fusiformes bipolares, densamente distribuidas de forma paralela a la superficie de la uretra y concentradas especialmente en la zona subepitelial. También aparecen en la uretra de rata, generalmente orientadas perpendicularmente al urotelio. Estas células resultaron ser inmunoreactivas a vimentina y c-kit (en la oveja), y algunas de ellas también poseían una cGMP-ir, condensada en el soma celular. El hecho de que esta cGMP-ir apareciera incluso en preparaciones tratadas con ODQ y L-NNA demuestra su inespecificidad y sugiere que no están implicadas en el proceso de neurotransmisión nitrérgica, a pesar de que la existencia de una densa red de nervios nitrérgicos en esta zona, y su estrecha relación estructural con ICC pudiera sugerir esta función. En la vejiga humana también se ha descrito la presencia de una densa red de ICC subepiteliales positivas para vimentina, débilmente para c-kit, y para Cx43, un marcador de GJ, sugiriendo su funcionamiento como un sincitio celular con una posible función en la transmisión de señales sensoriales durante el llenado vesical (Sui et al., 2002). Células similares, positivas a c-kit y de localización subepitelial han sido descritas en la uretra humana (Van der AA et al., 2004), y en la vejiga de cobaya las ICC subepiteliales densamente empaquetadas e inmunoreactivas a cGMP se hallan relacionadas con la presencia de células positivas para nNOS en la base del urotelio (Gillespie et al., 2005). Se sabe que las células epiteliales de la vejiga liberan ATP, ACh y NO en respuesta al estiramiento (Ferguson, 1999), por lo que es posible la existencia de una relación

funcional entre urotelio, ICC-LP y nervios sensoriales que participe en la función aferente tanto de la vejiga como de la uretra.

Otra subpoblación de ICC en la pared uretral son las denominadas ICC de la adventicia o ICC de la serosa (**ICC-SR**). Estas ICC también son positivas para vimentina en ambas especies y para c-kit en la oveja y se localizan en el tejido conectivo que rodea la uretra. Poseen morfologías más variadas, bipolares o multipolares, formando redes aparentemente interconectadas entre sí y en relación con vasos sanguíneos y troncos nerviosos. A pesar de esta relación estructural, y al igual que las ICC-LP, no parecen desempeñar una función reguladora mediada por NO ya que presentan una cGMP-ir no inhibida en preparaciones tratadas con ODQ y L-NNA. Hay que destacar la mayor abundancia de estas células en la rata, donde forman una auténtica corona celular que rodea la uretra. La presencia de células positivas a c-kit ha sido también descrita en la adventicia o serosa de la pared del tracto urinario de diversas especies, observándose, al igual que en nuestro estudio, un predominio de éstas en las especies animales de pequeño tamaño (rata, ratón y conejo) en comparación con las de mayor tamaño (cerdo, vaca y perro) (Metzger et al., 2005). En base a estas diferencias ínterespecíficas y asumiendo un papel de esta red celular como marcapasos de la actividad espontánea de la uretra, se podría argumentar que una abundante red de ICC-SR en especies de pequeño tamaño podría ser suficiente para modular la actividad eléctrica del músculo subyacente. En este sentido la continuidad de estas células con las que se introducen entre los septos de músculo liso (ICC-SEP) podría permitir la conducción de la actividad eléctrica a las profundidades de la capa muscular. Sin embargo, en especies de gran tamaño, al igual que ocurre en el tracto digestivo (Mazet y Raynier, 2004), un solo marcapasos externo sería insuficiente para transmitir la excitación a todo el espesor de la pared uretral y podría necesitar la ayuda de un segundo marcapasos situado en la submucosa. No conocemos la razón de que las ICC-SR posean cGMP-ir, al igual que ocurre con la población de ICC-LP, y si esta supuesta acumulación de cGMP pudiera estar relacionada con su funcionalidad. Estudios recientes han descrito la presencia de GC particulada en ICC de lámina propia y serosa, mientras que las ICC-IM están desprovistas de esta enzima (De Vente et al., 2007). Además, se ha comprobado que estas ICC son capaces de responder a varios péptidos natriuréticos, ANP y BNP, dando lugar a un acúmulo de cGMP en su interior, fenómeno que no resulta ser inhibido por ODQ (De Vente et al., 2007). En cualquier caso, nuestros resultados indican que las ICC presentes en lámina propia y serosa no están participando en la neurotransmisión nitrérgica en la uretra aunque podrían estar involucradas en la transmisión de la información sensorial desde la submucosa o la generación de actividad marcapasos.

Por último, las ICC distribuidas entre las capas de músculo liso (**ICC-IM**) de la uretra constituyen la población funcionalmente más importante ya que es la que muestra variaciones en la cGMP-ir en función del tratamiento del tejido (aumento de cGMP en respuesta a EFS y SNC y su consecuente inhibición por el tratamiento con los inhibidores de NOS y de sGC), lo que sugiere su participación en la neurotransmisión

nitrérgica uretral. Las ICC-IM uretrales también presentaron morfologías variables. Aunque las bipolares y fusiformes con largas prolongaciones fueron las más frecuentes, también se observaron otras multipolares, triangulares, o estrelladas. En función de su relación con las fibras musculares pueden a su vez subdividirse en varios tipos: ICC septales (ICC-SEP) situadas entre los septos de tejido conectivo que separan los fascículos musculares. Estas células presentan prolongaciones especialmente largas, sobre todo en la rata, donde se observó que se extendían a lo largo de toda la pared, interconectando unas con otras y formando así largas vías de conducción. Otras, las auténticas ICC-IM se localizan sobre y rodeando los propios fascículos musculares con una típica orientación paralela a la fibra muscular. Esta distribución es similar a la descrita para las ICC del tracto gastrointestinal, donde se ha sugerido que las ICC podrían estar situadas entre las terminales nerviosas y las SMC, actuando así como intermediarias en el proceso de la neurotransmisión (Ward, 2000).

Alternativamente a la teoría de la intercalación, en otras regiones del tracto gastrointestinal se ha sugerido un modelo de inervación paralela en el cual tanto SMC como ICC actuarían como efectores directos del NO liberado desde las terminaciones nerviosas nitrérgicas. Apoyando esta hipótesis, diversos estudios en el colon (Alberti et al., 2007) de ratas mutantes Ws/Ws y en el esfínter anal interno (Terauchi et al., 2005) y esfínter esofágico inferior (Sivarao et al., 2001) de ratones mutantes W/W^v muestran como la neurotransmisión purinérgica y nitrérgica no resulta afectada, sugiriendo que el NO liberado de las terminaciones nerviosas es capaz de actuar directamente sobre las SMC. Este modelo de inervación paralela también podría explicar nuestros resultados. Tanto las ICC como las SMC podrían establecer contactos lo suficientemente íntimos con las terminaciones nerviosas, permitiendo a ambas células responder al neurotransmisor liberado (en este caso el NO) cuando la preparación es estimulada por EFS, produciendo un acúmulo de cGMP en su interior de similar intensidad en ambas células. Estos resultados están en concordancia con la reciente propuesta de que ambos tipos celulares estarían implicados en la actividad marcapasos de la uretra (Hashitani et al., 2006; Hashitani y Suzuki, 2007), sugiriendo que las ICC y las SMC compartirían funciones en la uretra.

Además de que las ICC sean capaces de responder al NO produciendo cGMP, existe la controversia de si las ICC son también capaces de producir NO. Esta idea proviene de diversos estudios en el tubo digestivo que han descrito la presencia en ICC de nNOS y eNOS y esta característica ha sido interpretada como un posible efecto de amplificación por parte de las ICC de la respuesta mediada por el NO de origen nervioso (Vannuchi et al., 2002; Xue et al., 1994). Por el contrario otros estudios indican la ausencia de nNOS en ICC de intestino humano (Wang et al., 2003b) o solamente observan su aparición en situaciones de inflamación como en la colitis experimental (Altdorfer et al., 2002). En nuestro estudio, los resultados de los dobles marcajes nNOS/vimentina demuestran que no aparecen ICC (positivas para vimentina) que a su vez sean reactivas a nNOS. Aunque no podemos descartar la posible existencia de alguna variante de nNOS no detectada con los dos anticuerpos policlonales

empleados en el presente estudio. Así, en el colon del ratón se ha demostrado que las ICC poseen una variante de la isoforma nNOS (nNOS-α) unida a membranas que únicamente es detectada por anticuerpos monoclonales, mientras que la nNOS-β soluble en el citoplasma sí es detectada por anticuerpos policlonales (Vannuchi et al., 2002). Sin embargo y en consonancia con los resultados obtenidos, estudios previos empleando la técnica histoquímica inespecífica NADPH-diaforasa no han podido identificar ICC positivas en la uretra de oveja (García-Pascual y Triguero, 1994; González-Soriano et al., 2003), ni tampoco otros estudios en vejiga (Gillespie et al., 2004) y uretra de cobaya (Smet et al., 1996) han descrito inmunoreactividad a nNOS en ICC. En este sentido, nuestro estudio estaría en concordancia con el mecanismo de control propuesto en el Sistema Nervioso Central (Knowles et al, 1989), en el cual la sGC resultaría inactivada en una célula productora de NO por el mismo aumento en los niveles de Ca^{2+} necesarios para la activación de la NOS. De hecho, nuestros resultados muestran que ninguna de las estructuras positivas a cGMP mostró colocalización con nNOS o PGP 9.5 contrariamente a otros estudios que describen positividad a cGMP en troncos nerviosos en uretra de conejo (Fujiwara et al., 2000) o terminaciones nerviosas en la vejiga de ratón, cobaya y humana (Lagou et al., 2006; Gillespie et al., 2004; Smet et al., 1996). Sólo se detectó cGMP-ir en algunas estructuras paralelas a las fibras nerviosas que pudieran tratarse de células de la glia, en concreto células de Schwann que recubren los axones de las neuronas formando una vaina aislante de mielina. En el músculo liso visceral, las células de Schwann son capaces de responder a neurotransmisores endógenos, como por ejemplo el ATP, dando lugar a corrientes de Ca^{2+} (Lin y Bennet, 2006). De igual forma, estas células en la uretra podrían responder al NO liberado de las terminaciones nerviosas dando lugar a un acúmulo de cGMP en su interior, aunque se requiere el empleo de técnicas más específicas que lo demuestren.

El resultado más importante obtenido en el presente estudio del análisis de la relación entre ICC positivas a vimentina o cGMP y estructuras nerviosas en general (positivas a PGP 9.5) o específicamente nitrérgicas (positivas a nNOS) es la clara relación estructural entre ambos elementos que aunque independientes (no hay colocalización en ningún caso) se encuentran muy próximos, presentando incluso numerosos puntos de contacto entre ellos (especialmente entre las ICC y las terminaciones nitrérgicas). Este hecho constituye la base morfológica que sustenta el posible papel mediador de las ICC en la neurotransmisión nitrérgica ya que se sitúan en íntimo contacto con los terminales liberadores del neurotransmisor. Estos resultados están en concordancia con estudios previos realizados en vejiga y uretra de diferentes especies (Fujiwara et al., 2000; Gillespie et al., 2004; Lagou et al., 2006; Smet et al., 1996).

Por último, quisiéramos destacar la presencia de cGMP-ir en células uroteliales de la uretra de rata, y en el endotelio de los vasos sanguíneos de ambas especies. La producción de cGMP en células epiteliales en respuesta a NO puede estar asociada a funciones sensoriales (Gillespie et al., 2004) y parece ser que depende de la especie animal. De hecho ha sido descrita en la vejiga y uretra de cobaya (Gillespie et al., 2004;

Smet el at., 1996) pero no se ha podido observar en la vejiga de ratón (Fujiwara et al., 2000; Lagou et al., 2006), ni en vejiga y uretra humana (Smet et al., 1996). Respecto al endotelio vascular, se observó una cGMP-ir débil en condiciones basales que se incrementó cuando las preparaciones fueron estimuladas nitrérgicamente, sugiriendo el posible papel de la vía NO/cGMP en la regulación del flujo sanguíneo en la uretra. De igual modo, otros estudios han descrito cGMP-ir en el endotelio de la uretra humana y de cobaya donde colocaliza con eNOS (Werkström et al., 2006). A diferencia del endotelio nuestro estudio mostró en muy pocos casos cGMP-ir en el músculo liso vascular a pesar de la existencia de una gran densidad de nervios nitrérgicos perivasculares.

En resumen, este estudio muestra por vez primera la acumulación de cGMP en ICC de la uretra de rata y oveja en respuesta a la estimulación de los nervios nitrérgicos intramurales, sugiriendo su participación como mediadoras de la neurotransmisión. Aunque parece haber varios tipos de ICC inmunoreactivas a cGMP formando redes interconectadas en distintas localizaciones de la pared uretral (serosa, mucosa y capa muscular), solamente las ICC-IM parecen estar implicadas en la neurotransmisión nitrérgica, ya que la acumulación de cGMP pudo ser prevenida al bloquear la NOS o la sGC. Ninguna de las ICC presentaron nNOS-ir aunque si existe una cercana relación estructural, sugiriendo también una relación funcional, entre ICC y nervios nitrérgicos. Debido a que no sólo las ICC sino también las SMC responden con aumentos en cGMP-ir a consecuencia de la estimulación nitrérgica, nuestros resultados encajarían en un modelo de inervación paralela en el que ambos tipos celulares actuarían como efectores directos de la acción del NO liberado de los nervios.

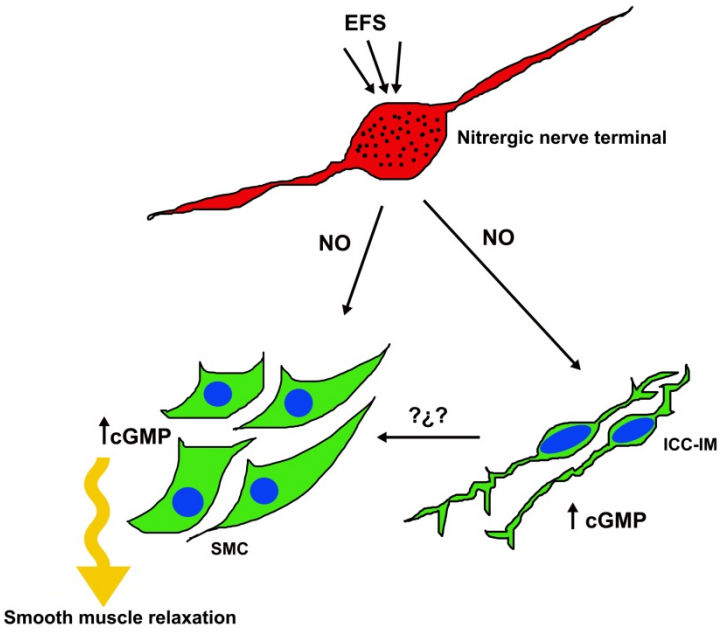

Figura XII. Modelo propuesto de inervación paralela en el cual tanto las SMC como las ICC-M actuarían como efectores directos del NO liberado desde las terminaciones nerviosas nitrérgicas dando lugar a un acúmulo de cGMP en su interior y mediando la relajación del músculo liso uretral.

2. Participación de los CNG en la neurotransmisión nitrérgica uretral: papel de las ICC

Aunque inicialmente los canales CNG fueron descritos en tejidos sensoriales, como las células fotorreceptoras u olfatorias (Fesenko et al., 1985; Nakamura y Gold, 1987), en la actualidad se sabe que están presentes en una gran variedad de tejidos no sensoriales como son el hipocampo, corazón, testículos, hígado, páncreas, glándula adrenal y colon, donde pudieran estar participando en la regulación temporal y espacial de muchos procesos celulares (Kaupp, 1995), aunque sus mecanismos de acción no han sido todavía esclarecidos (Matulef y Zagotta, 2003; Burns y Baylor, 2001). Hasta el momento no existe ningún estudio que haya descrito la presencia de canales CNG en el tracto urinario inferior, y en concreto en la uretra.

Los CNG son canales catiónicos no selectivos, débilmente activados por cambios en el potencial de membrana y cuya apertura o cierre depende fundamentalmente de la unión directa a nucleótidos cíclicos intracelulares (Fesenko et al., 1985; Kaupp y Seifert, 2002; Matulef y Zagotta, 2003), aunque también podrían ser directamente modulados por NO mediante S-nitrosilación de un residuo de cisteína (Broillet 2000; Broillet y Firestein, 2000). Esta ampliamente establecido que estos canales conducen principalmente corrientes de Na^+, Ca^{2+} y Mg^+ hacia el interior celular, provocando la despolarización de la membrana o cambios locales en los niveles de Ca^{2+} citosólico (Finn et al., 1996; Wei et al., 1998). En la actualidad se considera que estos canales podrían constituir una vía alternativa para la entrada de Ca^{2+} a la célula que es independiente del potencial de membrana y que relaciona la actividad de proteínas reguladas por Ca^{2+} con la señalización de nucleótidos cíclicos (cAMP y cGMP) sin necesidad de la actuación de proteínas kinasas. Incluso algunos estudios en el sistema nervioso central han sugerido que los CNG podrían estar entre los principales efectores del NO (Zufall et al., 1997; Savchenko et al., 1997).

El hecho de que las SMC y las ICC-IM presentes en la uretra de oveja y de rata exhiban un aumento en los niveles de cGMP cuando el tejido es estimulado nitrérgicamente (tanto con EFS como con SNC), nos lleva a pensar que los CNG, que son activados por este nucleótido, pudieran estar presentes en estas células participando en la neurotransmisión nitrérgica uretral. Apoyando esta hipótesis, estudios previos de nuestro grupo han descrito que L-cis-Diltiazem (bloqueante específico de los CNG regulados por cGMP), es capaz de inhibir la pronunciada relajación mediada por NOS y sGC que se produce como consecuencia de la depleción de las vesículas sinápticas inducida por las α-toxinas del veneno del escorpión en la uretra de oveja (Triguero et al., 2003). Este hecho además viene reforzado por una inhibición de la relajación del músculo liso uretral inducida por EFS en presencia de L-cis-Diltiazem (Triguero et al., 2003).

Con estos antecedentes, el objetivo de este trabajo fue examinar la posibilidad de que los CNG estén presentes en la uretra de la rata y analizar en mayor profundidad su

posible participación en la neurotransmisión nitrérgica. La potente y rápida inhibición de la relajación inducida por EFS por L-cis-Diltiazem, a una concentración (50 μM) que se encuentra dentro del rango normalmente empleado para inhibir los canales CNG en células fotorreceptoras (Stern et al., 1986) apoya esta sugerencia. Además, este efecto inhibitorio resultó ser cinco veces más potente que el descrito anteriormente en la uretra de oveja (Triguero et al., 2003), y también fue observado en experimentos preliminares (no publicados) en uretra de ratón, lo que sugiere que sea un hecho generalizado en la uretra de diferentes especies.

Por el contrario, las respuestas contráctiles inducidas por EFS, las cuales son fundamentalmente de carácter adrenérgico (García-Pascual et al., 1991d) sólo sufrieron una débil y lenta inhibición por la misma concentración (50 μM) de L-cis-Diltiazem que inhibía por completo las respuestas relajantes nitrérgicas. Este efecto es probablemente debido a la acción inespecífica de L-cis-Diltiazem sobre canales de Ca^{2+} dependientes de voltaje debido a su relación estructural con el compuesto D-Diltiazem, conocido bloqueante de los canales de Ca^{2+} tipo L. Así, la contracción inducida por una alta concentración de K^+, que es debida a la despolarización directa del músculo liso y la consecuente apertura de canales de Ca^{2+} dependientes de voltaje, fue inhibida tanto por D-Diltiazem como por L-cis-Diltiazem, pero este último necesitó concentraciones 10 veces superiores. Asimismo, D-Diltiazem se mostró dos órdenes de magnitud más potente que L-cis-Diltiazem en bloquear la contracción uretral inducida por EFS, mientras que fue completamente ineficaz en inhibir la relajación nitrérgica uretral. Además, el perfil temporal de inhibición de L-cis-Diltiazem, extremadamente rápido sobre las relajaciones nitrérgicas, pero de acción más lenta sobre las respuestas contráctiles podría reflejar la acción de este fármaco a diferentes niveles: un rápido bloqueo del sitio de unión del CNG a los nucleótidos cíclicos a dosis bajas y un lenta inhibición de los canales de Ca^{2+} tipo L que sólo se manifiesta a concentraciones elevadas. El hecho de que experimentos de "*patch clamp"* muestren que la administración extracelular de concentraciones bajas (orden micromolar) de L-cis-Diltiazem provocan una inhibición muy rápida (sólo limitada por el tiempo requerido para cambiar la solución) de las corrientes de Ca^{2+} activadas por cGMP, apoya esta posibilidad (Stern et al., 1986).

Reforzando el hecho de que la activación de los canales CNG desempeña un papel crucial en la relajación nitrérgica, L-cis-Diltiazem bloqueó casi por completo la relajación inducida por YC-1, utilizado para incrementar los niveles intracelulares de cGMP al actuar como potente activador de la sGC por mecanismos independientes de NO (Friebe y Koesling, 1998).

Existen dos subunidades distintas de CNG (A y B), que dan lugar a seis diferentes subtipos de canales en vertebrados: CNGA1, CNGA2, CNGA3, CNGA4, CNGB1 y CNGB3 (Craven and Zagotta, 2006). Estos subtipos pueden combinarse de múltiples maneras formando heterotetrámeros y, dando lugar a una gran variabilidad de canales CNG funcionales (Hofmann et al., 2005). Nuestros experimentos de RT-PCR en uretra de rata confirman la expresión del mRNA de los subtipos CNGA1 y CNGB1, que

componen el canal funcional CNGA1, también conocido como "*retinal-like CNG"* (subtipo de CNG descrito en la retina). El canal CNGA1 se activa únicamente por la unión a cGMP, posee una conductancia preferente a Ca^{2+} y es bloqueado específicamente por la aplicación intracelular de concentraciones micromolares de L-cis-Diltiazem. Sin embargo esta inhibición requiere la presencia de ambos subtipos con una única y determinada estequiometria: 3CNGA1:1CNGB1 (Weitz et al., 2002; Hofmann et al., 2005; Zhong et al., 2002). Aunque en este estudio no se ha realizado una cuantificación de ambas subunidades, la expresión del mRNA mediante RT-PCR muestra claramente como el subtipo CNGA1 se expresa con una intensidad claramente mayor que el subtipo CNGB1 en la uretra de rata, haciendo posible la existencia de una relación 3:1. El canal CNGA1 se encuentra altamente expresado en las células fotorreceptoras de la retina, mientras que en otros tejidos como cerebro, testículos, hígado y corazón se describe una expresión débil (Bradley et al., 2001), coincidente con nuestro caso, ya que se precisaron dos rondas de amplificación para que las bandas correspondientes a las dos subunidades pudieran ser visualizadas en el gel de agarosa. Esta débil expresión del canal CNGA1 es a priori sorprendente, dado el potente efecto inhibitorio de L-cis-Diltiazem sobre la relajación nitrérgica sugiriendo que su participación en el proceso de neurotransmisión se realice a nivel de algún proceso clave.

Nuestros resultados de inmunofluorescencia mostraron por otro lado, una intensa CNGA1-ir en una subpoblación de células alargadas presentes en la capa muscular de la uretra, que tanto por sus características morfológicas (largas y finas prolongaciones, núcleo ovoide y escaso citoplasma) como por su positividad a vimentina pueden ser consideradas como ICC. Estas ICC, serían ICC-IM que discurren en paralelo a las fibras de músculo liso, inmunoreactivas a α-actina, donde también se observó CNGA1-ir, aunque en este caso fue débil y difusa. Las estructuras nerviosas tales como fibras o troncos nerviosos intramurales no presentaron CNGA1-ir en ningún caso. Es destacable el hecho de que la distribución de esta CNGA1-ir es muy similar a la cGMP-ir anteriormente descrita en preparaciones de uretra de rata estimuladas tanto con EFS como con donantes de NO, lo cual sugiere que aquellas ICC que son capaces de producir un incremento de cGMP en respuesta a NO sean las que utilicen estos canales para provocar en última instancia la relajación uretral. Entre los diferentes efectores conocidos del cGMP, uno de los principales y más importantes es PKGI, cuya expresión en la uretra de ratón se ha descrito únicamente en el músculo liso y en algunas terminaciones nerviosas nitrérgicas, pero nunca en ICC (Persson et al., 2000). Este hallazgo podría explicar nuestros resultados, planteando la hipótesis de que exista una expresión preferencial de canales CNGA1 en las ICC-IM mientras que la participación de los mecanismos dependientes de PKGI podría ser más relevante en el músculo liso uretral. No obstante, se requiere el desarrollo de herramientas farmacológicas más selectivas que actúen específicamente sobre canales CNG y sobre PKGI para poder definir la importancia y participación relativa de cada uno de estos dos efectores funcionales de la vía del cGMP que finalmente conducen a la relajación del músculo liso uretral.

Hay que señalar que nuestros resultados indican que la activación del canal CNG, que supuestamente induciría la entrada de cationes, incluido Ca^{2+} al interior de la célula, estaría implicado en la relajación del músculo liso uretral mediada por cGMP, lo que contradictoriamente supone una disminución y no un aumento en la concentración de Ca^{2+} intracelular. Por lo tanto, sería condición indispensable que la entrada de Ca^{2+} a través de CNG no afectara a los filamentos contráctiles. En este sentido, hay que señalar que estudios previos realizados en nuestro grupo llevaron a la hipótesis de que el neurotransmisor nitrérgico en la uretra no fuera NO libre, sino algún precursor más estable, por ejemplo un nitrocompuesto, basándonos en el hecho de que este transmisor es resistente a la acción de radicales superóxido y sustancias secuestradoras de NO extracelular (García-Pascual y Triguero, 1994; García-Pascual et al., 2000). Entre los diferentes tipos de nitrocompuestos, se ha sugerido como posible candidato a un S-nitrosotiol dada la similitud de su respuesta relajante con la inducida por EFS (Kerr et al., 1992; Thornbury et al., 1992; García-Pascual et al., 1999; García-Pascual et al., 2000). Una explicación alternativa sería que las terminaciones nerviosas liberaran NO libre, el cual no sería accesible a los destructores de NO debido a la estrecha relación estructural entre éstas y las ICC, y estas células respondieran al efecto de NO liberando a su vez otro mediador químico capaz de inducir la relajación del músculo liso. Apoyando este razonamiento, la entrada de Ca^{2+} mediada por cGMP a través de los canales CNG en las ICC podría ser el estímulo necesario para la secreción de este segundo mediador químico. El hecho de que se haya demostrado previamente la existencia de uniones similares a sinapsis entre ambos tipos celulares (Harhun et al., 2004) y la implicación de CNG en el control de la exocitosis de las sinapsis en células fotorreceptoras refuerzan esta hipótesis (Rieke y Schwartz, 1994).

En conclusión, en este estudio se demuestra la expresión de canales CNGA1 en la uretra de rata, localizados en SMC de forma débil, pero mucho más intensamente en ICC-IM, desempeñando una función crítica en la relajación uretral inducida por la vía NO/cGMP.

3. Participación de canales CNG sobre la actividad espontánea y en los cambios inducidos por la activación de la vía NO/cGMP de ICC y SMC aisladas

Como continuación de los resultados obtenidos en el apartado anterior, se estudió el posible papel de los canales CNG tanto sobre las oscilaciones espontáneas de Ca^{2+} que se producen en SMC e ICC aisladas de la uretra de conejo, actividad que refleja su función como marcapasos, como sobre los cambios que se producen en dichas oscilaciones de Ca^{2+} en respuesta a NO o al aumento en los niveles intracelulares de su principal mediador, el cGMP.

Hemos observado que L-cis-Diltiazem, utilizado como inhibidor específico de CNG (Hofmann et al., 2005), produjo una reducción significativa en la frecuencia y amplitud media de las ondas espontáneas de Ca^{2+} y en el calcio basal tanto en SMC

como en ICC, mientras que el isómero D-Diltiazem solamente fue eficaz en SMC. La clara diferencia en el comportamiento de D-Diltiazem entre ambos tipos de células indica en primer lugar que las oscilaciones de Ca^{2+} en SMC, pero no en ICC, son dependientes de la entrada de Ca^{2+} a través de canales tipo L. Este hecho, ya ha sido descrito previamente. De hecho, estudios electrofisiológicos en ICC uretrales han demostrado el escaso efecto de nifepidina, una dihidropiridina bloqueante también de estos mismos canales, sobre la frecuencia de las ondas espontáneas (Johnston et al., 2005; Sergeant et al., 2006b). Como se ha señalado en el apartado anterior, la similitud de L-cis-diltiazem con su isómero D-Diltiazem permite que también este compuesto sea capaz de afectar, aunque a dosis más altas y de forma más lenta a los canales de Ca^{2+} tipo L (Triguero et al., 2009). Por lo tanto, no podemos descartar que la mayor parte del efecto bloqueante de L-cis-Diltiazem sobre las ondas espontáneas de Ca^{2+} en SMC, pero no en ICC, pueda ser debido al bloqueo de canales de Ca^{2+} dependientes de voltaje. En conjunto, estos resultados sugieren que el efecto inhibitorio de L-cis-Diltiazem sobre las ondas espontáneas de Ca^{2+} sólo podría ser atribuido al bloqueo específico de los canales CNG en ICC.

Aunque se ha determinado que la liberación de Ca^{2+} de depósitos intracelulares es el principal generador de la actividad marcapasos de las ICC uretrales (Sergeant et al., 2006b), la entrada de Ca^{2+} extracelular también parece jugar un papel importante. Hasta el momento no se ha esclarecido cual es la vía que utiliza el catión para entrar en la célula. Se ha sugerido la participación de la entrada capacitativa de Ca^{2+}, secundaria a la movilización de Ca^{2+} desde los almacenes intracelulares (Johnston et al., 2005), o la entrada de Ca^{2+} a través del intercambiador Na^{+}-Ca^{2+} funcionando en sentido inverso (Bradley et al., 2006). En este sentido, nuestros resultados sugieren que los canales CNG de las ICC podrían proporcionar una vía alternativa de entrada de Ca^{2+} que contribuya a la generación y/o mantenimiento de las ondas espontáneas de Ca^{2+}en estas células. Siguiendo este razonamiento, L-cis-Diltiazem como inhibidor de esta entrada de Ca^{2+} a través de CNG podría servir como una herramienta útil para la inhibición selectiva de la actividad espontánea en ICC sin afectar a las SMC. Sin embargo, sería necesaria la realización de estudios electrofisiológicos a nivel de los canales CNG en ambos tipos de células para comprobar esta hipótesis.

En apoyo a esta hipótesis y corroborando los resultados previos de inmunohistoquímica en secciones de uretra de rata (apartado anterior, Triguero et al., 2009), hemos observado en el presente estudio una intensa CNGA1-ir en ICC aisladas de la uretra de conejo, mientras que en SMC esta tinción fue muy débil y difusa, por lo que los CNG estarían mayoritariamente expresados en ICC.

Cuando las células aisladas, tanto SMC como ICC, fueron expuestas a diferentes procedimientos que dan lugar a un aumento en los niveles intracelulares de cGMP, se observó una reducción en la frecuencia y amplitud media de las ondas espontáneas de Ca^{2+}, así como en el calcio basal, aunque en diferente grado. Estos procedimientos incluyen tratamientos con: 1) un activador de sGC, YC-1; 2) un análogo permeable de cGMP, 8-Br-cGMP; 3) un cóctel de inhibidores de las PDE (IBMX + Zaprinast) y 4) un

donante de NO, DEA-NO. Los tratamientos con DEA-NO e YC-1 fueron los más potentes en reducir la frecuencia media de las oscilaciones de Ca^{2+}. En ambos casos se produce una activación intensa de la sGC que en el caso de NO, su activador natural, es debido a su unión al grupo hemo de la enzima (Denninger y Marletta, 1999), mientras que YC-1 activa directamente a sGC mediante su unión a un sitio diferente del grupo hemo (Friebe et al, 1996; Mülsch et al, 1997; Friebe y Koesling, 1998). Por el contrario, el análogo permeable de cGMP, 8-Br-cGMP, no modificó las oscilaciones de calcio, y los inhibidores de las PDE sólo redujeron ligeramente la frecuencia y amplitud de éstas. Puesto que 8-Br-cGMP debe de entrar en la célula a través de la membrana plasmática, se podría sugerir que esta entrada tan lenta no alcanzaría niveles de cGMP lo suficientemente altos como para afectar a los parámetros de Ca^{2+} estudiados. Por otro lado, los inhibidores de las PDE actúan reduciendo la degradación de cGMP y permitiendo su acumulación. En este caso hemos utilizado un cóctel compuesto por un inhibidor general de las PDE (IBMX) que puede actuar tanto sobre las PDE de cAMP como de de cGMP, y de un inhibidor específico de las PDE de cGMP tipo V (Zaprinast), que es el tipo de PDE más abundante en la uretra (Werkström et al., 2006). El modesto efecto de estos compuestos apoya la idea de que la producción basal de cGMP es baja y por lo tanto su acumulación por los inhibidores de PDE no permite alcanzar niveles de cGMP suficientemente grandes para afectar a las oscilaciones espontáneas de Ca^{2+}. Por lo tanto estos resultados sugieren que sólo con aquellos procedimientos que originan una rápida e intensa actividad de sGC se produce un efecto reductor claro de las oscilaciones de Ca^{2+}.

Nuestros resultados están en concordancia con estudios electrofisiológicos previos que muestran que tanto 8-Br-cGMP, donantes de NO, como agonistas de la PKG reducen tanto las despolarizaciones espontáneas transitorias (STDs) como las corrientes de entrada espontáneas transitorias (STICs) registradas en ICC aisladas bajo condiciones de fijación de corriente (*current-clamp*) y fijación de voltaje (*voltage-clamp*), respectivamente (Sergeant et al., 2006a). Además, otros estudios han mostrado como nitroprusiato sódico y 8-Br-cGMP son capaces de reducir la frecuencia de las ondas lentas en el musculo liso de la uretra de conejo (Hashitani et al., 1996), apoyando la idea de que NO media su efecto a través de la vía NO/cGMP/PKG.

Dado que los canales CNG son directamente activados por cAMP o cGMP, lo más lógico sería esperar que el bloqueo de éstos con L-cis-Diltiazem presentara efectos inhibitorios sobre los cambios en la actividad espontánea inducidos por el aumento de cGMP. Sin embargo, en ningún caso se observó un efecto antagonista de L-cis-Diltiazem sobre el efecto previo inducido por los diferentes procedimientos experimentales utilizados. Incluso en el caso de 8-Br-cGMP y los inhibidores de las PDE, que por sí mismos no modificaron las ondas de Ca^{2+} o sólo lo hicieron ligeramente, la adición de L-cis-Diltiazem se sumó al efecto anterior provocando una mayor reducción en las ondas espontáneas de Ca^{2+}. En los otros casos (DEA-NO e YC-1) en que el efecto inhibitorio de las oscilaciones espontáneas de Ca^{2+} fue más marcado, la adición posterior de L-cis-Diltiazem no produjo un efecto adicional significativo pero

en ningún caso antagonizó el efecto previo. El efecto inhibitorio de L-cis-Diltiazem sobre las oscilaciones de Ca^{2+}, se podría especular que es debido a su acción inespecífica sobre los canales de Ca^{2+} tipo L, como ha sido descrito anteriormente, y por lo tanto no estaría relacionado con su acción sobre los canales CNG. En cualquier caso, nuestros resultados llevarían a la conclusión que los canales CNG no participan en el mecanismo por el cual el cGMP reduce las ondas espontáneas y el Ca^{2+} basal. La activación de PKG por cGMP podría ser responsable de estos efectos, aunque de nuevo para comprobar esta posibilidad sería necesario el empleo de inhibidores selectivos de PKG.

Estos resultados son difíciles de relacionar con la hipótesis propuesta en el apartado anterior de que los canales CNG estén participando en el mecanismo por el que el NO conduce a la relajación del músculo liso de la uretra inducida por NO/cGMP. Sin embargo varias observaciones expuestas en este trabajo y el anterior son lo suficientemente sólidas para ser tenidas en cuenta: 1) L-cis-Diltiazem produce una inhibición rápida y casi completa de la relajación inducida por EFS o por YC-1 en la uretra de diferentes especies (rata, ratón y oveja; Triguero et al., 2003; Triguero et al., 2009), lo que sugiere que los canales CNG jueguen un papel clave en el proceso de la neurotransmisión nitrérgica uretral; 2) Se ha confirmado en la uretra de rata la expresión del mRNA de las subunidades CNGA1 y CNGB1, que conforman el canal funcional CNGA1, canal que se activa específicamente por cGMP y es bloqueado por concentraciones micromolares de L-cis-Diltiazem (Triguero et al., 2009); 3) Se ha observado una intensa CNGA1-ir localizada en una subpoblación de ICC inmunoreactivas a vimentina tanto en cortes histológicos (apartado anterior, Triguero et al., 2009) como en células aisladas (en el presente apartado), sugiriendo que los canales CNG se localizan principalmente en ICC y es allí donde desempeñan su principal función.

Una posible explicación a estos resultados sería que la apertura de canales CNG originara incrementos de Ca^{2+} en subdominios celulares sin afectar al nivel de Ca^{2+} en el conjunto del citoplasma y por lo tanto sin afectar a las ondas de Ca^{2+}. De hecho, se sabe que los canales CNG pueden estar agrupados en microdominios dentro de una misma célula (Yau y Baylor, 1989; Koutalos y Yau, 1996; Savchenko et al., 1997), lo que permite una modulación espacio-temporal muy precisa de las funciones celulares por parte de los nucleótidos cíclicos (Kaupp, 1995). Como ya hemos sugerido en el apartado anterior, el NO liberado desde las terminaciones nerviosas podría actuar sobre las ICC, con las que están estrechamente relacionadas. Aquí, los canales CNG podrían estar localizados en microdominos subcelulares, donde al ser activados por cGMP producirían una entrada localizada de Ca^{2+}. Ésta podría ser el estímulo necesario para inducir la secreción de un mediador químico que actuaría sobre las SMC vecinas. Así, los CNG estarían localizados estratégicamente cerca de los sitios de liberación del mediador químico y por tanto serían el estímulo necesario para acoplar la respuesta NO/cGMP a la secreción del mismo. En este sentido hay que señalar la intensa CNGA1-ir observada en múltiples y finas espinas o espículas que emergen del cuerpo

celular y de las prolongaciones de las ICC, lo que sugiere que los canales CNG estarían concentrados en regiones especializadas de la membrana que entran en contacto con células vecinas. Estudios previos han mostrado la producción y liberación desde las ICC de varios mediadores químicos tales como productos derivados de la COX con actividad sobre las SMC (Collins et al., 2009). Sin embargo la existencia e identidad de este posible mediador en la uretra no se conoce todavía y sería necesaria la realización de nuevas investigaciones utilizando métodos más resolutivos capaces de analizar los niveles de Ca^{2+} y segundos mensajeros en microdominios subcelulares.

En resumen, en este estudio se ha demostrado la expresión selectiva de CNGA1 en ICC aisladas de la uretra de conejo, donde podrían participar en las oscilaciones de Ca^{2+}intracelular que determinan su función como marcapasos. Sin embargo no ha podido demostrarse su implicación en las alteraciones de Ca^{2+}intracelular inducidas por la activación de la vía NO/cGMP.

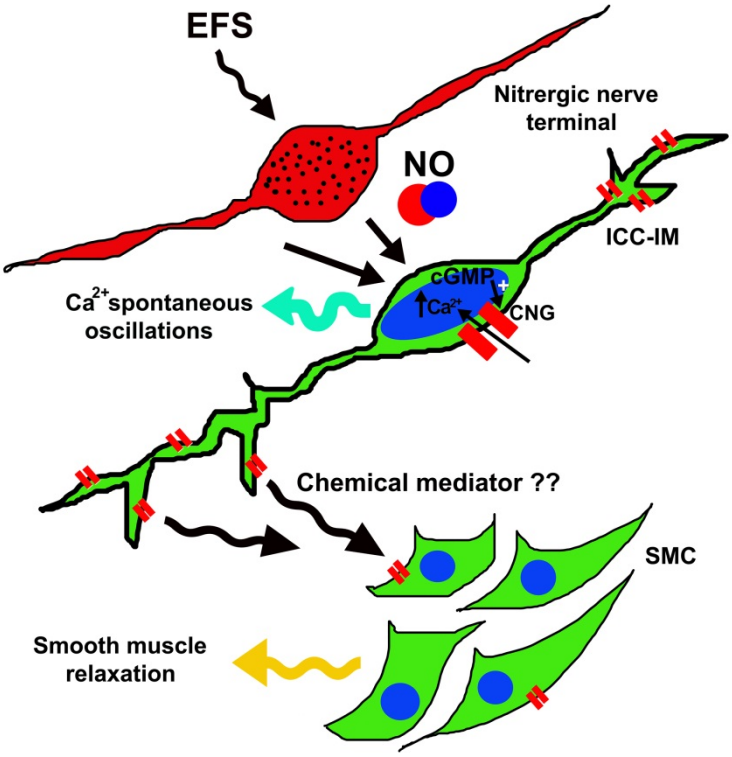

Figura XIII. Expresión de los canales CNG en SMC, pero fundamentalmente en ICC, donde podrían estar participando tanto en la generación y mantenimiento de las ondas espontáneas de Ca^{2+}, como en la relajación uretral mediada por la vía NO/cGMP.

4. Papel del acoplamiento eléctrico a través de uniones intercelulares comunicantes en la neurotransmisión uretral

En el tracto gastrointestinal, está generalmente aceptado que las ICC basan su función como células marcapasos en la conexión existente entre las células de la red de ICC mediante GJ, que permiten la rápida transmisión de señales eléctricas (Belzer et al.,

2002; 2004; Sanders, 1996). Del mismo modo, existen GJ que conectan unas SMC con otras, permitiéndoles coordinar la contracción de las paredes musculares de las vísceras gastrointestinales (Imtiaz et al., 2009). Igualmente son numerosos los autores que asumen que las ICC también tienen la capacidad de afectar al comportamiento de las SMC a través de sinapsis eléctricas rápidas (Sanders y Ward, 2006), permitiendo una rápida propagación de los cambios en el potencial de membrana a lo largo del sincitio muscular sin la necesidad de un mensajero químico que sea liberado a un espacio sináptico. Sin embargo, existe escasa evidencia estructural acerca de la presencia de GJ entre ICC y SMC, y de hecho muchos son los estudios que han fracasado en el intento de demostrar este tipo de conexión entre ambos tipos celulares (Daniel et al., 1998; Powley et al., 2008).

Una GJ está formada por la unión de dos hemicanales o conexones insertos en dos células contiguas, de tal forma que comunican ambos citoplasmas. Cada conexón está compuesto a su vez por la asociación de 6 subunidades proteicas llamadas Cx (Elfgang et al., 1995). Existen más de 20 tipos distintos de Cx, nombradas por su peso molecular (Willecke et al., 2002), dando lugar a una gran variabilidad de GJ, en términos de conductancia y permeabilidad, dependiendo de las Cx que lo formen (Kanaporis et al., 2008), lo que justifica la importancia de identificar que tipos de Cx están presentes en un determinado tejido.

Aunque cada Cx presenta una distribución tisular específica, muchos tipos celulares expresan más de un tipo de Cx (Malfait et al., 2001). Así, numerosos estudios en vejiga de diferentes especies animales y humanas han descrito la presencia de tres Cx diferentes: Cx37, Cx40 y Cx43, siendo esta última la más abundante (Haefliger et al., 2002; Ikeda et al., 2007; Neuhaus et al., 2002a; 2002b; 2009). Además, estos tres tipos de Cx están presente en ICC situadas en las capas submucosa (ICC-LP) y muscular (ICC-IM) de la vejiga (Sui et al., 2002), y se ha observado que en situaciones de hiperactividad vesical se producen alteraciones en la expresión vesical de Cx43 (Christ et al., 2003; Ikeda et al., 2007; Kuhn et al., 2008; Li et al., 2007) acompañadas de cambios en el número de las ICC (De Jongh et al., 2007), por lo que parece existir una asociación relevante desde el punto de vista clínico entre ICC, Cx y SMC, al menos en la vejiga urinaria.

En la uretra, hasta el momento no existen estudios acerca de la presencia de las diferentes Cx por lo que el objetivo de este apartado fue investigar la posible expresión y distribución de Cx43, Cx40 y Cx37 en la uretra de rata y oveja, así como su posible participación en la neurotransmisión uretral, tanto excitatoria (noradrenérgica) como inhibitoria (nitrérgica) mediante el uso de diferentes bloqueantes de GJ.

Nuestros resultados de PCR muestran por primera vez la expresión de Cx43, Cx40 y Cx37 en la uretra de rata, de forma similar a lo que ocurre en la vejiga urinaria de diferentes especies animales (Kuhn et al., 2008; Ikeda et al., 2007; Neuhaus et al., 2002a; 2002b, 2009). Cx43 fue la que presentó mayor intensidad y extensión en la pared uretral en experimentos de inmunofluorescencia, localizándose tanto en SMC,

como en ICC-LP e ICC-IM, así como en el urotelio (en la uretra de oveja). En las SMC, identificadas por su α-actina-ir, el marcaje de Cx43 apareció típicamente como un punteado fino e irregular, mientras que en ICC, inmunoreactivas a vimentina, además de este punteado algunas presentaron un marcaje mucho más intenso y uniforme a lo largo de toda la membrana celular o incluso en el citoplasma. La Cx43-ir desapareció por completo cuando las preparaciones fueron preincubadas con el péptido bloqueante específico para este anticuerpo, lo que demuestra la especificidad de la reacción. Por su parte, Cx37 presentó un marcaje más débil y menos extenso, presente también en SMC, ICC-LP e ICC-IM, mientras que la presencia de Cx40 fue observada en el endotelio de los vasos sanguíneos y con mucha menos intensidad en SMC, pero en ningún caso en ICC. En resumen, la expresión aparente de las diferentes Cx mediante inmunofluorescencia fue: Cx43>Cx37>Cx40, observándose sólo las dos primeras en ICC.

El típico patrón de distribución puntiforme de las Cx observado en la membrana plasmática tanto de SMC como de ICC es característico de GJ, sugiriendo por lo tanto la posible existencia de uniones funcionales en cualquiera de sus diferentes combinaciones (ICC-ICC, ICC-SMC o SMC-SMC). Hay que destacar la expresión tan marcada de Cx43 en ICC presentes en submucosa y capa muscular, similar a lo anteriormente descrito en vejiga (Sui et al., 2002) y en intestino grueso humano (Nemeth et al., 2000), y que sugiere un papel especial para este subtipo de Cx en la comunicación intercelular de ICC en diferentes órganos. El hecho de que en algunos casos la expresión de Cx43 se presentara más uniforme a lo largo de toda la membrana plasmática o incluso en el citoplasma de las ICC, podría reflejar el proceso de secreción y transporte de conexones desde el aparato de Golgi (Musil y Goodenough, 1993) hasta la membrana antes de su ensamblaje con otro conexón de una célula adyacente para conformar una GJ completa (Hutchings et al., 2008). La presencia en la membrana de conexones o hemicanales no incorporados en GJ podría servir también como vía de liberación de diferentes metabolitos al medio extracelular, como ocurre en los astrocitos del sistema nerviosos central (Kang et al., 2008; Stout et al., 2002). Por otro lado, está plenamente establecido que las GJ además de permitir el acoplamiento eléctrico entre células vecinas también pueden permitir el movimiento intercelular de una gran variedad de moléculas citoplasmáticas, incluyendo segundos mensajeros de bajo peso molecular como ATP, IP_3, nucleótidos, metabolitos, etc. (Lawrence et al., 1978), con diferente permeabilidad dependiendo de cuales sean las Cx constituyentes (Harris, 2007). En este sentido, se ha descrito que Cx43 presenta una mayor permeabilidad a cAMP que otras Cx como Cx40, Cx26 o Cx32 (Kanaporis et al., 2008; Bedner et al., 2006). La rápida difusión de cAMP de una célula a otra a través de GJ parece ser que es capaz de compensar la actividad de degradación de las PDE, y por lo tanto llegar a activar de forma efectiva ciertas funciones celulares (Kanaporis et al., 2008). De forma similar, podría producirse a través de GJ la difusión rápida de cGMP, el segundo mensajero de la acción del NO, aunque hasta el momento no existe ningún estudio que lo demuestre. En este escenario, incluso podría sugerirse que la distribución diferencial de distintas Cx en los distintos tejidos podría dar lugar a la formación de GJ

especializadas para el transporte de determinados metabolitos. Por lo tanto, la manipulación farmacológica selectiva de los diferentes tipos de GJ tendría un gran interés terapéutico.

El análisis del papel funcional de las GJ ha presentado el problema de la carencia de herramientas selectivas para su estudio ya que los bloqueantes clásicos de GJ, octanol, heptanol o carbenoxolona, presentan efectos no específicos que complican la interpretación de los resultados. En este sentido, el reciente descubrimiento de una nueva familia de péptidos, llamados péptidos GAP, ha proporcionado la primera herramienta farmacológica selectiva para estudiar la función de las GJ en un amplio rango de sistemas biológicos (Herve y Dhein, 2010). Estos péptidos actúan específicamente sobre el primer (GAP26) o el segundo (GAP27) bucle extracelular de Cx, y su acción es selectiva del tipo de Cx que se trate (Evans y Boitano, 2001); así por ejemplo el péptido GAP26 inhibe específicamente la transmisión de corrientes eléctricas a través de GJ compuestas por Cx43 (Desplantez et al., 2012). En nuestro estudio hemos utilizado una combinación de péptidos GAP26 y GAP27 con acción selectiva sobre las tres Cx presentes en la uretra: Cx43, Cx37 y Cx40.

Nuestros resultados funcionales en la uretra de rata y de oveja mostraron que las respuestas inducidas por EFS, tanto contráctiles como relajantes, no fueron modificadas significativamente por la preincubación con péptidos GAP durante largos periodos de tiempo (2h). La posibilidad de que existiera una pobre penetración de estas drogas quedó descartada por el hecho de que α-GA, un compuesto lipofílico conocido como bloqueante clásico de GJ (Davidson y Baumgarten, 1988), fue también incapaz de inhibir la transmisión nerviosa uretral, mientras que las contracciones inducidas por una alta concentración de K^+ si fueron significativamente reducidas por ambos bloqueantes en las dos especies estudiadas, demostrando la efectividad de ambos compuestos en inhibir la comunicación intercelular. Estos resultados están en concordancia con estudios que han mostrado que GAP27 y α-GA reducen la vasoconstricción miogénica en arterias mesentéricas pero no las contracciones inducidas con diferentes agonistas como fenilefrina (Earley et al., 2004) o que en ratones transgénicos con una delección específica de Cx43, las respuestas de las SMC intestinales a altas concentraciones de K^+ sean modificadas mientras que las respuestas inducidas por un agonista muscarínico, no resulten afectadas (Döring et al., 2007). En resumen, estos hallazgos sugieren una mayor implicación de GJ en la respuesta contráctil inducida por despolarización y la apertura de los canales de Ca^{2+} tipo L que en las respuestas inducidas por los neurotrasmisores NE y NO.

El hecho de que los bloqueantes de GJ no modifiquen las respuestas inducidas por neurotransmisores endógenos sugiere que la comunicación intercelular entre ICC-SMC, ICC-ICC o SMC-SMC no es esencial en la neurotransmisión de la uretra. Esta idea ya ha sido propuesta en otras estructuras como el intestino de ratón, donde diferentes péptidos GAP y otros bloqueantes de GJ tampoco son capaces de afectar a la neurotransmisión entérica (Daniel et al., 2007). Estos resultados sugieren que la respuesta de la uretra a los diferentes neurotransmisores no depende de la transmisión

de señales eléctricas en el sincitio muscular. Podría tratarse de musculo liso multiunitario, en el cual las unidades motoras son pequeñas, predominando aquellas en las que existe asociación de sólo una o pocas células musculares con cada terminación nerviosa, y por lo tanto cada fibra muscular se comportaría como una unidad independiente. Además, esta hipótesis pondría en duda la función de las ICC como supuestas mediadoras de la neurotransmisión. En este sentido, diversos estudios en tracto gastrointestinal consideran que las SMC por sí solas pueden responder directamente a los neurotransmisores liberados desde las varicosidades nerviosas (Cobine et al., 2010; Goyal y Chaudhury, 2010) y diversos estudios estructurales muestran que la distancia entre las terminaciones nerviosas y las SMC (50-200 nm) es suficiente para permitir la llegada por difusión de los diferentes neurotransmisores, incluido el NO (Wood y Garthwaite, 1994).

En la uretra, como se ha indicado en el apartado 1, hemos propuesto un modelo de inervación paralela en el cual tanto las SMC como las ICC podrían actuar como efectores directos del NO liberado por las terminaciones nerviosas nitrérgicas. Por lo tanto el papel de las ICC como mediadoras de la neurotransmisión podría ser sustituido por una función neuromoduladora más modesta, similar a la descrita en las sinapsis centrales para los astrocitos. Éstos son capaces de liberar mediadores difusibles como el ATP directamente al medio extracelular a través de los conexones que no están formando GJ completas (Kang et al., 2008; Stout et al., 2002). Se sabe que estos conexones son funcionalmente activos en la difusión selectiva de sustancias de bajo peso molecular al espacio extracelular, y que su permeabilidad puede ser regulada por despolarización o por fosforilación por PKC (Retamal et al., 2006). De acuerdo a esta hipótesis, las ICC responderían a la actividad neural con cambios en los niveles de los mensajeros secundarios como el cGMP, tal y como hemos observado en el presente estudio y a su vez estás células podrían modificar la liberación de sustancias activas a través de los conexones. Hay que resaltar que este mecanismo estaría en concordancia con el hecho de que los péptidos GAP no afecten a las respuestas nerviosas en la uretra, ya que la acción de estos bloqueantes es interrumpir el acoplamiento de conexones complementarios y con ello reducir el número de GJ activas (Evans y Boitano, 2001).

En conclusión, hemos demostrado por vez primera la expresión de tres tipos de Cx (Cx43, Cx37 y Cx40) en la uretra de rata y oveja, predominando la expresión de Cx43 en ICC y SMC. Sin embargo, la posible participación de mecanismos de comunicación intercelular eléctrica en la neurotransmisión uretral, tanto contráctil como relajante, no fue sustentada debido a la falta de efecto inhibitorio de diferentes inhibidores de GJ. Una posible alternativa que requiere posteriores estudios sería la participación de Cx presentes en ICC en funciones de neuromodulación mediante la liberación de sustancias con acción paracrina al medio extracelular.

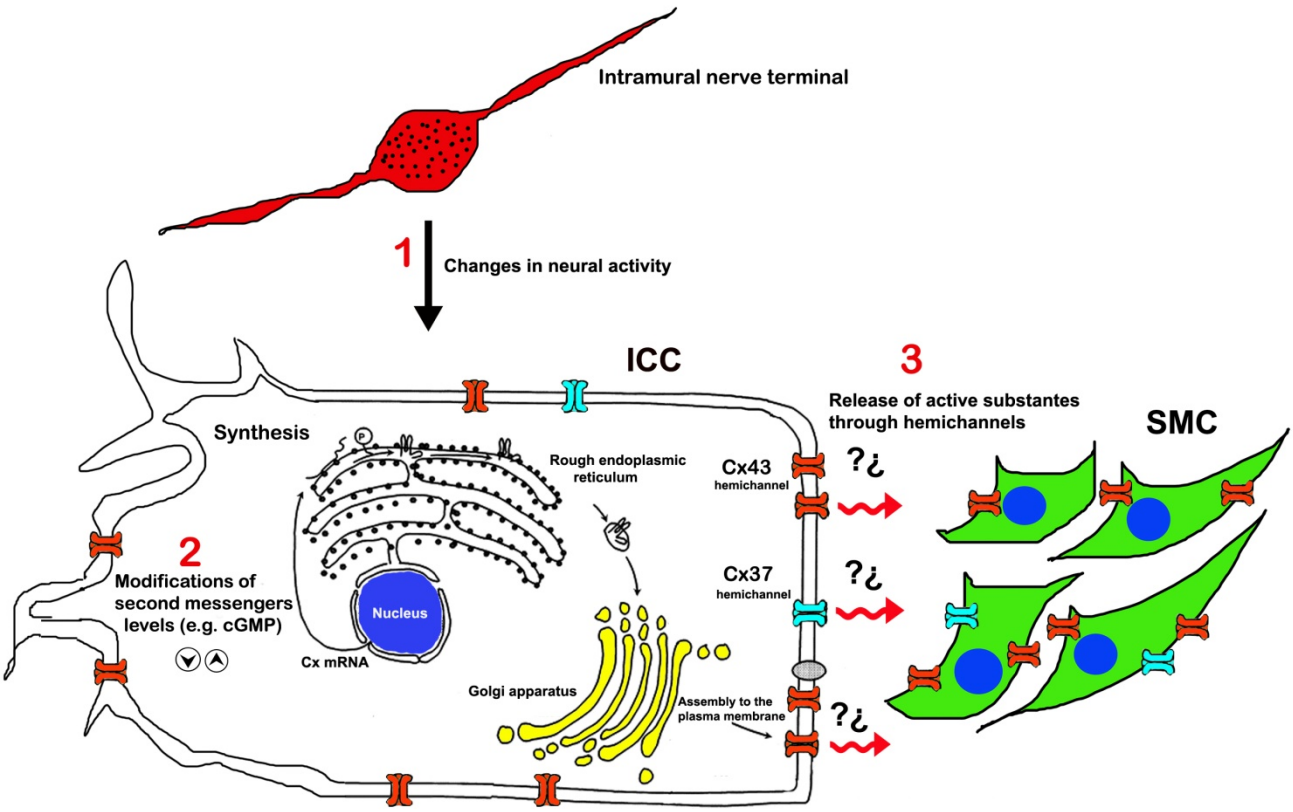

Figura XIV. Expresión de Cx43, Cx40, y Cx34 en la uretra de rata, predominando la expresión de Cx43 en ICC y SMC. Sin embargo, las GJ no participan en la neurotransmisión uretral, tanto contráctil como relajante, aunque las Cx presentes en ICC sí podrían participar en funciones de neuromodulación mediante la liberación de sustancias al medio extracelular.

5. Participación de CaCC en la neurotransmisión excitatoria uretral: papel de las ICC

En términos de excitabilidad celular, el potencial de membrana está generalmente definido por el balance existente entre los pequeños cationes, dada su distribución asimétrica a ambos lados de la membrana, mientras que el único anión permeable, el Cl^-, se encuentra en altas concentraciones a ambos lados de la membrana y generalmente se le considera en un segundo plano en cuanto a su participación en el estado iónico general de la célula. Sin embargo, en la uretra de conejo se ha descrito que la actividad marcapasos de las ICC está determinado por el balance iónico de Cl^- y la apertura de CaCC y que la NE, el principal mediador de la contracción uretral, podría actuar aumentando la frecuencia de las despolarizaciones espontáneas en ICC a través de la activación de estos CaCC (Sergeant et al., 2002).

El estudio de los CaCC es complicado dada la gran variedad de canales existentes, lo que explica el entusiasmo de los fisiólogos cuando el canal anoctamina1 (ANO1, también denominado TMEM16A) fue identificado, clonado y caracterizado como el principal CaCC funcional (Caputo et al., 2008, Schroeder et al., 2008, Yang et al., 2008). Además, recientemente ANO1 ha sido detectado en ICC del tracto gastrointestinal, pero no en músculo liso, donde incluso ha sido propuesto como nuevo

marcador específico de estas células, junto con el clásico c-kit, que permite su diferenciación de SMC y otras células vecinas (Gómez-Pinilla et al., 2009). Sin embargo este hecho no parece ser una regla común a todos los tejidos, y el primer estudio realizando con ANO1 en diferentes órganos, incluida la uretra, describe su ausencia en el tejido uretral de ratón (Huang et al., 2009).

En el presente estudio hemos analizado la expresión y distribución de ANO1 en la uretra de tres especies diferentes (oveja, rata y ratón), así como el papel funcional del Cl^- y de los CaCC en la actividad contráctil y relajante de la uretra inducida tanto por estimulación nerviosa como por agonistas exógenos.

Las respuestas contráctiles inducidas por EFS en la uretra se pueden considerar de carácter predominantemente adrenérgico, debido a la liberación de NE de las terminaciones nerviosas y la consecuente activación de receptores adrenérgicos postsinápticos. Este hecho había sido demostrado previamente en la uretra de la oveja (García-Pascual et al., 1991d) y ha sido también confirmado en el presente estudio en la uretra de rata y ratón. Así, las respuestas contráctiles inducidas por EFS fueron inhibidas casi por completo por TTX (bloqueante de canales de sodio) y por fentolamina (antagonista adrenérgico) mientras que el tratamiento posterior con el bloqueante muscarínico atropina no produjo mayor inhibición. Sin embargo, cuando la atropina se administró como tratamiento inicial si se provocó una inhibición parcial de las respuestas contráctiles inducidas por EFS. Estos resultados podrían explicarse por la existencia de un mecanismo modulador colinérgico de la transmisión adrenérgica (Mattiason et al., 1984), en el que la liberación de ACh actuara sobre receptores muscarínicos presinápticos presentes en las terminaciones nerviosas adrenérgicas provocando una mayor liberación del transmisor.

La función de los CaCC en las respuestas contráctiles del músculo liso todavía sigue siendo un aspecto controvertido, debido en parte a la falta de herramientas farmacológicas específicas, y a su amplia distribución y variabilidad. En nuestras condiciones experimentales, dos de los tres inhibidores de CaCC utilizados, ácido niflúmico y 9-AC, fueron capaces de reducir significativamente las respuestas contráctiles de la uretra, provocadas tanto por EFS como por la adición exógena de NE. Sin embargo, STIS (ácido 4-acetamido-4´-isotiocianato-2,2´-estilbenodisulfónico), otro antagonista putativo de los CaCC (Zoccoli y Karnovsky, 1980), no presentó ningún efecto inhibitorio significativo poniendo en duda su actividad como inhibidor específico de los CaCC. En este sentido, estudios previos han demostrado la carencia de efecto de STIS o de otro compuesto relacionado, DIDS (ácido 4,4´-diisotiocianatostilbeno-2,2-disulfónico), en modificar la concentración de cloro intracelular ($[Cl^-]_i$) en las fibras de Purkinje cardíacas de oveja (Vaughan-Jones, 1986) o en los conductos deferentes (Aickin y Brading, 1990) y uréter de cobaya (Aickin, 1990), aunque este derivado del ácido estilbenodisulfónico sí parece ser capaz de modificar la $[Cl^-]_i$ en otros sistemas (Hoffmann y Simonsen, 1989). También es posible que su papel como inhibidor del intercambio Cl^-/HCO_3 intervenga en este efecto (Chipperfield y Harper, 2000).

La exposición de las preparaciones a una solución Krebs libre de Cl^- ($[Cl^-]_o$), produjo una contracción rápida inicial que regresó al nivel basal pasados 10-20 min. Esta contracción fue similar en forma y magnitud al primer componente rápido de la contracción inducida por altas concentraciones de K^+ (García-Pascual et al., 1991d), sugiriendo que es debida a una despolarización de la membrana. Según establece el equilibrio de Donnan, las concentraciones fisiológicas de $[Cl^-]_i$ (intracelular) < $[Cl^-]_e$ (extracelular) hacen que E_m (potencial de membrana) = E_{Cl} (potencial de equilibrio para el Cl^-). Sin embargo, en la célula muscular lisa, los niveles fisiológicos de $[Cl^-]_i$ parecen ser mayores que los descritos por el equilibrio de Donnan, puesto que $E_m > E_{Cl}$, y por lo tanto el movimiento de Cl^- a través de la membrana provoca un efecto despolarizante neto (Chipperfield y Harper, 2000). La desviación de este equilibrio se ve aumentada cuando las preparaciones son sumergidas en soluciones salinas artificiales (como la solución Krebs), que contienen una mayor concentración de Cl^- que el medio extracelular (Koncz y Daugiras 1994). En estas condiciones, la eliminación de Cl^- externo es seguida de un aumento en la salida de Cl^- a través de la membrana siguiendo el fuerte gradiente de concentración y por lo tanto despolarizando la misma (Lamb y Barna, 1998). Cuando esta despolarización activa los canales de Ca^{2+} dependientes de voltaje, induce la contracción muscular. Este efecto también se ha descrito en preparaciones vasculares (Lamb y Barna, 1998).

Después de 30 min de exposición al medio $[Cl^-]_o$ y una vez que el efecto contráctil inicial había desaparecido, las contracciones inducidas por EFS fueron reducidas significativamente. Este hecho, junto con la inhibición que originaron los inhibidores de los CaCC sobre las contracciones inducidas tanto por EFS como por la adición exógena de ACh o NE, sugiere que la actividad contráctil del músculo liso uretral es dependiente de las corrientes de Cl^-. En el modelo de actividad marcapasos planteado previamente en la uretra de conejo (Sergeant et al., 2006b) se propuso que la estimulación de los CaCC ocurría tras un aumento en los niveles de Ca^{2+} intracelular, provocada a su vez por la activación de los receptores IP_3 del retículo sarcoplásmico. En nuestro estudio, sólo en las preparaciones de uretra de oveja, la preincubación durante 30 min con 2-APB (un bloqueante de los receptores IP_3) produjo una inhibición significativa de las contracciones inducidas por EFS. Por lo tanto, parecen existir diferencias entre especies con respecto a la contribución de las diferentes fuentes de Ca^{2+} (tanto intra- como extracelulares) que participan en la activación de los CaCC involucrados en la contracción uretral inducida por NE.

Dentro de la extensa y compleja familia de los CaCC, el recientemente clonado y caracterizado ANO1 ha sido identificado como el principal CaCC en tejidos excitables (Caputo et al., 2008; Schroeder et al., 2008; Yang et al., 2008). Sólo algunos miembros de la familia de las anoctaminas son capaces de producir corrientes de Cl^- dependientes de Ca^{2+} y ANO-1 es el que produce corrientes de mayor amplitud (Kunzelmann et al., 2011). En el presente trabajo, se detectó por inmunofluorescencia la presencia de ANO1-ir exclusivamente en SMC y células uroteliales de las tres especies estudiadas. El intenso y nítido marcaje para ANO1 en la capa muscular lisa se confirmó mediante

colocalización con α-actina. Sin embargo, en ningún caso se detectó ANO1-ir en ICC tanto de la lámina propia (ICC-LP) como las dispersas entre los haces musculares lisos (ICC-IM). Estos resultados están en claro contraste con los obtenidos previamente en tracto gastrointestinal (Huang et al., 2009), donde mientras las SMC no fueron marcadas se describe una fuerte ANO1-ir en una amplia red de ICC (Gómez-Pinilla et al., 2009). Nuestros resultados también están en contradicción con los únicos estudios previos en tejido uretral, donde no han sido capaces de demostrar ANO1-ir en la capa muscular lisa (Huang et al., 2009). Estas diferencias probablemente tengan un origen metodológico: distintos protocolos de inmunofluorescencia (Huang et al. utilizaron metanol y paraformaldehído como fijadores, pero sin crioprotección del tejido) o la utilización de diferentes anticuerpos primarios (un antisuero policlonal casero desarrollado en conejo frente a nuestro anticuerpo comercial, creado en conejo y que ha producido resultados satisfactorios en tracto gastrointestinal de diferentes especies; Gómez-Pinilla et al., 2009; Hwang et al., 2009; Zhu et al., 2009). Por lo tanto, la detección de ANO1 en distintos tejidos empleando el mismo procedimiento experimental hace improbable que nuestros resultados sean un mero artefacto.

La especificidad de la ANO1-ir fue además confirmada mediante el análisis de la expresión de su mRNA por RT-PCR utilizando dos pares diferentes de oligonucleótidos diseñados para dos secuencias de ANO1 conocidas, dirigidos a diferentes regiones del mRNA, y que producen productos de distinto tamaño y composición. En ambos casos, se amplificó una única banda del tamaño esperado, y aunque no se realizó una PCR cuantitativa, la aparente intensidad de las bandas correspondientes a la uretra fue claramente superior a las bandas amplificadas de la próstata, órgano utilizado como control positivo y que expresa ANO1 en intensidad sólo superada por el páncreas (Schreiber et al., 2010).

El resultado más significativo de este estudio es la ausencia de ANO1-ir en todas aquellas células que presentan marcaje con vimentina. Estos resultados a primera vista parecen sorprendentes, ya que estudios previos han descrito la presencia de CaCC en ICC aisladas de uretra de conejo, donde generan corrientes de Cl^- espontáneas (Sergeant et al., 2001) implicadas en su actividad como células "marcapasos" del tono miogénico uretral (Sergeant et al., 2000). Por el contrario, las SMC aisladas de la uretra de conejo apenas poseen CaCC y sólo una pequeña minoría son activas espontáneamente (Sergeant et al., 2000). Incluso se ha llegado a sugerir que el tratamiento con inhibidores de CaCC, como el ácido niflúmico o 9-AC, podría ser utilizado para la generación de un "*knockout* farmacológico" de las ICC en la uretra de conejo (Sergeant et al., 2002). La causa de estas discrepancias podría radicar en la existencia de diferencias específicas. Así, los mismos autores describen en uretra de oveja que los CaCC están presentes tanto en ICC como en SMC (Sergeant et al., 2001), siendo ambos tipos celulares capaces de generar corrientes espontáneas y por tanto sembrando la duda sobre el papel marcapasos exclusivo de las ICC en esta especie. Además, otros estudios en tracto urinario inferior (vejiga y uretra) de diferentes especies confirman la implicación de los CaCC en el

control de la contracción del músculo liso, por lo que la uretra de conejo parece ser la excepción a la norma (Chipperfield y Harper, 2000).

La ausencia de expresión de ANO1 en las ICC uretrales de las tres especies utilizadas en este estudio podría alternativamente explicarse por la posible existencia de un CaCC diferente en ICC uretrales todavía sin caracterizar. Además, la ausencia de canales ANO1 en las ICC uretrales en este estudio está en concordancia con el hecho de que los inhibidores de CaCC no modifiquen las relajaciones nitrérgicas del musculo liso uretral inducidas por EFS.

En conclusión, el presente estudio muestra que el Cl^- desempeña un papel central en la contracción uretral noradrenérgica, actuando directamente sobre el músculo liso, sin modificar la respuesta relajante nitrérgica. La acción del Cl^- podría ser debida a la participación de CaCC reactivos a ANO1 presentes en SMC y urotelio, pero nunca en ICC. Este hecho sorprendente diferencia las ICC uretrales, al menos de las especies estudiadas, de sus homólogas del tracto gastrointestinal y de nuevo sugiere la existencia de diferentes tipos de ICC, en distintos órganos o incluso dentro del mismo tejido, con diferentes características y que puedan desempeñar diferentes funciones.

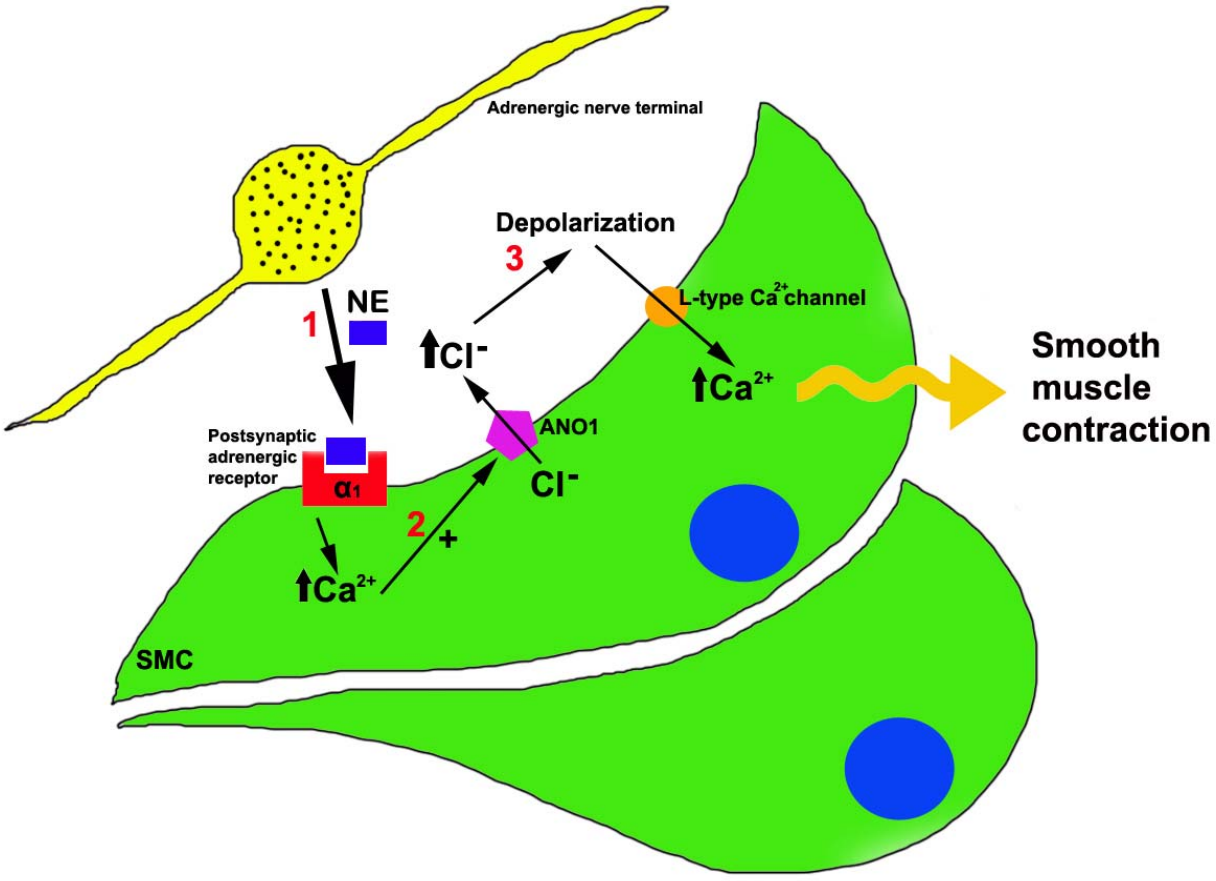

Figura XV. Participación de los CaCC en la contracción uretral noradrenérgica, actuando directamente sobre el músculo liso.

6. Cambios en la producción de NO en la vejiga y uretra en un modelo experimental de cistitis hemorrágica inducida por CYP en la rata

En este trabajo se ha utilizado la inducción de cistitis hemorrágica por CYP en la rata como un modelo de inflamación vesical bien establecido que nos permita analizar los cambios que se producen en la producción de NO durante un proceso inflamatorio tanto en la vejiga como en la uretra. Hay que señalar que este es el primer estudio que describe los efectos de CYP en la uretra. La cistitis inducida por CYP supone un serio efecto secundario de su uso como quimioterápico en tratamientos antineoplásicos. Por lo tanto, avanzar en el conocimiento de los mecanismos patogénicos que desencadenan la cistitis podría ayudar al desarrollo de nuevos tratamientos preventivos.

Los animales tratados con CYP en nuestro estudio mostraron claros síntomas de dolor e hiperactividad vesical con un aumento en el número de micciones totales y en el número de micciones de bajo volumen como ya ha sido descrito previamente (Bon et al., 1998; Yoshimura y de Groat, 1999). Acompañando a estos trastornos funcionales, se observaron claros síntomas de inflamación tanto en la vejiga como en la uretra. Estas alteraciones fueron aumentando con la duración del tratamiento, siendo especialmente evidentes en los animales sometidos a los tratamientos intermedio (48h) y crónico (10 días). Cabe destacar que la CYP también afectó a otros órganos como el riñón, pulmón o hígado, donde se observaron edema y hemorragias, incluso aproximadamente el 10% de los animales murieron antes de completar el tratamiento debido a trastornos hemorrágicos. Se piensa que la cistitis inducida por CYP es debida a su metabolización en el hígado a acroleína, la cual al eliminarse por la orina es capaz de erosionar el epitelio vesical, provocando una reacción inflamatoria que se extiende por toda la pared vesical (Cox, 1979). Sin embargo, la escasa aparición de lesión en el epitelio tanto vesical como uretral, unido a la existencia de lesiones vasculares generalizadas sugiere que el efecto de la acroleína no se circunscriba exclusivamente al urotelio, sino que también pueda actuar desde la sangre alterando la permeabilidad e integridad de los vasos sanguíneos (Korkmaz et al., 2007; Ramu et al., 1995). Esta sugerencia está también sustentada en el hecho de que las lesiones en vejiga y uretra fueron similares a pesar de la diferencia entre ambos órganos en el tiempo de contacto con la orina. Por ello, hay que tener en cuenta que el empleo de CYP como modelo de inflamación o hiperactividad vesical debería restringirse en términos de tiempo y dosis con objeto de minimizar los efectos sistémicos. En este sentido, el tratamiento que consideramos más adecuado como modelo de cistitis hemorrágica sería el intermedio (48h), ya que origina un proceso inflamatorio agudo en el tracto urinario, sin afectar de forma grave al estado general de los animales.

Se considera de forma general que un exceso en la producción de NO es el principal responsable de los trastornos vesicales propios de la cistitis hemorrágica inducida por CYP en la rata y que esta producción aumentada de NO proviene de la inducción de la isoforma inducible (iNOS; Souza-Filho et al., 1997; Alfieri y Cubeddu, 2000; Korkmaz et al., 2007; Andersson et al., 2008; Linares-Fernández y Alfieri, 2007;

Xu et al., 2001). Un aumento en la producción de radicales libres y citoquinas (TNF-α e interleucinas), que a su vez activan el factor de transcripción NF-kB, podrían provocar la inducción de la expresión de un gran número de genes (se han descrito hasta 60 genes distintos), entre ellos la iNOS (Baltrons y García, 1999; Morris y Billiar, 1994; Nazif et al., 2007; Oter et al., 2004). Esta enzima se caracteriza porque se expresa en las células tan sólo después de su estimulación con citoquinas, microbios o productos microbianos, y una vez sintetizada produce NO en altas concentraciones de forma no controlada. La combinación de altos niveles de NO y radicales libres (como el O_2^-) puede dar lugar a la formación de peroxinitrito, el cual a su vez origina peroxidación lipídica y daño tisular (Korkmaz et al., 2007). De hecho, se ha demostrado un aumento en la expresión de nitrotirosina, utilizado como marcador de la nitración de proteínas por NO/peroxinitrito y de poli-ADP ribosa polimerasa, como indicador de la lesión del DNA en la cistitis inducida por CYP en la rata (Abraham y Rabi, 2009).

En contra de lo esperado, nuestros resultados mostraron de forma clara la ausencia de inducción de iNOS en la vejiga y en la uretra en ninguno de los tratamientos con CYP empleados. Esta aseveración está basada tanto en experimentos de inmunofluorescencia e inmunotransferencia, que miden la expresión proteica, como en experimentos de PCR que determinan la expresión de mRNA. Hay que tener en cuenta que la idea de la participación fundamental de iNOS en la patogenia de la cistitis inducida por CYP no está sólidamente probada ya que procede de hallazgos poco contrastados. La mayoría de estos trabajos basan esta hipótesis en el efecto protector del tratamiento previo de los animales con inhibidores supuestamente selectivos de iNOS, como aminoguanidina (Abraham et al., 2009; Korkmaz et al., 2005) o S-metiltiosourea (Alfieri et al., 2001; Oter et al., 2004; Linares-Fernández y Alfieri, 2007). Sin embargo, la selectividad de estos compuestos es dosis-dependiente y por tanto a altas concentraciones también provocan la inhibición de las isoformas constitutivas de la NOS (eNOS y nNOS). En esta línea, recientemente se ha mostrado que la administración sistémica del inhibidor no selectivo de NOS, L-NAME atenúa la disminución de la actividad colinérgica del detrusor en ratas tratadas con CYP (Andersson et al., 2008).

Además, aunque algunos estudios describen aumentos en la expresión de iNOS (tanto mRNA como proteína) a consecuencia de la cistitis inducida por CYP en la rata (Matsuoka et al., 2008; Ribeiro et al., 2002) o incluso en biopsias de pacientes con cistitis intersticial (Koskela et al., 2008; Nazif et al., 2007), en todos los casos este aumento es moderado y sólo se localiza en el urotelio y células inflamatorias de la submucosa. Resulta difícil entender cómo la producción de NO exclusivamente en el urotelio pueda ser la responsable de las alteraciones y lesiones patológicas que aparecen en toda la pared vesical, teniendo en cuenta la corta vida media del NO y por lo tanto su limitada accesibilidad a capas más profundas. Además, el aumento en la expresión de iNOS parece ser transitorio, describiéndose tras 1 (Matsuoka et al., 2008), 12 (Ribeiro et al., 2002) y 24 horas (Sakura et al., 2008) de la inyección de CYP, pero nunca en un modelo crónico durante 60 horas (Giglio et al., 2005) o 7 días (Cho et al., 2010). De la

misma forma, se describe en la vejiga de ratón durante la cistitis inducida por LPS (lipopolisacárido bacteriano), SP, o estimulación por antígenos una sobrexpresión génica de iNOS a las 4 horas pero no tras 24 horas de dicha inducción (Saban et al., 2002). Por lo tanto no podemos descartar que puedan producirse aumentos transitorios en la expresión de iNOS en tiempos distintos a los ensayados en el presente trabajo, pero en ningún caso parece existir una inducción sostenida de iNOS que justifique los trastornos inflamatorios observados.

Apoyando nuestros resultados, Poljakovic y Persson (2003) observaron que ratones carentes de iNOS ($iNOS^{-/-}$) no eran diferentes de la cepa control ($iNOS^{+/+}$) en cuanto a su capacidad para defenderse de una infección inducida por la instilación vesical de E.Coli, induciéndose en ambas cepas la producción de nitrotirosina. Llama la atención que ambos tipos de ratones expresen nNOS y eNOS en las células inflamatorias, sugiriendo que el origen del NO producido en exceso no procede necesariamente de la actividad iNOS. En la línea de estas observaciones, se ha descrito que en las fases iniciales (primeras horas) de la cistitis inducida por CYP, el aumento en la producción de NO puede proceder de un aumento en la fosforilación de la isoforma endotelial (eNOS), por acción de la fosfatidil-inositol-3-kinasa (PI-3K), lo cual aumenta su actividad (Kang et al., 2004). Sin embargo, no existen datos previos que muestren cambios en la expresión de las isoformas constitutivas de NOS en animales con cistitis inducida por CYP.

Nuestros resultados han demostrado por vez primera modificaciones significativas en la expresión de ambas isoformas constitutivas (nNOS y eNOS) aunque en sentido inverso. Mientras nNOS sufre una disminución pasajera en su expresión, evidente en los tratamientos agudo e intermedio pero que desaparece en el tratamiento crónico, la expresión de eNOS sufre un aumento muy acusado y progresivo con la duración de la administración de CYP. eNOS que normalmente se expresa en los tejidos control en el endotelio y epitelio se extiende e intensifica en los tejidos inflamados hacia SMC, ICC y células inflamatorias infiltradas en todo el espesor de la pared de ambos órganos, pero especialmente en la vejiga. Por el contrario, nNOS mostró una expresión localizada fundamentalmente en el plexo nervioso intramural del trígono o base vesical y en la uretra, disminuyendo tanto la densidad de nervios nitrérgicos en estas zonas como la expresión proteica de esta enzima a consecuencia de los tratamientos agudo e intermedio.

Se ha descrito que la hiperreflexia temprana que acompaña a la cistitis se debe a una sobreexpresión de nNOS en los segmentos espinales (Lagos y Ballejo, 2004), aunque no se conoce lo que ocurre en los nervios periféricos intramurales. En la vejiga hipertrófica de la rata se ha mostrado una disminución de nNOS-ir y de actividad NOS Ca^{2+}-dependiente (Johansson et al., 2003), hecho que también ha sido demostrado en un modelo de inflamación del intestino en rata (Porras et al., 2006), estando estos efectos relacionados con la liberación de citoquinas pro-inflamatorias. Por lo tanto, estos antecedentes apoyan nuestros resultados y sugieren que algunos mediadores liberados

durante el proceso inflamatorio puedan ocasionar una disminución en la expresión de la isoforma neuronal de NOS en nervios nitrérgicos.

Estudios realizados en otros órganos muestran al igual que en nuestro caso la implicación de las isoformas constitutivas de NOS en procesos inflamatorios. En riñón de ratón, se ha demostrado la inducción de iNOS y eNOS, mientras que se reduce la expresión de nNOS a consecuencia de la inyección de LPS (Holmquist et al., 2005). Asimismo, en un modelo de colitis en rata se describe un aumento en la expresión tanto de eNOS como de iNOS en la submucosa intestinal, unido a un aumento del flujo sanguíneo que fue reducido por el inhibidor no selectivo (L-NNA), pero no por el inhibidor selectivo de iNOS (I-NIL), indicando que es la isoforma endotelial la responsable del trastorno (Petersson et al., 2007). También en la sepsis cerebral, se ha descrito que es la producción de NO por parte de eNOS la inductora de la inflamación, originando un aumento en la permeabilidad vascular y edema (Handa et al., 2008). Sin embargo, en otros casos el papel de la isoforma endotelial durante un proceso inflamatorio es protector. Así, se ha demostrado en ratones deficientes de la isoforma endotelial que la inflamación provocada en diferentes modelos de colitis es más severa que cuando esta enzima está presente (Vallance et al., 2004). Por lo tanto, el papel protector o perjudicial del NO puede variar dependiendo del tejido y las condiciones locales (cantidad producida, disponibilidad de radicales libres, antioxidantes, etc.). En nuestro caso, llama la atención la gravedad de las lesiones vasculares (ectasias, edema y profusas hemorragias) que acompañan a la cistitis inducida por CYP lo que sugiere la implicación en las mismas de un aumento en la producción de NO a nivel endotelial. El aumento en la expresión de eNOS en la vejiga también ha sido descrito previamente asociado a diversos procesos patológicos vesicales. Así, aparece en la capa urotelial y suburotelial de la vejiga en tratamientos con CYP durante 60 horas (Giglio et al., 2005), en un modelo de inflamación vesical inducida por LPS (Kang et al., 2004), así como en células inflamatorias en un modelo de hipertrofia vesical (Johansson et al., 2003). Por tanto, eNOS podría representar una nueva fuente de NO alternativa a la inducción de iNOS durante la cistitis inducida con CYP. El hecho de que en el presente estudio no se observe mediante PCR cuantitativa una sobreexpresión paralela en el mRNA de eNOS en el tratamiento intermedio con CYP podría deberse a la existencia de mecanismos post-transcripcionales o a una desincronización en la sobreexpresión del mRNA y de la proteína en cuestión. Sería necesario cuantificar la producción de mRNA a diferentes periodos del tratamiento con CYP para responder a esta cuestión.

Hay que destacar que en los experimentos de inmunotransferencia de eNOS no se observaron aumentos significativos en la densidad correspondiente a la proteína completa (133 KDa), mientras que se produjo la aparición de una banda muy intensa a valores aproximados de 60 KDa cuya densidad aumentó progresivamente a consecuencia del tratamiento. Es posible que esta banda represente un fragmento degradado de eNOS que conserve el epítopo específico. Así, se ha descrito que la asociación de NOS con la chaperona *"Heat Shock Protein 90"* (HSP90) confiere protección a la enzima contra el ataque proteolítico (Averna et al., 2008), y que mientras

nNOS se asocia con mayor cantidad de HSP90, lo que le confiere mayor resistencia (Averna et al., 2008), eNOS contiene menos HSP90 y es más susceptible de ser atacada por la acción de agentes proteolíticos como la calpaína. Podría argumentarse que la inflamación vesical y uretral inducida por CYP originara un aumento en la actividad proteolítica tisular que llevaría a una intensa destrucción de eNOS (la isoforma más susceptible). Sin embargo, nuestros resultados no permiten saber si la enzima antes de degradarse ha sido capaz de producir cantidades notables de NO o si por el contrario, pese a su sobreexpresión, la alta tasa de destrucción se traduzca en bajos niveles de la enzima funcionalmente activa. El hecho de que eNOS aparezca en otras células, tales como SMC, ICC y células inflamatorias en los animales tratados con CYP, unido a la presencia de extensas lesiones vasculares, sugiere la participación de una enzima capaz de producir cantidades apreciables de NO a pesar de su rápido *"turnover"*. En cualquier caso, para demostrar esta posibilidad sería necesario medir *in situ* la cantidad real de NO producido.

Una excesiva producción de NO por parte de eNOS localizada en estructuras vecinas, como el propio músculo o las ICC, podría ser también responsable directo de la disminución en la expresión de nNOS en las terminaciones nerviosas intramurales. Las consecuencias funcionales de estos cambios son extremadamente difíciles de predecir. Las propiedades fisicoquímicas del NO son tales que las alteraciones espacio-temporales en la expresión de las isoformas de NOS y sus efectos sobre las células vecinas son mucho más importantes que la producción global de NO. Otra posibilidad es que la actividad de NOS se "desacople" en los tejidos inflamados debido a deficiencias de sustratos o cofactores necesarios, de forma que su actividad de desvíe de la producción de NO a la generación de radicales superóxido (O_2^-), lo que conduciría a una situación de estrés oxidativo contribuyendo al daño tisular. Esta situación ha sido descrita en la disfunción del endotelio asociada con la hipertensión, diabetes y aterosclerosis (Chuang et al., 2009).

Mientras está sólidamente documentada la participación de las terminaciones aferentes vesicales en la hiperactividad del detrusor que acompaña a la cistitis inducida por CYP (Chuang et al., 2009), poco se sabe acerca de los cambios que se producen en la función eferente motora en la vejiga, y especialmente en la uretra. En este sentido, nuestros resultados están en concordancia con trabajos previos (Lagos y Ballejo, 2004; Giglio et al., 2005), que describen una reducción en la contractilidad del músculo detrusor tras un tratamiento agudo con CYP. Este efecto parece ser inespecífico ya que afectó de forma similar a las contracciones inducidas por altas concentraciones de K^+, EFS o la adición exógena de ACh. Además, esta reducción no parece estar relacionada con los niveles de NO puesto que el inhibidor de NOS, L-NNA, no fue capaz de modificar este efecto. Alternativamente, el daño tisular, especialmente el edema, que alcanza su punto máximo a las 48 h después del tratamiento con CYP, podría provocar un deterioro transitorio en la contractilidad del músculo detrusor que posteriormente revierte al disminuir este edema con el tratamiento crónico. En la uretra sin embargo, este efecto no parece ser lo suficientemente intenso como para modificar la

neurotransmisión eferente, tanto contráctil como relajante. En este sentido, se podría haber esperado una reducción en la relajación nitrérgica de la uretra a consecuencia de la reducción en la expresión de nNOS que acompaña a los tratamientos agudo e intermedio. No obstante, dada la alta densidad de inervación nitrérgica a este nivel (cuello vesical y uretra), se podría argumentar que una reducción incluso moderada en la densidad de nervios nitrérgicos no fuera suficiente para afectar significativamente a la relajación muscular. En conjunto, estos resultados sugieren que la hiperexcitabilidad vesical que acompaña a la cistitis no parece estar relacionada con los cambios en la actividad motora eferente tanto en la vejiga como en la uretra y por lo tanto estaría más relacionado con alteraciones de la inervación aferente que modifiquen el reflejo de micción.

En conclusión, este estudio demuestra que la prominente reacción inflamatoria inducida por CYP tanto en la vejiga como en la uretra, no se acompaña de inducción de iNOS mientras que si se modifica la expresión de las isoformas constitutivas. Se ha demostrado una reducción de la expresión de nNOS en nervios nitrérgicos, mientras que aumenta la expresión de eNOS en diferentes tipos celulares lo que podría contribuir a la patogenicidad del proceso.

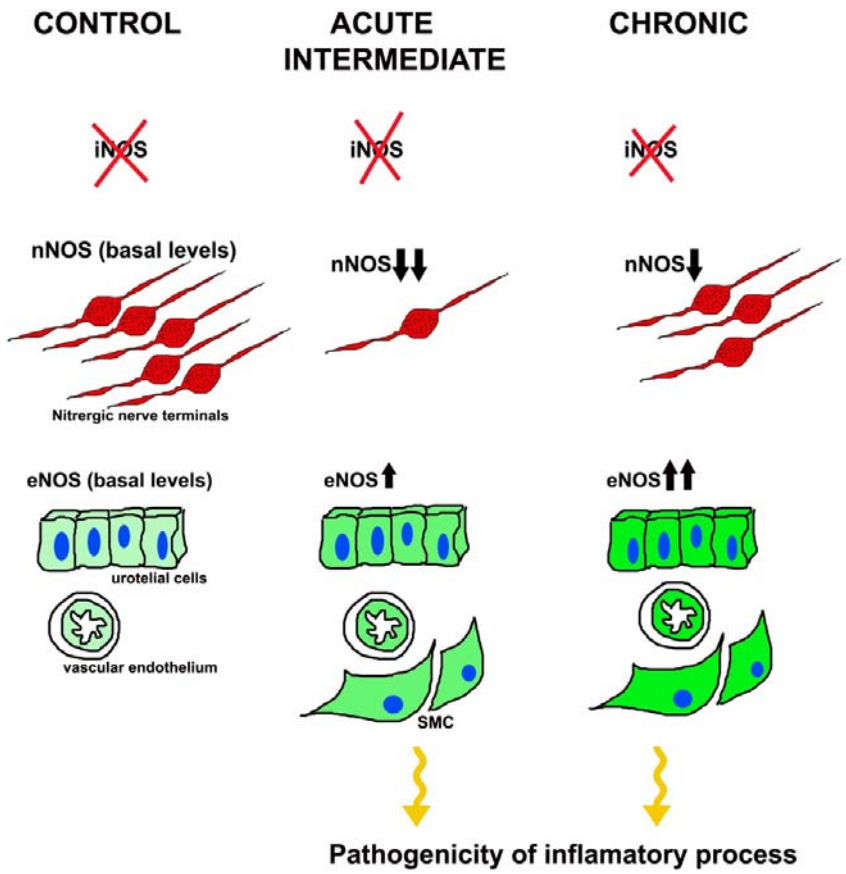

Figura XVI. Cambios producidos en las isoformas de la NOS en la cistitis inducida por CYP. No se produce en ningún caso la expresión de iNOS, mientras que si se modifica la expresión de las isoformas constitutivas. Se ha demostrado una reducción de la expresión de nNOS en nervios nitrérgicos, mientras que aumenta la expresión de eNOS en diferentes tipos celulares, lo que podría contribuir a la patogenicidad del proceso.

7. Participación de ICC en la cistitis inducida por CYP

La probada relación existente entre nervios nitrérgicos e ICC tanto en la uretra (manuscrito I) como en la vejiga (Gillespie et al., 2005) y la hipótesis de la participación de estas células como mediadoras del proceso de neurotransmisión nitrérgica (manuscrito I) hace pensar que una alteración en la producción de NO, como la descrita anteriormente durante la cistitis inducida por CYP, pudiera ir acompañada de cambios en la densidad y distribución de las ICC. El presente estudio muestra un incremento considerable en la densidad de células inmunoreactivas a diferentes marcadores de ICC y/o fibroblastos (c-kit, vimentina, CD34 y PDGFRα) en la pared vesical y uretral a medida que progresa el tratamiento con CYP.

No obstante, antes de intentar dar una explicación a este aumento generalizado de ICC es necesario hacer algunas consideraciones. En primer lugar, hay que tener en cuenta que ninguno de los anticuerpos utilizados es totalmente selectivo para ICC. Si c-kit es el marcador por excelencia de ICC en el intestino (Huizinga et al., 1995) y otros tejidos (Torihashi et al., 1997; Lammie et al., 1994; Vanderwinden et al., 1996), también marca otras células tales como mastocitos, melanocitos, neuronas y células de la glía (Zhang y Fedoroff, 1997). Además, incluso en el intestino, no todas las ICC son reactivas a c-kit, como por ejemplo las ICC-DMP del intestino delgado (Torihashi et al., 1999; Wang et al., 2003a), sugiriendo la existencia de subtipos de ICC con diferente reactividad a c-kit que pudieran tener diferentes características funcionales. En el tracto urinario inferior, se ha podido demostrar c-kit-ir en la vejiga de ratón (McCloskey et al., 2009), a diferencia de otros autores que describen una falta de reactividad a este anticuerpo, sirviéndose de vimentina para la identificación de estas célula tanto en vejiga como en uretra de diferentes especies (Sergeant et al., 2000; Gillespie et al., 2004; Pezzone et al., 2003; Koh et al., 2012). En nuestro estudio, aunque en un principio apenas obtuvimos marcaje con c-kit en uretra de rata fijada con paraformaldehído (manuscrito I), la utilización de un anticuerpo diferente (c-19, Santa Cruz Biotechnology) nos ha permitido obtener resultados satisfactorios tanto en la vejiga como en la uretra de esta especie. La reactividad a c-kit apareció principalmente en los somas de células con morfología típica de ICC y aunque también apareció un ligero marcaje inespecífico en células uroteliales y en el músculo liso de ambos órganos, en ningún caso dificultó el análisis de los resultados.

En comparación con c-kit, vimentina-ir parece ser menos dependiente de las condiciones experimentales. Así, en todos los casos en los que por cuestiones técnicas no se pudo demostrar c-kit-ir, si se observó una clara positividad a vimentina en las ICC uretrales (Sergeant et al., 2000; manuscrito I). Vimentina, tampoco es exclusiva de ICC, siendo capaz de marcar mastocitos, y fibroblastos o miofibroblastos. No obstante, la morfología peculiar de las ICC, células alargadas con escaso citoplasma, núcleo ovoide y largas prolongaciones, permite diferenciarlas fácilmente de macrófagos y mastocitos, de forma redondeada y carente de prolongaciones (Fig. 3 manuscrito VI). Hay que destacar el alto nivel de colocalización (75-80%) observado en nuestro estudio entre c-

kit y vimentina. En muchos otros casos, tanto en vejiga como en uretra, se ha demostrado la colocalización de ambos marcadores en estas células (Davidson y McCloskey, 2005; Smet et al., 1996; Johnston et al., 2010; manuscrito I). Este hecho es especialmente relevante ya que dadas las dificultades técnicas para obtener un adecuado marcaje con c-kit en tejidos fijados, la validación del uso de vimentina como marcador específico de ICC en estos tejidos es de gran importancia. Estos resultados vienen refrendados por estudios previos que describen la positividad a vimentina en ICC uretrales y vesicales en donde sin embargo no se demuestra su positividad a c-kit (Sergeant et al., 2000; Gillespie et al., 2004; Pezzone et al., 2003; Koh et al., 2012; manuscrito I).

Actualmente existe un amplio debate acerca de la presencia de otros marcadores en ICC. Entre ellos, CD34 es una glicoproteína transmembrana presente en células endoteliales y mesenquimatosas (Pusztaszeri et al., 2006) que es considerada por algunos investigadores como un marcador de fibroblastos (c-kit negativos) pero no de ICC tanto en tracto gastrointestinal como en vejiga, (Vanderwinden et al., 1999, 2000; Pieri et al., 2008; Rasmussen et al., 2007). Sin embargo, otros estudios han demostrado mediante PCR y microscopia confocal la coexpresión de c-kit con CD34, y por tanto la existencia de esta proteína en ICC (Robinson et al., 2000). También se ha demostrado que las células c-kit positivas de GIST también expresan CD34 (Hirota et al., 1998). Algo similar pasa con PDGFRα, recientemente propuesto como un nuevo marcador de células similares a ICC del tracto gastrointestinal que son negativas a c-kit (Iino et al., 2009; Iino y Nojyo, 2009; Chan et al., 2010; Kurahashi et al., 2012). En base a estos resultados se ha sugerido la existencia en el tracto digestivo de dos tipos de células intersticiales, las verdaderas ICC, y otra subpoblación de células denominadas "similares a fibroblastos" (*fibroblast-like cells*) que son PDGFRα positivas pero que no muestran reactividad a c-kit. En vejiga se ha descrito también una población de células inmunoreactivas a PDGFRα que muestran positividad a vimentina, no pudiéndose probar su colocalización con c-kit (Koh et al., 2012), y que al igual que en tracto gastrointestinal se encuentran próximas a SMC y en íntimo contacto con las terminaciones nerviosas (Horiguchi y Komuro, 2000, Lang, 2011; Cobine et al., 2011).

Nuestros resultados muestran la existencia de un alto grado de colocalización entre todas las parejas de marcadores ensayados. La colocalización de CD34 y PDGFRα con vimentina y c-kit (aunque este último sólo pudo ser enfrentado a CD34 al no disponer de anticuerpos eficaces en especies diferentes para PDGFRα), sugiere que a diferencia de lo indicado en el tracto digestivo (Iino et al., 2009; Iino y Nojyo, 2009; Chan et al., 2010; Kurahashi et al., 2012), la mayoría de las ICC también serían positivas a CD34 y PDGFRα. Llama la atención el alto grado de colocalización entre estos dos últimos marcadores (supera el 90%), que posiblemente no llega a su totalidad debido al marcaje de células endoteliales por parte de CD34 pero no de PDGFRα (Pieri et al., 2008). También en tracto gastrointestinal se ha demostrado la colocalización entre ambos marcadores mediante inmunohistoquímica (Robinson et al., 2000; Vanderwinden et al., 1999). El grado de colocalización es ligeramente inferior cuando se enfrentan

CD34 con vimentina o c-kit (50-80 %), sugiriendo la posible existencia de una segunda población celular que fuera marcada mayoritariamente por CD34 y PDGFRα. El debate actual se centra en si las células positivas a estos marcadores alternativos (CD34 y PDGFRα) pero negativas a c-kit serían verdaderas ICC con diferente función (Vanderwinden et al., 2000) o se trataría de fibroblastos o "células similares a fibroblastos" (Horiguchi y Komuro, 2000, Lang, 2011; Cobine et al., 2011). Aunque, teniendo en cuenta que para ambos tipos celulares se ha descrito su relación estructural y funcional con SMC y nervios intramurales y que por lo tanto ambos podrían actuar como mediadoras de la neurotransmisión (Horiguchi y Komuro, 2000, Lang, 2011; Cobine et al., 2011; Koh et al., 2012), las semejanzas entre ambos podrían ser mucho mayores de lo que sugieren sus diferentes nombres. Es posible que sea necesaria una reevaluación de lo que se considera una ICC que esté basada en aspectos funcionales, más allá de su reactividad a c-kit, o a cualquier otro marcador.

Se ha sugerido que las ICC localizadas en diferentes regiones de la pared uretral o vesical pudieran tener diferente especialización funcional. Así, las ICC localizadas a nivel subepitelial y en la lámina propia donde forman un sincitio conectado entre sí y con nervios aferentes (Hashitani, 2006), podrían participar en el procesamiento de la información aferente (Huizinga et al., 2008) o bien podrían tener una función marcapasos (Mazet y Ranier, 2004). Estas ICC en la uretra hemos visto que muestran aumentos de cGMP que no se modifican por la estimulación de los nervios nitrérgicos (manuscrito I), sugiriendo que su función principal no es ser efectores de la acción del NO. Por el contrario, las ICC de la capa muscular, estarían especialmente adaptadas a actuar como mediadoras entre los nervios intramurales y las SMC, ya que en éstas los aumentos de cGMP inducidos por la estimulación nitrérgica eran específicamente inhibidos al bloquear la enzima de síntesis de NO y de sGC (manuscrito I). En el presente estudio no se observó una distribución diferencial de células positivas a cualquiera de los cuatro marcadores empleados entre las capas submucosa y muscular tanto en la vejiga como la uretra. Estos resultados siguieren que los marcadores empleados no son capaces de discriminar entre los posibles tipos funcionales de ICC anteriormente descritas.

El tratamiento con CYP originó una acumulación muy marcada de células positivas a los cuatro marcadores empleados que fue muy similar entre ellos. Además, en ninguno de los casos el tratamiento con CYP modificó el grado de colocalización de ninguna de las parejas de anticuerpos analizados, lo que refuerza la sugerencia de que todos los marcadores empleados serían útiles para detectar las células que proliferan durante el proceso inflamatorio. Esta acumulación también fue similar en la capa submucosa y muscular, aunque destaca un especial empaquetamiento de células situadas debajo del urotelio, cuya densidad aumenta de forma progresiva con el tratamiento con CYP. Estos resultados son similares a los descritos por de Jongh y colaboradores (2007) en un modelo de obstrucción vesical en el cobaya, aunque en este caso las ICC son marcadas con un anticuerpo anti-cGMP. Hay que tener en cuenta que tanto en la cistitis como en la obstrucción uretral uno de los síntomas característicos es

un aumento en la excitabilidad del reflejo de micción que lleva a síntomas de hiperactividad vesical. Así, aumentan el número de micciones totales y de pequeño tamaño a consecuencia del tratamiento con CYP. Esta hiperexcitabilidad podría tener su origen en un incremento en la descarga aferente vesical originada por una mayor densidad de ICC a nivel subepitelial. Estas células podrían actuar directamente sobre las terminaciones aferentes como auténticos mecanorreceptores o podrían, como marcapasos, aumentar la actividad contráctil vesical que a su vez originaría la distorsión mecánica y la consecuente activación de las terminaciones aferentes.

En el modelo de obstrucción vesical inducida en cobayas descrito anteriormente (de Jongh et al., 2007) se describe un incremento en la densidad de ICC inmunoreactivas a cGMP en la capa muscular situadas especialmente en agrupaciones llamadas nodos intermusculares, donde se asocian con terminaciones nerviosas intramurales. En el presente estudio, un análisis más detallado de la distribución de células positivas a c-kit, vimentina, CD34 y PDFGRα dentro de la capa muscular, muestra que estas células fueron especialmente densas en la periferia de los haces musculares, expandiéndose hacia la serosa, donde forman una densa corona celular, fundamentalmente en el caso de la uretra. Además, esta densa red de ICC conecta a su vez con las distribuidas en la submucosa formando una macrored interconectada que se extiende por toda la pared vesical y uretral. Esta disposición permitiría que las ICC actuaran en la transmisión y coordinación de señales desde el urotelio o los nervios intramurales hasta el músculo y viceversa. De esta forma, un aumento en la densidad de ICC podría originar un incremento de la actividad contráctil inter-miccional que a su vez desencadenaría la situación de hiperreflexia. En apoyo de esta sugerencia se ha demostrado que en el síndrome de vejiga hiperactiva humana se da un prominente aumento en el número de ICC inmunoreactivas a c-kit en comparación con vejigas sanas (Biers et al., 2006). De la misma manera, en un modelo de obstrucción vesical parcial en cobayas, acompañado de hiperactividad vesical, se ha observado un incremento en la densidad de ICC positivas a c-kit y vimentina en la capa subserosa, así como una alteración en la distribución de ICC en la capa suburotelial (Kubota et al., 2008). En conjunto estos resultados sugieren una relación directa entre el aumento en el número de ICC y la hiperexcitabilidad vesical que caracterizan estos síndromes.

Nuestros resultados muestran también la expresión *de novo* de eNOS en células positivas a vimentina y CD34 en las diferentes capas de la pared vesical y uretral de los animales tratados con CYP. Aunque no pudieron realizarse dobles marcajes con c-kit y PDGFRα, la coincidencia con vimentina y CD34 y sus características morfológicas son suficientes para identificar estas células como ICC. Se ha descrito previamente que las ICC al menos en la uretra no expresan nNOS, aunque son efectoras del NO liberado de los nervios mediante aumentos en el cGMP intracelular (manuscrito I). Además, el presente trabajo muestra que estas células tampoco expresan la isoforma endotelial en ausencia de inflamación (preparaciones control). Por lo tanto, la expresión de eNOS en ICC, y la consiguiente producción de NO a partir de estas células podría contribuir a la patogenia del proceso inflamatorio. Como ya se ha indicado en el apartado anterior un

exceso en la producción de NO parece ser uno de los mecanismos centrales en el desarrollo de la cistitis (Souza-Filho et al., 1997; Alfieri y Cubeddu, 2000; Korkmaz et al., 2007) y este exceso de NO podría provenir de la expresión de la isoforma constitutiva endotelial en un gran número de ICC distribuidas por toda la pared vesical y uretral.

Las ICC también poseen funciones secundarias en procesos de inmunomodulación, crecimiento, reparación y fibrosis (Powell et al., 1999a; 1999b; Sanders 1996; Pucilowska et al., 2000; Schuppan et al., 2000; Van Assche, 2001). Numerosos estudios han mostrado la pérdida, reducción o daño de ICC en una gran diversidad de desórdenes de la motilidad intestinal (Sanders et al., 2002; Streutker et al., 2007). Por el contrario en procesos inflamatorios tales como la enfermedad intestinal inflamatoria y particularmente en la enfermedad de Crohn, se ha demostrado que las células mesenquimales (fibroblastos o ICC) se activan a un fenotipo fibrogénico dando lugar a la fibrosis del tejido mediante la secreción anormal de matriz extracelular (Burke et al., 2007). Además, se ha descrito la participación de PDGFR en afecciones fibróticas de diferentes tejidos (Andrae et al., 2008; Bonner, 2004; Powell et al., 1999a) y ratones con un aumento en la activación de PDGFRα desarrollan fibrosis gastrointestinal y sarcoma (Olson y Soriano, 2009). También se ha sugerido la participación de otros factores de crecimiento como scf (ligando natural del receptor c-kit), el factor de crecimiento epidérmico y el factor de crecimiento transformante-β, entre otros (Powell et al., 1999a; 1999b). Teniendo en cuenta la estrecha similitud entre las ICC gastrointestinales y las del tracto urinario se podría sugerir que la proliferación de ICC formaría parte de un proceso de fibrosis que contribuiría a la patogenia de la cistitis inducida por CYP.

Nuestros resultados muestran un claro efecto inhibitorio de Glivec sobre la proliferación de ICC tanto en la lámina propia como en la capa muscular lisa de la vejiga y de la uretra, así como de los síntomas de hiperactividad vesical que se inducen a consecuencia del tratamiento con CYP. Este hecho sugiere la participación del prominente aumento en el número de ICC que acompaña a nuestro modelo de cistitis hemorrágica en el desencadenamiento de los síntomas de hiperactividad. Glivec es un inhibidor selectivo de receptores tirosina quinasa que se sabe que es capaz de inhibir el receptor c-kit y el receptor PDGFR (Druker et al., 1996), y actualmente se utiliza para el tratamiento de GIST c-kit positivos (Kubota et al., 2004; Joensuu et al., 2001). Ya había sido previamente descrito que el tratamiento con Glivec inhibe el desarrollo de ICC-MY y la actividad eléctrica espontánea en el tracto gastrointestinal durante el último periodo de gestación (Beckett et al., 2007). Respecto a tracto urinario inferior, diversos autores han observado una reducción en la actividad vesical a consecuencia de la inhibición de c-kit (Sui et al., 2002; Biers et al., 2006; Vahabi et al., 2011; Kubota et al., 2006; 2004). Biers et al., (2006) demostraron que Glivec inhibe el aumento en la contractilidad vesical y en la actividad espontánea que se producen en el síndrome de vejiga hiperactiva y Kubota et al (2006) mostraron que Glivec es capaz de reducir la actividad espontánea vesical. El hecho de que Glivec sea capaz de prevenir el aumento en el

número de ICC así como los síntomas de hiperactividad vesical, permite sugerir su posible aplicación terapéutica en la prevención de los trastornos vesicales que acompañan a los tratamientos quimioterapéuticos con CYP. Además, su uso potencial podría extenderse a otras patologías inflamatorias del tracto urinario inferior que cursen también con proliferación de ICC y con síntomas de hiperactividad. Aunque se necesitan más estudios para clarificar del papel de las ICC en el desencadenamiento de dichos trastornos, un exceso en la producción de NO derivada de la expresión de eNOS en una población muy aumentada de ICC podría contribuir al proceso.

En resumen, este estudio muestra por vez primera que la prominente reacción inflamatoria inducida por CYP en la vejiga y uretra se acompaña de un aumento generalizado en la densidad de ICC positivas a c-kit, vimentina, CD34 y PDGFRα. Además, el proceso se acompaña de la inducción de la expresión de eNOS en dichas células, pudiendo constituir una nueva fuente de NO que contribuyera a la patogenicidad del proceso inflamatorio. Por último, Glivec fue capaz de inhibir tanto la proliferación de ICC como los síntomas de hiperactividad vesical, lo que nos lleva a sugerir su posible aplicación terapéutica en la prevención de los trastornos vesicales secundarios al tratamiento quimioterápico con CYP.

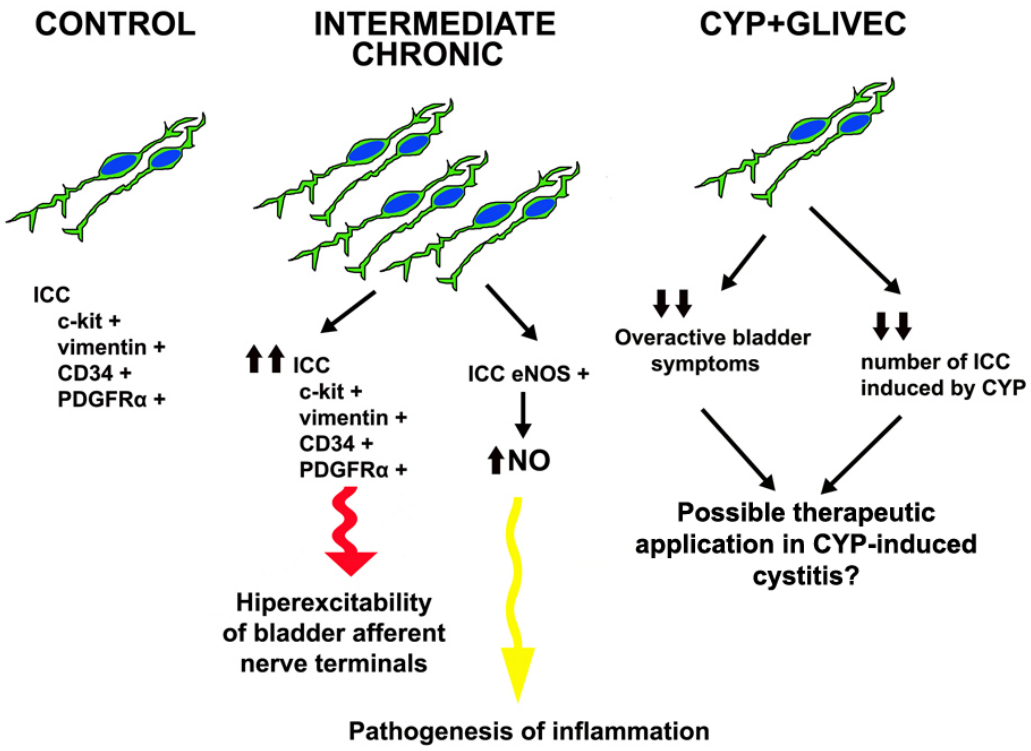

Figura XVII. Cambios en el número de ICC positivas a cuatro marcadores distintos y el efecto preventivo de Glivec en la cistitis inducida por CYP. El aumento en la expresión de eNOS en ICC podría contribuir a la patogenicidad del proceso.

CONCLUSIONES

1. La estimulación de los nervios nitrérgicos en la uretra provoca la acumulación de cGMP tanto en ICC como SMC por lo que proponemos un modelo de inervación paralela en el que ambos tipos celulares podrían ser efectores directos del NO liberado desde las terminaciones nerviosas. La estrecha relación estructural entre ICC y nervios nitrérgicos apoya esta sugerencia. Las ICC inmunoreactivas a cGMP se distribuyen en las distintas capas de la pared uretral, pero sólo las intramusculares (ICC-IM) parecen estar implicadas en la transmisión nitrérgica.

2. Se demuestra la expresión de canales CNG (subtipo CNGA1, activado por cGMP) en la uretra, localizados en SMC pero más intensamente en ICC. En ICC aisladas, la expresión de canales CNG1 es muy intensa en espículas que se proyectan desde las prolongaciones y el cuerpo celular. La funcionalidad de este canal parece ser esencial para el desarrollo de la relajación uretral provocada por la activación de la vía NO-cGMP, aunque hasta el momento no se conoce el mecanismo implicado.

3. Los canales CNG podrían también participar en la actividad marcapasos de las ICC, pero no de las SMC, proporcionando una vía alternativa para la entrada de Ca^{2+}. Sin embargo, no están implicados en la reducción de las ondas de Ca^{2+} provocada por cGMP, sugiriendo que éste no es el mecanismo por el cual los canales CNG median la relajación inducida por NO/cGMP en la uretra.

4. Se demuestra la expresión de las conexinas: Cx37, Cx40 y Cx43 en la uretra, localizadas tanto en SMC como en ICC. Sin embargo, el fracaso de los bloqueantes de GJ en modificar las respuestas contráctiles o relajantes inducidas por estimulación nerviosa no sustenta la participación de un mecanismo de comunicación eléctrica entre ICC y SMC en la neurotransmisión uretral.

5. Se demuestra una intensa expresión de CaCC del tipo ANO1 en SMC de la uretra que participan en la contracción uretral noradrenérgica, pero no en la relajante nitrérgica. En claro contraste con el tracto gastrointestinal, no se ha podido demostrar la expresión de ANO1 en ninguno de los diferentes subtipos de ICC uretrales.

6. El tratamiento con CYP en la rata induce una reacción inflamatoria tanto en la vejiga como la uretra, aunque sólo en la vejiga se altera la contractilidad muscular. Se demuestra la ausencia de expresión de iNOS en ambos órganos, mientras que si se modifica la expresión de las isoformas constitutivas. Una reducción pasajera en la expresión de nNOS se acompaña de un incremento progresivo en la expresión de eNOS

que además se extiende a SMC e ICC, las cuales podrían constituir nuevas fuentes de NO que podrían colaborar a la patogenicidad del proceso inflamatorio.

7. El tratamiento con CYP en la rata induce un aumento generalizado en el número de ICC positivas para c-kit, vimentina, CD34 y PDGFRα, en la vejiga y en la uretra que es acompañado de la expresión *de novo* de eNOS en estas células, constituyendo una nueva fuente de NO que podría contribuir a la patogenicidad del proceso inflamatorio. Glivec fue capaz de inhibir tanto la proliferación de las ICC como los síntomas de hiperactividad vesical que se producen como consecuencia del tratamiento con CYP, lo cual apoya el papel de las ICC en la patogenia del proceso y nos permite sugerir su posible aplicación terapéutica en la prevención de los trastornos vesicales secundarios al tratamiento quimioterápico con CYP.

BIBLIOGRAFÍA

Abraham P, Rabi S, Kulothungan P. Aminoguanidine, selective nitric oxide synthase inhibitor, ameliorates cyclophosphamide-induced hemorrhagic cystitis by inhibiting protein nitration and PARS activation. *Urology* 73: 1402-1406, 2009.

Abraham P, Rabi S. Protein nitration, PARP activation and NAD+ depletion may play a critical role in the pathogenesis of cyclophosphamide-induced hemorrhagic cystitis in the rat. *Cancer Chemother Pharmacol* 64:279-85, 2009.

Abrams P. Describing bladder storage function: overactive bladder syndrome and detrusor overactivity. *Urology* 62 (5): 28-37, 2003.

Abu-Shoud HM, Stuehr DJ. Nitric oxide synthases reveal a role for calmodulin in controlling electron transfer. *Proc. Natl. Acad. Sci. U.S.A* 90: 10769-10772, 1993.

Aickin CC, Brading AF. The effect of loop diuretics on Cl^- transport in smooth muscle of the guinea-pig vas deferens and taenia from caecum. *J Physiol* 421: 33-53, 1990.

Aickin CC. Chloride transport across the sarcolema of vertebrate smooth muscle. In: Chloride and Carriers in Nerve, Muscle and Glial Cells, edited by Alvarez-Leefmans FJ and Russel JM. New York: Plenum, 1990, p. 209-249.

Alberti E, Mikkelsen HB, Wang XY, Díaz M, Larsen JO, Huizinga JD, Jimenez M. Pacemaker activity and inhibitory neurotransmission in the colon of Ws/Ws mutant rats. *Am J Physiol Gastrointest Liver Physiol* 292: 1499-1510, 2007.

Alfieri AB, Cubeddu LX. Nitric oxide and NK_1-tachykinin receptors in cyclophosphamide-induced cystitis in rats. *J Pharmacol Exp Ther* 295: 824-829, 2000.

Alfieri AB, Malave A, Cubeddu LX. Nitric oxide synthases and cyclophosphamide-induced cystitis in rats. *Naunyn Schmiedebergs Arch Pharmacol* 363: 353-357, 2001.

Alm P. Cholinergic innervations of the human urethra and urinary bladder: a hystochemical study and review of methodology. *Acta Pharmacol Toxicol* 43: 56-62, 1978.

Altdorfer K, Bagaméri G, Donáth T, Fehér E. Nitric oxide synthase immunoreactivity of interstitial cells of Cajal in experimental colitis. *Inflamm. Res* 51:569-571, 2002.

Alvarez B, Denicola A, Radi R. Reaction between peroxynitrite and hydrogenperoxide: formation of oxygen and slowing of peroxynitrite descomposition. *Chem Res Toxicol* 8(6):859-864, 1995.

Andersson KE, Arner A Urinary bladder contraction and relaxation: physiology and pathophysiology. *Physiol Rev* 84: 935-986, 2004.

Andersson KE, García-Pascual A, Forman A, TØttrupt A. Non-adrenergic, non-cholinergic nerve mediated relaxation of rabbit urethra is caused by nitric oxide. *Acta Physiol Scand* 141: 133-134, 1991.

Andersson KE, García-Pascual A, Persson A, Forman A, TØttrupt A. Electrically-induced nerve-mediated relaxation of rabbit urethra involves nitric oxide. *J.Urol* 147: 253-259, 1992.

Andersson KE. Pharmacology of urinary tract smooth muscles and penile erectile tissues. *Pharmacol Rev* 45:253-288, 1993.

Andersson KE, Wein AJ. Pharmacology of the Lower Urinary Tract: Basis for Current and Future Treatments of Urinary Incontinence. *Pharmacol Rev* 56(4): 581-631, 2004.

Andersson MC, Tobin G, Giglio D. Cholinergic nitric oxide release from the urinary bladder mucosa in cyclophosphamide-induced cystitis of the anaesthetized rat. *Br J Pharmacol* 153: 1438-1444, 2008.

Andersson PO, Malmgren A, Uvelius B. Functional responses of different muscle types of the female rat urethra in vitro. *Acta Physiol Scand* 140: 365-372, 1990.

Andrae J, Gallini R, Betsholtz C. Role of platelet-derived growth factors in physiology and medicine. *Genes Dev* 22: 1276-1312, 2008

Augsburger HR, Cruz-Orive LM, Arnold S. Morphology and Steorology of the Female Canine Urethra Correlated with the Urethral Pressure Profile. *Acta Anat* 148**:** 197-205, 1993.

Averna M, Stifanese R, De Tullio R, Passalacqua M, Salamino F, Pontremoli S, Melloni E. Functional role of HSP90 complexes with endothelial nitric-oxide synthase (eNOS) and calpain on nitric oxide generation in endothelial cells. *J Biol Chem* 283: 29069-29076, 2008.

Azadzoi KM, Tarcan T, Kozlowski R, Krane RJ, Siroky MB. Overactivity and structural changes in the chronically ischemic bladder. *J Urol* 162: 1768-1778, 1999.

Bagot K, Chess-Williams R. Alpha 1A/L-adrenoceptors mediate contraction of the circular smooth muscle of the pig urethra. *Auton Autacoid Pharmacol* 26: 345-353, 2006.

Baltrons MA, García A. Nitric oxide-independent down-regulation of soluble guanylyl cyclase by bacterial endotoxin in astroglial cells. *J Neurochem* 73:2149-2157, 1999.

Batista CK, Brito GA, Souza ML, Leitao BT, Cunha FQ, Ribeiro RA. A model of hemorrhagic cystitis induced with acrolein in mice. *Braz J Med Biol Res* 39(11): 1475-1481, 2006.

Bauer AJ, Publicover NG, Sanders KM. Origin and spread of slow waves in canine gastric antral circular muscle. *Am J Physiol* 249: 800-806, 1985.

Beckett EA, Horiguchi K, Khoyi M, Sanders KM, Ward SM. Loss of enteric motor neurotransmission in the gastric fundus of Sl/Sl^{d} mice. *J. Physiol* 543: 871-887, 2002.

Beckett EA, Ro S, Bayguinov Y, Sanders KM, Ward SM. Kit signaling is essential for development and maintenance of interstitial cells of Cajal and electrical rhythmicity in the embryonic gastrointestinal tract. *Dev Dyn* 236: 60-72, 2007.

Bedner P, Niessen H, Odermatt B, Kretz M, Willecke K, Harz H. Selective permeability of different connexion channels to the second messenger cyclic AMP. *J Biol Chem* 281: 6673-6681, 2006.

Belzer V, Kobilo T, Rich A, Hanani M. Intercellular coupling among interstitial cells of Cajal in the guinea pig small intestine. *Cell Tissue Res* 307:15-21, 2002.

Belzer V, Nissan A, Freund HR, Hanani M. Coupling among interstitial cells of Cajal in the human ileum. *Neurogastroenterol Motil* 16: 75-80, 2004.

Bender AT, Beavo JA. Cyclic nucleotide phosphodiesterases: molecular regulation to clinical use. *Pharmacol Rev* 58: 488-520, 2006.

Bennett BC, Kruse MN, Roppolo JR, Flood HD, Fraser, de Groat WC. Neuronal control of urethral outlet activity in vivo: role of nitric oxide. *J. Urol* 153: 2004-2009, 1995.

Biers SM, Reynard JM, Doore T, Brading AF. The functional effects of a c-kit tyrosine inhibitor on guinea-pig and human detrusor. *BJU Int* 97(3): 612-616, 2006.

Billiard TR, Curran RD, Stuerh DJ, Stadler J, Simmons RL, Murray SA. Inducible cytosolic enzyme activity for the production of nitrogen oxides from L-arginine in hepatocytes. *Biochem Biophys Res Commun* 168: 1034-1040, 1990.

Birder LA. Urinary bladder urothelium: Molecular sensors of chemical/thermal/mechanical stimuli. *Vascul Pharmacol* 45:221-226, 2006.

Bon K, Lanteri-Minet M, Michiels JF, Menetrey D. Cyclophosphamide cystitis as a model of visceral pain in rats: a c-fos and Krox-24 study at telencephalic levels, with a note on pituitary adenylate cyclase activating polypeptide (PACAP). *Exp Brain Res* 122: 165-174, 1998.

Bonner JC. Regulation of PDGF and its receptors in fibrotic diseases. *Cytokine Growth Factor Rev* 15: 255-273, 2004.

Boucher M, Meen M, Codron JP, Coudore F, Kemeny JL, Eschailer A. Cyclophosphamide-induced cystitis in freely-moving conscious rats: behavioural approach to a new model of visceral pain. *J Urol* 164(1): 203-208, 2000.

Brading AF, McCloskey KD. Mechanisms of disease: specialized interstitial cells of the urinary tract- an assessment of current knowledge. *Nat Clin Pract Urol* 2: 546-554, 2005.

Brading AF, McCoy R, Dass N. α1-Adrenoreceptors in urethral function. *Eur Urol* 36(1): 74-79, 1999.

Brading AF. The physiology of the mammalian urinary outflow tract. *Exp. Physiol* 84: 215-221, 1999.

Bradley E, Andersson AU, Woolsey SM, Thornbury KD, McHale NG, Hollywood MA. Characterization of T-type calcium current and its contribution to electrical activity in rabbit urethra. *Am J Physiol Cell Physiol* 286: 1078-1088, 2004.

Bradley E, Hollywood MA, Johnston L, Large RJ, Matsuda T, Baba A, McHale NG, Thornbury KD, Sergeant GP. Contribution of reverse Na^{+}-Ca^{2+} exchange to spontaneous activity in interstitial cells of Cajal in the rabbit urethra. *J. Physiol* 574(3):651-661, 2006.

Bradley E, Hollywood MA, McHale NG, Thornbury KD, Sergeant GP. Pacemaker activity in urethral interstitial cells is not dependent on capacitative calcium entry. *Am J Physiol Cell Physiol* 289:625-632, 2005.

Bradley E, Kadima S, Drumm B, Hollywood MA, Thornbury KD, McHale NG, Sergeant GP. Novel excitatory effects of adenosine triphosphate on contractile and pacemaker activity in rabbit urethral smooth muscle. *J Urol* 183: 801-811, 2010.

Bradley J, Frings S, Yau KW, Reed R. Nomenclature for ion channels subunits. *Science* 294: 2095-2096, 2001.

Bredt DS. Endogenous nitric oxide synthesis:biological functions and pathophysiology. *Free Radic Res* 31:577-596, 1999.

Bredt DS, Snyder SH. Isolation of nitric oxide synthetase, a calmodulin-requiring enzyme. *Proc Natl Acad Sci USA* 87: 682-685, 1990.

Brock N, Pohl J, Stekar J. Studies on the urotoxicity of oxazaphosphorine cytostatics and its prevention. I. Experimental studies on the urotoxicity of alkylating compounds. *Eur J Cancer* 17(6): 595-607, 1981.

Broillet MC. A single intracellular cysteine residue is responsible for the activation of the olfactory cyclic nucleotide-gated channels by NO. *J Biol Chem* 275: 15135-15141, 2000.

Broillet MC, Firestein S. Beta subunits of the olfactory cyclic nucleotide-gated channel from a nitric oxide activated Ca^{2+} channel. *Neuron* 18: 951-958, 2000.

Bryan NS, Bian K, and Murad F. Discovery of the nitric oxide signaling pathway and targets for drug development. *Front Biosci* 14: 1–18, 2009.

Burke JP, Mulsow JJ, O´Keane C, Docherty NG, Watson RW, O´Connel PR. Fibrogenesis in Crohn´s disease. *Am J Gastroenterol* 102: 439-448, 2007.

Burnett AL, Calvin DC, Chamness SL, Liu JX, Nelson RJ, Klein SL, Dawson VL, Dawson TM, Snyder SH. Urinary bladder-urethral sphincter dysfunction in mice with targeted disruption of neuronal nitric oxide synthase models idiopathic voiding disorders in humans. *Nat Med* 3: 571-574, 1997.

Burns AJ, Lomax AE, Torihashi S, Sanders KM, Ward SM. Interstitial cells of Cajal mediates inhibitory neurotransmission in the stomach. *Proc. Natl. Acad. Sci. USA* 93:12008-12013, 1996.

Burns ME, Baylor DA. Activation, deactivation, and adaptation in vertebrate photoreceptor cells. *Annu. Rev. Neurosci.* 24:779–805, 2001.

Burnstock G, Lavin S. Interstitial cells of Cajal and purinergic signalling. *Auton Neurosci* 97: 68-72, 2002.

Cajal SR. Histologie du système nerveux de l´homme et des vertébrés. Paris: Maloine, 891-942, 1911.

Cajal SR. Los ganglios y plexus nerviosos del intestine de los mamíferos. Imprenta y Librería de Nicolás Moya. Madrid. 1893.

Caputo A, Caci E, Ferrera L, Pedemonte N, Barsanti C, Sondo E, Pfeffer U, Ravazzolo R, Zegarra-Moran O, Galietta JV. TMEM16A, a membrane protein associated with calcium-dependent chloride channel activity. *Science* 322: 590–594, 2008.

Cayabyab FS, deBruin H, Jimenez M, Daniel EE. Ca^{2+} role in myogenic and neurogenic activities of canine ileum circular muscle. *Am J Physiol* 271: 1053-1066, 1996.

Chan F, Liu Y, Sun H, Li X, Shang H, Fan D, An J, Zhou D. Distribution and possible role of PDGF-AA and PDGFR-α in the gastrointestinal tract of adult guinea pigs. *Virchows Arch* 457: 381-388, 2010.

Charles IG, Palmer RM, Hickery MS, Bayliss MT, Chubb AP, Hall VS, Moss DW, Moncada S. Cloning, characterization, and expression of a cDNA encoding an inducible nitric oxide synthase from the human chondrocyte. *Proc Natl Acad Sci U S A*. 90(23): 11419-11423, 1993.

Chen H, Redelman D, Ro S, Ward SM, Ordog T, Sanders KM. Selective labeling and isolation of functional classes of interstitial cells of Cajal of human and murine small intestine. *Am J Physiol Cell Physiology* 292: 497-507, 2007.

Chipperfield AR, Harper AA. Chloride in smooth muscle. *Prog Biophys Mol Biol* 74: 175-221, 2000.

Cho HJ, Xie QW, Calaycay J, Mumford RA, Swiderek KM, Lee TD, Nathan C. Calmodulin is a subunit of nitric oxide synthase from macrophages. *J Exp Med* 176: 599-604, 1992.

Cho KH, Hyun JH, Chang YS, Na YG, Shin JH, Song KH. Expression of nitric oxide synthase and aquaporine-3 in cyclophosphamide treated rat bladder. *Int Neurourol J* 24: 149-156, 2010.

Christ GJ, Day NS, Day M, Zhao W, Persson K, Pandita RJ, Andersson KE. Increased connexin43-mediated intercellular communication in a rat model of bladder overactivity in vivo. *Am J Physiol Regul Integr Comp Physiol* 284: 1241-1248, 2003.

Chuang YC, Yoshimura N, Huang CC, Wu M, Chiang PH, Chancellor MB. Intravesical botulism toxin A administration inhibits COX-2 and EP4 expression and suppresses bladder hyperactivity in cyclophosphamide-induced cystitis in rats. *Eur Urol* 56: 159-167, 2009.

Cobine CA, Henning GW, Bayguinov YR, Halton WJ, Ward SM, Keef KD. Interstitial cells of Cajal in the cynomolgus monkey rectoanal region and their relationship to sympathetic and nitrergic nerves. *Am J Physiol Gastrointest Liver Physiol* 298: 643-656, 2010.

Cobine CA, Henning GW, Kurahashi M, Sanders KM, Ward SM, Keef KD. Relationship between interstitial cells of Cajal, fibroblast-ike cells and inhibitory motor nerves in the internal anal sphincter. *Cell Tissue Res* 344: 17-30, 2011.

Coggins PR, Ravdin RG, Eisman SH. Clinical evaluation of a new alkylating agent: cytoxan (cyclophosphamide). *Cancer* 13: 1254-1260, 1960.

Collins C, Klausner AP, Herrick B, Koo HP, Miner AS, Henderson SC, Ratz PH. Potential for control of detrusor smooth muscle spontaneous rhythmic contraction by cyclooxygenase products released by interstitial cells of Cajal. *J Cell Mol Med* 13(9B): 3236-3250, 2009.

Corbett JA, Tilton RG, Chang K, Hasan KS, Ido Y, Wang JL, Sweetland MA, Lancaster JR Jr, Williamson JR, McDaniel ML. Aminoguanidine, a novel inhibitor of nitric oxide formation, prevents diabetic vascular dysfunction. *Diabetes* 41 :552-6, 1992.

Cox PJ. Cyclophosphamide cystitis—identification of acrolein as the causative agent. *Biochem Pharmacol* 28(13): 2045-2049, 1979.

Craven KB and Zagotta WN. CNG and HCN channels: Two peas, one pod. *Annu. Rev. Physiol* 68:375-401, 2006.

Cunningham RMJ, Larkin P, McCloskey KD. Ultraestructural properties of interstitial cells of Cajal in the guinea pig bladder. *J Urol* 185(3): 1123-1131, 2011.

Daniel EE, Boddy G, Bong A, Cho W. A new model of pacing in the mouse intestine. *Am J Physiol Gastrointest Liver Physiol* 286: 253-262, 2004.

Daniel EE. Communication between interstitial cells of Cajal and gastrointestinal muscle. *Neurogastrointerol Motil* 16 (1): 118-122, 2004.

Daniel EE, Wang YF, Cayabyab F. Role of Gap junctions in structural arrangements of interstitial cells of Cajal and canine ileal smooth muscle. *Am J Physiol Gastrointestinal Liver Physiol* 274:1125-1141, 1998.

Daniel EE, Yazbi AE, Mannarino M, Galante G, Boddy G, Livergant J, Oskouei TE. Do gap junctions play a role in nerve transmissions as well as pacing in mouse intestine? *Am J Physiol Gastrointest Liver Physiol* 292: 734-745, 2007.

Dass N, McMurray G, Greeland JE, Brading AF. Morphological aspects of the female pig bladder neck and urethra of guinea pig, quantitative analysis using computer assisted 3-dimensional reconstruction. *Journal of Urology* 165: 1294-1299, 2001.

Davidson JS, Baumgarten IM. Glycyrrhetinic acid derivatives: a novel class of inhibitors of gap-junctional intercellular communication. Structure-activity relationships. *J Pharmacol Exp Ther* 246: 1104-1107, 1988.

Davidson RA, McCloskey KD. Morphology and localization of interstitial cells in the guinea-pig bladder: structural relationships with smooth muscle and neurons. *J Urol* 173: 1385-1390, 2005.

Debiec-Rychter M, Cools J, Dumez H, Sciot R, Stul M, Mentens N, Vranckx H, Wasag B, Prenen H, Roesel J, Hagemeijer A, van O.A, Marynen P. Mechanisms of resistance to imatinib mesylate in gastrointestinal stromal tumors and activity of the PKC412 inhibitor against imatinib-resistant mutants. *Gastroenterology* 128, 270–279, 2005.

De Jongh R, van Koeveringe GA, van Kerrebroeck PEV, Markerink-van Ittersum M, de Vente J, Gillespie JI. Alterations to network of NO/cGMP-responsive interstitial cells induced by outlet obstruction in guinea-pig bladder. *Cell Tissue Res* 330: 147-160, 2007.

Demetri, GD, van Oosterom AT, Garrett CR, Blackstein ME, Shah MH, Verweij J, McArthur G, Judson IR, Heinrich MC, Morgan JA, Desai J, Fletcher CD, George S, Bello C, Huang X, Baum CM, Casali PG. Efficacy and safety of sunitinib in patients with advanced gastrointestinal stromal tumour after failure of imatinib: a randomised controlled trial. *Lancet* 368, 1329–1338, 2006.

Denninger JW, Marletta MA. Guanylate cyclase and the NO/cGMP signaling pathway. *Biochim Biophys Acta* 1414 (2-3): 334-350, 1999.

Desplantez T, Verma V, Leybaert L, Evans WH, Weingart R. Gap26, a connexion mimetic peptide, inhibits currents carried by connexin43 hemichannels and gap junction channels. *Pharmacol Res* 65: 546-552, 2012.

De Vente J, Markerink-van Ittersum M, Gillespie JI. Natriuretic peptide responsive, cyclic guanosine monophosphate producing structures in the guinea pig bladder. *J Urol* 177: 1191-1194, 2007.

Dickens EJ, Hirst GSD, Tomita T. Identification of rhythmically active cells in guinea-pig stomach. *J. Physiol* 514:515-531, 1999.

Digesu GA, Khullar V, Cardozo L, Salvatore S. Overactive bladder symptoms: do we need urodynamics? *Neurourol Urodyn* 22(2): 105-108, 2003.

Dinerman JL, Dawson TM, Schell MJ, Snowman A, Snyder SH. Endothelial nitric oxide synthase localized to hippocampal pyramidal cells: Implications for synaptic plasticity. *Proc Natl Acad Sci USA* 91: 4214-4218, 1994.

Dokita S, Morgan WR, Wheeler MA, Yoshida M, Latif-Pour J, Weiss R. N^G-nitro-L- arginine inhibits non-adrenergic, non-cholinergic relaxation in rabbit urethral muscle. *Life Science* 48:2429-2436, 1991.

Dokita S, Smith SD, Nishimoto T, Wheeler MA, Weiss RM. Involvement of nitric oxide and cyclic GMP in rabbit urethral relaxation. *Eur J Pharmacol* 266:269-275, 1994.

Döring B, Pfitzer G, Adam B, Liebregts T, Eckardt D, Holtmann G, Hofmann F, Feil S, Feil R, Willecke K. Ablation of connexin43 in smooth muscle cells of the mouse intestine: functional insights into physiology and morphology. *Cell Tissue Res* 327: 333-342, 2007.

Druker BJ, Tamura S, Buchdunger E, Ohno S, Segal GM, Fanning S, Zimmermann J, Lydon NB. Effects of a selective inhibitor of the Abl tyrosine kinase on the growth of Bcr-Abl positive cells. *Nat Med* 2: 561-566, 1996.

Du CA, Conklin JL. Origin of slow waves in the isolated proximal colon of the cat. *J Auton Nerv Syst* 28:167-177, 1989.

Dun NJ, Dun SL, Wu SY, Forstermann U. Nitric oxide synthase immunoreactivity in rat superior cervical ganglia and adrenal glands. *Neurosci Lett* 158: 51-54, 1993.

Dun NL, Dun SL, Forstermann U, Tseng LF. Nitric oxide synthase immunoreactivity in rat spinal cord. *Neurosci Lett* 147: 217-220, 1992.

Duquette RA, Shymygol A, Vaillant C, Mobasheri A, Pope M, Burdyga T, Wray S. Vimentin-positive, c-KIT-Negative Interstitial Cells in Human and Rat Uterus: A Role in Pacemaking? *Biol Reprod* 72: 276-283, 2005.

Earley S, Resta TC, Walker BR. Disruption of smooth muscle gap junctions attenuates myogenic vasoconstriction of mesenteric resistance arteries. *Am J Physiol Heart Circ Physiol* 287: 2677-2686, 2004.

Edvarsen, P. Nervous control of urinary bladder in cats. IV. Effects of autonomic blocking agents on responses to peripheral nerve stimulation. *Acta Physiol Scand* 72: 234-247, 1968.

Elbadawi A, Schenk, EA. Dual innervation of the mammalian urinary bladder. A histochemical study of the distribution of cholinergic and adrenergic nerves. *Am J Anat* 119: 405-428, 1966.

Elfgang C, Eckert R, Lichtenberg-Fraté H, Butterweck A, Traub O, Klein RA, Hülser DF, Willecke K. Specific permeability and selective formation of gap junction channels in connexin-transfected HeLa cells. *J Cell Biol* 129: 805-817, 1995.

Epperson A, Hatton WJ, Callaghan B, Doherty P, Walker RL, Sanders KM, Ward SM, Horowitz B. Molecular markers expressed in cultured and freshly isolated interstitial cells of Cajal. *Am J Physiol* 279:529-539, 2000.

Evans WH, Boitano S. Connexin mimetic peptides: specific inhibitors of gap-junctional intercellular communication. *Biochem Soc Trans* 29: 606-612, 2001.

Exintaris B, Klemm MF, Lang R. Spontaneous slow wave and contractile activity of the guinea pig prostate. *J. Urol*. 168:315-322, 2002.

Faussone-Pellegrini MS, Cortesini C, Romagnoli P. Ultrastructure of the túnica muscularis of the cardial portion of the human esophagus and stomach, with special reference to the so-called Cajal´s interstitial cells. *Arch Ital Anat Embriol* 82: 157-177, 1977.

Faussone-Pellegrini MS. Histogenesis, structure, and relationships of interstitial cells of Cajal (ICC): form morphology to functional interpretation. *Eur J Morphol* 30: 137-148, 1992.

Faussone-Pellegrini MS, Pantalone D, Cortesini C. An ultrastructural study of the interstitial cells of Cajal of the human stomach. *J Submicrosc Cytol Pathol* 21: 439-460, 1989.

Faussone-Pellegrini MS, Thuneberg L. Guide to the identification of interstitial cells of Cajal. *Microsc Res Tech* 47:248-266, 1999.

Ferguson DR. Urothelial function. *BJU International*. 84: 235-242, 1999.

Fesenko EE, Kolesnikov SS, Lyubarsky AL. Induction by cyclic GMP of cationic conductance in plasma membrane of retinal rod outer segment. *Nature* 313:310–13, 1985.

Finn JT, Grunwald ME, Yau KW. Cyclic nucleotide-gated channels: an extended family with diverse functions. *Annu Rev Physiol* 58: 395-426, 1996.

Fleming I, Busse R. NO: the primary EDRF. *J Mol Cell Cardiol* 31:5-14, 1999.

Forrest AS, Ordog T, Sanders KM. Neural regulation of slow-wave frequency in the murine gastric antrum. *Am J Physiol Gastrointest Liver Physiol* 290:486-495, 2006.

Förstermann U, Pollock JS, Schmidt HH, Heller M, Murad F. Calmodulin-dependent endothelium-derived relaxing factor/nitric oxide synthase activity is present in the particulate and cytosolic fractions of bovine aortic endothelial cells. *Proc Natl Acad Sci USA* 88(5):1788-92, 1991.

Fowler CJ, Griffiths D, de Groat WC. The neural control of micturition. *Nat Rev Neurosci* 9:453-466, 2008.

Fox EA, Phillips RJ, Martinson FA, Baronowsky EA, Powley TL. Vagal afferent innervations of smooth muscle in the stomach and duodenum of the mouse: morphology and topography. *J Comp Neurol* 428: 558-576, 2000.

Francis SH, Noblett BD, Todd BW, Wells JN, Corbin JD. Relaxation of vascular and tracheal smooth muscle by cyclic nucleotide analogs that preferentially activate purified cGMP-dependent protein kinase. *Mol Pharmacol* 34: 506-517, 1988.

Frenier SL, Knowlen GG, Speth RC, Moore MP. Urethral pressure response to α-adrenergic agonist and antagonist drugs in anesthezised healthy male cats.*Am J Vet Res* 53:1161-1165, 1992.

Friebe A, Koesling D. Mechanism of YC-1-induced activation of soluble guanylyl cyclase. *Mol Pharmacol* 53: 123-127, 1998.

Friebe A, Schultz G, Koesling D. Sensitizing soluble guanylyl cyclase to become a highly CO-sensitive enzyme. *EMBO J* 15(24):6863-6868, 1996.

Fry CH, Sui GP, Kanai AJ, Wu C. The function of suburothelial myofibroblasts in the bladder. *Neurourol Urodyn* 26 :914-9, 2007.

Fujiwara M, Andersson KE, Persson K. Nitric-oxide-induced cGMP accumulation in the mouse bladder is not related to smooth muscle relaxation. *Eur J Pharmacol* 401:241-250, 2000.

García-Pascual A, Costa G, García-Sacristán A, Andersson KE. Calcium dependence of contractile activation of isolated sheep urethra. I. Responses to electrical stimulation. *Pharmacol Toxicol* 69: 263-269, 1991d.

García-Pascual A, Costa G, García-Sacristán A, Andersson KE. Relaxation of sheep urethral muscle induced by electrical stimulation of nerves: involvement of nitric oxide. *Acta Physiol Scand* 141:531-539, 1991c.

García-Pascual A, Costa G, Isla M, García-Sacristán A. Characterization of α-adrenoreceptors in the preprostatic uretra of sexually immature male lambs. *Eur J Pharmacol* 203**:**259-265, 1991a.

García-Pascual A, Costa G, Isla M, Jimenez E, García-Sacristán A. Potassium-induced contraction in the lamb proximal urethra: Involvement of norepinephrine and different calcium entry pathways. *J Pharmacol Exp Ther* 256: 127-134, 1991b.

García-Pascual A, Costa G, Labadía A, Jiménez E, Triguero D. Differential mechanisms of urethral smooth muscle relaxation by several NO donors and nitric oxide. *Naunyn Schmiedebergs Arch Pharmacol* 360(1):80-91, 1999.

García-Pascual A, Costa G, Labadía A, Jiménez E, Triguero D, Rodríguez- Veiga E, González-Soriano J. Partial nicotinic receptor blockade unmasks a modulatory role of nitric oxide on urethral striated neuromuscular transmission.*Nitric Oxide* 13: 98-110, 2005.

García-Pascual A, Costa G, Labadía A, Persson K, Triguero D. Characterization of nitric oxide synthase activity in sheep urinary tract: functional implications. *Br J Pharmacol* 118: 905-914, 1996.

García-Pascual A, Labadía A, Costa G, Triguero D. Effects of superoxide anion generators and thiol modulators on nitrergic transmission and relaxation to exogenous nitric oxide in the sheep urethra. *Br J Pharmacol* 129: 53-62, 2000.

García-Pascual A, Triguero D. Relaxation mechanism induced by stimulation of nerves and by nitric oxide in sheep urethral muscle. *J. Physiol* 476: 333-347, 1994.

Gartner LP, Hiatt JL. Sistema urinario. En: Texto-Atlas de Histología. 2ª Edición. Mc Graw-Hill Interamericana S.A. México DF. Pág 415-438, 2002.

Garvey EP, Oplinger JA, Furfine ES, Kiff RJ, Laszlo F, Whittle BJ, Knowles RG. 1400W is a slow, tight binding, and highly selective inhibitor of inducible nitric-oxide synthase in vitro and in vivo. *J Biol Chem* 272:4959–4963, 1997.

Ghosh, DK, Stuehr, DJ. Macrophage NO synthase: characterization of isolated oxygenase and reductase domains reveals a head-to-head subunit interaction. *Biochemistry* 34:801-807, 1995.

Giglio D, Ryberg AT, To K, Delbro DS, Tobin G. Altered muscarinic receptor subtype expression and fuctional responses in cyclophosphamide induced cystitis in rats. *Auton Neurosci: Basic & Clinical* 122: 9-20, 2005.

Gillespie JL, Drake MJ. The actions of sodium nitroprusside and the phosphodiesterase inhibitor dipyridamole on phasic activity in the isolated guinea-pig bladder. *BJU International* 93:851-858, 2004.

Gillespie JI, Markerink- van Ittersum M, de Vente J. cGMP generating cells in the bladder wall: identification of distinct networks of interstitial cells. *BJU International* 94:1114-1124, 2004.

Gillespie JI, Markerink- van Ittersum M, de Vente J. Expression of neural nitric oxide synthase (nNOS) and nitric-oxide-induced changes in cGMP in the urothelial layer of the guinea pig bladder. *Cell Tissue Res* 321: 341-351, 2005.

Gomes TN, Santos CC, Souza-Filho MV, Cunha FQ, Ribeiro RA. Participation of TNF-alpha and IL-1 in the pathogenesis of ciclophosphamide-induced hemorrhagic cystitis. *Braz J Med Biol Res* 28(10): 1103-1108, 1995.

Gomez-Pinilla PJ, Gibbons SJ, Bardsley MR, Lorincz A, Pozo MJ, Pasricha PJ, Van de Rijn M, West RB, Sarr MG, Kendrick ML, Cima RR, Dozois EJ, Larson DW, Ordog T, Farrugia G. Ano1 is a selective marker of interstitial cells of Cajal in the human and mouse gastrointestinal tract. *Am J Physiol Gastrointest Liver Physiol* 296: 1370–1381, 2009.

González-Soriano J, Martín- Palacios S, Rodriguez-Veiga E, Triguero D, Costa G, García-Pascual A. Nitric oxide synthase in the external urethral sphincter of the sheep: immunohistochemical and functional study. *J Urol* 169: 1901-1906, 2003.

Goodman VL, Rock EP, Dagher R, Ramchandani RP, Abraham S, Gobburu JV, Booth BP, Verbois SL, Morse DE, Liang CY, Chidambaram N, Jiang JX, Tang, S, Mahjoob K, Justice R, Pazdur R. Approval summary: sunitinib for the treatment of imatinib refractory or intolerant gastrointestinal stromal tumors and advanced renal cell carcinoma. *Clin Cancer Res* 13, 1367–1373, 2007.

Gordge MP. How cytotoxic is nitric oxide. *Exp Nephrol* 6:12-16, 1998.

Goyal RK, Chaudhury A. Mounting evidence aganist the role of ICC in neurotransmission to smooth muscle in the gut. *Am J Physiol Gastrointest Liver Physiol* 298: 10-13, 2010.

Grol S, van Koeveringe GA, de Vente J, van Kerrebroeck PE, Gillespie JI. Regional differences in sensory innervation and suburothelial interstitial cells in the bladder neck and urethra. *BJU Int* 102(7): 870-7, 2008.

Gross SS, Wolin MS. Nitric oxide: Pathophysiological mechanisms. *Annu Rev. Physiol* 57: 737-769, 1995.

Growney JD, Clark JJ, Adelsperger J, Stone R, Fabbro D, Griffin JD, Gilliland DG. Activation mutations of human c-KIT resistant to imatinib mesylate are sensitive to the tyrosine kinase inhibitor PKC412. *Blood* 106, 721–724, 2005.

Grozdanovic Z, Christova, Gossrau R. Differences in the localization of the postsynaptic oxide synthase I and acetylcholinesterase suggest a heterogeneity of neuromuscular junctions in rat and mouse skeletal muscles. *Acta histochem* 99:47-53, 1997.

Gupta K, Hooton TM, Naber KG, Wullt B, Colgan R, Miller LG, Moran GJ, Nicolle LE, Raz R, Schaeffer AJ, Soper DE. International clinical practice guidelines for the treatment of acute uncomplicated cystitis and pyelonephritis in women: A 2010 update by the Infectious Diseases Society of America and the European Society for Microbiology and Infectious Diseases. *Clin Infect Dis* 52: 103-120, 2011.

Haefliger JA, Tissières P, Tawadros T, Formenton A, Bény JL, Nicod P, Frey P, Meda P. Connexin 43 and 26 are differentially increased after rat bladder obstruction. *Exp Cell Res* 274: 216-225, 2002.

Hamberger B, Norberg KA. Adrenergic synaptic terminals and nerve cells in bladder ganglia of the cat. *Inter J Neuropharmacol* 4:41-45, 1965.

Hanani M, Farrugia G, Komuro, T. Intercellular coupling of interstitial cells of Cajal in the digestive tract. *Int. Rev. Cytol.* 242, 249–282, 2005.

Handa O, Stephen J, Cepinskas G. Role of endothelial nitric oxide synthase-derived nitric oxide in activation and dysfunction of cerebrovascular endothelial cells during early onsets of sepsis. *Am J Physiol Heart Circ Physiol* 295: 1712-1719, 2008.

Hanno PM, Chapple CR, Cardozo LD. Bladder pain syndrome/interstitial cystitis: a sense of urgency. *World J Urol* 27(6): 717-721, 2009.

Harhun MI, Gordienko DV, Povstyan OV, Moss RF, Bolton TB. Function of Interstitial Cells of Cajal in the Rabbit Portal Vein. *Circ. Res*. 95:619-626, 2004.

Harhun MI, Pucovsky V, Povstyan OV, Gordienko DV, Bolton TB. Interstitial cells in the vasculature. *J Cell Mol Med* 9:232-243, 2005.

Harris AL. Connexin channel permeability to cytoplasmic molecules. *Prog Biophys Mol Biol* 94: 120-143, 2007.

Hashitani H, Edwards FR. Spontaneous and neurally activated depolarisations in smooth muscle cells of the guinea-pig urethra. *J Physiol* 514:459-470, 1999.

Hashitani H, Fukuta H, Takano H, Klemm M, Suzuki H. Origin and propagation of spontaneous excitation in smooth muscle of the guinea-pig urinary bladder. *J Physiol* 530: 273-286, 2001.

Hashitani H, García-Londoño AP, Hirst GS, Edwards FR. Atypical slow waves generated in gastric corpus provide dominant pacemaker activity in guinea pig stomach. *J Physiol* 569:459-465, 2005.

Hashitani H. Interaction between interstitial cells and smooth muscles in the lower urinary tract and penis. *J Physiol* 576: 707-714, 2006.

Hashitani H, Lang R, Suzuki H. Role of perinuclear mitochondria in the spatiotemporal dynamics of spontaneous Ca^{2+} waves in interstitial cells of Cajal-like cells of the rabbit urethra. *Br J Pharmacol* 161: 680-694, 2010.

Hashitani H, Suzuki H. Identification of interstitial cells of Cajal in corporal tissues of the guinea-pig penis. *Br J Pharmacol* 141: 199-204, 2004.

Hashitani H, Suzuki H. Properties of spontaneous Ca^{2+} transients recorded from interstitial cells of Cajal-like cells of the rabbit urethra in situ. *J Physiol* 583: 505-519, 2007.

Hashitani H, Van Helden DF, Suzuki H. Properties of spontaneous depolarisations in circular smooth muscle cells of rabbit urethra. *Br J Pharmacol* 118:1627-1632, 1996.

Hashitani H, Yanai Y, Kohri K, Suzuki H. Heterogeneous CPA sensitivity of spontaneous excitation in smooth muscle of the rabbit urethra. *Br J Pharmacol* 148: 340-349, 2006.

Hashitani H, Yanai Y, Suzuki H. Role of interstitial cells and gap junctions in the transmission of spontaneous Ca^{2+} signals in detrusor smooth muscles of the guinea-pig urinary bladder. *J Physiol* 559:567-581, 2004.

Hassouna M, Abel-Rahman M, Galeano C, Elhilali MM. Responses of the urethral smooth muscles to pharmacological agents I. Cholinergics and adrenergics agonist and antagonist. *J Urol* 129:1262-1264, 1983.

Henning GW, Hirst GDS, Park KJ, Smith CB, Sanders KM, Ward SM, Smith TK. Propagation of pacemaker activity in the guinea-pig antrum. *J Physiol* 556:585-599, 2004.

Herve JC, Dhein S. Peptides targeting gap junctional structures. *Curr Pharm Des* 16: 3056-3070, 2010.

Hevel JM, White KA, Marletta MA. Purification of the inducible murine macrophage nitric oxide synthase. Identification as a flavoprotein. *J Biol Chem* 266:22789-22791, 1991.

Hibbs JB, Taintor RR, Vavrin Z, Rachlin EM. Nitric oxide: a citotoxic activated macrophage effector molecule. *Biochem Biophys Res Commun* 157:87-94, 1988.

Hirota S, Isozaki K, Moriyama Y, Hashimoto K, Nishida T, Ishiguro S, Kawano K, Hanada M, Kurata A, Takeda M, Muhammad Tunio G, Matsuzawa Y, Kanakura Y, Shinomura Y, Kitamura Y. Gain-of-function mutations of c-kit in human gastrointestinal stromal tumors. *Science* 279(5350): 577-580, 1998.

Hirst GD. An additional role for ICC in the control of gastrointestinal motility? *J Physiol* 537: 1, 2001.

Hirst GD, Bramich NJ, Teramoto N, Suzuki H, Edwards FR. Regenerative component of slow waves in the guinea-pig gastric antrum involves a delayed increase in ‹Ca^{2+}›i and Cl^- channels. *J Physiol. London* 540:907-919, 2002.

Hirst GD, Ward SM. Interstitial cells: involvement in rhythmicity and neural control of gut smooth muscle. *J Physiol* 550: 337.346, 2003.

Hoffmann EK, Simonsen LO. Membrane mechanisms in volume and pH regulation in vertebrate cells. *Physiol Rev* 69: 315-382, 1989.

Hofmann F, Biel M and Kaupp UB. International Union of Pharmacology. LI. Nomenclature and structure-function relationships of cyclic nucleotide-regulated channels. *Pharmacol. Rev*. 57 (4): 455-462, 2005.

Ho KM, Ny L, McMurray G, Andersson KE, Brading AF, Noble JG. Co-localization of carbón monoxide and nitric oxide synthesizing enzymes in the human urethral sphincter. *J Urol* 161 (6): 1968-1972, 1999.

Hollywood MA, Sergeant GP, McHale NG, Thornbury KD. Activation of Ca^{2+}-activated Cl^- current by depolarizing steps in rabbit urethral interstitial cells. *Am J Physiol Cell Physiol* 285:327-333, 2003.

Holmquist B, Olsson CF, Svensson ML, Svanborg C, Forsell J, Alm P. Expression of nitric oxide synthase isoforms in the mouse kidney: cellular localization and influence by lipopolysaccharide and toll-like receptor 4. *J Mol Hist* 36: 499-516, 2005.

Homma Y. Lower urinary tract symptomatology: its definition and confusion. *Int J Urol* 15: 35-43, 2008.

Horiguchi K, Komuro T. Ultrastructural observations of fibroblast-like cells forming gap junctions in the W/W^V mouse small intestine. *J Auton Nerv Syst* 80: 142-147, 2000.

Horiguchi K, Semple GS, Sanders KM, Ward SM. Distribution of pacemaker function through the tunica muscularis of the canine gastric antrum. *J Physiol* 537: 237-250, 2001.

Horowitz B, Ward SM, Sanders KM. Cellular and molecular basis for electrical rhythmicity in gastrointestinal muscles. *Annu Rev Physiol* 61:19-43, 1999.

Hossein A, Ghofrani HA, Osterloh IH, Grimminger F. Sildenafil: from angina to erectile dysfunction to pulmonary hypertension and beyond. *Nature Reviews Drug Discovery* 5: 689-702, 2006.

Huang F, Rock JR, Harfe BD, Cheng T, Huang X, Jan YN, Jan LY. Studies on expression of the TMEM16A calcium-activated chloride channel. *Proc Natl Acad Sci USA* 106: 21413–21418, 2009.

Huizinga JD. Physiology and pathophysiology of the interstitial cell of Cajal: from bench to bedside II. Gastric motility: lessons from mutant mice on slow waves and innervation. *Am. J. Physiol*. 281:1129-1134, 2001.

Huizinga JD, Reed DE, Berezin I, Wang XY, Valdez DT, Liu LW, Diamant NE. Survival dependency of intramuscular ICC on vagal afferent nerves in the cat esophagus. *Am J Physiol regul Integr Comp Physiol* 294: 302-310, 2008.

Huizinga JD, Thuneberg L, Klüppel M, Malysz J, Mikkelsen HB, Bernstein A. W/kit gene required for intestinal pacemaker activity. *Nature* 373: 347-349, 1995.

Huizinga JD, Zhu Y, Ye J, Molleman A. High-conductance chloride channels generate pacemaker currents in interstitial cells of Cajal. *Gastroenterol* 123:1627-1636, 2002.

Hutchings S, Gevaert T, Deprest J, Roskams T, Van Lommel A, Nilius B, De Ridder D. Immunochemistry using an antibody to unphosphorilated connexion 43 to identify human myometrial interstitial cells. *Reprod Biol Endocrinol* 6:43, 2008.

Hwang SJ, Blair PJ, Britton FC, O´Driscoll KE, Henning GW, Bayguinov YR, Rock JR, Harfe BD, Sanders KM, Ward SM. Expression of anoctamin1/TMEM16A by interstitial cells of Cajal is fundamental for slow wave activity in gastrointestinal muscles. *J Physiol* 587: 4887-4904, 2009.

Iino S, Horiguchi K, Horiguchi S, Nojyo Y. c-Kit-negative fibroblast-like cells express platelet-derived growth factor receptor *a* in the murine gastrointestinal musculature. *Histochem Cell Biol* 131: 691-702, 2009.

Iino S, Horiguchi K. Interstitial cells of cajal are involved in neurotransmission in the gastrointestinal tract. *Acta Histochem Cytochem* 39: 145-153, 2006.

Iino S, Horiguchi K, Nojyo Y. Interstitial cells of Cajal in nitric oxide neurotransmission. *Auton Neurosci* 119:147, 2005.

Iino S, Horiguchi S, Horiguchi K. Interstitial cells of Cajal in the gastrointestinal musculature of W^{jic} c-kit mutant mice. *J Smooth Muscle Res* 47: 111-121, 2011.

Iino S, Nojyo Y. Immunohistochemical demonstration of c-kit-negative fibroblast-like cells in murine gastrointestinal musculature. *Arch Histol Cytol* 72(2): 107-115, 2009.

Iino S, Nojyo Y. Muscarinic M2 acetylcholine receptor distribution in the guinea-pig gastrointestinal tract. *Neuroscience* 138:549-559, 2006.

Iino S, Ward SM, Sanders KM. Interstitials cells of Cajal are functionally innervated by excitatory motor neurones in the murine intestine. *J Physiol* 556:521-530, 2004.

Ikeda Y, Fry C, Hayashi F, Stolz D, Griffiths D, Kanai A. Role of gap junctions in spontaneous activity of the rat bladder. *Am J Physiol Renal Physiol* 293: 1018- 1025, 2007.

Imtiaz MS, Von der Weid P-Y, Van Helden DF. Synchronization of Ca2+ oscillations: a coupled oscillator-based mechanism in smooth muscle. *FEBS J* 277: 278-285, 2009.

Jain L, Chen XJ, Brown LA, Eaton DC. Nitric oxide inhibits lung sodium transport through a cGMP-mediated inhibition of epithelial cation channels. *Am. J. Physiol. Lung Cell Mol. Physiol*. 274: L475-484, 1998.

Joensuu H, Roberts PJ, Sarlomo-Rikala M, Andersson LC, Tervahartiala P, Tuveson D, Silberman S, Capdeville R, Dimitrijevic S, Druker B, Demetri GD. Effect of the tyrosine kinase inhibitor STI571 in a patient with a metastaticgastrointestinal stromal tumor. *N. Engl J Med* 344, 1052–1056, 2001.

Johansson R, Pandita RK, Poljakovic M, García-Pascual A, de Vente J, Persson K. Activity and expression of nitric oxide synthase in the hipertrophied rat bladder and the effect of nitric oxide on bladder smooth muscle growth. *J Urol* 168: 2689-2694, 2003.

Johnston L, Carson C, Lyons AD, Davidson RA, McCloskey KD. Cholinergic-induced Ca^{2+} signaling an interstitial cells of Cajal from the guinea pig bladder. *Am J Physiol Renal Physiol* 294: 645-655, 2008.

Johnston L, Sergeant GP, Hollywod MA, Thornbury KD, McHale NG. Calcium oscillation in the interstitial cells of the rabbit urethra. *J Physiol* 565:449-461, 2005.

Johnston L, Woolsey S, Cunningham R, O´Kane H, Duggan B, Keane P, McCloskey KD. Morphological expression of KIT positive interstitial cells of Cajal in human bladder. *J Urol* 184: 370-377, 2010.

Ju H, Zou R, Venema VJ, Venema RC. Direct interaction of endotelial nitric-oxide synthase and caveolin-1 inhibits synthase activity. *J Biol Chem* 272:18522-25, 1997.

Kanaporis G, Mese G, Valiuniene L, White TW, Brink PR, Valiunas V. Gap junction channels exhibit connexin-specific permeability to cyclic nucleotides. *J Gen Physiol* 131: 293-305, 2008.

Kang J, Kang N, Lovatt D, Torres A, Zhao Z, Lin J, Nedergaard M. Connexin 43 hemichannels are permeable to ATP. *J Neurosci* 28: 4702-4711, 2008.

Kang WS, Tamarkin FJ, Wheeler MA, Weiss RM. Rapid up-regulation of endothelial nitric-oxide synthase in a mouse model of Escherichia coli lipopolysaccharide-induced bladder inflammation. *J Pharmacol Exp Ther* 310: 452-8, 2004.

Kass DA, Takimoto E, Nagayama T, Champion HC. Phosphodiesterase regulation of nitric oxide signaling. *Cardiovasc Res* 75:303-14, 2007.

Kaupp UB. Family of cyclic nucleotide gated ion channels. *Curr Opin Neurobiol* 5: 432-445, 1995.

Kaupp UB, Seifert R. Cyclic nucleotide-gated ion channels. *Physiol. Rev*. 82:769–824, 2002.

Kelly RA, Balligand JL, Smith TW. Nitric oxide and cardiac function. *Circ Res* 79(3): 363-380, 1996.

Kerr SW, Buchanan LV, Bunting S, Mathews WR. Evidence that S-nitrosothiols are responsible for the smooth muscle relaxing activity of the bovine retractor penis inhibitory factor. *J Pharmacol Exp Ther* 263: 285-292, 1992.

Kim YC, Koh SD, Sanders KM. Voltage-dependent inward currents of interstitial cells of Cajal from murine colon and small intestine. *J Physio London.*541:797-810, 2002.

Kleemann R, Rothe H, Kolb-Bachofen V, Xie QW, Nathan C, Martin S, Kolb H. Transcription and translation of inducible nitric oxide synthase in the pancreas and prediabetic BB rats. *FEBS Lett* 328: 9-12, 1993.

Klinger MB, Dattilio A, Vizzard MA. Expression of cyclooxygenase-2 in urinary bladder in rats with cyclophosphamide-induced cystitis. *Am J Physiol Regul Integr Comp Physiol* 293: 677-685, 2007.

Knowles RG, Moncada S. Nitric oxide synthases in mammals. *Biochem J* 298(2): 249-258, 1994.

Knowles RG, Palacios M, Palmer RMJ, Moncada S. Formation of nitric oxide from L-arginine in the central nervous system: a transduction mechanism for the stimulation of soluble GC. *Proc Natl Acad Sci USA* 86: 5159-5162, 1989.

Kobzik L, Reid MB, Bredt DS, Stamler JS. Nitric oxide in skeletal muscle. *Nature* 372: 546-548, 1994.

Kobzik L, Stringer B, Ballingand JK, Reid MB, Stamler JS. Endothelial type nitric oxide synthase in skeletal muscle fibers: mitochondrial relationship.*Biochem Biophys Res Commun* 211(2): 375-381, 1995.

Koch KW, Kaupp UB. Cyclic GMP directly regulates a cation conductance in membranes of bovine rods by a cooperative mechanism. *J. Biol. Chem.* 260:6788-6800, 1985.

Koh BH, Roy R, Hollywood MA, Thornbury KD, McHale NG, Sergeant GP, Hatton WJ, Ward SM, Sanders KM, Koh SD. Platelet-derived growth factor receptor-a cells in mouse urinary bladder: a new class of interstitial cells. *J Cell Mol Med* 16(4): 691-700, 2012.

Komuro T. Structure and organization of interstitial cells of Cajal in the gastrointestinal tract. *J Physiol* 576: 653-658, 2006.

Koncz C, Daugiras JT. Use of MQAE for measurements of intracelular [Cl^-] in cultured aortic smooth muscle cells. *Am J Physiol Heart Circ Physiol* 267: 2114-2123, 1994.

Korkmaz A, Oter S, Sadir S, Coskun O, Topal T, Ozler M, Bilgic H. Peroxynitrite may be involved in bladder damage caused by cyclophosphamide in rats. *J Urol* 173: 1793-1796, 2005.

Korkmaz A, Topal T, Oter S. Pathophysiological aspects of cyclophosphamide and ifosfamide induced hemorrhagic cystitis; implication of reactive oxygen and nitrogen species as well as PARP activation. *Cell Biol Toxicol* 23: 303-312, 2007.

Koskela LR, Thiel T, Ehrén I, De Verdier PJ, Wiklund NP. Localization and expression of inducible nitric oxide synthase in biopsies from patients with interstitial cystitis. *J Urol* 180: 737-41, 2008.

Koutalos Y, Yau KW. Regulation of sensivity in vertebrate rod photoreceptors by calcium. *Trends Neurosci* 19(2): 73-81, 1996.

Kubes P, Suzuki M, Granger DN. Nitric oxide: an endogenous modulator of leukocyte adhesion. *Proc. Natl. Acad. Sci. USA* 88:4651-4655, 1991.

Kubota Y, Biers SM, Kohri K, Brading AF. Effects of imatinib mesylate (Glivec) as a c-kit tyrosine kinase inhibitor in the guinea-pig urinary bladder. *Neurourol Urodyn* 25: 205-210, 2006.

Kubota Y, Hashitani H, Shirasawa N, Kojima Y, Sasaki S, Mabuchi Y, Soji T, Suzuki H, Kohri K. Altered distribution of interstitial cells in the guinea pig bladder following bladder outlet obstruction. *Neurourol Urodyn* 27: 330-340, 2008.

Kubota Y, Kajioka S, Biers M, Yokota E, kohri K, Brading AF. Investigation of the effect of the c-kit inhibitor Givec on isolated guinea-pig detrusor preparations. *Auton Neurosci* 115: 64-73, 2004.

Kuhn A, Stadlmayr W, Monga A, Cameron I, Anthony F. A pilot study of Connexin 43 (Cx43) in human bladder tissue in patients with idiopathic detrusor overactivity. *Eur J Obstet Gynecol Reprod Biol.*141: 83-86, 2008.

Kunisawa Y, Komuro T. Interstitial cells of Cajal in the guinea-pig gastric antrum. Distribution and Ultrastructure. *Proc 8APEM*, 945-946, 2004.

Kunzelmann K, Tian Y, Martins JR, Faria D, Kongsuphol P, Ousingsawat J, Thevenod F, Roussa E, Rock J, Schreiber R. Anoctamins. *Pflügers Arch* 462: 195-208, 2011.

Kurahashi M, Nakano Y, Hennig GH, Ward SM, Sanders KM. Platelet-derived growth factor receptor α-positive cells in the tunica muscularis of human colon. *J Cell Mol Med* 16: 1397-1404, 2012.

Lagos P, Ballejo G. Role of spinal nitric oxide synthase-dependent processes in the initation of the micturition hyperreflexia associated with cyclophosphamide-induced cystitis. *Neuroscience* 125: 663-670, 2004.

Lagou, M, Drake MJ, Markerink-Van ittersum M, De Vente J, Gillespie, J I. Interstitial cells and phasic activity in the isolated mouse bladder. *BJU International*.98: 643-650, 2006.

Laine R, Montellano PR. Neuronal nitric oxide synthase isoforms alpha and mu are closely related calpain-sensitive proteins. *Mol. Pharmacol* 54: 305-312, 1998.

Lamb F, Barna TJ. Chloride ion currents contribute functionally to norepinephrine-induced vascular contraction. *Am J Physiol Heart Circ Physiol* 275: 151-160, 1998.

Lammie A, Drobnjak M, Gerald W, Saad A, Cote R, Cordon-Cardo C. Expression of c-kit and kit ligand proteins in normal human tissues. *J. Histochem. Cytochem*. 42: 1417, 1994.

Lander H M, Ogiste JS, Frieda S, Pearce A, Levi R, Novogrodsky A. Nitric Oxide-stimulated Guanine Nucleotide Exchange on $p21^{ras}$. *J Biol. Chem* 270:7017-7020, 1995.

Landry DW, Oliver JA. The pathogenesis of vasodilatory shock. *N Engl J Med* 345: 588-595, 2001.

Lang, RJ. Do fibroblast-like cells´intercede during enteric inhibitory motor neurotransmission in gastrointestinal smooth muscles? *J Physiol* 589: 453- 454, 2011.

Lang RJ, Tonta MA, Zoltkowski BZ, Meeker WF, Wendt I, Parkington HC. Pyeloureteric peristalsis: role of atypical smooth muscle cells and interstitial cells of Cajal-like cells as pacemakers. *J Physiol* 576(3): 695-705, 2006.

Lantéri-Minet M, Bon K, de Pommery J, Michiels JF, Menétrey D. Cyclophosphamide cystitis as a model of visceral pain in rats: model elaboration and spinal structures involved as revealed by the expression of c-Fos and Krox-24 proteins. *Exp Brain Res* 105(2): 220-232, 1995.

Latifpour J, Kondo S, O´Hollaren B, Morita T, Weiss RM. Autonomic receptors in urinary tract: sex and age differences. *J Pharmacol Exp Ther* 253: 661-667, 1990.

Lawrence TS, Beers WH, Gilula NB. Transmission of hormonal stimulation by cell-to-cell communication. *Nature* 272:501–506, 1978.

Lecoin L, Gabella G, Le Douarin N. Origin of the c-kit-positive interstitial cells in the avian bowel. *Development* 122:725-733, 1996.

Lee HW, Baak CH, Lee MY, Kim YC. Spontaneous contractions augmented by cholinergic and adrenergic systems in the human ureter. *Korean J Physiol Pharmacol* 15: 37-41, 2011.

Le Feber J, Van Asselt E. Pudendal nerve stimulation induces urethral contraction and relaxation. *Am J Physiol Regulatory Integrative Comp Physiol* 277: 1368-1375, 1999.

Lei SZ, Pan ZH, Aggarwal SK, Chen HSV, Hartman J, Sucher NJ, Lipton SA. Effect of nitric oxide production on the redox modulatory site of the NMDA receptor-channel complex. *Neuron* 8: 1087-1099, 1992.

Leone AM, Wilklund NP, Hökfelt T, Brundin L, Moncada S. Release of nitric oxide by nerve stimulation in the human urogenital tract. *Neuroreport* 5: 733-736, 1994.

Levine LA, Richie JP. Urological complications of cyclophosphamide. *J Urol* 141: 1063-1069, 1989.

Levin RM, Wein AJ. Quantitative analysis of α and β adrenergic receptor densities in the lower urinary tract of the dog and the rabbit. *Investig Urol* 17: 75-77, 1979.

Li L, Jiang C, Hao P, Li W, Song C, Song B. Changes of gap junctional cell-cell communication in overactive detrusor in rats. *Am J Physiol Cell Physiol* 293: 1627-1635, 2007.

Li Q, Lancaster JR Jr. Calibration of nitric oxide flux generation from diazeniumdiolate *NO donors. *Nitric Oxide* 21(1): 69-75, 2009.

Linares-Fernández BE, Alfieri AB. Cyclophosphamide-induced cystitis: Role of nitric oxide synthase, cyclooxygenase-1 and 2, and NK_1 receptors. *J Urol* 177: 1531-1536, 2007.

Lincoln J, Burnstock G. Autonomic innervation of the urinary bladder and urethra. En: *The autonomic Nervous System*, vol. III*: Nervous control of the urogenital System* (ed. Maggi CA), pp 33-68. London: Harwood Academic, 1993.

Lincoln TM, Komalavilas P, Boerth NJ, MacMillan-Crow LA, Cornwell TL. cGMP signalling through cAMP and cGMP-dependent protein kinases. *Adv Pharmacol* 34: 305-322, 1995.

Lin CS, Lau A, Bakircioglu E, Tu R, Wu F, Week S, Nunes L, Lue TF. Analysis of Neuronal Nitric Oxide Synthase Isoform Expression and Identification of Human nNOS-μ. *Biocheml Biophysical Res Comm* 253: 388-394, 1998.

Lin YQ, Bennet MR. Schawnn cells in rat vascular autonomic nerves activated via purinergic receptors. *Neuroreport* 17: 531-535, 2006.

Liu LW, Thuneberg L, Huizinga JD. Cyclopiazonic acid, inhibiting the endoplasmic reticulum calcium pump, reduces the canine colonic pacemarker frecuency. *J Pharmacol Exp Ther* 275:1058-1068, 1995.

Liu M, Geddis MS, Wen Y, Setlik W, Gershon MD. Expression and function of $5\text{-}HT_4$ receptors in the mouse enteric nervous system. *Am J Physiol Gastrointest Liver Physiol* 289: 1148-1163, 2005.

Lyons AD, Gardiner TA, McCloskey KD. Kit-positive interstitial cells in the rabbit urethra: structural relationships with nerves and smooth muscle. *BJU Int* 99: 687-694, 2007.

Macedo FY, Mourao LT, Freitas HC, Lima RC Jr, Wong DV, Oriá RB, Vale ML, Brito GA, Cunha FQ, Ribeiro RA. Interleukin-4 modulates the inflammatory response in ifofosfamide-induced hemorrhagic cystitis. *Inflammation* 35(1): 297-307, 2012.

Macedo FY, Mourao LT, Palheta RC Jr, Juca DM, Lima RC Jr, Neto J de S, Magalhaes PJ, Santos AA, Souza MH, Brito GA, Ribeiro RA. Cyclooxygenase-2 contributes to functional changes seen on experimental hemorrhagic cystitis induced by ifofosfamide in rat urinary bladder. *Cancer Chemother Pharmacol* 67: 935-943, 2011.

Maeda H, Yamagata A, Nishikawa S, Yoshinga K, Kobayashi S, Nishi K, Nishikawa S-I. Requirement of c-kit for development of intestinal pacemaker system. *Development* 116:369-375, 1992.

Magee T, Fuentes AM, Garban H, Rajavashisth T, Marquez D, Rodriguez JA, Rajfer J, González-Cadavid NF. Cloning of a novel neuronal nitric oxide synthase expressed in penis and lower urinary tract. *Biochem Biophys Res Commun* 226(1): 145-151, 1996.

Maggi CA, Lecci A, Santicioli P, Del Bianco E, Giuliani S. Cyclophosphamide cistitis in rats: involvement of capsaicin-sensitive primary afferents. *J Auton Nerv Syst* 38(3): 201-208, 1992.

Maggi CA, Santicioli P, Del Bianco E, Lecci A, Guliani S. Evidence for the involvement of bradykinin in chemically-evoked cystitis in anaesthetized rats. Naunyn Schmiedebergs *Arch Pharmacol* 347(4): 432-437, 1993.

Malfait M, Gomez P, van Veen TAB, Parys JB, De Smadt H, Vereecke J, Himpens B. Effects of hyperglycemia and protein kinase C on connexin43 expression in cultured rat retinal pigment epithelial cells. *Membrane Biol* 181: 31-40, 2001.

Malley SE, Vizzard MA. Changes in urinary bladder cytokine mRNA and protein after cyclophosphamide-induced cystitis. *Physiol Genomics* 9: 5-13, 2002.

Manneschi LI, Pacini S, Corsani L, Bechi P, Faussone-Pellegrini MS. Interstitial cells of Cajal in the human stomach: distribution and relationship with enteric innervation. *Histol Histopathol* 19:1153-1164, 2004.

Matsuoka Y, Masuda H, Yokoyama M, Kihara K. Protective effects of bilirubin aganist cyclophosphamide induced hemorrhagic cistitis in rats. *J Urol* 179: 1160-1166, 2008.

Mattiason A, Andersson KE, Sjögren C. Adrenoceptors and cholinoceptors controlling the release of noradrenaline from adrenergic nerves in the isolated urethra from rabbit and man. *J Urol* 131: 1190-1195, 1984.

Matulef K, Zagotta WN. Cyclic nucleotide-gated ion channels. *Annu Rev.Cell Dev. Biol.* 19:23–44, 2003.

Mayer B, John M, Bohme E. Purification of a calcium/calmodulin-dependent nitric oxide synthase from porcine cerebellum. Cofactor role of tetrahydrobiopterin. *FEBS Lett* 277: 215-219, 1990.

Mazet B, Raynier C. Interstitial cells of Cajal in the guinea pig antrum: distribution and regional density. *Cell Tissue Res*. 316(1):23-34, 2004.

McCloskey KD, Anderson UA, Davidson RA, Bayguinov YR, Sanders KM, Ward SM. Comparison of mechanical and electrical activity and interstitial cells of Cajal in urinary bladders from wild-type and W/W^v mice. *Br J Pharmacol* 156(2): 273-283, 2009.

McCloskey KD, Gurney AM. Kit-positive cells in the guinea pig bladder. *J Urol* 168: 832-836, 2002.

McCloskey KD. Interstitial cells in the urinary bladder--localization and function. *Neurourol Urodyn*, 29(1):82-7, 2010.

McCloskey KD. Interstitial cells of Cajal in the urinary tract. *Handb Exp Pharmacol* 202: 233-254, 2011.

McHale NG, Hollywood MA, Sergeant GP, Shafei M, Thornbury KT, Ward SM. Organization and function of ICC in the urinary tract. *J Physiol* 576(3): 689-694, 2006.

McMillan K, Masters BS. Prokaryotic expression of the heme- and flavin-binding domains of rat neuronal nitric oxide synthase as distinct polypeptides: identification of the heme-binding proximal thiolate ligand as cysteine-415. *Biochemistry* 34: 3686-3693, 1995.

McMurray G, Casey JH, Naylor AM. Animal models in urological disease and sexual dysfunction. *Br J Pharmacol* 147: 562-579, 2006.

McNeil DL, Traugh NE Jr, Vaidya AM, Hua HT, Papka RE. Origin and distribution of NADPH-diaphorase-positive neurons and fibbers innervating the urinary bladder of the rat. *Neurosci Lett* 147:33-36, 1992.

Medina P, Segarra G, Torondel B, Chuan P, Doménech C, Vila JM, Lluch S. Inhibition of neuroeffector transmission in human vas deferens by sidenafil. *Br J Pharmacol* 131: 871-874, 2000.

Meisenberg B, Lassiter M, Hussein A, Ross M, Vredenburgh JJ, Peters WP. Prevention of hemorrhagic cystitis after high-dose alkylating agent chemotherapy and autologous bone marrow support. *Bone Marrow Transplant* 14: 287-291, 1994.

Melikian N, Seddom MD, Casadei B, Chowienczyk PJ, Shah AM. Neuronal nitric oxide synthase and human vascular regulation. *Trends Cardiovasc Med* 19: 256-62, 2009.

Metzger R, Neugebauer A, Rolle U, Böhlig L, Till H. c-Kit receptor (CD117) in the porcine urinary tract. *Pediatr Surg Int* 24: 67-76, 2008.

Metzger R, Schuster T, Till H, Franke FE, Dietz HG. Cajal-like cells in the upper urinary tract: comparative study in various species. *Pediatr Surg Internat* 21:169-174, 2005.

Metzger R, Schuster T, Till H, Stehr M, Franke FE, Dietz HG. Cajal-like cells in the human upper urinary tract. *J Urol* 172:769-772, 2004.

Mevorach RA, Bogaert GA, Kogan BA. Role of nitric oxide in fetal lower urinary tractfunction. *J Urol* 152: 510-514, 1994.

Michel T, Li GK, Busconi L. Phosphorylation and subcellular translocation of endothelial nitric oxide synthase. *Proc Natl Acad Sci USA* 90: 6252-56, 1993.

Mohr S, Stamler JS, Brune B. Posttranslational Modification of Glyceraldehyde-3-phosphate Dehydrogenase by S-Nitrosylation and Subsequent NADH Attachment. *J. Biol. Chem* 271: 4209-4214, 1996.

Moncada S. Nitric oxide release accounts for the biological activity of endothelium-derived relaxing factor. *Nature* 327: 524-526, 1987.

Moncada S, Palmer RMJ, Higgs EA. Nitric oxide: physiology, pathophysiology and pharmacology. *Pharmacol Rev* 43: 109-42, 1991.

Morais MM, Belarmino-Filho JN, Brito GA, Ribeiro RA. Pharmacological and histopathological study of cyclophosphamide-induced hemorrhagic cystitis-comparision of the effects of dexamethasone and Mesna. *Braz J Med Biol Res* 32(10): 1211-1215, 1999.

Morris SM, Billiar TR. New insights into the regulation of inducible nitric oxide synthase. *Am J Physiol* 266:829-839, 1994.

Mülsch A, Bauersachs J, Schäfer A, Stasch JP, Kast R, Busse R. Effect of YC-1, an NO-independent, superoxide-sensitive stimulator of soluble guanylyl cyclase, on smooth muscle responsiveness to nitrovasodilators. *Br J Pharmacol* 120(4): 681-689, 1997.

Mungrue IN, Bredt DS. nNOS at a glance: implications for brain and brawn. *J Cell Sci* 117: 2627-2629, 2004.

Musil LS, Goodenough DA. Multisubunit assembly of an integral plasma membrane channel protein gap junction connexin43 occurs after exit from the ER. *Cell* 74: 1065-1077, 1993.

Nakamura T, Gold GH. A cyclic nucleotide gated conductance in olfatoy receptor cilia. *Nature* 325: 442-444, 1987.

Nakane M, Schimidt HHHW, Pollock JS, Forstermann U, Murad F. Cloned human brain nitric oxide synthase is highly expressed in skeletal muscle. *FEBS Lett* 316: 175-180, 1993.

Nathan CF. Nitric oxide as a secretory product of mammalial cells. *FASEB J* 6: 3051-3064, 1992.

Nathan C, Xie QW. Regulation of biosynthesis of nitric oxide. *J Biol Chem* 269: 13725-13728, 1994.

Nazif O, Teichman JM, Gebhart GF. Neural upregulation in interstitial cystitis. *Urology* 69:24-33, 2007.

Nemeth L, Maddur S, Puri P. Immunocolocalization of the gap junction protein Connexin43 in the interstitial cells of Cajal in the normal and Hirchsprung´s disease bowel. *J Pediatr Surg* 35: 823-828, 2000.

Neuhaus J, Heinrich M, Schwalenberg T, Stolzenburg J-U. TGF-β1 inhibits Cx43 expression and formation of functional syncitia in cultured smooth muscle cells from human detrusor. *Eur Urol* 55: 491-498, 2009.

Neuhaus J, Weimann A, Stolzenburg J-U, Wolburg H, Horn L-C, Dorschner W. Smooth muscle cells from human urinary bladder express connexin 43 in vivo and in vitro. *World J Urol* 20: 250-254, 2002a.

Neuhaus J, Wolburg H, Hermsdorf T, Stolzenburg J-U, Dorschner W. Detrusor smooth muscle cells of the guinea-pig are functionally coupled via gap junctions in situ and in cell culture. *Cell Tissue Res* 309: 301-311, 2002b.

Okishio Y, Niioka S, Takeuchi T, Nishio H, Hata F, Takatsuji K. Differences in mediator of nonadrenergic, noncholinergic relaxation of the distal colon between Wistar-ST and Sprague-Dawley strains of rats. *Eur J Pharmacol* 388:97-105, 2000.

Olson LE, Soriano P. Increased PDGFRα activation disrupts connective tissue development and drives systemic fibrosis. *Dev Cell* 16: 303-313, 2009.

Omori K, Kotera J. Overview of PDEs and their regulation. *Circ Res* 100:309-327, 2007.

Ördög T, Ward SM, Sanders KM. Interstitial cells of Cajal generates electrical slow waves in the murine stomach. *J Physiol* 518:257-269, 1999.

Oter S, Korkmaz A, Oztas E, Yildirim I, Topal T, Bilgic H. Inducible nitric oxide synthase inhibition in cyclophosphamide induced hemorrhagic cystitis in rats. *Urol Res* 32: 185-189, 2004.

Patel AK, Chapple CR. Anatomy of the lower urinary tract. *Surgery* 26: 127-132, 2008.

Patterson LM, Zheng H, Ward SM, Berthoud HR. Immunohistochemical identification of cholecystokinin A receptors on interstitial cells of Cajal, smooth muscle, and enteric neurons in rat pylorus. *Cell Tissue Res*, 305:11-23, 2001.

Persson CG, Andersson KE. Adrenoreceptor and cholinoceptor mediated effects in the isolated urethra of cat and guinea-pig. *Clin Exp Pharmacol Physiol* 3: 415-426, 1976.

Persson K, Alm P, Johansson K, Larsson B, Andersson KE. Co-existence of nitrergic, peptidergic and acetylcholine esterase-positive nerves in the pig lower urinary tract. *J Auton Nerv Syst* 52: 225-236, 1995.

Persson K, Alm P, Johansson K, Larsson B, Andersson KE. Nitric oxide synthase in pig lower urinary tract: inmunohistochemistry, NADPH diaphorase histochemistry and functional effects. *Br J Pharmacol* 110: 521-530, 1993.

Persson K, Andersson KE. Nitric oxide and relaxation of the lower urinary tract. *Br J Pharmacol* 106: 416-422, 1992.

Persson K, Andersson KE. Non-adrenergic, non-cholinergic relaxation and levels of cyclic nucleotides in rabbit lower urinary tract. *Eur J Pharmacol* 268: 159-167, 1994.

Persson K, Igawa, Mattiasson A, Andersson KE. Effects of inhibition of the L-arginine/nitric oxide pathway in the rat lower urinary tract in vivo and in vitro. *Br J Pharmacol* 107: 178-184, 1992.

Persson K, Johansson K, Alm P, Larsson B, Andersson KE. Morphological and functional evidence aganist a sensory and sympathetic origin of nitric oxide synthase nerves in the rat urinary tract. *Neuroscience* 77: 271-281, 1997.

Persson K, Pandita RK, Aszodi A, Ahmad M, Pfeifer A, Fässler R, Andersson KE. Functional characteristic of urinary tract smooth muscles in mice laking cGMP protein kinase type I. *Am J Physiol* 279: 1112-1120, 2000.

Persson K, Poljakovic M, Johansson K, Larsson B. Morphological and biochemical investigation of nitric oxide synthase and related enzymes in the rat and pig urothelium. *J Histochem Cytochem* 47: 739-750, 1999.

Petersson J, Schreiber O, Steege A, Patzak A, Hellsten A, Phillipson M, Holm L. eNOS involved in colitis-induced mucosal blood flow increase. *Am J Physiol Gastrointest Liver Physiol* 293: G1281-1287, 2007.

Petras JM, Cummings JF. Sympathetic and parasympathetic innervations of the urinary bladder and urethra. *Brain Res* 153: 363-369, 1978.

Pezzone MA, Watkins SC, Alber SM, King WE, de Groat WC, Chancellor MB, Fraser MO. Identification of c-kit-positive cells in the mouse ureter: the interstitial cells of Cajal of the urinary tract. *Am J Physiol Renal Physiol* 284:925-929, 2003.

Philips FS, Stenberg SS, Cronin AP, Vidal PM. Cyclophosphamide and urinary bladder toxicity. *Cancer Res* 21: 1577-1589, 1961.

Piaseczna Piotrowska A, Rolle U, Solari V, Puri P. Interstitial cells of Cajal in the human normal urinary bladder and in the bladder of patients with megacystis-microcolon intestinal hypoperistalsis syndrome. *BJU Int* 94:143-146, 2004.

Pieri L, Vannucchi MG, Faussone-Pellegrini MS. Histochemical and ultrastructural characteristics of an interstitial cell type different from ICC and resident in the muscle coat of human gut. *J Cell Mol Med* 12:1944-1955, 2008.

Pineda, J., Kogan, J.H., Aghajanian, G.K. Nitric oxide and carbon monoxide activate locuscoeruleus neurons through a cGMP-dependent protein kinase: involvement of a nonse-lective cationic channel. *J Neurosci.* 16: 1389-1399, 1996.

Pinna C, Eberini I, Puglisi L, Burnstock G. Presence of constitutive endothelial nitric oxide synthase immunoreactivity in urothelial cells of hamster proximal urethra. *Eur J Pharmacol* 367: 85-89, 1999.

Pinna C, Puglisi L, Burnstock G. A pharmacological and histochemical study of hamster urethra and the role of urothelium. *B J Pharmacol* 116: 655-662, 1996.

Pluja L, Alberti E, Fernández E, Mikkelsen HB, Thuneberg L, Jiménez M. Evidence supporting presence of two pacemakers in rat colon. *Am J Physiol Grastrointest Liver Physiol* 281: 255-266, 2001.

Poljakovic M, Persson K. Urinary tract infection in iNOS-deficient mice with focus on bacterial sensitivity to nitric oxide. *Am J Physiol Renal Physiol* 284: 22-31, 2003.

Pollock JS, Nakane M, Buttery LK, Martinez A, Springall D, Polak JM, Forstermann U, Murad F. Characterization and localization of endothelial nitric oxide synthase using specific monoclonal antibodies. *Am J Physiol* 265: C1379-1387, 1993.

Poole DP, Van Nguyen T, Kawai M, Furness JB. Protein kinases expressed by interstitial cells of Cajal. *Histochem Cell Biol* 121:21-30, 2004.

Poole DP, Xu B, Koh SL, Hunne B, Coupar IM, Irving HR, Shinjo K, Furness JB. Identification of neurons that express 5-hydroxytryptamine4 receptors in intestine. *Cell Tissue Res* 325:413-422, 2006.

Popescu LM, Hinescu ME, Ionescu N, Ciontea SM, Cretoiu D, Ardelean C. Interstitial cells of Cajal in páncreas. *J Cell Mol Med* 9:169-190, 2005.

Porcher C, Baldo M, Henry M, Orsoni P, Jule Y, Ward SM. Deficiency of interstitial cells of Cajal in the small intestine of patients with Crohn´s disease. *Am J Gastroenterol* 97:118-125, 2002.

Porcher C, Juhem A, Peinnequin A, Bonaz B. Bombesin receptor subtype-3 is expressed by the enteric nervous system and by interstitial cells of Cajal in the rat gastrointestinal tract. *Cell Tissue Res* 320:21-31, 2005.

Porras M, Martin MT, Torres R, Vergara P. Cyclic upregulated iNOS and long-term downregulated nNOS are the bases for relapse and quiescent phases in a rat model of IBD. *Am J Physiol Gastrointest Liver Physiol* 290: 423-430, 2006.

Povstyan OV, Gordienko DV, Harhun MI, Bolton TB. Identification of interstitial cells of Cajal in the rabbit portal vein. *Cell Calcium* 33: 223-239, 2003.

Powell DW, Mifflin RC, Valentich JD, Crowe SE, Saada JI, West AB. Myofibroblasts I. Paracrine cells important in health and disease. *Am J Physiol Cell Physiol* 277: 1-19, 1999a.

Powell DW, Mifflin RC, Valentich JD, Crowe SE, Saada JI, West AB. Myofibroblasts II. Intestinal subepithelial myofibroblasts. *Am J Physiol Cell Physiol* 277: 183-201, 1999b.

Powley TL, Wang, X-Y, Fox EA, Phillips, RJ, Liu LWC, Huizinga, JD. Ultrastructural evidence for communication between intramuscular vagal mechanoreceptors and interstitial cells of Cajal in the rat fundus. *Neurogastroenterol Motil* 20: 69-79, 2008.

Prabhakar P, Thatte HS, Goetz RM, Cho MR, Golan DE, Michel T. Receptor-regulated translocation of endothelial nitric-oxide synthase. *J Biol Chem* 273: 27383-27388, 1998.

Prosser CL, Smith CE, Melton CE. Conduction of action potentials in the ureter of the rat. *Am J Physiol* 181: 651-660, 1955.

Pucilowska JB, Williams KL, Lund PK. Fibrogenesis. IV. Fibrosis and inflammatory bowel disease: celular mediators and animal models. *Am J Physiol Gastrointest Liver Physiol* 279: 653-659, 2000.

Pusztaszeri MP, Seelentag W, Bosman FT. Immunohistochemical expression of endothelial markers CD31, CD34, von Willebrand factor, and Fli-1 in normal tissues. *J Histochem Cytochem* 54(4):385-95, 2006.

Qiao LY, Vizzard MA. Cystitis-induced upregulation of tyrosine kinase (TrkA, TrkB) receptor expression and phosphorylation in rat micturition pathways. *J Comp Neurol* 454(2): 200-211, 2002.

Qiao LY, Vizzard MA. Up-regulation of phosphorylated CREB but not c-Jun in bladder afferent neurons in dorsal root ganglia after cystitis. *J Comp Neurol* 469(2): 262-274, 2004.

Radziszewski P, Ekblad W, Sundler F, Mattiasson A. Distribution of neuropeptide-tyrosine hydroxylase and nitric oxide synthase containing fibers in the external urethral sphincter of the rat. *Scand J Urol Nephrol Suppl* 179:81-85, 1996.

Ramu K, Fraiser LH, Mamiya B, Ahmed T, Kehrer JP. Acrolein mercapturates: synthesis, characterization and assessment of their role in the bladder toxicity of cyclophosphamide. *Chem Res Toxicol* 8: 515-524, 1995.

Rand MJ, Li CG. Nitric oxide as a neurotransmitter in peripheral nerves: Nature of transmitter and mechanism of transmission. *Ann. Rev. Physiol* 57: 659-682, 1995.

Rasmussen H, Hansen A, Smedts F, Rumessen JJ, Horn T. CD34-positive interstitial cells in the human detrusor. *APMIS* 115: 1260-1266, 2007.

Rasmussen H, Rumessen JJ, Hansen A, Smedts F, Horn T. Ultrastructure of Cajal-like interstitial cells in the human detrusor. *Cell Tissue Res* 335: 517-527, 2009.

Ravi K, Brennan LA, Levic S, Ross PA, Black SM. S-nitrosylation of endothelial nitric oxide synthase is associated with monomerization and decreased enzyme activity. *PNAS* 101: 2619-2624, 2004.

Ress DD, Palmer RM, Schulz R, Hodson HF, Moncada S. Characterization of three inhibitors of endothelial nitric oxide synthase in vitro and in vivo. *Br J Pharmacol.*101:746-52, 1990.

Retamal MA, Cortés CJ, Reuss L, Bennet MVL, Sáez JC. S-nitrosylation and permeation through connexin 43 hemichannels in astrocytes: induction by oxidant stress and reversal by reducing agents. Proc Natl Acad Sci USA 103: 4475-4480, 2006.

Ribeiro RA, Freitas HC, Campos MC, Santos CC, Figueiredo FC, Brito GA, Cunha FQ. Tumor necrosis factor-alpha and interleukin-1beta mediate the production of nitric oxide involved in the pathogenesis of ifofosfamide induced hemorrhagic cystitis in mice. *J Urol* 167(5): 2229-2234, 2002.

Ribeiro RA, Lima RC Jr, Leite CA, Mota JM, Macedo FY, Lima MV, Brito GA. Chemotherapy-induced hemorrhagic cystitis: pathogenesis, pharmacological approaches and new insights. *J Exp Integr Med* 2(2): 95-112, 2012.

Richards MK, Marletta, MA. Characterization of neuronal nitric oxide synthase and a C415H mutant, purified from a baculovirus overexpression system. *Biochemistry* 33: 14723-14732, 1994.

Rieke F, Schwartz EA. A cGMP-gated current can control exocytosis at cone synapses. *Neuron* 13: 863-873, 1994.

Robinson TL, Sircar K, Hewlett BR, Chorneyko K, Riddell RH, Huizinga JD. Gastrointestinal stromal tumors may originate from a subset of CD34-positive interstitial cells of Cajal. *Am J Pathol* 156: 1157-1163, 2000.

Roosen A, Datta SN, Chowdhury RA, Patel PM, Kalsi V, Elneil S, Dasgupta P, Kessler TM, Khan S, Panicker J, Fry CH, Brandner S, Fowler CJ, Apostolidis A. Suburothelial myofibroblasts in the human overactive bladder and the effect of botulinum neurotoxin Type A treatment. *Eur Urol* 55: 1440-1448, 2009.

Ro S, Park C, Jin J, Zheng H, Blair PJ, Redelman D, Ward SM, Yan W, Sanders KM. A model to study the phenotypic changes of interstitial cells of Cajal in gastrointestinal diseases. *Gastroenterology* 138: 1068-1078, 2010.

Ruiz-Velasco V, Zhong J, Hume JR, Keef KD. Modulation of Ca^{2+} channels by cyclic nucleotide cross activation of opposing protein kinases in rabbit portal vein. *Circ Res* 82: 557-565, 1998.

Rumessen JJ, Mikkelsen HB, Thuneberg L. Ultrastructure of interstitial cells of Cajal associated with deep muscular plexus of human small intestine. *Gastroenterology* 102: 56-68, 1992.

Rumessen JJ, Thuneberg L. Pacemaker cells in the gastrointestinal tract: interstitial cells of Cajal. *Scand J Gastroenterol Suppl* 216:82-94, 1996.

Saban MR, Nguyen NB, Hammond TG, Saban R. Gene expression profiling of mouse bladder inflammatory responses to LPS, substance P, and antigen-stimulation. *Am J Pathol* 160: 2095-2110, 2002.

Sakura M, Masuda H, Matsuoka Y, Yokoyama M, Kawakami S, Kihara K. Rolipram, a specific type-4 phospodiesterase inhibitor, inhibits cyclophosphamide-induced haemorrhagic cystitis in rats. *BJU Int* 103: 264-269, 2008.

Salkowski CA, Detore G, McNally R, van Rooijen N, Vogel SN. Regulation of inducible nitric oxide synthase messenger RNA expression and nitric oxide production by lipopolysaccharide in vivo: the roles of macrophages, endogenous IFN-gamma, and TNF receptor-1-mediated signaling. *J Immunol* 158(2): 905-912, 1997.

Salmhofer HWL, Neuhuber P, Ruth P, Huber A, Russwurm M, Allescher HD. Pivotal role of the interstitial cells of Cajal in the nitric oxide signalling pathway of rat small intestine. Morphological evidence. *Cell Tiss Res* 305:331-340, 2001.

Sanders KM. A case for interstitial cells of Cajal as pacemakers and mediators of neurotransmission in the gastrointestinal tract. *Gastroenterology* 111:492-515, 1996.

Sanders KM. Interstitial cells of Cajal at the clinical and scientific interface. *J Physiol* 576 (3): 683-687, 2006.

Sanders KM, Ordog T, Koh SD, Ward SM. A novel pacemarker mechanism drives gastrointestinal rhythmicity. *News Physiol Sci* 15:291-298, 2000.

Sanders KM, Ördög T, Ward SM. Physiology and Pathophysiology of the Interstitial Cells of Cajal: From Bench to Bedside IV. Genetic and animal models of GI motility disorders caused by loss of intestinal cells of Cajal. *Am J Physiol Gastrointest Liver Physiol* 282:G747-G756, 2002.

Sanders KM. Postjunctional electrical mechanisms of enteric neurotransmission. *Gut* 47:23-25, 2000.

Sanders KM, Ward SM. Interstitial cells of Cajal: a new perspective on smooth muscle function. *J Physiol* 576: 721-726, 2006.

Sanders KM, Ward SM. Kit mutants and gastrointestinal physiology. *J Physiol* 578.1: 33-42, 2007.

Sautet JY, Amara A, Cabanie P, Van Haverbeke G, More J. The urethral muscle (musculus urethralis) of the female calf. Anatomical, histological, histochemical and morphometrical data. *Acta Anat (Basel)* 130 (4): 366-372, 1987.

Savchenko A, Barnes S, Kramer R. Cyclic-nucleotide gated channels mediate synaptic feedback by nitric oxide. *Nature* 390: 694-697, 1997.

Scaife CL, Hunt KK, Patel SR, Benjamin RS, Burgess MA, Chen LL, Trent J, Raymond AK, Cormier J.N, Pisters PW, Pollock RE, Feig BW. Is there a role for surgery in patients with qunresectableq cKIT+ gastrointestinal stromal tumors treated with imatinib mesylate? *Am. J. Surg*. 186, 665–669, 2003.

Schimidt HW, Gagne GD, Nakane M, Pollock JS, Miller MF, Murad F. Mapping of neural nitric oxide synthase in the rat suggests frequent colocalization with NADPH diaphorase but not with soluble guanylyl cyclase, and novel paraneural functions for nitrinergic signal transduction. *J Histochem Cytochem* 40: 1439-1456, 1992a.

Schmidt HW, Lohmann SM, Walter U. The nitric oxide and cGMP signal transduction system: regulation and mechanism of action. *Biochem Biophys Acta* 1178: 153-175, 1993.

Schimidt HW, Warner TD, Ishii K, Sheng H, Murad F. Insulin secretion from pancreatic B cells caused by L-arginine-derived nitrogen oxides. *Science* 255: 721-723, 1992b.

Schreiber R, Uliyakina I, Kongsuphol P, Warth R, Mirza M, Martins JR, Kunzelmann K. Expression and function of epithelial anoctamins. *J Biol Chem* 285: 7838-7845, 2010.

Schroeder BC, Cheng T, Jan YN, Jan LY. Expression cloning of TMEM16A as a calcium-activated chloride channel subunit. *Cell* 134: 1019–1029, 2008.

Schuppan D, Koda M, Hahn EG. Fibrosis of liver, pancreas and intestine: common mechanisms and clear targets? *Acta Gastroenterol Belg* 63: 366-370, 2000.

Searles CD. Transcriptional and posttranscriptional regulation of endothelial nitric oxide synthase expression. *Am J Physiol Cell Physiol* 291: 803-816, 2006.

Seber A, Shu XO, Defor T, Sencer S, Ramsay N. Risk factors for severe hemorrhagic cystitis following BMT. *Bone Marrow Transplant* 23 (1): 35-40, 1999.

Sergeant GP, Bradley E, Drumm B, Hollywood MA, McHale NG, Thornbury KD. Regulation of spontaneous activity in interstitial cells of Cajal of the rabbit urethra by ATP. *Proc Physiol Soc* 15: 139, 2009.

Sergeant GP, Bradley E, Thornbury KD, McHale NG, Hollywood MA. Role of mitochondria in modulation of spontaneous Ca^{2+} waves in freshly dispersed interstitial cells of Cajal from the rabbit urethra. *J Physiol* 586: 4631-4642, 2008.

Sergeant GP, Hollywood MA, McCloskey KD, McHale NG, Thornbury KD. Role of IP(3) in modulation of spontaneous activity in pacemakers cells of rabbit urethra. *Am J Physiol Cell Physiol* 280:C1349-1356, 2001b.

Sergeant GP, Hollywood MA, McCloskey KD, Thornbury KD, McHale NG. Specialised pacemaking cells in the rabbit urethra. *J Physiol* 526:359-366, 2000.

Sergeant GP, Hollywood MA, McHale NG, Thornbury KD. Ca^{2+} signalling in urethral interstitial cells of Cajal. *J Physiol* 576: 715-720, 2006a.

Sergeant GP, Hollywood MA, McHale NG, Thornbury KD. Spontaneous Ca2+ activated Cl- currents in isolated urethral smooth muscle cells. *J. Urol* 166: 1161-1166, 2001a.

Sergeant GP, Johnston L, McHale NG, Thornbury KD, Hollywood MA. Activation of the cGMP/PKG pathway inhibits electrical activity in rabbit urethral interstitial cells of Cajal by reducing the spatial spread of Ca^{2+} waves. *J Physiol* 574: 167-181, 2006b.

Sergeant GP, Thornbury KD, McHale NG, Hollywood MA. Characterization of norepinephrine-evoked inward currents in interstitial cells isolated from the rabbit urethra. *Am J Physiol Cell Physiol* 283: 885-894, 2002.

Sethi S, Dikshit M. Modulation of polymorphonuclear leukocytes function by nitric oxide. *Thromb Res* 100(3):223-247, 2000.

Shafik A, El-Sibai O, Shafik AA, Shafik I. Identification of interstitial cells of Cajal in human urinary bladder: concept of vesical pacemaker. *Urology* 64:809-813, 2004b.

Shafik A, El-Sibai O, Shafik I. Identification of c-kit-positive cells in the uterus. *Int J Gynaecol Obstet* 87: 254-255, 2004a.

Shafik A, El-Sibai O, Shafik I, Shafik AA. Immunohistochemical identification of the pacemaker cajal cells in the normal human vagina. *Arch Gynecol Obstet* 272: 13-16, 2005b.

Shafik A, Shafik I, El-Sibai O. Identification of c-kit positive cells in the human prostate: the interstitial cells of Cajal. *Arch Androl* 51: 345-351, 2005a.

Shafik A. Study of interstitial cells in the penis: human study. *J Sex Med* 4:66-71, 2007.

Shaul PW, Smart EJ, Robinson LJ, German Z, Yuhanna IS, Ying Y, Anderson RG, Michel T. Acylacion targets endothelial nitric-oxide synthase to plasmalemmal caveoale. *J Biol Chem* 271: 6518-6522, 1996.

Sheng H, Gagne GD, Matsumoto T, Miller MF, Forstermann U, Murad F. Nitric oxide synthase in bovine superior cervical ganglion. *J Neurochem* 61: 1120-1126, 1993.

Shepherd JD, Pringle LE, Barnett MJ, Klingemann HG, Reece DE, Phillips GL. Mesna versus hyperhydration for the prevention of cyclophosphamide-induced hemorrhagic cystitis in bone marrow transplantation. *J Clin Oncol* 9: 2016-2020, 1991.

Shuttleworth CW, Xue C, Ward SM, de Vente J, Sanders KM. Inmunohistochemical localization of 3´5´-cyclic guanosine monophosphate in the canine proximal colon: Responses to nitric oxide and electrical stimulation of enteric inhibitory neurones. *Neuroscience* 56:513-522, 1993.

Sivarao DV, Mashimo HL, Thatte MS, Goyal RK. Lower esophageal sphincter is achalasic in nNOS (-/-) and hypotensive in W/W (v) mutant mice. *Gastroenterology* 121: 34-42, 2001.

Smaldone MC, Vodovotz Y, Tyagi V, Barclay D, Philips BJ, Yoshimura N, Chancellor MB, Tyagi P. Multiplex analysis of urinary cytokine levels in rat model of cyclophosphamide-induced cystitis. *Urology* 73(2): 421-426, 2009.

Smart EJ, Robinson LJ, German Z, Yuhanna IS, Ying Y, Anderson RG, Michel T. Acylacion targets endothelial nitric-oxide synthase to plasmalemmal caveoale. *J Biol Chem* 271: 6518-6522, 1996.

Smet PJ, Edyvane KA, Jonavicius J, Marshall VR. Distribution of NADPH-diaphorase-positive nerves supplying the human urinary bladder. *J Auton Nerv Syst* 47:109-113, 1994.

Smet PJ, Jonavicius J, Marshall VR, de Vente J. Distribution of nitric oxide synthase-immunoreactive nerves and identification of the cellular targets of nitric oxide in guinea-pig and human urinary bladder by cGMP immunohistochemistry. *Neuroscience* 71:337-348, 1996.

Smith SD, Wheeler MA, Weiss RM. Nitric oxide synthase: An endogenous source of elevated nitrite in infected urine. *Kidney Int* 45:568-591, 1994.

Smith TK, Reed JB, Sanders KM. Interaction of two electrical pacemakers in muscularis of canine proximal colon. *Am J Physiol* 252:290-299, 1987.

Soderling SH, Beavo JA. Regulation of cAMP and cGMP signalling: new phosphodiesterases and new functions. *Curr Opin Cell Biol* 12(2): 174, 2000.

Sohal GS, Ali MM, Farooqui FA. A second source of precursor cells for the developing enteric nervous system and interstitial cells of Cajal. *Int J Dev Neurosci* 20:619-626, 2002.

Southwell BR. Localization of protein kinase C theta immunoreactivity to interstitial cells of Cajal in guinea-pig grastrointestinal tract. *Neurograstroenterol Motil* 15:139-147, 2003.

Souza-Filho MVP, Lima MVA, Pompeu MML, Ballejo G, Cunha FQ, Ribeiro RA. Involvement of nitric oxide in the pathogenesis of cyclophosphamide-induced hemorrhagic cystitis. *Am J Pathol* 150: 247-256, 1997.

Stamler JS, Simon DI, Jaraki O, Osborne JA, Francis S, Mullins M, Singel D, Loscalzo J. S-nitrosylation of tissue-type plasminogen activator confers vasodilatory and antiplatelet properties on the enzyme.*Proc. Natl. Acad. Sci USA* 89:8087-8091, 1992b.

Stamler JS, Simon DI, Osborne JA., Mullins ME, Jaraki OM, Singel DJ, Loscalzo J. S-nitrosylation of proteins with nitric oxide: synthesis and characterization of biologically active compounds. *Proc Natl Acad Sci USA* 89: 444-448, 1992a.

Sternini C, Wong H, Wu SV, de Giorgio R, Yang M, Reeve Jr J, Brecha NC, Walsh JH. Somatostatin 2A receptor is expressed by enteric neurons, and by interstitial cells of Cajal and enterochromaffin-like cells of the gastrointestinal tract. *J Comp Neurol* 386:396-408, 1997.

Stern JH, Kaupp UB, MacLeish PR. Control of the light-regulated current in rod photoreceptors by cyclic cGMP, calcium and L-diltiazem. *Proc Natl Acad Sci USA* 83: 1163-1167, 1986.

Stewart WF, Van Rooyen JB, Cundiff GW, Abrams P, Herzog AR, Corey R, Hunt TL, Wein AJ. Prevalence and burden of overactive bladder in the United States. *World J Urol* 20(6): 327-336, 2003.

Stillwell TJ, Benson RC Jr. Cyclophosphamide-induced hemorrhagic cystitis: a review of 100 patients. *Cancer* 61: 451-457, 1988.

Stout CE, Costantin JL, Naus CC, Charles AC. Intercellular calcium signalling in astrocytes via ATP release through connexin hemichannels. *J Biol Chem* 277: 10482-10488, 2002.

Strasser H, Ninkovic M, Hess M, Bartsch G, Stenzl A. Anatomic and functional studies of the male and female urethral sphincter. *World J. Urol* 18: 324-329, 2000.

Streutker CJ, Huizinga JD, Driman DK., Riddell R.H. Interstitial cells of Cajal in health and disease. Part II: ICC and gastrointestinal stromal tumours. *Histopathology* 50:190–202, 2007.

Stuehr DJ, Cho HJ, Know NS, Weise MF, Nathan CF. Purification and characterization of the cytokine-induced macrophage nitric oxide synthase: An FAD and FMN-containing flavoprotein. *Proc Natl Acad Sci USA* 88:7773-7777, 1991b.

Stuehr DJ. Mammalian nitric oxide synthases. *Biochem Biophys Acta* 1411:217-230, 1999.

Stuehr DJ, Soo Kwon N, Nathan CF, Griffith OW, Feldman PL, Wiseman J. N^{w}-Hidroxy-L-arginine Is a Intermediate in the Biosynthesis of Nitric Oxide from L-Arginine. *J Biol Chem* 266: 6259-6263, 1991a.

Sui GP, Rothery S, Dupont E, Fry CH, Severs NJ. Gap junctions and connexion expression in human suburothelial interstitial cells. *BJU Int* 90:118-129, 2002.

Sui GP, Wu C, Fry CH. Electrical characteristics of suburothelial cells isolated from the human bladder. *J Urol* 171: 938-943, 2004.

Sui GP, Wu C, Roosen A, Ikeda Y, Kanai AJ, Fry CH. Modulation of bladder myofibroblast activity: implications for bladder function. *Am J Physiol Renal Physiol* 295: 688-697, 2008.

Sutherland RS, Kogan BA, Piechota HJ, Bredt DS. Vesicourethral function in mice with genetic disruption of neuronal nitric oxide synthase. *J Urol* 157: 1109-1116, 1997.

Suzuki H, Takano H, Yamamoto Y, Komuro T, Saito M, Kato K, Mikoshiba K. Properties of gastric smooth muscles obtained from mice which lack inositol trisphosphate receptor. *J Physiol. London* 525:105-111, 2000.

Szurszewski JH, Farrugia G. Carbon monoxide is an endogenous hyperpolarizing factor in the gastrointestinal tract. *Neurogastroenterol Motil* 16:81-85, 2004.

Takaki M. Gut pacemaker cells: the interstitial cells of Cajal (ICC). *J Smooth Muscle Res* 39: 137-161, 2003.

Takayama I, Horiguchi K, Daigo Y, Mine T, Fujino MA, Ohno S. The interstitial cells of cajal and a gastroenteric pacemarker system. *Arch. Histol. Cytol.* 65:1-26, 2002.

Takeda H, Matsuzawa A, Igawa Y, Yamazaki Y, Kaidoh K, Akahane S, Kojima M, Miyata H, Akahane M, Nishizawa O. Functional characterization of beta-adrenoceptor subtypes in the canine and rat lower urinary tract. *J. Urol* 170: 654-658, 2003.

Takeda Y, Koh SD, Sanders KM, Ward SM. Differential expression of ionic conductances in interstitial cells of Cajal in the murine gastric antrum. *J Physiol* 586: 859-873, 2008.

Taniguchi M, Nishida T, Hirota S, Isozaki K, Ito T, Nomura T, Matsuda H, Kitamura Y. Effect of c-kit Mutation on Prognosis of Gastrointestinal Stromal Tumors. *Cancer Res* 59:4297-4300, 1999.

Terauchi A, Kobayashi D, Mashimo H. Distinct roles of nitric oxide synthases and interstitial cells of Cajal in rectoanal relaxation. *Am J Physiol Gastrointest Liver Physiol* 289: 291-299, 2005.

Thornbury KD, Hollywood MA, McHale NG. Mediation by nitric oxide of neurogenic relaxation of the urinary bladder neck muscle in sheep. *J Physiol* 451: 133-144, 1992.

Thuneberg L. Interstitial cells of Cajal: intestinal pacemaker cells. *Adv Anat Embryol Cell Biol* 71: 1-130, 1982.

Thuneberg L. Interstitial cells of Cajal. In:Wood, JD (Ed), Handbook of physiology. The gastrointestinal system, vol 1. Am Physiol Soc, Bethesda, MD, 349-386, 1989.

Thuneberg L, Peters S. Toward a concept of stretch-coupling in smooth muscle. I. Anatomy of intestinal segmentation and sleeve contractions. *Anat Rec* 262: 110-124, 2001.

Torihashi S, Horisawa M, Watanabe Y. c-Kit inmunoreactive interstitial cells in the human gastrointestinal tract. *J Auton Nerv Syst* 75:38-50, 1999.

Torihashi S, Ward SM, Nishikawa S, Nishi K, Kobayashi S, Sanders KM. c-kit-dependent development of interstitial cells and electrical activity in the murine gastrointestinal tract. *Cell Tissue Res*. 280:97-111, 1995.

Torihashi S, Ward SM, Sanders KM. Development of c-kit-positive cells and the onset of electrical rhythmicity in murine small intestine. *Gastroenterology* 112:144-155, 1997.

Tracey WR, Pollock JS, Murad F, Nakane M, Forstermann U. Identification of a type III (endothelial-like) particulate nitric oxide synthase in LLC-PK1 kidney tubular epithelial cells. *Am J Physiol* 266: C22-26, 1994.

Triguero D, González M, García-Pascual A, Costa G. Atypical relaxation by scorpion venom in the lamb urethral smooth muscle involves both NO-dependent and –independent responses. *Naunyn-Schmiedeberg´s Arch Pharmacol* 361: 151-159, 2003.

Triguero D, Prieto D, García-Pascual A. NADPH-diaphorase and NANC relaxations are correlated in the sheep urinary tract. *Neurosci Lett* 163:93-96, 1993.

Triguero D, Sancho M, García-Flores M, García-Pascual, A. Presence of cyclic nucleotide-gated channels in the rat urethra and their involvement in nerve-mediated nitrergic relaxation. *Am J Physiol Renal Physiol* 297: 1353-1360, 2009.

Vahabi B, McKay NG, Lawson K, Sellers DJ. The role of c-kit positive interstitial cells in mediating phasic contractions of bladder strips from streptozotocin-induced diabetic rats. *BJU Int* 107: 1480-1487, 2011.

Vallance BA, Dijkstra G, Qiu B, van der Waaij LA, van Goor H, Jansen PL, Mashimo H, Collins SM. Relative contributions of NOS isoforms during experimental colitis: endothelial-derived NOS maintains mucosal integrity. *Am J Physiol Gastrointest Liver Physiol* 287: 865-874, 2004.

Van Assche G. Can we influence fibrosis in Crohn's disease? *Acta Gastroenterol Belg* 64: 193-196, 2001.

Van Der AA F, Roskams T, Blyweert W, Ost D, Bogaert G, De Ridder D. Identification of kit positive cells in the human urinary tract. *J Urol*. 171: 2492-2496, 2004.

Vanderwinden JM, Rumessen JJ, De Laet MH, Vanderhaeghen JJ, Schiffmann SN. CD34 immunoreactivity and interstitial cells of Cajal in the human and mouse gastrointestinal tract. *Cell Tissue Res* 302: 145-153, 2000.

Vanderwinden JM, Rumessen JJ, De Laet MH, Vanderhaeghen JJ, Schiffmann SN. CD34+ cells in human intestine are fibroblast adjacent to, but distinct from, interstitial cells of Cajal. *Lab Invest* 79: 59-65, 1999.

Vanderwinden JM, Rumessen JJ, Liu H, Descamps D, De Laet MH, Vanderhaeghen JJ. Interstitial cells of Cajal in human colon and in Hirchsprung´s disease. *Gastroenterology* 111:901-910, 1996.

Van Nassauw L, Costagliola A, Van Op Den Bosch J, Cecio A, Vanderwinden JM, Burnstock G, Timmermans JP. Region-specific distribution of the $P2Y_4$ receptor in enteric glial cells and interstitial cells of Cajal within the guinea-pig gastrointestinal tract. *Auton Neurosci* 126-127: 299-306, 2006.

Vannucchi MG, Corsani L, Bani D, Faussone Pellegrini MS. Myenteric neurons and interstitial cells of Cajal of mouse colon express several nitric oxide synthase isoforms. *Neurosci letters* 326:191-195, 2002.

Vaughan-Jones RD. An investigation of chloride-bicarbonate exchange in the sheep cardiac Prurkinge fibre. *J Physiol* 379: 377-406, 1986.

Vera PL, Nadelhaft I. Afferent and sympathetic innervations of the dome and the base of the urinary bladder of the female rat. *Brain Res Bull* 29: 651-658, 1992.

Verweij J, Casali PG, Zalcberg J, LeCesne A, Reichardt P, Blay JY, Issels R, van OA, Hogendoorn PC, van GM, Bertulli R, Judson I. Progression-free survival in gastrointestinal stromal tumours with high-dose imatinib: randomised trial. *Lancet* 364, 1127–1134, 2004.

Villanueva V. Incontinencia urinaria- Parte I. Revista de Postgrado de la Cátedra VIa Medicina N&deg**; 108**: 12-16, 2001.

Vishwajit S, Andersson KE. Terminology of lower urinary tract symptoms. Helping or confusing? *Scientific World Journal* 9: 17-22, 2009.

Vizzard MA. Alterations in growth-associated protein (GAP-43) expression in lower urinary tract pathways following chronic spinal cord injury. *Somatosens Motor Res* 16(4): 369-381, 1999.

Vizzard MA. Alterations in neuropeptide expression in lumbosacral bladder pathways following chronic cystitis. *J Chem Neuroanat* 21(2): 125-138, 2001.

Vizzard MA. Up-regulation of pituitary adenylate cyclase-activating polypeptide in urinary bladder pathways after chronic cystitis. *J Comp Neurol* 420(3): 335-348, 2000.

Vose JM, Reed EC, Pippert GC, Anderson JR, Bierman PJ, Kessinger A, Spinolo J, Armitage JO. Mesna compared with continous bladder irrigation as uroprotection during high-dose chemotherapy and transplantation: a randomized trial. *J Clin Oncol* 11: 1306-1310, 1993.

Waldeck K, Ny L, Persson K, Andersson KE. Mediators and mechanisms of relaxation in rabbit urethral smooth muscle. *BrJ Pharmacol* 123:617-624, 1998.

Walden PD, Durkin MM, Lepor H, Wetzel JM, Gluchowski, Gustafson EL. Localization of mRNA and receptor binding sites for the a1A-adrenoceptor subtype in the rat, monkey and human urinary bladder and prostate. *J.Urol* 157: 1032–1038, 1997.

Walerczyk M, Fabczak H, Fabczak S. Detection and localization of a putative cyclic-GMP-activated channel protein in the protozoan ciliate Stentor coeruleus. *Protoplasma* 227:139-146, 2006.

Wang J, Ma M, Locovei S, Keane RW, Dahl G. Modulation of membrane channel currents by gap junctions protein mimetic peptides: size matters. *Am J Physiol Cell Physiol* 293: 1112-1119, 2007.

Wang XY, Paterson C, Huizinga JD. Cholinergic and nitrergic innervation of ICC-DMP and ICC-IM in the human small intestine. *Neurogastroenterol Motil* 15:531-543, 2003a.

Wang XY, Sanders KM, Ward SM. Relationship between interstitial cells of Cajal and enteric motor neurons in the murine proximal colon. *Cell Tissue Res* 302:331-342, 2000.

Wang XY, Ward SM, Gerthoffer WT, Sanders KM. PKC-ε translocation in enteric neurons and interstitial cells of Cajal in response to muscarinic stimulation. *Am J Physiol Gastrointest Liver Physiol* 285: 593-601, 2003b.

Ward SM, Beckett EA, Wang X, Baker F, Khoyi M, Sanders KM. Interstitial cells of Cajal mediate cholinergic neurotransmission from enteric motor neurons. *J Neurosci* 20:1393-1403, 2000b.

Ward SM, Burns AJ, Torihashi S, Sanders KM. Mutation of the proto-oncogene c-kit blocks development of interstitial cells and electrical rhythmicity in murine intestine. *J Physiol* 480(1):91-97, 1994.

Ward SM. Interstitial cells of Cajal in enteric neurotransmission. *Gut* 47:40-43, 2000.

Ward SM, McLaren GJ, Sanders KM. Interstitial cells of Cajal in the deep muscular plexus mediate enteric motor neurotransmission in the mouse small intestine. *J Physiol* 573:147-159, 2006.

Ward SM, Ordog T, Koh SD, Abu Baker S, Jun JY, Amberg G, Monaghan K, Sanders KM. Pacemaking of interstitial cells of Cajal depends upon calcium handling by endoplasmic reticulum and mitochondria. *J Physiol* 525:355-361, 2000a.

Ward SM, Sanders KM. Pacemaker activity in septal structures of canine colonic circular muscle. *Am J Physiol* 259: 264-273, 1990.

Ward SM, Sanders KM. Physiology and pathophysiology of the interstitial cell of Cajal: from bench to bedside. I. Functional development and plasticity of interstitial cells of Cajal networks. *Am J. Physiol. Gastrointest. Liver Physiol*. 281: 602-611, 2001.

Warner T, Mitchell JA, Sheng H, Murad F. Effects of cyclic GMP on smooth muscle relaxation. *Adv Pharmacol* 26: 171-194, 1994.

Watson NA, Notley RG. Urological complications of cyclophosphamide. *Br J Urol* 45: 606-609, 1973.

Wei JY, Samanta RD, Leconte L, Barnstable CJ. Molecular and pharmalogical analysis of cyclic nucleotide-gated cannel function in the central nervous system. *Prog Neurobiol* 56: 37-64, 1998.

Weitz D, Ficek N, Kremmer E, Bauer PJ, Kaupp UB. Subunit stoichiometry of the CNG channel of rod photoreceptors. *Neuron* 36:881–89, 2002.

Werkstrom V, Svensson A, Andersson KE, Hendlund P. Phospodiesterase 5 in the female pig and human urethra: morphological and functional aspects. *BJU Int* 98:414-423, 2006.

West NJ. Prevention and treatment of hemorrhagic cystitis. *Pharmacotherapy* 17(4): 696-706, 1997.

Willecke K, Eiberger J, Degen J, Eckardt D, Romualdi A, Guldenagel M, Deutsch U, Söhl G. Structural and functional diversity of conexin genes in the mouse and human genome. *Biol Chem* 383:725-737, 2002.

Wiseman OJ, Fowler CJ, Landon DN. The role of the human bladder lamina propria myofibroblast. *BJU Int* 91: 89-93, 2003.

Won KJ, Sanders KM, Ward SM. Interstitial cells of Cajal mediate mechanosensitive responses in the stomach. *Proc Natl Acad Sci USA* 102: 14913-14918, 2005.

Wood J, Garthwaite J. Models of the diffusional spread of nitric oxide: implications for neural nitric oxide signalling and its pharmacological properties. *Neuropharmacology* 33: 1235-1244, 1994.

Wu SY, Dun NJ. Potentiation of IPSC by nitric oxide in immature rat sympathetic preganglionic neurones in vitro. *J Physiol* 495: 479-490, 1996.

Xue C, Pollock J, Schimidt HHHW, Ward SM, Sanders KM. Expression of nitric oxide synthase immunoreactivity by interstitial cells of the canine proximal colon. *J Auton Nerv Syst* 49: 1-14, 1994.

Xu E, Leung S, Wright J, Guggino, SE. Expression of cyclic nucleotide-gated cation channels in airway epithelial cells. *J Membr Biol* 171: 117-126, 1999.

Xu X, Cubbedu LX, Malave A. Expression of inducible nitric oxide synthase in primary culture of rat bladder smooth muscle cells by plasma from cyclophosphamide-treated rats. *Eur J Pharmacol* 416: 1-9, 2001.

Yang YD, Cho H, Koo JY, Tak MH, Cho Y, Shim WS, Park SP, Lee J, Lee B, Kim BM, Raouf R, Shin YS, Oh U. TMEM16A confers receptor-activated calcium-dependent chloride conductance. *Nature* 455: 1210–1215, 2008.

Yau KW, Baylor DA. Cyclic GMP-activated conductance of retinal photoreceptor cells. *Annu Rev Neurosci* 12: 289-327, 1989.

Yoshimura N, de Groat WC. Increased excitability of afferent neurons innervating rat urinary bladder after chronic bladder inflammation. *J Neurosci* 19(11): 4644-4653, 1999.

Young HM, Ciampoli D, Southwell BR, Newgreen DF. Origin of interstitial cells of Cajal in the mouse intestine. *Dev Biol* 180: 97-107, 1996.

Young HM. Embryological origin of interstitial cells of Cajal. *Microsc Res Tech* 47:303-308, 1999.

Zhang SC, Fedoroff S. Cellular localization of stem cell factor and c-kit receptor in the mouse nervous system. *J Neurosci Res* 47: 1-15, 1997.

Zhong H, Molday LL, Molday RS, Yau KW. The heteromeric cyclic nucleotide-gated channel adopts a 3A:1B stoichiometry. *Nature* 420:193–98, 2002.

Zhou Y, Ling E.A. Neural nitric oxide synthase in the neural pathways of the urinary bladder. *J Anat* 194: 481-496, 1999.

Zhu MH, Kim TW, Ro S, Yan W, Ward SM, Koh SD, Sanders KM. A Ca(2+)-activated Cl(-) conductance in interstitial cells of Cajal linked to slow wave currents and pacemaker activity. *J Physiol* 587: 4905-4918, 2009.

Zoccoli MA, Karnovsky ML. Effect of two inhibitors of anion transport on the hydrolysis of glucose 6-phosphate by rat liver microsomes. *J Biol Chem* 255: 1113-1119, 1980.

Zufall F, Shepherd GM, Barnstable CJ. Cyclic nucleotide gated channels as regulators of CNS development and plasticity. *Curr Opin Neurobiol* 7: 404-412, 1997.

Zygmunt PM, Zygmunt PKE, Högestätt ED, Andersson KE. Effects of ω-conotoxin on adrenergic, cholinergic and NANC neurotransmission in the rabbit urethra and detrusor. *Br J Pharmacol* 110: 1285-1290, 1993.

ANEXO

Los estudios de esta tesis se han publicado o están pendientes de publicarse en los siguientes artículos:

I- Angeles Garcia-Pascual, Maria Sancho, Gonzalo Costa and Domingo Triguero. Interstitial Cells of Cajal in the urethra are cyclic GMP-Mediated Targets of Nitrergic Neurotransmission. *Am J Physiol Renal Physiol* 295: 971-983, 2008.

II- Domingo Triguero, Maria Sancho, Marta Garcia-Flores and Angeles Garcia-Pascual. Presence of cyclic nucleotide- gated channels in the rat urethra and their involvement in nerve mediated nitrergic relaxation. *Am J Physiol Renal Physiol* 297:1353-1360, 2009.

III- Maria Sancho, Angeles Garcia-Pascual, Domingo Triguero and Gerard P. Sergeant. Involvement of cyclic nucleotide–gated channels in Ca2+ oscillations under control conditions and in the presence of increased cyclic GMP levels in isolated interstitial cells of Cajal from the rabbit urethra. **(Unpublished)**

IV- Maria Sancho, Domingo Triguero and Angeles Garcia-Pascual. Direct coupling through Gap Junctions is not involved in Urethral Neurotransmission. *Am J Physiol Renal Physiol,* 300:864-872, 2011.

V- Maria Sancho, Angeles Garcia-Pascual and Domingo Triguero. Presence of the Ca^{2+}-activated chloride channel anoctamin 1 in the urethra and its role in excitatory neurotransmission. *Am J Physiol Renal Physiol,* 302 (3): 390-400, 2012.

VI- Maria Sancho, Jose Ferrero, Domingo Triguero and Angeles Garcia-Pascual. Altered neuronal and endothelial nitric oxide synthase expression in the bladder and urethra of cyclophosphamide-treated rats. **(Unpublished)**

VII- Maria Sancho, Domingo Triguero and Angeles Garcia-Pascual. Involvement of bladder and urethral interstitial cells in the cyclophosphamide-induced cystitis in the rat: preventive effect of Glivec. **(Unpublished)**

MANUSCRITO I

Am J Physiol Renal Physiol 295: F971–F983, 2008.
First published July 16, 2008; doi:10.1152/ajprenal.90301.2008.

Interstitial cells of Cajal in the urethra are cGMP-mediated targets of nitrergic neurotransmission

Ángeles García-Pascual, María Sancho, Gonzalo Costa, and Domingo Triguero
Department of Physiology, Veterinary Faculty, Complutense University, Madrid, Spain

Submitted 9 May 2008; accepted in final form 11 July 2008

García-Pascual A, Sancho M, Costa G, Triguero D. Interstitial cells of Cajal in the urethra are cGMP-mediated targets of nitrergic neurotransmission. *Am J Physiol Renal Physiol* 295: F971–F983, 2008. First published July 16, 2008; doi:10.1152/ajprenal.90301.2008.—While interstitial cells of Cajal (ICC) in the urethra respond to nitric oxide (NO) donors by increasing cGMP, it remains unclear whether urethral ICC are functionally innervated by nitrergic nerves. We have addressed this issue in the rat and sheep urethra, where cGMP production and relaxation were compared in preparations subjected to electrical field stimulation (EFS; 2 Hz, 4 min) of nitrergic nerves or to exogenous *S*-nitroso-L-cysteine (SNC; 0.1 mM, 4 min). Upon EFS, cGMP immunoreactivity (cGMP-ir) was observed in both smooth muscle cells (SMC) and in spindle-shaped cells that contained c-kit and vimentin, features of ICC. Similarly, cGMP-ir was preferentially, but inconsistently, found in ICC of the outer muscle layer on exposure to SNC. We found separate functional groups of ICC within the urethra. Thus only ICC present in the muscle layers (ICC-M) but not those in the serosa (ICC-SR) and lamina propia (ICC-LP) seem to be specifically influenced by activation of neuronal NO synthase (nNOS). Thus the increase in cGMP-ir in the ICC-M induced by EFS was prevented by N^{ω}-nitro-L-arginine and ODQ. Urethral ICC did not express nNOS, although they were closely associated with nitrergic nerves. cGMP-ir was also present in the urothelium (in the rat but not in the sheep) and the vascular endothelium but not in neural structures, such as the nerve trunks and nerve terminals. Together, these results suggest a model of parallel innervation in which both SMC and ICC-M are effectors of nerve-released NO in the urethra.

ICC; nitric oxide; cGMP immunofluorescence; urinary tract

INTERSTITIAL CELLS OF CAJAL (ICC) were first described in the intestine by Santiago Ramón y Cajal nearly a century ago (6). They are branched, noncontractile but excitable cells that are believed to act as pacemakers of the slow waves and to be important mediators of enteric neurotransmission, or to even act as mechanoreceptors (see Ref. 27).

Similarly, smooth muscles in the urinary tract have spontaneous electrical and mechanical activities that are controlled by a rich supply of autonomic nerves. Therefore, it is not surprising that cells that are morphologically and functionally similar to gastrointestinal ICC have been described throughout the urinary tract, from the ureter to the bladder and in the urethra of different species, including humans (for a review, see Ref. 4). In urinary tissues, it is now accepted that these cells, previously named interstitial cells (IC), ICC, ICC-like cells, or myofibroblasts, should all be considered as ICC in accordance with the nomenclature used in the gut (Fifth International Symposium on Interstitial Cells of Cajal, Ireland, 2007). However, studies concerning their role in the urinary tract are scarce and somewhat controversial. In enzymatic dispersal from the rabbit urethra, a small population of noncontractile, vimentin-immunoreactive (vimentin-ir) cells that spontaneously displayed Ca^{2+} oscillations coupled to firing of transient inward currents was described, while smooth muscle cells (SMC) were electrically quiescent (28). These features suggested an obvious pacemaking role for the ICC in this structure. Careful studies of the ionic basis of this spontaneous excitation revealed that this activity comes from the spontaneous release of Ca^{2+} from intracellular stores and the subsequent activation of Ca^{2+}-activated Cl^- channels (19). However, in the guinea pig (15) and sheep (29) urethras not only ICC but also SMC were able to develop spontaneous depolarization mediated by Ca^{2+}-activated Cl^- channels. Recently, on the basis of the heterogeneous effect of cyclopiazonic acid, a known inhibitor of Ca^{2+} uptake into intracellular stores, it was suggested that both ICC and SMC may simultaneously be involved in urethral pacemaking in the intact rabbit urethra (16). Indeed, spontaneous Ca^{2+} transients in rabbit urethral ICC "in situ" were not temporally correlated with neighboring SMC, which generated Ca^{2+} transients by themselves (17).

The urethral smooth muscle sphincter has a high spontaneous tone during continence, which is augmented by neurally released norepinephrine (NE) and abruptly lost during micturition by neurally released nitric oxide (NO; reviewed in Ref. 2). It has been shown that NE increased the frequency of the spontaneous depolarizations in ICC isolated from the rabbit urethra through the activation of Ca^{2+}-activated Cl^- channels (30). By contrast, this electrical activity was inhibited by the NO donor DEA-NO, as well as activators of the cGMP pathway, probably by inhibiting the inositol 1,4,5-trisphosphate-mediated Ca^{2+} release from intracellular stores (31). Indeed, SIN-1 (another NO donor) reduced the amplitude of ICC Ca^{2+} transients in the intact rabbit urethra, while phenylephrine increased their frequency and induced a sustained rise in Ca^{2+} (17). These results suggest that, like the gut, neurotransmitters in the urethra may act through ICC, although this hypothesis has yet to be tested in experiments where the release of the endogenous neurotransmitters from intramural nerves is elicited.

One of the main features of urinary tract ICC from both the bladder and the urethra is their ability to accumulate cGMP upon exposure to NO donors (10, 13, 22, 34, 40, 43). Hence, ICC appear to express the second messengers necessary to transduce NO signals, including guanylate cyclase (GC). However, the involvement of ICC in the relaxation induced by selective stimulation of nitrergic nerves in the urethra has yet to be demonstrated. It is well known that urethral nitrergic

Address for reprint requests and other correspondence: A. García-Pascual, Dept. of Physiology, Veterinary Faculty, Complutense Univ., Avda. Puerta de Hierro s/n, 28040 Madrid, Spain (e-mail: angarcia@vet.ucm.es).

The costs of publication of this article were defrayed in part by the payment of page charges. The article must therefore be hereby marked "*advertisement*" in accordance with 18 U.S.C. Section 1734 solely to indicate this fact.

relaxation is mediated by GC activation and cGMP accumulations (11, 25). However, urethral tissue responds quite differently to exogenous NO or NO donors and to the endogenous release of the nitrergic transmitter (12).

In the present study, we have used cGMP immunofluorescence to identify the specific cell types in the sheep and rat urethra that respond to nitrergic stimulation by elevating their intracellular cGMP. Tissues were subjected to electrical field stimulation (EFS) of nitrergic nerves or exposed to *S*-nitroso-L-cysteine (SNC), the NO donor that produces the fastest relaxation and highest levels of cGMP in the sheep urethra (12). Both relaxations and cGMP immunoreactivity (cGMP-ir) were compared directly. Furthermore, immunoreactivity for the protein gene product (PGP 9.5) or the neuronal isoform of NO synthase (nNOS) in nerve structures was combined with cGMP labeling to identify nerves and their relationship with the effector cells. Finally, vimentin/cGMP and c-kit/cGMP double labeling was used to confirm the mesenchymal nature of the cGMP-containing cells. Preliminary data from this study were presented at the Third International Conference on cGMP Generators, Effectors and Therapeutic Implications (Dresden, Germany, 2007).

EXPERIMENTAL PROCEDURES

Drugs and Solutions

NE, atropine sulfate, guanethidine monosulfate, D-tubocurarine hydrochloride, IBMX, L-cysteine, N^{ω}-nitro-L-arginine (L-NNA), and sodium nitrite were obtained from Sigma-Aldrich Chemie (Steinheim, Germany). Both 1,4-dihydro-5[2-propoxy-phenyl]-7H-1,2,3 triazolo [4,5 d] pyrimidine-7-one (zaprinast) and 1H-(1,2,4)oxadiazolo (4,3) alquinoxalin-1-one (ODQ) were purchased from Alexis (Alexis Biochemicals, Lausen, Switzerland), and SQ22536 was obtained from Calbiochem (Darmstadt, Germany). Most drugs were dissolved in distilled water except IBMX and zaprinast, which were dissolved in DMSO, and ODQ in acetonitrile. Solutions were stored at −20°C, and the drugs were diluted to the working concentrations in 0.9% NaCl. Solutions of SNC were prepared by adding a sodium nitrite (100 mM) solution to the same volume of a solution containing 250 mM HCl, 1 mM EDTA, and 100 mM L-cysteine. The SNC concentration was determined spectrophotometrically (Shimadzu UV-1601 UV-visible spectrophotometer, Shimadzu, Tokyo, Japan), assuming a molar absorption coefficient of $\varepsilon_{544} = 16.6$ M/cm. Working dilutions were prepared in deoxygenated distilled water immediately before use, and they were kept on ice and maintained in the dark.

Tissue Preparation

Lower urinary tracts from female sheep (4–6 mo old) and female Wistar rats (6–8 wk old and 200–300 g) were used in this study. Sheep urinary tracts were collected at the local slaughterhouse shortly after death and maintained at 4°C in Krebs solution (in mM): 119 NaCl, 4.6 KCl, 1.5 $CaCl_2$, 1.2 $MgCl_2$, 15 $NaHCO_3$, 1.2 KH_2PO_4, 0.01 EDTA, and 11 glucose. From each urinary tract, the urethra was dissected out, and the fat and connective tissue were removed. Rats were killed by cervical dislocation followed by exsanguination, and after the abdomen was opened, the whole lower urinary tract was removed. All procedures were approved by the Complutense University Ethical Committee and were performed in accordance with European guidelines. Transverse strips (~3-mm wide and 5-mm long) or rings (3-mm wide) were obtained from the proximal sheep or rat urethras, respectively, immediately caudal to the bladder neck. Care was taken not to damage the mucosal and serosal layers to maintain the integrity of the tissue.

Nitrergic Stimulation of Urethral Preparations

The preparations in which cGMP immunofluorescence was assessed were previously subjected to functional experiments, facilitating the direct comparison between the relaxant responses to nitrergic stimulation and the accumulation of the cyclic nucleotide. Urethral preparations (strips or rings) were mounted between two stainless steel hooks in 5-ml organ baths containing Krebs solution at 37°C and bubbled with a mixture of 95% O_2-5% CO_2 (pH 7.4). The isometric tension was recorded with Grass FT03C transducers (Grass Instruments, Quincy; MA) and displayed on a MacIntosh computer with a MacLab analog-to-digital converter v5.5 (AD Instruments, Hastings, East Sussex, UK). Preparations were equilibrated at a resting tension of either 15 (sheep) or 5 mN (rat) for 60 min.

Guanethidine (50 μM) and atropine (1 μM) were present throughout the experiment to prevent the release of NE from nerves or the effects of the released acetylcholine on muscarinic receptors, respectively. D-Tubocurarine 0.1 mM was also present in the rat experiments to avoid the effect of somatic nerve stimulation that innervates the striated muscle of the urethra. Tissues were precontracted with 50 μM NE and relaxed by the addition of SNC (0.1 mM for 4 min) or by selective EFS of nitrergic nerves. EFS was achieved with a Grass S-48 stimulator (Grass Instruments) connected to platinum electrodes placed parallel to the preparation and coupled to a Med-Lab stimulus splitter (Med-Lab Instruments, Loveland, CO). Square-wave pulses of 0.8-ms duration, supramaximal voltage (current strength, 200 mA), train duration of 5 s, and a frequency of 2 Hz were delivered for 4 min, supramaximal parameters to stimulate nitrergic-inhibitory nerves in this preparation (38). Preparations that did not relax properly were excluded from the study. In all experiments, tissues were exposed to the phosphodiesterase (PDE) inhibitors IBMX (1 mM) and zaprinast (0.1 mM), 30 s before stimulation, to prevent the breakdown of cyclic nucleotides, and these inhibitors were present throughout the stimulation period (4 min). This treatment enabled the accumulation of sufficient cGMP to be visualized by immunofluorescence. Control preparations were processed identically except that the tissues were not exposed to SNC or EFS. Furthermore, some preparations were pretreated with the NO synthase inhibitor L-NNA (0.1 mM) or the GC inhibitor ODQ (0.1 mM) for 30 min before the addition of NE, and these inhibitors remained present throughout the experiment (see Fig. 1 for examples of the experimental procedure). All samples were immediately processed for immunofluorescence.

Immunofluorescence

Urethral strips were fixed partially stretched to 110% of their length by pinning them to a Sylgard base, while the urethral rings were immersion-fixed following the method described by De Vente et al. (8). After fixation for 30 min in ice-cold 4% paraformaldehyde in 0.1 M phosphate buffer (PB; pH 7.0), the tissue was incubated in mixed solutions of paraformaldehyde in 0.1 M PB and increasing concentrations of sucrose (10% sucrose for 90 min followed by 20% sucrose for 120 min), and cryoprotection was terminated by incubating overnight in 30% sucrose in PB at 4°C. Tissues were snap-frozen in liquid nitrogen-cooled isopentane and stored at −80°C for up to 15 days. Cryostat sections transverse to the mucosal surface (10 μm: CM1850 UV, Leica Microsystems, Barcelona, Spain) of the urethras embedded in Tissue-Tek OCT compound were thawed onto poly-L-lysine-coated slides. From each urethra, consecutive sections were collected on 4–5 slides, and thus each contained a similar collection of 10–15 serial sections from the same animal. The slides were air-dried at room temperature for 12–24 h and then processed directly or stored at −80°C for no more than 30 days.

Urethral sections were washed three times for 5 min with PB and to avoid nonspecific antibody binding; they were then incubated for 60 min with 3% normal donkey antiserum (Chemicon International, Temecula, CA) containing 0.3% Triton X-100. The sections were incubated with the primary antibody (or antibodies for dual labeling)

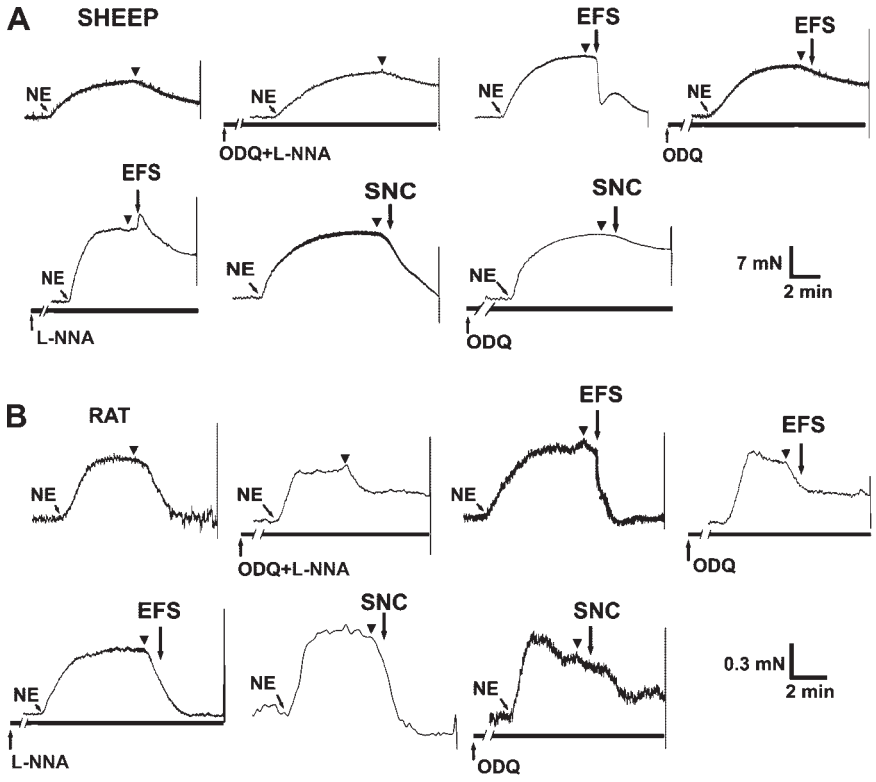

Fig. 1. Representative tracings showing the relaxation responses induced in sheep (*A*) and rat (*B*) urethral preparations under different conditions of nitrergic stimulation. Electrical field stimulation (EFS; 2 Hz, 4 min) or *S*-nitroso-L-cysteine (SNC; 0.1 mM, 4 min) in the presence or the absence of N^{ω}-nitro-L-arginine (L-NNA) and/or ODQ (0.1 mM, 30 min pretreatment) compared with control unstimulated preparations is shown. All preparations were precontracted with norepinephrine (NE; 50 μM), and the black arrowheads indicate the point at which phosphodiesterase (PDE) inhibitors (IBMX 1 mM and zaprinast 0.1 mM) were added, which were present throughout the experiment. The final vertical lines indicate the rapid removal of tissues to be processed for immunofluorescence.

diluted in 2% normal donkey serum and 0.3% Triton X-100 for 24 h at 4°C in a humidified chamber. To visualize cGMP in rat urethral sections, we used a sheep anti-formaldehyde-fixed cGMP antibody (1:2,000; a generous gift from Dr. J. De Vente, Maastricht University, Maastricht, The Netherlands), the selectivity and detection limits of which were described previously (8). For the sheep urethra, we used a rabbit anti-cGMP polyclonal antiserum (1:3,000; Chemicon International). Two anti-c-kit rabbit polyclonal antisera were used: c-kit Ab-1 (1:25; Oncogene Research Products, San Diego, CA) and c-kit H-300 (1:50; sc-5535, Santa Cruz Biotechnology, Santa Cruz, CA). The other primary antibodies used were a mouse monoclonal anti-vimentin antibody (clone V9; 1:100; Chemicon International), a mouse monoclonal anti-NOS brain (clone NOS-B1; 1:3,000; Sigma-Aldrich Chemie), a rabbit nNOS polyclonal antiserum (1:300; Cayman Chemical, Ann Arbor, MI), and a mouse monoclonal antibody against the neuronal marker protein gene product 9.5 (PGP9.5; 1:50; Abcam, Cambridge, UK). Double labeling for cGMP and vimentin, nNOS, or PGP9.5 and c-kit with vimentin involved the use of the polyclonal antisera for cGMP and c-kit and the monoclonal antibodies for vimentin, nNOS, and PGP 9.5, although the polyclonal nNOS antiserum was used for the vimentin-nNOS double labeling.

The following secondary antibodies were used, appropriately matched to the species in which the primary antibody was raised: donkey anti-rabbit FITC, donkey anti-sheep FITC, and donkey anti-mouse rhodamine (all 1:100; Chemicon International). Sections were incubated with the secondary antibodies for 2 h in the dark in a humidified chamber at room temperature. After a washing (3 times, 10 min each) with PB, the nuclei were counterstained with 4′,6-diamino-2-phenylindole dihydrochloride (DAPI; 10.9 mM for 20–30 min; Sigma-Aldrich Chemie), and the sections were washed again and mounted with Prolong Gold antifade reagent (Molecular Probes, Eugene, OR). In all cases, a number of controls were performed in which the specificity of the immunoreactions was established by omitting the primary antibody or antibodies.

The labeled sections were examined under an Axioplan 2 fluorescence microscope (Carl Zeiss Microimaging, Göttingen, Germany) equipped with the appropriate filter sets. They were photographed with a Spot-2 digital camera (Diagnostic Instruments, Sterling Heights, MI), and the images were stored digitally as 12-bit images using MetaMorph 6.1 software (MDS Analytical Technologies, Toronto, ON, Canada). Some sections were examined by confocal laser-scanning microscopy using a spectral confocal microscope (TCS-SP2, Leica Microsystems, Barcelona, Spain). The confocal micrographs shown are digital composites of Z-series scans of 10–12 optical sections through a depth of 10–12 μm obtained with Leica Confocal Software (LCS, Leica Microsystems). Digital images were subsequently transferred to Adobe Photoshop 8.0 (San Jose, CA) for compilation of the figures. Images of the whole-rat urethral ring were constructed using the "photomerge" tool of Adobe Photoshop software from 20–25 different microphotographs (magnification ×20) taken from the different regions of the ring.

Data Analysis

Urethral relaxations were expressed as the percentage of the tension elicited by NE immediately before each stimulation. In rat preparations, the time to reach 50% of the total relaxation (half-relaxation time) was also measured since the pronounced relaxant effect of PDE inhibitors unmasks the effect of stimulation with either SNC or EFS. Each experiment was carried out using a different animal, and at least five animals were included in each experimental group.

The intensity of cGMP-ir was quantified using MetaMorph 6.1 image analysis software (MDS Analytical Technologies). For each experimental group, this measurement was performed in no more than three randomly selected tissue sections per animal from at least three animals and from at least three different staining procedures (performed on different days). Images at ×20 magnification were obtained at a constant time exposure to permit direct comparisons between them. In each image, an area comprising the outer muscular [250,713 (35,829) μm^2, $n = 42$], inner muscular [198,335 (101,298) μm^2, $n = 43$], or mucosal [300,896 (185,011) μm^2, $n = 35$] layer of

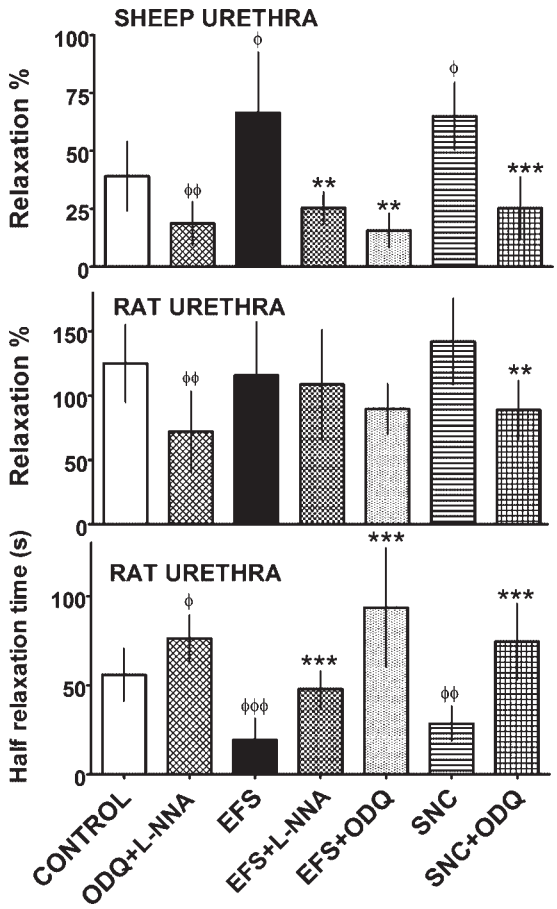

Fig. 2. Relaxant responses induced by EFS and SNC in the presence or absence of L-NNA and/or ODQ, and compared with control unstimulated preparations from the sheep and rat urethra. The experimental protocol is as shown in Fig. 1, and the results are means (SD) from 4–13 different animals expressed as the percentage of the contractile tension induced by NE (Relaxation %) or the time to reach 50% of total relaxation (half-relaxation time). $\Phi P < 0.05$, $\Phi\Phi P < 0.01$, $\Phi\Phi\Phi P < 0.001$ differences compared with controls. $^{**}P < 0.01$ and $^{***}P < 0.001$ differences with preparations stimulated with EFS or SNC but not treated with L-NNA or ODQ (ANOVA followed by *t*-test applying the false discovery rate procedure).

the sheep urethra, or the complete smooth muscle coat [166,720 (110,358) μm^2, $n = 85$] of the rat urethra, was selected, and a threshold was established to subtract the background immunofluorescence. The proportion of the selected area exceeding the threshold values was quantified. For all images, the threshold was kept constant and it was set to a level that gave a relative threshold area of <5% in the least-intense images (corresponding to the preparations treated with ODQ).

The results are given as means (SD) from *n* experiments. One-way ANOVA was used for multiple comparisons followed by the unpaired *t*-test. The level of significance was determined by applying the false discovery rate procedure (7). Data were compared using GraphPad Prism 5 software (GraphPad Software, San Diego, CA).

RESULTS

Functional Responses

In all sheep and rat urethra preparations used here, a direct comparison was made between the relaxation responses and cGMP-ir in response to different stimuli (EFS, addition of SNC, and pretreatment with the NOS inhibitor L-NNA or the GC inhibitor ODQ). For sufficient cGMP to accumulate in tissues for immunohistochemical assays, preparations must be pretreated with PDE inhibitors (32). However, a 30-min incubation with PDE inhibitors completely precluded the increase in contractile tension produced by NE (incubation time used in previous studies where isometric tension was not monitored: 13, 20, 34, 40, 43) and hence, the study of relaxant responses. Accordingly, the exposure to PDE inhibitors was limited to 30 s before EFS or SNC, and these compounds remained present throughout the experiment (a total time in the presence of PDE inhibitors of 4 min). Exposure to PDE inhibitors for 30 s relaxed NE-precontracted preparations by 6.9 (5.0)% ($n = 20$) in the sheep and 24.4 (12.7)% ($n = 12$) in the rat preparations. This relaxation reached 39.1 (15.0)% ($n = 7$) in the sheep and 125.1 (30.2)% ($n = 7$) in the rat, after a 4-min exposure (control preparations exposed to PDE inhibitors alone) (Figs. 1 and 2; Table 1). This prominent relaxant effect of PDE inhibitors was nearly halved upon exposure to ODQ (0.1 mM), although additional inhibition of NOS by L-NNA (0.1 mM) produced no further reduction (Table 1; Figs. 1 and 2). Furthermore, incubation with the specific adenylate cyclase inhibitor SQ22536 (0.2 mM) significantly reduced PDE inhibitor-induced relaxation in the sheep, but not in the rat preparations, although this inhibition was not further enhanced by ODQ (Table 1).

Upon specific nitrergic stimulation (EFS in the presence of guanethidine and atropine, and with the addition of D-tubocurarine in the rat), a very rapid and prominent relaxant response was induced that peaked after 30 s at 63.7 (27.5)%, $n = 13$ in the sheep and 113.4 (33.1)%, $n = 12$ in the rat. This response was followed by a partial reversion and a sustained relaxation (Fig. 1), which was significantly higher than that produced by

Table 1. *Effects of inhibiting guanylate cyclase with ODQ, adenylate cyclase with SQ22536, and nitric oxide synthase with L-NNNA on the relaxant response induced by PDE inhibitors in urethras from sheep and rats*

	Rats			Sheep		
	Relaxation, %	*n*	*P*	Relaxation, %	*n*	*P*
Control	125.1 (30.2)	7		39.1 (15.0)	7	
ODQ (0.1 mM)	64.6 (27.2)	8	0.001	20.7 (5.1)	6	0.037
ODQ+L-NNA (0.1 mM)	72.1 (31.4)	7	0.007	18.6 (9.5)	5	0.023
SQ22536 (0.2 mM)	109.8 (45.6)	7	0.456	18.5 (6.8)	7	0.007
SQ22536+ODQ	76.3 (20.5)	7	0.004	19.7 (5.5)	5	0.040

Values are means (SD). *n,* No of animals; L-NNA, N^{ω}-nitro-L-arginine; PDE, phosphodiesterase. Preparations were precontracted with norepinephrine (NE; 50 μM) and exposed to IBMX (1 mM) and zaprinast (0.1 mM) for 4 min in the presence or absence (control) of the treatment indicated (applied 30 min before NE). ANOVA followed by *t*-test and the false discovery rate procedure were applied. *P* values express the difference with respect to the control conditions.

PDE inhibitors in control preparations in the sheep ($P = 0.021$), but not in the rat ($P = 0.613$; Fig. 2). However, a comparison of the half-relaxation times unmasked a significant ($P < 0.0001$) enhancement in the speed of relaxation upon EFS in the rat tissue (Fig. 2).

The addition of SNC (0.1 mM for 4 min) induced slightly slower relaxations that were as pronounced as those induced by EFS in both species (Fig. 1). As with EFS, the magnitude of relaxation was significantly higher ($P = 0.005$) than that induced by PDE inhibitors in the sheep tissue. Both relaxations were of a similar magnitude in the rat ($P = 0.358$), and only by measuring the half-relaxation time was a more rapid response to SNC observed ($P = 0.0027$; Fig. 2). Pretreatment with either L-NNA (0.1 mM) or ODQ (0.1 mM) induced pronounced inhibition of the relaxant responses to EFS and, similarly, ODQ reduced the response to SNC (Figs. 1 and 2).

cGMP Immunoreactivity in Sheep and Rat Urethras Under Different Experimental Conditions of Nitrergic Stimulation

In control preparations (from a total of 7 sheep and 4 rat preparations), which were immediately fixed after contraction with NE (50 μM) and incubated with PDE inhibitors for 4 min but not exposed to nitrergic stimulation, basal cGMP-ir was observed in some cells with a characteristic ICC morphology. These cells were located in the serosa (ICC-SR), especially in the rat (Fig. 3*A*) and in the lamina propia (ICC-LP), particularly in the sheep (see Fig. 5*B*). Few cGMP-ir ICC were observed in the muscle layers (ICC-M), although they were more abundant in the outer muscle layer of the sheep (Figs. 3*A* and 4*A*). cGMP-ir was also evident in some urothelial cells, especially in the most superficial cell layer in the rat (Fig. 3*A*), but not in the sheep urethra (Figs. 4, *E* and *F*), as well as in the vascular endothelium in both species (not shown).

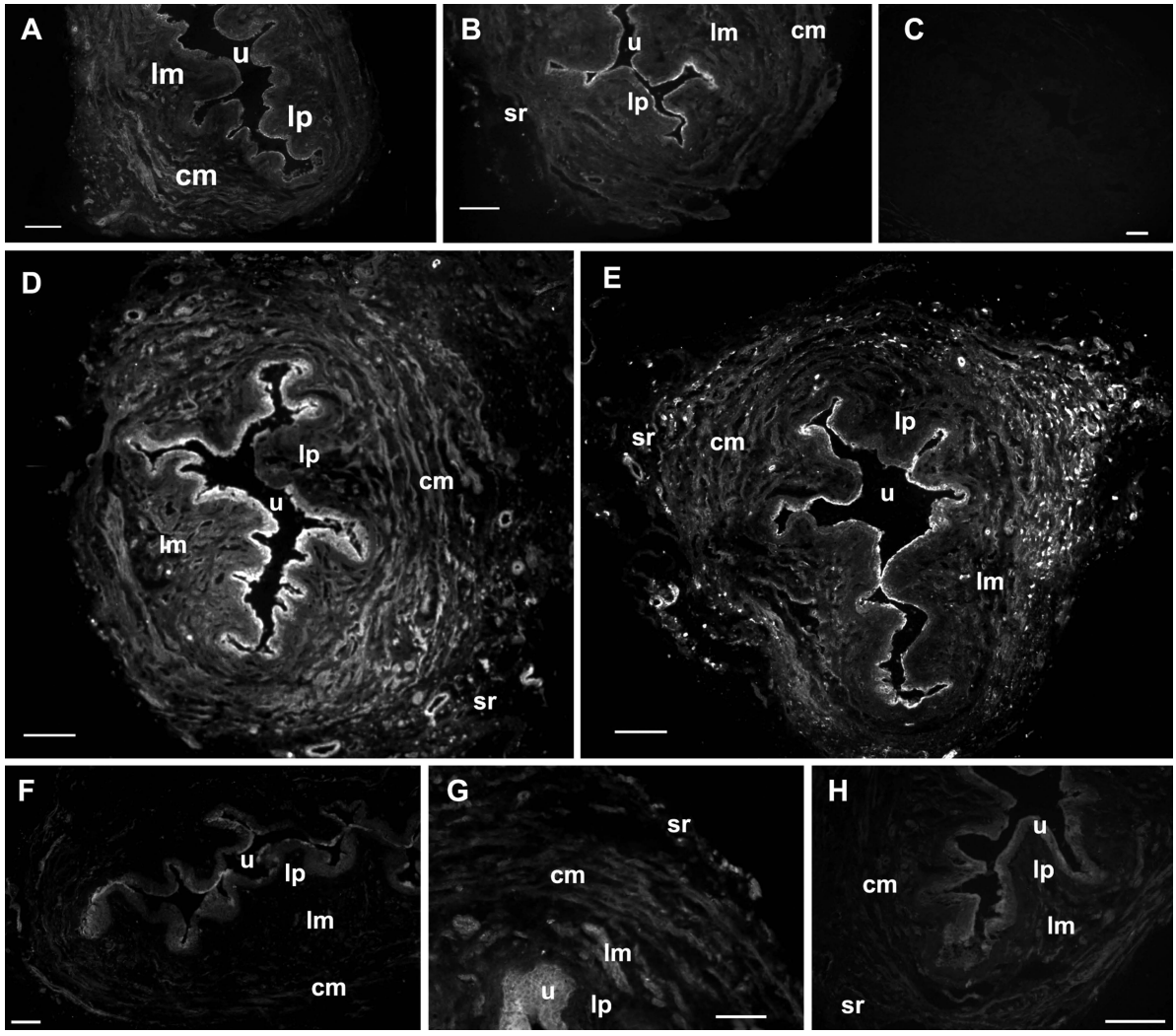

Fig. 3. Comparison of cGMP immunoreactivity (cGMP-ir) in ring sections of the rat urethra. *A*: under control conditions, there is a weak immunoreactivity in the epithelium and in some cells of the outer muscle layer. *B*: a mild reduction in basal cGMP-ir occurs in unstimulated preparations treated with L-NNA and ODQ. *C*: cGMP-ir is absent in a negative control (without primary antibody). *D*: prominent increase in cGMP-ir in a preparation subjected to EFS, showing an intense reaction in the smooth muscle cells (SMC), interstitial cells of Cajal (ICC), intramural vessels, and urothelium. *E*: ring stimulated with SNC displaying dense groups of highly cGMP-ir ICC in the outer circular muscle layer. *F–H*: pronounced inhibition of cGMP-ir in preparations stimulated by EFS in the presence of ODQ (*F*) or L-NNA (*G*) and in a preparation stimulated by SNC in the presence of ODQ (*H*). The experimental protocol is as shown in Fig. 1, and the images of the whole ring were constructed from 20–25 different microphotographs (×20) taken from the different regions of the ring. u, Urothelium; lp, lamina propia; lm, longitudinal muscle; cm, circular muscle; sr, serosa. Bars = 100 μm.

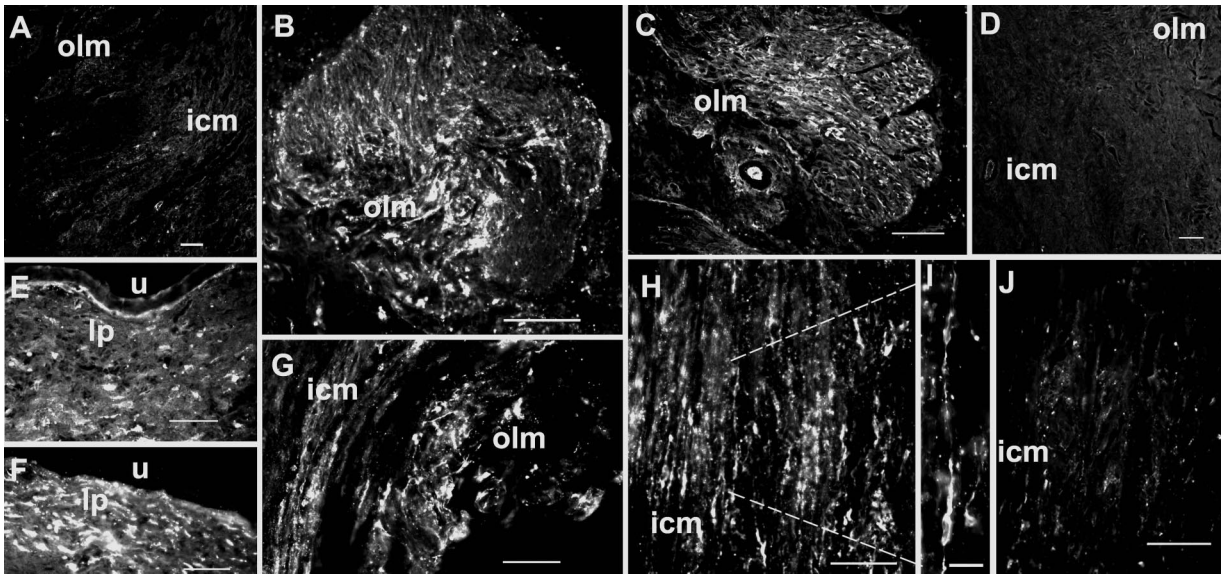

Fig. 4. Comparison of cGMP-ir in the sheep urethra. *A*: faint reaction in muscle layers under control conditions. *B* and *C*: prominent cGMP-ir in ICC scattered in the outer muscle layer of SNC- stimulated preparations. *D*: pronounced inhibition of the cGMP-ir induced by SNC due to the presence of ODQ. *E* and *F*: mucosal layer showing the absence of urothelial cGMP-ir and the presence of strong cGMP-ir in the ICC of the lamina propia, which did not change after stimulation with SNC (*E*) and was not inhibited by the presence of ODQ in a EFS-stimulated preparation (*F*). *G* and *H*: intense cGMP-ir in muscle layers of preparations stimulated by EFS where some ICC (ICC-M) can be clearly visualized. *I*: higher magnification of *H* showing 2 bipolar ICC-M with long interconnected prolongations running parallel to the SMC of the inner circular muscle layer. *J*: reduction in cGMP-ir in the inner circular muscle layer in a preparation stimulated by EFS in the presence of L-NNA. The experimental protocol is as shown in Fig. 1. olm, Outer longitudinal muscle; icm, inner circular muscle; u, urothelium; lp, lamina propia. Bars = 100 μm except in *I* (bar = 20 μm).

There seemed to be less cGMP-ir in preparations pretreated with ODQ and L-NNA (both at 0.1 mM; 5 from sheep and 3 from rats) than in control preparations (Fig. 3*B*), although the difference in the % area above threshold was not statistically significant in any of the urethral layers examined from sheep (outer muscle layer, $P = 0.333$ and inner muscle layer, $P = 0.324$), or the rat muscle wall ($P = 0.133$; Fig. 5*A*). Moreover, the fluorescence intensity did not seem to change in either the epithelium (Fig. 3*B*) or in the serosa and lamina propia (Fig. 5*B*).

Selective stimulation of nitrergic nerves by EFS (2 Hz, 4 min) induced a pronounced increase in cGMP-ir in the urethral muscle wall in both the rat (10 urethras; Figs. 3*D* and 5*A*) and the sheep (13 urethras; Figs. 4, *G–I*, and 5*A*). We observed cGMP-ir in cells with a characteristic ICC morphology as well as in SMC. This muscle staining makes the differentiation of cGMP-ir ICC-M more difficult as ICC-M were scattered in between the SMC or surrounding the muscle bundles. Other ICC-M were observed within the septa that separated muscle bundles. For instance, two strong cGMP-ir spindle-shaped intramuscular ICC-M with long interconnected prolongations running parallel to the inner circular SMC in the sheep urethra are shown in Fig. 4, *H* and *I*. The presence of cGMP-ir in ICC-LP in the sheep urethra was not affected by EFS (Fig. 5*B*), nor were ICC-SR affected in the rat urethra (Fig. 3*D*). After EFS, cGMP-ir was also conspicuous in the rat epithelium and vascular endothelium (Fig. 3*D*).

Exposure to SNC (0.1 mM for 4 min; 8 sheep and 6 rat preparations) induced very conspicuous cGMP-ir in ICC found in compact groups throughout the serosa and outer smooth muscle layers of the rat (Fig. 3*E*) and sheep (Fig. 4, *B* and *C*) urethra. Paradoxically, cGMP-ir in the SMC seemed to be weaker than in EFS-stimulated preparations, making the ICC stand out against a less intense background. Furthermore, the cGMP-ir ICC were distributed heterogeneously, with dense groups of cells appearing at certain sites in the urethral wall, while other areas were devoid of them (Fig. 3*E*). Furthermore, despite showing similar relaxation responses, significant cGMP-ir ICC populations were not identified in some preparations exposed to SNC (2 of 6 in the rat and 3 of 8 in the sheep). The less intense staining of SMC together with the variability in ICC labeling may explain the lack of significant differences in the % area above the threshold when SNC-stimulated preparations of sheep urethra were compared with control unstimulated ones ($P = 0.066$ in the inner muscle layer and $P = 0.093$ in the outer muscle layer; Fig. 5*A*). Intense cGMP-ir was also detected in the ICC-LP of the sheep urethra (Figs. 4*E* and 5*B*), the urothelium of the rat urethra (Fig. 3*E*), and the vascular endothelium in both species (Figs. 3*E* and 4*C*).

Inhibiting NOS with L-NNA (0.1 mM) impaired the increase in cGMP-ir induced by EFS (Figs. 3*G*, 4*J*, and 5*A*), showing that cGMP accumulation was directly related to NOS activation in nitrergic nerves (4 preparations from sheep and rats). Selective inhibition of soluble GC with ODQ (0.1 mM) also produced pronounced inhibition of cGMP-ir in preparations stimulated by EFS (4 sheep and 6 rats, Figs. 3*F* and 5*A*) or SNC (5 sheep and 6 rats, Figs. 3*H*, 4*D*, and 5*A*). As stated above, the high variability in ICC labeling in SNC-stimulated preparations could underlie the failure to detect significant differences in the % area above the threshold for SNC and SNC plus ODQ treatment in the sheep urethra ($P = 0.852$ in the inner and $P = 0.088$ in the outer muscle layers, Fig. 5*A*). The epithelium (Fig. 3, *F–H*) and vascular endothelium (not shown) of the rat urethra seemed to be less intensely stained following exposure to L-NNA, and especially ODQ than the EFS- or SNC-stimulated tissue. Surprisingly, most of the cGMP-ir ICC-LP in the sheep urethra (Figs. 4*F* and 5*B*) as well as the

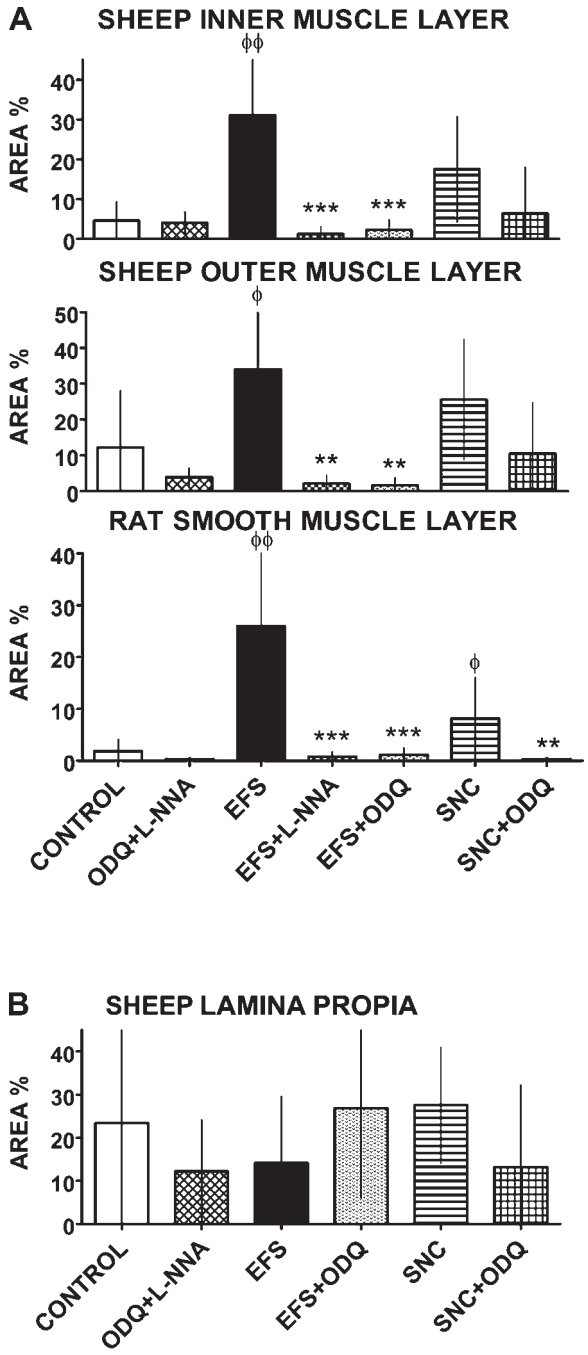

Fig. 5. Quantification of cGMP-ir in the sheep and rat urethra under different conditions of nitrergic stimulation. Preparations were stimulated by EFS (2 Hz, 4 min) or SNC (0.1 mM, 4 min) in the presence or the absence of L-NNA (0.1 mM) and/or ODQ (0.1 mM) and compared with unstimulated tissues. All preparations were precontracted with NE (50 μ) and pretreated with PDE inhibitors (See Fig. 1 for details of the experimental procedure), and they were all fixed immediately and processed for cGMP immunofluorescence. Hand-drawn fields of urethral sections were selected, and the percent area above the intensity threshold was measured (Area %; see text for details). In the sheep urethra, measurements were made independently in the inner circular muscle layer and outer longitudinal muscle layer (*A*) and the lamina propia (*B*), whereas the whole muscle coat was selected in the rat sections (*A*). Values are means ± SD of 5–13 different fields from at least 3 different animals. $\Phi P < 0.05$, $\Phi\Phi P < 0.01$ differences with respect to the controls. $^{**}P < 0.01$ and $^{***}P < 0.001$ differences with respect to preparations stimulated with EFS or SNC but not treated with L-NNA or ODQ (ANOVA followed by *t*-test applying the false discovery rate procedure).

ICC-SR in the rat urethra (not shown) were not affected by exposure to either L-NNA or ODQ.

Pyriform or spindle cell bodies containing a big ovoid nucleus surrounded by scant cytoplasm was the most common cGMP-ir ICC morphology (Fig. 4*I* and see Figs. 7*J* and 8, *A*, *E*, *F*, and *G*). In these cells, cGMP-ir was mainly observed in the cell body, extending into the cellular processes in some cases (Figs. 4, *G–I* and see Figs. 7*J* and 8, *A* and *D–H*), while in other cases cGMP-ir was distributed in irregular patches that did not clearly define the cell contour (not shown). cGMP-ir ICC were distributed irregularly throughout the urethral wall, and in the serosa, cGMP-ir ICC-SR formed groups of interconnected cells around the urethral surface (Fig. 3, *A*, *D*, and *E*). In both circular and longitudinal muscle layers, some cGMP-ir ICC-M had long cytoplasmic extensions that typically ran parallel to muscle fibers within the smooth muscle bundles (Figs. 4, *G–I* and see Fig. 8*A*). There were also cGMP-ir ICC that seemed to run between muscular bundles with long processes that formed interconnected "networks" (Figs. 4, *B* and *C* and see Fig. 8*H*). The population of cGMP-ir ICC-LP in the sheep urethra consisted of bipolar cells parallel to the urethral surface, particularly evident beneath the epithelium, and in which cGMP-ir was condensed in the soma (Figs. 4, *E* and *F*). Some cGMP-ir ICC in the lamina propia of the rat were orientated perpendicular to the epithelial surface (not shown).

Vimentin, cGMP/Vimentin, and c-kit/Vimentin Immunolabeling: Are ICC-Like Cells in the Urethra Real ICC?

In paraformaldehyde-fixed preparations, urethral ICC are at best only weakly stained by antibodies against c-kit, the tyrosine kinase receptor that specifically marks ICC in the gastrointestinal tract, although they are stained for vimentin (26, 28). Since we must use prefixed tissues (the cGMP antibodies were developed against cGMP in fixed tissues), we assessed whether vimentin is a suitable marker for ICC in the urethra and whether vimentin-ir cells are true ICC.

A total of 23 sheep and 14 rat urethras were immunostained for vimentin, and in both species vimentin-ir prominently stained cell processes (Fig. 6). Vimentin-ir cells were distributed throughout the urethral wall, and their morphology and distribution were similar but denser than for cGMP-ir cells. Thus spindle-shaped cells with one or more processes were found in the serosa (ICC-SR), muscular (ICC-M), and lamina propia (ICC-LP), forming interconnected networks (Fig. 6, *A–C* and *F*). In some cases, multiple interconnected cells formed "tracks" running across the entire urethral surface (Fig. 6*A*). In the muscle layers, both interfascicular and intramuscular vimentin-ir cells were observed (Fig. 6, *C–E*). Finally, in the sheep lamina propia bipolar cells accumulated densely parallel to the urothelial surface (Fig. 6*F*). In the rat, some cells lay perpendicular to the urothelium (Fig. 6*B*), and a dense ring of labeled cells was located between the inner longitudinal muscle layer and the lamina propia (Fig. 6*A*). Smooth muscle cells or nerve structures were not stained for vimentin.

The c-kit-ir was determined in four sheep and six rat urethras with two different antibodies (c-kit Ab-1 from Oncogene and c-kit H-300 from Santa Cruz). While neither antibody produced considerable c-kit-ir in rat preparations (not shown), the c-kit H-300 antibody produced weak c-kit-ir in the sheep urethra ICC. The cells recognized by this antibody had a

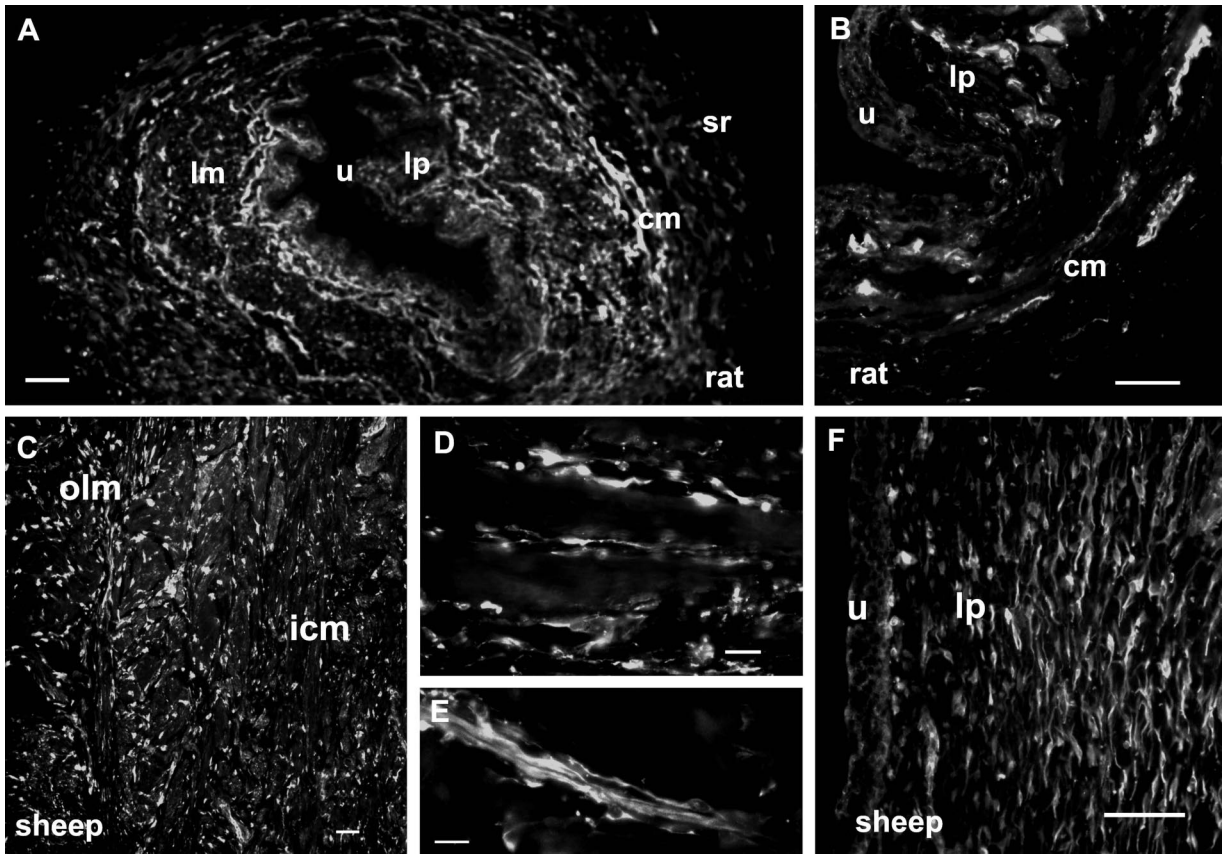

Fig. 6. Vimentin-ir in sheep and rat urethra. Low-power magnification of a complete ring (*A*), or a higher magnification of a section (*B*) of 2 different rat preparations, shows dense networks of vimentin-ir ICC in the lamina propia and muscle layers of the rat urethra. Note the presence of long interconnected processes surrounding the whole ring, which were especially dense at the junction of the lamina propia with the muscle layer, and at the outer circular muscle coat (*A*). In *B*, note the presence of vimentin-ir ICC distributed perpendicularly to the urothelial surface. *C–F*: vimentin-ir in sheep urethral sections. *C*: dense vimentin-ir ICC-M in between or inside smooth muscle bundles in both muscle layers of the urethral wall. *D* and *E*: high-magnification images showing parallel distribution of ICC-M along the smooth muscle fibers (*D*) and interconnected interfascicular ICC-M in between smooth muscle bundles (*E*). *F*: dense vimentin-ir in bipolar ICC in the lamina propia running parallel to the urothelium. u, Urothelium; lp, lamina propia; lm, longitudinal muscle; cm, circular muscle; olm, outer longitudinal muscle; icm, inner circular muscle. Bars = 100 μm (*A–C* and *F*) and = 20 μm (*D* and *E*).

morphology and distribution similar to those described for vimentin-ir and cGMP-ir, although there was a mild nonspecific reaction in SMC and epithelial cells (Fig. 7, *A* and *D*).

Double-labeling confirmed that both vimentin and c-kit colocalized in the sheep tissue, as did cGMP and vimentin in EFS or SNC stimulated tissues (Fig. 7). However, while all ICC from the sheep urethra that were labeled for c-kit were also vimentin-ir (Fig. 7, *A–F*), only a fraction of the vimentin-ir ICC were cGMP-ir in urethral preparations stimulated by SNC or EFS from both species (Fig. 7, *G–L*). It is noteworthy that vimentin-ir was concentrated at the periphery of the cell and particularly in the cell processes, which were much more clearly labeled by vimentin than by cGMP antibodies (Figs. 6 and 7).

Double Labeling for cGMP/nNOS and cGMP/PGP9.5: Relationship of ICC to Neuronal Structures

A total of 12 sheep preparations (6 stimulated by EFS and 6 by SNC) and 11 rat preparations (6 stimulated by EFS and 5 by SNC) were used to study the relationship between the ICC and neurons. Both combinations of double labeling showed that cGMP never colocalized with nNOS or PGP 9.5, although they were closely related (Figs. 8, 9, and 10). Nerve varicosities with PGP 9.5-ir or nNOS-ir were frequently found in close contact with cGMP-ir ICC throughout the urethral wall, in the muscle layer (Fig. 8, *A–C*, *E*, *F*, and *H*), lamina propia (Figs. 8*D* and 9, *A–C*), and serosa (Fig. 8*G*). Perivascular nNOS-ir nerves were found in intramural vessels with cGMP-ir in the endothelium (Fig. 9, *D–F*). By contrast, there was no nNOS-ir in ICC in sheep or rat urethras when they were double labeled for cGMP/nNOS (Fig. 8, *A–G*) or vimentin/nNOS (Fig. 8, *I* and *J*), indicating that these cells did not contain the enzymatic machinery for NO synthesis. Finally, no cGMP-ir was detected in nNOS-ir or PGP 9.5-ir nerve terminals in the muscle layer (Fig. 8, *A–C*, *E*, *F*, and *H*) or the lamina propia (Fig. 8*D*). Furthermore, when either nNOS-ir or PGP 9.5-ir nerve trunks were observed, cGMP-ir was present in adjacent and long nonneural cells that could be glia (Fig. 10).

DISCUSSION

This study presents the first evidence of cGMP production in both SMC and ICC in response to selective stimulation of urethral nitrergic nerves, supporting the functional innervation of ICC in the urethra. The specificity of this reaction was demonstrated, as NOS and GC inhibition impaired both the relaxation response and cGMP accumulation. In addition, the close association between EFS-stimulated ICC and nitrergic

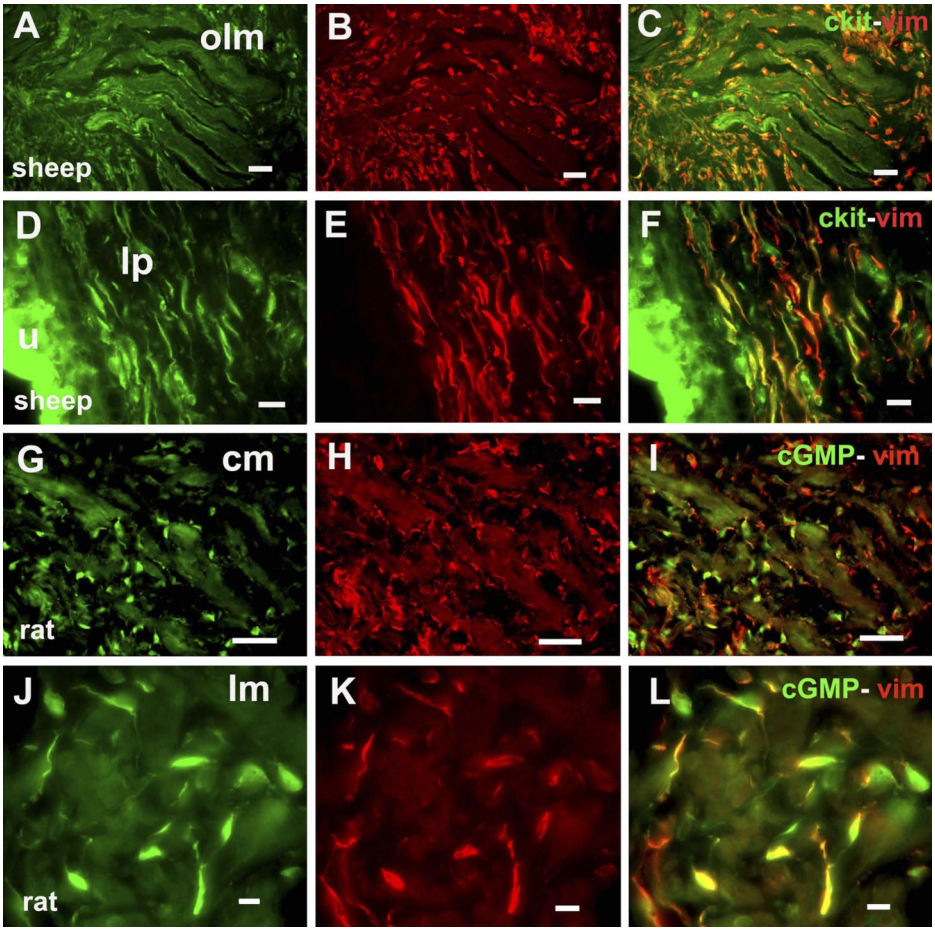

Fig. 7. Colocalization of vimentin-ir (red) with c-kit-ir (green) and cGMP-ir (green) in ICC from the sheep and rat urethra. Examples of c-kit-ir (*A* and *D*) and vimentin-ir (*B* and *E*) are shown along with their respective merged images (*C* and *F*) in the outer longitudinal muscle coat (*A–C*) and lamina propia (*D–F*) of the sheep urethra. Examples of cGMP-ir (*G* and *J*) and vimentin-ir (*H* and *K*) are shown, along with their respective merged images (*I* and *L*), in the muscle layer of a rat urethra subjected to EFS (*G–I*) or to SNC (*J–L*). u: urothelium; lp: lamina propia. Bars = 100 μm (*A–I*) and = 20 μm (*J–L*).

intramural nerve terminals provides further morphological evidence of this relationship.

Only one previous study has examined the accumulation of cGMP-ir in ICC by EFS of intrinsic nitrergic nerves, carried out in the canine proximal colon (32). In this tissue, cGMP-ir was present in ICC located at the internal surface of the circular muscle layer but not in the ICC-M. By contrast, strong cGMP-ir was observed in networks of urethral ICC-M upon exposure to NO donors (SNP or DEA-NO) in rabbits, pigs, guinea pigs, and humans (34, 40, 43). Here, SNC induced a similar pattern of strong cGMP-ir in groups of interconnected ICC in the outer muscle layers of the urethra in both sheep and rats. Moreover, we found weaker cGMP-ir in SMC similar to that described in the rabbit (40) and pig (43) when challenged with SNP or DEA-NO, respectively. These differences may reflect the higher capacity of ICC to accumulate cGMP in response to the relatively high concentrations of NO released by the NO donors in the presence of PDE inhibitors. It should be noted that the cGMP levels found in sheep urethral preparations exposed to SNC or NO gas were two orders of magnitude higher than those found upon EFS for the same level of relaxation (11, 12). Thus the functional significance of this cGMP accumulation remains unclear, and it does not seem to be related to relaxation. Where nitrergic innervation is scarce in the bladder and NO does not induce muscle relaxation (37), the accumulation of cGMP-ir induced by NO donors was localized exclusively to networks of ICC similar to those found here (13, 22). It is also noteworthy that in the gastric fundus of *Sl/Sl*^{d} or *W/W*^{v} mutant mice that specifically lack ICC-M the hyperpolarization response to the nitrergic transmitter or to exogenously added SNP was greatly diminished, while relaxation induced by this NO donor remained unaffected (3, 5). Together, these results strongly suggest that NO donors and the nitrergic neurotransmitter have different mechanisms of action, and some caution should be exerted when these compounds are used as exogenous nitrergic stimulants.

By contrast to NO donors, a similar increase in cGMP-ir was observed in either the ICC or SMC upon EFS in both sheep and rat urethras. In the gastrointestinal tract, it was suggested that the ICC may be interposed between nerves and SMC, acting as mediators in a serial process of neurotransmission. Indeed, while the gastric fundus of *Sl/Sl*^{d} or *W/W*^{v} mutant mice did not develop inhibitory or excitatory junction potentials in response to enteric nerves stimulation, the responses to exogenous acetylcholine were maintained (3, 5), suggesting that the loss of ICC led to the loss of neurotransmission. Alternatively, parallel ICC and SMC innervation has been proposed in some regions of the gut. In the colon of *W/W*^{v} rats, both rapid ATP-derived and the slow NO-mediated inhibitory neurotransmission is preserved, suggesting that NO released by nerves may directly affect SMC (1). Similarly, nitrergic relaxation of both the internal anal sphincter (36) and the lower esophageal sphincter in vivo (33) remains in *W/W*^{v} mice. This model of parallel innervation could explain our results, whereby ICC

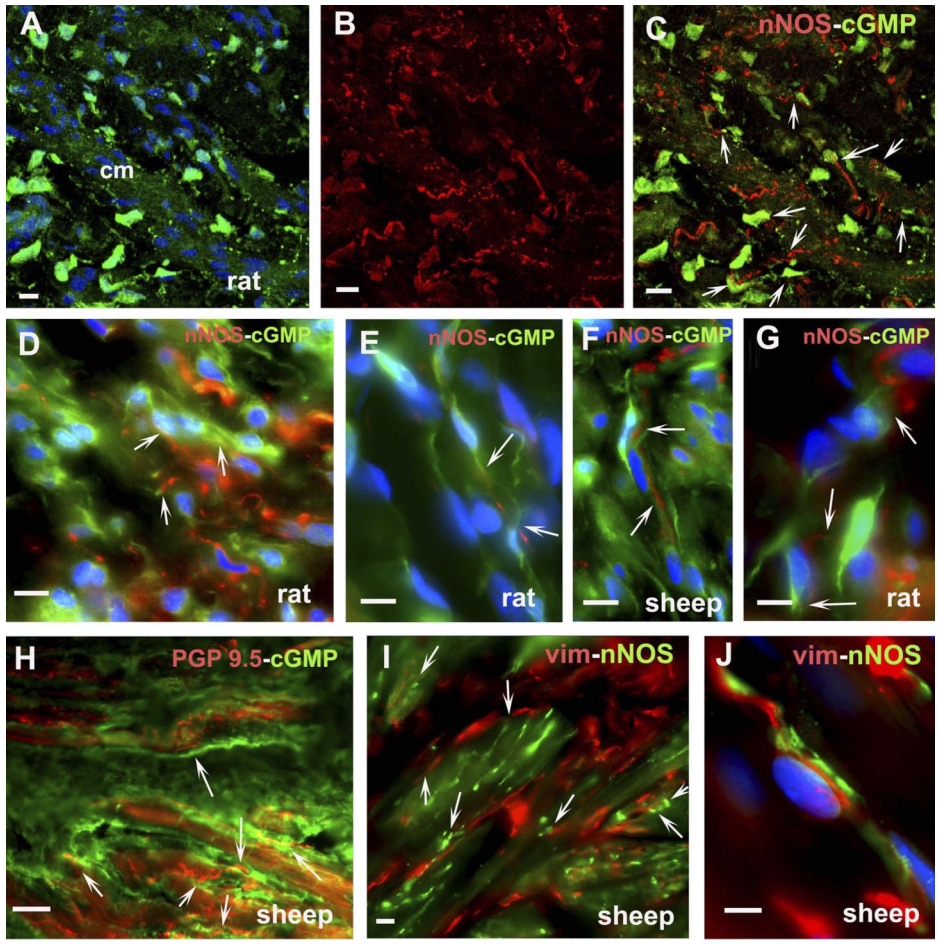

Fig. 8. There is no colocalization but rather a close relationship between cGMP-ir ICC and neuronal nitric oxide synthase (nNOS)-ir or PGP9.5-ir nerve structures. *A–C*: confocal images showing *z*-stacks of a 12-μm section of the circular muscle layer from a sheep urethra stimulated by SNC. cGMP-ir (green) in ICC together with nuclear counterstaining with 4′,6-diamino-2-phenylindole dihydrochloride (DAPI; blue, *A*) and nNOS-ir (red) in intramural nerves (*B*) are shown, along with the merged image (*C*). *D–F*: higher magnification of double cGMP-ir(green)/nNOS-ir (red) and nuclear counterstaining with DAPI (blue), showing the close relationship between cGMP-ir ICC and nNOS containing nerve terminals in the rat lamina propia treated with ODQ (*D*), in the muscular (*E*) and serosal (*G*) layers of rat urethra upon exposure to SNC, and in the muscular layer of sheep urethra following EFS (*F*). Double labeling for PGP9.5-ir (red)/cGMP-ir (green) in the muscular layers of sheep urethra exposed to SNC (*H*) shows no colocalization. Similarly, vimentin-ir (red) never colocalized with nNOS-ir (green) in double-labeled sections (*I* and *J*) of the muscular layer of the sheep urethra, although some vimentin-ir ICC were observed in close apposition to nitrergic nerves (*J*). Arrows indicate the points of close contact between ICC and nerve structures. cm, Circular muscle. Bars = 20 μm except in *H* (100 μm).

and SMC make sufficiently close contact with nerve terminals to allow both cells to respond to the transmitter released. These results agree with the recent proposal that both ICC and SMC may be simultaneously involved in urethral pacemaking (16, 17), and they suggest that both cell types may share several functions in the urethra. Whether ICC are regulatory or modulatory and how they affect neurotransmission and/or other SMC functions remain to be determined.

Our results show that only the population of cGMP-ir ICC found within the muscle layers of the urethras from sheep and rats (ICC-M) would be functionally coupled to nitrergic neurotransmission. Thus they accumulate more cGMP following EFS, which can be prevented by both L-NNA and ODQ. In addition, the cGMP-ir induced by SNC was blocked in the presence of ODQ. These features correlate with the pronounced relaxations induced by EFS and SNC in the same urethral preparations, which were also inhibited by L-NNA and/or ODQ. In contrast, the dense networks of ICC-SR and ICC-LP showed permanent and conspicuous cGMP-ir under all experimental conditions. Indeed, the presence of cGMP-ir is not sufficient to consider a cell responsive to NO, or even as a mediator of nitrergic neurotransmission. More recently, particulate GC was shown to be present in ICC of both the lamina propia and the serosa of the guinea pig bladder, but not in the ICC within the muscle coat (9). Moreover, these ICC responded to the natriuretic peptides ANP and BNP by augmenting their cGMP-ir, a phenomenon that was not inhibited by ODQ. Whether activation of particulate GC is behind the nonspecific accumulation of cGMP in ICC-SR and ICC-LP remains unclear. Together, these data suggest separate roles for ICC throughout the urethral wall. Only ICC-M seem to act as NO-dependent modulators of contractile activity, while ICC in the lamina propia and serosa could be involved in other functional aspects like sensorial perception or act as pacemaker cells.

It should be noted that the preparations here were exposed to PDE inhibitors for 4 min. While considerably shorter than that used when the effect of NO donors on cGMP-ir was studied previously in urinary tissues (~30 min) (13, 20, 34, 40, 43), a prominent relaxant effect was observed in basal conditions (without EFS or SNC stimulation), especially high in the rat urethra. In the human urethra, the PDE-5 inhibitors sildenafil, vardenafil, and tadalafil also induced complete relaxation of NE-precontracted strips, and they increased cGMP levels but not those of cAMP (43). Thus strong basal NO or GC activity may induce the basal cGMP-ir detected in some cells, including ICC, urothelium, and vascular endothelium. However, since both basal cGMP-ir and PDE inhibitor-induced relaxation were only partially reduced by ODQ and L-NNA, nonspecific mechanisms unrelated to GC or NOS activation may also be involved. There is significant activation of adenylate cyclase and the ensuing accumulation of cAMP that was inhibited by SQ22536 in the sheep but not the rat urethra. This activation seems likely to be secondary to the increase in cGMP because it was not further inhibited by ODQ treatment, and it could be related to cGMP-dependent modulation of PDE

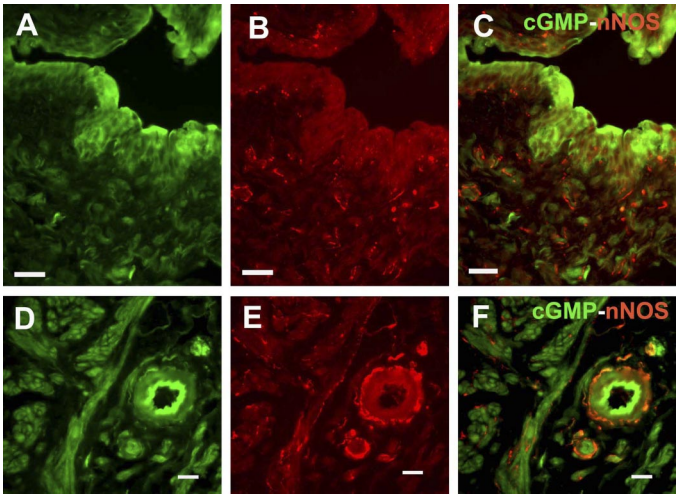

Fig. 9. *A–C*: double cGMP-ir (green)/nNOS-ir (red) in the rat urethra showing the presence of cGMP-ir in urothelial cells and the relationship between ICC and nitrergic nerves in the lamina propia. *D–F*: cGMP-ir (green) in the endothelium of an intramural vessel in the muscle layer of a sheep urethra and the perivascular distribution of nNOS-ir (red) nerves. cGMP-ir (*A* and *D*) and nNOS-ir (*B* and *E*) are shown along with their merged images (*C* and *F*). Bars = 20 μm.

for cAMP. In addition, we cannot rule out the involvement of other ODQ-independent mechanisms such as the activation of particulate GC (9) or the direct effects of PDE inhibitors on K^+ channels (24).

ICC in the urethra appear to be very weakly labeled for c-kit (a tyrosine kinase receptor encoded by the *c-kit* proto-oncogene), which has become the standard means of recognizing ICC in the gastrointestinal tract (18). Similarly, a small population of dispersed noncontractile cells in the rabbit urethra contained vimentin but were not c-kit-ir (28). Indeed, no c-kit-ir was detected in paraformaldehyde-fixed mouse urinary bladder and urethra, while networks of c-kit-ir ICC were described in the ureter (26). Similarly, in fixed gut tissue, no c-kit-ir were detected in ICC from the deep muscular plexus, a type of gastrointestinal ICC clearly involved in neurotransmission (41), bringing into question the use of c-kit as an exclusive marker for ICC. Despite the relatively weak c-kit-ir in our preparations, we considered that cells present in the rat and sheep urethras that showed vimentin- and cGMP-ir can be considered as true ICC for the following reasons: *1*) their characteristic spindle-shaped morphology with long processes, a big ovoid nucleus, and scant cytoplasm; *2*) vimentin-ir and c-kit-ir colocalized in the sheep urethra; and *3*) these cells were around and within muscle bundles, following the long the axis of the bundle and maintaining intimate contacts with intramural nerves, including nitrergic nerves. It cannot be ruled out that other cell types besides ICC were present, such as fibroblasts that are also immunoreactive for vimentin or c-kit. In fact, cells with morphological characteristics very similar to ICC were described as myofibroblasts in the bladder lamina propia (35), although, these ICC-LP play no role in nitrergic neurotransmission. It should also be noted that only a fraction of the total vimentin-ir ICC population in the urethra seems to respond to NO by accumulating cGMP, as found in the guinea pig and human bladder (34). Consequently, ICC might have different functions other than being the target for the NO action and they might develop distinctly into different types of ICC.

It has been suggested that ICC in the gut are themselves able to produce NO and, indeed, both nNOS and endothelial NOS have been identified in the ICC of the colon (39, 44). As in the human intestinal ICC (42), nNOS-ir was never found in the ICC from either the rat or sheep urethra. While the expression of an nNOS isoform not recognized by our nNOS antibodies cannot be ruled out, this possibility is not supported by the fact that NADPH-diaphorase histochemistry did not identify ICC in the sheep urethra (11, 14). Moreover, our results agree with those from the guinea pig urethra (34) and bladder (13) where no nNOS-ir was observed in ICC. In fact no cGMP-ir structures detected here colocalized with nNOS-ir. This concords with the control mechanism proposed in the central nervous system (21) by which GC would be inactivated by the same rise in Ca^{2+} needed to activate NOS in the NO-synthesizing cell. Indeed, our results do not confirm the presence of cGMP-ir in nerve structures, as described in the nerve trunks of the rabbit urethra (10) and in the varicose nerve terminals of the bladder from guinea pigs, humans (13, 34), or mice (22). It should also be noticed that in both the rat and sheep urethra, neither nNOS nor PGP 9.5 colocalized with cGMP in intramural nerve trunks, although cGMP-ir was present in nucleated structures parallel to nerve fibers that could be glia. Similar,

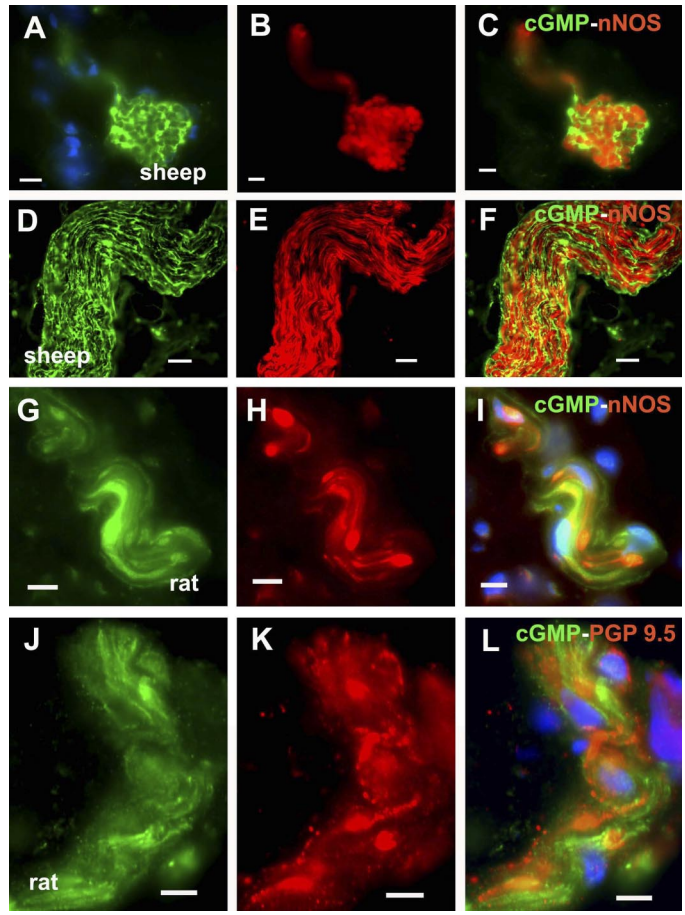

Fig. 10. Double cGMP-ir (green)/nNOS-ir (red; *A–I*) or cGMP-ir (green)/PGP9.5-ir (red; *J–L*) showing no colocalization of either pair of markers in intramural nerve trunks in the sheep (*A–F*) and rat (*G–L*) urethra. cGMP-ir (*A*, *D*, *G*, and *J*) and either nNOS-ir (*B*, *E*, and *H*) or PGP9.5-ir (*K*) are shown along with their merged images (*C*, *F*, *I*, and *L*). In *A*, *I*, and *L*, the nuclei are counterstained with DAPI (blue). Bars = 20 μm.

parallel staining of thin nerve terminals was observed (not shown) that may be due to the close apposition of Schwann cells. In visceral smooth muscle, it is known that Schwann cells of axon varicosities respond to endogenous transmitters such as ATP, producing Ca^{2+} transients (23). Whether Schwann cells in the urethra also respond to the neurally derived NO via cGMP requires further study. Nevertheless, it is clear that there is a close relationship between cGMP-ir ICC and nerve terminals, especially those containing nNOS, which is in accordance with previous studies (10, 13, 22, 34).

Finally, besides ICC and SMC, cGMP-ir was also observed in urothelial cells (although only in the rat urethra) and in the vascular endothelium. The presence of cGMP-ir in epithelial cells in response to NO donors is thought to be associated with sensory functions (13), and it seems to be species dependent. Indeed, this feature was described in the guinea pig urethra (34) and bladder (13) but not in the mouse bladder (10, 22) or in the human bladder and urethra (34). In the endothelium, cGMP-ir was observed under basal conditions, and it appears to increase upon stimulation, suggesting a role for cGMP in regulating blood flow to the urethra. Similar endothelial cGMP-ir in the wall of the human and pig urethra has also been described, where it colocalizes with endothelial NOS (43). Nevertheless, cGMP-ir has only rarely been observed in the vascular smooth muscle (not shown), even though perivascular nitrergic nerves are present.

Conclusions

In conclusion, for the first time we demonstrated that cGMP-ir accumulates in ICC following stimulation of intramural nitrergic nerves in the rat and sheep urethra, suggesting that they may act as cells responsive to nitrergic neurotransmission. Different functional types of cGMP-ir ICC form interconnecting networks at different locations in the urethral wall: serosa, mucosa, and muscle layer. Only muscular ICC (ICC-M) seem to be clearly involved in nitrergic transmission, in which nerve stimulation-induced cGMP responses were specifically prevented by NOS and GC inhibitors. No ICC were nNOS-ir, although there was a close relationship between cGMP-ir ICC and nNOS-containing nerve terminals, suggesting a functional relationship between them. Since, cGMP-ir was induced in both ICC-M and SMC upon EFS, these results agree with a parallel innervation model, in which both type of cells are effectors of the NO released by nerves. Whether ICC act as mediators and/or as regulators of neurotransmission is still to be elucidated.

ACKNOWLEDGMENTS

The authors are grateful to Jean de Vente (Department of Psychiatry and Neuropsychology, European Graduate School of Neuroscience, University of Maastricht, Maastricht, The Netherlands) for kindly providing the sheep antiserum against cGMP. The microphotographs were acquired and analyzed at the Microscopy and Cytometry Center (Complutense University, Madrid, Spain). Also, we thank Alfonso Cortés and Luis M. Alonso for technical assistance with the fluorescence and confocal microscopy.

GRANTS

This work was supported by grants from the Spanish "Ministerio de Educación y Ciencia" (BFU2006-15135-C02-01) and the "Comunidad de Madrid-Universidad Complutense de Madrid" (UCMGR85/06-920307).

REFERENCES

1. **Alberti E, Mikkelsen HB, Wang XY, Díaz M, Larsen JO, Huizinga JD, Jimenez M.** Pacemaker activity and inhibitory neurotransmission in the colon of Ws/Ws mutant rats. *Am J Physiol Gastrointest Liver Physiol* 292: G1499–G1510, 2007.
2. **Andersson KE, Wein AJ.** Pharmacology of the lower urinary tract: basis for current and future treatment of urinary incontinence. *Pharmacol Rev* 56: 581–631, 2004.
3. **Beckett EA, Horiguchi K, Khoyi M, Sanders KM, Ward SM.** Loss of enteric motor neurotransmission in the gastric fundus of Sl/Sld mice. *J Physiol* 543: 871–887, 2002.
4. **Brading AF, McCloskey KD.** Mechanisms of disease: specialized interstitial cells of the urinary tract-an assessment of current knowledge. *Nat Clin Pract Urol* 2: 546–554, 2005.
5. **Burns AJ, Lomax AEJ, Torihashi S, Sanders KM, Ward SM.** Interstitial cells of Cajal mediate inhibitory neurotransmission in the stomach. *Proc Natl Acad Sci USA* 93: 12008–12013, 1996.
6. **Cajal SR.** Histologie du système nerveux de l'homme et des vertébrés. Paris: Maloine, 1911.
7. **Curran-Everett D.** Multiple comparisons: philosophies and illustrations. *Am J Physiol Regul Integr Comp Physiol* 279: R1–R8, 2000.
8. **De Vente J, Hopkins DA, Markerink-van Ittersum M, Emson PC, Schmidt HHHW, Steinbusch HWM.** Distribution of nitric oxide synthase and nitric oxide-receptive, cyclic GMP-producing structures in the rat brain. *Neuroscience* 87: 207–241, 1998.
9. **De Vente J, Markerink-van Ittersum M, Gillespie JI.** Natriuretic peptide responsive, cyclic guanosine monophosphate producing structures in the guinea pig bladder. *J Urol* 177: 1191–1194, 2007.
10. **Fujiwara M, Andersson KE, Persson K.** Nitric oxide-induced cGMP accumulation in the mouse bladder is not related to smooth muscle relaxation. *Eur J Pharmacol* 401: 241–250, 2000.
11. **García-Pascual A, Triguero D.** Relaxation mechanisms induced by stimulation of nerves and by nitric oxide in sheep urethral muscle. *J Physiol* 476: 333–347, 1994.
12. **Garcia-Pascual A, Costa G, Labadia A, Jimenez E, Triguero D.** Differential mechanisms of urethral smooth muscle relaxation by several NO donors and nitric oxide. *Naunyn-Schmiedeberg's Arch Pharmacol* 360: 80–91, 1999.
13. **Gillespie JI, Markerink-van Ittersum M, de Vente J.** cGMP generating cells in the bladder wall: identification of distinct networks of interstitial cells. *BJU Int* 94: 1114–1124, 2004.
14. **Gonzalez-Soriano J, Martín-Palacios S, Rodriguez-Veiga E, Triguero D, Costa G, García-Pascual A.** Nitric oxide synthase in the external urethral sphincter of the sheep: immunohistochemical and functional study. *J Urol* 169: 1901–1906, 2003.
15. **Hashitani H, Edwards FR.** Spontaneous and neurally activated depolarization in smooth muscle cells of the guinea-pig urethra. *J Physiol* 514: 459–470, 1999.
16. **Hashitani H, Yanai Y, Kohri K, Suzuki H.** Heterogeneous CPA sensitivity of spontaneous excitation in smooth muscle of the rabbit urethra. *Br J Pharmacol* 148: 340–349, 2006.
17. **Hashitani H, Suzuki H.** Properties of spontaneous Ca^{2+} transients recorded from interstitial cells of Cajal-like cells of the rabbit urethra in situ. *J Physiol* 583: 505–519, 2007.
18. **Huizinga JD, Thuneberg L, Klüppel M, Malysz J, Mikkelsen HB, Bernstein A.** W/kit gene required for interstitial cells of Cajal and for intestinal pacemaker activity. *Nature* 373: 347–349, 1995.
19. **Johnston L, Sergeant GP, Hollywood MA, Thornbury KD, McHale NG.** Calcium oscillation in interstitial cells of the rabbit urethra. *J Physiol* 565: 449–461, 2005.
20. **Jongh RJ, van Koeveringe GA, van Kerrebroeck PEV, Markerink-van Ittersum M, de Vente J, Gillespie JI.** Alterations to network of NO/cGMP-responsive interstitial cells induced by outlet obstruction in guinea-pig bladder. *Cell Tiss Res* 330: 147–160, 2007.
21. **Knowles RG, Palacios M, Palmer RMJ, Moncada S.** Formation of nitric oxide from L-arginine in the central nervous system: a transduction mechanism for the stimulation of soluble GC. *Proc Nat Acad Sci USA* 86: 5159–5162, 1989.
22. **Lagou M, Drake MJ, Markerink-van Ittersum M, de Vente J, Gillespie JI.** Interstitial cells and phasic activity in the isolated mouse bladder. *BJU Int* 98: 643–650, 2006.
23. **Lin YQ, Bennett MR.** Schwann cells in rat vascular autonomic nerves activated via purinergic receptors. *Neuroreport* 17: 531–535, 2006.

24. **Medina P, Segarra G, Torondel B, Chuan P, Doménech C, Vila JM, Lluch S.** Inhibition of neuroeffector transmission in human vas deferens by sildenafil. *Br J Pharmacol* 131: 871–874, 2000.
25. **Persson K, Andersson KE.** Non-adrenergic, non-cholinergic relaxation and levels of cyclic nucleotides in rabbit lower urinary tract. *Eur J Pharmacol* 268: 159–167, 1994.
26. **Pezzone MA, Watkins SC, Alber SM, King WE, de Groat WC, Chancellor MB, Fraser MO.** Identification of c-kit-positive cells in the mouse ureter: the interstitial cells of Cajal of the urinary tract. *Am J Physiol Renal Physiol* 284: F925–F929, 2003.
27. **Sarna SK.** Are interstitial cells of Cajal plurifunction cells in the gut? *Am J Physiol Gastrointest Liver Physiol* 294: G372–G390, 2008.
28. **Sergeant GP, Hollywood MA, McCloskey KD, Thornbury KD, McHale NG.** Specialised pacemaking cells in the rabbit urethra. *J Physiol* 526: 359–366, 2000.
29. **Sergeant GP, Hollywood MA, McHale NG, Thornbury KD.** Spontaneous Ca^{2+} activated Cl^- currents in isolated urethral smooth muscle cells. *J Urol* 166: 1161–1166, 2001.
30. **Sergeant GP, Thornbury KD, McHale NG, Hollywood MA.** Characterization of norepinephrine-evoked inward currents in interstitial cells isolated from the rabbit urethra. *Am J Physiol Cell Physiol* 283: C885–C894, 2002.
31. **Sergeant GP, Johnston L, McHale NG, Thornbury KD, Hollywood MA.** Activation of the cGMP/PKG pathway inhibits electrical activity in rabbit urethral interstitial cells of Cajal by reducing the spatial spread of Ca^{2+} waves. *J Physiol* 574: 167–181, 2006.
32. **Shuttleworth CW, Xue C, Ward SM, de Vente J, Sanders KM.** Immunohistochemical localization of 3′,5′-cyclic guanosine monophosphate in the canine proximal colon: responses to nitric oxide and electrical stimulation of enteric inhibitory neurons. *Neuroscience* 56: 513–522, 1993.
33. **Sivarao DV, Mashimo HL, Thatte HS, Goyal RK.** Lower esophageal sphincter is achalasic in nNOS (−/−) and hypotensive in W/W (v) mutant mice. *Gastroenterology* 121: 34–42, 2001.
34. **Smet PJ, Jonavicius J, Marshall VR, De Vente J.** Distribution of nitric oxide synthase-immunoreactive nerves and identification of the cellular targets of nitric oxide in guinea-pig and human urinary bladder by cGMP immunohistochemistry. *Neuroscience* 71: 337–348, 1996.
35. **Sui GP, Wu C, Fry CH.** Electrical characteristics of suburothelial cells isolated from the human bladder. *J Urol* 171: 938–943, 2004.
36. **Terauchi A, Kobayashi D, Mashimo H.** Distinct roles of nitric oxide synthases and interstitial cells of Cajal in rectoanal relaxation. *Am J Physiol Gastrointest Liver Physiol* 289: G291–G299, 2005.
37. **Triguero D, Prieto D, García-Pascual A.** NADPH-diaphorase and NANC relaxations are correlated in the sheep urinary tract. *Neurosci Lett* 163: 93–96, 1993.
38. **Triguero D, Costa G, Labadia A, Jimenez E, Garcia-Pascual A.** Spontaneous photo-relaxation of urethral smooth muscle from sheep, pig and rat and its relationship with nitrergic neurotransmission. *J Physiol* 522: 443–456, 2000.
39. **Vannucchi MG, Corsani L, Bani D, Faussone-Pellegrini MS.** Myenteric neurons, and interstitial cells of Cajal of mouse colon express several nitric oxide synthase isoforms. *Neurosci Lett* 326: 191–195, 2002.
40. **Waldeck K, Ny L, Persson K, Andersson KE.** Mediator and mechanisms of relaxation in rabbit urethral smooth muscle. *Br J Pharmacol* 123: 617–624, 1998.
41. **Wang XY, Paterson C, Huizinga JD.** Cholinergic and nitrergic innervation of ICC-DMP and ICC-IM in the human small intestine. *Neurogastroenterol Motil* 15: 531–543, 2003a.
42. **Wang XY, Ward SM, Gerthoffer WT, Sanders KM.** PKC-ε translocation in enteric neurons and interstitial cells of Cajal in response to muscarinic stimulation. *Am J Physiol Gastrointest Liver Physiol* 285: G593–G601, 2003.
43. **Werkström V, Svensson A, Andersson KE, Hedlund P.** Phosphodiesterase 5 in the female pig and human urethra: morphological and functional aspects. *BJU Int* 98: 414–423, 2006.
44. **Xue C, Pollock J, Schmidt HHHW, Ward SM, Sanders KM.** Expression of nitric oxide synthase immunoreactivity by interstitial cells of the canine proximal colon. *J Auton Nerv Syst* 49: 1–14, 1994.

MANUSCRITO II

Am J Physiol Renal Physiol 297: F1353–F1360, 2009.
First published August 26, 2009; doi:10.1152/ajprenal.00403.2009.

Presence of cyclic nucleotide-gated channels in the rat urethra and their involvement in nerve-mediated nitrergic relaxation

Domingo Triguero, María Sancho, Marta García-Flores, and Ángeles García-Pascual

Department of Physiology, Veterinary School, Complutense University, Madrid, Spain

Submitted 16 July 2009; accepted in final form 20 August 2009

Triguero D, Sancho M, García-Flores M, García-Pascual A. Presence of cyclic nucleotide-gated channels in the rat urethra and their involvement in nerve-mediated nitrergic relaxation. *Am J Physiol Renal Physiol* 297: F1353–F1360, 2009. First published August 26, 2009; doi:10.1152/ajprenal.00403.2009.—We have addressed the distribution of cGMP-gated channels (CNG) in the rat urethra for the first time, as well as their putative role in mediating of the relaxation elicited by electrical field stimulation of nitrergic nerves. Functional studies have shown that specifically blocking CNG with L-*cis*-diltiazem leads to the rapid inhibition of urethral relaxation induced either by nitric oxide (NO) released by the nerves or by soluble guanylate cyclase activated with YC-1. By contrast, nerve-mediated noradrenergic contractions were only slowly and mildly reduced by L-*cis*-diltiazem. This effect was mimicked by lower concentrations of the D-diltiazem isomer, probably due to the nonspecific inhibition of voltage-dependent calcium channels. However, D-diltiazem did not affect relaxation responses. The expression of heteromeric retinal-like CNGA1 channels was demonstrated by conventional PCR on mRNA from the rat urethra. These channels were located in a subpopulation of intramuscular interstitial cells of Cajal (ICC) as well as in smooth muscle cells, although they were less abundant in the latter. CNG channels could not be visualized in any nervous structure within the urethral wall, in agreement with the emerging view that a subset of ICC serves as a target for NO. These channels could provide a suitable ionic mechanism to associate the changes in cytosolic calcium with the activation of the nitric NO-cGMP pathway and relaxation although the precise mechanisms involved remain to be elucidated.

nitric oxide; cGMP

MICTURITION IS INITIATED BY an abrupt loss of urethral smooth muscle sphincter tone that is mediated by the release of nitric oxide (NO) from the local nitrergic fiber network (see Ref. 1 for a review). It is generally accepted that this process involves the NO-dependent activation of soluble guanylate cyclase (GC), which provokes a transient increase in intracellular cGMP levels and the subsequent activation of PKG in urethral smooth muscle cells (1, 20). Some recent reports suggest that the interstitial cells of Cajal (ICC) act as a new cellular element in the NO-cGMP pathway. These cells are of mesenchymal origin, and they exist as interconnected networks in all the layers of the urethral wall. Many authors have described the ability of vesical and urethral ICC to accumulate cGMP upon exposure to exogenous NO donors (12, 26, 30). Furthermore, we recently reported that only a muscle subpopulation of urethral ICC undergo a significant increase in cGMP upon functional nitrergic activation (11), suggesting that these cells could be also targets of the NO released by nerves.

Address for reprint requests and other correspondence: D. Triguero, Dept. of Physiology, Veterinary School, Complutense Univ., Avda Puerta de Hierro s/n, 28040 Madrid, Spain (e-mail: dtriguer@vet.ucm.es).

Urethral ICC are far from electrically quiescent since they generate spontaneous Ca^{2+} oscillations, supporting their role as pacemakers. In a tonic organ like the urethra, pacemaker cells have been suggested to support the asynchronous recruitment of muscle units to maintain tone, very much like in skeletal muscle (22). The ionic mechanism thought to underlie this activity is initiated by inositol 1,4,5-triphosphate (IP_3)-mediated Ca^{2+} release from intracellular stores and the subsequent opening of Ca^{2+}-activated Cl^- channels in the rabbit urethra (17). In addition, extracellular Ca^{2+} entry through non-voltage-dependent Ca^{2+} channels is also needed for the spontaneous Ca^{2+} oscillations (24), and a Na^+/Ca^{2+} exchanger (NCX) working in a reverse mode has been suggested (4). The physiological relevance of the spontaneous ICC depolarization is reinforced by the fact that they can be modified by endogenous neurotransmitter release, suggesting that ICC act as mediators of neurotransmission as in the gut. Therefore, to define the involvement of ICC in the regulation of urinary motor function and their relationship with autonomic nervous control will require an analysis of the mechanisms of communication between all the cells involved in this pathway.

The hyperpolarization-activated (HCN) and the cyclic nucleotide-gated (CNG) channels are ion channels directly gated by the binding of intracellular cAMP and/or cGMP to a cytoplasmic cyclic nucleotide-binding domain. The functional roles of these ion channels are thought to be complex, and they are poorly understood (see updated reviews in Refs. 5 and 15). In clear contrast to the structurally related subfamily of HCN channels, CNG channels are weakly activated by changes in membrane potential, and their opening and gating are directly defined by the intracellular binding of cyclic nucleotides. These channels mainly carry an inward Na^+ and Ca^{2+} current which provokes membrane depolarization or local changes in cytosolic Ca^{2+} concentrations. Although initially described in bovine rod photoreceptors (19), their involvement in the control of photoresponse is already found as early as in ciliate protozoa (29). Indeed, it is now generally accepted that they may be found in sensory receptors, epithelia, and blood vessels and even in spermatozoa (see Ref. 5), participating in a plethora of physiological processes from sensory transduction to the control of fluid reabsorption at the alveolar epithelia (16). However, in most of these cases the specific role of CNG channels is unknown. Although CNG channels can conduct currents carried by mono- and divalent cations, there is growing interest in this family as they provide an alternative pathway for Ca^{2+} entry that is virtually independent of membrane voltage and that couples the activity of Ca^{2+}-regulated proteins to cAMP/cGMP signaling without involving protein kinases.

One of the most widely used specific inhibitors of cGMP-gated CNG channels is L-*cis*-diltiazem (15), while the D-isomer blocks voltage-gated Ca^{2+} channels. When analyzing the ef-

fect of synaptic vesicle depletion induced by the scorpion venom α-toxins in the sheep urethra, we observed that their depolarizing effect lead to pronounced NO synthase (NOS)- and GC-mediated relaxation that could be inhibited by L-*cis*-diltiazem (28). Similarly, L-*cis*-diltiazem was shown to inhibit relaxation elicited by electrical field stimulation (EFS) of intrinsic nitrergic nerves (28). These data strongly suggest that CNG channels are involved in the NO-cGMP signaling pathway active in the urethra.

In the present work, we further examine the possibility that retinal-like CNG channels (CNGA1), a functional subtype selectively gated by cGMP, are present in the rat urethra. We studied the cellular distribution of CNGA1 channels by immunofluorescence as well as the mRNA expression of the different subunits that form the functional channel. We show that CNGA1 channels are mainly present in a subpopulation of urethral ICC, and they are only weakly expressed in smooth muscle cells. In addition, the characterization of the functional effects of L-*cis*-diltiazem on both relaxant and contractile nerve-mediated responses induced by EFS provides new insights into the relevance of CNG channels in the regulation of urethral motility. We hypothesize that CNG could be a suitable link between the activation of the NO-cGMP pathway and the modulation of the nitrergic control of smooth muscle activity by the ICC.

EXPERIMENTAL PROCEDURES

Drugs and Solutions

Arginine vasopressin (AVP), atropine sulfate, guanethidine monosulfate, *d*-tubocurarine hydrochloride, 3-(5′-hydroxymethyl-2-furyl)-1-benzyl indazole (YC-1), and D-diltiazem were obtained from Sigma-Aldrich Chemie (Steinheim, Germany). L-*cis*-Diltiazem was obtained from Biomol International. The drugs were all dissolved in distilled water and stored at −20°C, and the working concentrations were reached by dilution in 0.9% NaCl.

Tissue Preparation

The lower urinary tract was obtained from 60 female Wistar rats (6–8 wk old and weighing 200–300 g) killed by cervical dislocation followed by exsanguination. After opening of the abdomen, the whole lower urinary tract was removed and maintained at 4°C in Krebs solution (in mM): 119 NaCl, 4.6 KCl, 1.5 $CaCl_2$, 1.2 $MgCl_2$, 15 $NaHCO_3$, 1.2 KH_2PO_4, 0.01 EDTA, and 11 glucose. All procedures were approved by the Complutense University Ethical Committee, and they were performed in accordance with European guidelines. Longitudinal strips (~3 mm wide and 5 mm long), or rings (3 mm wide) were obtained from the proximal urethra and used to study the relaxant and contractile responses, respectively.

Recording of Isometric Tension

Urethral preparations (strips or rings) were mounted between two stainless steel hooks in 5-ml organ baths containing Krebs solution at 37°C, and they were bubbled with a mixture of 95% O_2-5% CO_2 (pH 7.4). The isometric tension was recorded with Grass FT03C transducers (Grass Instruments, Quincy, MA) and displayed on a MacIntosh computer with a MacLab analog-to-digital converter, v 5.5 (AD Instruments, Hastings, East Sussex, UK). Preparations were equilibrated at a resting tension of 5 mN for 60 min, and their viability was tested by the contractile response elicited by exposure to high external K^+ (120 mM).

Urethral relaxation of nitrergic origin was achieved through EFS of strip preparations precontracted with AVP (0.1 μM), and in the continued presence of atropine (1 μM) and guanethidine (50 μM) to avoid cholinergic and adrenergic excitatory influences. D-Tubocurarine (10 μM) was also added to block the activation of urethral striated muscle. EFS was achieved with a Grass S-48 stimulator (Grass Instruments) connected to platinum electrodes placed parallel to the preparation and coupled to a Med-Lab stimulus splitter (Med-Lab Instruments, Loveland, CO). To construct relaxant frequency-response curves, square-wave pulses of 0.8 ms at supramaximal voltage (current strength, 200 mA) were delivered at 2-min intervals in trains of 5 s at a frequency ranging from 0.5 to 12 Hz. Subsequently, long-train duration (60 s) single relaxations at a frequency of 2 and 35 Hz were performed at 1-min intervals. After washing, the preparations were pretreated for 30 min with either L-*cis*-diltiazem (50 μM) or D-diltiazem (1 μM) before the contraction (AVP)-relaxation (EFS) protocol was again followed in the continued presence of these inhibitors. In a separate set of experiments, AVP-precontracted preparations were subjected to repetitive EFS (5 s, 10 Hz, at 1-min intervals) and L-*cis*-diltiazem (50 μM) was added at the peak of contraction while the repetitive EFS was maintained.

Urethral contractile responses were assessed on ring preparations by either EFS or exposure to a 120 mM K^+ solution. EFS delivered on basal tone consisted of 10–12 stimuli of 0.8-ms pulses in 5-s trains at a frequency of 35 Hz and at 1-min intervals. This stimulation paradigm was repeated at 10-min intervals, during which the preparations were incubated with increasing concentrations of L-*cis*-diltiazem (0.01 to 50 μM). Finally, the effect of L-*cis*-diltiazem (50 μM) on repetitive EFS was studied in a similar way to that described previously, except that the EFS was delivered at a frequency of 35 Hz on basal tone.

Depolarization induced by high external K^+ (120 mM) was used to assess the possible effect of both diltiazem isomers on voltage-dependent calcium channel activation. After challenging twice with K^+ (120 mM), preparations were incubated for 30 min with atropine (1 μM) and guanethidine (50 μM), which remained present for the rest of the experiment to avoid the release of excitatory neurotransmitters by the depolarizing stimuli. The preparations were then challenged again with high K^+, pretreated for 30 min with either L-*cis*- or D-diltiazem isomers (50 and 1 μM, respectively), and contracted again with 120 mM K^+. After extensive washing, the reversibility of the diltiazem inhibition was tested by a final exposure to high K^+. The effect of YC-1 (50 μM), a specific activator of soluble GC, was studied when added at the peak of contraction induced by AVP (0.1 μM) in the absence of or after a 15-min incubation with L-*cis*-diltiazem (50 μM).

Control preparations that were not exposed to drugs were run in parallel and subjected to the same protocols.

Immunofluorescence

Urethral preparations were processed for immunofluorescence studies as described previously (11). In brief, the tissue was fixed in ice-cold 4% paraformaldehyde in 0.1 M phosphate buffer (PB; pH 7.0), cryoprotected at 4°C with increasing concentrations of sucrose in PB (10 to 30%), snap-frozen in liquid nitrogen-cooled isopentane, and stored at −80°C for up to 15 days. Cryostat sections (10 μm: CM1850 UV, Leica Microsystems, Barcelona, Spain) of the urethra embedded in Tissue-Tek OCT compound were thawed onto poly-L-lysine-coated slides. From each urethra, consecutive sections were collected on separate slides to obtain 10–15 serial sections from the same animal. The slides were air-dried at room temperature for 12–24 h and then processed directly or stored at −80°C for no more than 30 days.

Urethral sections were washed with PB (3x, 5 min) and incubated for 60 min with 3% normal donkey antiserum (Chemicon International, Temecula, CA) containing 0.3% Triton X-100. The sections were incubated with primary antibodies diluted in 2% normal donkey serum and 0.3% Triton X-100 for 24 h at 4°C in a humidified chamber. The primary antibodies used were raised against CNGA1 (affinity-purified rabbit antiserum, 1:100) and vimentin (a mouse

monoclonal, clone V9; 1:100), both from Chemicon International, and α-smooth muscle actin (a mouse monoclonal antibody, 1:1,000) from Sigma-Aldrich Chemie. The sections were then incubated with the secondary antibodies for 2 h in the dark in a humidified chamber at room temperature. The secondary antibodies used were appropriately matched to the species in which the primary antibody was raised: donkey anti-rabbit Alexa Fluor 488 and donkey anti-mouse Alexa Fluor 594 (both diluted at 1:200; Molecular Probes, Eugene, OR). After washing (3 times, 10 min each) with PB, the nuclei were counterstained with 4′,6-diamino-2-phenylindole dihydrochloride (DAPI; 10.9 mM for 20–30 min; Sigma-Aldrich Chemie), and the sections were washed again and mounted with Prolong Gold antifade reagent (Molecular Probes). In all cases, a number of controls were performed in which the specificity of the immunoreactions was established by omitting the primary antibodies.

The labeled sections were examined under an Axioplan 2 fluorescence microscope (Carl Zeiss Microimaging, Göttingen, Germany) equipped with the appropriate filter sets. They were photographed with a Spot-2 digital camera (Diagnostic Instruments, Sterling Heights, MI), and the images were stored digitally as 12-bit images using MetaMorph 6.1 software (MDS Analytical Technologies, Toronto, ON). Digital images were subsequently transferred to Adobe Photoshop 8.0 (San Jose, CA).

RT-PCR

After dissection, samples of female rat urethra and retina were immediately frozen in liquid N_2 and total RNA was extracted with a Qiagen Rneasy Fibrous Tissue minikit. Conventional RT-PCR to amplify transcripts of CNGA1 and CNGB1 subunits was performed on a PerkinElmer thermocycler (Gene Amp PCR System 2400) in a 25-μl reaction volume using the Access RT-PCR system (Promega). The RT-PCR protocol involved: an incubation at 45°C for 45 min, and then at 94°C for 2 min; 35 cycles of 94°C for 30 s, 60°C for 45 s, and 68°C for 45 s; an elongation step was at 68°C for 7 min. Specific primers for CNGA1 amplification were designed based on the published sequence (accession number: NM_053497); forward primer 5-GTGCTGGATTCCGAGTATGT-3′ (positions 1081–1100) and reverse primer 5′-GCTTGAGTTTCTGCTGCATC-3′ (1923–1942). An aliquot of 0.5 μl from the first reaction was used as a template for a second round of amplification of 15 cycles, using two previously described nested primers (18); the forward primer was 5′-GCCACCATTGTCGGTAACATAGG-3′ (positions 1141–1163), and the reverse primer was 5′-TCATACTCAGCCAAGATTCGGGCA-3′ (positions 1895–1918). To amplify CNGB1, we used the primers described by Bönigk et al. (2): forward primer 5′-TGACGTCACCTCCGATGAGG-3′ (positions 612–631) and reverse primer 5′-GTAGGCTTTGCTGAGGATGG-3′ (1187–1206). An additional round of amplification was performed over a further 15 cycles with the same primers using 2 μl of the first PCR product. Similar procedures were performed on the retina, except for the second round of amplification, which was omitted. The sizes of the amplified fragments were verified in a 2% agarose gel stained with SYBR gold and visualized in a Bio-Rad Fluor-S MultiImager (Hercules CA).

Data Analysis

Urethral relaxation was expressed as the percentage of the tension elicited by AVP immediately before each stimulation, while contractions were expressed as a percentage of that elicited by control 120 mM K^+. The results are given as means ± SE from *n* experiments (from *n* different animals), and one-way ANOVA was used for multiple comparisons followed by the unpaired Student's *t*-test. Data were compared using GraphPad Prism 5 software (GraphPad Software, San Diego, CA).

RESULTS

Effects of L-Cis-Diltiazem and D-Diltiazem on Nitrergic Relaxation

The exposure of AVP (0.1 μM) precontracted rat urethral preparations to L-*cis*-diltiazem (50 μM) significantly inhibited the relaxation induced by nitrergic stimulation at all frequencies tested, following both short and long trains of EFS (Fig. 1, *A* and *B*). It should be noted that these rat urethral preparations were more sensitive to the effect of L-*cis*-diltiazem than sheep preparations, which showed a similar inhibition at 300 μM L-*cis*-diltiazem (28).

The inhibitory effect of L-*cis*-diltiazem (50 μM) on nitrergic relaxation had a rapid onset (Fig. 2). Repetitive short EFS (5 s, 10 Hz, at 1-min intervals) elicited a fairly constant and rapid urethral relaxation with a mild and progressive decay in the contractile tension (Fig. 2, *A* and *B*). The onset of the inhibitory effect of L-*cis*-diltiazem (50 μM) was rapid, inducing significant inhibition after the fourth EFS ($P < 0.05$), its effect being completed within the next six EFS (Fig. 2*B*).

When rat urethral preparations were exposed to D-diltiazem at a concentration routinely used to effectively block voltage-gated Ca^{2+} channels in urethral preparations (1 μM) (8), nitrergic relaxation remained unaffected at all the frequencies and durations of EFS tested (Fig. 3, *A* and *B*).

Effects of L-Cis-Diltiazem and D-Diltiazem on Nerve-Mediated Contractile Responses

L-*cis*-diltiazem exerted a dose-dependent inhibition of EFS-induced contractions (10–12 stimuli, 5 s, 35 Hz, 1-min intervals, Fig. 4*A*). Contractile responses were almost abolished on exposure to 50 μM L-*cis*-diltiazem, while a similar effect was obtained with D-diltiazem at 1 μM (data not shown). The time-dependent effect of L-*cis*-diltiazem (50 μM) was then tested by its addition after the fourth EFS in a protocol of short repetitive EFS (5 s, 35 Hz, 1-min intervals) on basal tone (Fig. 4*B*). As can be seen, the effect of L-*cis*-diltiazem on EFS-induced contractions had a much longer latency than on EFS-

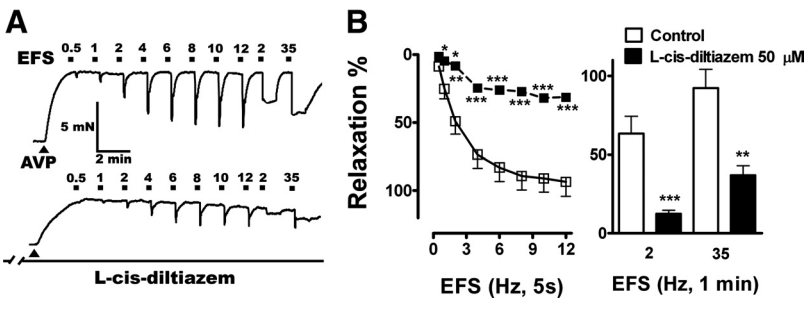

Fig. 1. Effects of L-*cis*-diltiazem on frequency-response nitrergic relaxations. *A*: representative traces showing the relaxation elicited by electrical field stimulation (EFS; 5 s, 0.5–12 Hz, and 1-min duration, 2 and 35 Hz) in AVP (0.1 μM)-precontracted rat urethral preparations in control (*top*) and after 30-min pretreatment with L-*cis*-diltiazem (50 μM, *bottom*). *B*: frequency-response curves in precontracted rat urethras induced by short (5 s, *left*) and long (1 min, *right*) EFS in the absence (open symbols and bars) and presence of L-*cis*-diltiazem (50 μM, filled symbols and bars). Values are means ± SE ($n = 6$ from different animals). $^{**}P < 0.01$, $^{***}P < 0.001$: significantly different from controls (1-way ANOVA followed by Student's *t*-test for unpaired observations).

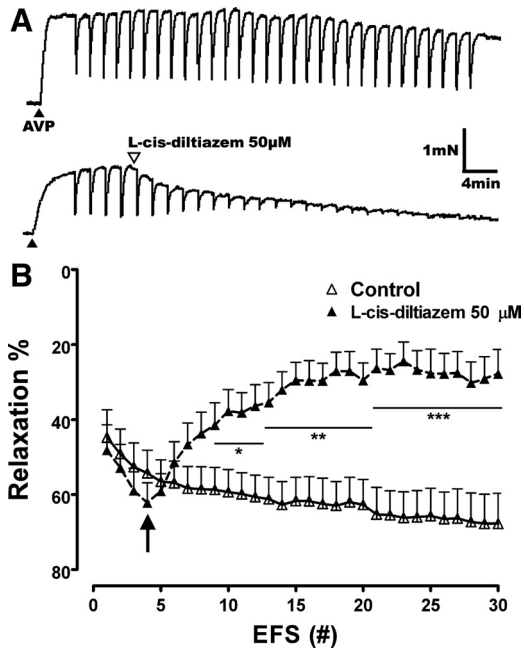

Fig. 2. Fast inhibitory effect of L-*cis*-diltiazem on nitrergic relaxation. *A*: representative traces showing the relaxation elicited by repetitive EFS (5 s, 10 Hz, at 1-min interval) in AVP (0.1 μM)-precontracted rat urethral preparations in control conditions (*top*) and when L-*cis*-diltiazem (50 μM) was added after the fourth EFS (*bottom*). *B*: temporal evolution of rat urethral relaxations induced by repetitive EFS (5 s, 10 Hz, 1-min interval; # indicates the stimulus number) in control preparations (open symbols) and following L-*cis*-diltiazem addition (50 μM, arrow, filled symbols). Values are means ± SE ($n = 6–8$ from different animals). $^{*}P < 0.05$, $^{**}P < 0.01$, $^{***}P < 0.001$: significantly different from controls (1-way ANOVA followed by Student's *t*-test for unpaired observations).

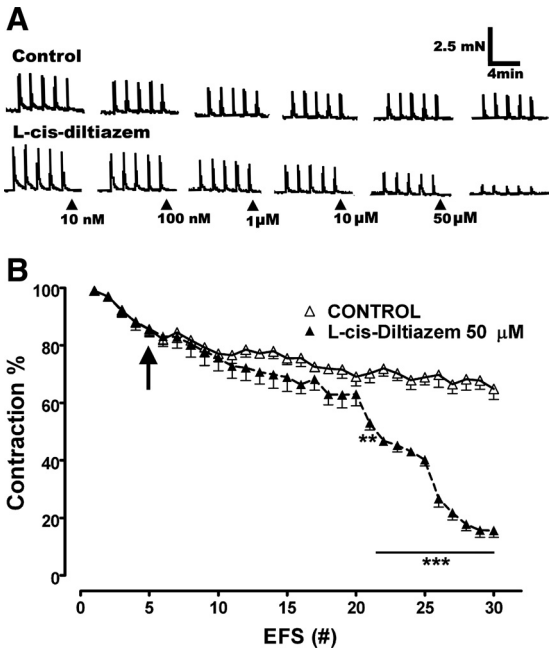

Fig. 4. Effects of L-*cis*-diltiazem on nerve-mediated contractile responses. *A*: representative traces showing the rat urethral contractions elicited by 5 pulses train EFS (5 s, 35 Hz, 1-min interval) on basal tension every 10 min in control conditions (*top*) and following 10-min incubation with increasing doses of L-*cis*-diltiazem. *B*: temporal evolution of rat urethral contractions induced by repetitive single EFS (5 s, 35 Hz, 1-min interval; # indicates the stimulus number) in control preparations (open symbols) and following L-*cis*-diltiazem addition (50 μM, arrow, filled symbols). Values are means ± SE ($n = 6$ from different animals). $^{**}P < 0.01$, $^{***}P < 0.001$: significantly different from controls (1-way ANOVA followed by Student's *t*-test for unpaired observations).

induced relaxations since it required an average of 15 additional EFS to significantly inhibit urethral contractions ($P < 0.05$, Fig. 4*B*).

Effects of L-Cis-Diltiazem and D-Diltiazem on 120 mM K^+-Induced Contractions

The effect of both diltiazem isomers on contraction elicited by the depolarization induced by high extracellular K^+ concentrations was subsequently tested. As can be seen, the contractile response induced by 120 mM K^+ was mildly decreased by blocking excitatory influences with atropine and guanethidine (Fig. 5, *A* and *B*). The remaining contraction can therefore be considered as due to direct smooth muscle depolarization. Preincubation with either L-*cis*-diltiazem or D-diltiazem (50 and 1 μM, respectively) significantly inhibited this residual high-K^+ contraction, an effect that was partially reversed by extensive washout of both isomers (Fig. 5, *A* and *B*). Thus L-*cis*-diltiazem seems to also affect L-type voltage-gated Ca^{2+} channel properties, although it seems to be >50 times weaker than the D-isomer.

Effects of L-Cis-Diltiazem on YC-1-Induced Relaxations

Exposure of AVP-precontracted urethral preparations to YC-1, a NO-independent specific activator of soluble GC, elicits a rapid relaxation that is thought to be due to the rise in intracellular cGMP levels subsequent to GC activation (Fig. 6, *A* and *B*). Such relaxation was completely abolished by preincubation with L-*cis*-diltiazem (50 μM), suggesting that it is mediated by the binding of intracellular cGMP to the cyclic binding domain of the putative CNG channel.

CNGA1 and CNGB1 mRNA Expression in the Rat Urethra

No CNG channels have been formerly identified in the urethra, although the functional results obtained in this study

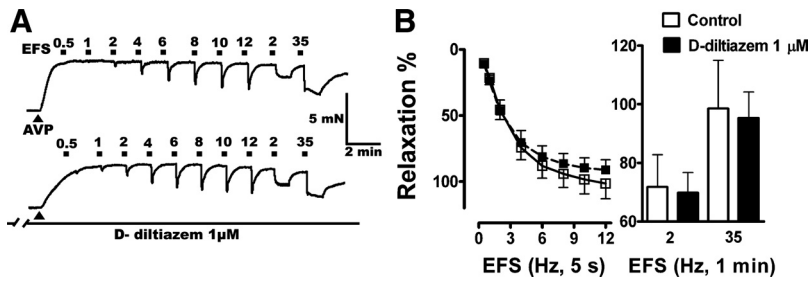

Fig. 3. Effects of D-diltiazem on frequency-response nitrergic relaxation. *A*: representative traces showing the relaxation elicited by EFS (5 s, 0.5–12 Hz, and 1-min duration, 2 and 35 Hz) in AVP (0.1 μM)-precontracted rat urethral preparations in control conditions (*top*) and after a 30-min pretreatment with D-diltiazem (1 μM, *bottom*). *B*: frequency-response curves in precontracted rat urethras for short (5 s, *left*) and long duration (1 min, *right*) in the presence (filled symbols and bars) and absence (open symbols and bars) of D-diltiazem pretreatment (1 μM). Values are means ± SE ($n = 6$ from different animals). No statistically significant differences were found between both groups (1-way ANOVA).

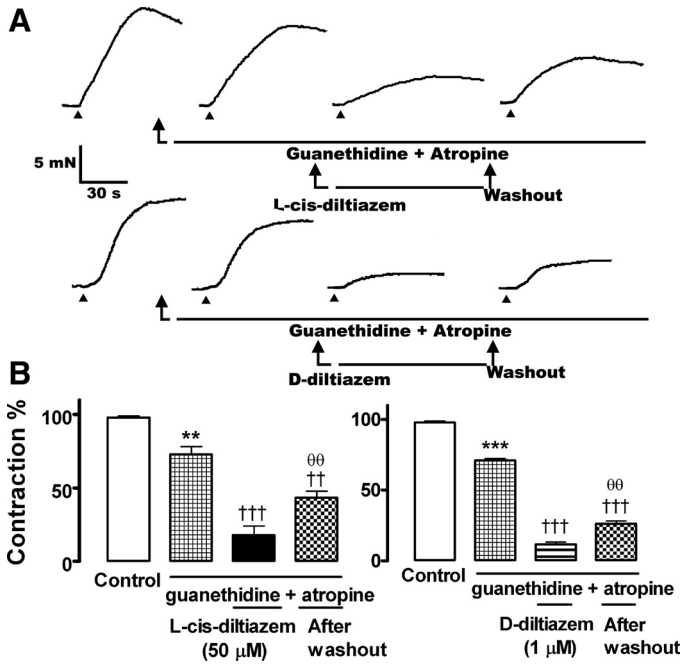

Fig. 5. Effects of L-*cis*-diltiazem and D-diltiazem on 120 mM K^+-induced contractions. *A*: representative traces showing the rat urethral contractions induced by 120 mM K^+ addition (triangle, from *left* to *right*) in control conditions, in the presence of guanethidine (10 μM) and atropine (1 μM), after treatment with L-*cis*-diltiazem (50 μM, *top* tracings) or D-diltiazem (1 μM, *bottom* tracings); and after washout of the diltiazem isomers. *B*: mean values of the 120 mM K^+-induced contraction in rat urethral preparations under the different experimental conditions detailed in *A*. Values are means ± SE (n = 6 from different animals). $^{**}P < 0.01$, $^{***}P < 0.001$: significantly different from controls. ††$P < 0.01$, †††$P < 0.001$: compared with guanethidine+atropine. ΘΘ$P < 0.01$ compared with the presence of diltiazem isomers (1-way ANOVA followed by Student's *t*-test for unpaired observations).

suggest that the heteromeric retinal-like CNG channel is likely to exist in this tissue. We carried out RT-PCR using specific primers based on the known sequences of the mRNA encoding CNGA1 and CNGB1 channel subunits, and a band of the predicted size was amplified that showed 99% identity with the rodtype CNGA1 sequence when sequenced. Another band was also identified of a similar size to that of the CNGB1 fragment obtained in the retina used as a positive control (Fig. 7). No bands were detected when the reactions were carried out without reverse transcriptase (data not shown), eliminating the possibility of genomic DNA contaminating the preparation. Nested primers were used in a second round of CNGA1 amplification to eliminate nonspecific fragments, and two rounds of amplification with the same primers pair were sufficient to obtain a visible band corresponding to CNGB1.

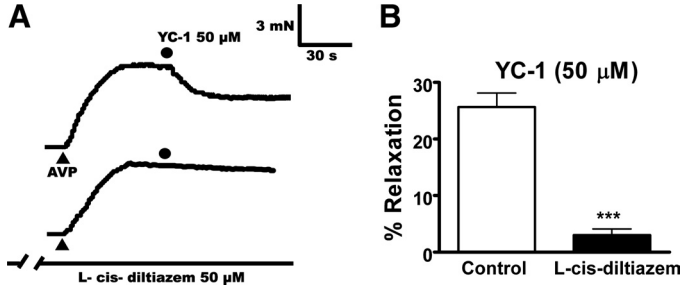

Fig. 6. *A*: representative traces showing the relaxant effect of YC-1 (50 μM) added at the peak (dot) AVP (0.1 μM)-precontracted rat urethral preparations (*top* tracing) and its inhibition by treatment with L-*cis*-diltiazem (50 μM, *bottom* tracing). *B*: bars graphs showing the effect of L-*cis*-diltiazem (50 μM, filled bar) on YC-1-induced relaxation (open bar). Values are means ± SE (n = 6 from different animals). $^{***}P < 0.001$ significantly different from control (Student's *t*-test for unpaired observations).

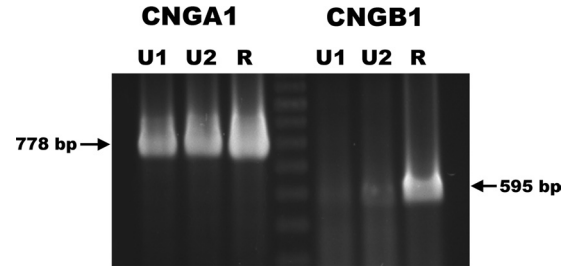

Fig. 7. Amplification of CNGA1 and CNGB1 cyclic nucleotide-gated channel subunits visualized in 2% agarose gels stained with SYBR gold. The mRNA transcripts of appropriate sizes for both subunits were expressed in rat urethral samples from different animals (U1 and U2; 778 bp for CNGA1 and 595 bp for CNGB1; *middle* lane, 100-bp ladder) compared with the transcripts in the rat retina (R) used as controls.

Immunofluorescence Detection of CNG1 Channels in the Urethral Wall

Specific CNG1 channel immunoreactivity (ir) was evident in two cell types in the rat urethra (Fig. 8), and it was not detected in the absence of the primary antibody (data not shown). Weak and diffuse CNG1-ir was present in smooth muscle cells where it colocalized with α-actin (Fig. 8, *A–C*). In addition, intense CNG1-ir was evident in spindle-shaped cells that were scattered between the smooth muscle bundles or in the connective septa (Fig. 8, *A–C*). These CNG1-ir cells were a subpopulation of the vimentin-ir cells present in the rat urethra (Fig. 8, *D–F*), confirming that they were ICC. These cells had long and thin cytoplasmic prolongations, usually running parallel to the corresponding smooth muscle fibers. CNG1-ir was not detected in any nervous structure such as nerve fibers, nerve trunks, or ganglia (data not shown).

DISCUSSION

In the present study, we further extend our understanding of the role of functional CNG channels in the urethra and in the relaxation response mediated by the NO-cGMP pathway. This activity was largely based on the effect of L-*cis*-diltiazem, a specific blocker of most cGMP-regulated CNG channels (15). Here, we demonstrate inhibition by L-*cis*-diltiazem in rat urethral preparations, which was fivefold more potent than that previously observed in sheep (28), being within the concentration range described in intact rod photoreceptors (27). Moreover, we observed a similar effect of L-*cis*-diltiazem in preliminary experiments on mouse preparations (Triguero D, unpublished observations). Hence this effect might be a general feature in different species.

By contrast, rat urethral noradrenergic contractions elicited by EFS (8) were only slowly and mildly inhibited by the same concentration of L-*cis*-diltiazem. This effect probably comes from a nonspecific action of L-*cis*-diltiazem rather than by inhibiting noradrenergic neurotransmission. In fact, L-*cis*-diltiazem inhibited contractile responses induced by either NE (28)

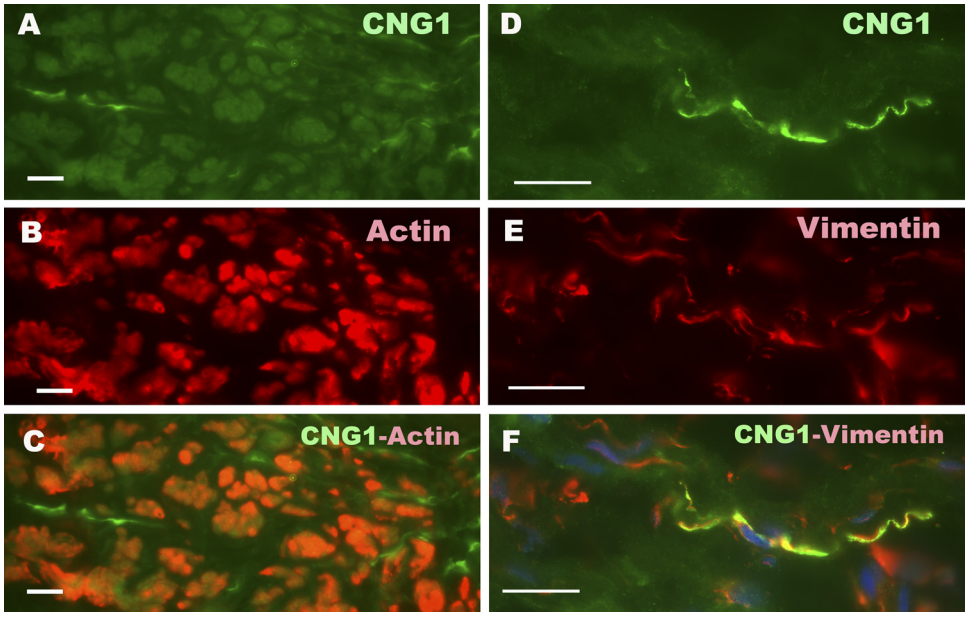

Fig. 8. Representative photomicrographs showing the immunolocalization of CNGA1 (green, *A*, *C*, *D*, and *F*), α-actin (red, *B* and *C*), and vimentin (red, *E* and *F*) within the smooth muscle layer of the rat urethra. Faint CNGA1-immunoreactivity (ir) can be observed in smooth muscle cells given its colocalization with α-actin-ir, while intense CNGA1-ir was evident in spindle-shaped cells scattered at the septa in between the muscle bundles (*A*–*C*). As shown in *D* to *F*, CNGA1-ir was coexpressed in a subpopulation of vimentin-ir interstitial cells of Cajal (ICC) of the rat urethral smooth muscular layer, characterized by their long cytoplasmic prolongations. Nuclei were counterstained with DAPI (blue) in *F*. Scale bars = 50 μm.

or AVP (present study). In addition, direct smooth muscle depolarization induced by high K^+ was similarly inhibited by L-*cis*-diltiazem, possibly due to its structural similarity with D-diltiazem, the most representative benzothiazepine calcium channel blocker. Indeed, while D-diltiazem is two orders of magnitude more potent than L-diltiazem in inhibiting the urethral contraction induced by both EFS and high K^+, it is completely ineffective on EFS-induced relaxations. In addition, the temporal profile of the inhibition elicited by L-*cis*-diltiazem, being extremely rapid on relaxations, could reflect the action of L-*cis*-diltiazem on different targets: a rapid blockade of the cyclic nucleotide-binding site of a CNG channel and a slower inhibition of L-type Ca^{2+} channels. Significantly, inhibition of cGMP-gated currents by low-micromolar concentrations of L-*cis*-diltiazem applied extracellularly in patch-clamp studies was described to be limited by the time required to change the solution, while D-diltiazem had little effect when applied intracellularly even at millimolar concentrations (27).

Alternatively, L-*cis*-diltiazem could abrogate the relaxation elicited by YC-1 in rat urethral preparations. YC-1 has been used to increase cGMP by directly and strongly activating soluble GC by NO-independent mechanisms (7). Therefore, the almost complete inhibition of the YC-1-induced relaxation of the rat urethra by L-*cis*-diltiazem strongly favors our proposal that its main effect on relaxation is mediated by the specific blockade of CNG channels.

All the members of the CNG channel subfamily are heterotetramers of the A and B subunits, with different subtypes, and the varying stoichiometries produce a wide variety of functional channels (15). Our RT-PCR experiments confirmed the expression of mRNA for the CNGA1 and CNGB1 subunits in the rat urethra which have been described to form the functional CNGA1 channel, usually referred as retinal-like CNG. The CNGA1 channel is considered to be specifically activated by cGMP, as it has a preferential Ca^{2+} conductance and it is specifically blocked by micromolar L-*cis*-diltiazem when applied intracellularly. However, this inhibition requires the presence of both subunits with a stoichiometry of 3 CNGA1:1 CNGB1 (15). Although not quantified, the apparent expression of transcripts for both subunits mRNAs suggests that the CNGA1 subunit is more strongly expressed. Although this channel is highly expressed in retinal cells, few CNG transcripts were found in a variety of tissues as brain, testis, kidney, and heart (3) as seems to occur in the urethra since two rounds of amplification were needed to visualize both bands. Such weak expression was initially surprising given the prominent inhibitory effect of L-*cis*-diltiazem on EFS-induced relaxation, suggesting their association to the abundant urethral nitrergic innervation.

CNGA1-ir was localized in a subpopulation of spindle-shaped vimentin-ir cells, the intramuscular urethral ICC, and more weakly in smooth muscle cells. However, CNGA1-ir was absent from nervous structures. This distribution of CNGA1-ir is very similar to that found for cGMP-ir in rat urethral preparations challenged with EFS or NO donors (11). Thus the same cells that produce an increase in cGMP in response to NO also express CNGA1, strongly suggesting that these channels mediate the effect of cGMP. One of the main known effectors of cGMP is cGMP-dependent protein kinase I (PKGI). In the mouse urethra, PKGI expression is restricted to smooth muscle and some non-nitrergic nerves, and it has not been described in ICC-like cells (20). Preferential expression of CNGA1 channels in ICC, while PKG-mediated mechanisms were more relevant in smooth muscle, might explain our results. New tools acting selectively on CNG channels and PKG are needed to define the relative importance of these two functional pathways in the downstream effects of cGMP in the urethra.

We believe that the most relevant result presented here is that CNG channel activation has a key role in nitrergic relaxation and that this control is mainly exerted through ICC. The morphology and distribution of urethral CNGA1-ir ICC resemble that of vimentin/cGMP-ir ICC, which has a close relationship with neuronal NOS- or PGP 9.5-ir nerve structures (11), suggesting a regulatory role for ICC in nitrergic transmission through CNG channels. Indeed, ICC in the urethra have been suggested to mediate neurotransmission (14, 23, 24) and to act

as pacemakers of the spontaneous myogenic tone (22). However, whether both functions are related and mediated by common mechanisms is unclear. It has been shown that ICC electrical activity is increased by neurally released NE through the activation of Ca^{2+}-activated Cl^- channels (23) while it is inhibited by NO donors and GC activators, probably by inhibiting the IP_3-mediated Ca^{2+} release (14, 24). Although the role of Ca^{2+} stores in the spontaneous transient depolarization of urethral ICC has been firmly established, some caveats remain (see 25). It has been suggested that capacitive calcium entry could contribute to the Ca^{2+}-propagating waves (17). However, the dependence of ICC on Ca^{2+} entry by alternative routes has also been highlighted. One of the proposed pathways involves Ca^{2+} influx through the NCX working in a reverse mode (4). However, they do not explain the physiological conditions that could change the ionic balance in the vicinity of the NCX to reverse its activity. The presence of CNG channels in ICC could provide another pathway for Ca^{2+} entry, participating in the generation and maintenance of Ca^{2+} waves.

It has to be stressed that our results indicate that CNG channel activation is involved in cGMP-mediated relaxation, which presupposes a decrease rather an increase in intracellular Ca^{2+} concentrations. Thus Ca^{2+} entry through CNG should not affect contractile filaments. In the gastrointestinal tract, it has been suggested that the ICC communicate with smooth muscle cells by electrical coupling through gap junctions (6). In addition, diffusible mediators released by ICC act on smooth muscle, and synapse-like junctions have been observed between ICC and smooth muscle cells (13). In previous studies, we suggested that the urethral nitrergic transmitter is not NO but a more stable nitrocompound, based on the fact that it was not sensitive to superoxide generators and to an extracellular NO scavenger (9, 10). An alternative explanation is that NO was released at tightly associated one-to-one communication sites between nerve terminals and the ICC, where it is not readily accessible to exogenous NO destructors, while another chemical mediator is released by the ICC to finally induce the smooth muscle relaxation. The cGMP-mediated entry of Ca^{2+} through CNG channels strategically located near to the release sites of ICC may be the stimulus needed to couple NO-cGMP responses to secretion. Indeed, control of exocytosis by CNG channels has been demonstrated previously at the cone synapses (21).

Conclusions

In conclusion, we have described the expression of CNG channels of the retinal-like type (CNGA1) in the rat urethra located in smooth muscle cells and, more remarkably, in a subpopulation of ICC. These channels seem to mediate the urethral relaxation elicited by functional activation of the NO-cGMP pathway, and they could be viewed as a suitable link between NOS activity in nitrergic nerves and the balance of ions such as Ca^{2+} in effector cells. The possible involvement of CNG channels in either the pacemaker function of ICC or in their function as mediators of neurotransmission should be considered.

ACKNOWLEDGMENTS

The microphotographs were acquired and analyzed at the Microscopy and Cytometry Centre (Complutense University, Madrid, Spain), and we thank Alfonso Cortés and Luis M. Alonso for technical assistance with the fluorescence microscopy. Sequence analysis of CNGA1 cDNA was carried out by the Genomic and Proteomic Service (Complutense University, Madrid, Spain). The authors are also indebted to Dr. Magdalena Torres (Dept. of Biochemistry and Molecular Biology IV, Complutense University) for assistance with the RT-PCR experiments. D. Triguero and A. García-Pascual were responsible for the conceptual and experimental design, data acquisition and analysis, and drafting of the manuscript; M. Sancho and M. García-Flores performed the work's organ bath (M. Sancho), RT-PCR (M. García-Flores), and immunofluorescence (M. Sancho) studies, as well as drafting and reviewing parts of the manuscript.

GRANTS

This work was supported by grants from the Spanish "Ministerio de Educación y Ciencia" (BFU2006-15135-C02-01) and the "Universidad Complutense de Madrid" (GR58/08-920307).

REFERENCES

1. **Andersson KE, Wein AJ.** Pharmacology of the lower urinary tract: basis for current and future treatment of urinary incontinence. *Pharmacol Rev* 56: 581–631, 2004.
2. **Bönigk W, Bradley J, Müller F, Sesti F, Boekhoff I, Ronnett GV, Kaupp B, Frings S.** The native rat olfactory cyclic nucleotide-gated channel is composed of three distinct subunits. *J Neurosci* 19: 5332–5347, 1999.
3. **Bradley J, Frings S, Yau KW, Reed R.** Nomenclature for ion channels subunits. *Science* 294: 2095–2096, 2001.
4. **Bradley E, Hollywood MA, Johnston L, Large RJ, Matsuda T, Baba A, McHale NG, Thornbury KD, Sergeant GP.** Contribution of reverse Na^+/Ca^{2+} exchange to spontaneous activity in interstitial cells of Cajal in the rabbit urethra. *J Physiol* 574: 651–661, 2006.
5. **Craven KB, Zagotta WN.** CNG and HCN channels: two peas, one pod. *Annu Rev Physiol* 68: 375–401, 2006.
6. **Daniel EE, Thomas J, Ramnarain M, Bowes TJ, Jury J.** Do gap junctions couple interstitial cells of Cajal pacing and neurotransmission to gastrointestinal smooth muscle? *Neurogastroenterol Motil* 13: 297–307, 2001.
7. **Friebe A, Koesling D.** Mechanism of YC-1-induced activation of soluble guanylyl cyclase. *Mol Pharmacol* 53: 123–127, 1998.
8. **García-Pascual A, Costa G, García-Sacristán A, Andersson KE.** Calcium dependence of contractile activation of isolated sheep urethra. I. Responses to electrical stimulation. *Pharmacol Toxicol* 69: 263–269, 1991.
9. **García-Pascual A, Triguero D.** Relaxation mechanisms induced by stimulation of nerves and by nitric oxide in sheep urethral muscle. *J Physiol* 476: 333–347, 1994.
10. **García-Pascual A, Labadía A, Costa G, Triguero D.** Effects of superoxide anion generators and thiol modulators on nitrergic transmission and relaxation to exogenous nitric oxide in the sheep urethra. *Br J Pharmacol* 129: 53–62, 2000.
11. **García-Pascual A, Sancho M, Costa G, Triguero D.** Interstitial cells of Cajal in the urethra are cGMP-mediated targets of nitrergic neurotransmission. *Am J Physiol Renal Physiol* 295: F971–F983, 2008.
12. **Gillespie JI, Markerink-van Ittersum M, DeVente J.** cGMP generating cells in the bladder wall: identification of distinct networks of interstitial cells. *BJU Int* 94: 1114–1124, 2004.
13. **Harhun MI, Gordienko DV, Povstyan OV, Moss RF, Bolton TB.** Function of interstitial cells of Cajal in the rabbit portal vein. *Circ Res* 95: 619–626, 2004.
14. **Hashitani H, Suzuki H.** Properties of spontaneous Ca^{2+} transients recorded from interstitial cells of Cajal-like cells of the rabbit urethra in situ. *J Physiol* 583: 505–519, 2007.
15. **Hofmann F, Biel M, Kaupp UB.** International Union of Pharmacology. LI. Nomenclature and structure-function relationships of cyclic nucleotide-regulated channels. *Pharmacol Rev* 57: 455–462, 2005.
16. **Jain L, Chen XJ, Brown LA, Eaton DC.** Nitric oxide inhibits lung sodium transport through a cGMP-mediated inhibition of epithelial cation channels. *Am J Physiol Lung Cell Mol Physiol* 274: L475–L484, 1998.
17. **Johnston L, Sergeant GP, Hollywood MA, Thornbury KD, McHale NG.** Calcium oscillations in interstitial cells of the rabbit urethra. *J Physiol* 565: 449–461, 2005.
18. **Kingston PA, Zufall F, Barnstable CJ.** Rat hippocampal neurons express genes for both rod retinal and olfactory cyclic nucleotide-gated

channels: novel targets for cAMP/cGMP function. *Proc Natl Acad Sci USA* 93: 10440–10445, 1996.
19. **Koch KW, Kaupp UB.** Cyclic GMP directly regulates a cation conductance in membranes of bovine rods by a cooperative mechanism. *J Biol Chem* 260: 6788–6800, 1985.
20. **Persson K, Pandita RK, Aszodi A, Ahmad M, Pfeifer A, Fässler R, Andersson KE.** Functional characteristics of urinary tract smooth muscles in mice lacking cGMP protein kinase type I. *Am J Physiol Regul Integr Comp Physiol* 279: R1112–R1120, 2000.
21. **Rieke F, Schwartz EA.** A cGMP-gated current can control exocytosis at cone synapses. *Neuron* 13: 863–873, 1994.
22. **Sergeant GP, Hollywood MA, McCloskey KD, Thornbury KD, McHale NG.** Specialised pacemaking cells in the rabbit urethra. *J Physiol* 526: 359–366, 2000.
23. **Sergeant GP, Thornbury KD, McHale NG, Hollywood MA.** Characterization of norepinephrine-evoked inward currents in interstitial cells isolated from the rabbit urethra. *Am J Physiol Cell Physiol* 283: C885–C894, 2002.
24. **Sergeant GP, Johnston L, McHale NG, Thornbury KD, Hollywood MA.** Activation of the cGMP/PKG pathway inhibits electrical activity in rabbit urethral interstitial cells of Cajal by reducing spatial spread of Ca^{2+} waves. *J Physiol* 574: 167–181, 2006.
25. **Sergeant GP, Hollywood MA, McHale NG, Thornbury KD.** Ca^{2+} signalling in urethral interstitial cells of Cajal. *J Physiol* 576: 715–720, 2006.
26. **Smet PJ, Jonavicius J, Marshall VR, DeVente J.** Distribution of nitric oxide synthase-immunoreactive nerves and identification of the cellular targets of nitric oxide in guinea-pig and human urinary bladder by cGMP immunohistochemistry. *Neuroscience* 71: 337–348, 1996.
27. **Stern JH, Kaupp UB, MacLeish PR.** Control of the light-regulated current in rod photoreceptors by cyclic GMP, calcium and L-diltiazem. *Proc Natl Acad Sci USA* 83: 1163–1167, 1986.
28. **Triguero D, González M, García-Pascual A, Costa G.** Atypical relaxation by scorpion venom in the lamb urethral smooth muscle involves both NO-dependent and -independent responses. *Naunyn-Schmiedeberg's Arch Pharmacol* 361: 151–159, 2003.
29. **Walerczyk M, Fabczak H, Fabczak S.** Detection and localization of a putative cyclic-GMP-activated channel protein in the protozoan ciliate Stentor coeruleus. *Protoplasma* 227: 139–146, 2006.
30. **Werkström V, Svensson A, Andersson KE, Hedlund P.** Phosphodiesterase 5 in the female pig and human urethra: morphological and functional aspects. *BJU Int* 98: 414–423, 2006.

MANUSCRITO III

Involvement of cyclic nucleotide–gated channels in Ca^{2+} oscillations under control conditions and in the presence of increased cyclic GMP levels in isolated interstitial cells of Cajal from the rabbit urethra

Maria Sancho[a,*], Angeles Garcia-Pascual[a], Domingo Triguero[a]and Gerard P. Sergeant[b]

From:

[a]Department of Physiology, School of Veterinary Medicine, Complutense University, Madrid, Spain.

[b]Smooth Muscle Research Centre, Dundalk Institute of Technology, Dublin Road, Dundalk, Co. Louth, Ireland.

***Corresponding Author**:

Maria Sancho, Department of Physiology, School of Veterinary Medicine, Avda. Puerta de Hierro s/n, Complutense University, 28040 Madrid, Spain.

Telephone:3413943842; Fax: 3413943864; e-mail: mariasanchogonzalez@hotmail.com

Abstract

The cyclic nucleotide-gated channels (CNG1) are ion channels gated by the binding of intracellular cGMP, which would allow the entry of Ca^{2+} inside the cell. Although they are known to link nitric oxide (NO)-cGMP pathway activation to urethral relaxation, the precise mechanisms involved remain to be elucidated. We have addressed the expression of CNG1 channels in smooth muscle cells (SMC) and interstitial cells of Cajal (ICC) isolated from the rabbit urethra, as well as the effects of their specific blockade by L-cis-Diltiazem, on spontaneous Ca^{2+} waves as well as on Ca^{2+} oscillations recorded in the presence of raised cGMP levels. These cGMP increases were provoked by different treatments acting in separate elements of the NO-cGMP pathway. Confocal imaging on freshly dispersed SMC and ICC showed that L-cis-Diltiazem significantly reduced the frequency and amplitude of Ca^{2+} waves as well as in the basal calcium in both type of cells. In contrast, the isomer D-diltiazem was only efective in SMC by acting on L-type voltage-gated Ca^{2+} channels. Reduction of intracellular Ca^{2+} events were observed when both type of cells were exposed to different procedures of increasing cGMP levels with the following order of potency: DEA-NO > YC-1 > PDE inhibitors > 8-Br-cGMP. L-cis-Diltiazem did inhibit these changes and its effect was additive to the previous reduction in Ca^{2+} oscillations, probably due to their unspecific effect on L-type Ca^{2+} channels. The expression of heteromeric retinal-like CNG1 channels was demonstrated by immunocitochemistry in both isolated SMC and ICC with big differences in intensity between both type of cells. Weak and diffuse CNG1- immnoreactivity (ir) was present in SMC (also showing α-actin-ir), while very intense CNG1-ir was evident in vimentine-ir ICC, mostly located in very thin spines emerging from the ICC body and prolongations. Together, these results indicate that CNG channels could provide a new and exclusive pathway for Ca^{2+} entry in ICC that participates in the generation and maintenance of spontaneous Ca^{2+} waves, but not in the reduction in Ca^{2+} events induced by cGMP in both cells. The mechanisms behind the involvement of CNG channels in the proposed function of ICC as intermediaries of nitrergic neurotransmission await further investigations.

1. Introduction

ICC were first described in the gastrointestinal tract, where they are believed to generate and propagate pacemaker activity, to act as stretch receptors, or being intermediaries between nerve and SMC in both cholinergic and nitrergic neurotransmission [1, 2]. Today, cells similar to gastrointestinal ICC have been described in a wide variety of smooth muscle organs, including the urinary tract [3].

The rabbit urethra contains a vimentin-ir population of cells with many characteristics of the gastrointestinal ICC [4]. While smooth muscle cells (SMC) are electrically quiescent, urethral ICC are spontaneously active, displaying Ca^{2+} oscillations coupled to firing of transient inward currents that supports their role as pacemakers [4]. In urethral ICC, a Ca^{2+} wave is initiated by a localized release of Ca^{2+} through ryanodine receptors (RyR) present in intracellular stores and propagated by regenerative release from inositol 1,4,5-triphosphate receptors (IP_3R). Calcium oscillations also require extracellular Ca^{2+} [5, 6] and a role for reverse mode Na^{2+}/Ca^{2+} exchange (NCX) across the plasma membrane has been proposed [7].

Isolated urethral ICC are known to respond to both excitatory and inhibitory neurotransmitters. Thus, norepinephrine (NE) acting via Ca^{2+}-activated Cl^- channels (CaCC) increased the frequency of spontaneous Ca^{2+} oscillations [8]. By contrast, spontaneous electrical activity was inhibited by the NO donor DEA-NO, as well by the GC activator YC-1 or by cell permeant analogues of cGMP (8-Br-cGMP). These effects seem to be mediated by interfering with IP_3 signaling by inhibiting Ca^{2+} release from IP_3R [9]. In addition, immunohistochemical studies suggest a close contact between ICC and nitrergic nerve terminals in the urethra from several species [10, 11], and ICC from both the bladder and the urethra seem to accumulate cGMP upon exposure to NO donors [10- 16]. Furthermore, increased immunoreactivity for cGMP in SMC as well as in intramuscular ICC (ICC-M) following selective stimulation of nitrergic nerves by electrical field stimulation (EFS) have been described in the sheep and rat urethra [10]. Since it was prevented by inhibiting neuronal NO synthase (nNOS) and GC, a model of parallel innervation in which both SMC and ICC-M are effectors of nerve-released NO has been suggested.

CNG ion channels are directly gated by the binding of intracellular cAMP and/or cGMP to a cytoplasmic cyclic nucleotide-binding domain, while they are weakly activated by changes in membrane potential [17]. These channels mainly carry Na^+ and/or Ca^{2+} inward currents, which provokes membrane depolarization or local changes in cytosolic Ca^{2+} levels, providing an alternative pathway for Ca^{2+} entry that couples the activity of Ca^{2+} regulated proteins to cAMP/cGMP signaling without involving protein kinases (PK). We recently demonstrated the expression of CNG1 (selectively activated by cGMP) in SMC and, more abundant in ICC-M of the rat urethra [18]. In addition, blocking CNG with L-cis-Diltiazem almost completely inhibited urethral relaxations induced either by EFS or by GC activation with YC-1 [18, 19], as well as the GC-

mediated relaxation induced by α-toxins of scorpion venom [19]. By contrast, adrenergic nerve-mediated contractions were not selectively affected by L-cis-Diltiazem [18]. These results strongly suggest that CNG channels play a key role in the process that links NO-cGMP pathway activation with urethral SMC relaxation, although the precise mechanisms involved remain to be elucidated.

In the present study, we used confocal imaging on freshly dispersed ICC and SMC from the rabbit urethra to examine the effects of L-cis-Diltiazem on spontaneous Ca^{2+} waves as well as on those changes in Ca^{2+} waves induced by increases in intracellular cGMP levels elicited by treatment with: 1) a cGMP permeant-analogue (8-Br-cGMP); 2) a GC activator (YC-1); 3) a mixture of phosphodiesterase (PDE) inhibitors (IBMX, Zaprinast); or 4) a NO donor (DEA-NO). Furthermore, we analyze the immunoreactivity of CNG1 by immunofluorescence in isolated ICC and SMC.

2. Material and Methods

2.1 Cell dispersal

All experiments conducted in this study were approved by the Dundalk Institute of Technology Animal Use and Care Committee. The urethra was removed from both male and female New Zealand white rabbits immediately after sacrifice by lethal injection of pentobarbitone (i.v.). The proximal urethra was partly removed (3 cm) and placed in Krebs solution. This was then opened up longitudinally and the urothelium removed by sharp dissection. Strips of tissue, 0.5 cm in width were cut into $1mm^3$ pieces and stored in Ca^{2+}-free Hanks solution for 30 min at 4ºC prior to cell dispersal. Dispersal medium consisted of Ca^{2+}-free Hanks solution (see Solutions) containing (per 5 ml): 15 mg collagenase (type 1A), 1 mg protease (type XXIV), 10 mg bovine serum albumin and 10 mg trypsin inhibitor (all from Sigma-Aldrich, Steinheim, Germany). Tissue pieces were incubated for 10- 15 min at 37ºC and then transferred to Ca^{2+}-free Hanks solution and stirred for 15-30 min to release single SMC and ICC. Dispersed cells were plated in Petri dishes containing 100 μM Ca^{2+} Hanks solution and stored at 4ºC for use within 8h. Both ICC and SMC could be easily distinguished each other as previously described [4]. These cells were either used immediately in electrophysiological experiments or plated on glass coverslips for immunocitochemistry.

2.2 Ca^{2+} imaging of single SMC and ICC

Isolated single cells were placed in Hanks solution and allowed to settle in glass-bottomed Petri dishes (WillCo) until they had stuck down. Then, they were incubated in 0.5 μM Fluo-4AM (Molecular Probes, Eugene OR) in Hanks solution containing 100 μM Ca^{2+} for 15 min in the dark at room temperature, and washed with warmed (36 ± 1ºC) normal Hanks solution for 30 min prior to experimentation. During the

experiments, the dish containing the cells was continuously perfused with Hanks solution and additionally the cell under study was superfused by means of a custom built close delivery system consisting of a pipette of 200 μm tip diameter placed approximately 300 μm apart from the cell, which allowed a fast solution switch (< 5 s).

Cells were imaged using an iXon 887 EMCCD camera (Andor Technology, Belfast, Ireland; 512 pixels x 512 pixels, pixel size 16 μm x 16 μm) coupled to a Nipkow spinning disk confocal head (CSU22, Yokogawa, Japan). A krypton-argon laser (Melles Griot UK) at 488 nm was used to excite the Fluo-4, and the emitted light was detected at wavelengths of 510 nm. Experiments were performed using a x60 objective (Olympus) resulting in images of pixel size 0.266 μm x 0.266 μm and images were acquired at five frames per second. Background fluorescence, obtained by using a null frame, was substracted from each frame to obtain '*F*'. F_0 was determined as the minimum fluorescence measured between oscillations under control conditions. Post hoc line-scan images of the entire cell were obtained and handled by using Image J software (Bethesda, Maryland, USA) to obtain plots of F/F_0 and intensity profiles.

2.3 Data analysis

Summary data are presented as the mean ± S.E.M., and statistical differences in wave frequency and amplitude were compared using Student's paired *t* test, taking $P < 0.05$ as significant. 'Basal Ca^{2+}, during oscillatory activity was defined as the "diastolic Ca^{2+} levels" (in F/F_0 units) just before an experimental intervention. In the presence of drugs, basal Ca^{2+} was also measured between oscillations and in those cases in which they were abolished; basal Ca^{2+} was determined as the mean Ca^{2+} level during the last 30 s before drug application. $\Delta F/F_0$ refers to the change in Ca^{2+} levels from basal to peak. Throughout, '*n*' refers to the number of cells in each experimental series, which were obtained from a minimum of two animals. Data were compared using GraphPad Prism 5 software (GraphPad Software, San Diego, CA, USA).

2.4 Immunofluorescence of single SMC and ICC

Cells were fixed in ice-cold 4% paraformaldehyde in PBS for 20 min, washed in PBS (3 x 5 min) at 4ºC and then incubated in normal donkey antiserum (10% in PBS + 0.05% Triton X-100) for 1h at room temperature. They were incubated overnight at 4ºC in primary antibody: anti-CNG1 (affinity-purified rabbit antiserum; Chemicon International, Temecula, CA, USA), anti-vimentin (mouse monoclonal, clone V9; Chemicon International, Temecula, CA, USA) or anti-α-smooth muscle actin (mouse monoclonal antibody; Sigma-Aldrich, Steinheim, Germany). The antibodies were diluted 1:100 (anti-CNG and anti-vimentin) or 1:800 (anti-α-actin) in PBS containing 0.1% Triton X-100 and 5% donkey serum. The cells were then incubated with the secondary antibodies for 1h at room temperature. Secondary antibodies used were

appropriately matched to the species in which the primary antibody was raised: donkey anti-rabbit Alexa Fluor 488 and donkey anti-mouse Alexa Fluor 594 (both diluted at 1:200 in PBS; Molecular Probes, Eugene OR). Controls were prepared by omitting the primary antibody from the first incubation solution. Specimens were examined under an Axioplan 2-fluorescence microscope (Carl Zeiss Microimaging, Göttingen, Germany) equipped with the appropriate filter sets. They were photographed with a Spot-2 digital camera (Diagnostic Instruments, Sterling Heights, MI, USA), and the images were stored digitally as 12-bit images using MetaMorph 6.1 software (MDS Analytical Technologies, Toronto, ON). Some cells were examined by confocal laser-scanning microscopy using a spectral confocal microscope (TCS-SP2, Leica Microsystems, Barcelona, Spain), and three-dimensional shadow projections were constructed from the resulting stacks using the Leica Confocal software (LCS, Leica Microsystems, Barcelona, Spain). Digital images were subsequently transferred to Adobe Photoshop 8.0.1 (San Jose, CA, USA).

2.5 Solutions and drugs

The compositions of the Hanks solution used was (mM): NaCl (125), KCl (5.36), glucose (10), sucrose (2.9), $NaHCO_3$ (4.17), KH_2PO_4 (0.44), Na_2HPO_4 (0.33), $MgSO_4$ (0.4), $MgCl_2$ (0.5), $CaCl_2$ (1.8) and Hepes (10); pH adjusted to 7.4 with NaOH. Ca^{2+}-free Hanks solution was of the same composition as Hanks solution except that $MgSO_4$, $MgCl_2$ and $CaCl_2$ were omitted and substituted by $NaHCO_3$ (15.5 mM); pH adjusted to 7.4 with NaOH. Krebs solution was composed of: NaCl (120), KCl (5.9), $NaHCO_3$ (1.2), glucose (5.5), CaCl (12.5), $MgCl_2$ (6); pH maintained at 7.4 by bubbling with 95% O_2- 5% CO_2.

The following drugs were used: L-cis-Diltiazem, D-Diltiazem and 1*H*-[1,2,4] oxadiazolo[4,3-*a*]quinoxalin-1-one (ODQ) were obtained from Ascent (Cambridge, UK); 3-(5-hydroxymethyl-2-furyl)-1-benzyl indazole (YC-1), diethylamine nitric oxide (DEA-NO) and 1,4-dihydro-5-(2-propoxyphenyl)-7H-1,2,3-triazolo(4,5-d)pyrimidin-7-one (Zaprinast) were from Sigma-Aldrich (Steinheim, Germany); 8-Br-cGMP and 3,7-dihydro-1-methyl-3-(2-methylpropyl)-1*H*-purine-2,6-dione (IBMX) were purchased from Tocris (Bristol, UK). Stock solutions were prepared in water, except for ODQ, zaprinast, and 8-Br-cGMP, which were dissolved in DMSO and DEA-NO in 10mM NaOH before being diluted to their final concentrations in Hanks solution. Drug vehicles had no effect on the Ca^{2+}oscillations studied.

3. Results

3.1 Effects of Diltiazem isomers on spontaneous Ca^{2+} events in isolated SMC and ICC

About 5% of the freshly dispersed cells showed (under bright field illumination) the highly branched appearance typical of ICC [4]. Of these, more than 50% showed regular spontaneous increases in fluorescence intensity when viewed with the confocal microscope. In contrast SMC, identified by their smooth spindle-shape, rarely exhibited spontaneous Ca^{2+} waves.

Freshly dispersed cells loaded with the Ca^{2+} indicator Fluo4-AM showed Ca^{2+} oscillations that were quite variable from cell to cell as noted previously [5]. These ocurred at a mean frequency of 16.12 ± 2.60 min^{-1} in SMC, and 10.73 ± 1.25 min^{-1} in ICC; and had a mean amplitude of 3,07 ± 0.22 F/F_0 in SMC and 2.62 ± 0.16 F/F_0 in ICC. **Figure 1** shows that the addition of L-cis-Diltiazem (50 μM) induced a significant reduction in the frequency (10.21 ± 2.48 min^{-1} in n= 13 SMC; and 6.57 ± 0.78 min^{-1} in n= 23 ICC) and the amplitude of the Ca^{2+} waves (2.07 ± 0.25 F/F_0 in n=13 SMC, and 1.84 ±0.13 F/F_0 in n=23 ICC) as well as in the basal Ca^{2+} (0.74 ± 0.05 F/F_0 in n= 13 SMC, and 0.77 ± 0.03 F/F_0 in n= 23 ICC) in both type of cells. The effects of L-cis-Diltiazem were not reversed upon washout.

The addition of D-Diltiazem (50 μM) elicited a significant reduction of both the mean frequency and the mean amplitude of Ca^{2+} waves in SMC (4.44 ± 0.88 min^{-1} and 1.98 ± 0.27 F/F_0, respectively, n= 14), but not in ICC (8.09 ± 0.93 min^{-1} and 2.34 ± 0.14 F/F_0, respectively, n= 21) (**Fig. 2**). While a mild reduction in basal calcium were observed in both type of cells, this effect was stronger in SMC (0.82 ± 0.04 F/F_0, n= 14) than in ICC (0.96 ± 0.01 F/F_0; P= 0.09, n= 21). The effects of D-Diltiazem were not reversed upon washout.

3.2 Effects of L-cis-Diltiazem on Ca^{2+} events following increases in intracellular cGMP levels and in the presence of a NO donor (DEA-NO)

We next assessed the effects of L-cis-Diltiazem on spontaneous Ca^{2+} waves and basal Ca^{2+} after inducing cGMP accumulation inside the cell by either 8-Br-cGMP, IBMX+Zaprinast or YC-1 treatments.

Figure 3 shows an example of spontaneous waves in the presence of 8-Br-cGMP (1 mM) and following addition of L-cis-Diltiazem (50 μM). As can be seen, waves that propagated throughout the cell under control conditions were not significantly affected in their mean frequency or mean amplitude by application of 8-Br-cGMP, either in SMC or ICC. Only basal calcium was effectively reduced in both cell types. Upon addition of L-cis-Diltiazem (50 μM) a significant reduction in both the frequency, and the amplitude of Ca^{2+} waves was noted, and basal calcium was further

diminished in both cells. The effect of L-cis-Diltiazem was partly reversed upon washout.

As PDE are known to hydrolyze both cAMP and cGMP, we used a cocktail of a non-specific PDE inhibitor (IBMX) and a selective type V PDE inhibitor (Zaprinast; 0.1 mM each) to reduce the degradation of cGMP and then induce its accumulation into the cell. As shown in **Figure 4**, the application of PDE inhibitors lightly, but significantly, reduced the mean frequency, amplitude of calcium events and basal calcium in both type of cells. The subsequent addition of L-cis-Diltiazem (50 μM) further reduced all the parameters and these effects were reversed upon washout.

As shown in **Figure 5,** YC-1 (60 μM) induced a pronounced and reversibly reduction in the mean frequency, the mean amplitude of Ca^{2+} waves, and the basal calcium in both cell types. Upon application of L-cis-Diltiazem (50 μM) no further changes were observed in all the parameters analyzed.

Figure 6 shows a representative recording of spontaneously active SMC and ICC and the effect of DEA-NO. As expected, the addition of DEA-NO (60 μM) induced prominent reductions in both the mean frequency and the mean amplitude of Ca^{2+} events as well as the basal Ca^{2+} in both type of cells. As mentioned before for YC-1, the subsequent addition of L-cis-Diltiazem (50 μM), both in the absence or in the presence of DEA-NO, did not induce any further change of these parameters. The DEA-NO effects were reversible upon washout.

When comparing the degree of inhibition of Ca^{2+} waves by the different treatments, significant differences were observed in their effects on the frequency of Ca^{2+} waves, giving the following order of potency in SMC; DEA-NO > YC-1(P= 0.035) > PDE inhibitors (P= 0.020) > 8-Br-cGMP (P= 0.026) and in ICC: DEA-NO > YC-1(P= 0.024) > PDE inhibitors (P= 0.020) = 8-Br-cGMP (P= 0.285). However, no significant differences were observed when comparing values of amplitude and basal Ca^{2+}.

3.3 CNG1 Immunofluorescence on isolated SMC and ICC

When the cells were stained with vimentin antibody SMC were almost invisible (**Fig. 9A, E**) while ICC were clearly imaged (**Figs. 8, 9A** and **9E)**. The opposite pattern was observed in the case of α-actin which selectively marked SMC (**Fig. 7**). SMC showed a typical spindle shape but the morphology of ICC was highly variable as previously described [4]. Thus, some cells had a stellate appearance with many branches radiating from a central region containing the nucleus (**Figs. 8D-F** and **9**), while others were bipolar with a centrally placed nucleus and long and thin cytoplasmic prolongations (**Fig. 8 G-I**).

Specific CNG1-ir was evident in both SMC and ICC from the rabbit urethra although with very different intensity (**Figs. 7, 8,** and **9**). Weak and diffuse CNG1-ir was present in SMC (α-actin-ir) (**Figs. 7B, E,** and **9B, D**), while very intense CNG1-ir was evident in ICC (vimentin-ir) (**Figs. 8,** and **9**). Note the intense CNG-ir present in multiple and very thin spines emerging from the ICC body and prolongations (**Figs. 8 B, E, I**, and **9F**, arrowed). CNG1-ir was not detected in the absence of the primary antibody (data no shown).

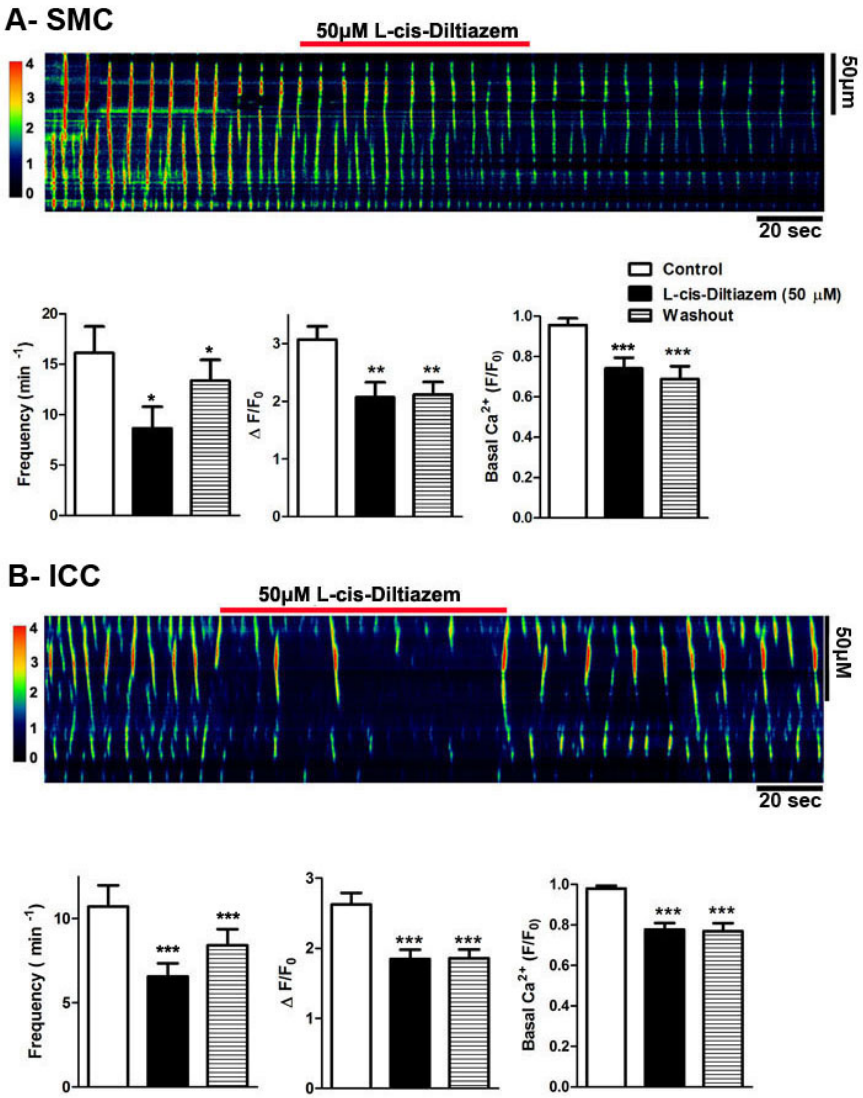

Figure 1. The effects of L-cis-Diltiazem on spontaneous Ca^{2+} events in SMC (**A**) and ICC (**B**) isolated from the rabbit uretra and incubated with Fluo-4AM. Upper panels show representative pseudo-line scan images and lower panels summarize the values of mean frequency (min^{-1}; left), mean amplitude ($\Delta F/F_0$; centre), and basal Ca^{2+} levels (F/F_0; right). L-cis-Dilitiazem were added at 50µM and present for 60-90 s before washout. Data are expressed as means ± SEM (n = 13 SMC, n = 23 ICC). * $P < 0.05$, ** $P < 0.01$, *** $P < 0.001$ compared with controls (Student's t-test for paired observations).

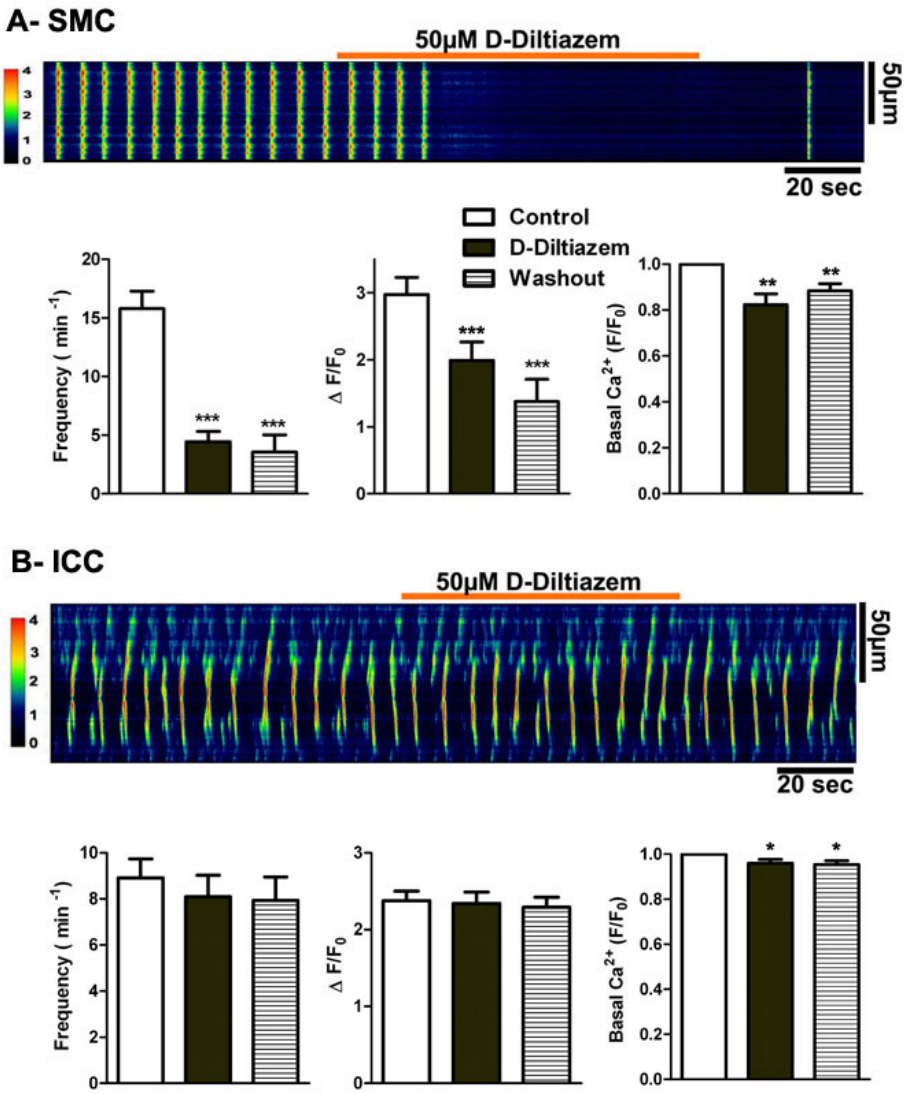

Figure 2. The effects of D-Diltiazem on spontaneous Ca^{2+} events in SMC (**A**) and ICC (**B**) isolated from the rabbit uretra and incubated with Fluo-4AM. Upper panels show representative pseudo-line scan images and lower panels summarize the values of mean frequency (min^{-1}; left), mean amplitude ($\Delta F/F_0$; centre), and basal Ca^{2+} levels (F/F_0; right). D-Dilitiazem was added at 50µM for 60-90 s before washout. Data are expressed as means ± SEM (n = 14 SMC, n = 21 ICC). * $P < 0.05$, ** $P < 0.01$, *** $P < 0.001$ compared with controls (Student's t-test for paired observations).

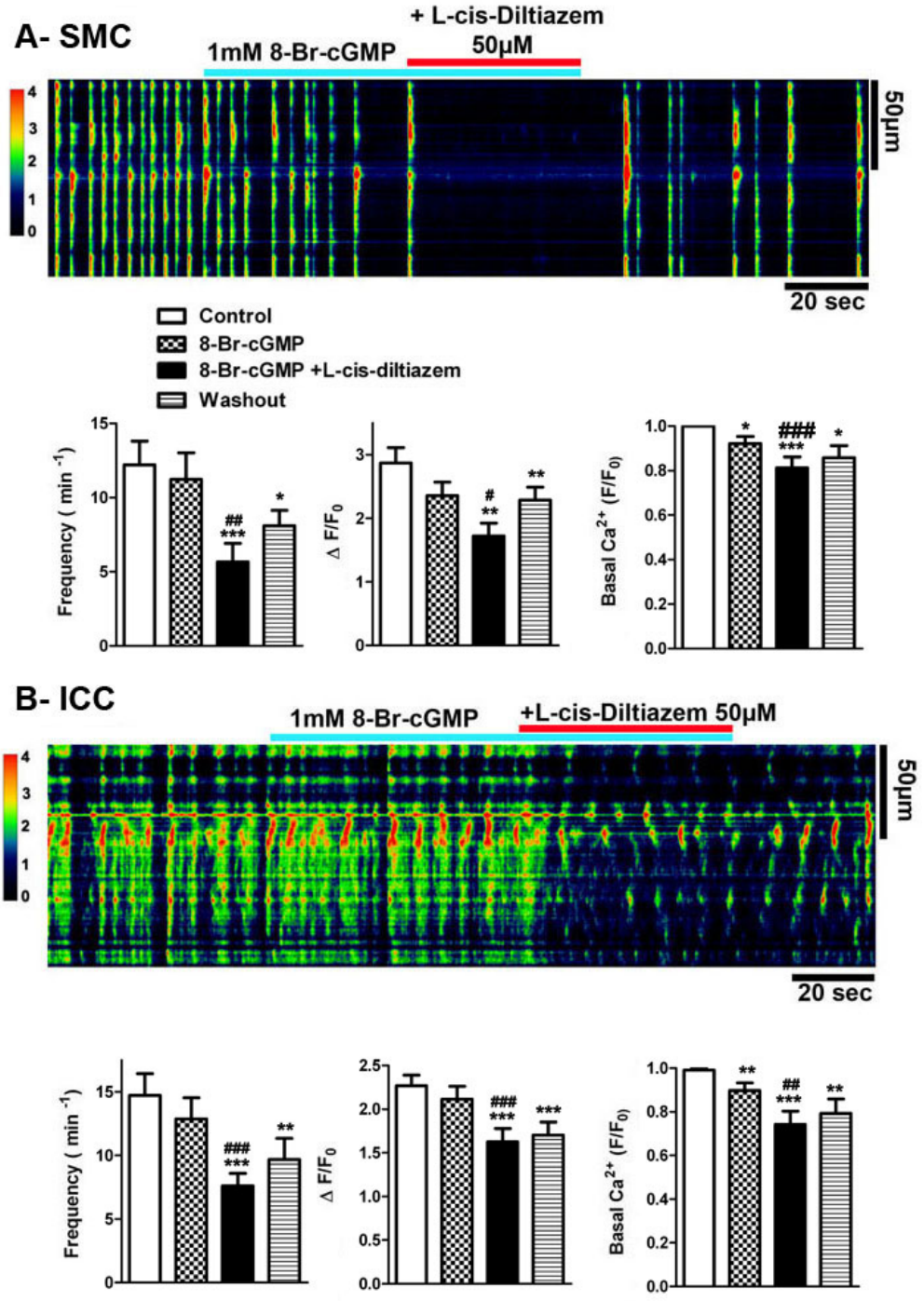

Figure 3. The effects of L-cis-Diltiazem on Ca^{2+} events following treatment with 8-Br-cGMP in SMC (**A**) and ICC (**B**) isolated from the rabbit uretra and incubated with Fluo-4AM. Upper panels show representative pseudo-line scan images and lower panels summarize the values of mean frequency (min^{-1}; left), mean amplitude (Δ F/F_0; centre), and basal Ca^{2+} levels (F/F_0; right). 8-Br-cGMP was added at 1 mM followed by the subsequent addition of L-cis-Diltiazem at 50µM 40-60 s later. Both drugs were present for another 40-60 s before washout. Data are expressed as means ± SEM (n = 21 SMC, n = 22 ICC). * $P < 0.05$, ** $P < 0.01$, *** $P < 0.001$ compared with controls; # $P < 0.05$ ## $P < 0.01$, ### $P < 0.001$ compared with 8- Br-cGMP alone (Student's t-test for paired observations).

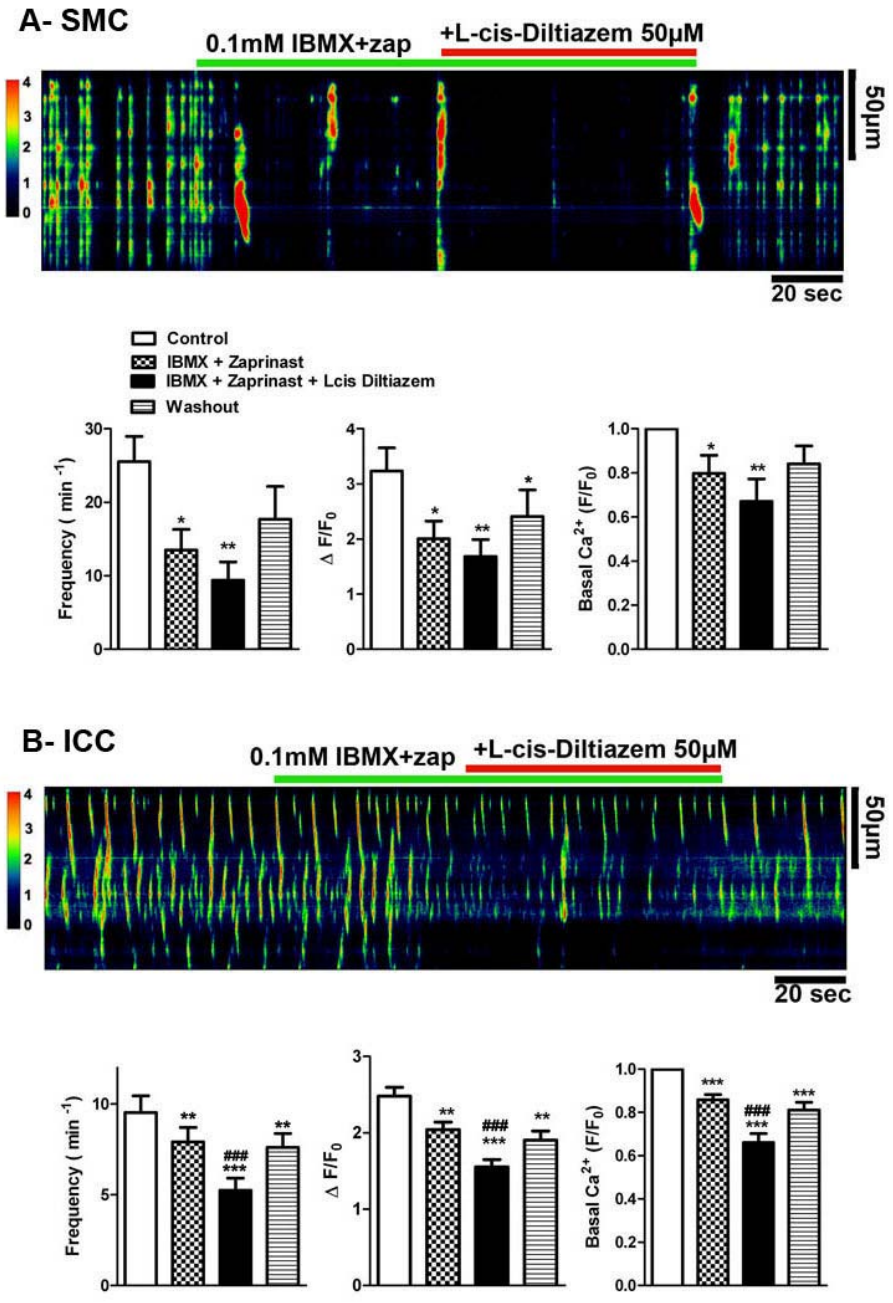

Figure 4. The effects of L-cis-Diltiazem on Ca^{2+} events following inhibition of PDE with IBMX and zaprinast in SMC (**A**) and ICC (**B**) isolated from the rabbit uretra and incubated with Fluo-4AM. Upper panels show representative pseudo-line scan images and lower panels summarize the values of mean frequency (min^{-1}; left), mean amplitude (Δ F/F_0; centre), and basal Ca^{2+} levels (F/F_0; right). IBMX and Zaprinast (zap) were added at 0.1 mM each followed by the subsequent addition of L-cis-Diltiazem at 50µM 40-60 s later. All drugs were present together for another 40-60 s before. Data are expressed as means ± SEM (n = 7 SMC, n = 23 ICC). * $P < 0.05$, ** $P < 0.01$, *** $P < 0.001$ compared with controls; ### $P < 0.001$ compared with IBMX + Zaprinast alone (Student's t-test for paired observations).

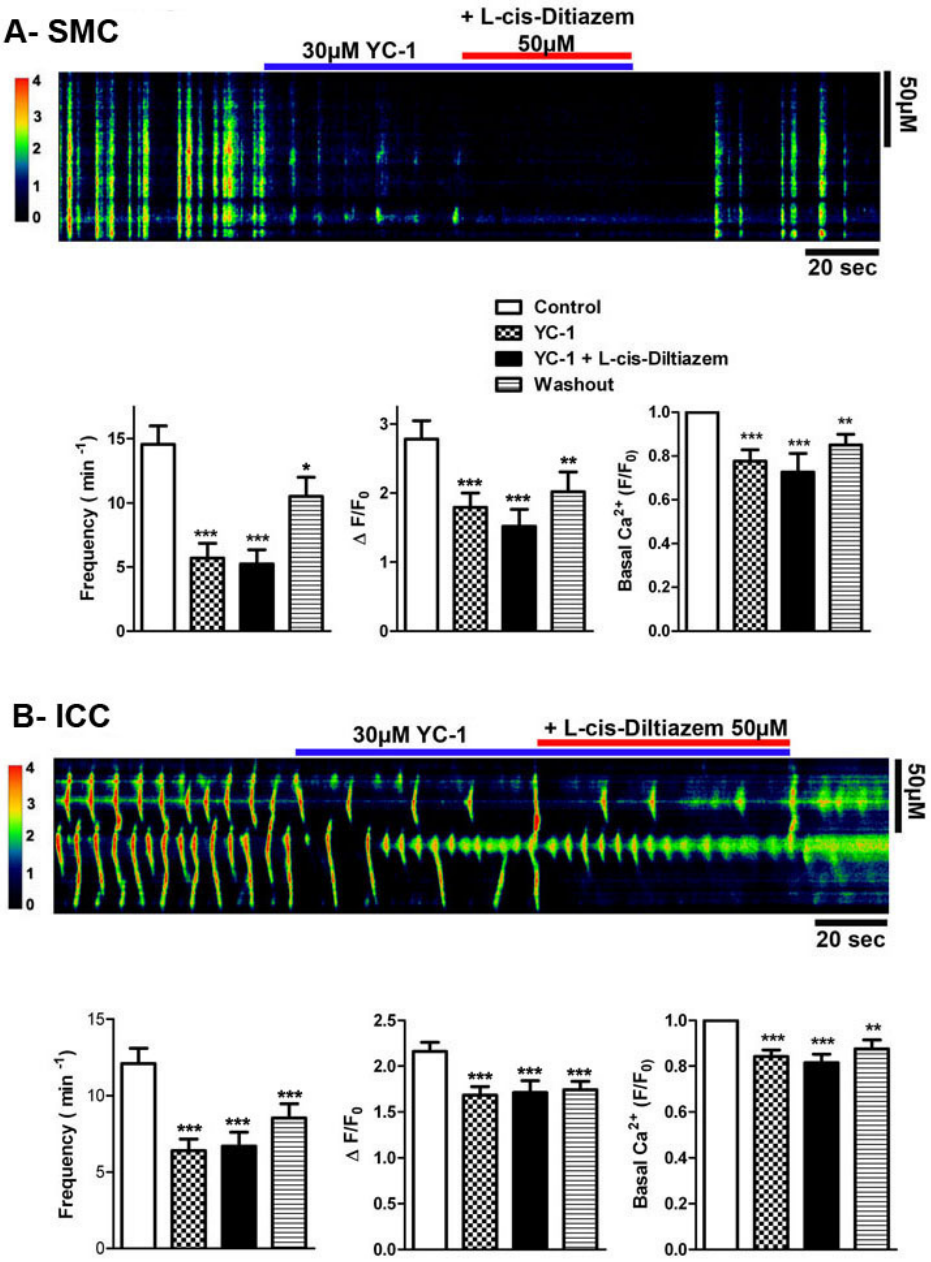

Figure 5. The effects of L-cis-Diltiazem on Ca^{2+} events following activation of soluble guanylyl cyclase by YC-1 in SMC (**A**) and ICC (**B**) isolated from the rabbit uretra and incubated with Fuo-4AM. Upper panels show representative pseudo-line scan images and lower panels summarize the values of mean frequency (min^{-1}; left), mean amplitude (Δ F/F_0; centre), and basal Ca^{2+} levels (F/F_0; right). YC-1 was added at 30 μM followed by the subsequent addition of L-cis-Diltiazem at 50μM 40- 60 s later. Both drugs were present for another 40-60 s before washout. Data are expressed as means ± SEM (n = 15 SMC, n = 23 ICC). * $P < 0.05$, ** $P < 0.01$, *** $P < 0.001$ compared with controls (Student's t-test for paired observations).

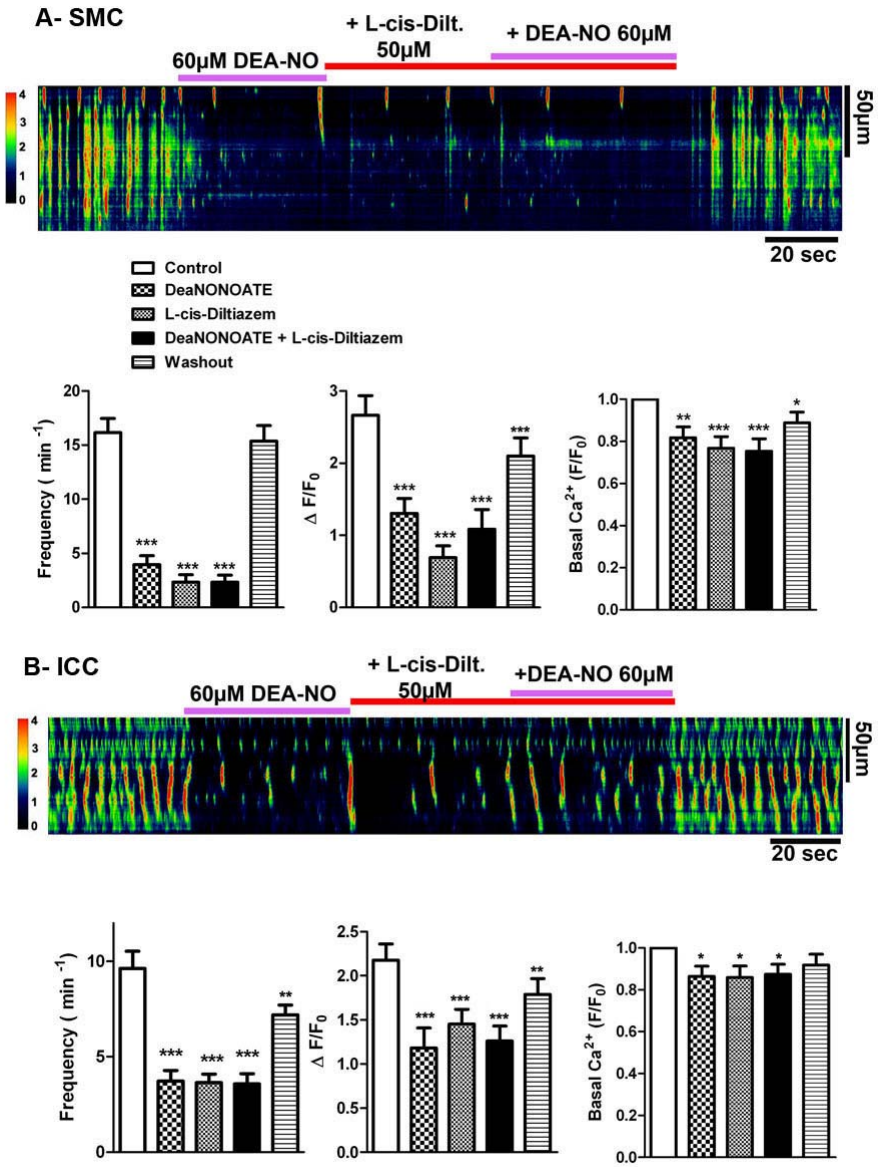

Figure 6. The effects of L-cis-Diltiazem on Ca^{2+} events following the addition of the NO donor, DEA-NO, in SMC (**A**) and ICC (**B**) isolated from the rabbit uretra and incubated with Fluo-4AM. Upper pannels show representative pseudo-line scan images and lower pannels summarize the values of mean frequency (min^{-1}; left), mean amplitude (Δ F/F_0; centre), and basal Ca^{2+} levels (F/F_0; right). DEA-NO were added at 60 µM for 40- 50 s before washout followed by the addition of L-cis-Diltiazem at 50µM for 40- 50 s. After that, a new application of DEA-NO (60 µM) was done and both drugs were present for the last 40-50 s before washing. Data are expressed as means ± SEM (n = 17 SMC, n = 14 ICC). * $P <$ 0.05, ** $P < 0.01$, *** $P < 0.001$ compared with controls (Student's t-test for paired observations).

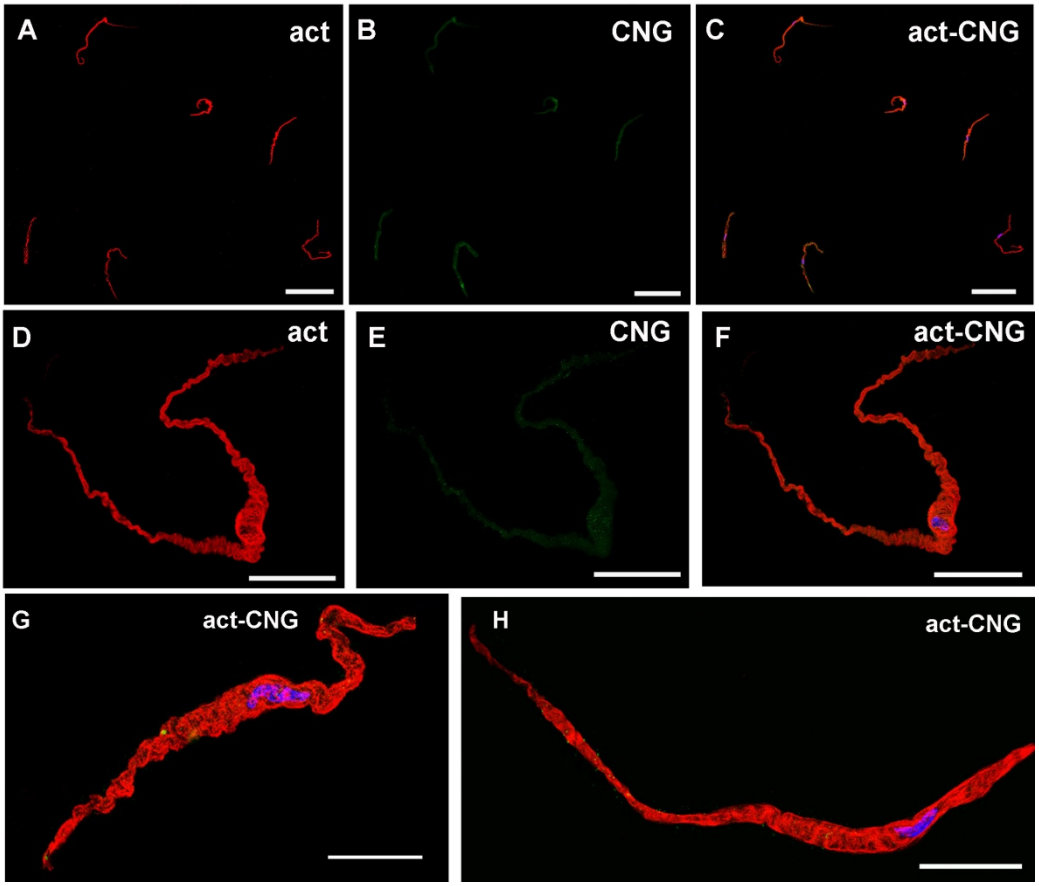

Figure 7. CNG1 immunoreactivity (CNG1-ir) in isolated SMC from the rabbit urethra. Representative photomicrographs show the immunocolocalization of the weak and diffuse CNGA1-ir (green **B, E**) and the more intense α-actin-ir (**A, D**). **C, F, G, H** are merged images where the prominent red α-actin-ir is masking the slight green CNGA1-ir. Nuclei were counterstained with DAPI (blue). Scale bars = 25 μm except in A-C (100 μm).

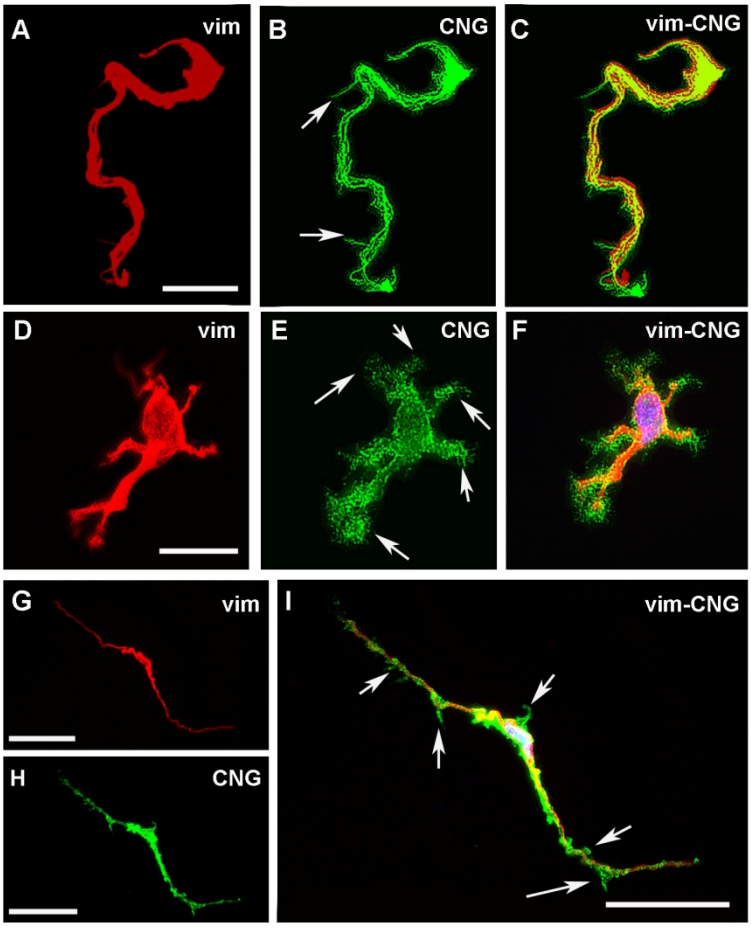

Figure 8. CNG1 immunoreactivity (CNG1-ir) in isolated ICC from the rabbit urethra. Representative photomicrographs show very intense CNGA1-ir (green **B, E, H**) in the same ICC that present also intense vimentin-ir (**A, D, G**). **C, F** and I are merged images where the yellow color denotes co-localization. Note the intense CNG-ir detected in very thin spines emerging from the body main branches (arrows). Nuclei were counterstained with DAPI (blue). Scale bars = 25 μm.

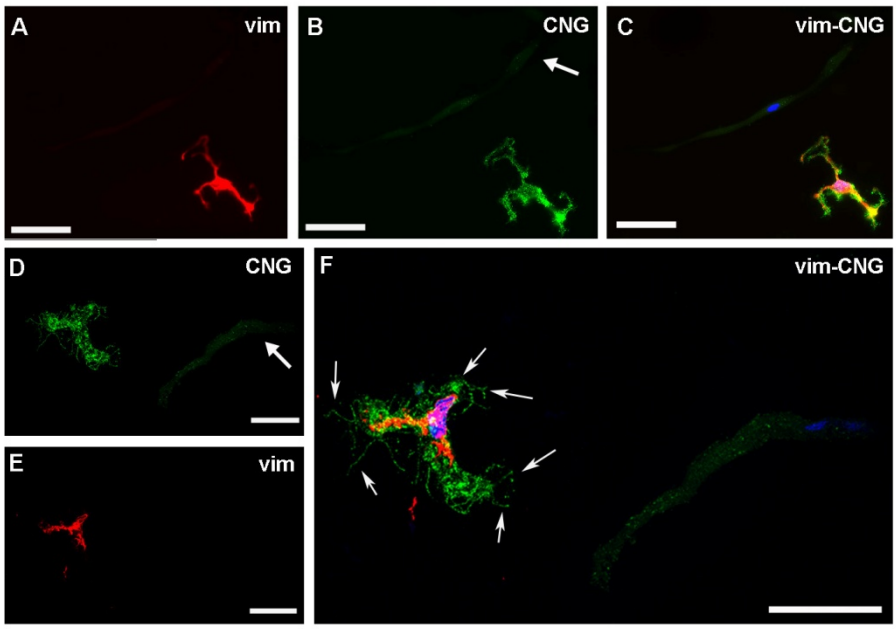

Figure 9. Comparative CNG1 immunoreactivity (CNG1-ir) in isolated SMC and ICC from the rabbit urethra. Representative microphotographs show the difference in CNGA1-ir (green) between a SMC and an ICC that are present in the same field (**B** and **D**, arrows denote SMC). Faint CNG1-ir can be observed in SMC, while intense CNG1-ir was evident in stellate-shaped ICC. ICC but not SMC were also positive to vimentin (red **A, E**), which co-localize with CNG-ir (**C** and **F**). Note the presence of CNG-ir in very thin spines emerging from the body and main branches (arrows). Nuclei were counterstained with DAPI (blue). Scale bars = 25 μm.

4. Discussion

In the present study, we tested the possible role of CNG channels on spontaneous Ca^{2+} oscillations as well as on those changes in Ca^{2+} waves recorded in the presence of raised cGMP levels in both isolated SMC and ICC from the rabbit urethra. We used L-cis-Diltiazem as one of the most widely used specific inhibitors of cGMP-gated CNG channels known to date [20].

Here, we demonstrated a significant reduction by L-cis-Diltiazem of the mean frequency and amplitude of spontaneous Ca^{2+} waves and basal calcium in both SMC and ICC, while the D-Diltiazem isomer was only effective in SMC. D-diltiazem is a benzothiazepine widely used to block L-type voltage-gated Ca^{2+} channels [21, 22]. Thus, non-specific effects of L-cis-Diltiazem on spontaneous Ca^{2+} waves acting through the inhibition of L-type Ca^{2+} channel cannot be discarded, possibly due to its structural similarity with the D-Diltiazem isomer. In fact, it has been previously shown a partial inhibition by L-cis-Diltiazem of contractile responses induced by direct smooth muscle depolarization in the rat urethra [18], although at a much higher dose than that found to inhibit urethral nitrergic relaxation through the selective blockade of CNG channels [18]. In a similar way, in the present work most of the inhibiting effect of L-cis-Diltiazem on spontaneous Ca^{2+} waves in SMC could be ascribed to the blockade of L-type Ca^{2+} channels. It is known that Ca^{2+} waves are more dependent of Ca^{2+} entry through voltage-dependent Ca^{2+} channels in SMC than in ICC. In fact, electrophysiological studies in ICC have shown that nifepidine had little effect on the frequency of waves, although it sometimes shortened their duration, suggesting that these channels do not appear to participate in a great extent in initiating pacemaking [5, 6]. The clear differential effect of D-Diltiazem observed in the present study between SMC and ICC supports the suggestion that the inhibitory effect of L-cis-Diltiazem on spontaneous Ca^{2+} waves in ICC were attributable to specific inhibition of CNG channels. These results suggest distinct involvement of CNG channels in the spontaneous Ca^{2+} waves between both types of cells. It has been previously shown that alternative routes of extracellular Ca^{2+} entry could operate in isolated urethral ICC [6], such as a capacitive calcium entry due to Ca^{2+} mobilization from internal stores [5] or the involvement of Ca^{2+} influx through Na^{+}/Ca^{2+} exchanger working in a reverse mode [7]. In light of our results, CNG channels in ICC could provide a new selective pathway for Ca^{2+} entry in these cells that further differentiates the mechanisms of generation and maintenance of spontaneous Ca^{2+} waves between SMC and ICC. Indeed, we found an intense CNGA1-ir in ICC while only a faint and diffuse staining was detected in SMC, further supporting the abovementioned suggestion that CNG channels would be involved in generation of spontaneous Ca^{2+} waves only in ICC. Under this suggestion, L-cis-Diltiazem could be viewed as a new selective tool for inhibiting ICC spontaneous activity without affecting SMC. However, electrophysiological studies at the level of the CNG channels in both types of cells are needed to probe this suggestion.

When isolated cells, both ICC and SMC, were exposed to different procedures to inducing increases in cGMP levels, a reduction in the mean frequency and the mean amplitude of Ca^{2+} oscillations as well as in the basal calcium were consistently observed although at different degrees. These procedures include treatments with 1) the soluble GC activator YC-1; 2) the membrane-permeant cGMP analogue 8-Br-cGMP; 3) a cocktail of PDE inhibitors and 4) the NO donor DEA-NO. DEA-NO and YC-1 were the most potent in reducing the frequency of Ca^{2+} oscillations. NO is considered to be the natural activator of soluble GC, giving cGMP production by acting on the heme moiety of the enzyme [23]. By the other hand, YC-1 directly and strongly activates soluble GC by its binding to a site other than the GC heme group and it is therefore considered as NO-independent [24- 26]. In contrast, 8-Br-cGMP did not modify the Ca^{2+} oscillations and the PDE inhibitors lightly reduced the frequency and amplitude of Ca^{2+} waves. Since 8-Br-cGMP must enter the cell through the plasma membrane, it can be suggested that this slow entry might not get sufficiently high levels of cGMP to affect the Ca^{2+} parameters studied. On the other hand, PDE inhibitors, increases cGMP levels by reducing its degradation. We have used a cocktail composed of a general PDE inhibitor (IBMX), which may act on both cAMP and cGMP PDEs and a specific inhibitor of PDE V (Zaprinast), the more abundant type of PDE in the urethra [16]. The modest effect of these compounds further support the suggestion that slow accumulations of basally produced cGMP or slowly entry of cGMP analogs are of lower efficacy in inhibiting Ca^{2+} oscillations than when GC is rapidly activated to produce higher levels of cGMP, as occur with NO and YC-1.

Our observation of reduced Ca^{2+} oscillations and basal Ca^{2+} levels in situations of increased cGMP levels is in accordance with previous electrophysiological studies showing that 8-Br-cGMP, NO donors as well as protein kinase G (PKG) agonists reduced spontaneous transient depolarizations (STDs) and spontaneous transient inward currents (STICs) recorded on isolated ICC under current-clamp and voltage-clamp conditions, respectively [9]. Furthermore, sodium nitroprusside, and 8-Br-cGMP both reduced the frequency of electrical slow waves in rabbit urethral smooth muscle [27], supporting the idea that NO mediates its effect via the cGMP/PKG pathway. Abrogation of urethral NO-mediated relaxation induced by EFS in the PKGI-null mice further support this suggestion [28]. The effects of all these compounds that increased cGMP levels were comparable to the inhibitory action of the IP_3R blocker, 2-APB on spontaneous activity of isolated ICC [9], which is consistent with the idea that NO/cGMP mediates their effects by interfering with IP_3 signaling. This is also supported by several studies in other smooth muscles showing that PKG can reduce IP_3 production [29] and can inhibit Ca^{2+} release from intracellular stores through IP_3R [30, 31].

Since CNG channels are directly activated by cAMP or cGMP, we would have expected to find that their blockade by L-cis-Diltiazem had inhibitory effects on the changes in Ca^{2+} waves induced by cGMP increases in SMC and ICC loaded with Fluo4-AM. However, we found in some cases that the effect of L-cis-Diltiazem was additive

to the previous effect provoking a further reduction in Ca^{2+} oscillations. That was the case with 8-Br-cGMP and PDE inhibitors. In others (YC-1 and DEANO), L-cis-Diltiazem had negligible effects but it was never inhibitory. It is still now unclear the mechanism behind this unexpected inhibitory effect of L-cis-Diltiazem on Ca^{2+} waves, but it is tempting to speculate that it might be due to their unspecific effect on L-type Ca^{2+} channels, as described above, and then unrelated to its action on CNG channels. In any case, the results clearly showed that CNG channels do not seem to participate in the mechanisms by which cGMP leads to reduction in Ca^{2+} oscillations and basal Ca^{2+}. Alternatively, as suggested above, PKG activation might be behind these effects. However, the lack of specific PKG inhibitors makes it difficult to test this hypothesis under our experimental conditions and further studies are needed to solve this question.

The results presented here are difficult to relate to the hypothesis that CNG channels are behind the mechanisms by which NO leads to urethral smooth muscle relaxation through the cGMP pathway. Nevertheless, several observations made in this and previous works are sufficiently strong to take them into consideration: 1) L-cis-Diltiazem induces a fast and almost complete inhibition of the urethral nitrergic relaxation induced by EFS or by YC-1 in the urethra of several species (rat, mouse and sheep; [18, 19]) strongly suggesting that CNG channels play a central clue in the nitrergic neurotransmission process; 2) It has been confirmed the expression of mRNA for the CNGA1 and CNGB1 subunits in the rat urethra which have been described to form the functional CNGA1 channel in photoreceptors and in other neurons, usually referred as retinal-like CNG or CNGA1 channel. This channel is considered to be specifically activated by cGMP, it has a preferential Ca^{2+} conductance and it is specifically blocked by micromolar L-cis-Diltiazem acting on the intracellular CNG-binding domain [18]; 3) The localization of CNGA1-ir was clearly observed in a subpopulation of spindle-shaped vimentin-ir ICC and more weakly in SMC. These observations have been made both in tissue sections [18] and isolated cells (present study), strongly suggesting that the role played by CNG are mainly located in ICC. Especially the present study showed a tremendous difference in CNGA-ir between isolated SMC and ICC that pointed to these later cells as playing the main character. In addition, CNGA1-ir has been found located in the same cells (ICC) that also showed cGMP-ir after challenge with EFS of intramural nitrergic nerves or NO donors [10]. The fact that the same cells that produced an increase in cGMP in response to NO also expressed CNG channels is in according to the suggestion that they mediate the effect of cGMP.

All these features strongly support the proposed role of ICC as mediator of the nitrergic neurotransmission process, being CNG channel activation a central element in that function. It is quite obvious that cGMP-mediated relaxation presupposes a decrease rather an increase in intracellular Ca^{2+} concentrations in SMC and then Ca^{2+} entry through CNG should not affect contractile filaments. The facts that these cells contained very few CNG channels and the reduction in Ca^{2+} events induced by cGMP accumulating drugs was not inhibited by L-cis-Diltiazem support that CNG channels do

not affect the relaxation mechanisms at the smooth muscle level. The situation could be different in ICC. Here we showed that these cells responded to increases in cGMP by lowering their intracellular Ca^{2+} concentration, as it did SMC, and these changes were similarly not inhibited by L-cis-Diltiazem. A possible explanation for these results could be that Ca^{2+} oscillations in the bulk of the cytoplasm were not the variable that changed in response to CNG channel opening, so probably we could have not been looking at the right place. It is known that CNG channels can be clustered in separate microdomains within a single cell [32- 34] thereby permitting a finely tuned temporal-spatial modulation of cell functions by cyclic nucleotides [35]. We hypothesize that NO released from nitrergic nerve terminals act on ICC, where CNG channels located at cellular subdomains were activated by cGMP and inducing localized Ca^{2+} influx, without affecting the entire cytoplasm and then not reflected in calcium waves. The cGMP-mediated entry of Ca^{2+} through CNG channels might be involved in the release of another chemical mediator, which may regulate the tone of the nearby smooth muscle. CNG channels strategically located near to the release sites of ICC may be the stimulus needed to couple NO-cGMP responses to secretion. Indeed, control of exocytosis by CNG channels has been demonstrated previously at the cone synapses [36]. In this sense, it is worthy the intense CNG1-ir present in multiple and very thin spines or spicules emerging from the ICC body and their prolongations, suggesting that CNG channels are heavily concentrated in specialized regions that can contact with neighbouring cells. Supporting this, the presence of synapse-like structures between ICC and SMC have been previously described [37] and several chemical mediators such as some cyclooxygenase derived products acting on SMC have been suggested to be produced and released by ICC [38]. However, to the best of our knowledge the existence and identity of this possible mediator in the urethra is still not known. An alternative hypothesis, first suggested in the gastrointestinal tract, is that the ICC communicate with SMC by electrical coupling through gap junctions [39]. However, recent studies have proved that several gap junction uncoplers and connexin inhibitors were not able to affect urethral nitrergic neurotransmission, speaking against this possibility [40]. Further investigations using adequate approaches are needed to solve these questions.

Conclusions

In conclusion, we have described the expression of CNG1 channels of the retinal-like type (CNGA1) especially concentrated in isolated ICC from the rabbit urethra. These channels could provide a new pathway for Ca^{2+} entry in ICC that participates in the generation and maintenance of spontaneous Ca^{2+} waves. However, CNG channels do not seem to participate in the mechanisms by which cGMP leads to reduction in Ca^{2+} oscillations and basal Ca^{2+}, suggesting that this is not the key element by which these channels contributes to the NO/cGMP mediated relaxation of the urethra. Further investigations are needed to solve the mechanisms behind the urethral nitrergic neurotransmission process that are controlled by CNG channels.

References

[1] **Cajal SR.** Histologie du système nerveux de l´homme et des vertebras. *Paris Maloine* 2:891-942, 1991.

[2] **Sanders KM, Ward SM.** Interstitial cells of Cajal: a new perspective on smooth muscle function. *J Physiol* 576: 721-726, 2006.

[3] **McCloskey KD**. Interstitial cells of Cajal in the urinary tract. *Handb Exp Pharmacol* 202: 233-54, 2011.

[4] **Sergeant GP, Hollywood MA, McCloskey KD, Thornbury KD, McHale NG.** Specialized pacemaking cells in the rabbit urethra. *J Physiol* 526: 359-366, 2000.

[5] **Johnston L, Sergeant GP, Hollywood MA, Thornbury KD, McHale NG.** Calcium oscillations in interstitial cells of the rabbit urethra. *J Physiol* 565: 449-461, 2005.

[6] **Sergeant GP, Hollywood MA, McHale NG, Thornbury KD**. Ca^{2+} signaling in urethral interstitial cells of Cajal. J Physiol 576: 715-720, 2006a.

[7] **Bradley E, Hollywood MA, Johnston L, Large RJ, Matsuda T, Baba A, McHale NG, Thornbury KD, Sergeant GP.** Contribution of reverse Na^{+}-Ca^{2+} exchange to spontaneous activity in interstitial cells of Cajal in the rabbit urethra. *J. Physiol* 574(3):651-661, 2006.

[8] **Sergeant GP, Thornbury KD, McHale NG, Hollywood MA.** Characterization of norepinephrine-evoked inward currents in interstitial cells isolated from the rabbit urethra. *Am J Physiol Cell Physiol* 283: 885-894, 2002.

[9] **Sergeant GP, Johnston L, McHale NG, Thornbury KD, Hollywood MA**. Activation of the cGMP/PKG pathway inhibits electrical activity in rabbit urethral interstitial cells of Cajal by reducing the spatial spread of Ca^{2+} waves. *J Physiol* 574: 167-181, 2006b.

[10] **García-Pascual A, Sancho M, Costa G, Triguero D.** Interstitial cells of Cajal in the urethra are cGMP-mediated targets of nitrergic neurotransmission. *Am J Physiol Renal Physiol* 295: 971-983, 2008.

[11] **Smet PJ, Jonavicius J, Marshall VR, de Vente J.** Distribution of nitric oxide synthase-immunoreactive nerves and identification of the cellular targets of nitric oxide in guinea-pig and human urinary bladder by cGMP immunohistochemistry. *Neuroscience* 71:337-348, 1996.

[12] **Fujiwara M, Andersson KE, Persson K.** Nitric oxide-induced cGMP accumulation in the mouse bladder is not related to smooth muscle relaxation. *Eur J Pharmacol* 401: 241–250, 2000.

[13] **Gillespie JI, Markerink- van Ittersum M, de Vente J.** cGMP generating cells in the bladder wall: identification of distinct networks of interstitial cells. *BJU International* 94:1114-1124, 2004.

[14] **Lagou M, Drake MJ, Markerink-van Ittersum M, de Vente J, Gillespie JI.** Interstitial cells and phasic activity in the isolated mouse bladder. *BJU Int* 98: 643–650, 2006.

[15] **Waldeck K, Ny L, Persson K, Andersson KE.** Mediator and mechanisms of relaxation in rabbit urethral smooth muscle. *Br J Pharmacol* 123: 617–624, 1998.

[16] **Werkström V, Svensson A, Andersson KE, Hendlund P**. Phospodiesterase 5 in the female pig and human urethra: morphological and functional aspects. *BJU Int* 98:414-423, 2006.

[17] **Craven KB, Zagotta WN.** CNG and HCN channels: two peas, one pod. *Annu Rev Physiol* 68: 375-401, 2006.

[18] **Triguero D, Sancho M, García-Flores M, García-Pascual, A**. Presence of cyclic nucleotide-gated channels in the rat urethra and their involvement in nerve-mediated nitrergic relaxation. *Am J Physiol Renal Physiol* 297: 1353-1360, 2009.

[19] **Triguero D, González M, García-Pascual A, Costa G.** Atypical relaxation by scorpion venom in the lamb urethral smooth muscle involves both NO-dependent and –independent responses. *Naunyn-Schmiedeberg´s Arch Pharmacol* 361: 151-159, 2003.

[20] **Hofmann F, Biel M, Kaupp UB**. International Union of Pharmacology LI. Nomenclature and structure-function relationships of cyclic nucleotide regulated channels. *Pharmacol Rev* 57: 455-462, 2005.

[21] **Koch KW, Kaupp UB.** Cyclic GMP directly regulates a cation conductance in membranes of bovine rods by a cooperative mechanism. *J Biol Chem* 260: 6788-6800, 1985.

[22] **Stern JH, Kaupp UB, MacLeish PR**. Control of the light-regulated current in rod photoreceptors by cyclic GMP, calcium and L-diltiazem. *Proc Natl Acad Sci USA* 83: 1163-1167, 1986.

[23] **Denninger JW, Marletta MA.** Guanylate cyclase and the NO/cGMP signaling pathway. *Biochim Biophys Acta* 1414 (2-3): 334-350, 1999.

[24] **Friebe A, Schultz G, Koesling D.** Sensitizing soluble guanylyl cyclase to become a highly CO-sensitive enzyme. *EMBO J* 15(24):6863-6868, 1996.

[25] **Mülsch A, Bauersachs J, Schäfer A, Stasch JP, Kast R, Busse R.** Effect of YC-1, an NO-independent, superoxide-sensitive stimulator of soluble guanylyl cyclase, on smooth muscle responsiveness to nitrovasodilators. *Br J Pharmacol* 120(4): 681-689, 1997.

[26] **Friebe A, Koesling D,** Mechanism of YC-1-induced activation of soluble guanylyl cyclase. *Mol Pharmacol* 53: 123-127, 1998.

[27] **Hashitani H, Van Helden DF, Suzuki H.** Properties of spontaneous depolarizations in circular smooth muscle cells of rabbit urethra. *Br J Pharmacol* 118: 1627-1632, 1996.

[28] **Persson K, Pandita RK, Aszodi A, Ahmad M, Pfeifer A, Fassler R, Andersson KE.** Functional characteristics of urinary tract smooth muscles in mice lacking cGMP protein kinase type I. *Am J Physiol Regul Integr Comp Physiol* 279: 1112-1120, 2000.

[29] **Ruth P, Wang GX, Boekhoffi I, May B, Pfeifera A, Penner R, Korth M, Breer H, Hofmann F.** Transfected cGMP-dependent protein kinase suppresses calcium transients by inhibition of inositol 1,4,5-trisphosphate production. *Proc Natl Acad Sci USA*, 90: 2623-2627, 1993.

[30] **Komalavilas P, Lincoln TM.** Phosphorylation of the inositol 1,4,5-trisphosphate receptor. Cyclic GMP-dependent protein kinase mediates cAMP and cGMP dependent phosphorylation in the intact rat aorta. *J Biol Chem* 271: 21933-21938, 1996.

[31] **Feil R, Gappa N, Rutz M, Schlossmann J, Rose CR, Konnerth A, Brummer S, Kühbandner S, Hofmann F.** Functional reconstitution of vascular smooth muscle cells with cGMP-dependent protein kinase I isoforms. *Circ Res* 90: 1080-1086, 2002.

[32] **Yau KW, Baylor DA.** Cyclic GMP-activated conductance of retinal photoreceptor cells. *Annu Rev Neurosci* 12: 289-327, 1989.

[33] **Koutalos Y, Yau KW.** Regulation of sensivity in vertebrate rod photoreceptors by calcium. *Trends Neurosci* 19(2): 73-81, 1996.

[34] **Savchenko A, Barnes S, Kramer RH**. Cyclic-nucleotide-gated channels mediate synaptic feedback by nitric oxide. *Nature* 390(6661): 694-698, 1997.

[35] **Kaupp UB.** Family of cyclic nucleotide gated ion channels. *Curr Opin Neurobiol* 5(4): 434-442, 1995.

[36] **Rieke F, Schwartz EA.** A cGMP-gated current can control exocytosis at cone synapses. *Neuron* 13: 863-873, 1994.

[37] **Harhun MI, Gordienko DV, Povstyan OV, Moss RF, Bolton TB.** Function of interstitial cells of Cajal in the rabbit portal vein. *Circ Res* 95: 619-626, 2004.

[38] **Collins C, Klausner AP, Herrick B, Koo HP, Miner AS, Henderson SC, Ratz PH.** Potential for control of detrusor smooth muscle spontaneous rhythmic contraction by cyclooxygenase products released by interstitial cells of Cajal. *J Cell Mol Med* 13(9B): 3236-3250, 2009.

[39] **Daniel EE, Thomas J, Ramnarain M, Bowes TJ, Jury J.** Do gap junctions couple interstitial cells of Cajal pacing and neurotransmission to gastrointestinal smooth muscle? *Neurogastroenterol Motil* 13: 297-307, 2001.

[40] **Sancho M, Triguero D, García-Pascual A.** Direct coupling through gap junctions is not involved in urethral neurotransmission. *Am J Physiol Renal Physiol* 300: F-864-872, 2011.

MANUSCRITO IV

Am J Physiol Renal Physiol 300: F864–F872, 2011.
First published January 19, 2011; doi:10.1152/ajprenal.00641.2010.

Direct coupling through gap junctions is not involved in urethral neurotransmission

Maria Sancho, Domingo Triguero, and Angeles Garcia-Pascual

Department of Physiology, Veterinary Faculty, Complutense University, Madrid, Spain

Submitted 1 November 2010; accepted in final form 18 January 2011

Sancho M, Triguero D, Garcia-Pascual A. Direct coupling through gap junctions is not involved in urethral neurotransmission. *Am J Physiol Renal Physiol* 300: F864–F872, 2011. First published January 19, 2011; doi:10.1152/ajprenal.00641.2010.—Interstitial cells of Cajal (ICC) are believed to participate in urethral neurotransmission and it was proposed that direct coupling of ICC and smooth muscle cells (SMC) through gap junctions (GJ) is involved, although this still remains unclear. Hence, we investigated the distribution of different connexins (Cx 43, Cx40, and Cx37) in the sheep and rat urethra, as well as their possible role in neurotransmission. Conventional PCR confirmed that three Cxs are expressed in the urethra. Moreover, both Cx43 and Cx37-immunoreactivity (-ir) were present in SMC, ICC, and the urothelium, although Cx37-ir was significantly weaker and Cx40-ir was limited to the endothelium. While these results indicate that GJ intercellular communication could occur between SMC and ICC, neither the contractile (noradrenergic) nor the relaxant (nitrergic) responses of the rat and sheep urethra to electrical field stimulation were significantly modified by two different GJ inhibitors: 18α-glycyrrhetinic acid and a cocktail of Cx mimetic peptides (^{Cx43}Gap 26, $^{Cx37,\ Cx43}$Gap 27, and ^{Cx40}Gap 27). By contrast, contractions induced by high K^+ were effectively reduced by both blockers, evidence that they effectively inhibit intercellular communication. These results indicate that GJ are not implicated in urethral neurotransmission, although the question of whether ICC modulate neurotransmission through some other mechanism remains to be determined.

interstitial cells of Cajal; connexin; nitric oxide; norepinephrine

URINARY CONTINENCE IS MAINTAINED at rest by a high spontaneous urethral tone, which is augmented by neurally released norepinephrine (NE). This high tone is abruptly lost during micturition by the release of nitric oxide (NO) from the nitrergic nerve network (reviewed in Ref. 1). Several investigations in the last decade led to the suggestion that the neurotransmission processes in the urethra are mediated by interstitial cells of Cajal (ICC) (15, 42, 43), similar to that described in the gastrointestinal tract (3, 5). In the lower urinary tract, it is now accepted the presence of a population of branched noncontractile cells with ultrastructural characteristics similar to those of the gut (41), which are ICC following the nomenclature guidelines approved in the Fifth International Symposium on Interstitial Cells of Cajal, Ireland, 2007. However, studies concerning their role in the urinary tract are scarce. In the urethra, the first description of vimentin-positive cells that accumulated cGMP immunoreactivity upon addition of NO donors, and with a remarkable resemblance to ICC of the intestine, was made by Smet et al. (45). Extensive studies using isolated rabbit ICC revealed the ionic mechanisms that are behind their proposed pacemaker role and these mechanisms are very similar to the activity of ICC seen in the gut (see Ref. 44 for a review). Furthermore, the presence of close contacts between ICC and nitrergic nerves in the urethra from several species has been described (15, 45), suggesting a functional relationship between them. This is further supported by the fact that spontaneous electrical activity of ICC isolated from the rabbit urethra is modified by both excitatory and inhibitory neurotransmitters. Thus, norepinephrine (NE) increases the frequency of spontaneous depolarization in ICC through the activation of Ca^{2+}-activated Cl^- channels (42), while this electrical activity was inhibited by the NO donor, DEA-NO, as well as by activators of the cGMP pathway that probably inhibit IP_3-mediated Ca^{2+} release from intracellular stores (43). Indeed, we recently showed that cGMP immunoreactivity (-ir) increases in interconnected networks of intramuscular ICC in response to selective stimulation of nitrergic nerves by electrical field stimulation (EFS). This increase was prevented by inhibiting NO synthase and guanylate cyclase, suggesting that it is specifically caused by activation of neuronal NO synthase and that ICC are direct effectors of nerve-released NO (15).

However, the underlying mechanism of communication between ICC, nerves and the final effectors, the smooth muscle cells (SMC) is still not known. In the gastrointestinal tract, it is generally believed that ICC are connected to each other through gap junctions (GJ). This enables electrical messages to be rapidly transmitted between cells in the ICC network, facilitating their behavior as pacemakers (4). SMC can also communicate through GJ, coordinating the contraction of the walls of hollow organs (23). However, there is scant structural evidence for the existence of GJ between ICC and SMC, and some studies failed to demonstrate they connect these two cell types (8, 38). Nevertheless, it has been often assumed that ICC can influence the behavior of SMC through rapid electrical synapses (40), involving the rapid spread of shifts in membrane potential to the muscular syncitium. Alternatively, low-molecular-weight second messengers (cGMP, IP3, calcium, etc.) could freely diffuse through GJ from the ICC to interconnected SMC (29).

GJ are intercellular channels formed by the docking of two connexons or hemichannels in neighbouring cells. Each connexon is composed of 6 associated connexin (Cx) subunits and at least 20 different types of Cxs have been described, named according to their expected molecular weight (48). Furthermore, the Cxs associated in a given connexon may be homomeric or heteromeric, and equivalent or distinct connexons can dock to form homotypic or heterotypic GJ. Thus, a wide variety of GJ can exist, with different attributes in terms of their permeability to low-molecular-weight substances such as ATP, cAMP, IP_3, or several dyes (25), justifying the need to identify the Cxs present in any given tissue. Several studies

Address for reprint requests and other correspondence: A. García-Pascual, Dept. of Physiology, Veterinary Faculty, Complutense Univ., Avda. Puerta de Hierro s/n, 28040 Madrid, Spain (e-mail: angarcia@vet.ucm.es).

described the presence of Cx43, Cx40, and Cx37 in the bladder of different animal species, including humans, Cx43 being the most abundant (22, 34, 35, 37). Indeed, Cx43 has been localized in the subepithelial and intramuscular ICC of the bladder (46), suggesting that it may be implicated in homocellular or heterocellular GJ communication involving ICC. Furthermore, changes in the expression of Cx43 were recently demonstrated in cases of bladder outlet obstruction (17), bladder overactivity (6, 22, 28, 30), or patients with urge incontinence (36), suggesting that this Cx may be involved in the pathogenesis of urinary disorders. However, no studies are yet available on the presence of Cxs in the urethra.

Here, we used RT-PCR and immunofluorescence to demonstrate the expression and location of Cx43, Cx40, and Cx37 in the sheep and rat urethra. Furthermore, the possible functional involvement of GJ in both the excitatory (noradrenergic) or inhibitory (nitrergic) neurotransmission in the urethra was evaluated by using GJ blockers in tissues subjected to EFS. We used 18α-glycyrrhetinic acid (α-GA) as a nonselective GJ blocker (10), as well as a mixture of different Cx mimetic peptides (GAP peptides) that are considered to be more selective tools to block GJ formed by specific Cxs (13, 47).

EXPERIMENTAL PROCEDURES

Drugs and Solutions

Atropine sulphate, guanetidine monosulphate, NE bitartrate salt, D-tubocurarine hydrochloride, [Arg^8] vasopressin acetate salt (AVP), and α-GA were obtained from Sigma Chemie GmbH (Steinheim, Germany). Both ^{Cx43}Gap 26, $^{Cx37,\ Cx43}$Gap 27 and ^{Cx40}Gap 27 were acquired from Severn Biotech (Kidderminster, Worcs., UK). All drugs were dissolved in distilled water except α-GA, which was dissolved in ethanol. Stock solutions were stored at −20°C and working dilutions were made up in 0.9% NaCl.

Tissue Preparation

Lower urinary tracts from 40 female sheep (3–6 mo old) and 45 female Wistar rats (6–8 wk old and 200–300 g) were used in this study. Sheep urinary tracts were collected at the local slaughterhouse shortly after death and they were transported to the laboratory in cold Krebs solution (in mM): 119 NaCl, 4.6 KCl, 1.5 $CaCl_2$, 1.2 $MgCl_2$, 15 $NaHCO_3$, 1.2 KH_2PO_4, 0.01 EDTA, and 11 glucose. Rats were killed by cervical dislocation followed by exsanguination and after opening the abdomen, the whole lower urinary tract was removed. All procedures were approved by the Complutense University Ethical Committee and they were performed in accordance with the current European guidelines (Council Directive 86/609/EEC). From each urinary tract, the urethra was dissected out and cleaned from the fat and connective tissue, taking care not to damage either the mucosal and serosal layers and to maintain the integrity of the tissue. Transverse strips (~3-mm wide and 5-mm long in sheep and rats) or rings (3-mm wide in rats only) were taken from the proximal urethras, immediately caudal to the bladder neck. All preparations were studied on the day the animals were killed.

Reverse Transcription and PCR Amplification

Total RNA was extracted from a proximal female rat urethra ring (≤30 mg) using the Qiagen RNeasy Fibrous Tissue mini-kit with DNase digestion step, and its quality was determined by agarose gel electrophoresis. Conventional RT-PCR of Cx43, Cx40, and Cx37 transcripts was performed in a 25-μl reaction volume using the Access RT-PCR System (Promega, Madison, WI) on a Perkin Elmer thermocycler (Gene Amp PCR System 2400). The RT-PCR protocol involved heating to 45°C for 45 min and then to 94°C for 2 min; 35 cycles at 94°C for 30 s, 60°C for 45 s, and 68°C for 45 s; and a final termination step at 68°C for 7 min. The specific primer sets for the rat Cx sequences (Metabion International, Deutschland) were Cx43 forward 5′-taggtgcatgttctgcaagc-3′, reverse 5′-gactgcttcctctcacgtcc-3′; Cx40 forward 5′-cgaggacaatcttcccgttca-3′, reverse 5′-ctgaagaagccaactccagc-3′; and Cx37 forward 5′-aaggagatgacccctacca-3′, reverse 5′-tcgagtgtaacacagcccag-3′. The specificity of all these primers has been demonstrated previously (2) and positive controls were included by amplifying of rat heart RNA samples. To rule out any possible genomic DNA contamination in the RNA samples, RT-PCR was also performed without reverse transcriptase. The size of the fragments amplified was verified in a 2% agarose electrophoresis gel stained with ethidium bromide and visualized in Biorad Fluor-S MultiImager (Hercules, CA).

Immunofluorescence

Urethral strips were fixed when partially stretched to 110% their length by pinning them to a sylgard base, while the urethral rings were fixed by immersion, in both cases for 30 min in ice-cold 4% paraformaldehyde in 0.1 M phosphate buffer (PB; pH 7.4). The tissue was then incubated in solutions of paraformaldehyde in 0.1 M PB with increasing concentrations of sucrose (10% sucrose for 90 min followed by 20% sucrose for 120 min) and cryoprotection was terminated by incubating overnight in 30% sucrose in PB at 4°C. Tissues were then snap-frozen in liquid nitrogen-cooled isopentane and stored at −80°C for up to 15 days. Cryostat sections (10 μm: CM1850 UV, Leica Microsystems, Barcelona, Spain) transverse to the mucosal surface of the urethra embedded in Tissue-Tek OCT compound were thawed onto poly-L-lysine-coated slides. From each urethra, consecutive sections were collected on 4–5 slides and thus, each slide contained a similar collection of 10–15 serial sections from the same animal. The slides were air-dried at room temperature for 12–24 h and then processed directly or stored at −80°C for no more than 30 days.

Urethral sections were washed three times for 5 min each with PB and to avoid nonspecific antibody binding, they were then incubated for 2 h with 3% normal donkey serum (Chemicon International, Temecula, CA) containing 0.3% Triton X-100. The sections were incubated with the primary antibody (or antibodies for dual labeling) diluted in 2% normal donkey serum and 0.3% Triton X-100 for 24 h at 4°C in a humidified chamber. The primary antibodies used were a rabbit anti-Cx43 polyclonal antiserum, a rabbit anti-Cx40 polyclonal antiserum, a rabbit anti-Cx37 polyclonal antiserum (all diluted 1:200; Alpha Diagnostic International, San Antonio, TX), a mouse anti-vimentin monoclonal antibody (clone V9; 1:100; Chemicon), and a mouse anti-α-smooth muscle actin monoclonal antibody (clone 1A4, 1:1,000; Sigma). The secondary antibodies used were an Alexa 488-conjugated donkey anti-rabbit and an Alexa 594-conjugated donkey anti-mouse (all 1:100; Molecular Probes, Eugene, OR). The sections were incubated with the secondary antibodies for 2 h in a humidified chamber at room temperature in the dark. After being washed with PB (3 times, 10 min each), the nuclei were counterstained with 4′,6-diamino-2-phenylindole (10.9 mM; Sigma) for 20–30 min and the sections were mounted with Prolong Gold antifade reagent (Molecular Probes). In all cases, negative controls involved the omission of the primary antibody and for Cx43 immunostaining, the specificity of binding was verified by preincubation (overnight at 4°C) of the primary antibody with the corresponding blocking peptide (mouse Cx43 blocking peptide, 1:200; Alpha Diagnostic International).

The sections were visualised on an Axioplan 2 fluorescence microscope (Carl Zeiss Microimaging GmbH, Göttingen, Germany) equipped with the appropriate filter sets. They were photographed with a Spot-2 digital camera (Diagnostic Instruments, Sterling Heights, MI) and the images were stored digitally as 12-bit images using MetaMorph 6.1 software (MDS Analytical Technologies, Toronto, Canada). Digi-

tal images were subsequently processed using Adobe Photoshop 8.0 (San José, CA).

Organ Bath Studies

Isometric tension was recorded as described previously (14), whereby urethral preparations were mounted between two stainless-steel hooks in 5-ml organ baths containing Krebs solution at 37°C and bubbled with a mixture of 95% O_2-5% CO_2 (pH 7.4). The isometric tension was recorded by means of Grass FT03C transducers (Grass Instruments, Quincy, MA) and it was displayed on a MacIntosh computer with a MacLab analog-to-digital converter v5.5 (AD Instruments, Hastings, East Sussex, UK). Preparations were equilibrated at a resting tension of either 15 mN (sheep) or 5 mN (rat preparations) for 60 min, changing the bath fluid every 15 min.

EFS was achieved with a Grass S-48 stimulator (Grass Instruments) connected to platinum electrodes placed parallel to the preparation and coupled to a Med-Lab stimulus splitter (Med-Lab Instruments, Loveland, CO, USA). Square-wave pulses of 0.8-ms duration, supramaximal voltage (current strength, 200 mA), and with a train duration of 5 s or 1 min to different frequencies were delivered at 2-min intervals.

Experimental Protocol

EFS-induced noradrenergic contractions (1–50 Hz, 5-s train duration at 2-min intervals) were assessed in sheep strips and rat rings at baseline in the presence of L^G-nitro-L-arginine (0.1 mM) to prevent the interference of NO released by the nerves and D-tubocurarine (0.1 mM) to avoid the effect of somatic nerve stimulation that innervates the striated muscle of the rat urethra. Urethral relaxation of nitrergic origin was obtained by EFS of sheep and rat strip preparations precontracted with NE (50 μM, in the sheep) or AVP (0.1 μM, in the rat) in the continuous presence of guanethidine (50 μM) to prevent the release of NE from nerves and atropine (1 μM) to impair the effects of the acetylcholine released on muscarinic receptors. D-Tubocurarine (0.1 mM) was also added. Both frequency-response curves from 0.5 to 12 Hz with a 5-s train duration (at 2-min intervals) and single relaxations during 1 min at a frequency of 2 or 35 Hz were elicited.

The involvement of GJ in urethral neurotransmission was assessed by the use of drugs that interfere with their function, coupling, gating, and synthesis. α-GA (50 μM, 30 min) was used as a nonspecific inhibitor of intercellular communication through GJ, and a cocktail (0.3 mM each for 2 h) of three Cx mimetic peptides (^{Cx43}Gap 26, ^{Cx37,43}Gap 27, and ^{Cx40}Gap 27) was chosen to specifically inhibit the Cx types present in the urethra. The effects of ethanol (α-GA solvent) were tested in control preparations obtained from the same animal in parallel. Contractile responses to 120 mM KCl (high K^+) were induced before and after incubation with the GJ inhibitors to test their effects on the direct activation of smooth muscle by depolarization and the opening of L-type calcium channels.

Data Analysis

As previously described, urethral relaxation was expressed as a percentage of the tension elicited by the contractile agent recorded immediately before each stimulation. Similarly, the contractions were expressed as a percentage of the maximum control contraction before treatment in each preparation (14). The results are given as means ± SE from *n* experiments (from different animals). The Student's *t*-test (2-tailed for unpaired data) was used for statistical comparisons and a value of $P < 0.05$ was considered significant. The data were compared using GraphPad Prism 5 software (GraphPad Software, San Diego, CA).

RESULTS

Expression of Cx mRNA in the Rat Urethra

The expression of Cx43, Cx40, and Cx37 mRNA was examined by RT-PCR using total RNA extracts from the rat urethra as the template (Fig. 1). Cx43, Cx40, and Cx37 transcripts of the correct predicted sizes, 627, 503, and 509 bp, respectively, were amplified from both rat urethra and heart RNA, the latter used as a positive control. No bands were detected when the reactions were carried out in the absence of reverse transcription, eliminating the possible contamination of the preparation with genomic DNA.

Expression and Localization of Cx Proteins in the Rat and the Sheep Urethra by Immunofluorescence

Strong and widespread Cx43-ir was found in the SMC of both the sheep (Fig. 2, *A* and *B*) and rat urethra (Fig. 3*A*), where it colocalized with α-actin-ir (Fig. 3, *A–C*). This labeling appeared as fine punctuate (Fig. 2*A*) or patchy staining (Fig. 2*B*). In addition, intense Cx43-ir was present in spindle-shaped cells with multiple long processes that were scattered between the smooth muscle bundles and muscle cells (Fig. 2, *D* and *E*) or that formed a ramifying network in the submucosal layer making contacts with one another (Fig. 3, *D* and *E*). These Cx43-ir cells represented a subpopulation of the vimentin-ir cells present in the urethra, suggesting that they were putative ICC (Fig. 3, *D–K*). The Cx43 staining pattern observed in ICC was more uniform and intense, and this Cx was present along the whole membrane rather than adopting a punctuate distribution, or it was even detected in the cytoplasm (Figs. 2, *D* and *E*, and 3, *F* and *I*). Furthermore, strong Cx43-ir was observed in the urothelium from the sheep (Fig. 2*F*) but not from the rat urethra (not shown). No significant CX43-ir was evident when

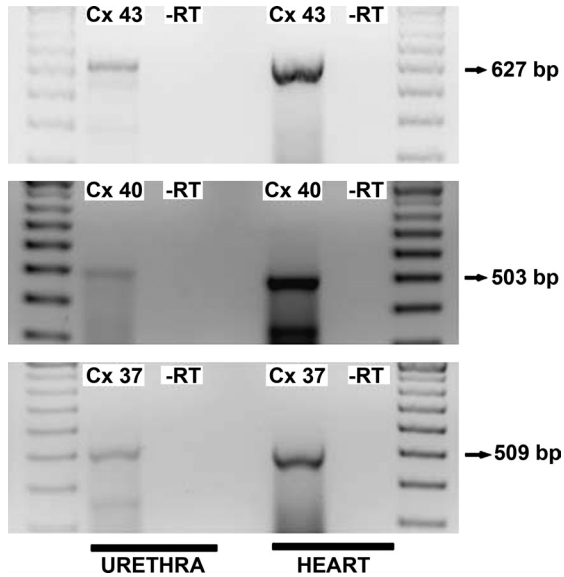

Fig. 1. PCR products amplified from connexin (Cx)43, Cx40, and Cx37 transcripts (from *top* to *bottom*) and visualized in 2% agarose gel stained with ethidium bromide. The mRNA transcripts for the 3 Cxs expressed in rat urethra corresponded to the sizes expected and to the transcripts in the rat heart that was used as a positive control: 627 bp for Cx43, 503 bp for Cx40, and 509 bp for Cx37 (*left* and *right* lanes 100-bp ladder). Negative controls were run without performing reverse transcription (−RT).

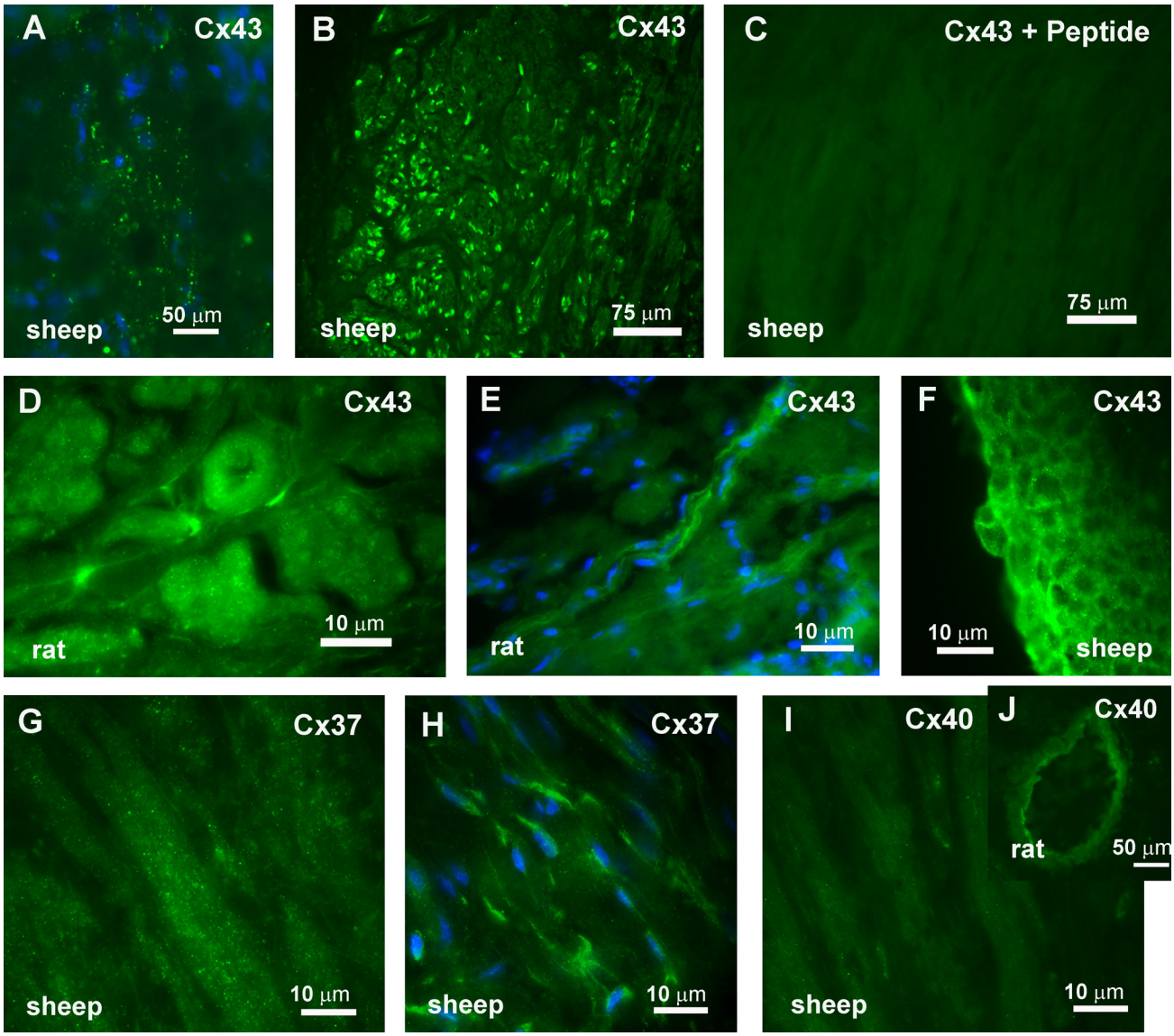

Fig. 2. Cx43, Cx37, and Cx40 immunoreactivity in sheep and rat urethra. Note the expression of Cx43 in a punctuate pattern (*A*) or as a patchy staining (*B*) in the smooth muscle cells (SMC) of the sheep urethra, which was not evident in the presence of the corresponding blocking peptide (*C*). *D* and *E* show the especially intense labeling of intramuscular (*D*) and serosal (*E*) interstitial cells of Cajal (ICC) in the rat urethra, while *F* shows Cx43-immunoreactivity (ir) in the sheep urothelium. Cx37-ir was less intense in both the muscular layer (*G*) and the submucosal ICC (*H*), and only faint Cx40-ir was observed in the muscular layer (*I*). *J* shows labeling of a large vessel. Bar = 50 μm in *A* and *J*, 75 μm in *B* and *C*, 10 μm in *D–I*.

the antibody was adsorbed to the corresponding blocking peptide before its use (Fig. 2*C*).

Cx37-ir was also observed in the SMC (Fig. 2*G*) and ICC located in the muscle and submucosal layer (Fig. 2*H*), although the staining was weaker and less extended than that for Cx43. Finally, Cx40-ir was found in the vascular endothelium (Fig. 2*J*) and very weakly in the SMC (Fig. 2*I*), but it was never associated to vimetin-ir ICC. In all the cases, no staining was observed when the primary antibody was omitted (data not shown).

Effects of GJ Inhibitors on Contractile and Relaxant Nerve-Mediated Responses in the Rat and Sheep Urethra

The administration of GJ inhibitors, either α-GA (50 μM) for 30 min or a cocktail of GAP peptides, ^{Cx43}Gap 26, ^{Cx37,43}Gap 27, and ^{Cx40}Gap 27 (0.3 mM each) for 2 h, had no effect on either rat or sheep urethral EFS-induced noradrenergic contractions at all the frequencies tested (1–50 Hz; Figs. 4 and 5). Nitrergic relaxation also remained unaffected by the two GJ inhibitors at all the frequencies used (1–12 Hz) in precontracted preparations of both species when both short- and long-duration EFS protocols were employed (Figs. 6 and 7). Thus, intercellular communication through GJ does not seem to be essential for the nerve-mediated functional responses of the urethra.

Effects of GJ Inhibitors on High K^+-Induced Contractions in the Rat and Sheep Urethra

By contrast to their effects on the EFS responses, GJ inhibitors did inhibit contractile responses induced by depolarization

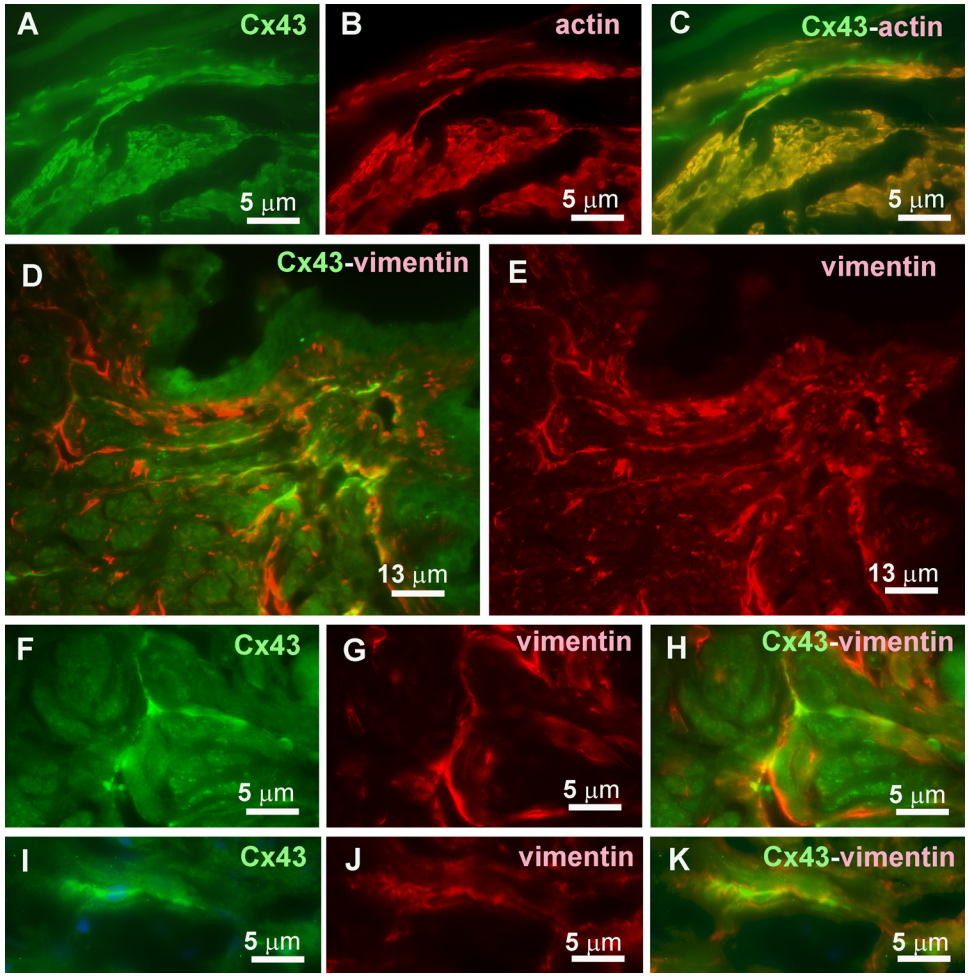

Fig. 3. Dual Cx43 (green)/actin (red) or Cx43 (green)/vimentin (red) staining of the rat urethra indicating the presence of Cx43 in both SMC (colocalization with actin) and ICC (colocalization with vimentin). Cx43 (*A*, *F*, *I*) and actin (*B*) or vimentin (*E*, *G*, *J*) immunoreactivity is shown along with their merged images (*C*, *D*, *H*, *K*). Bar = 5 μm except in *D* and *E* (13 μm).

by high concentrations of extracellular K^+ (Fig. 8). Thus, contractile responses induced by 120 mM K^+ were reduced to 60.5 ± 8.2% (n = 13, P = 0.0009) in the sheep and to 76.7 ± 6.3% (n = 8, P = 0.02) in the rat urethra by α-GA (50 μM for 30 min). Likewise, the GAP peptide cocktail (0.3 mM for 2 h) reduces these responses to 66.2 ± 11.5% (n = 10, P = 0.01) in the sheep and to 64.6 ± 9.2% (n = 9, P = 0.005) in the rat urethra. These responses confirm that both GJ inhibitors are effective in blocking intercellular communication in the urethral preparations.

DISCUSSION

In the present study, we tested the possible role of GJ in the urethral excitatory (noradrenergic) as well as inhibitory (nitrergic) neurotransmission. We confirm that Cx37, Cx40, and Cx43 are all expressed in the urethra, extending previous reports of their expression in the bladder (17, 22, 30, 34–37, 46). Indeed, like the bladder, Cx43 was the most intensely and extensively expressed in the urethra, being in the SMC, ICC, and the urothelium. Cx43-ir was found in both the submucosal and intramuscular ICC populations. The intensity of protein expression when evaluated by immuohistochemistry was Cx43>Cx37>Cx40. Cx40-ir was very scant, and it was mainly observed in the endothelium, seldom in the SMC and not at all in the ICC. By contrast, Cx37-ir was also observed in the SMC and ICC, although to a lesser extent than Cx43.

It has to be noted that interstitial cells were identified as true urethral ICC due to their staining for vimentin while their

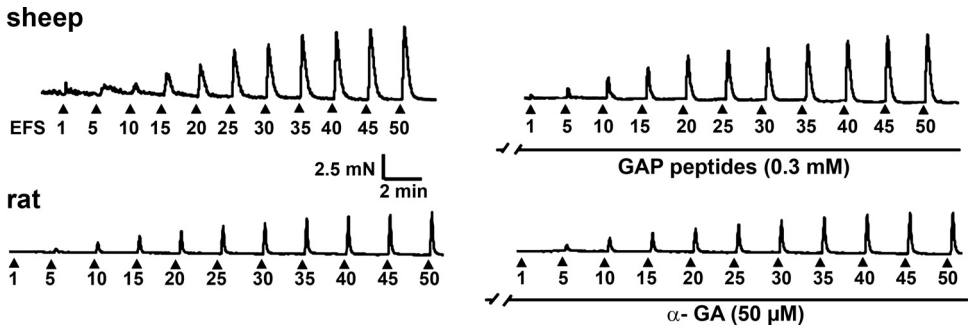

Fig. 4. Representative traces showing the contractions elicited by electrical field stimulation (EFS; 5 s, 1 to 50 Hz) on the basal tension in sheep (*top*) and rat (*bottom*) urethral preparations in control conditions (*left*) and following incubation with the gap junction (GJ) inhibitors (*right*): GAP peptides (0.3 mM, 2 h, *top*) and 18α-glycyrrhetinic acid (α-GA; 50 μM, 30 min, *bottom*).

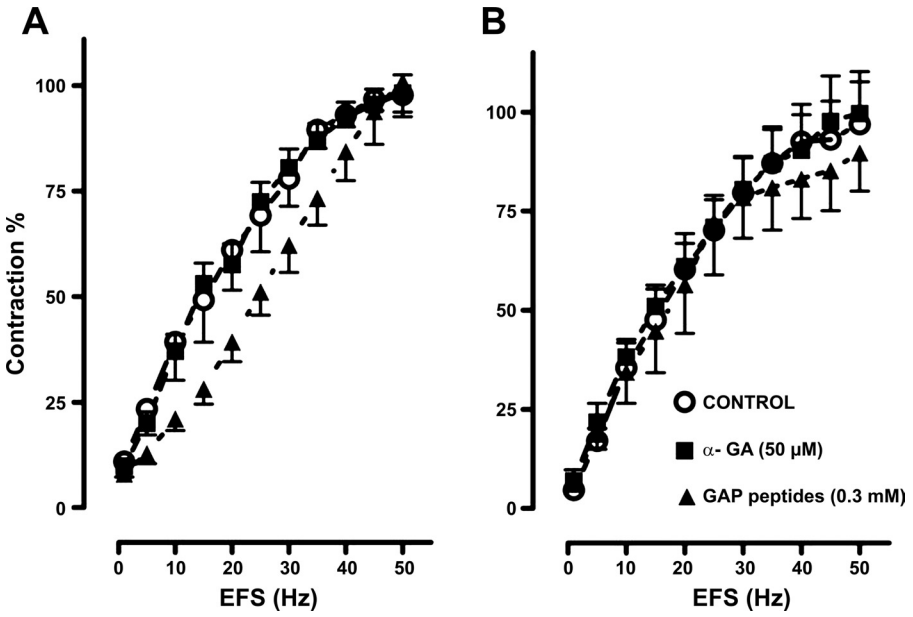

Fig. 5. Contractile frequency-response curves in the sheep (*A*) and rat urethra (*B*) in the presence and absence (open symbols) of GJ inhibitors: α-GA (50 μM, 30 min, ■) and GAP peptides (0.3 mM, 2 h, ▲). The data are expressed as means ± SE ($n = 7$ from different animals in both species). No statistically significant differences were found between groups (1-way ANOVA).

positivity for c-kit was not considered. C-kit is a tyrosine kinase receptor encoded by the *c-kit* proto-oncogene, which has become the standard means of recognizing ICC in the gastrointestinal tract (19). However, the ICC in the urethra (15, 41) as well as in the bladder (32) are weakly labeled for c-kit and their number did not changed in W/W^v mice (31). In fact, now is considering that c-kit positivity may not be an essential criterion for ICC, even in the gut, and that their phenotypic expression may change in the different stages of development and in the different types of ICC (27).

Immunofluorescence for these three Cxs showed the typical punctuate pattern characteristic of GJ in the plasma membrane, making it possible that GJ form through the association of these Cxs between SMC and ICC in any combination (ICC-ICC, SMC-SMC, or ICC-SMC). The prominent expression of Cx43 in the ICC is noteworthy, similar to that previously found in the bladder (46) and large intestine (33). Furthermore, Cx43-ir was sometimes observed as uniform staining of the membrane or in the cytoplasm of ICC, which could represent the connexons or hemichannels formed in the cytosol and transported to the entire cell membrane before their docking to form complete GJ (21).

It is known that GJ formed by different Cxs have different permeability to several second messengers, such as ATP, IP_3, cyclic nucleotides, etc. (18) and Cx43 has been described as more permeable to cAMP than Cx40 or Cx26 (25). The rapid diffusion of cAMP from cell to cell through Cx43 but not Cx40 or 26 would increase this nucleotide sufficiently to overcome the extremely effective phosphodieterase degradation and to trigger relevant cellular functions (25). Although no data yet exist, it seems likely that similar selective diffusion could take place for cGMP, the second messenger for NO. It could be argued that specific GJ between ICC and SMC drive the selective diffusion of second messengers, which could be fine tuned by the differential distribution of Cx types within a nonuniform GJ population. Such a scenario would justify the specific pharmacological manipulation of these GJ for therapeutic purposes.

However, the functional role of GJ has been difficult to analyze due to the lack of selective pharmacological tools. Classical GJ blockers, such as octanol, heptanol, or carbox-

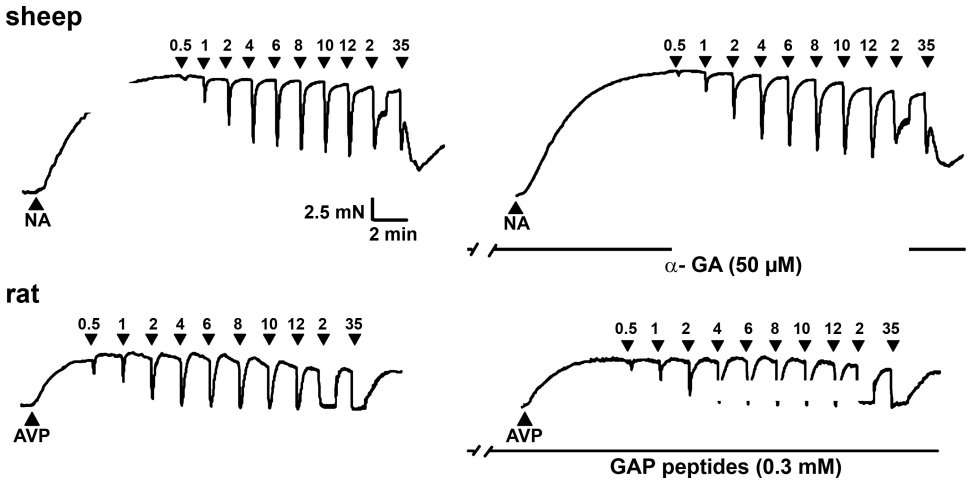

Fig. 6. Representative traces showing the relaxation elicited by EFS (0.5 to 12 Hz for 5 s and 2 and 35 Hz for 1 min) in sheep (*top*) and rat (*bottom*) urethral preparations previously contracted with NE (50 μM) and AVP (0.1 μM), respectively, both in control conditions (*left*) and after pretreatment with GJ inhibitors (*right*): α-GA (50 μM, 30 min: *top*) and GAP peptides (0.3 mM, 2 h: *bottom*).

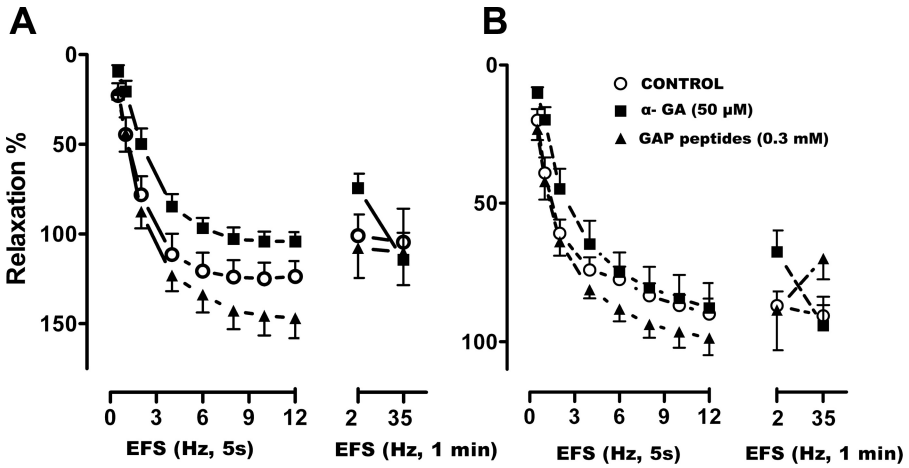

Fig. 7. Frequency-response curves in precontracted sheep (*A*) and rat (*B*) urethras for short (5 s, *left*) and long (1 min, *right*) EFS in the presence or absence (open symbols) of GJ inhibitor pretreatment: α-GA (50 μM, 30 min: filled squares) and GAP peptides (0.3 mM, 2 h: ▲). The data are expressed as means ± SE ($n = 7$ from different animals in both species). No statistically significant differences were found between groups (1-way ANOVA).

enolone, have nonspecific effects that complicate the interpretation of their effects. The new family of GAP peptides appears to be the first selective tool to investigate the function of GJ. They act specifically on the first (GAP 26) or second (GAP 27) extracellular loop of the Cx molecule and they have been shown to be selective for the different Cxs (13). In the present study, we used a cocktail of GAP 26 and GAP 27 peptides that are active on the three types of Cxs present in the urethra: Cx43, Cx37, and Cx40. However, neither contractile nor relaxant responses to EFS were significantly modified in the rat and sheep urethra by the cocktail of GAP peptides. The possibility of poor tissue penetration of the peptides can be

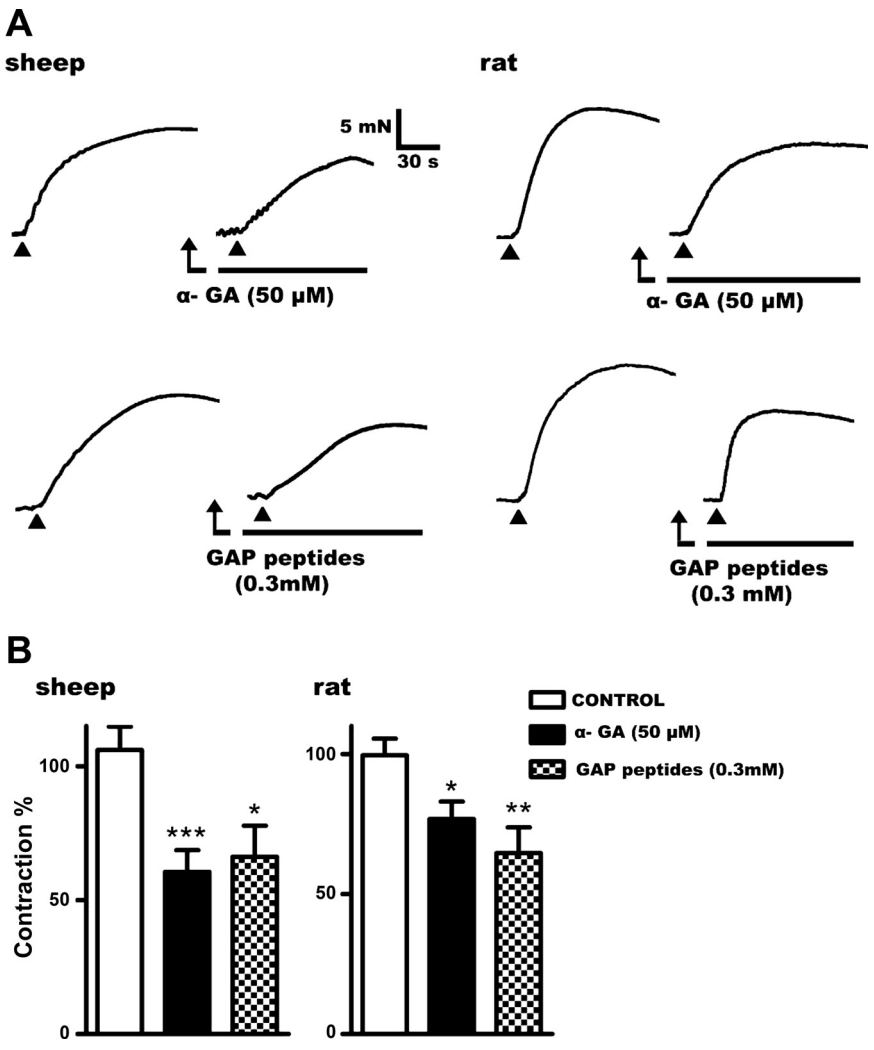

Fig. 8. Effects of GJ inhibitors on high K^+-induced contractions. *A*: representative traces from sheep (*left*) and rat (*right*) urethral preparations showing the contractions induced by addition of 120 mM K^+ (triangle) in control conditions and after treatment with α-GA (50 μM, 30 min: *top*) or GAP peptides (0.3 mM each, 2 h: *bottom*). *B*: mean values of the high K^+-induced contraction in the sheep (*left*) and rat (*right*) urethra under the different experimental conditions detailed in *A*. Data are expressed as means ± SE ($n = 10$ from different animals in both species). $^*P < 0.05$, $^{**}P < 0.01$, $^{***}P < 0.001$ significantly different from controls (1-way ANOVA followed by Student's *t*-test for unpaired observations).

ruled out since the lipophilic compound α-GA, a classic GJ uncoupler (10), also failed to inhibit nerve transmission. Furthermore, the contractions induced by high K^+ were effectively reduced to a similar extent (~25–30%) by both blockers in both species, reflecting the effectiveness of both compounds in inhibiting intercellular communication. Similarly, GAP 27 and α-GA reduced myogenic vasoconstriction of mesenteric arteries but not the contractions induced by agonists, such as phenylephrine (12). Moreover, the responses of intestinal SMC to high K^+ but not carbachol were modified in transgenic mice with a conditional deletion of Cx43 (11). These differences suggest a greater involvement of GJ in the contractile response induced by depolarization and L-type calcium channel opening than in the responses induced by the neurotransmitters NE and NO.

The failure of the GJ blockers to affect the responses induced by endogenous neurotransmitters suggests that direct intercellular communication, either ICC-SMC, ICC-ICC, or SMC-SMC, is not essential for neurotransmission in the urethra. This conclusion was also reached in other structures, like the mouse intestine, where several GAP peptides and other GJ blockers also failed to affect neurotransmission (9). These results suggest that transmission of electrical signals throughout the SMC syncitium is not involved in the urethral response to neurotransmitters, which point to a multi-unitary type of smooth muscle with a high nerve/SMC ratio. Furthermore, this challenges the proposed role of ICC as mediators of neurotransmission between nerves and SMC, as suggested on the basis of the observation that neurotransmission was lost in the gastric fundus of mutant mice lacking ICC (3, 5). Recently, and in contrast to previous studies, the stomach of such mutant mice was shown to respond to NO and other neurotransmitters released by the nerves, and only a mild increase in general excitability was observed (20). Moreover, studies in gastrointestinal tissues questioned whether ICC were necessary for neurotransmission, showing that SMC can respond directly to the transmitters released (7, 16). Indeed, structural studies show that nerve varicosities and SMC are separated by a distance of 50–200 nm, suggesting that there is no barrier for the diffusion of neurotransmitters, including NO (49). In the urethra, we previously observed an increase in cGMP-ir in both ICC and SMC in response to stimulation of intramural nitrergic nerves, suggesting a parallel innervation in which both cell types are targets for the released NO (15).

As a result, we believe that the hypothesis that ICC play a key role as mediators of neurotransmission should be reconsidered, since they appear to have a more modest modulatory effect. Indeed, the modulation of central synapses by astrocytes could be considered as an analogous system, whereby diffusible mediators like ATP are released through hemichannels (26). It is also known that hemichannels that do not form GJ are functionally active in the selective movement of different low-molecular-weight substances into the extracellular space and that this permeability can be regulated by depolarization or phosphorylation by protein kinase C (39). Thus, active connexons in the ICC membrane might permit the release of autocrine or paracrine substances acting on neighboring cells. A new mechanism of ICC modulation would imply that changes in neural activity would modify the levels of second messengers in ICC (e.g., cGMP) and that these cells would then modify the release of active substances through hemichannels. This proposal is compatible with failure of GAP peptides to affect the nerve-mediated responses of the urethra, since they are believed to disrupt the docking of complementary hemichannels and thereby reduce the number of active GJ (13). Indeed, long incubations (1–2 h) with GAP peptides seem to be needed to significantly reduce the number of effective GJ (13). However, direct alterations of channel gating cannot be excluded (13) and further studies into the modifications of hemichannel permeability to specific messengers (e.g., cGMP) by GAP peptides are needed.

Finally, the possibility that Cxs fulfill a functional role on lower urinary tract motility seems to be supported by altered Cx43 expression in the bladder (6, 22, 28, 30) and the changes in the number of ICC (24) in cases of detrusor overactivity and bladder outlet obstruction. Hence, there appears to be a clinical relevant association between ICC, GJ, and smooth muscle excitability.

Conclusions

In conclusion, we demonstrate for the first time the expression of three Cxs (Cx37, Cx40, and Cx43) in the urethra, the expression of Cx43 predominating in both the SMC and ICC, and permitting these cell types to communicate. However, the failure of GAP peptides and α-GA to modify either noradrenergic contraction or nitrergic relaxation induced by EFS in the rat and sheep urethra suggests that GJ are not implicated in urethral smooth muscle neurotransmission. Whether ICC are mediators and/or modulators of neurotransmission and the way they act remain to be elucidated.

ACKNOWLEDGMENTS

The microphotographs were acquired and analyzed at the Microscopy and Cytometry Centre (Complutense University, Madrid, Spain), and we thank A. Cortés and L. M. Alonso for technical assistance with the fluorescence microscopy.

GRANTS

This work was supported by grants from the Spanish Ministerio de Educación y Ciencia (BFU2006-15135-C02-01) and the Comunidad de Madrid-Universidad Complutense de Madrid (UCMGR85/06-920307).

DISCLOSURES

No conflicts of interest, financial or otherwise, are declared by the author(s).

REFERENCES

1. **Andersson KE, Wein AJ.** Pharmacology of the lower urinary tract: basis for current and future treatment of urinary incontinence. *Pharmacol Rev* 56: 581–631, 2004.
2. **Arensbak B, Mikkelsen HB, Gustafsson F, Christensen T, Holstein-Rathlou NH.** Expression of connexin 37, 40 and 43 mRNA and protein in renal preglomerular arterioles. *Histochem Cell Biol* 115: 479–487, 2001.
3. **Beckett EA, Horiguchi K, Khoyi M, Sanders KM, Ward SM.** Loss of enteric motor neurotransmission in the gastric fundus of Sl/Sld mice. *J Physiol* 543: 871–887, 2002.
4. **Belzer V, Kobilo T, Rich A, Hanani M.** Intercellular coupling among interstitial cells of Cajal in the guinea pig small intestine. *Cell Tissue Res* 307: 15–21, 2002.
5. **Burns AJ, Lomax AEJ, Torihashi S, Sanders KM, Ward SM.** Interstitial cells of Cajal mediate inhibitory neurotransmission in the stomach. *Proc Natl Acad Sci USA* 93: 12008–12013, 1996.
6. **Christ GJ, Day NS, Day M, Zhao W, Persson K, Pandita RJ, Andersson KE.** Increased connexin43-mediated intercellular communication in a rat model of bladder overactivity in vivo. *Am J Physiol Regul Integr Comp Physiol* 284: R1241–R1248, 2003.

7. **Cobine CA, Henning GW, Bayguinov YR, Halton WJ, Ward SM, Keef KD.** Interstitial cells of Cajal in the cynomolgus monkey rectoanal region and their relationship to sympathetic and nitrergic nerves. *Am J Physiol Gastrointest Liver Physiol* 298: G643–G656, 2010.
8. **Daniel EE, Wang YF, Cayabyab F.** Role of Gap junctions in structural arrangements of interstitial cells of Cajal and canine ileal smooth muscle. *Am J Physiol Gastrointest Liver Physiol* 274: G1125–G1141, 1998.
9. **Daniel EE, El Yazbid A, Mannarino M, Galante G, Boddy G, Livergant J, Oskouei E.** Do gap junctions play a role in nerve transmissions and well as pacing in mouse intestine? *Am J Physiol Gastrointest Liver Physiol* 292: G734–G745, 2007.
10. **Davidson JS, Baumgarten IM.** Glycyrrhetinic acid derivatives: a novel class of inhibitors of gap-junctional intercellular communication. Structure-activity relationships. *J Pharmacol Exp Ther* 246: 1104–1107, 1988.
11. **Döring B, Pfitzer G, Adam B, Liebregts T, Eckardt D, Holtmann G, Hofmann F, Feil S, Feil R, Willecke K.** Ablation of connexin43 in smooth muscle cells of the mouse intestine: functional insights into physiology and morphology. *Cell Tissue Res* 327: 333–342, 2007.
12. **Earley S, Resta TC, Walker BR.** Disruption of smooth muscle gap junctions attenuates myogenic vasoconstriction of mesenteric resistance arteries. *Am J Physiol Heart Circ Physiol* 287: H2677–H2686, 2004.
13. **Evans WH, Boitano S.** Connexin mimetic peptides: specific inhibitors of gap-junctional intercellular communication. *Biochem Soc Trans* 29: 606–612, 2001.
14. **García-Pascual A, Costa G, Labadia A, Persson K, Triguero D.** Characterization of nitric oxide syntase activity in sheep urinary tract: functional implications. *Br J Pharmacol* 118: 905–914, 1996.
15. **García-Pascual A, Sancho M, Costa G, Triguero D.** Interstitial cells of Cajal in the urethra are cGMP-mediated targets of nitrergic neurotransmission. *Am J Physiol Renal Physiol* 295: F971–F983, 2008.
16. **Goyal RK, Chaudhury A.** Mounting evidence against the role of ICC in neurotransmission to smooth muscle in the gut. *Am J Physiol Gastrointest Liver Physiol* 298: G10–G13, 2010.
17. **Haefliger JA, Tissières P, Tawadros T, Formenton A, Bény JL, Nicod P, Frey P, Meda P.** Connexins 43 and 26 are differentially increased after bladder outlet obstruction. *Exp Cell Res* 274: 216–225, 2002.
18. **Harris AL.** Connexin channel permeability to cytoplasmic molecules. *Prog Biophys Mol Biol* 94: 120–143, 2007.
19. **Huizinga JD, Thuneberg L, Klüppel M, Malysz J, Mikkelsen HB, Bernstein A.** W/kit gene required for interstitial cells of Cajal and for intestinal pacemaker activity. *Nature* 373: 347–349, 1995.
20. **Huizinga JD, Liu LWC, Fitzpatrick A, White E, Gill S, Wang XY, Zarate N, Krebs L, Choi C, Starret T, Dixit D, Ye J.** Deficiency of intramuscular ICC increases fundic muscle excitability but does not impede nitrergic innervations. *Am J Physiol Gastrointest Liver Physiol* 294: G589–G594, 2008.
21. **Hutchings S, Gevaert T, Deprest J, Roskams T, Van Lommel A, Nilius B, De Ridder D.** Immunohistochemistry using an antibody to unphosphorilated connexin 43 to identify human myometrial interstitial cells. *Reprod Biol Endocrinol* 6: 43, 2008.
22. **Ikeda Y, Fry C, Hayashi F, Stolz D, Griffiths D, Kanai A.** Role of gap junctions in spontaneous activity of the rat bladder. *Am J Physiol Renal Physiol* 293: F1018–F1025, 2007.
23. **Imtiaz MS, Von der Weid P-Y, Van Helden DF.** Synchronization of Ca^{2+} oscillations: a coupled oscillator-based mechanism in smooth muscle. *FEBS J* 277: 278–285, 2009.
24. **De Jongh R, van Koeveringe GA, van Kerrebroeck PEV, Markerink-van Ittersum M, de Vente J, Gillespie JI.** Alterations to network of NO/cGMP-responsive interstitial cells induced by outlet obstruction in guinea-pig bladder. *Cell Tissue Res* 330: 147–160, 2007.
25. **Kanaporis G, Mese G, Valiuniene L, White TW, Brink PR, Valiunas V.** Gap junction channels exhibit connexin-specific permeability to cyclic nucleotides. *J Gen Physiol* 131: 293–305, 2008.
26. **Kang J, Kang N, Lovatt D, Torres A, Zhao Z, Lin J, Nedergaard M.** Connexin 43 hemichannels are permeable to ATP. *J Neurosci* 28: 4702–4711, 2008.
27. **Komuro T.** Structure and organization of interstitial cells of Cajal in the gastrointestinal tract. *J Physiol* 576: 653–658, 2006.
28. **Kuhn A, Stadlmayr W, Monga A, Cameron I, Anthony F.** A pilot study of connexin 43 (Cx43) in human bladder tissue in patients with idiopathic detrusor overactivity. *Eur J Obstet Gynecol Reprod Biol* 141: 83–86, 2008.
29. **Kumar NM, Gilula NB.** The gap junction communication channels. *Cell* 84: 381–388, 1996.
30. **Li L, Jiang C, Hao P, Li W, Song C, Song B.** Changes of gap junctional cell-cell communication in overactive detrusor in rats. *Am J Physiol Cell Physiol* 293: C1627–C1635, 2007.
31. **McCloskey KD, Anderson UA, Davidson RA, Bayguinov YR, Sanders KM, Ward SM.** Comparison of mechanical and electrical activity and interstitial cells of Cajal in urinary bladders from wild-type and *W/W^v* mice. *Br J Pharmacol* 156: 273–283, 2009.
32. **McCloskey KD.** Interstitial cells in the urinary bladder–localization and function. *Neurourol Urodyn* 29: 82–87, 2010.
33. **Nemeth L, Maddur S, Puri P.** Immunolocalization of the gap junction protein Connexin43 in the interstitial cells of Cajal in the normal and Hirschsprung's disease bowel. *J Pediatr Surg* 35: 823–828, 2000.
34. **Neuhaus J, Weimann A, Stolzenburg JU, Wolburg H, Horn LC, Dorschner W.** Smooth muscle cells from human urinary bladder express connexin 43 in vivo and in vitro. *World J Urol* 20: 250–254, 2002.
35. **Neuhaus J, Wolburg H, Hermsdorf T, Stolzenburg JU, Dorschner W.** Detrusor smooth muscle cells of the guinea-pig are functionally coupled via gap junctions in situ and in cell culture. *Cell Tissue Res* 309: 301–311, 2002.
36. **Neuhaus J, Pfeiffer F, Wolburg H, Horn LC, Dorschner W.** Alterations in connexin expression in the bladder of patients with urge symptoms. *BJU Int* 96: 670–676, 2005.
37. **Neuhaus J, Heinrich M, Schwalenberg T, Stolzenburg JU.** TGF-β1 inhibits Cx43 expression and formation of functional syncitia in cultured smooth muscle cells from human detrusor. *Eur Urol* 55: 491–498, 2009.
38. **Powley TL, Wang XY, Fox EA, Phillips RJ, Liu LWC, Huizinga JD.** Ultrastructural evidence for communication between intramuscular vagal mechanoreceptors and interstitial cells of Cajal in the rat fundus. *Neurogastroenterol Motil* 20: 69–79, 2008.
39. **Retamal MA, Cortés CJ, Reuss L, Bennett MVL, Sáez JC.** S-nitrosylation and permeation through connexin 43 hemichannels in astrocytes: induction by oxidant stress and reversal by reducing agents. *Proc Natl Acad Sci USA* 103: 4475–4480, 2006.
40. **Sanders KM, Ward SM.** Interstitial cells of Cajal: a new perspective on smooth muscle function. *J Physiol* 576.3: 721–726, 2006.
41. **Sergeant GP, Hollywood MA, McCloskey KD, Thornbury KD, McHale NG.** Specialised pacemaking cells in the rabbit urethra. *J Physiol* 526: 359–366, 2000.
42. **Sergeant GP, Thornbury KD, McHale NG, Hollywood MA.** Characterization of norepinephrine-evoked inward currents in interstitial cells isolated from the rabbit urethra. *Am J Physiol Cell Physiol* 283: C885–C894, 2002.
43. **Sergeant GP, Johnston L, McHale NG, Thornbury KD, Hollywood MA.** Activation of the cGMP/PKG pathway inhibits electrical activity in rabbit urethral interstitial cells of Cajal by reducing the spatial spread of Ca^{2+} waves. *J Physiol* 574: 167–181, 2006.
44. **Sergeant GP, Thornbury KD, McHale NG, Hollywood MA.** Interstitial cells of Cajal in the urethra. *J Cell Mol Med* 10: 280–291, 2006.
45. **Smet PJ, Jonavicius J, Marshall VR, De Vente J.** Distribution of nitric oxide synthase-immunoreactive nerves and identification of the cellular targets of nitric oxide in guinea-pig and human urinary bladder by cGMP immunohistochemistry. *Neuroscience* 71: 337–348, 1996.
46. **Sui GP, Rothery S, Dupont E, Fry CH, Severs NJ.** Gap junctions and connexin expression in human suburothelial interstitial cells. *BJU Int* 90: 118–129, 2002.
47. **Wang J, Ma M, Locovei S, Keane RW, Dahl G.** Modulation of membrane channel currents by gap junction protein mimetic peptides: size matters. *Am J Physiol Cell Physiol* 293: C1112–C1119, 2007.
48. **Willecke K, Eiberger J, Degen J, Eckardt D, Romualdi A, Guldenagel M, Deutsch U, Söhl G.** Structural and functional diversity of conexin genes in the mouse and human genome. *Biol Chem* 383: 725–737, 2002.
49. **Wood J, Garthwaite J.** Models of the diffusional spread of nitric oxide: implications for neural nitric oxide signaling and its pharmacological properties. *Neuropharmacology* 33: 1235–1244, 1994.

MANUSCRITO V

Am J Physiol Renal Physiol 302: F390–F400, 2012.
First published November 23, 2011; doi:10.1152/ajprenal.00344.2011.

Presence of the Ca^{2+}-activated chloride channel anoctamin 1 in the urethra and its role in excitatory neurotransmission

Maria Sancho, Angeles García-Pascual, and Domingo Triguero

Department of Physiology, Veterinary School, Complutense University, Madrid, Spain

Submitted 22 June 2011; accepted in final form 16 November 2011

Sancho M, García-Pascual A, Triguero D. Presence of the Ca^{2+}-activated chloride channel anoctamin 1 in the urethra and its role in excitatory neurotransmission. *Am J Physiol Renal Physiol* 302: F390–F400, 2012. First published November 23, 2011; doi:10.1152/ajprenal.00344.2011.—We investigated the cellular distribution of the calcium-activated chloride channel (CaCC), anoctamin 1, in the urethra of mice, rats, and sheep by both immunofluorescence and PCR. We studied its role in urethral contractility by examining the effects of chloride-free medium and of several CaCC inhibitors on noradrenergic and cholinergic excitatory responses, and on nitrergic relaxations in urethral preparations. In all species analyzed, CaCC played a key role in urethral contractions, influencing smooth muscle cells activated by increases in intracellular calcium, probably due to calcium influx but with a minor contribution by IP_3-mediated calcium release. The participation of CaCC in relaxant responses was negligible. Strong anoctamin 1 immunoreactivity was detected in the smooth muscle cells and urothelia of sheep, rat, and mouse urethra, but not in the interstitial cells of Cajal (ICC) in any of these species. RT-PCR confirmed the expression of anoctamin 1 mRNA in the rat urethra. This anoctamin 1 in urethral smooth muscle probably mediates the activity of chloride in contractile responses in different species, However, the lack of anoctamin 1 in ICCs challenges its proposed role in regulating urethral contractility in a manner similar to that observed in the gut.

noradrenergic neurotransmission; interstitial cells of Cajal

MEMBRANE POTENTIAL is usually defined as the balance between small cations asymmetrically distributed across the cell membrane. Chloride, the only permeable anion, is present at very high concentrations on both sides of the membrane and it is usually considered in a second plane when considering other important ions. The complex role of chloride in maintaining the membrane potential is reflected by the wide variety of chloride channels known to exist (some of which are no longer included in this group). The recently cloned and characterized anoctamin 1 (ANO1; also known as TMEM16A) was identified as the main calcium-activated chloride channel (CaCC) (6, 26, 34). Only some members of the anoctamin family can produce measurable Ca^{2+}-dependent Cl^- currents and since ANO-1 can elicit currents of much larger amplitude than other anoctamine paralogs (19), it is considered to be a reliable indicator of CaCC activity in excitable tissues.

The expression and function of ANO1 have been analyzed in different tissues from normal and ANO1-deficient mice (16). While ANO-1 is absent from smooth muscle cells in the gastrointestinal tract, it has been localized to a conspicuous network of interstitial cells of Cajal (ICC) (16) thought to mediate autorhythmicity and neurotransmission (6, 24). Thus, ANO-1 has been proposed as a specific marker of ICCs in the smooth muscle in the gut (12). The lack of ANO-1 in both smooth muscle and ICCs of the mouse urethra suggests differences between gastrointestinal ICCs and those of urinary tissues (16).

The pacemaker activity of isolated rabbit urethral ICCs is defined by the ionic balance of chloride. Moreover, specific CaCC inhibitors have been proposed as tools for their "pharmacological ablation" in ICCs, based on the abolition of chloride currents in smooth muscle cells (30). However, the rabbit urethra appears to reflect the exception to the rule as chloride-dependent currents have been described in muscle preparations of the lower urinary tract of several other species (bladder and urethra), in which they are implicated in the control of smooth muscle contraction (7).

Due to the aforementioned species and tissue differences, it is difficult to draw generalized conclusions regarding ICC function. In the present study, we analyzed the distribution of ANO1 in the urethra of sheep, rat, and mouse, using conventional PCR and immunohistochemistry. In addition, the role of chloride in the contractile and relaxant activity of the urethra mediated by norepinephrine (NE), acetylcholine (ACh), and nitric oxide (NO) was investigated in functional studies. These mediators were either released by intrinsic nerves via electrical field stimulation (EFS) or added as exogenous agonists. Our results demonstrate that chloride plays a key role in excitatory urethral contraction by acting directly on smooth muscle, having a negligible influence on relaxation. Moreover, no significant differences in chloride activity were detected between species. Intense ANO1 immunolabeling was consistently observed in the smooth muscle layers and the urothelium, but not in the ICC, strongly suggesting that ANO1 is not specific to ICCs in the urethra, in contrast to the gastrointestinal tract (12).

MATERIALS AND METHODS

Drugs and solutions. ACh, atropine sulphate, 2-aminoethoxydiphenyl borate (2-APB), guanethidine monosulphate, L^G-nitro-L-arginine, norepinephrine bitartrate salt (NE), D-tubocurarine hydrochloride, [Arg^8] vasopressin acetate salt (AVP), niflumic acid, anthracene 9-carboxylate (9-AC), and 4-acetamido-4′-isothiocyanato-2,2′-stilbenedisulfonic acid disodium salt hydrate (SITS) were all obtained from Sigma (Steinheim, Germany). Tetrodotoxin (with citrate, TTX) was obtained from Alomone Labs (Jerusalem, Israel). All drugs were dissolved in distilled water, except for niflumic acid and 9-AC, which were dissolved in DMSO. Stock solutions were stored at −20°C and working dilutions were prepared in 0.9% NaCl.

Tissue preparation. Studies were carried out on the lower urinary tracts from female sheep (3 to 6 mo old), Wistar rats (6 to 8 wk old, weighing 200–300 g), and Swiss mice (6 to 8 wk old, weighing 25–30 g). Sheep urinary tracts were collected at the local abattoir shortly after death and transported to the laboratory in cold Krebs solution,

Address for reprint requests and other correspondence: D. Triguero, Dept. of Physiology, Veterinary School, Complutense Univ., Avda. Puerta de Hierro s/n, 28040 Madrid, Spain (e-mail: dtriguer@vet.ucm.es).

composed of (in mM) 119 NaCl, 4.6 KCl, 1.5 $CaCl_2$, 1.2 $MgCl_2$, 15 $NaHCO_3$, 1.2 KH_2PO_4, 0.01 EDTA, and 11 glucose. Rats and mice were obtained from Harland Ibérica and housed on a 12:12-h light-dark cycle with ad libitum access to food and water. Rats and mice were killed by cervical dislocation and then exsanguinated, before the abdomen was opened to remove the entire lower urinary tract. All procedures were approved by the Ethical Committee at the Complutense University and performed in accordance with European guidelines (Council Directive 86/609/EEC). The urethra was dissected out from each urinary tract, and cleaned of fat and connective tissue, taking care not to damage the mucosal and serosal layers of the rat and mouse preparations, and to maintain the integrity of the tissue. The mucosa was removed from the sheep preparations. Subsequently, transverse strips (~3 mm wide and 5 mm long) or rings (3 mm wide in rats and mice) were taken from the proximal urethra and used to study the relaxant and contractile responses, respectively.

Recording of isometric tension. Urethral preparations (strips or rings) were mounted between two stainless steel hooks in 5-ml organ baths containing Krebs solution at 37°C, and they were bubbled with a mixture of 95% O_2-5% CO_2 (pH 7.4). The isometric tension was recorded with Grass FT03C transducers (Grass Instruments, Quincy, MA) and displayed on a MacIntosh computer with a MacLab analog-to-digital converter v5.5 (AD Instruments, Hastings, East Sussex, UK). Preparations were equilibrated at a resting tension of 15 mN (sheep) or 5 mN (rat and mice) for 60 min, and their viability was tested by twice inducing the contractile response by exposure to a high concentration of external K^+ (120 mM).

EFS was applied using a Grass S-48 stimulator (Grass Instruments) that was connected to platinum electrodes placed parallel to the preparation and coupled to a Med-Lab stimulus splitter (Med-Lab Instruments, Loveland, CO). Square-wave pulses (0.8 ms) at a supramaximal voltage (current strength, 200 mA) and a train of 5-s pulses at different frequencies were delivered at 2-min intervals.

Basal urethral excitatory contractile responses were assessed by EFS (1 to 50 Hz, 5-s train duration, 2-min intervals) in the presence of L^G-nitro-L-arginine (0.1 mM) to prevent interference by the NO released from nerves, and of D-tubocurarine (0.1 mM) to prevent stimulation of the somatic nerves that innervate the striated muscle of the urethra in rats and mice. After being washed, the preparations were pretreated for 30 min with the IP_3 receptor inhibitor 2-APB (50 μM) in chloride-free Krebs solution (in mM: 119 C_2H_5COONa, 3.5 $C_6H_{11}KO_7$, 1.5 $CaCl_2$, 1.2 $MgSO_4$, 15 $NaHCO_3$, 1.2 NaH_2PO_4, 0.01 EDTA, and 11 glucose) or with one of the following chloride channel inhibitors: niflumic acid (0.1 mM), SITS (0.1 mM), or 9-AC (1 mM). The stimulation protocol was then repeated.

The relative contribution of NE and ACh to EFS-induced contractions was assessed by testing the effects of atropine (1 μM) before and after the addition of phentolamine (10 μM). The final addition of TTX (1 μM) served to test the nerve dependency of the contraction. Cumulative dose-response curves for NE (0.01 to 100 μM) and ACh (0.01 μM to 10 mM) were obtained and the effects of chloride channel inhibitors were evaluated by repeating the dose-response curve after a 30-min treatment.

The effect of niflumic acid on EFS-induced nitrergic relaxation was also analyzed. Accordingly, strip preparations were precontracted with AVP (0.1 μM) in the continuous presence of atropine (1 μM) and guanethidine (10 μM) to avoid cholinergic and adrenergic excitatory influences. D-Tubocurarine (10 μM) was also added to both rat and mouse preparations. To construct relaxant frequency-response curves, EFS were delivered at 2-min intervals in trains of 5 s at frequencies that ranged from 0.5 to 12 Hz. Long-train duration (60 s) single relaxations at a frequency of 2 and 35 Hz were subsequently performed at 1-min intervals. All responses were completely blocked by TTX (1 μM) and L^G-nitro-L-arginine (0.1 mM), highlighting their nitrergic origin (4). Niflumic acid (0.1 mM) was added 30 min before the next contraction (AVP)-relaxation (EFS) protocol. Control preparations were run in parallel with experimental preparations, receiving the same volume of drug solvents and subjected to the same protocols.

Immunofluorescence. Urethral preparations were analyzed by immunofluorescence as described previously (11). The tissue was first fixed in ice-cold 4% paraformaldehyde in 0.1 M phosphate buffer (PB; pH 7.4) and then incubated in paraformaldehyde solutions with increasing concentrations of sucrose in 0.1 M PB (10% sucrose for 90 min followed by 20% sucrose for 120 min). Cryoprotection was terminated by incubating overnight in 30% sucrose in PB at 4°C, after which the tissues were snap-frozen in liquid nitrogen-cooled isopentane and stored at −80°C for up to 15 days. Cryostat sections (10 μm) transverse to the mucosal surface were obtained from urethras embedded in Tissue-Tek OCT (CM1850 UV, Leica Microsystems, Barcelona, Spain) and they were thawed onto poly-L-lysine-coated slides. Consecutive sections were collected from each urethra on separate slides to obtain 10 to 15 similar serial sections from the same animal. The slides were air-dried at room temperature for 12 to 24 h and then processed directly or stored at −80°C for no more than 30 days.

The urethral sections were washed three times with PB (5 min each) and incubated for 2 h with 3% normal donkey serum (Chemicon International, Temecula, CA) containing 0.3% Triton X-100. The sections were then incubated in a humidified chamber for 24 h at 4°C with the primary antibody (or antibodies for dual labeling) diluted in 2% normal donkey serum and 0.3% Triton X-100. In both sheep and rat preparations, the following primary antibodies were used: rabbit polyclonal antiserum raised against ANO1 (1:100; Abcam, Cambridge, UK), mouse monoclonal anti-vimentin antibody (clone V9, 1:100; Chemicon International), and mouse monoclonal anti-α-smooth muscle actin (1:800; Sigma). Mouse preparations were analyzed using the same primary rabbit antiserum against ANO1 as above and a rabbit polyclonal antiserum against α-smooth muscle actin (1:100; Abcam). Alexa fluor 488 donkey anti-rabbit and Alexa fluor 594 donkey anti-mouse (both at 1:200; Molecular Probes, Eugene, OR) were used as the secondary antibodies. For mouse preparations, primary antibodies for ANO1 and actin (both of rabbit origin) were examined on separate slides containing alternate sections, which were exposed individually to Alexa fluor 488 and Alexa fluor 594 donkey anti-rabbit secondary antibodies, respectively (both at 1:200; Molecular Probes). The sections were incubated with the secondary antibodies for 2 h in the dark in a humidified chamber at room temperature. After three washes with PB (10 min each), the nuclei were counterstained with DAPI (10.9 mM for 30 min; Sigma), and the sections were washed again and mounted with ProLong Gold antifade reagent (Molecular Probes). In all cases, multiple controls were performed in which the specificity of the immunoreactions was established by omitting the primary antibodies.

Sections were examined on an Axioplan 2 fluorescence microscope (Carl Zeiss MicroImaging GmbH, Göttingen, Germany) equipped with the appropriate filter sets, photographed with a Spot-2 digital camera (Diagnostic Instruments, Sterling Heights, MI), and the images were stored digitally as 12-bit images using MetaMorph 6.1 software (MDS Analytical Technologies, Toronto, Canada). Digital images were subsequently processed using Adobe Photoshop 8.0 (San José, CA).

Data analysis. Relaxation was normalized as a fraction of the tension induced by AVP immediately before stimulation. The contractile responses and normalized relaxations were expressed as a percentage of the maximum response obtained during the first stimulation, before the treatment of each preparation (% of control), and the results are presented as means ± SE of n experiments (from n different animals). One-way ANOVA was used for multiple comparisons followed by an unpaired Student's t-test (2-tailed). Data were compared using GraphPad Prism 5 software (GraphPad Software, San Diego, CA).

RT-PCR. Upon removal, the female rat urethra and male rat prostate glands were immediately frozen in liquid nitrogen and total

RNA was extracted using the Qiagen RNeasy Fibrous Tissue Mini Kit with a DNase digestion step. RNA quality was determined by agarose gel electrophoresis. Conventional RT-PCR was performed to amplify the ANO1 transcript in a 25-μl reaction volume using the Access RT-PCR system (Promega, Madison, WI) on a Perkin Elmer thermocycler (GeneAmp PCR System 2400). The RT-PCR protocol involved the following: an incubation at 45°C for 45 min and at 94°C for 2 min; 35 cycles at 94°C for 30 s, 60°C for 45 s, and 68°C for 45 s; and a final extension at 68°C for 7 min. Two sets of specific primers for ANO1 amplification were designed based on the published sequence (Acc. Number: NM_001107564): ANO1 *set 1* gave a product of 637 bp, forward primer 5′-GCGCGTGCCAGTCACCTCTT-3′ (positions 1482 to 1501) and reverse primer was 5′-GCCGACCAACAAACCG-GCCT-3′ (positions 2099 to 2118); ANO1 *set 2* gave a product of 308 bp, forward primer 5′-TGGAGGAGTGTGCCCCAGGC-3′ (positions 2155 to 2174) and reverse primer 5′-TGGGGCCAGAGGGAAGGACG-3′ (positions 2443 to 2462). Positive controls included the amplification of rat prostate cDNAs, which are reported to strongly express ANO1 mRNA (25) and to rule out the possibility of contamination with genomic DNA, RT-PCR was performed without reverse transcription. The fragments amplified were verified in 2% agarose gel electrophoresis stained with ethidium bromide and visualized by Bio-Rad Fluor-S MultiImager (Hercules, CA).

RESULTS

Effects of chloride channel inhibition on excitatory responses. When exposed to the anion transport inhibitor SITS (0.1 mM), the urethral contractions induced by both EFS and NE in sheep, rats, and mice remained unaffected at all frequencies (1 to 50 Hz) and NE doses (0.01 to 300 μM) tested (Figs. 1 and 2). However, in

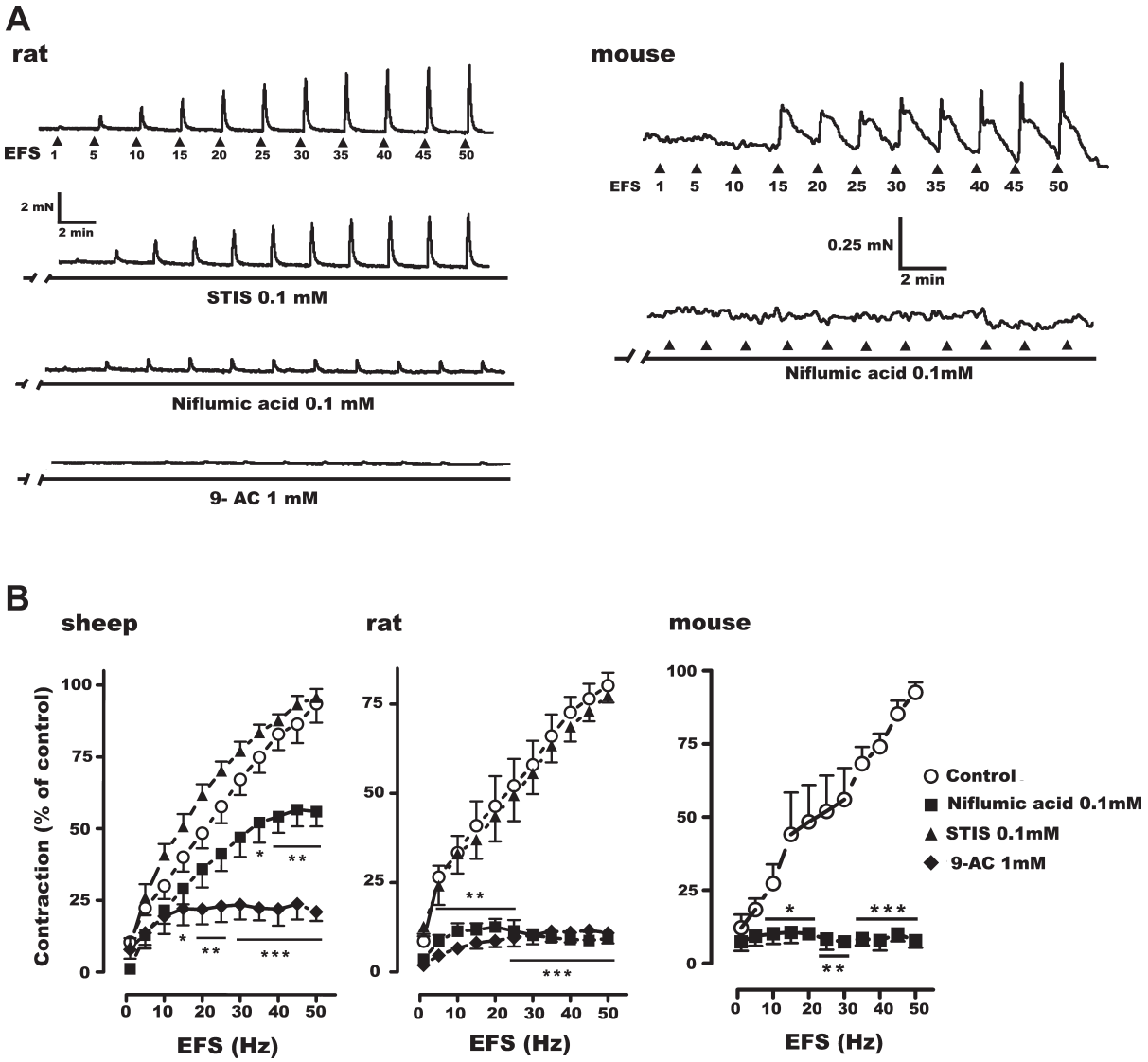

Fig. 1. Effects of chloride channel inhibitors on frequency-dependent contractile responses. *A*: representative traces showing rat (*left*) and mouse (*right*) urethral contractions elicited by electrical field stimulation (EFS; 5 s, 1 to 50 Hz) at a basal tension in control conditions (*top*) and following a 30-min incubation with the following chloride channel inhibitors: 4-acetamido-4′-isothiocyanato-2,2′-stilbenedisulfonic acid disodium salt hydrate (SITS; 0.1 mM), niflumic acid (0.1 mM), and anthracene 9-carboxylate (9-AC; 1 mM; *bottom*). *B*: changes in the frequency-response contraction curves at basal tension (expressed as a percentage of their respective control curves) in sheep (*left*), rat (*middle*), and mouse (*right*) urethra in the absence (open symbols) or the presence (30-min pretreatment) of SITS (0.1 mM), niflumic acid (0.1 mM), or 9-AC (1 mM; filled symbols). The data are expressed as means ± SE ($n = 6$ in sheep, $n = 5$ in rats and mice). $^*P < 0.05$, $^{**}P < 0.01$, $^{***}P < 0.001$ when compared with controls (1-way ANOVA followed by Student's *t*-test for unpaired observations).

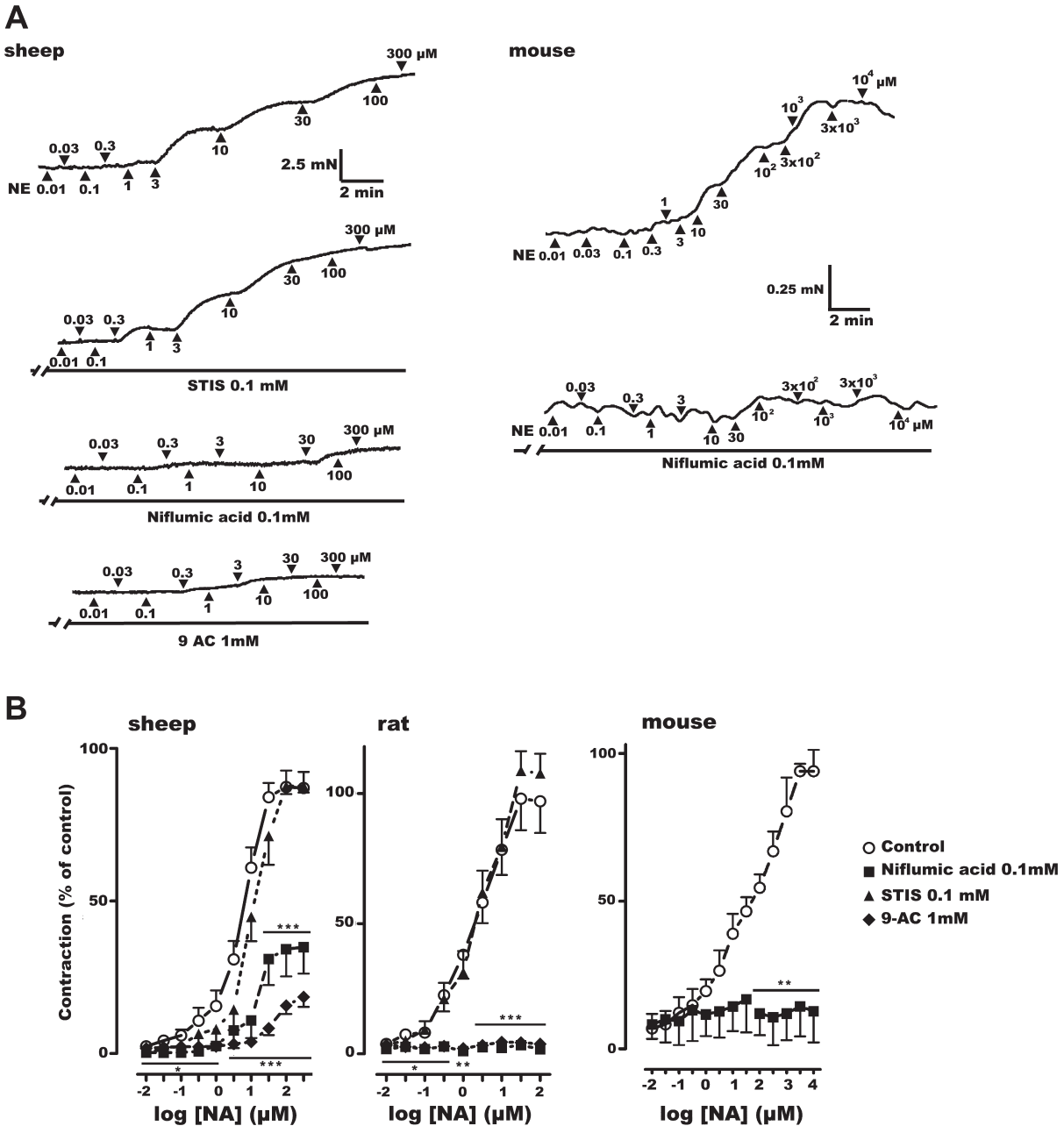

Fig. 2. Effects of chloride channel inhibitors on concentration-dependent contractions induced by norepinephrine (NE). *A*: representative traces showing sheep (*left*) and mouse (*right*) urethral contractions induced by cumulative addition of NE (0.01 to 100 μM) at basal tension in control conditions (*top*) and following a 30-min incubation with the following chloride channel inhibitors: SITS (0.1 mM), niflumic acid (0.1 mM), or 9-AC (1 mM; *bottom*). *B*: changes in the dose-response contraction curves induced by NE on basal tension (expressed as the percentage of the respective control curves) in sheep (*left*), rat (*middle*), and mouse (*right*) urethra in the presence (30-min pretreatment: filled symbols) or the absence (open symbols) of SITS (0.1 mM), niflumic acid (0.1 mM), or 9-AC (1 mM) pretreatment. Data are expressed as means ± SE ($n = 8$ in sheep, $n = 5$ in rats and mice). *$P < 0.05$, **$P < 0.01$, ***$P < 0.001$ when compared with controls (1-way ANOVA followed by Student's *t*-test for unpaired observations).

the presence of more specific inhibitors of fenamate and anthracene chloride channels, such as niflumic acid (0.1 mM) and 9-AC (1 mM), respectively (8), nerve-mediated contractions (Fig. 1) and the contractions elicited by cumulative addition of NE (Fig. 2) were inhibited, especially in rat and mouse urethras. Sheep urethra was more resistant to the effects of these chloride inhibitors (Figs. 1 and 2).

In agreement with previous findings in sheep (10), phentolamine (10 μM) inhibited EFS-induced contraction in rats (Fig. 3*A*) and mice. Maximal responses at 50 Hz were decreased to 16 ± 3.4% of the control preparations ($n = 9$, $P < 0.01$), which were not reduced further by TTX (1 μM; not shown) or subsequent addition of atropine (1 μM; Fig. 3*A*), suggesting that NE is the main excitatory neurotransmitter in the urethra. However, when atropine (1 μM) was added before phentolamine, EFS-induced contractions were reduced significantly in both the rat (Fig. 3*B*) and mouse (maximal responses at 50 Hz were reduced to 54 ± 3.6% of control preparations; $n = 9$,

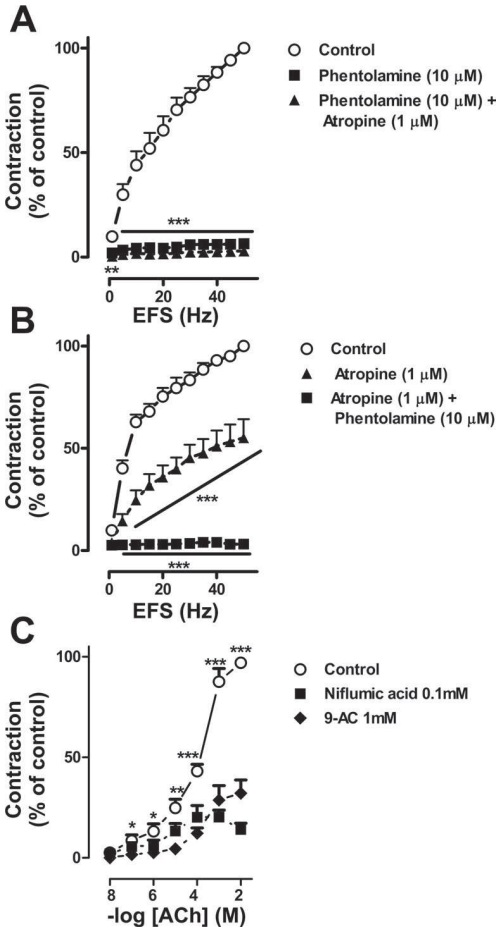

Fig. 3. Cholinergic participation in excitatory contractile responses and its inhibition by chloride channel inhibitors. Changes in the frequency-response (EFS) contraction curves at basal tension (expressed as a percentage of the respective control curves) in rat urethra in the presence (30-min pretreatment, filled symbols) or the absence (open symbols) of *A*: phentolamine (10 μM), followed by atropine (1 μM) or *B*: atropine, followed by phentolamine. *C*: changes in the dose-response contraction curves induced by ACh at basal tension (expressed as the percentage of the respective control curves) in rat urethra in the presence (30-min pretreatment, filled symbols) or the absence (open symbols) of niflumic acid (0.1 mM) or 9-AC (1 mM). Data are expressed as means ± SE ($n = 8$). *$P < 0.05$, **$P < 0.01$, ***$P < 0.001$ compared with controls (1-way ANOVA followed by Student's *t*-test for unpaired observations).

$P < 0.01$), and the remaining responses were subsequently abolished by phentolamine (10 μM; Fig. 3*B*). ACh elicited dose-dependent contraction in rat preparations (Fig. 3*C*), which were significantly inhibited by both niflumic acid (0.1 mM) and 9-AC (1 mM).

Significant fast contraction was induced when urethral preparations were exposed to chloride-free Krebs solution, which returned to the basal level of tension within 10 to 20 min (Fig. 4*A*). In both sheep and rat preparations, contractions of a similar shape and comparable magnitude were observed (40% of their respective preliminary responses to 120 mM K^+), which were very similar to the first rapid component of the contraction induced by high external K^+ concentrations (10). Indeed, these responses may reflect a shift in membrane potential to a more positive value, due to an increase in the outward Cl^- gradient that is not balanced by the impermeant anions that replace extracellular Cl^-. Exposure to chloride-free Krebs solution for 30 min resulted in a significant reduction in EFS-induced contractions at all the frequencies tested (1 to 50 Hz), with greater sensitivity in the rat rather than the sheep urethra (Fig. 4, *B* and *C*). However, in both species, this effect was much weaker than that observed with niflumic acid or 9-AC (0.1 and 1 mM, respectively; compare Figs. 2 and 4).

Effect of 2-APB on contractile responses. In a model of pacemaker activity proposed previously (29), CaCC stimulation occurs following the rise in intracellular Ca^{2+} levels that results from the activation of intracellular IP_3-sensitive calcium stores. When the effect of IP_3 receptor inhibition with 2-APB was investigated, significant inhibition of EFS-induced contractions was only observed in sheep urethral preparations following a 30-min exposure to 2-APB (50 μM; Fig. 5).

Effect of niflumic acid on nitrergic relaxant responses. We limited the study of the effects of niflumic acid to rat urethral preparations, as these were the most sensitive to the effects of chloride channel inhibitors. Niflumic acid was the most effective inhibitor of EFS-induced contractions, although pretreatment of rat urethral preparations with niflumic acid (50 μM) did not modify the magnitude or shape of nitrergic relaxations at any frequency or duration of EFS tested (0.5 to 12 Hz, 5 s; 2 and 35 Hz, 1 min; Fig. 6). Furthermore, pretreatment with 2-APB (50 μM, 30 min) did not modify EFS-induced rat urethral relaxations (data not shown).

Expression and distribution of ANO1 chloride channels in the urethral wall. ANO1 channel immunoreactivity (-ir) was exclusively detected in smooth muscle and urothelial cells in all three species studied (no such staining was detected in control preparations when the primary antibody was omitted: data not shown). The strong and clear ANO1 signal observed in smooth muscle colocalized with α-actin (Fig. 7, *A* to *C* and *D* to *F*). In mouse preparations, the restrictions imposed by the antibodies used (see MATERIALS AND METHODS) precluded determination of ANO1 and α-actin in the same section. However, when immunoreactions were performed on contiguous sections, the profile of both markers revealed similar patterns (Fig. 7, *G* and *H*) to those seen in sheep and rat. Analysis of the colocalization of ANO1 with vimentin revealed ANO1 in vimentin-expressing ICCs in the lamina propia or between smooth muscle bundles (Fig. 8). Furthermore, ANO1 was not detected in any nervous structures, including nerve fibers and nerve trunks.

ANO1 mRNA expression in the rat urethra. RT-PCR was performed using two sets of specific primers designed from known ANO1 sequences, directed against different regions of the mRNA, and producing products of different sizes and compositions, to ensure accurate assessment of ANO1 gene expression. In both cases, each set of primers amplified a specific band of the predicted size from RNA obtained from both urethra and prostate tissue, the latter serving as a positive control. Indeed, the product amplified from urethral tissue produced a band of stronger intensity. No bands were detected in reactions lacking reverse transcriptase, discounting the possibility of genomic DNA contamination of the preparations (Fig. 9).

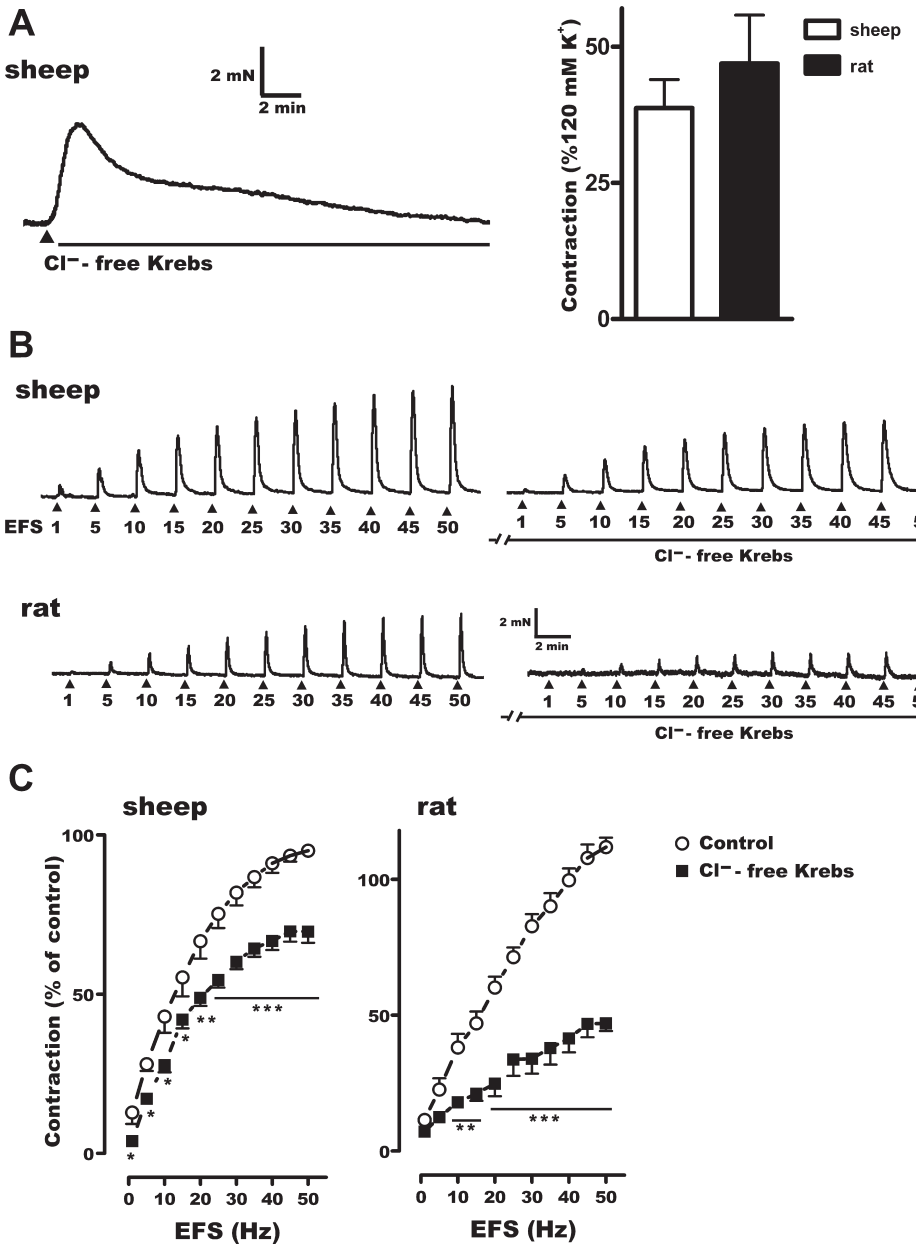

Fig. 4. Effects of chloride-free Krebs solution on nerve-mediated contractile responses. *A*: representative traces (*left*) showing the transient urethral contraction elicited on switching to chloride-free Krebs (arrowhead). *Right*: bar diagrams showing the magnitude of contraction compared with that induced by 120 mM K^+ solution in the same preparation. *B*: representative traces showing sheep (*top*) and rat (*bottom*) urethral contractions elicited by EFS (5 s, 1 to 50 Hz) at basal tension in control conditions (*left*) and following a 30-min incubation with the chloride-free Krebs solution (*right*). *C*: changes in the frequency-response contraction curves at basal tension (expressed as a percentage of the respective control curves) in sheep (*left*) and rat (*right*) urethra in chloride-free Krebs solution presence (pretreatment for 30 min, filled symbols) or in normal Krebs solution (open symbols). Data are expressed as means ± SE ($n = 8$ in sheep, $n = 7$ in rats). $^*P < 0.05$, $^{**}P < 0.01$, $^{***}P < 0.001$ when compared with controls (1-way ANOVA followed by Student's *t*-test for unpaired observations).

DISCUSSION AND CONCLUSIONS

We performed a comparative study of the distribution of the recently cloned ANO1 in three species, considered to be the main CaCC (6, 26, 34). In addition, we assessed how the movement of chloride participated in both contractile and relaxant responses in the urethra, and we analyzed the modulatory role of ICCs in the urinary tract by studying the involvement of CaCC.

Excitatory urethral contractile responses are generally considered to be of adrenergic origin, as confirmed here. While other transmitters may contribute to evoked contractions in several species (3), their role has not yet been clearly established. Evoked contractions may have a cholinergic component, involving either direct action of ACh on discrete smooth muscle layers (14) or on the modulation of NE release (21). Since atropine partial inhibits nerve-mediated excitatory urethral contractions in all three species studied, there does indeed seem to be some cholinergic input to these events. However, blocking this effect with phentolamine suggests that ACh acts on presynaptic muscarinic receptors in adrenergic nerve terminals, supporting a modulatory effect of ACh on NE release (21). Indeed, the effect of CaCC inhibitors on cholinergic responses could not be distinguished from that of adrenergic inhibitors, pointing to NE as the true mediator of smooth muscle activation.

Although classically linked to the development and maintenance of contractile responses in smooth muscle structures (7), the physiology of chloride channels remains controversial, in part due to the lack of specific pharmacological tools, and their widespread distribution and variability. In our experimental conditions, the CaCC inhibitors niflumic acid and 9-AC effectively inhibit urethral contractile responses in all species tested.

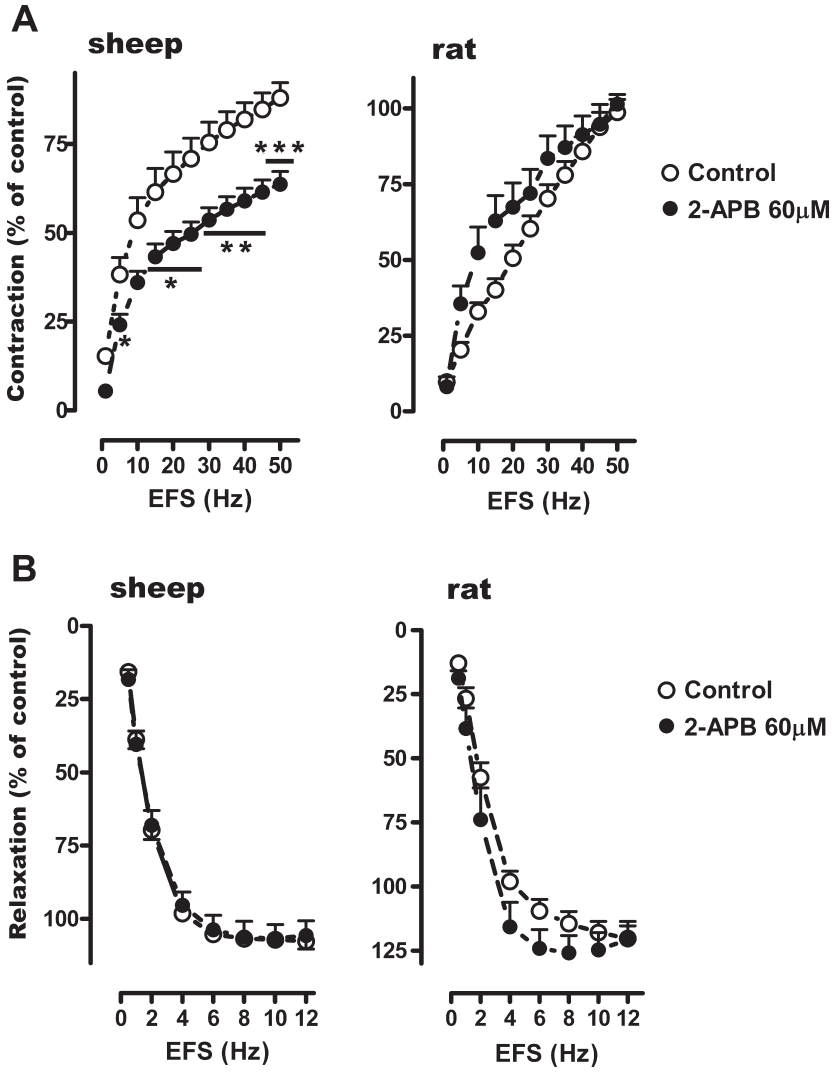

Fig. 5. Effects of the IP_3 receptor inhibitor 2-APB on contractions induced by EFS. Changes in the frequency-response contraction curves (EFS, 5 s, 1 to 50 Hz) at basal tension (expressed as percentage of the respective control curves) in sheep (*left*) and rat (*right*) urethra in the presence (●) or absence (○) of 2-APB (60 μM). Data are expressed as means ± SE ($n = 7$ in sheep, $n = 6–8$ in rats). $^*P < 0.51$, $^{**}P < 0.01$, $^{***}P < 0.001$ compared with controls (1-way ANOVA followed by Student's *t*-test for unpaired observations).

The sheep urethra was slightly more resistant to the inhibitory action of these compounds than that of the rat and mouse. However, the putative CaCC antagonist SITS (36) consistently had no effect in any of the three species under each experimental condition, challenging its activity as a specific CaCC inhibitor. Indeed, previous studies reported no effect of SITS or 4,4′-diisothiocyanatostilbene-2,2′-disulfonic acid on intracellular chloride levels ($[Cl^-]_i$) in sheep cardiac Purkinje fibers (32), or in guinea pig vas deferens (2) or ureter (1). It has been well-established that this stilbenedisulfonic acid derivative modifies $[Cl^-]_i$ in other systems (15), although its activity as an inhibitor of Cl^-/HCO_3^- exchange may also account for this effect (reviewed in Ref. 7).

While a discussion of the mechanisms regulating chloride movements is beyond the scope of the present study, some basic concepts should be considered. Physiological levels of $[Cl^-]_i$ in smooth muscle cells are higher than those predicted by the Donnan equilibrium, since $E_m > E_{Cl}$ and thus, Cl^- movements have a net depolarizing effect (7). Deviation from the equilibrium is augmented further when smooth muscle cells are immersed in artificial saline solutions (e.g., Krebs) containing much higher $[Cl^-]$ than the extracellular milieu, thereby raising the $[Cl^-]_i$ even further (18). In these conditions, removal of external chloride is followed by an increase in Cl^- efflux across the membrane along a strong concentration gradient, leading to a membrane depolarization that is augmented when external Cl^- is replaced by impermeant anions (20). When depolarization is sufficient to activate voltage-gated Ca^{2+} channels, the increase in $[Ca^{2+}]_i$ can induce contraction. As shown in vascular preparations (20), this membrane depolarization depends on the length of exposure to low extracellular chloride $[Cl^-]_o$ conditions, with the initially significant effect shortly after exposure progressively diminishing thereafter. By contrast, a low $[Cl^-]_o$ potentiates NE-induced vascular contraction through CaCCs that are activated by NE-mediated increases in $[Ca^{2+}]_i$ (potentiation by low $[Cl^-]_o$ disappears at 0 Ca^{2+}) (20). In the urethra of all three species studied here, contractions induced by both EFS and exogenous NE or ACh were dependent on Cl^- currents, as witnessed by the strong inhibitory effect of low $[Cl^-]_o$, and their inhibition by 9-AC and niflumic acid. However, variation between species regarding the contribution of different Ca^{2+} sources to CaCC activity in NE-induced contraction cannot be ruled out. The Cl^- current in the rat and mouse urethra is most likely

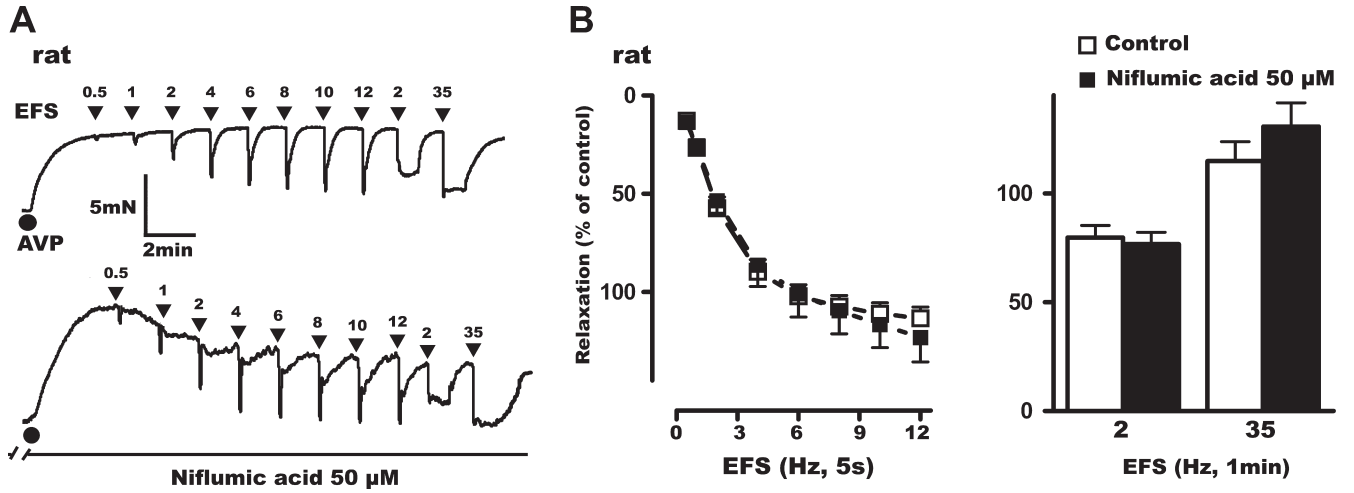

Fig. 6. Effects of niflumic acid on the frequency-dependent nitrergic relaxations. *A*: representative traces showing the relaxation elicited by EFS (5 s, 0.5 to 12 Hz, and 1-min duration, 2 and 35 Hz) in AVP (0.1 μM) precontracted rat urethral preparations under control conditions (*top*) and after 30-min pretreatment with 50 μM niflumic acid (*bottom*). *B*: changes in the frequency-response curves in precontracted rat urethras following short (5 s; *left*)- and long-duration EFS (1 min; *right*) in the presence (filled symbols and bars) or the absence (open symbols and bars) of 50 μM niflumic acid. Data are expressed as means ± SE (n = 7). No significant differences were found between the 2 groups (1-way ANOVA).

activated by Ca^{2+} influx, consistant with the failure of 2-APB to affect NE-induced contractions. By contrast, Ca^{2+} mobilization from IP_3-sensitive stores triggered by NE receptor activation in the sheep urethra may be partly responsible for Ca^{2+}-mediated CaCC activation.

Despite these differences, our functional results are consistent with chloride movements via chloride channels representing a major component of smooth muscle contractility in the urethra. The earlier failure to detect ANO1 in the mouse urethra (16) clearly contradicts our current results. While this

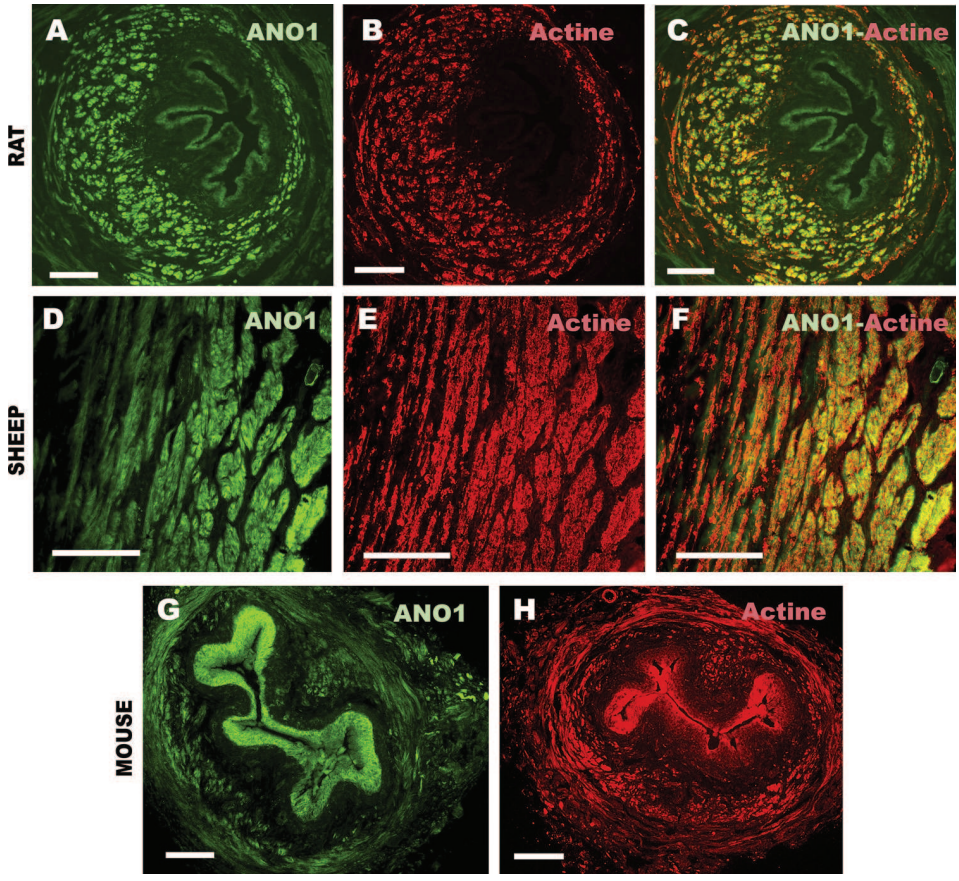

Fig. 7. Colocalization of anoctamin 1 (ANO1) channels and α-actin in smooth muscle of the urethra. Representative photomicrographs showing immunolocalization of ANO1 (green: *A*, *D*, and *G*) and α-actin (red: *B*, *E*, and *H*) within the smooth muscle layer of rat (*top*), sheep (*middle*), and mouse (*bottom*) urethra. Intense ANO1-immunoreactivity (ir) can be observed colocalized with α-actin in smooth muscle cells (*C* and *F*). Faint but positive ANO1-ir was detected in the rat and mouse urothelium (*A* and *G*). Scale bars = 50 μm.

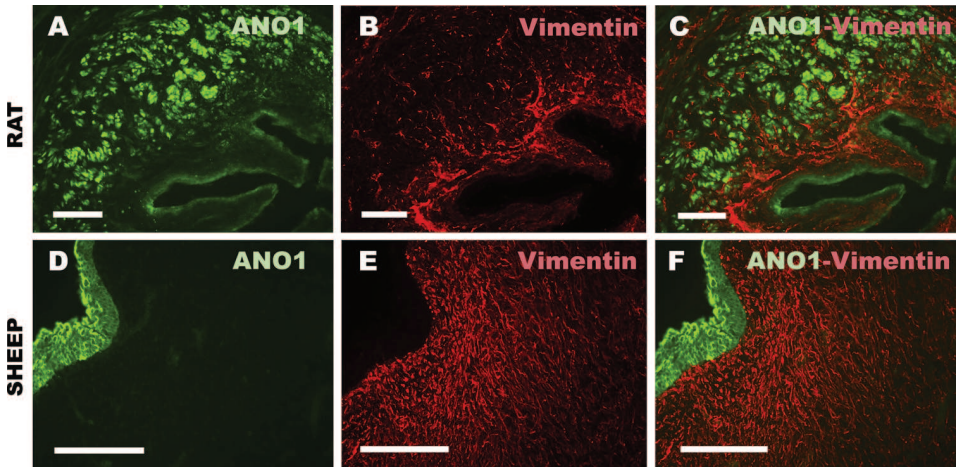

Fig. 8. ANO1 channels and vimentin do not colocalize in urethral interstitial cells of Cajal (ICCs). Representative photomicrographs showing intense ANO1-ir (green) within the rat smooth muscle coat (*A*) and sheep urothelium (*D*). No ANO1-ir was detected in the submucosal layer, which exhibited abundant vimentin-positive ICCs (*B*, *E*). ANO1 (green) did not colocalize with vimentin (red), which was distributed in the submucosa (*F*) and between the muscle bundles (*C*). Scale bars = 50 μm.

may be due to differences in the immunohistochemical protocols used (the earlier study used methanol or paraformaldehyde as fixatives, with no cryoprotection), it is more likely that these conflicting findings are due to the use of different antibodies (i.e., a rabbit polyclonal antiserum generated in-house vs. a commercially available ANO1 rabbit antibody that produced similar results in the gastrointestinal tract) (12, 17, 35). Given the successful detection of ANO1 in independent studies, it is unlikely that our results are a mere artefact. Moreover, the specificity of the immunoreactivity was further confirmed by assessing the distribution of ANO1 mRNA using two different probes targeting separate regions of the mRNA sequence. In both cases, a clear, unique band of the predicted size was amplified and while we did not perform quantitative PCR, the apparent intensity of the bands amplified from the urethra was

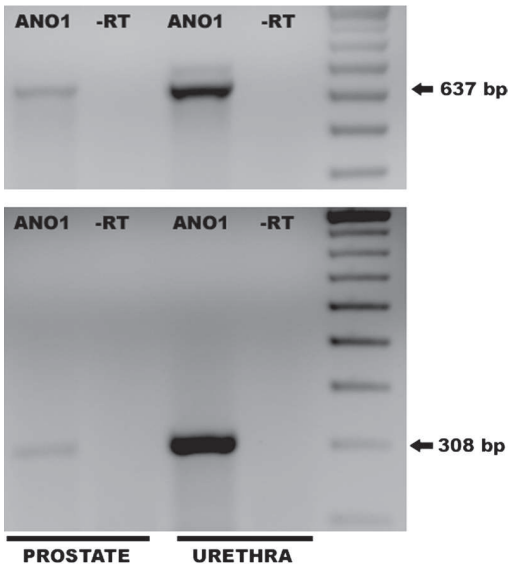

Fig. 9. ANO1 mRNA expression in rat urethra. Amplification products of ANO1 visualized on 2% agarose gels stained with ethidium bromide. The mRNA transcripts of the expected sizes for this channel were amplified from rat urethral tissue [637 bp for the first set of ANO1 primers (*top*) and 308 bp for the second set of ANO1 primers (*bottom*)] and corresponded to the transcripts amplified from rat prostate tissue (positive control). Negative controls were performed without the reverse-transcriptase enzyme (-RT). Right lane: 100-bp ladder.

stronger than that amplified from the prostate, which was used as a positive control and strongly expresses ANO1 (surpassed only by the pancreas) (25). Thus, the results of PCR amplification are consistent with the ANO1 immunolabeling findings.

Our structural data revealed the restriction of ANO1 to smooth muscle cells (expressing smooth muscle actin) and epithelial cells of the urothelium. Anoctamins have been described in almost all secretory epithelia and they are considered essential for the secretion process (see Ref. 19 for a recent review). However, the urothelium is generally considered not to have a secretory function, except for its role in Na^+, K^+, and Cl^- transport in the bladder, which is triggered by an increase in hydrostatic pressure (33). Interestingly, before its identification as a CaCC, ANO-1 was associated with tumoural cells and malignancy (measured as migratory ability), due to its participation in regulating cell volume during mechanical deformation (19). Indeed, ANO-1 itself has been directly described as a mediator of mechanosensitive secretion in biliary epithelium (9). While we found no significant changes in urethral contractions in preparations naturally devoid of urothelium (sheep strips) or in which it has been removed (rat rings, not shown), the participation of ANO-1 in mechanoreception by urothelium (routinely subject to large changes in both stretching and fluid pressure) appears plausible and should be analyzed further using different experimental approaches.

ANO1-ir was consistently absent from cells expressing vimentin, despite the distinct subtypes of ICC described in different layers of the urethra (11). These results appear surprising at first glance, as CaCCs are thought to be present in rabbit urethral ICCs, where they generate large-amplitude spontaneous Cl^- currents (28) and may act as "pacemakers" of urethral slow wave activity (27). Moreover, the use of specific CaCC inhibitors, such as 9-AC and niflumic acid, has been proposed for "pharmacological knock-out" of ICCs in the rabbit urethra (30), emphasizing the important role of CaCCs in the origin of this spontaneous oscillator.

ICCs were initially proposed to act as cytosolic Ca^{2+} oscillators in the gut, based on the observed activation of CaCC by Ca^{2+} released from IP_3-dependent stores and the subsequent Ca^{2+} influx (5). However, this mechanism does not appear to persist in the urethra given the lack of correlation between Ca^{2+} transients in ICCs and smooth muscle cells in different regions of the urinary tract, and in different species (13).

Furthermore, the ICC-Ca^{2+} oscillator model suggests electrical coupling between ICCs and smooth muscle cells via gap junctions (5). However, this direct coupling appears not to be relevant in urethral neurotransmission despite the existence of gap junctions between these cells, suggesting chemical rather than electrical communication (23). In agreement, the present findings do not support the ICC-Ca^{2+} oscillator model in whole urethral preparations from sheep, rats, or mice, as no spontaneous or slow wave activity was detected and IP_3 inhibitors had no effect on EFS-induced urethral contractions.

The absence of ANO1 in urethral ICCs from the three species studied may be explained by the presence of a different and as-yet uncharacterized CaCC in these cells. Alternatively, ANO1 may only be expressed in rabbit urethral ICC. The lack of ANO1 channels in urethral ICC is consistent with the failure of CaCC inhibitors to modify EFS-induced nitrergic relaxation. Although significant increases in cGMP have been observed in a subset of urethral ICCs upon functional nitrergic stimulation (11), this appears to be at least partially mediated by a different ionic mechanism, involving cyclic nucleotide-gated (CNG) channels (31). CNG channels are thought to modify $[Ca^{2+}]_i$ in different cellular microdomains, possibly leading to the release of some chemical mediators (22).

In conclusion, we detected strong ANO1 expression in the smooth muscle cells of the urethra in three different species, where it played a crucial role in the development and maintenance of excitatory contractile responses, but it did not participate significantly in urethral relaxation. Moreover, ANO1 was absent from all urethral ICC subtypes, in sharp contrast to the strong expression in ICCs of the gastrointestinal tract. Therefore, despite their morphological resemblance, the functional differences between distinct ICCs prevent us from drawing generalized conclusions regarding their function.

ACKNOWLEDGMENTS

The microphotographs were acquired and analyzed at the Microscopy and Cytometry Centre (Complutense University, Madrid, Spain). We thank Alfonso Cortés and Luis M. Alonso for technical assistance with the fluorescence microscopy.

GRANTS

This work was supported by grants from the "Comunidad de Madrid–Universidad Complutense de Madrid" (UCMGR85/06-920307), UCM-Santander (GR35/10-A-920307), and Fundación Mutua Madrileña (FMM2011).

DISCLOSURES

No conflicts of interest, financial or otherwise, are declared by the author(s).

AUTHOR CONTRIBUTIONS

Author contributions: M.S., A.G.-P., and D.T. performed experiments; M.S. and D.T. analyzed data; M.S. and D.T. prepared figures; M.S., A.G.-P., and D.T. edited and revised manuscript; M.S., A.G.-P., and D.T. approved final version of manuscript; A.G.-P. and D.T. conception and design of research; A.G.-P. and D.T. interpreted results of experiments; A.G.-P. and D.T. drafted manuscript.

REFERENCES

1. **Aickin CC.** Chloride transport across the sarcolemma of vertebrate smooth and skeletal muscle. In: *Chloride Channels and Carriers in Nerve, Muscle and Glial Cells*, edited by Alvarez-Leefmans FJ and Russell JM. New York: Plenum, 1990, p. 209–249.
2. **Aickin CC, Brading AF.** The effect of loop diuretics on Cl^- transport in smooth muscle of the guinea pig vas deferens and taenia from caecum. *J Physiol* 421: 33–53, 1990.
3. **Andersson KE, Sjögren C.** Aspects of the physiology and pharmacology of the bladder and urethra. *Prog Neurobiol* 19: 71–89, 1982.
4. **Andersson KE, García-Pascual A, Forman A, Töttrup A.** Nonadrenergic, noncholinergic nerve mediated relaxation of rabbit urethra is caused by nitric oxide. *Acta Physiol Scand* 141: 133–134, 1991.
5. **Berridge MJ.** Smooth muscle cell calcium activation mechanisms. *J Physiol* 586: 5047–5061, 2008.
6. **Caputo A, Caci E, Ferrera L, Pedemonte N, Barsanti C, Sondo E, Pfeffer U, Ravazzolo R, Zegarra-Moran O, Galietta JV.** TMEM16A, a membrane protein associated with calcium-dependent chloride channel activity. *Science* 322: 590–594, 2008.
7. **Chipperfield AR, Harper AA.** Chloride in smooth muscle. *Prog Biophys Mol Biol* 74: 175–221, 2000.
8. **Chu LL, Adaikan PG.** Role of chloride channels in the regulation of corpus cavernosum tone: a potential therapeutic target for erectile dysfunction. *J Sex Med* 5: 813–821, 2008.
9. **Duna AK, Khimji AKS, Kresge C, Rockey DC, Alpini G, Feranchak AP.** Mechanosensitive secretion in biliary epithelium mediated through a novel Cl^- channel, TMEM16A. *Hepatology* 52: 433A, 2010.
10. **García-Pascual A, Costa G, García-Sacristán A, Andersson KE.** Calcium dependence of contractile activation of isolated sheep urethra. I. Responses to electrical stimulation. *Pharmacol Toxicol* 69: 263–269, 1991.
11. **García-Pascual A, Sancho M, Costa G, Triguero D.** Interstitial cells of Cajal in the urethra are cGMP-mediated targets of nitrergic neurotransmission. *Am J Physiol Renal Physiol* 295: F971–F983, 2008.
12. **Gomez-Pinilla PJ, Gibbons SJ, Bardsley MR, Lorincz A, Pozo MJ, Pasricha PJ, Van de Rijn M, West RB, Sarr MG, Kendrick ML, Cima RR, Dozois EJ, Larson DW, Ordog T, Farrugia G.** Ano1 is a selective marker of interstitial cells of Cajal in the human and mouse gastrointestinal tract. *Am J Physiol Gastrointest Liver Physiol* 296: G1370–G1381, 2009.
13. **Hashitani H, Lang RJ.** Functions of ICC-like cells in the urinary tract and male genital organs. *J Cell Mol Med* 14: 1199–1211, 2010.
14. **Hassouna M, Abdelhakim A, Abdelrahman M, Galeano C, Elhilali MM.** Response of the urethral smooth muscle to pharmacological agents. *J Urol* 129: 1262–1264, 1983.
15. **Hoffmann EK, Simonsen LO.** Membrane mechanisms in volume and pH regulation in vertebrate cells. *Physiol Rev* 69: 315–382, 1989.
16. **Huang F, Rock JR, Harfe BD, Cheng T, Huang X, Jan YN, Jan LY.** Studies on expression of the TMEM16A calcium-activated chloride channel. *Proc Natl Acad Sci USA* 106: 21413–21418, 2009.
17. **Hwang SJ, Blair PJA, Britton FC, O'Driscoll KE, Hennig G, Bayguinov YR, Rock JR, Harfe BD, Sanders KM, Ward SM.** Expression of anoctamin 1/TMEM16A by interstitial cells of Cajal is fundamental for slow wave activity in gastrointestinal muscles. *J Physiol* 587: 4887–4904, 2009.
18. **Koncz C, Daugiras JT.** Use of MQAE for measurements of intracellular $[Cl^-]$ in cultured aortic smooth muscle cells. *Am J Physiol Heart Circ Physiol* 267: H2114–H2123, 1994.
19. **Kunzelmann K, Tian Y, Martins JR, Faria D, Kongsuphol P, Ousingsawat J, Thevenod F, Roussa E, Rock J, Schreiber R.** Anoctamins. *Pflügers Arch* 462: 195–208, 2011.
20. **Lamb F, Barna TJ.** Chloride ion currents contribute functionally to norepinephrine-induced vascular contraction. *Am J Physiol Heart Circ Physiol* 275: H151–H160, 1998.
21. **Mattiasson A, Andersson KE, Sjögren C.** Adrenoceptors and cholinoceptors controlling the release of noradrenaline from adrenergic nerves in the isolated urethra from rabbit and man. *J Urol* 131: 1190–1195, 1984.
22. **Rieke F, Schwartz EA.** A cGMP-gated current can control exocytosis at cone synapses. *Neuron* 13: 863–873, 1994.
23. **Sancho M, Triguero D, García-Pascual A.** Direct coupling through gap junctions is not involved in urethral neurotransmission. *Am J Physiol Renal Physiol* 300: F864–F872, 2011.
24. **Sanders KM.** A case for interstitial cells of Cajal as pacemakers and mediators of neurotransmission in the gastrointestinal tract. *Gastroenterology* 111: 492–515, 1996.
25. **Schreiber R, Uliyakina I, Kongsuphol P, Warth R, Mirza M, Martins JR, Kunzelmann K.** Expression and function of epithelial anoctamins. *J Biol Chem* 285: 7838–7845, 2010.
26. **Schroeder BC, Cheng T, Jan YN, Jan LY.** Expression cloning of TMEM16A as a calcium-activated chloride channel subunit. *Cell* 134: 1019–1029, 2008.

27. **Sergeant GP, Hollywood MA, McCloskey KD, Thornbury KD.** Specialised pacemaking cells in the rabbit urethra. *J Physiol* 526: 359–366, 2000.
28. **Sergeant GP, Hollywood MA, McHale NG, Thornbury KD.** Spontaneous Ca^{2+} activated Cl^- currents in isolated urethral smooth musle cells. *J Urol* 166: 1161–1166, 2001.
29. **Sergeant GP, Hollywood MA, McHale NG, Thornbury KD.** Ca^{2+} signalling in urethral interstitial cells of Cajal. *J Physiol* 576: 715–720, 2006.
30. **Sergeant GP, Thornbury KD, McHale NG, Hollywood MA.** Characterization of norepinephrine-evoked inward currents in interstitial cells isolated from the rabbit urethra. *Am J Physiol Cell Physiol* 283: C885–C894, 2002.
31. **Triguero D, Sancho M, García-Flores M, García-Pascual A.** Presence of cyclic nucleotide-gated channels in the rat urethra and their involvement in nerve-mediated nitrergic relaxation. *Am J Physiol Renal Physiol* 297: F1353–F1360, 2009.
32. **Vaughan-Jones RD.** An investigation of chloride-bicarbonate exchange in the sheep cardiac Purkinje fibre. *J Physiol* 379: 377–406, 1986.
33. **Wang ECY, Lee JM, Johnson JP, Kleyman TR, Bridges R, Apodaca G.** Hydrostatic pressure-regulated ion transport in bladder uroepithelium. *Am J Physiol Renal Physiol* 285: F651–F663, 2003.
34. **Yang YD, Cho H, Koo JY, Tak MH, Cho Y, Shim WS, Park SP, Lee J, Lee B, Kim BM, Raouf R, Shin YS, Oh U.** TMEM16A confers receptor-activated calcium-dependent chloride conductance. *Nature* 455: 1210–1215, 2008.
35. **Zhu MH, Kim TW, Ro S, Yan W, Ward SM, Koh SD, Sanders KM.** A Ca^{2+}-activated Cl^- conductance in interstitial cells of Cajal linked to slow wave currents and pacemaker activity. *J Physiol* 587: 4905–4918, 2009.
36. **Zoccoli MA, Karnovsky ML.** Effect of two inhibitors of anion transport on the hydrolysis of glucose 6-phosphate by rat liver microsomes. *J Biol Chem* 255: 1113–1119, 1980.

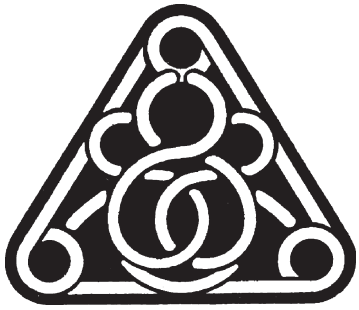

MANUSCRITO VI

Altered neuronal and endothelial nitric oxide synthase expression in the bladder and urethra of cyclophosphamide-treated rats

Maria Sancho, Jose Ferrero, Domingo Triguero and Angeles Garcia-Pascual*

From:

Department of Physiology, School of Veterinary Medicine, Complutense University, Madrid, Spain.

***Corresponding Author**:

Angeles Garcia-Pascual, Department of Physiology, School of Veterinary Medicine, Avda. Puerta de Hierro s/n, Complutense University, 28040 Madrid, Spain.
Telephone: 3413943843; Fax: 3413943864; e-mail: angarcia@vet.ucm.es

Abstract

Increased nitric oxide (NO) production plays a key role in cyclophosphamide (CYP)-induced cystitis, although the underlying mechanisms and the relative involvement of the different NO synthase (NOS) isoforms remain to be elucidated. Moreover, the role of the urethra in this process is unclear. In this study, we have analyzed the changes in the expression and distribution of the inducible (iNOS), endothelial (eNOS) and neuronal (nNOS) isoforms of NOS, and the alterations in nerve-mediated contractility in the bladder and urethra of CYP-treated rats. Accordingly, Wistar rats were treated with 150 mg kg^{-1} CYP for 4 (acute treatment) or 48 hours (intermediate treatment), or with 70 mg kg^{-1} CYP every 3 days for 10 days (chronic treatment), and the changes in protein expression were assessed by immunohistofluorescence and quantified in Western blots, while mRNA expression was assessed by conventional/quantitative PCR. Similarly, nerve-mediated contractility was quantified *in vitro*. Unexpectedly, no iNOS expression was detected in CYP-treated animals, while a transient downregulation of nNOS expression and a progressive upregulation of eNOS was observed. Similar qualitative changes were observed in the bladder and urethra, although contractility only diminished in the bladder. These findings suggest that spatiotemporal alterations in NO production by constitutive NOS may be involved in the pathogenicity of CYP. As a result, further studies will be necessary to fully characterize the contribution of eNOS to the increases in NO associated with bladder inflammation.

Highlights

► No iNOS expression was observed in CYP-treated bladders or urethras. ► CYP treatment induced a transient downregulation of nNOS coincident with a progressive upregulation of eNOS. ► Changes in contractility were not associated with NO synthesis. ► Changes in NO production mediated by constitutive NOS isoforms may contribute to CYP pathogenicity.

Abbreviations

Ach, acetylcholine chloride; AVP, arginine vasopressin; CYP, cyclophosphamide; DAPI, 4',6-diamino-2-phenylindole dihydrochloride; EFS, electrical field stimulation; H&E, haematoxylin and eosin; ir, immunoreactivity or immunoreaction; NA, noradrenaline; L-NOARG, N^{w}-nitro-L-arginine; NO, nitric oxide; iNOS, inducible nitric oxide synthase; eNOS, endothelial nitric oxide synthase; nNOS, neuronal nitric oxide synthase; PB, phosphate buffer, RT-PCR, real time PCR; SNC, S-nitroso-L-cysteine.

Key words: cyclophosphamide, cystitis, eNOS, nNOS, bladder, urethra.

1. Introduction

Haemorrhagic cystitis is a common clinical complication of cyclophosphamide (CYP) treatment, which is used both in chemotherapy for solid tumours and in conditioning for hematopoietic cell transplantation [1]. In experimental animals, mainly rats, CYP-induced cystitis is a common model of bladder inflammation in which symptoms of an overactive bladder develop [2, 3]. Among the many mediators implicated in CYP-induced cystitis, the overproduction of nitric oxide (NO) is known to play a key role [4-8]. This increased NO production is often assumed to result from the expression of the inducible isoform of NO synthase (iNOS) [4, 8, 9], while the production of NO by the other two constitutively expressed NOS isoforms, endothelial (eNOS) and neural (nNOS), has attracted little attention. Constitutive NOS can produce controlled amounts of NO, mainly from the endothelium (eNOS) and nerve structures (nNOS) [10]. Changes in NO release from these different sources may alter efferent contractile and/or afferent sensory functions, affecting distinct target cell types including smooth muscle cells, sensory nerves, urothelial cells and interstitial cells.

CYP-induced cystitis is thought to be triggered by the accumulation of its hepatic metabolite, acrolein, in the urine. Acrolein is a highly reactive aldehyde that attacks the epithelium and which initiates an inflammatory process that spreads throughout the bladder wall [7]. Thus, other organs in the urinary system that are not in contact with the urine for long periods should not be as strongly affected by CYP-treatment, such as the urethra. However, despite the possible contribution of urethral inflammation to the symptomatology of overactive bladder, the effect of CYP on the urethra remains largely unexplored.

In the present study, we investigated the changes in the expression and distribution of iNOS, eNOS and nNOS, and the alterations in nerve-mediated contractility in both the bladder and urethra of rats subjected to acute, intermediate or chronic CYP treatment regimens. We observed prominent inflammatory reactions in the urethra and bladder, although contractility was only modified in the bladder. A surprising lack of iNOS expression was observed in both organs in response to CYP treatment, while nNOS and eNOS expression decreased and increased, respectively.

2. Materials and Methods

2.1 Drugs

Acetylcholine chloride (ACh), atropine sulphate, cyclophosphamide monohydrate (CYP), guanethidine monosulphate, noradrenaline bitartrate salt (NE), D-tubocurarine hydrochloride, N^G–nitro-L-arginine (L-NOARG) and [Arg^8] vasopressin acetate salt (AVP) were all obtained from Sigma Chemie GMbH (Steinheim, Germany). All drugs were dissolved in distilled water, except for CYP, which was dissolved in NaCl (0.9 %). Solutions were stored at -20ºC and the drugs were diluted to working

concentrations in 0.9% NaCl. Solutions of S-nitrocysteine (SNC) were prepared by adding sodium nitrite (100 mM) to an equivalent volume of a solution containing 250 mM HCl, 1 mM EDTA, and 100 mM L-cysteine. SNC concentrations were determined spectrophotometrically (Shimadzu UV-1601 UV-visible spectrophotometer; Shimadzu, Tokyo, Japan), assuming a molar absorption coefficient of ε_{544} = 16.6 Mcm^{-1}. Working dilutions were prepared in deoxygenated distilled water immediately before use, kept on ice and stored in the dark.

2.2 CYP treatment

Haemorrhagic cystitis was induced by CYP administration to 77 adult female Wistar rats (200-250 g). Rats were housed individually and were maintained under standard laboratory conditions (12 h light/dark cycle) with *ad libitum* access to food and water. CYP was administered according to the following regimes: (i) acute treatment: 150 mg kg^{-1} i.p., 4 h before sacrificing; (ii) intermediate treatment: 150 mg kg^{-1} i.p., 48 h before sacrificing; or (iii) chronic treatment: 70 mg kg^{-1} i.p., administered every 3 days for 10 days. Control animals received a corresponding volume of saline (0.9%) alone instead of CYP. All procedures were approved by the Ethical Committee of the Complutense University and performed in accordance with European guidelines (EU Directive 86/609/EEC).

2.3 Voiding frequency test

Micturition frequency was analyzed in all the rats as described previously [11]. Drinking water was removed one hour before testing and the rats were left in cages lined with filter paper for 30 min. A UV light source was used to visualize and trace the urine spots on the filter paper, and the total number of urine spots and those of small diameter (<0.5 cm) was counted and expressed as the number of voids per hour.

2.4 Histology and immunofluorescence

Animals were anesthetized (40 mg kg^{-1} ketamine + 5 mg kg^{-1} xylazine, i.p.) and then subjected to cardiac perfusion with heparinised 0.1 M phosphate buffer (PB), followed by 4% paraformaldehyde in PB for 30 min. The lower urinary tract was removed from the rats and tissue samples (5 x 5 mm) were obtained from the mid detrusor, the trigone or the proximal urethra, and fixed in ice-cold 4% paraformaldehyde in 0.1 M PB (pH 7.0). The tissue was then processed as described previously [12], cryoprotecting the samples with increasing concentrations of sucrose (10-30%) and then snap-freezing it in liquid nitrogen-cooled isopentane and storing at -80ºC for up to 15 days. The tissues were embedded in Tissue-Tek OTC compound and cryostat sections (7 μm: CM1850 UV, Leica Microsystems, Barcelona, Spain) cut transversal to the mucosal surface were recovered on poly-L-lysine-coated slides. The slides were air-dried at room temperature for 24 h and then processed directly or stored at -80ºC for no more than 30 days.

The sections were stained with haematoxylin and eosin (H&E) to evaluate the histological damage, two different researchers who were blind to the treatment of each section examining the stained sections for oedema, haemorrhage, vascular congestion, cell infiltration and epithelial damage (including epithelial denudation or proliferation). Accordingly, the lesions were classified as non-existent (0), mild (1), moderate (2) or severe (3).

Immunofluorescence was performed as described previously [14] using the antibodies listed in Table 1. Briefly, sections were washed with PB (3 x 5 min) and incubated for 1 h with 3% normal donkey serum (Chemicon International, Temecula, CA, USA) containing 0.3% Triton X-100. The sections were incubated for 24 h in a humidified chamber at 4ºC with the primary antibody diluted in 2% normal donkey serum and 0.3% Triton X-100, and for 2 h at room temperature in the dark with the secondary antibodies. After washing with PB (3 times, 10 min each), the nuclei were counterstained for 20-30 min with 4′,6-diamino-2-phenylindole (DAPI, 10.9 mM; Sigma-Aldrich) and the sections were then mounted with Prolong Gold® antifade reagent (Molecular Probes, Eugene, OR, USA). In all cases, negative controls from which the primary antibody was omitted were run in parallel. The sections were visualised on an Axioplan 2 fluorescence microscope (Carl Zeiss Microimaging, Göttingen, Germany) and photographed with a Spot-2 digital camera (Diagnostic Instruments Sterling Heights, MI, USA). Images were stored digitally as 12-bit images using MetaMorph 6.1 software (MDS Analytical Technologies, Toronto, ON, Canada) and the intensity of immunofluorescence was quantified by measuring the proportion of the selected area that exceeded the threshold value, as described previously [12]. For each experimental group, this measurement was made on no more than 3 randomly selected tissue sections per animal taken from at least 3 animals and for at least 3 different staining procedures (performed on different days). Images at ×20 magnification were obtained at a constant time exposure to permit the direct comparison between images. A threshold was established to subtract background immunoreactivity (ir) and the proportion of the selected area where the staining exceeding the threshold value was analyzed separately in the lamina propria and the muscle layer. Finally, to avoid the interfering effect of oedema, measurements were normalized according to the number of cells in the area of interest, dividing by the percentage of the area stained with DAPI.

2.5 Western Blotting

Whole urethras and urinary bladders from each group of animals (control, acute, intermediate and chronic) were homogenized separately in cold lysis buffer containing a protease inhibitor mix (1 mM PMSF, 1 μM pepstatin A, 2 μM leupeptin and 1 mM DTT: Sigma Aldrich). The homogenate was centrifuged at 10,000 *g* for 15 minutes and the supernatant was collected and divided into aliquots. Samples (6 μg) were resolved by SDS-PAGE (7.5% acrylamide/bisacrylamide) and electrotransferred onto nitrocellulose membranes. The membranes were probed with the same primary

antibodies for the NOS isoforms used in the immunofluorescence experiments (**Table 1**), which were diluted in blocking solution containing 0.2% Tween-20. A mouse monoclonal anti-β-actin antibody (1:3000: Sigma) was used as a loading control. Sufficient antibody solution was used to completely cover the membrane, after which it was washed (6 x 10 min) at room temperature in PB + 0.2% Tween-20 with gentle shaking. The membranes were then incubated for 45 min at room temperature in the dark with the secondary antibody (Table 1) diluted in blocking solution containing 0.2% Tween-20 + 0.02% SDS. After washing (6 x 10 min), images were acquired using the Odyssey infrared imaging system (LI-COR Biosciences, NE, USA). The density of the bands was quantified by measuring the integrated fluorescence intensity using the Odyssey Application Software 2.1 program. These values were normalized to those of the loading control and expressed in function of the control sample for each individual test.

2.6 Standard PCR for iNOS

Total RNA was extracted from the bladder and the proximal urethra (from control and intermediate CYP-treated animals) using the Qiagen RNeasy® Fibrous Tissue mini-kit. RNA quality was determined by agarose gel electrophoresis. Standard PCR of iNOS transcripts was performed in a 25 µl reaction volume using the Access RT-PCR System (Promega, Madison, USA) in a Perkin Elmer thermocycler (Gene Amp PCR System 2400). The PCR protocol was as follows: heating to 45ºC for 45 min, and to 94ºC for 2 min; 35 cycles at 94ºC for 30 s, 60ºC for 45 s and 68ºC for 45 s; and a final termination step at 68ºC for 7 min. The three specific primer sets for iNOS amplification were designed using Primer-BLAST (Acc. Number: NM_012611.3). The primer sequences were as follows (Metabion International, Deutschland): 1-forward 5′-GAAGTCCAGCCGCACCACCC-3′, reverse 5′-ACGCTGAACACCTCGTCGGC-3′; 2-forward: 5′-TCGAGTTCCCAGCCTGCCCC-3′, reverse: 5′-AGGCTGCCCGGAAGGTTT -3′; and 3- forward: 5′-GCAACCCTTCCGGGCAGCCT-3′, reverse: 5′-CTTGCACCAGGGCCGTCTGG-3′. To rule out any possible genomic DNA contamination of the RNA samples, standard PCR was also performed without reverse transcriptase. The size of the amplified fragments was verified in a 2% agarose electrophoresis gel stained with ethidium bromide and visualized using a Biorad Fluor-S MultiImager (Hercules CA, USA). Mouse macrophage iNOS cDNA (a generous gift from Dr I. Rodriguez Crespo, Complutense University, Madrid, Spain) was used as a positive control.

2.7 Real time (RT)-PCR of eNOS

Quantitative RT-PCR of eNOS was performed using bladder and urethra samples from control and intermediate CYP-treated animals. We used the predesigned primers and MGB probes for eNOS (Rn02132634 s1, Applied Biosystems: forward 5′-TCCGCTACCAGCCTGACCCC-3′ and reverse 5′-CTCAGGCCGAGGGGAGCTGT), together with the GAPDH amplification kit (VIC®/MGB Probe, Primer Limited) as an

endogenous control. PCR reactions were performed in a 9800 Fast Thermal Cycler (Applied Biosystems) with TaqMan Gold PCR reagents.

2.8 *In vitro* contractility

Transverse strips (~3 mm wide, 5 mm long) from the mid-detrusor and trigone region, and urethral rings (3 mm wide) were obtained from control and CYP-treated rats sacrificed by cervical dislocation. The isometric tension was recorded as described previously [13] in urethral preparations mounted between two stainless-steel hooks in 5-ml organ baths containing Krebs solution at 37ºC (in mM: 119 NaCl, 4.6 KCl, 1.5 $CaCl_2$, 1.2 $MgCl_2$, 15 $NaHCO_3$, 1.2 KH_2PO_4, 0.01 EDTA, and 11 glucose) and bubbled with a mixture of 95% O_2 and 5% CO_2 [pH 7.4]. The isometric tension was recorded using Grass FT03C transducers (Grass Instruments, Quincy; MA, USA) and it was displayed on a MacIntosh computer using a MacLab analogue-to-digital converter v5.5 (AD Instruments Ltd., Hastings, East Sussex, UK). Preparations were equilibrated at a resting tension of 10 mN for 60 min and their viability was determined by eliciting a contractile response at a high concentration of external K^+ (120 mM).
Electrical field stimulation (EFS) was applied using a Grass S-48 stimulator (Grass Instruments Quincy, MA, USA) using platinum electrodes placed parallel to the preparation and coupled to a Med-Lab stimulus splitter (Med-Lab Instruments, Loveland, CO, USA). Square-wave pulses of 0.8 ms duration, supra-maximal voltage (current strength, 200 mA), with a train duration of 5 s at different frequencies were delivered at 2 min intervals. EFS (1-50 Hz) mainly induces noradrenergic contractions in the urethra and cholinergic contractions in the bladder [10] and the effects of EFS were compared with those induced by the cumulative addition of NE or ACh, at concentrations ranging from 0.01 μM to 1 mM. N^w-nitro-L-arginine (L-NOARG, 0.1 mM) was added to investigate the contribution of NO to contractility. Urethral relaxation of nitrergic origin was induced by applying EFS to preparations precontracted with arginine vasopressine (AVP, 0.1 μM) in the presence of guanethidine (50 μM), in order to prevent the neuronal release of NE, and atropine (1 μM) to block the effects of the ACh released. D-tubocurarine (0.1 mM) was also added to prevent the stimulation of somatic nerves that innervate the striated muscle of the urethra. Urethral relaxations were also induced by the cumulative addition of the NO donor SNC (0.01 μM to 1 mM).

2.9 Data Analysis

Contractile responses were expressed as a percentage of the KCl-induced response of each preparation or in absolute values (mN), while relaxation was normalized by expressing it as a fraction of the tension induced by AVP at the point prior to stimulation. Histological damage is expressed as the median and the corresponding range, while all the other data are presented as the mean ± SEM. Means were compared by ANOVA followed by an unpaired *t*-test, and the medians were

compared using the Mann-Whitney non-parametric test. *P* values of <0.05 were considered significant.

3. Results

3.1 Pathological signs induced by CYP Treatment

After CYP treatment, rats showed clear symptoms of pain that included decreased movement, piloerection and the characteristic immobile rounded-back posture. In addition, some chronically-treated animals bled from the eyes and muzzle, and approximately 10% died before completing the treatment (usually on day 9), displaying signs of haemorrhage in various organs (liver, kidney and lungs) and blood in the urine. These animals were excluded from the analysis.

The total voiding frequency and in particular, the number of low volume voids, increased with the duration of treatment (**Fig. 1**). Similarly, the wet weight of the lower urinary tract increased significantly in animals that received intermediate and chronic treatments (**Fig. 2A**). The bladders and urethras of CYP-treated rats, especially those receiving intermediate and chronic treatments, exhibited clear signs of inflammation (**Fig. 2B, Table 2**). Microscopic evaluation revealed haemorrhagic cystitis of varying degrees of severity, characterized by oedema, vascular congestion, haemorrhage, cell infiltration, and erosion or proliferation of the urothelium (**Fig. 2C-F, Table 2**). CD163-ir revealed a progressive increase of infiltrated macrophages in the muscle layer and particularly in the lamina propria of both organs, which was correlated with increasing CYP treatment duration (**Fig. 3**). The vascular lesion and haemorrhage scores were similar in the bladder and urethra (**Table 2**).

3.2 Lack of iNOS expression

No significant iNOS-ir was observed in either the bladder or urethra and accordingly, no iNOS protein was detected in Western blots (**Fig. 4A-D**). The specificity of the primary antibody was verified using two recombinant proteins as positive controls (**Fig. 4E**). Finally, using 3 different primer pairs, no mRNA transcripts encoding for iNOS were amplified from the bladders or urethras of control animals, or from those treated for 48 h with CYP, while clear bands of the predicted size were amplified from the positive control sample (mouse macrophage iNOS cDNA: **Fig. 4F**).

3.3 CYP-induced changes in nNOS and eNOS expression

As nitrergic nerves are sparse in the bladder, we focused our analyses on the urethra and trigone. Neuronal nNOS-ir decreased in response to acute and intermediate CYP treatment but partially recovered after chronic treatment (**Fig. 5**), as corroborated in Western blots (**Fig. 6**). In the urethra, and particularly in the bladder, the weak eNOS-ir detected in the vascular endothelium and urothelium of control tissues was

dramatically and progressively enhanced by CYP-treatment, even extending to neighbouring smooth muscle and other cells of the interstitium (**Fig. 7**). Two specific bands for eNOS were evident in western blots of CYP-treated bladder and urethras, and the expression of the smaller isoform (60 kDa) increased dramatically after intermediate and chronic CYP-treatment, especially in the bladder (**Fig. 8A-B**). However, no significant increase in eNOS mRNA expression was detected by RT-PCR in either tissue following intermediate CYP treatment (**Fig. 8C**)

3.4 Changes in bladder and urethral contractility

The detrusor contractions induced by high concentrations of K^+, EFS or ACh were significantly reduced following intermediate CYP treatment (by about 40%), an effect that was reversed in chronically-treated animals (**Fig. 9A, B** and **D**). However, CYP treatment had no effect on any contractile (induced by high concentrations of K+, NE or EFS: **Fig. 10A, B** and **D**, respectively) or relaxant urethral responses (induced by EFS or SNC: **Fig. 10F** and **G**, respectively). EFS-induced relaxations were abolished by L-NOARG in all groups, demonstrating their nitrergic origin (data not shown). However, no further changes were observed in the contractile responses of the bladder (Fig. **9C** and **E**) or urethra (**Fig. 10C** and **E**) following pre-treatment with L-NOARG.

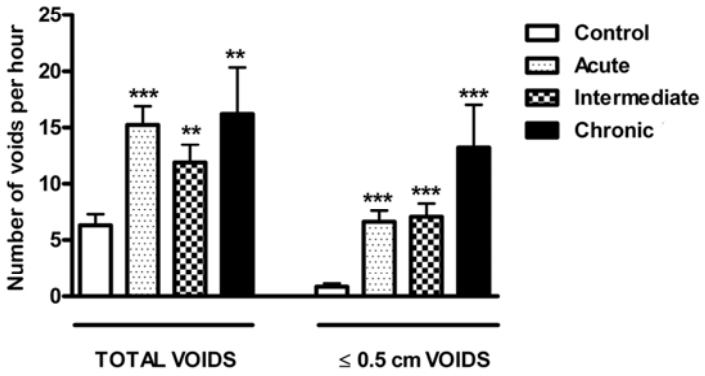

Figure 1. **Changes in voiding frequency in CYP-treated rats**. The total number and the number of small-volume voids are expressed per hour in animals treated with CYP for 4 h (acute), 48 h (intermediate) or 10 days (chronic). The data are expressed as the mean ± SEM (n = 13-20 per group): $^{**}P < 0.01$, $^{***}P < 0.001$ vs controls (one-way ANOVA followed by t-test for unpaired observations).

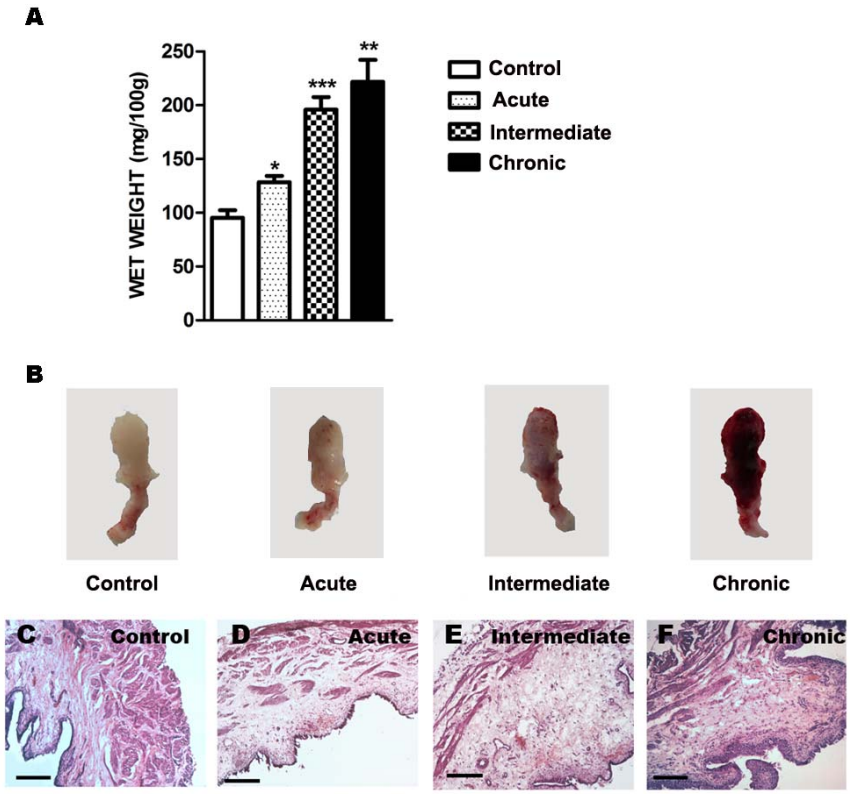

Figure 2. **Histomorphological alterations in the bladder and urethra of CYP-treated rats**. (*A*) Ratio of urinary tract weight to body weight. (*B*) Macroscopic alterations and (*C-F*) representative H&E staining of urinary bladder sections from control animals and those treated with CYP for 4 h (acute), 48 h (intermediate) or 10 days (chronic). Scale bar = 100 µm.

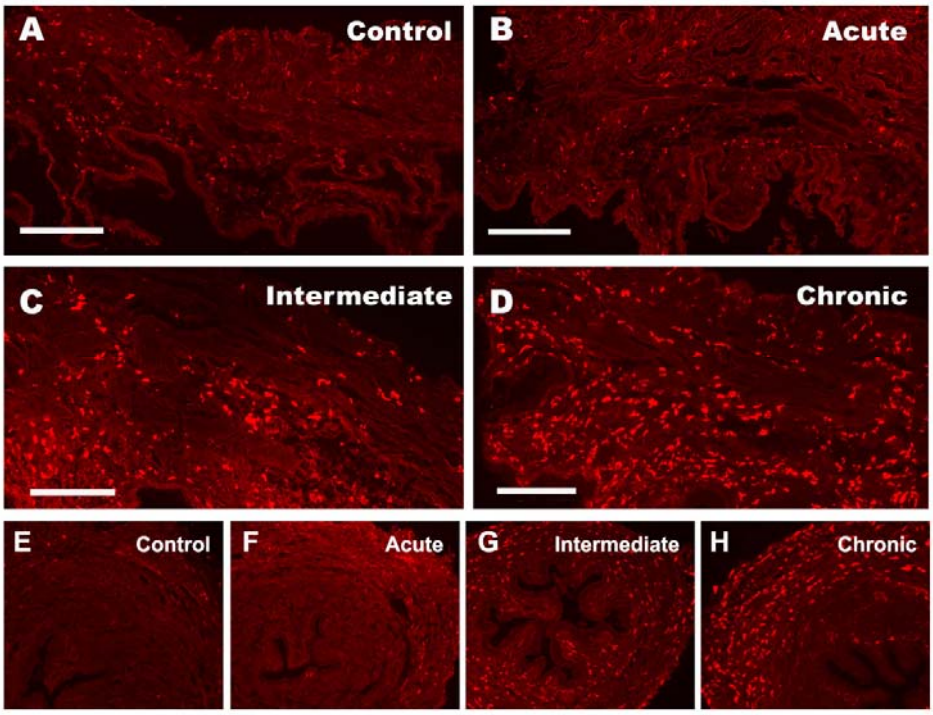

Figure 3. CYP treatment induces a progressive increase in the number of CD163-positive macrophages. Representative images of CD163-ir in the bladder (B-D) and urethra (F-H) of CYP-treated rats and their corresponding controls (A, E). Scale bar = 100 µm.

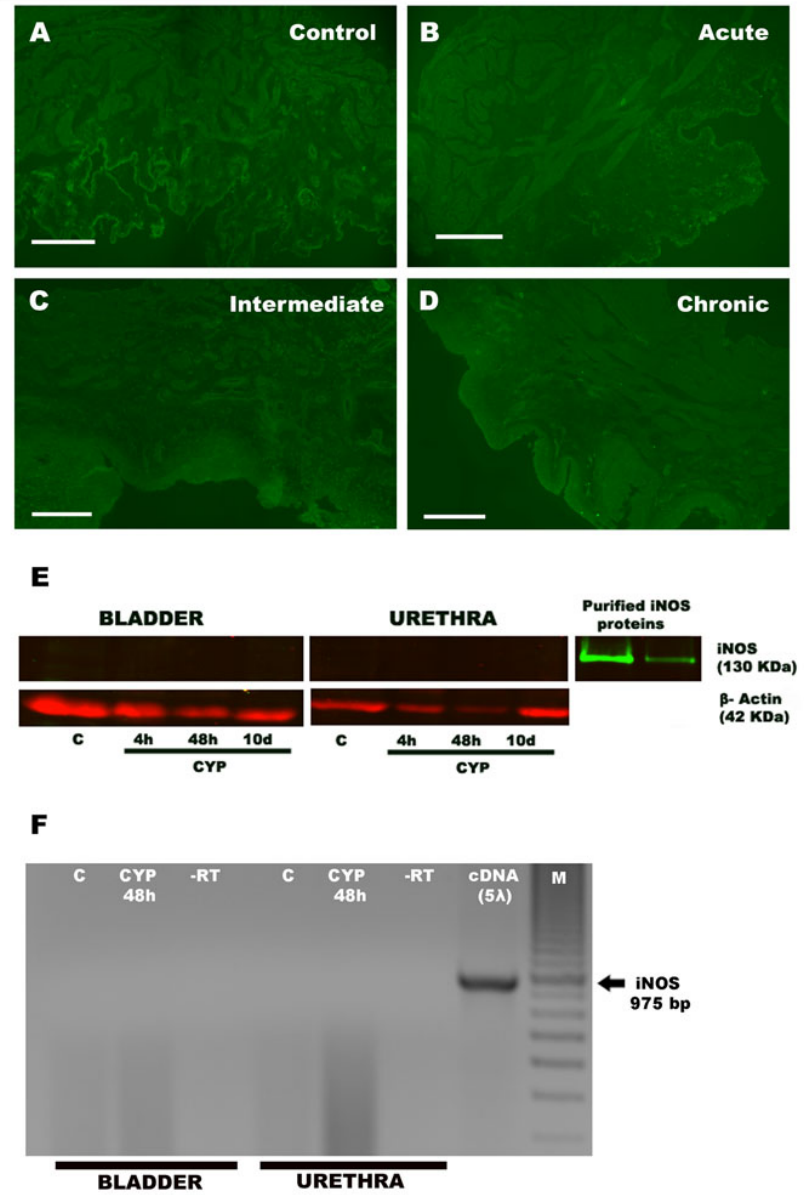

Figure 4. **iNOS expression in the bladder and urethra is unchanged following CYP treatment.** (A-D) Representative images showing the absence of iNOS-ir in the bladders of control rats and those treated with CYP for 4 h (acute), 48 h (intermediate) or 10 days (chronic). Scale bar = 100 μm. (*E*) Western blot analysis of iNOS protein in the bladder (*left*) and urethra (*centre*) of control and CYP-treated rats. Two purified iNOS proteins (130 kDa) were included as positive controls (*right*, iNOS standard and recombinant iNOS protein from mouse macrophage, respectively). The membranes were probed for β-actin as a loading control. (***F***) Real time PCR products showing the absence of amplified iNOS mRNA transcripts in the bladder (*left*) and urethra (*right*) of control and CYP-treated (48 h) rats. Mouse macrophage iNOS cDNA was amplified as a positive control, while the template for the negative controls was untranscribed RNA (-RT). M: Molecular marker.

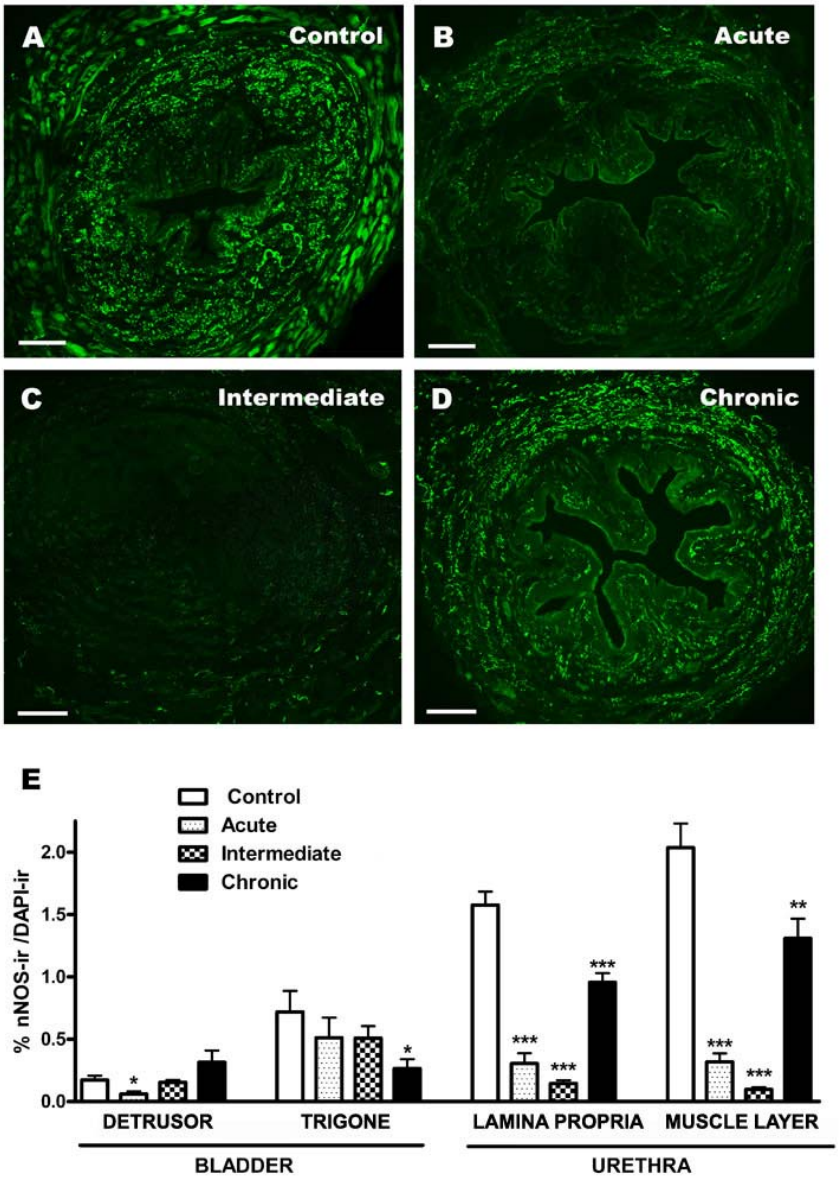

Figure 5. **Effects of CYP treatment on nNOS immunofluorescence in the bladder and urethra. (***A-D***)** Representative images of nNOS-ir in the urethra, and (*E*) quantification of nNOS-ir in the bladder (*left*) and urethra (*right*) of rats treated with CYP for 4 h (acute), 48 h (intermediate) or 10 days (chronic), compared with the corresponding controls. Scale bar = 50 μm. Measurements were recorded independently in the detrusor and trigone of the bladder, and in the lamina propria and smooth muscle layer of the urethra. The area above the intensity threshold was measured and normalized according to the number of cells in the region of interest (DAPI-labelled nuclei). Values represent the mean ± SEM of 6-7 different fields from at least 4 different animals: **P* < 0.05, ***P* < 0.01, ****P* < 0.001 vs controls (one-way ANOVA followed by *t*-test for unpaired observations).

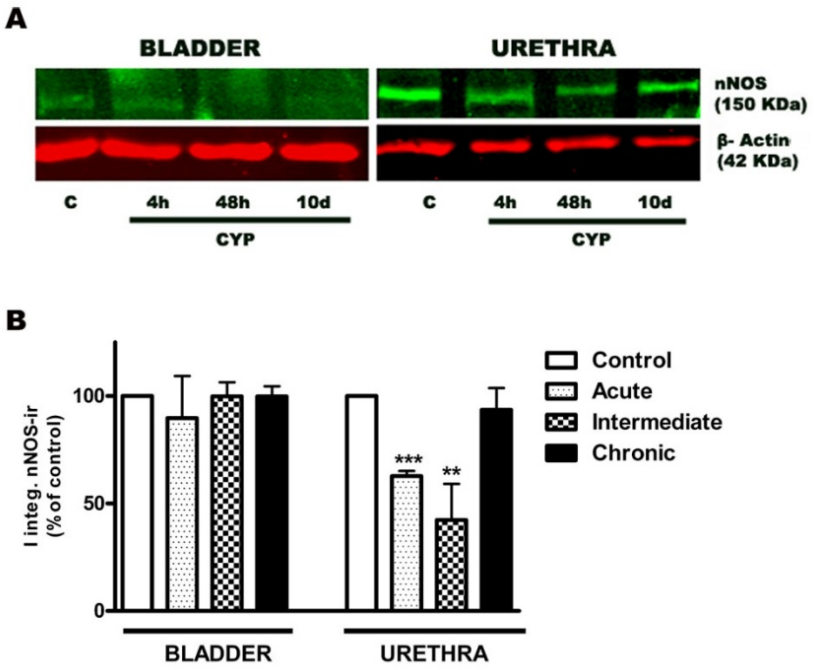

Figure 6. **Effects of CYP treatment on nNOS protein expression in the bladder and urethra.** (**A**) Representative images of Western blots and (***B***) quantification of nNOS protein expression in control conditions and after CYP treatment for 4 h (acute), 48 h (intermediate) or 10 days (chronic). Results are normalized to β-actin levels and expressed as a percentage of the controls. The data represent the mean ± SEM (n = 4): $^{**}P < 0.01$, $^{***}P < 0.001$ vs controls (one-way ANOVA followed by t-test for unpaired observations).

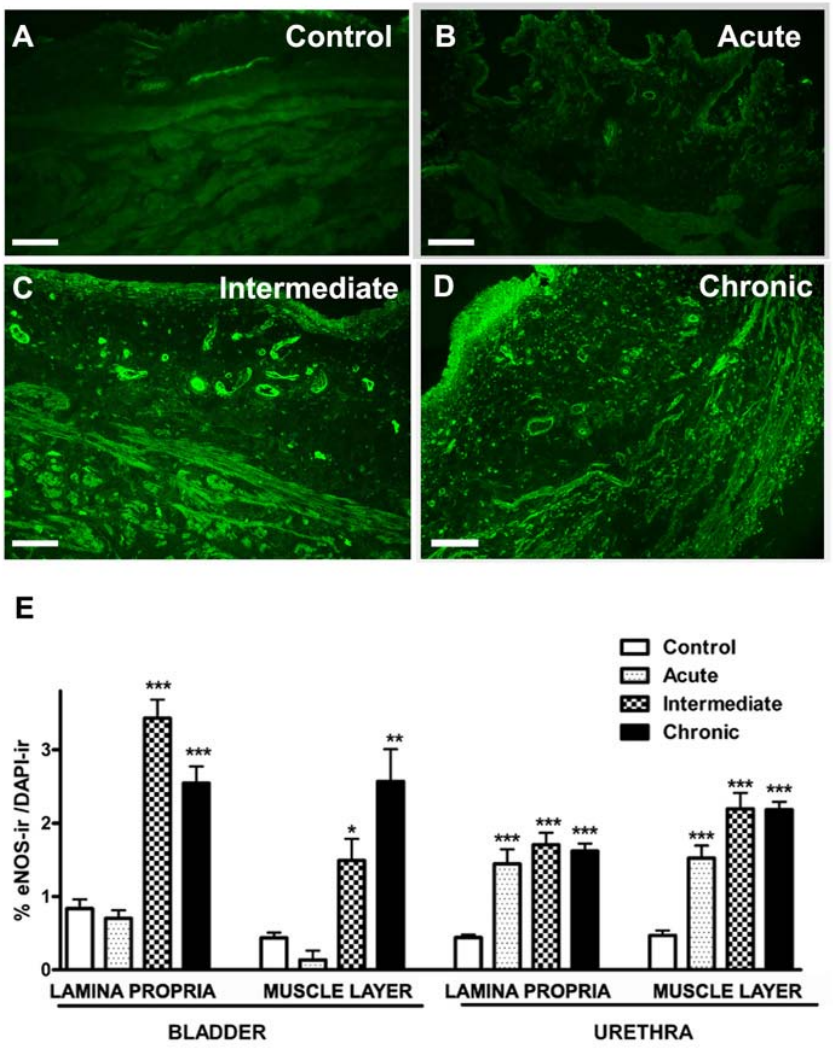

Figure 7. **Effects of CYP treatment on eNOS immunofluorescence in the bladder and urethra.** Representative images of the bladder (A-D) and quantification of eNOS-ir in the bladder (E, *left*) and urethra (E, *right*) of rats treated with CYP for 4 h (acute), 48 h (intermediate) or 10 days (chronic), and compared with the corresponding controls. Scale bar = 50 μm. Measurements were recorded independently in the lamina propria and muscle layer in both organs. The area above the intensity threshold was measured and normalized according to the number of cells in the region of interest (DAPI-labelled nuclei). Values represent the mean ± SEM of 6-7 different fields from at least 4 different animals: $*P < 0.05$, $**P < 0.01$, $***P < 0.001$ vs controls (one-way ANOVA followed by *t*-test for unpaired observations).

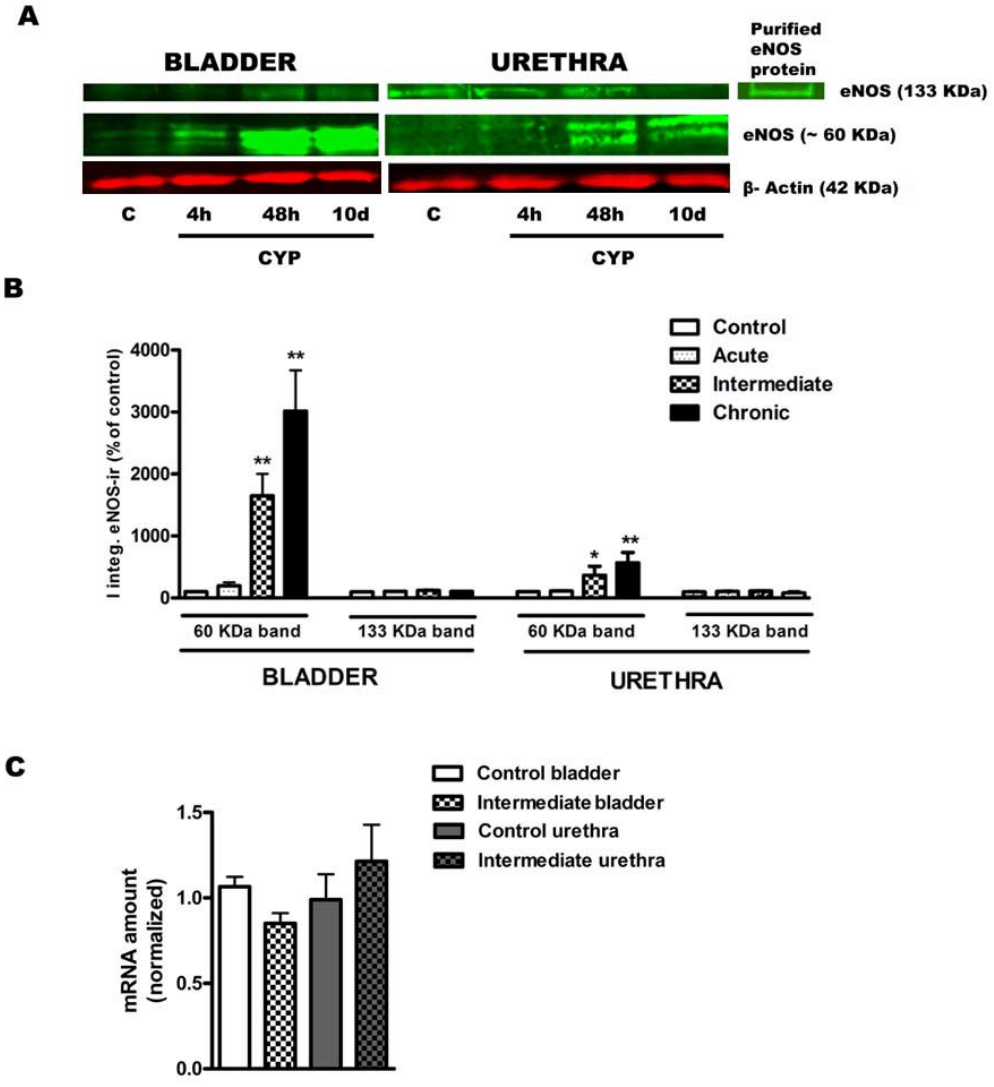

Figure 8. **Effects of CYP treatment on eNOS expression in the bladder and urethra.** (A) Representative Western blots and (***B***) quantification of eNOS protein expression in control conditions and after CYP treatment for 4 h (acute), 48 h (intermediate) or 10 days (chronic). A purified eNOS protein (~133kDa, *right*) was included as a positive control (bovine eNOS protein). Quantitative results independently represent the 60 and 133 kDa bands, expressed as the percentage of the control samples using β-actin as a loading control. (*C*) RT-PCR quantification of eNOS in the bladder (*left*) and urethra (*right*) of rats subjected to intermediate (48 h) CYP treatment. Values represent the mean ± SEM ($n = 4$): *$P < 0.05$, **$P < 0.01$ compared with the corresponding controls (one-way ANOVA followed by *t*-test for unpaired observations).

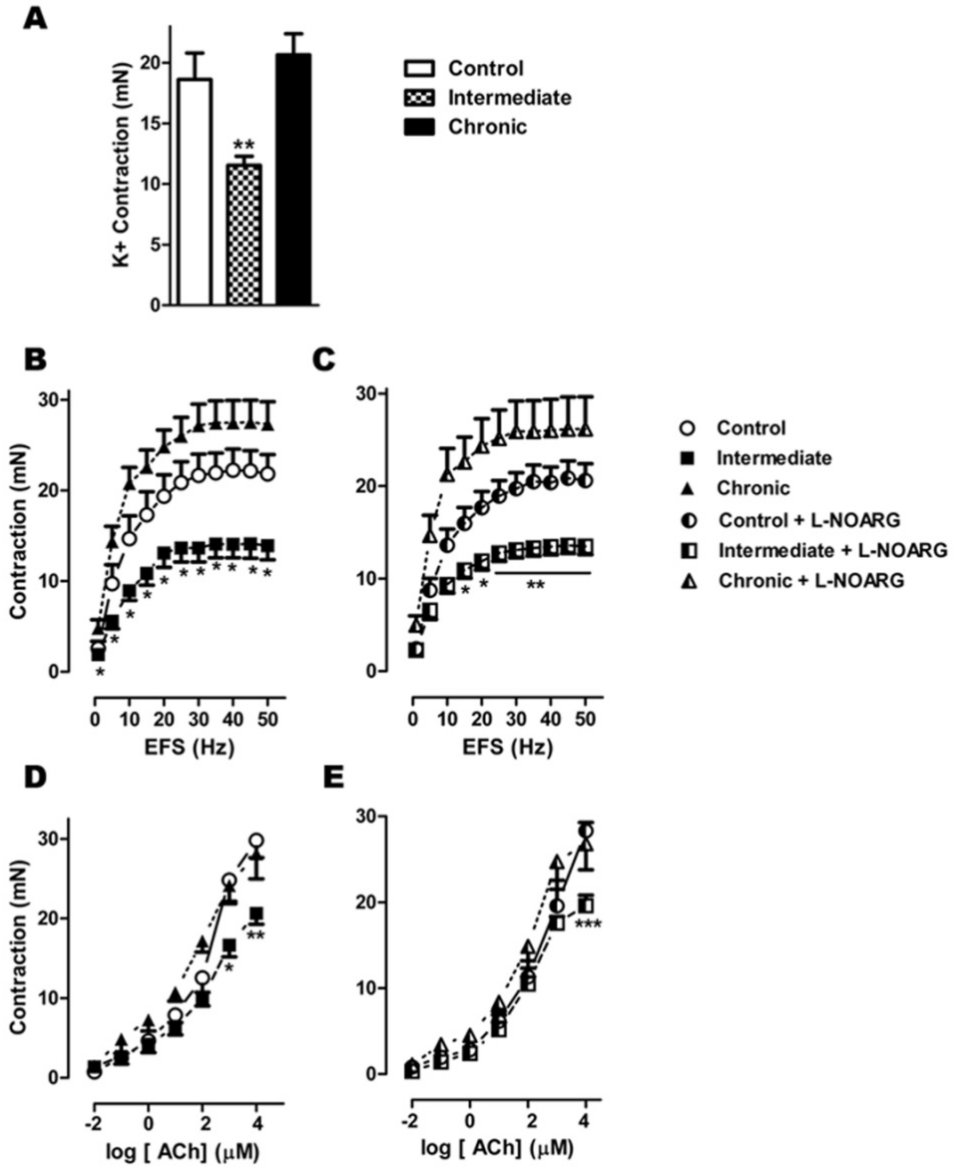

Figure 9. **Effects of CYP treatment on bladder contractility.** (*A*) Contractions induced by 120 mM K^+. (***B***-*C*) Frequency-response and (*D*-*E*) concentration-response curves induced by ACh in control conditions (open circles) and after intermediate (48 h, filled squares) or chronic (10 days, filled triangles) CYP treatment, in the presence (*C, E*) or absence (A,B,D) of L-NOARG (0.1 mM, half-filled symbols). Results are expressed as absolute values (mN) and they represent the mean ± SEM (n =6 per group): **P* <0.05; ***P* < 0.01 compared with the corresponding controls (one-way ANOVA followed by *t*-test for unpaired observations).

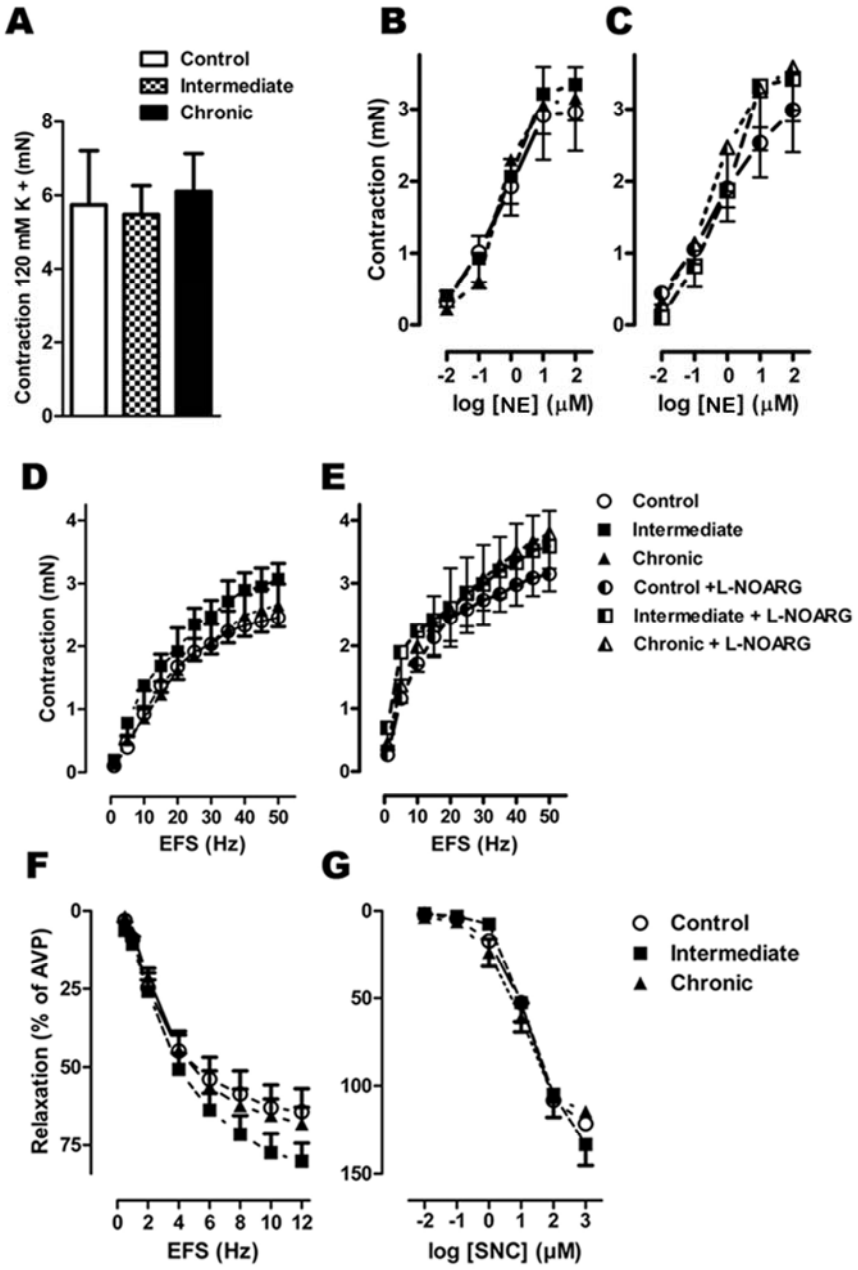

Figure 10. **Effects of CYP treatment on urethra contractility.** (*A*) Contractions induced by 120 mM K^+. (*B-C*) Concentration-response curves induced by NE. (*D-E*) Contractile and (*F*) relaxant frequency-response curves, and (*G*) concentration-response curves for SNC in the urethra in control conditions (open circles) and after intermediate (48 h, filled squares) or chronic (10 days, filled triangles) CYP treatment, in the presence (*C, E*) or absence (A, B, D, F and G) of L-NOARG (0.1 mM, half-filled symbols). The data are expressed as absolute values (mN) or as a percentage of the previous AVP-induced tone (relaxation responses), and they represent the mean ± SEM (n = 6 per group). No significant differences were detected between groups (one-way ANOVA).

Table 1. Primary and secondary antibodies, and their dilutions, applications and sources

Antibody	***Dilution***	***Application***	***Source***
Primary			
Rabbit anti-nNOS polyclonal antiserum	1:1000	IF*, WB**	Cayman Chemical (USA)
Rabbit anti-iNOS polyclonal antiserum	1:1000	IF, WB	Cayman Chemical (USA)
Rabbit anti-eNOS polyclonal antiserum	1:1000	IF, WB	Abcam (UK)
Mouse anti-CD163 monoclonal antibody	1:20	IF	HyCult biotech. (The
Secondary			Netherlands)
Alexa 488 conjugated donkey anti-rabbit	1:200	IF	Molecular Probes (USA)
Alexa 594 conjugated donkey anti-mouse	1:200	IF	Molecular Probes (USA)
IRDye 800CW goat anti-rabbit antibody	1:15,000	WB	LI-COR biosciences (USA)
IRDye 680CW goat anti-mouse antibody	1:15,000	WB	LI-COR biosciences (USA)
Nuclear staining			
4′6-diamino-2 phenylindole			
dihydrochloride (DAPI)	10.9 mM	IF	Sigma-Aldrich (USA)

* *IF, immunofluorescence;* ***WB, Western blotting.*

Table 2. Microscopic lesions in the urinary bladder and urethra of cyclophosphamide-treated rats. Lesions were scored as absent (**0**), mild (**1**), moderate (**2**) and severe (**3**), and they are represented as the median and range.

	BLADDER			**URETHRA**		
	Acute	**Intermediate**	**Chronic**	**Acute**	**Intermediate**	***Chronic***
Oedema	1 (1-2)*	3 (2-3)*	2 (2-3)*	1 (0-2)*	3 (2-3)**	2 (1-3)*
Haemorrhage	1 (0-2)*	2.5 (2-3)*	1.5 (0-2)*	1 (0-3)*	2 (0-3)*	3 (1-3)*
Vascular congestion	1 (0-1)*	1 (1-1)*	0.5 (0-2)*	1 (0-3)*	1 (1-2)**	1 (0-2)*
Cell infiltration	1.5 (1-2)*	3 (2-3)*	3 (2-3)*	1 (0-2)*	2 (0-3)*	2 (1-3)*
Epithelial damage	1.5 (1-2)*	3 (1-3)*	3 (1-3)*	1 (0-3)	2 (1-2)*	2 (1-2)*

** P < 0.05, ** P < 0.01 vs. control group (Mann-Whitney test, n = 5-7).*

4. Discussion

The results of this study demonstrate that CYP treatment of rats induces an inflammatory reaction in the bladder that is accompanied by bladder hyperactivity [2, 14], as witnessed by an increase in voiding frequency and small volume voids. These alterations were particularly evident following chronic treatment. Similar effects were observed in the urethra, where histological lesions also occurred to the same extent as in the bladder, such as oedema, haemorrhage, cell infiltrates and ulcerative or proliferative alterations of the urothelial layer.

Surprisingly, CYP failed to induce iNOS protein or mRNA expression, casting doubt on the general assumption that the increase in NO production observed in these conditions is mediated by iNOS activation [4, 8, 9]. It should be noted that this rationale is based on indirect evidence, including the reduction in bladder damage, urinary NO metabolites and protein nitration levels observed following treatment with selective iNOS inhibitors such as aminoguanidine [1, 15] and S-methylisothiourea [8, 16, 17]. However, the selectivity of these inhibitors is highly dose-dependent and inhibition of the constitutive isoforms can occur at elevated concentrations.

The expression of iNOS in the epithelium and inflammatory cells of the lamina propria has been described in the rat bladder 1 [18], 12 [19] and 24 [20] hours after CYP treatment, but not following chronic CYP administration for 7 days [3] or 60 hours [21]. Similarly, it remains controversial whether iNOS expression is induced in human interstitial cystitis [22]. The time course of iNOS gene expression in the mouse bladder during cystitis induced by LPS, substance P and antigen-stimulation reveals iNOS upregulation at 4 but not at 24 hours [23]. Thus, we cannot rule out the possibility that transient increases in iNOS expression occurred at times other than those assayed in the present study. As such, the involvement of iNOS in CYP-induced cystitis remains unclear.

In contrast to the iNOS findings, CYP administration produced significant alterations in the expression of constitutive NOS isoforms. Accordingly, nNOS expression was initially reduced by CYP administration but subsequently returned to its basal levels, while eNOS protein expression increased strongly and progressively in both structures, particularly in the bladder. The early micturition hyperreflexia reported when CYP induced cystitis has been attributed to the upregulation of nNOS in spinal segments [24], although no information is available regarding its expression in intramural nerves. Diminished nNOS-ir and Ca^{2+}-dependent NOS activity have been described in the hypertrophied rat bladder [25]. Moreover, downregulation of nNOS also occurs in the kidneys of LPS-treated mice [26] and in the intestine in a rat model of inflammatory bowel disease [27], effects attributed to the release of pro-inflammatory cytokines. On the other hand, increases in eNOS expression were described in the urothelium and suburothelial layer after 60 h CYP treatment [21] in a mouse model of LPS-induced bladder inflammation [28], as well as in inflammatory cells of

hypertrophied rat bladders [25]. Thus, eNOS may be an alternative source of NO in the bladder during CYP-induced cystitis. The fact that no significant upregulation of eNOS mRNA was observed following intermediate treatment may be explained by the involvement of post-transcriptional mechanisms or the differential timing of mRNA and protein upregulation. Further studies quantifying mRNA expression at different time points will be necessary to investigate this hypothesis.

It should be noted that of the two specific bands detected for eNOS in Western blots, the 60 kDa band augmented dramatically after intermediate and chronic CYP-treatment, suggesting the accumulation of degradation fragments due to increased proteolytic activity during inflammation. Association with the heat shock protein 90 (HSP90) chaperone protects NOS from proteolytic attack [29]. However, eNOS is more susceptible to damage by proteolytic agents [29] as it associates less with HSP90 than nNOS, and thus, enhanced proteolytic activity during inflammation may augment the metabolic turnover of eNOS. It remains to be determined whether eNOS enzymatic activity is sufficiently high as to increase NO levels in this scenario of upregulation and rapid turnover.

In addition to the endothelium, during inflammation increased eNOS expression was observed in other cells types, including smooth muscle cells and interstitial cells. By upregulating eNOS expression, these cells may become important sources of NO at the same time that NO release from nitrergic nerves is reduced due to the downregulation of nNOS. The functional consequences of these changes are extremely difficult to predict. The physicochemical properties of NO are such that spatiotemporal alterations in the expression of NOS isoforms and their effects on neighboring cells are far more significant than global NO production. Another possibility is that NOS activity becomes "uncoupled" in the inflamed tissues due to substrate or co-factor deficiency, and its activity is diverted from producing NO to generating the superoxide radical (O_2^-). This scenario has been described in dysfunctional endothelia associated with hypertension, diabetes and atherosclerosis [30]. Furthermore, this excess O_2^- may in turn lead to oxidative stress and contribute to tissue damage.

While the role of bladder afferents in CYP-induced detrusor overactivity is well documented [30, 31], little is known about the changes in efferent motor function induced by CYP in the bladder, and more particularly in the urethra. Our results are consistent with previous reports [21, 24] of reduced detrusor contractility after acute CYP administration. This effect appears to be unspecific, as responses to high K^+ concentrations, EFS or exogenously added ACh were similarly affected. Moreover, this reduction appears to be unrelated to NO levels, as it was not altered by L-NOARG. Tissue damage such as oedema, which peaked 48 h after treatment, may provoke the transient impairment of detrusor contraction and its subsequent reversal in chronically-treated animals. In the urethra, this effect was not strong enough to modify efferent neurotransmission, as neither contractile nor relaxant nerve-mediated urethral responses were altered by CYP treatment. Accordingly, a decrease in the nitrergic relaxation

induced by the intermediate CYP regime might have been expected, coinciding with the decrease in nNOS expression. Given the high density of nitrergic nerves in the urethra [12], a mild loss of these nerves would not significantly affect relaxation. Our results suggest that the bladder hyperexcitability that accompanies CYP-induced cystitis is not related to changes in the efferent motor activity of smooth muscle in either the bladder or the urethra. However, the effect of NO and other mediators produced by CYP treatment on the afferent pathways may underlie this hypersensitization of the bladder.

Finally, our data suggest that the toxic effects of CYP are not exclusively due to the accumulation of acrolein in the bladder, where it alters the epithelial barrier leading to an inflammatory reaction that spreads throughout the organ [7, 32]. This conclusion is based on several observations: (i) similar qualitative alterations were seen in the bladder and urethra despite the different periods of exposure to urine; (ii) proliferative changes in the epithelium were more common than degenerative alterations; (iii) vascular lesions were the most prominent form of damage; and (iv) haemorrhage in many other organs was observed to varying degrees. Thus, acrolein (or other CYP metabolites) in the blood may produce generalized vascular damage that is not limited to the urinary tract, although its accumulation in the urine may worsen the inflammatory process in the bladder. We propose that the use of CYP-induced cystitis in the rat as a model of inflammation should be restricted in terms of dose and time to minimize the systemic effects.

Conclusions

In conclusion, this study demonstrates that CYP administration induces prominent inflammatory reactions in the rat urethra and bladder, although contractility was only modified in an NO-independent manner in the bladder. The main finding was a lack of iNOS expression in both organs following CYP treatment, which was accompanied by a decrease in nNOS and an increase in eNOS expression. Several cells expressed eNOS *de novo*, representing new sources of NO that may contribute to the pathogenicity of CYP-induced cystitis.

Acknowledgements

This work was supported by grants from the “Comunidad de Madrid - Universidad Complutense de Madrid” (UCMGR85/06-920307), UCM-Santander (GR35/10-A-920307) and the Fundación Mutua Madrileña (FMM2011). The microphotographs were acquired and analyzed at the Microscopy and Cytometry Centre (Complutense University, Madrid, Spain). We thank Alfonso Cortés and Luis M. Alonso for their technical assistance with the fluorescence microscopy and Dr I. Rodriguez Crespo (Complutense University, Madrid) for the generous gift of mouse macrophage iNOS cDNA, the mouse macrophage recombinant iNOS and the bovine eNOS proteins.

References

[1] **Korkmaz A, Topal T, Oter S**. Pathophysiological aspects of cyclophosphamide and ifosfamide induced haemorrhagic cystitis. *Cell Biol. Toxicol.* 23: 303-312, 2007.

[2] **Yoshimura N, De Groat WC**. Increased excitability of afferent neurons innervating rat urinary bladder after chronic bladder inflammation. *J. Neurosci.* 19: 4644-4653, 1999.

[3] **Cho KH, Hyun JH, Chang YS, Na YG, Shin JH, Song KH**. Expression of nitric oxide synthase and aquaporine-3 in cyclophosphamide treated rat bladder. *Int. Neurourol. J*. 24: 149-156, 2010.

[4] **Souza-Filho MVP, Lima MVA, Pompeu MML, Ballejo G, Cunha FQ, Ribeiro RA.** Involvement of nitric oxide in the pathogenesis of cyclophosphamide-induced hemorrhagic cystitis. *Am. J. Pathol.* 150: 247-256, 1997.

[5] **Alfieri AB, Cubeddu LX.** Nitric oxide and NK1-tachykinin receptors in cyclophosphamide-induced cystitis in rats. *J. Pharmacol. Exp. Ther*. 295: 824-829, 2000.

[6] **Andersson MC, Tobin G, Giglio D.** Cholinergic nitric oxide release from the urinary bladder mucosa in cyclophosphamide-induced cystitis of the anaesthetized rat. *Br. J. Pharmacol*. 153: 1438-1444, 2008.

[7] **Korkmaz A, Topal T, Oter S.** Pathophysiological aspects of cyclophosphamide and ifosfamide induced hemorrhagic cystitis. *Cell Biol. Toxicol.* 23: 303-312, 2007.

[8] **Linares-Fernandez BE, Alfieri AB.** Cyclophosphamide-induced cystitis: Role of nitric oxide synthase, cyclooxygenase-1 and 2, and NK_1 receptors. *J. Urol.* 177: 1531-1536, 2007.

[9] **Xu X, Cubeddu LX, Malave A**. Expression of inducible nitric oxide synthase in primary culture of rat bladder smooth muscle cells by plasma from cyclophosphamide-treated rats. *Eur. J. Pharmacol.* 416: 1-9, 2001.

[10] **Andersson KE, Wein A.** Pharmacology of the urinary tract: Basis for current and future treatments of urinary incontinence. *Pharmacol Rev.* 56: 581-631, 2004.

[11] **Dickson A, Avelino A, Cruz A, Ribeiro-da-Silva F.** Peptidergic sensory and parasympathetic fiber sprounting in the mucosa of the rat urinary bladder in a chronic model of cyclophosphamide-induced cystitis. *Neuroscience* 141: 1633-1647, 2006.

[12] **García-Pascual A, Sancho M, Costa G, Triguero D.** Interstitial cells of Cajal in the urethra are cGMP-mediated targets of nitrergic neurotransmission. *Am. J. Physiol. Renal Physiol.* 295: 971-983, 2008.

[13] **García-Pascual A, Costa G, Labadia A, Persson K, Triguero D.** Characterization of nitric oxide synthase activity in sheep urinary tract: functional implications. *Br. J. Pharmacol.*118: 905-914, 1996.

[14] **Bon K, Lanteri-Minet M, Michiels JF, Menetrey D.** Cyclophosphamide cystitis as a model of visceral pain in rats: a c-fos and Krox-24 study at telencephalic levels, with a note on pituitary adenylate cyclase activating polypeptide (PACAP). *Exp. Brain Res.* 122: 165-174, 1998.

[15] **Abraham P, Rabi S, Kulothungan P.** Aminoguanidine, selective nitric oxide synthase inhibitor, ameliorates cyclophosphamide-induced hemorrhagic cystitis by inhibiting protein nitration and PARS activation. *Urology* 73: 1402-1406, 2009.

[16] **Alfieri AB, Malave A, Cubeddu LX.** Nitric oxide synthases and cyclophosphamide-induced cistitis in rats. *Naunyn-Schmiedeberg´s Arch. Pharmacol.* 363: 353-357, 2001.

[17] **Oter S, Korkmaz A, Oztas E, Yildirim I, Topal T, Bilgic H.** Inducible nitric oxide synthase inhibition in cyclophosphamide induced hemorrhagic cystitis in rats. *Urol. Res.* 32: 185-189, 2004.

[18] **Matsuoka Y, Masuda H, Yokoyama M, Kihara K.** Protective effects of bilirubin against cyclophosphamide induced hemorrhagic cistitis in rats. *J. Urol.* 179: 1160-1166, 2008.

[19] **Ribeiro RA, Freitas HC, Campos MC, Santos CC, Figueiredo FC, Brito GAC, Cunha FQ.** Tumor necrosis factor-α and interleukin-1β mediate the production of nitric oxide involved in the pathogenesis of ifosfamide induced hemorragic cistitis in mice. *J. Urol.* 167: 2229-2234, 2002.

[20] **Sakura M, Masuda H, Matsuoka Y, Yokoyama M, Kawakami S, Kihara K.** Rolipram, a specific type-4 phosphodiesterase inhibitor, inhibits cyclophosphamide-induced haemorrhagic cystitis in rats. *BJU international* 103: 264-269, 2008.

[21] **Giglio D, Ryberg AT, To K, Delbro DS, Tobin G.** Altered muscarinic receptor subtype expression and functional responses in cyclophosphamide induced cystitis in rats. *Auton Neurosci: Basic & Clinical* 122: 9-20, 2005.

[22] **Nazif O, Teichman JMH, Gebhart GF**. Neural upregulation in interstitial cystitis, *Urology* 69: 24-33, 2007.

[23] **Saban MR, Nguyen NB, Hammond TG, Saban R.** Gene expression profiling of mouse bladder inflammatory responses to LPS, substance P, and antigen-stimulation. *Am. J. Pathol.* 160: 2095-2110, 2002.

[24] **Lagos P, Ballejo G.** Role of spinal nitric oxide synthase-dependent processes in the initiation of the micturition hyperreflexia associated with cyclophosphamide-induced cystitis. *Neuroscience* 125: 663-670, 2004.

[25] **Johansson R, Pandita RK, Poljakovic M, Garcia-Pascual A, De Vente J, Persson K.** Activity and expression of nitric oxide synthase in the hypertrophied rat bladder and the effect of nitric oxide on bladder smooth muscle growth. *J. Urol.* 168: 2689-2694, 2003.

[26] **Holmqvist B, Olsson CF, Svensson ML, Svanborg C, Forsell J, Alm P**. Expression of nitric oxide synthase isoforms in the mouse kidney: cellular localization and influence by lipopolysaccharide and toll-like receptor 4. *J. Mol. Hist*. 36: 499-516, 2005.

[27] **Porras M, Martin MT, Torres R, Vergara P.** Cyclic upregulated iNOS and long-term downregulated nNOS are the bases for relapse and quiescent phases in a rat model of IBD. *Am. J. Physiol. Gastrointest. Liver Physiol*. 290: G423-G430, 2006.

[28] **Kang WS, Tamarkin FJ, Wheeler MA, Weiss RM.** Rapid up-regulation of endothelial nitric-oxide synthase in a mouse model of *Escherichia coli* lipopolysaccharide-induced bladder inflammation. *J. Pharmacol. Exp. Ther.* 310: 452-458, 2004.

[29] **Averna M, Stifanese R, De Tullio R, Passalacqua M, Salamino F, Pontremoli S, Melloni E.** Functional role of HSP90 complexes with endothelial nitric-oxide synthase (eNOS) and calpain on nitric oxide generation in endothelial cells. *J. Biol. Chem*. 283: 29069-29076, 2008.

[30] **Chuang YC, Yoshimura N, Huang CC, Wu M, Chiang PH, Chancellor MB.** Intravesical botulism toxin A administration inhibits COX-2 and EP4 expression and suppresses bladder hyperactivity in cyclophosphamide-induced cystitis in rats. *Eur. Urol.* 56: 159-167, 2009.

[31] **Chang CH, Peng HY, Wu HC, Lai CY, Hsieh MC, Lin TB.** Cyclophosphamide induces NR2B phosphorylation-dependent facilitation on spinal reflex potentiation. *Am. J. Physiol. Renal Physiol.* 300: F692-F699, 2011.

[32] **Ramu K, Fraiser LH, Mamiya B, Ahmed T, Kehrer JP.** Acrolein mercapturates: synthesis, characterization and assessment of their role in the bladder toxicity of cyclophosphamide. *Chem. Res. Toxicol.* 8: 515-524, 1995.

MANUSCRITO VII

Involvement of bladder and urethral interstitial cells in the cyclophosphamide-induced cystitis in the rat: preventive effect of Glivec

Maria Sancho, Domingo Triguero, Angeles Garcia-Pascual*

From:

Department of Physiology, School of Veterinary Medicine, Complutense University, Madrid, Spain.

***Corresponding author:**

Angeles Garcia-Pascual, Department of Physiology, School of Veterinary Medicine, Avda. Puerta de Hierro s/n, Complutense University, 28040 Madrid, Spain.
Telephone: 3413943843; Fax: 3413943864; e-mail: angarcia@vet.ucm.es

Abstract

Changes in the density and distribution of interstitial cells of Cajal (ICC) immunoreactives to four different markers: c-kit, vimentin, CD34 and PDGFRα, were analyzed by immunofluorescence in the bladder and urethra of CYP-treated rats. In addition, we investigated the possible protective effect of Glivec (imatinib mesylate). Finally, endothelial isoform of nitric oxide synthase (eNOS) expression in ICC was analyzed. Two cyclophosphamide (CYP)-treatments were performed: intermediate (48 h; 150 mg Kg^{-1}), and chronic (10 days, 50 mg Kg^{-1} every 3 days), with their respective controls. Pronounced increases in the density of ICC positive to all the four markers used were found in CYP-treated animals. These increases were similar in both the lamina propria and the muscle layer of the bladder and the urethra, and progressively increased with the duration of the CYP treatment. There were a remarkable accumulation of cells beneath the urothelium. The degree of colocalization in the same cell was higher than 60% for all the pairs of antibodies assayed (c-kit-vimentin, c-kit-CD34, vimentin-CD34, vimentin-PDGFRα y CD34-PDGFRα) in both tissue layers. The treatment with CYP did not modify in any case the colocalization percentages, suggesting that all the antibodies are equally useful in marking those cells that proliferate upon CYP treatment. In addition, we showed the expression of eNOS in cells positive to vimentin or CD34 and with morphological characteristics of ICC in the CYP treated bladder and urethra, but not in controls. Finally, pretreatment with Glivec significantly inhibited ICC proliferation as well as the increases in voiding frequency and urinary tract weight that accompanied the treatment with CYP. These results strongly suggest that ICC proliferation is behind the pathogenicity of CYP induced cystitis and eNOS expression may be involved. Glivec may have a possible therapeutic application in preventing bladder disorders which are secondary to chemotherapy treatment with CYP.

1. Introduction

Haemorrhagic cystitis is a known adverse effect of cyclophosphamide (CYP), a cytotoxic alkylating agent, which is used in the treatment of various malignant and nonneoplastic diseases. Well-known animal models of CYP-induced cystitis [1, 2] have been developed in rats and mice, which are characterized by the induction of bladder inflammation and interstitial cystitis accompanied by overactive bladder symptoms [3, 4]. It is well known that an increased nitric oxide (NO) production is implicated in the pathogenicity of CYP-induced cystitis [5- 7], and this is often assumed to result for the expression of the inducible isoform of NO synthase (iNOS) [5].

In the urinary tract, especially the urethra, interstitial cells of Cajal (ICC) have been suggested as mediators of the nitrergic neurotransmission process [8]. It could be suggested that alterations in NO production such as that produced by CYP-induced cystitis, could be accompanied by changes in the density and distribution of ICC. Indeed, in a model of bladder obstruction [9], accompanied by bladder overactivity, it has been reported an increase in the density of ICC immunoreactives to cGMP.

Among the different ICC markers, c-kit is a receptor tyrosine kinase extensively used as an ICC marker in gastrointestinal tract [10, 11] although not all ICC are reactive to c-kit, such as the ICC-DMP located in the small intestine [12, 13], suggesting the existence of ICC subtypes with different reactivity to c-kit and different functional characteristics. In the urinary tract, the first studies described urethral ICC as not positive to c-kit [14], but recent studies have effectively demonstrated c-kit staining in ICC throughout the urinary tract [15- 17]. It has to be pointed out that c-kit does not always mark “ICC-like cells” [12, 13, 18] as it can also be present in other cells including mast cells, melanocytes, nerve cells and glial cells [19]. Another alternative marker used for the recognition of ICC in the urinary tract is vimentin [14, 18, 20, 21], which also reacted to mast cells and fibroblasts or myofibroblasts. Other alternative ICC markers used has been CD34, a glycoprotein present in endothelial and mesenchymal cells [22], although some researchers believe that it is present in fibroblasts but not in ICC [23, 24]. Finally, the platelet-derived growth factor receptor α (PDGFRα) has recently been proposed as a new marker of a sub-population of c-kit negative ICC in gastrointestinal tract [25- 27] and urinary bladder [21]. The current debate focus on whether vimentin, CD34 or PDGFRα positive, but c-kit negative, cells would be true ICC and if so, the possible existence of different types of ICC with different functions [23].

Glivec (imatinib mesylate), is a drug currently used for the treatment of lymphomas and c-kit positive solid tumors of the gastrointestinal tract (GIST) [28, 29]. It is a receptor tyrosine kinase inhibitor and it is known to be able of inhibiting c-kit and PDGFR receptors [30], whose activation appears to be critical to maintain ICC phenotypic characteristics and regulate their proliferation [31, 32]. In the urinary tract, several authors have showed a reduction by Glivec in the bladder spontaneous activity and increased contractility induced in the overactive bladder syndrome [33, 34].

Therefore it would be interesting to investigate the possible preventive effect of Glivec in the CYP-induced cystitis.

In the present study, we investigated the possible changes in the number and distribution of ICC in the bladder and urethra of CYP-treated rats by using immunofluorescence with the four different markers: c-kit, vimentin, CD34 and PDGFRα. In addition we analyzed the possible protective effect of Glivec (imatinib mesylate) and the expression of the endothelial isoform of NO synthase (eNOS) in ICC of the bladder and urethra of animals treated with CYP.

2. Material and Methods

2.1 CYP and Glivec treatment

Haemorrhagic cystitis was induced by Cyclophosphamide monohydrate (CYP; Sigma Chemie GMbH, Steinheim, Germany dissolved in NaCl 0.9 %) administration to 48 adult female Wistar rats (200-250 g). Rats were housed individually and were maintained under standard laboratory conditions (12 h light/dark cycle) with *ad libitum* access to food and water. CYP was administered according to the following regimes: (i) intermediate treatment: 150 mg Kg^{-1} i.p., 48h before sacrificing; or (ii) chronic treatment: 50 mg Kg^{-1} i.p., administered every 3 days for 10 days. Control animals received a corresponding volume of saline (0.9%) instead of CYP. Meanwhile, other experimental groups were pretreated with imatinib mesylate (Glivec, LC Laboratories, USA; 10 mg Kg^{-1}, oral administration, five days before and during both CYP treatments). All procedures were approved by the Ethical Committee of the Complutense University and performed in accordance with European guidelines (EU Directive 86/609/EEC).

2.3 Voiding frequency test

Micturition frequency was analyzed in all the rats as described previously [35]. Drinking water was removed one hour before testing and the rats were left in cages lined with filter paper for 30 min. A UV light source was used to visualize and trace the urine spots on the filter paper, and the total number of urine spots and those of small diameter (<0.5 cm) was counted and expressed as the number of voids per hour.

2.4 Immunofluorescence

Animals were anesthetized (40 mg kg^{-1} ketamine + 5 mg kg^{-1} xylazine, i.p.) and then subjected to cardiac perfusion with heparinised 0.1 M phosphate buffer (PB), followed by 4% paraformaldehyde in PB for 30 min. The lower urinary tract was removed from the rats and tissue samples (5 x 5 mm) were obtained from the mid detrusor or the proximal urethra, and fixed in ice-cold 4% paraformaldehyde in 0.1 M

PB (pH 7.0). The tissue was then processed as described previously [8], cryoprotecting the samples with increasing concentrations of sucrose (10-30%) and then snap-freezing it in liquid nitrogen-cooled isopentane and storing at -80ºC for up to 15 days. The tissues were embedded in Tissue-Tek OTC compound and cryostat sections (7 µm: CM1850 UV, Leica Microsystems, Barcelona, Spain) cut transversal to the mucosal surface were recovered on poly-L-lysine-coated slides. The slides were air dried at room temperature for 24 h and then processed directly or stored at -80ºC for no more than 30 days.

Immunofluorescence was performed as described previously [8]. Briefly, sections were washed with PB (3 x 5 min) and incubated for 2h with 3% normal donkey serum (Chemicon International, Temecula, CA, USA) containing 0.3% Triton X-100. The sections were then incubated for 24 h in a humidified chamber at 4ºC with the primary antibody (or antibodies for dual labeling) diluted in 2% normal donkey serum and 0.3% Triton X-100. In both bladder and urethral preparations, the following primary antibodies were used: rabbit polyclonal anti-c-kit antibody (C-19; 1:100, Santa Cruz Biotechnology, Santa Cruz, CA), mouse monoclonal anti-vimentin antibody (clone V9; 1:200; Chemicon International), goat polyclonal anti-CD34 (1:100; Santa Cruz Biotechnology, Santa Cruz, CA), rabbit polyclonal anti-PDGFRα (1:100; Santa Cruz Biotechnology, Santa Cruz, CA), rabbit polyclonal anti-eNOS (1:100; Cayman Chemical, USA). Alexa fluor 488 donkey anti-rabbit, Alexa 488 donkey anti-goat, Alexa 594 donkey anti-rabbit and Alexa 594 donkey anti-mouse (all at 1:200; Molecular Probes, Eugene, OR) were used as the secondary antibodies. The sections were incubated with the secondary antibodies for 2 h in the dark in a humidified chamber at room temperature. After washing with PB (3 times, 10 min each), the nuclei were counterstained for 20-30 min with 4′,6-diamino-2-phenylindole (DAPI, 10.9 mM; Sigma-Aldrich) and the sections were then mounted with Prolong Gold® antifade reagent (Molecular Probes, Eugene, OR, USA). In all cases, negative controls from which the primary antibody was omitted were run in parallel.

Sections were visualized on an Axioplan 2 fluorescence microscope (Carl Zeiss Microimaging, Göttingen, Germany) and photographed with a Spot-2 digital camera (Diagnostic Instruments Sterling Heights, MI, USA). Images were stored digitally as 12-bit images using MetaMorph 6.1 software (MDS Analytical Technologies, Toronto, ON, Canada) and the intensity of immunofluorescence was quantified by measuring the proportion of the selected area that exceeded the threshold value, as described previously [8]. For each experimental group, this measurement was made on no more than 3 randomly selected tissue sections per animal taken from at least 4 animals and for at least 3 different staining procedures (performed on different days). Images at ×20 magnification were obtained at a constant time exposure to permit the direct comparison between images. A threshold was established to subtract background immunoreactivity (ir) and the proportion of the selected area where the staining exceeding the threshold value was analyzed separately in the lamina propria and the muscle layer. Finally, to avoid the interfering effect of oedema, measurements were normalized according to the

number of cells in the area of interest, dividing by the percentage of the area stained with DAPI.

The degree of colocalization between different ICC markers was assayed in pairs by dual labeling. It was expressed as percentage of cells that showed both markers respect to the total number of cells positive to each of the antibodies. Images at x40 magnification were analyzed separately in the lamina propria and the muscle layer.

2.5 Data Analysis

All data are presented as the mean ± SEM. Means were compared by one way ANOVA followed by Bonferroni and Newman-Keuls tests. *P* values of <0.05 were considered significant.

3. Results

3.1 Changes in density and distribution of ICC immunoreactive to c-kit, vimentin, CD34 and PDGFRα.

The antibodies used were reactive to c-kit (**Fig. 1**), vimentin (**Fig. 2**), CD34 (**Fig. 3**), and PDGFRα (**Fig. 4**). We analyzed the relative immunoreactivity to the four different markers of ICC, by determining the colocalization degree between them. We attempted to use antibodies generated in different species in order to perform the more possible pair of combinations (see **Table 1**).

As shown in **Figures 1-4**, CYP treatment induced a very pronounced increase in the density of ICC positives to the four markers used, which was evident in both the lamina propria and the muscle layer of the bladder and the urethra, and that progressively increased with the duration of the treatment. It is remarkable the dramatic increase in ICC at the subepithelial level, forming a compact cellular layer, which makes difficult the differentiation of individual cells (**Figs. 2B, 4I, 5J, N, Q)**. In the muscle layer, ICC were especially dense in the periphery of muscle bundles, expanding into the serosa, where they form a dense cellular crown, primarily in the urethra (**Figs. 2 H-I, 3 H-I**). It should be noted that not all antibodies marked ICC in the same way, while vimentin, CD34 and PDGFRα are present in the contour and ICC prolongations, c-kit is particularly concentrated in the cell bodies (**Figs. 1-5**).

Double labelings, using pairs of antibodies generated in different species, showed the existence of a high degree of colocalization in the same cell (**Fig. 5**), with colocalization percentages higher than 60% in all cases. These data are summarized in **Table 1**. The highest degree of colocalization was observed between CD34 and PDGFRα, reaching more than 90% in both organs, while the lowest degree corresponds to vimentin-CD34. Colocalization percentages were similar in the lamina propria and the smooth muscle layer **(Table 1)**.

CYP treatment did not modify the degree of colocalization of any of the antibody pair tested (**Table 1**), indicating that the ICC population that proliferates as a result of CYP treatment is positive to the four markers used.

3.2 Preventive effect of the treatment with Glivec

Pretreatment with Glivec significantly reduced the number of total and low volume voids (**Fig. 6**), indicating their protective effect on the hyperactivity symptoms that accompany CYP-induced cystitis. Glivec also significantly minimized the increase in lower urinary tract wet weight following the intermediate CYP treatment (**Fig. 7**). Similar histological lesions to those described in CYP-treated animals were still observed when Glivec was also administered (oedema, vascular congestion, hemorrhage, cell infiltration, and erosion or proliferation of the urothelium), although semiquantitative estimation was not performed in the present study.

Immunofluorescence results showed a dramatic reduction in the number of ICC in animals subjected to pretreatment with Glivec, which was manifested with the four antibodies used, in both the lamina propria and the smooth muscle layer of the bladder and the urethra, and in both CYP intermediate and chronic treatments (**Figs. 1-4**).

3.3 Induction of eNOS expression in ICC: a new source of NO during inflammation

eNOS expression were observed in cells with the characteristic morphology of ICC in CYP-treated animals. Double-labeling of eNOS with two different ICC markers were performed in order to demonstrate the nature of these cells. Only direct comparisons could be made between eNOS and vimentin or CD34, due to the impossibility to find out effective antibodies against c-kit and PDGFRα that were not generated in rabbit, the same specie where the eNOS antibody was obtained.

The results showed colocalization of eNOS with vimentin or CD34 in cells with elongated morphology, scant cytoplasm and long cell processes, and therefore identifiable as ICC (**Fig. 8 D-F**). This expression occurred in bladder and urethral ICC of the lamina propria (ICC-LP; **Fig. 8 A-C**), within the muscle bundles (ICC-IM; **Fig. 8 D-F**), or surrounding the muscle bundles (ICC-SEP, **Fig. 8 G-I**). Vimentin and/or CD34 positive ICC showed no eNOS-ir in control animals (not shown).

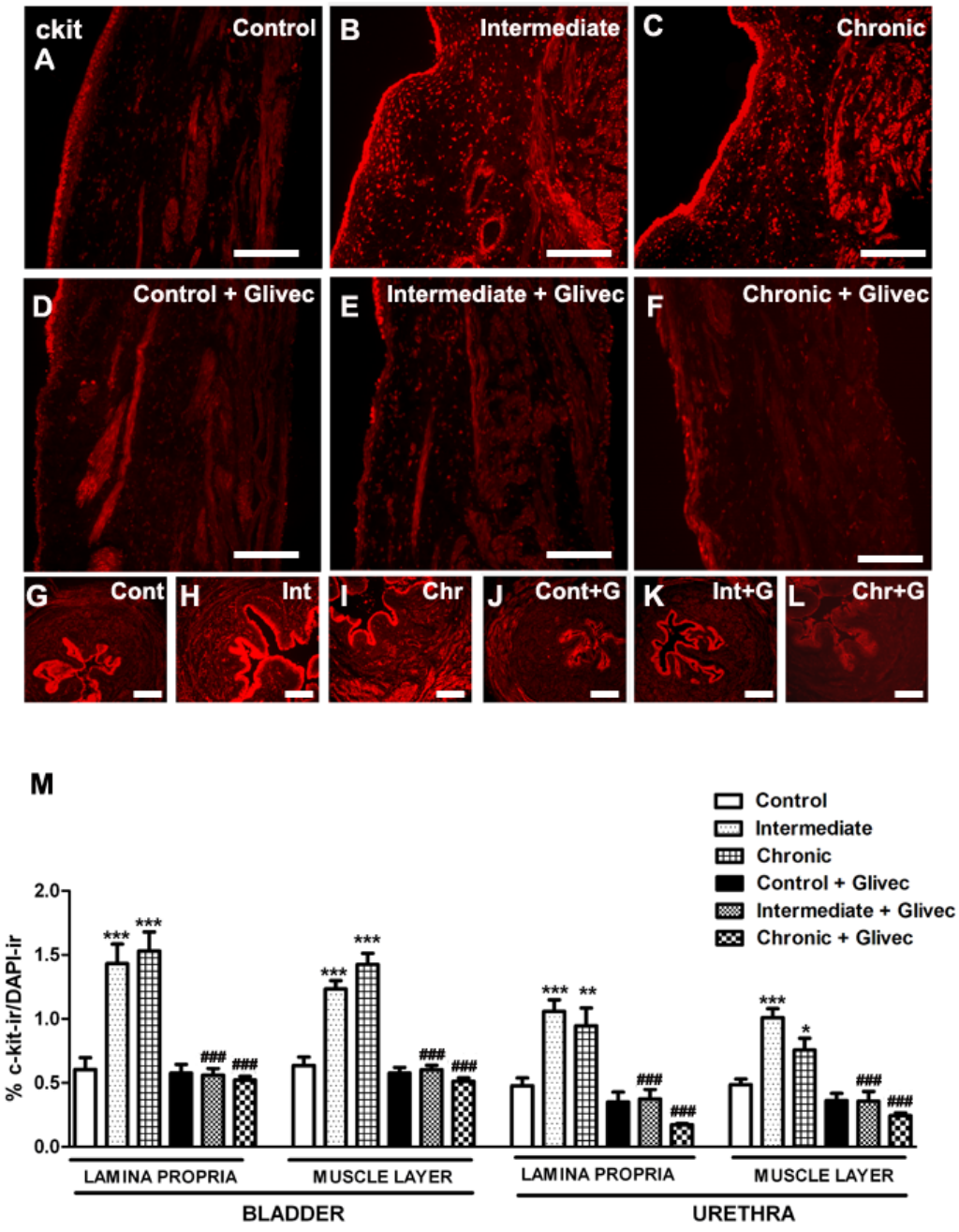

Figure 1. Prominent increases in the immunoreactivity to c-kit induced by the CYP treatment in the bladder and the urethra, and the preventive effect of Glivec. Animals were treated with CYP for 48h (150 mg Kg^{-1}; intermediate) or 10 days (50 mg Kg^{-1} every 3 days, chronic) and compared with controls and with those pre-treated with Glivec (10 mg Kg^{-1}, 5 days before and during CYP treatment).*A-F*: Representative images of the bladder. Bars = 100 µm. *G-L*: Representative images of the urethra. Bars = 50 µm. *M*: Quantification of c-kit-ir in the bladder and urethra. Measurements were made independently in the lamina propria and muscle layer in both organs. The area above the intensity threshold was measured and normalized according to the number of cells in the region of interest (DAPI- labeled nuclei). Values represent the mean ± SEM (*n*= 6-7 different fields from at least 4 different animals). **P* <0.05, ***P* < 0.01, *** *P* <0.001, compared with controls; $^{###}$ *P* <0.001, compared with the corresponding treatment without Glivec (one-way ANOVA followed by Bonferroni and Newman-Keuls tests).

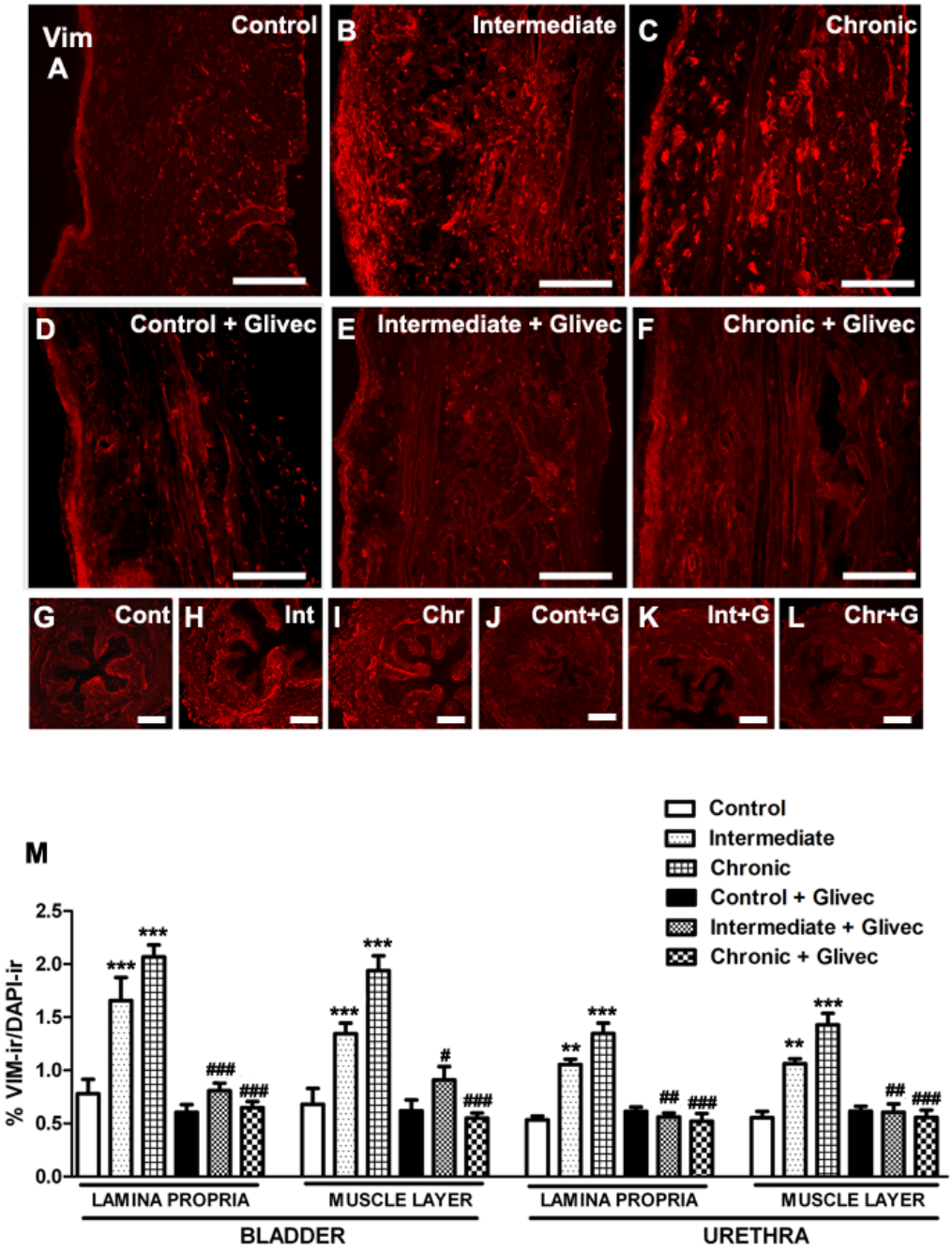

Figure 2. Prominent increases in the immunoreactivity to vimentin induced by the CYP treatment in the bladder and the urethra, and the preventive effect of Glivec. Animals were treated with CYP for 48h (150 mg Kg^{-1}; intermediate) or 10 days (50 mg Kg^{-1} every 3 days, chronic) and compared with controls and with those pre-treated with Glivec (10 mg Kg^{-1}, 5 days before and during CYP treatment).*A-F*: Representative images of the bladder. Bars = 100 µm. *G-L*: Representative images of the urethra. Bars = 50 µm. *M*: Quantification of vimentin-ir in the bladder and urethra. Measurements were made independently in the lamina propria and muscle layer in both organs. The area above the intensity threshold was measured and normalized according to the number of cells in the region of interest (DAPI-labeled nuclei). Values represent the mean ± SEM (*n*= 6-7 different fields from at least 4 different animals). $^{**}P < 0.01$, $^{***}P < 0.001$, compared with controls; $^{\#}P < 0.05$, $^{\#\#}P < 0.01$, $^{\#\#\#}P < 0.001$, compared with the corresponding treatment without Glivec (one-way ANOVA followed by Bonferroni and Newman-Keuls tests).

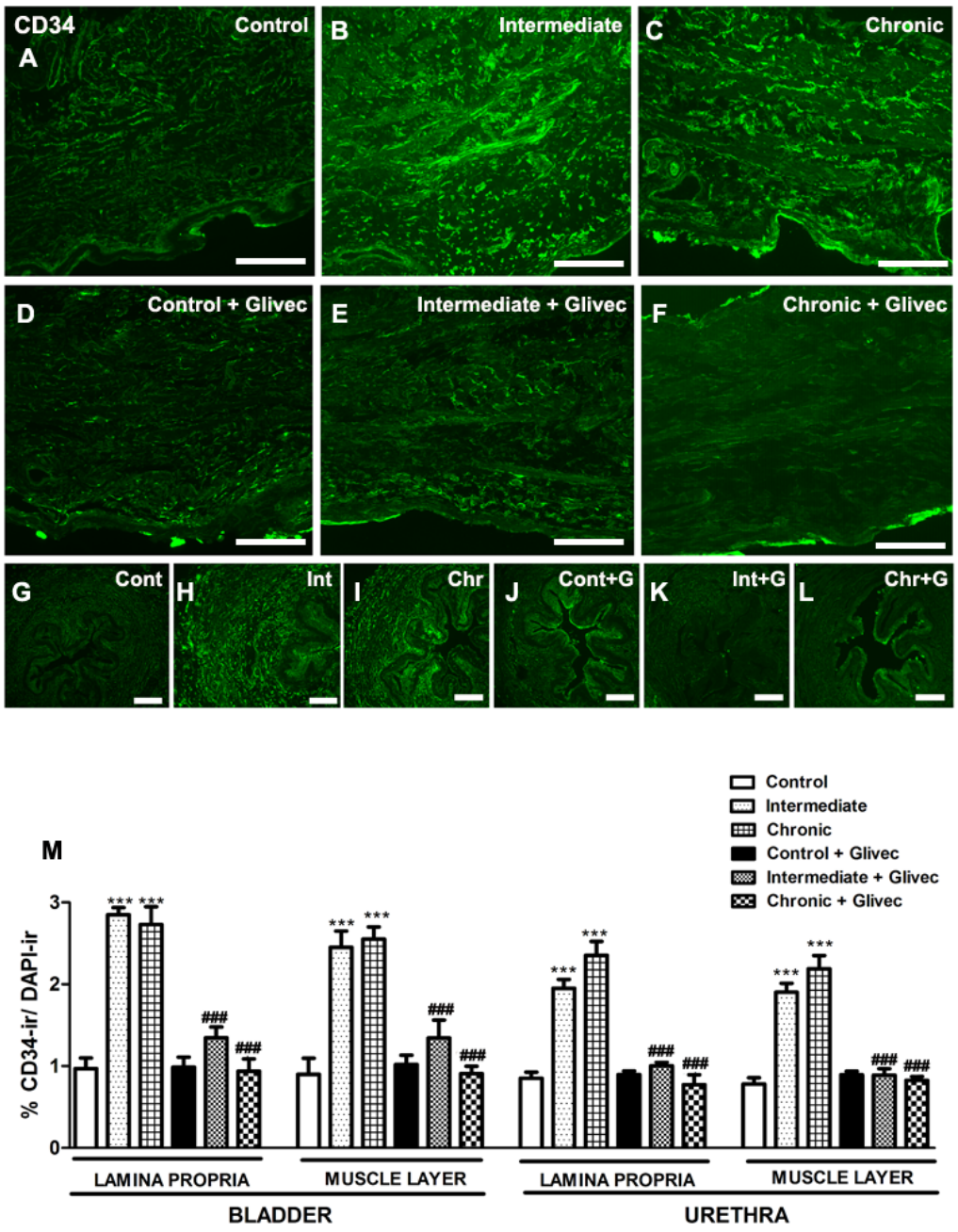

Figure 3. Prominent increases in the immunoreactivity to CD34 induced by the CYP treatment in the bladder and the urethra, and the preventive effect of Glivec. Animals were treated with CYP for 48h (150 mg Kg^{-1}; intermediate) or 10 days (50 mg Kg^{-1} every 3 days, chronic) and compared with controls and with those pre-treated with Glivec (10 mg Kg^{-1}, 5 days before and during CYP treatment).*A-F*: Representative images of the bladder. Bars = 100 µm. *G-L*: Representative images of the urethra. Bars = 50 µm. *M*: Quantification of CD34-ir in the bladder and urethra. Measurements were made independently in the lamina propria and muscle layer in both organs. The area above the intensity threshold was measured and normalized according to the number of cells in the region of interest (DAPI-labeled nuclei). Values represent the mean ± SEM (*n*= 6-7 different fields from at least 4 different animals). *** P <0.001, compared with controls; $^{\#\#}P$ < 0.01, $^{\#\#\#}$ P <0.001, compared with the corresponding treatment without Glivec (one-way ANOVA followed by Bonferroni and Newman-Keuls tests).

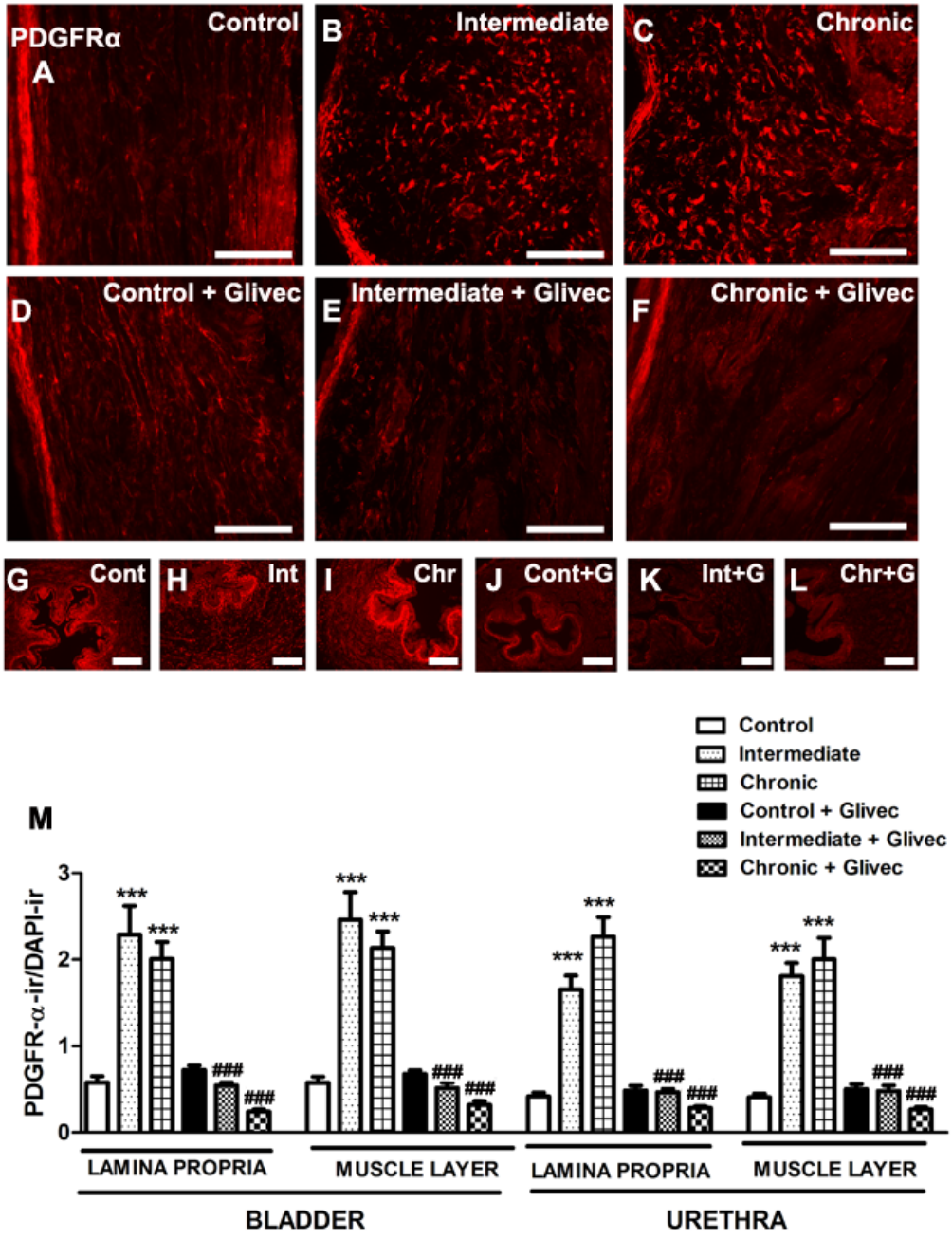

Figure 4. Prominent increases in the immunoreactivity to PDGFRα induced by the CYP treatment in the bladder and urethra, and the preventive effect of Glivec. Animals were treated with CYP for 48h (150 mg Kg^{-1}; intermediate) or 10 days (50 mg Kg^{-1} every 3 days, chronic) and compared with controls and with those pre-treated with Glivec (10 mg Kg^{-1}, 5 days before and during CYP treatment). *A-F*: Representative images of the bladder. Bars = 100 µm. *G-L*: Representative images of the urethra. Bars = 50 µm. *M*: Quantification of PDGFRα-ir in the bladder and the urethra. Measurements were made independently in the lamina propria and muscle layer in both organs. The area above the intensity threshold was measured and normalized according to the number of cells in the region of interest (DAPI-labeled nuclei). Values represent the mean ± SEM (*n*= 6-7 different fields from at least 4 different animals). *** P <0.001, compared with controls; ### P <0.001, compared with the corresponding treatment without Glivec (one-way ANOVA followed by Bonferroni and Newman-Keuls tests).

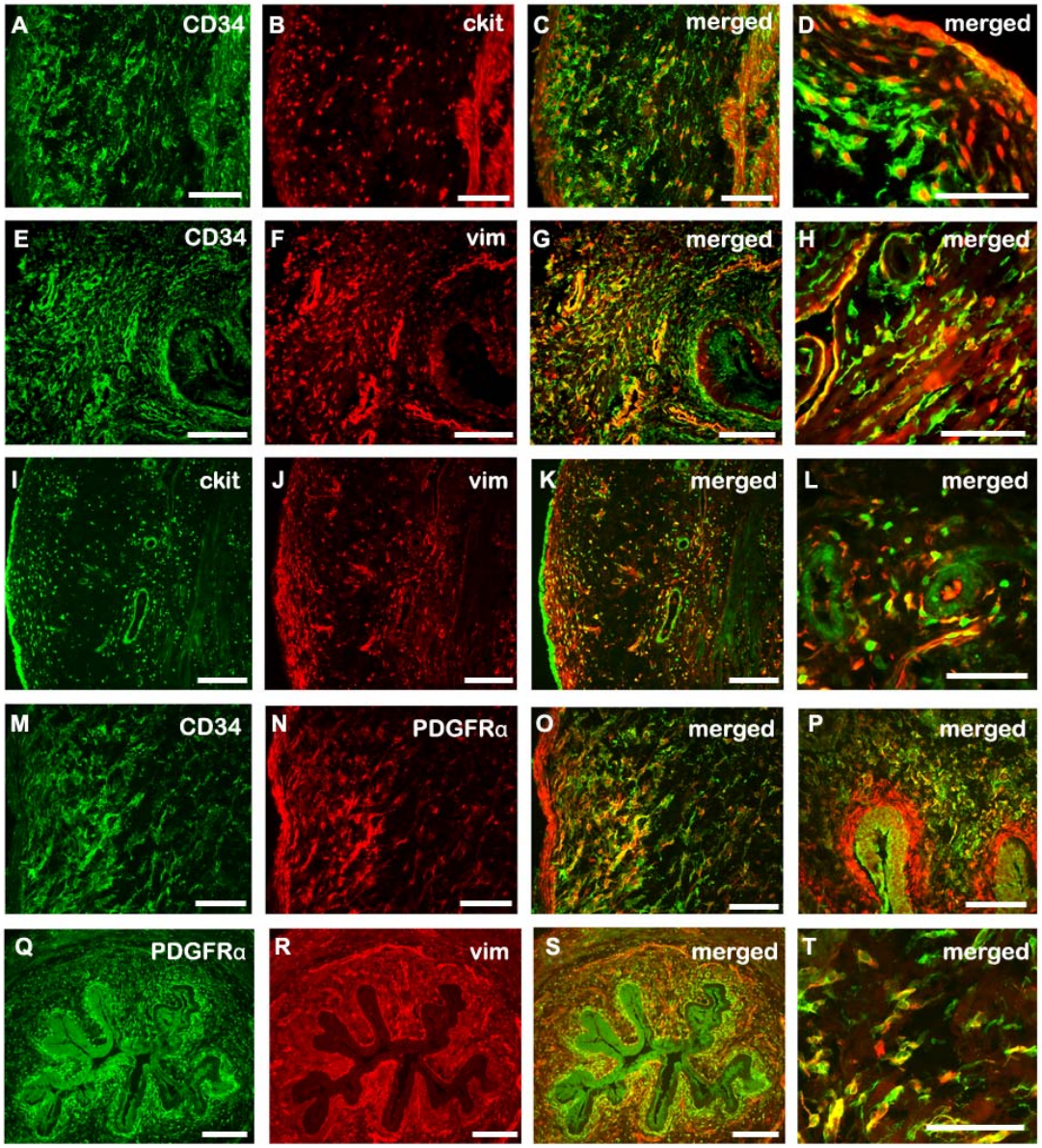

Figure 5. Representative photomicrographs showing the colocalization between the different ICC markers. All examples are from rats treated with CYP for 48 h (150 mg Kg^{-1}; intermediate treatment). *A-D*: CD34 (green)-c-kit (red) in the bladder. (*D*) The subepithelial layer of the same preparation at higher magnification. *E-H*: CD34 (green)-vimentin (red) in the bladder. (*H*) The submucosal layer of the same preparation at higher magnification. *I-L*: c-kit (green)-vimentin (red) in the bladder. (*L*) The submucosal layer of the same preparation at higher magnification. *M-P*: CD34 (green)- PDGFRα (red) in the bladder (*M-O*) and urethra (*P*). *Q-T*: PDGFRα (green)- vimentin (red) in the urethra. (*T*) The outer muscle layer of the same preparation at higher magnification. Bars = 100 μm, except *Q-S* (50 μm) y *D, H, L, T* (25 μm).

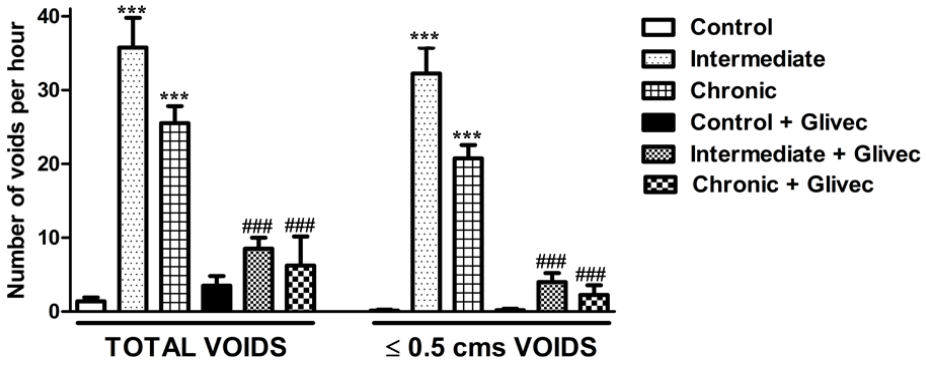

Figure 6. Changes in voiding frequency in CYP-treated rats, and the preventive effect of Glivec. The total number and the number of small-volume voids per hour were measured in animals treated with CYP for 48h (150 mg Kg^{-1}; intermediate) or 10 days (50 mg Kg^{-1} every 3 days; chronic), in animals previously treated with Glivec (10 mg Kg^{-1}, 5 days before and during CYP treatment) as well as in control animals. The data are expressed as the mean ± SEM (n = 6 per group). *** P <0.001, compared with controls; $^{\#\#}P < 0.01$, $^{\#\#\#}P < 0.001$ compared with the corresponding treatment without Glivec (one-way ANOVA followed by Bonferroni and Newman-Keuls tests).

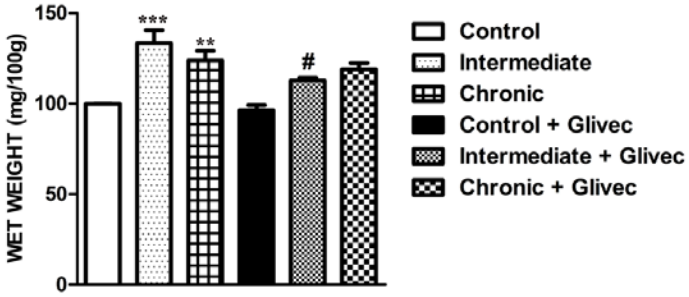

Figure 7. Changes in the urinary tract weight to body weight ratio in CYP-treated rats, and the preventive effect of Glivec. Measurements were performed in animals treated with CYP for 48h (150 mg Kg^{-1}; intermediate) or 10 days (50 mg Kg^{-1} every 3 days; chronic), and animals previously treated with Glivec (10 mg Kg^{-1}, 5 days before and during CYP treatment), as well as in controls. The data are expressed as the mean ± SEM (n = 6 per group). ** P <0.01, compared with controls; $^{\#}P < 0.05$ compared with the corresponding treatment without Glivec (one-way ANOVA followed by Bonferroni and Newman-Keuls tests).

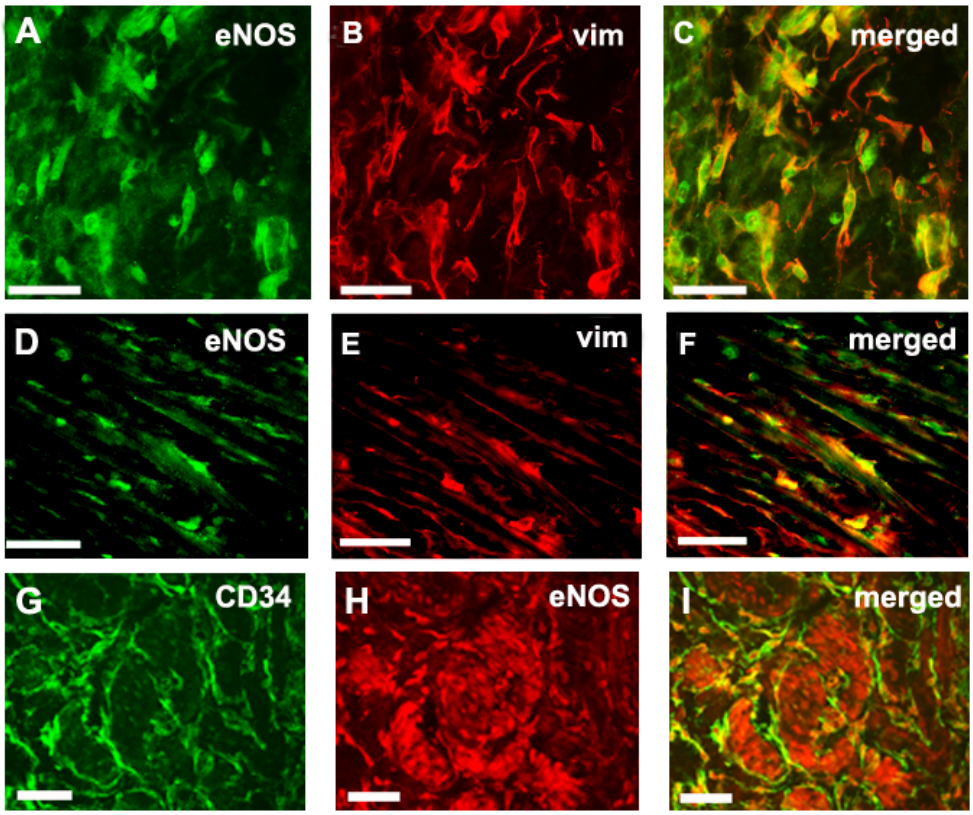

Figure 8. Colocalization of eNOS-ir (green, *A, C, D,F;* or red, *H* and *I*) with vimentin-ir (red, *B, C, E,* and *F*) or CD34-ir (green, *G* and *I*) in ICC present in the lamina propria (ICC-LP, *A-C*), parallel to the smooth muscle bundles (ICC-IM, *D-F*), or in between the smooth muscle bundles (ICC-SEP, *G-I*) of CYP-treated bladders (intermediate treatment) Bars = 50 μm.

	% COLOCALIZATION							
	BLADDER				URETHRA			
	CONTROL		CYP (Intermediate)		CONTROL		CYP (Intermediate)	
	LAMINA PROPRIA	MUSCLE LAYER	LAMINA PROPRIA	MUSCLE LAYER	LAMINA PROPRIA	MUSCLE LAYER	LAMINA PROPRIA	MUSCLE LAYER
c-kit/ CD34	72.6 ± 1.2	76.0 ± 3.4	74.6 ± 3.4	75.3 ± 3.1	75.8 ± 2.6	73.8 ± 3.2	78.2 ± 1.5	79.1 ± 1.3
CD34/ c-kit	85.7 ± 2.0	90.6 ± 1.2	88.2 ± 2.3	91.0 ± 2.0	85.9 ± 1.8	87.2 ± 1.5	89.6 ± 2.1	90.3 ± 1.6
Vimentin/ CD34	47.8 ± 2.0	49.2 ± 1.9	43.6 ± 1.4	47.4 ± 2.8	65.1 ± 3.5	68.4 ± 1.5	72.3 ± 2.0	71.3 ± 2.6
CD34/ Vimentin	60.7 ± 2.5	58.1 ± 1.9	58.9 ± 1.0	62.3 ± 2.7	77.9 ± 3.0	81.3 ± 1.4	81.6 ± 1.7	82.5 ± 1.9
PDGFRα/ Vimentin	87.3 ± 1.3	88.2 ± 1.4	89.0 ± 1.6	88.0 ± 1.4	81.0 ± 2.4	79.8 ± 1.2	81.2 ± 2.2	81.6 ± 1.7
Vimentin/PDGFRα	78.8 ± 1.9	76.0 ± 1.4	80.0 ± 2.1	80.6 ± 1.9	66.0 ± 1.1	66.3 ± 1.0	66.3 ± 1.0	67.4 ± 1.4
c-kit/ Vimentin	76.8 ± 0.8	77.6 ± 2.4	76.0 ± 2.5	77.4 ± 2.2	75.0 ± 1.4	77.4 ± 1.5	79.4 ± 2.8	79.6 ± 2.1
Vimentin/ c-kit	83.8 ± 1.0	84.4 ± 2.6	86.2 ± 1.3	86.5 ± 1.1	84.0 ± 1.8	82.4 ± 0.7	83.8 ± 0.7	84.1 ± 2.0
CD34/ PDGFRα	94.0 ± 0.9	94.2 ± 0.6	96.4 ± 0.8	94.0 ± 2.4	94.0 ± 2.1	93.9 ± 0.6	92.5 ± 1.4	91.0 ± 2.5
PDGFRα / CD34	91.2 ± 0.6	90.1 ± 0.5	93.1 ± 0.5	92.9 ± 1.3	91.0 ± 0.8	91.4 ± 0.8	91.2 ± 1.7	91.1 ± 0.7

Table 1. Colocalization between the different ICC markers in the lamina propria and the smooth muscle layer of the rat bladder and urethra in control situation and following intermediate treatment with CYP. Animals were treated with CYP for 48h (150 mg Kg^{-1}; intermediate) and compared with controls. The different antibodies were assayed in pairs by double immunofluorescence, and the results are expressed as percentage of cells that showed colocalization respect to the total number of cells positive to each of the antibodies. Data are the mean ± SEM (n = 6-8 different fields from at least 4 different animals). No significant differences were observed between tissue layers as well as between controls and CYP-treated animals (one-way ANOVA followed by Bonferroni and Newman-Keuls tests)

4. Discussion

The relationship between nitrergic nerves and ICC in both the urethra [8] and the bladder [36], and the hypothesis of the involvement of these cells as mediators of the nitrergic neurotransmission process [8] suggest that alterations in NO production such as that produced by CYP-induced cystitis [5- 7], could be accompanied by changes in the density and distribution of ICC. This study showed significant and progressive increases in the density of cells that are immunoreactive to different ICC and/or fibroblast markers (c-kit, vimentin, CD34 and PDGFRα) following CYP treatments in the bladder and the urethral wall.

Before attempting to give an explanation to this pronounced increase of ICC it would be worthwhile taking some aspects into considerations. Firstly, it should be noted that none of the antibodies used are completely selective of ICC. Even, c-kit which is considered as the main marker of ICC in the intestine [37] and other tissues [10, 11, 38] also labels other cell types such as mast cells, melanocytes, neurons, and glial cells [19]. Moreover, even in the intestine, not all ICC are reactive to c-kit, such as the ICC-DMP located in the small intestine [12, 13], suggesting ICC subtypes with different reactivity to c-kit and different functional characteristics. In the lower urinary tract c-kit-ir has been demonstrated in the mouse bladder [17], unlike other authors who described a lack of reactivity to this antibody and alternatively used vimentin to the identification of these cells in both the bladder and the urethra of different species [14, 18, 20, 21]. In our study, although c-kit-ir was not observed initially in the rat urethra fixed with paraformaldehyde [8], the use of a different antibody (c-19, Santa Cruz Biotechnology) allowed us to obtain satisfactory results in both the bladder and the urethra of this specie (present results). Here, c-kit-ir was concentrated mainly in the soma of cells with typical ICC morphology. Although non-specific staining also appeared in the urothelium and SMC in both organs, in any case it made the analysis of the results difficult.

Compared to c-kit, vimentin-ir seems to be less dependent on the experimental conditions. Thus, in all cases in which c-kit-ir could not be demonstrated, there was clear vimentin positivity in urethral ICC [8, 14]. Vimentin is also not exclusive for ICC, being able to mark also mast cells and fibroblasts or myofibroblasts. However, the peculiar ICC morphology, elongated cells with scant cytoplasm, ovoid nucleus and long prolongations, allows them to be easily differentiated from macrophages and mast cells, which are cells rounded and devoid of prolongations. It should be noted the high level of colocalization (75-80%) observed in the present study between c-kit and vimentin. Colocalization of both markers has been previously shown in these cells in both the bladder and urethra of different species [8, 39-41]. This fact is especially relevant given the technical difficulties to obtain adequate c-kit-ir in fixed tissues, and it allows us to validate the use of vimentin as a specific ICC marker in these organs. These results are supported by previous studies describing vimentin but not c-kit positivity in bladder and urethral ICC [8, 14, 18, 20, 21].

Currently, there is much debate about the presence of other markers in ICC. Among them, CD34 is a transmembrane glycoprotein present in endothelial and mesenchymal cells [22], which is considered by some researchers as a fibroblasts, but not a ICC, marker (c-kit negative) in both the gastrointestinal tract and the bladder [23, 24, 42, 43]. However, other studies have demonstrated, by immunofluorescence and PCR, the coexpression of c-kit and CD34, and therefore the existence of this protein in ICC [44]. It has also been shown that c-kit positive cells from GIST also express CD34 [45]. Something similar happens with PDGFRα, recently proposed as a new marker of ICC-like cells of the gastrointestinal tract that are c-kit negative [25- 27, 46]. Based on these results it has been suggested the existence of two different types of ICC in the digestive system: true ICC and another subpopulation called "fibroblast-like cells" that are immunoreactive to PDGFRα, but not to c-kit. In the bladder it has also been reported the existence of a cell population immunoreactive to PDGFRα and vimentin, but they were not able to probe its colocalization with c-kit [21]. These cells, as in the gastrointestinal tract, are close to SMC and in intimate contact with nerve endings [47-49].

Our results show a high degree of colocalization between all pairs of markers tested. Colocalization of CD34 and PDGFRα with vimentin and c-kit (the latter could only be tested with CD34 because of the absence of effective antibodies to PDGFRα in other species than the rabbit), suggest that unlike the digestive tract [25- 27, 46], the majority of ICC would also be CD34 and PDGFRα positive cells. It is remarkable the high degree of colocalization between these last two markers (more than 90%), which is not complete possibly due to the endothelial cell staining by CD34 but not by PDGFRα [24]. This colocalization has also been shown in the gastrointestinal tract [23, 42, 44]. The degree of colocalization was slightly lower between CD34 and vimentin or c-kit (50-80%), suggesting the possible existence of a cell population that would be mostly marked by CD34 and PDGFRα. The current debate focuses on whether positive cells to these alternative markers (CD34 and PDGFRα) but c-kit negatives would be true ICC with different functions [23] or alternatively they would represent fibroblasts or fibroblast-like cells [47- 49]. In any case, considering that it has been described structural and functional relationships between SMC and intramural nerves with both cell types, at least theoretically both of them could act as neurotransmission mediators [21, 47- 49]. Thus, similarities between them may be much higher than suggested by their different names. It is possible that a re-evaluation of what is considered an ICC based on functional aspects, beyond to its reactivity to c-kit or any other marker, is needed.

It has been suggested that ICC located in different regions of the bladder or the urethral wall might have different functional specialization. Thus, ICC located at subepithelial level and in the lamina propria, where they form a syncytium interconnected each other and with afferent nerves [50], could participate in afferent information processing [51] or they could have a pacemaker function [52]. These ICC in the urethra showed increases in cGMP that were not modified by nitrergic nerve

stimulation [8], suggesting that its main function is not to be effectors of the NO action. By contrast, ICC located in the muscle layer may be particularly adapted to act as mediators between intramural nerves and SMC, and thus their increases in cGMP induced by nitrergic stimulation were specifically inhibited by blocking NOS and sGC enzymes [8]. The present study did not show a differential distribution of cells positive for any of the four markers employed in either the lamina propria or the muscle layer of both the bladder and the urethra. These results suggest that these markers are not able to discriminate between the potential functional types of ICC previously described.

CYP treatment caused a pronounced accumulation of cells positive to the four markers used, which was very similar to each other. Furthermore, in any case treatment with CYP modified the degree of colocalization of the different pairs of antibodies analyzed, further supporting the suggestion that all markers employed would be equally useful for detecting cells that proliferate during the inflammatory process. This accumulation was similar in the lamina propria and the muscle layer, but it stand out a special accumulation of cells beneath the urothelium, whose density increased progressively with the treatment with CYP. These results are similar to those described by de Jongh et al (2007) [9] in a model of bladder obstruction in the guinea-pig, although in this case ICC are marked with an anti-cGMP antibody. It should be noted that a characteristic symptom of both cystitis and bladder obstruction is an increase in the excitability of the reflex voiding which leads to bladder hyperactivity symptoms. Thus, the number of total and low volume voids increased as a result of CYP treatment. This hyperexcitability could be caused by an increase in bladder afferent discharge induced by a higher density of ICC at subepithelial level. These cells may act on afferent endings as authentic mechanoreceptors, or they could, as pacemakers, increase bladder contractility and cause mechanical distortion with the consequent activation of afferent endings.

In the model of bladder obstruction in the guinea-pig previously described, de Jongh et al., 2007 [9] showed an increase in the density of cGMP positive cells in the muscle layer, which were especially located in groups named intermuscular nodes. Here they could associate with intramural nerve endings. In the present study, a more detailed analysis of the distribution of c-kit, vimentin, CD34 and PDGFRα positive cells within the muscle layer showed that these cells were denser in the periphery of the muscle bundles, expanding into the serosa, where they formed a dense cellular crown, particularly in the urethra. In addition, this dense pack of ICC was connected as well with ICC distributed in the lamina propria and they together formed an interconnected network that extended throughout the bladder and urethral wall. This would allow ICC to act in the transmission and coordination of signals from the urothelium or intramural nerves to the muscle and *vice versa*. Thus, an increase in the density of ICC could cause an increase in the inter-voiding contractile activity, which would trigger the hyperreflexia situation. In support of this suggestion, in the human overactive bladder syndrome a prominent increase in the number of c-kit positive ICC was observed compared to healthy bladders [33]. Similarly, in a model of partial bladder outlet

obstruction in guinea-pig, accompanied by bladder overactivity, it was observed an increase in the density of c-kit and vimentin positive cells in the subserosal layer, as well as an alteration in the distribution of ICC in the suburothelial layer [53]. All these facts suggest a direct relationship between the increase in the number of ICC and the bladder hyperexcitability that characterize these syndromes.

ICC also have secondary functions such as immunomodulation, growth, repair and fibrosis [54- 59]. Many studies have reported loss, reduction, or damage to ICC networks in a variety of intestinal motility disorders [60, 61]. By contrast, inflammatory process such as the inflammatory bowel disease and particularly Crohn's disease leads to tissue fibrosis through an abnormal secretion of extracellular matrix by mesenchymal cells (fibroblasts or ICC), which are activated to a fibrogenic phenotype [62]. Furthermore, PDGFR has been implicated in the fibrotic changes of several organs [54, 63, 64], and mice with enhanced activation of PDGFRα developed gastrointestinal fibrosis and sarcoma [65]. The involvement of other growth factors such as scf (natural ligand of c-kit receptor), epidermal growth factor and transforming growth factor-β has also been suggested [54, 55]. Given the close similarity between gastrointestinal and urinary ICC it could be suggested that they could also participate in a fibrogenic process that would contribute to the pathogenicity of CYP-induced cystitis.

Our results also demonstrated expression of eNOS *de novo* in vimentin and CD34 positive cells present in the different layers of the bladder and urethral wall of the CYP-treated animals. Although double labeling with c-kit and PDGFR-α could not be performed, colocalization with vimentin and CD34, and their morphological characteristics are sufficient to identify these cells as ICC. It has previously described that urethral ICC did not express nNOS, although they act as effectors of the NO released by intramural nerves by increases in intracellular cGMP [8]. Furthermore, this study showed that these cells did not express the endothelial isoform in the absence of inflammation (control preparations). Therefore, the expression of eNOS in ICC, and the subsequent production of NO from these cells may contribute to the pathogenesis of the inflammatory process. As already mentioned in the previous section, an excess in NO production seems to be one of the central mechanisms in the development of cystitis [5-7], and this excess of NO may result from the endothelial constitutive isoform expression in a large number of ICC distributed throughout the bladder and urethral wall.

Our results show a clear inhibitory effect of Glivec on ICC proliferation in the lamina propria and the smooth muscle layer of the bladder and the urethra, as well as on the increase in voiding frequency that were both induced by the treatment with CYP. This fact further suggests the involvement of increases in ICC in the development of symptoms of bladder hyperactivity. Glivec is a receptor tyrosine kinase inhibitor which is known to block c-kit and PDGFR receptors [30], and it is currently used for the treatment of lymphomas and solid tumors of the gastrointestinal tract characterized as c-kit positive [28, 29]. Treatment with Glivec was previously reported to inhibit development of ICC-MY and spontaneous electrical activity of the gastrointestinal tract

during the last period of gestation [66]. Regarding the lower urinary tract, several authors have observed a reduction in bladder activity following inhibition of c-kit [29, 33, 34, 67, 68]. Biers et al (2006) [33] demonstrated that Glivec inhibits the increase in bladder contractility and in spontaneous activity that are induced in the overactive bladder syndrome, and Kubota et al (2006) [34] showed that Glivec reduces bladder spontaneous activity. The fact that Glivec prevented both the increase in the number of bladder and urethral ICC and the bladder hyperactivity symptoms that occur as a result of CYP treatment, suggest its possible therapeutic application in the prevention of the bladder disorders that accompanied chemotherapy treatments with CYP. Even its potential use could be extended to other inflammatory diseases of the lower urinary tract that showed proliferation of ICC and overactive bladder symptoms. Although more studies are needed to clarify the role of ICC in these disorders, an excessive NO production derived from the expression of eNOS in an increased population of ICC could contribute to the process.

Conclusions

In conclusion, this study shows for the first time that the inflammatory reaction induced by CYP in the bladder and urethra is accompanied by a prominent increase in the density of c-kit-, vimentin-, CD34- and PDGFRα-positive cells, which would be considered as ICC. Furthermore, the process is accompanied by the induction of eNOS expression in these cells, which may constitute a new source of NO that contribute to the pathogenicity of the process. Finally, Glivec effectively inhibited both ICC proliferation and bladder symptoms of hyperactivity, suggesting a possible therapeutic application in preventing secondary effects on the bladder during chemotherapy treatments with CYP.

Acknowledgements

This work was supported by grants from the "Comunidad de Madrid-Universidad Complutense de Madrid" (UCMGR85/06-920307), UCM-Santander (GR35/10-A-920307) and the Fundación Mutua Madrileña (FMM2011). The microphotographs were acquired and analyzed at the Microscopy and Cytometry Centre (Complutense University, Madrid, Spain) and we thank Alfonso Cortés and Luis M. Alonso for their technical assistance with the fluorescence microscopy.

References

[1] **Cox PJ**. Cyclophosphamide cystitis—identification of acrolein as the causative agent. *Biochem Pharmacol* 28(13): 2045-2049, 1979.

[2] **Bon K, Lanteri-Minet M, Michiels JF, Menetrey D**. Cyclophosphamide cystitis as a model of visceral pain in rats: a c-fos and Krox-24 study at telencephalic levels, with a note on pituitary adenylate cyclase activating polypeptide (PACAP). *Exp Brain Res* 122: 165-174, 1998.

[3] **Yoshimura N, De Groat WC.** Increased excitability of afferent neurons innervating rat urinary bladder after chronic bladder inflammation. *J Neurosci* 19: 4644-4653, 1999.

[4] **Cho KH, Hyun JH, Chang YS, Na YG, Shin JH, Song KH.** Expression of nitric oxide synthase and aquaporine-3 in cyclophosphamide treated rat bladder. *Int Neurourol J* 24: 149-156, 2010.

[5] **Souza-Filho MVP, Lima MVA, Pompeu MML, Ballejo G, Cunha FQ, Ribeiro RA.** Involvement of nitric oxide in the pathogenesis of cyclophosphamide-induced hemorrhagic cystitis. *Am J Pathol* 150: 247-256, 1997.

[6] **Alfieri AB, Cubeddu LX**. Nitric oxide and NK_1-tachykinin receptors in cyclophosphamide-induced cystitis in rats. *J Pharmacol Exp Ther* 295: 824-829, 2000.

[7] **Korkmaz A, Topal T, Oter S**. Pathophysiological aspects of cyclophosphamide and ifosfamide induced hemorrhagic cystitis; implication of reactive oxygen and nitrogen species as well as PARP activation. *Cell Biol Toxicol* 23: 303-312, 2007.

[8] **García-Pascual A, Sancho M, Costa G, Triguero D.** Interstitial cells of Cajal in the urethra are cGMP-mediated targets of nitrergic neurotransmission. *Am J Physiol Renal Physiol* 295: 971-983, 2008.

[9] **De Jongh R, van Koeveringe GA, van Kerrebroeck PEV, Markerink-van Ittersum M, de Vente J, Gillespie JI.** Alterations to network of NO/cGMP-responsive interstitial cells induced by outlet obstruction in guinea-pig bladder. *Cell Tissue Res* 330: 147-160, 2007.

[10] **Torihashi S, Ward SM, Sanders KM**. Development of c-kit-positive cells and the onset of electrical rhythmicity in murine small intestine. *Gastroenterology* 112:144-155, 1997.

[11] **Vanderwinden JM, Rumessen JJ, Liu H, Descamps D, De Laet MH, Vanderhaeghen JJ.** Interstitial cells of Cajal in human colon and in Hirchsprung´s disease. *Gastroenterology* 111:901-910, 1996.

[12] **Torihashi S, Horisawa M, Watanabe Y**. c-Kit inmunoreactive interstitial cells in the human gastrointestinal tract. *J Auton Nerv Syst* 75:38-50, 1999.

[13] **Wang XY, Paterson C, Huizinga JD**. Cholinergic and nitrergic innervation of ICC-DMP and ICC-IM in the human small intestine. *Neurogastroenterol Motil* 15:531-543, 2003.

[14] **Sergeant GP, Hollywood MA, McCloskey KD, Thornbury KD, McHale NG.** Specialised pacemaking cells in the rabbit urethra. *J Physiol* 526:359-366, 2000.

[15] **McHale NG, Hollywood MA, Sergeant GP, Shafei M, Thornbury KT, Ward SM**. Organization and function of ICC in the urinary tract. *J Physiol* 576(3): 689-694, 2006.

[16] **Lyons AD, Gardiner TA, McCloskey KD**. Kit-positive interstitial cells in the rabbit urethra: structural relationships with nerves and smooth muscle. *BJU Int* 99: 687-694, 2007.

[17] **McCloskey KD, Anderson UA, Davidson RA, Bayguinov YR, Sanders KM, Ward SM**. Comparison of mechanical and electrical activity and interstitial cells of Cajal in urinary bladders from wild-type and W/W^v mice. *Br J Pharmacol* 156(2): 273-283, 2009.

[18] **Pezzone MA, Watkins SC, Alber SM, King WE, de Groat WC, Chancellor MB, Fraser MO.** Identification of c-kit-positive cells in the mouse ureter: the interstitial cells of Cajal of the urinary tract. *Am J Physiol Renal Physiol* 284:925-929, 2003.

[19] **Zhang SC, Fedoroff S**. Cellular localization of stem cell factor and c-kit receptor in the mouse nervous system. *J Neurosci Res* 47: 1-15, 1997.

[20] **Gillespie JI, Markerink- van Ittersum M, de Vente J.** cGMP generating cells in the bladder wall: identification of distinct networks of interstitial cells. *BJU International* 94:1114-1124, 2004.

[21] **Koh BH, Roy R, Hollywood MA, Thornbury KD, McHale NG, Sergeant GP, Hatton WJ, Ward SM, Sanders KM, Koh SD.** Platelet-derived growth factor receptor-a cells in mouse urinary bladder: a new class of interstitial cells. *J Cell Mol Med* 16(4): 691-700, 2012.

[22] **Pusztaszeri MP, Seelentag W, Bosman FT.** Immunohistochemical expression of endothelial markers CD31, CD34, von Willebrand factor, and Fli-1 in normal tissues. *J Histochem Cytochem* 54(4):385-95, 2006.

[23] **Vanderwinden JM, Rumessen JJ, De Laet MH, Vanderhaeghen JJ, Schiffmann SN**. CD34 immunoreactivity and interstitial cells of Cajal in the human and mouse gastrointestinal tract. *Cell Tissue Res* 302: 145-153, 2000.

[24] **Pieri L, Vannucchi MG, Faussone-Pellegrini MS**. Histochemical and ultrastructural characteristics of an interstitial cell type different from ICC and resident in the muscle coat of human gut. *J Cell Mol Med* 12:1944-1955, 2008.

[25] **Iino S, Horiguchi K, Horiguchi S, Nojyo Y.** c-Kit-negative fibroblast-like cells express platelet-derived growth factor receptor *a* in the murine gastrointestinal musculature. *Histochem Cell Biol* 131: 691-702, 2009.

[26] **Iino S, Nojyo Y**. Immunohistochemical demonstration of c-kit-negative fibroblast-like cells in murine gastrointestinal musculature. *Arch Histol Cytol* 72(2): 107-115, 2009.

[27] **Kurahashi M, Nakano Y, Hennig GH, Ward SM, Sanders KM.** Platelet-derived growth factor receptor α-positive cells in the tunica muscularis of human colon. *J Cell Mol Med* 16: 1397-1404, 2012.

[28] **Joensuu H, Roberts PJ, Sarlomo-Rikala M, Andersson LC, Tervahartiala P, Tuveson D, Silberman S, Capdeville R, Dimitrijevic S, Druker B, Demetri GD.** Effect of the tyrosine kinase inhibitor STI571 in a patient with a metastaticgastrointestinal stromal tumor. *N Engl J Med*.344, 1052–1056, 2001.

[29] **Kubota Y, Kajioka S, Biers M, Yokota E, kohri K, Brading AF.** Investigation of the effect of the c-kit inhibitor Givec on isolated guinea-pig detrusor preparations. *Auton Neurosci* 115: 64-73, 2004.

[30] **Druker BJ, Tamura S, Buchdunger E, Ohno S, Segal GM, Fanning S, Zimmermann J, Lydon NB.** Effects of a selective inhibitor of the Abl tyrosine kinase on the growth of Bcr-Abl positive cells. *Nat Med* 2: 561-566, 1996.

[31] **Maeda H, Yamagata A, Nishikawa S, Yoshinga K, Kobayashi S, Nishi K, Nishikawa S-I**. Requirement of c-kit for development of intestinal pacemaker system. *Development* 116:369-375, 1992.

[32] **Torihashi S, Ward SM, Nishikawa S, Nishi K, Kobayashi S, Sanders KM.** c-kit-dependent development of interstitial cells and electrical activity in the murine gastrointestinal tract. *Cell Tissue Res*. 280:97-111, 1995.

[33] **Biers SM, Reynard JM, Doore T, Brading AF**. The functional effects of a c-kit tyrosine inhibitor on guinea-pig and human detrusor. *BJU Int* 97(3): 612-616, 2006.

[34] **Kubota Y, Biers SM, Kohri K, Brading AF.** Effects of imatinib mesylate (Glivec) as a c-kit tyrosine kinase inhibitor in the guinea-pig urinary bladder. *Neurourol Urodyn* 25: 205-210, 2006.

[35] **Dickson A, Avelino A, Cruz A, Ribeiro-da-Silva F.** Peptidergic sensory and parasympathetic fiber sprounting in the mucosa of the rat urinary bladder in a chronic model of cyclophosphamide-induced cistitis. *Neurosci* 141: 1633-1647, 2006.

[36] **Gillespie JI, Markerink- van Ittersum M, de Vente J.** Expression of neural nitric oxide synthase (nNOS) and nitric-oxide-induced changes in cGMP in the urothelial layer of the guinea pig bladder. *Cell Tissue Res* 321: 341-351, 2005.

[37] **Huizinga JD, Thuneberg L, Klüppel M, Malysz J, Mikkelsen HB, Bernstein A**. W/kit gene required for intestinal pacemaker activity. *Nature* 373: 347-349, 1995.

[38] **Lammie A, Drobnjak M, Gerald W, Saad A, Cote R, Cordon-Cardo C**. Expression of c-kit and kit ligand proteins in normal human tissues. *J. Histochem. Cytochem*. 42: 1417, 1994.

[39] **Davidson RA, McCloskey KD**. Morphology and localization of interstitial cells in the guinea-pig bladder: structural relationships with smooth muscle and neurons. *J Urol* 173: 1385-1390, 2005.

[40] **Smet PJ, Jonavicius J, Marshall VR, de Vente J.** Distribution of nitric oxide synthase-immunoreactive nerves and identification of the cellular targets of nitric oxide in guinea-pig and human urinary bladder by cGMP immunohistochemistry. *Neuroscience* 71:337-348, 1996.

[41] **Johnston L, Woolsey S, Cunningham R, O´Kane H, Duggan B, Keane P, McCloskey KD**. Morphological expression of KIT positive interstitial cells of Cajal in human bladder. *J Urol* 184: 370-377, 2010.

[42] **Vanderwinden JM, Rumessen JJ, De Laet MH, Vanderhaeghen JJ, Schiffmann SN.** CD34+ cells in human intestine are fibroblast adjacent to, but distinct from, interstitial cells of Cajal. *Lab Invest* 79: 59-65, 1999.

[43**] Rasmussen H, Hansen A, Smedts F, Rumessen JJ, Horn T.** CD34-positive interstitial cells in the human detrusor. *APMIS* 115: 1260-1266, 2007.

[44**] Robinson TL, Sircar K, Hewlett BR, Chorneyko K, Riddell RH, Huizinga JD.** Gastrointestinal stromal tumors may originate from a subset of CD34-positive interstitial cells of Cajal. *Am J Pathol* 156: 1157-1163, 2000.

[45] **Hirota S, Isozaki K, Moriyama Y, Hashimoto K, Nishida T, Ishiguro S, Kawano K, Hanada M, Kurata A, Takeda M, Muhammad Tunio G, Matsuzawa Y, Kanakura Y, Shinomura Y, Kitamura Y.** Gain-of-function mutations of c-kit in human gastrointestinal stromal tumors. *Science* 279(5350): 577-580, 1998.

[46] **Chan F, Liu Y, Sun H, Li X, Shang H, Fan D, An J, Zhou D.** Distribution and possible role of PDGF-AA and PDGFR-α in the gastrointestinal tract of adult guinea pigs. *Virchows Arch* 457: 381-388, 2010.

[47] **Horiguchi K, Komuro T**. Ultrastructural observations of fibroblast-like cells forming gap junctions in the W/W^{V} mouse small intestine. *J Auton Nerv Syst* 80: 142-147, 2000.

[48] **Lang, RJ.** Do fibroblast-like cells´intercede during enteric inhibitory motor neurotransmission in gastrointestinal smooth muscles? *J Physiol* 589: 453- 454, 2011.

[49] **Cobine CA, Henning GW, Kurahashi M, Sanders KM, Ward SM, Keef KD.** Relationship between interstitial cells of Cajal, fibroblast-ike cells and inhibitory motor nerves in the internal anal sphincter. *Cell Tissue Res* 344: 17-30, 2011.

[50] **Hashitani H.** Interaction between interstitial cells and smooth muscles in the lower urinary tract and penis. *J Physiol* 576: 707-714, 2006.

[51] **Huizinga JD, Reed DE, Berezin I, Wang XY, Valdez DT, Liu LW, Diamant NE.** Survival dependency of intramuscular ICC on vagal afferent nerves in the cat esophagus. *Am J Physiol regul Integr Comp Physiol* 294: 302-310, 2008.

[52] **Mazet B, Raynier C.** Interstitial cells of Cajal in the guinea pig antrum: distribution and regional density. *Cell Tissue Res* 316(1):23-34, 2004.

[53] **Kubota Y, Hashitani H, Shirasawa N, Kojima Y, Sasaki S, Mabuchi Y, Soji T, Suzuki H, Kohri K.** Altered distribution of interstitial cells in the guinea pig bladder following bladder outlet obstruction. *Neurourol Urodyn* 27: 330-340, 2008.

[54] **Powell DW, Mifflin RC, Valentich JD, Crowe SE, Saada JI, West AB.** Myofibroblasts I. Paracrine cells important in health and disease. *Am J Physiol Cell Physiol* 277: 1-19, 1999.

[55] **Powell DW, Mifflin RC, Valentich JD, Crowe SE, Saada JI, West AB.** Myofibroblasts II. Intestinal subepithelial myofibroblasts. *Am J Physiol Cell Physiol* 277: 183-201, 1999.

[56] **Sanders KM**. A case for interstitial cells of Cajal as pacemakers and mediators of neurotransmission in the gastrointestinal tract. *Gastroenterology* 111:492-515, 1996.

[57] **Pucilowska JB, Williams KL, Lund PK**. Fibrogenesis. IV. Fibrosis and inflammatory bowel disease: celular mediators and animal models. *Am J Physiol Gastrointest Liver Physiol* 279: 653-659, 2000.

[58] **Schuppan D, Koda M, Hahn EG.** Fibrosis of liver, pancreas and intestine: common mechanisms and clear targets? *Acta Gastroenterol Belg* 63: 366-370, 2000.

[59] **Van Assche G**. Can we influence fibrosis in Crohn's disease? *Acta Gastroenterol Belg* 64: 193-196, 2001.

[60] **Sanders KM, Ördög T, Ward SM.** Physiology and Pathophysiology of the Interstitial Cells of Cajal: From Bench to Bedside IV. Genetic and animal models of GI motility disorders caused by loss of intestinal cells of Cajal. *Am J Physiol Gastrointest Liver Physiol* 282:G747-G756, 2002.

[61] **Streutker CJ, Huizinga JD, Driman DK., Riddell R.H.** Interstitial cells of Cajal in health and disease. Part II: ICC and gastrointestinal stromal tumours. *Histopathology* 50: 190–202, 2007.

[62] **Burke JP, Mulsow JJ, O´Keane C, Docherty NG, Watson RW, O´Connel PR**. Fibrogenesis in Crohn´s disease. *Am J Gastroenterol* 102: 439-448, 2007.

[63] **Andrae J, Gallini R, Betsholtz C.** Role of platelet-derived growth factors in physiology and medicine. *Genes Dev* 22: 1276-1312, 2008.

[64] **Bonner JC**. Regulation of PDGF and its receptors in fibrotic diseases. *Cytokine Growth Factor Rev* 15: 255-273, 2004.

[65] **Olson LE, Soriano P.** Increased PDGFRα activation disrupts connective tissue development and drives systemic fibrosis. *Dev Cell* 16: 303-313, 2009.

[66] **Beckett EA, Ro S, Bayguinov Y, Sanders KM, Ward SM.** Kit signaling is essential for development and maintenance of interstitial cells of Cajal and electrical rhythmicity in the embryonic gastrointestinal tract. *Dev Dyn* 236: 60-72, 2007

[67] **Sui GP, Rothery S, Dupont E, Fry CH, Severs NJ**. Gap junctions and connexion expression in human suburothelial interstitial cells. *BJU Int* 90:118-129, 2002.

[68] **Vahabi B, McKay NG, Lawson K, Sellers DJ.** The role of c-kit positive interstitial cells in mediating phasic contractions of bladder strips from streptozotocin-induced diabetic rats. *BJU Int* 107: 1480-1487, 2011.